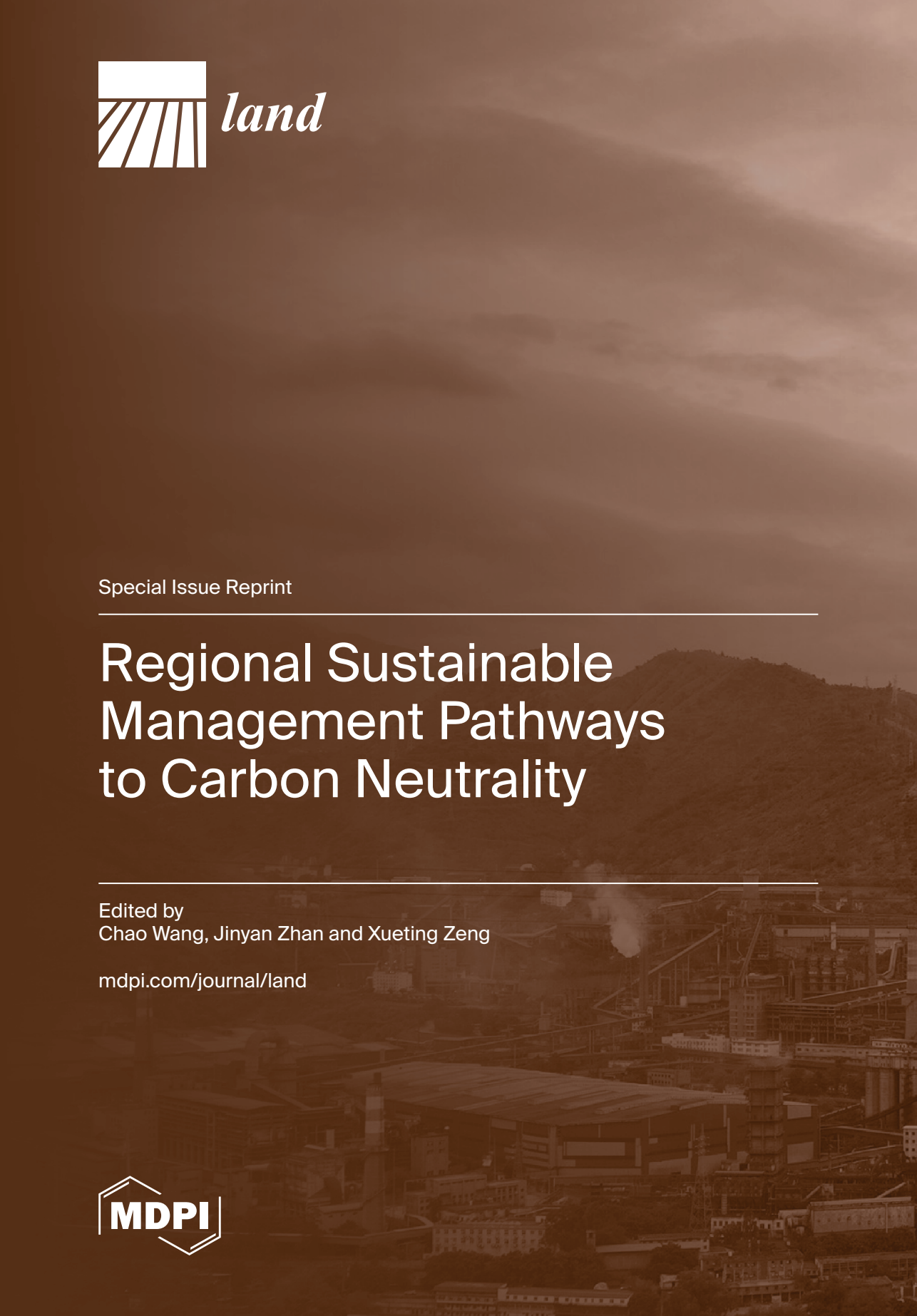

land

Special Issue Reprint

Regional Sustainable Management Pathways to Carbon Neutrality

Edited by
Chao Wang, Jinyan Zhan and Xueting Zeng

mdpi.com/journal/land

MDPI

Regional Sustainable Management Pathways to Carbon Neutrality

Regional Sustainable Management Pathways to Carbon Neutrality

Guest Editors

Chao Wang
Jinyan Zhan
Xueting Zeng

MDPI

Basel • Beijing • Wuhan • Barcelona • Belgrade • Novi Sad • Cluj • Manchester

Guest Editors

Chao Wang
School of Labor Economics
Capital University of
Economics and Business
Beijing
China

Jinyan Zhan
State Key Laboratory of Water
Environment Simulation
School of Environment
Beijing Normal University
Beijing
China

Xueting Zeng
School of Labor Economics
Capital University of
Economics and Business
Beijing
China

Editorial Office
MDPI AG
Grosspeteranlage 5
4052 Basel, Switzerland

This is a reprint of the Special Issue, published open access by the journal *Land* (ISSN 2073-445X), freely accessible at: https://www.mdpi.com/journal/land/special_issues/ZX12G8DDUJ.

For citation purposes, cite each article independently as indicated on the article page online and as indicated below:

Lastname, A.A.; Lastname, B.B. Article Title. *Journal Name* **Year**, *Volume Number*, Page Range.

ISBN 978-3-7258-2641-4 (Hbk)
ISBN 978-3-7258-2642-1 (PDF)
https://doi.org/10.3390/books978-3-7258-2642-1

Cover image courtesy of Chao Wang

Contents

Preface

Controlling carbon emissions has become an important way to realize regional sustainable development. This Reprint aims to encourage scholars to share their theories, methods and results on carbon emissions and carbon neutrality pathways. The Reprint focuses on carbon peak and carbon neutrality, belonging to environmental science, and is suitable for anyone who cares about climate change and carbon neutrality, including scholars, administrators, students, etc. It can be used as a textbook, extracurricular reading, case library, etc. This Reprint effectively summarizes the research progress about carbon emissions, fills the corresponding research gap, and provides the scientific basis for the realization pathways and strategy formulation of the carbon neutrality target.

This Reprint includes 13 articles covering the entire cascade framework from spatiotemporal variations to policy recommendations. There are three papers focusing on carbon emission accounting and spatial distribution characteristics, two papers considering carbon sequestration and carbon balance analysis, three papers exploring the complex relationships between carbon emission and the nature–social–economic system, one paper especially carrying out scenario analysis, and four papers contributing to policy recommendation. The contents include literature reviews, theoretical innovations, case analyses, policy refinements, and so on.

As the editors of the Reprint, we thank the editors of journal *Land* for the publication platform and the editing and publishing work. We thank all the authors of the 13 articles published in the Special Issue. All the authors provide their novel findings and perspectives in the direction of carbon neutrality pathways.

This Reprint and Special Issue was funded by the National Natural Science Foundation of China (Grant No. 72304192).

Chao Wang, Jinyan Zhan, and Xueting Zeng
Guest Editors

land

MDPI

Editorial

Regional Sustainable Management Pathways to Carbon Neutrality

Chao Wang [1], Jinyan Zhan [2,*] and Xueting Zeng [1]

[1] School of Labor Economics, Capital University of Economics and Business, Beijing 100070, China; wangc@cueb.edu.cn (C.W.); zxting1231@163.com (X.Z.)
[2] State Key Laboratory of Water Environment Simulation, School of Environment, Beijing Normal University, Beijing 100875, China
* Correspondence: zhanjy@bnu.edu.cn

With the background of global climate change and rapid economic growth, there are increasing problems threatening regional sustainable development [1]. Many global climate actions have been implemented. Carbon neutrality is gradually becoming a common development goal all over the world. Achieving carbon neutrality requires carbon reduction and a carbon sink increase. Carbon reduction is directly closed to the socioeconomic system, involving industrial structure, productive technology, energy consumption, and so on [2]. While carbon sequestration enhancement should improve carbon sink from the perspective of a natural ecosystem, many studies have been carried out centered on carbon emissions. Carbon emission accounting is basic work. Assessing carbon sinks and analyzing carbon balance states can help judge whether ecological objectives can be achieved. Clarifying the relationship between carbon emissions and socioeconomic systems and assessing the socioeconomic impacts of carbon reduction are crucial for upgrading industrial structures, optimizing energy consumption structures, and so on. Carbon emission prediction is the key to exploring the future realization path to carbon neutrality, such as target planning scenario analysis. Comprehensive management plans and frameworks need to be further and supplemented and improved, including promoting nature-based solutions, establishing ecological product realization mechanisms, standardizing carbon trading markets, and improving negotiation and compensation mechanisms.

This Special Issue, entitled "Regional Sustainable Management Pathways to Carbon Neutrality", presents 13 high-quality original research papers, covering the cascade framework of "spatiotemporal variations–balance analysis–socioeconomic impacts–scenario analysis–policy recommendations" centered on carbon emissions.

Carbon emissions accounting can be based on sector classification or administrative boundaries. Yang and Yan (2024) assessed and analyzed the characteristics of transportation CO_2 emissions and revealed their influencing factors. They classified thirty Chinese provinces into six characteristic types (Types I to VI) and proposed priority control directions and indicators for carbon reduction as well as typological strategies and key performance indicators (KPIs) for each type. The periodic development characteristics of carbon emissions were further explored. Lu et al. (2023) revealed the carbon emission development stage of three urban agglomerations in the Yangtze River Economic Belt. At the same time, the impacts of influencing factors were analyzed. Moreover, the preparation method of carbon emission spatial data was also innovated and developed [3]. Liu et al. (2023) established a carbon emission assessment model based on the "NPP–VIIRS–like" nighttime light data. The spatiotemporal variation of carbon emissions at three different levels and the spatial correlation at the county level were analyzed in the nine provinces along the Yellow River.

Carbon sequestration, as a typical regulation service that can absorb CO_2 and release O_2, becomes a key element in exploring how natural ecosystems contribute to carbon

Citation: Wang, C.; Zhan, J.; Zeng, X. Regional Sustainable Management Pathways to Carbon Neutrality. *Land* **2024**, *13*, 1611. https://doi.org/10.3390/land13101611

Received: 19 September 2024
Revised: 24 September 2024
Accepted: 30 September 2024
Published: 3 October 2024

neutrality. Yang et al. (2024) used the carbon absorption coefficient method to estimate the carbon sink in the Beijing–Tianjin–Hebei Region and explored the carbon sink enhancement potential based on different land use scenarios. They found that the expansion and optimization of arable land, garden land, and forest can effectively enhance carbon sinks. Based on the assessment of carbon source and carbon sink, carbon balance analysis can help with spatial zoning and optimization management. Fan et al. (2024) estimated the grid-scale net ecosystem productivity (NEP), explored the spatiotemporal evolution of carbon budgets, and conducted carbon balance zoning for the 31 cities in the middle reaches of the Yangtze River urban agglomerations (MRYRUA). They found that carbon sink functional zones were distributed in areas with rich ecological resources and proposed specific regional collaborative reduction policies.

The generation of carbon emissions is closely related to socioeconomic system. Most processes of economic production are accompanied by the generation of carbon emissions and pollutants. Many representative indexes have been established to assess environmental performance. Wang et al. (2024) assessed the carbon emission efficiency (CEE) and identified the main influence factors in the Beijing–Tianjin–Hebei Urban Agglomeration (BTHUA). They found that the input-related factors (carbon emissions per capita, employment per ten thousand people, total assets per capita, and energy intensity) had a negative effect on CEE, DP per capita, urbanization level, and proportion of the tertiary sector's GDP had positive impacts on CEE. Xue et al. (2023) considered various environmental pollutants into eco-efficiency (EE) assessment and established an index system to evaluate urbanization efficiency, aiming at analyzing the correlation between EE and urbanization efficiency in the 64 cities in China. Besides efficiency assessment, the impacts of carbon neutrality on land use were also investigated. Yang et al. (2023) analyzed the characteristics and driving mechanism of urban construction land under rapid urbanization and carbon neutrality targets.

The forecast of carbon emission trends can be used as an effective reference for policy-making. Meng et al. (2023) employed an extended STIRPAT model and ridge regression to simulate the projections of carbon peaks under different development scenarios. Moreover, Yang et al. (2024) also used scenario analysis to explore the carbon sink enhancement potential.

As the ultimate export of scientific research, this Special Issue published several papers on policy recommendations. Aligning with the Kunming-Montreal Global Biodiversity Framework (GBF) and other frameworks that support nature-based solutions, the policies and strategies should conform to the correct laws of nature, have a certain priority, and pay attention to harmony between nature and the socio-economy. The articles include carbon compensation zoning, carbon emission trading, ecological products, and synergistic carbon reduction policies. Chen et al. (2023) constructed a more comprehensive per capita carbon compensation zoning model, divided Chinese counties into per capita carbon compensation-type zones, and put forward the suggestions for optimizing low-carbon development. Li and Liu (2023) used a difference-in-differences model and verified that China's carbon emissions trading policy and the horizontal mobility experience of the provincial governors exert a significant positive effect on carbon emission reduction. Moreover, they identified the correlation between political factors and carbon emissions and provided specific suggestions for carbon reduction policy formulation. Wang et al. (2023) focused on the realization mechanism of ecological products and considered conversion efficiency as a convincing method to present the transformation degree of ecological production into economic benefits and the degree of eco–economic synergy. Forest Ecological Products (FEPs) value was evaluated to analyze the conversion efficiency in the Pearl River Delta (PRD). Chen et al. (2023) integrated the game model and general spatial equilibrium model, revealing the formation of regional comparative advantages in emission reductions and their impacts on synergistic emission reductions. Moreover, a form of synergy was proposed to provide trade, industry, and economic growth policies, which complement emission reduction policies.

Author Contributions: Conceptualization, C.W. and J.Z.; writing—original draft preparation, C.W., J.Z., and X.Z.; writing—review and editing, J.Z. and X.Z.; project administration, C.W. All authors have read and agreed to the published version of the manuscript.

Funding: This research was supported by the research funds from the National Natural Science Foundation of China (No. 72304192).

Data Availability Statement: No new data were created or analyzed in this study. Data sharing is not applicable to this article.

Acknowledgments: We are grateful to the authors who submitted papers to this Special Issue, the editors, and the reviewers for their constructive work.

Conflicts of Interest: The authors declare no conflicts of interest.

List of Contributions

1. Yang, Y.; Yan, F. An Inquiry into the Characteristics of Carbon Emissions in Inter-Provincial Transportation in China: Aiming to Typological Strategies for Carbon Reduction in Regional Transportation. *Land* **2024**, *13*, 15. https://doi.org/10.3390/land13010015.
2. Lu, Q.; Lv, T.; Wang, S.; Wei, L. Spatiotemporal Variation and Development Stage of CO_2 Emissions of Urban Agglomerations in the Yangtze River Economic Belt, China. *Land* **2023**, *12*, 1678. https://doi.org/10.3390/land12091678.
3. Liu, Y.; Liu, W.; Qiu, P.; Zhou, J.; Pang, L. Spatiotemporal Evolution and Correlation Analysis of Carbon Emissions in the Nine Provinces along the Yellow River since the 21st Century Using Nighttime Light Data. *Land* **2023**, *12*, 1469. https://doi.org/10.3390/land12071469.
4. Yang, H.; Zhao, S.; Qin, Z.; Qi, Z.; Jiao, X.; Li, Z. Differentiation of Carbon Sink Enhancement Potential in the Beijing–Tianjin–Hebei Region of China. *Land* **2024**, *13*, 375. https://doi.org/10.3390/land13030375.
5. Fan, Y.; Wang, Y.; Han, R.; Li, X. Spatial-Temporal Dynamics of Carbon Budgets and Carbon Balance Zoning: A Case Study of the Middle Reaches of the Yangtze River Urban Agglomerations, China. *Land* **2024**, *13*, 297. https://doi.org/10.3390/land1303029.
6. Wang, C.; Kong, Y.; Lu, X.; Xie, H.; Teng, Y.; Zhan, J. Rethinking Regional High-Quality Development Pathways from a Carbon Emission Efficiency Perspective. *Land* **2024**, *13*, 1441. https://doi.org/10.3390/land13091441.
7. Xue, S.; Wang, C.; Zhang, S.; Weng, C.; Zhang, Y. Eco-Efficiency of the Urban Agglomerations: Spatiotemporal Characteristics and Determinations. *Land* **2023**, *12*, 1275. https://doi.org/10.3390/land12071275.
8. Yang, H.; Ma, J.; Jiao, X.; Shang, G.; Yan, H. Characteristics and Driving Mechanism of Urban Construction Land Expansion along with Rapid Urbanization and Carbon Neutrality in Beijing, China. *Land* **2023**, *12*, 1388. https://doi.org/10.3390/land12071388.
9. Meng, Q.; Li, B.; Zheng, Y.; Zhu, H.; Xiong, Z.; Li, Y.; Li, Q. Multi-Scenario Prediction Analysis of Carbon Peak Based on STIRPAT Model-Take South-to-North Water Diversion Central Route Provinces and Cities as an Example. *Land* **2023**, *12*, 2035. https://doi.org/10.3390/land12112035.
10. Chen, J.; Wu, S.; Zhang, L. Spatiotemporal Variation of Per Capita Carbon Emissions and Carbon Compensation Zoning in Chinese Counties. Land **2023**, *12*, 1796. https://doi.org/10.3390/land12091796.
11. Li, Z.; Liu, B. Understanding Carbon Emissions Reduction in China: Perspectives of Political Mobility. *Land* **2023**, *12*, 903. https://doi.org/10.3390/land12040903.
12. Wang, J.; Liu, W.; Kong, F. Research on Forest Ecological Product Value Evaluation and Conversion Efficiency: Case Study from Pearl River Delta, China. *Land* **2023**, *12*, 1803. https://doi.org/10.3390/land12091803.
13. Chen, D.; Chang, X.; Hong, T.; Ma, T. Domestic Regional Synergy in Achieving National Climate Goals—The Role of Comparative Advantage in Emission Reduction. *Land* **2023**, *12*, 1723. https://doi.org/10.3390/land12091723.

References

1. Wang, H.H.; Zhan, J.Y.; Wang, C.; Chen, B.; Yang, Z.; Bai, C.Y. Short-term fluctuations of ecosystem services beneath long-term trends. *Resour. Conserv. Recycl.* **2024**, *203*, 107454. [CrossRef]

2. Zhan, J.; Wang, C.; Wang, H.; Zhang, F.; Li, Z. Pathways to achieve carbon emission peak and carbon neutrality by 2060: A case study in the Beijing-Tianjin-Hebei region, China. *Renew. Sustain. Energy Rev.* **2024**, *189*, 113955. [CrossRef]
3. Wang, C.; Yang, Y.; Bai, Y.; Teng, Y.; Zhan, J. Land use data can improve the accuracy of carbon emission spatial inversion model. *Land Degrad. Dev.* **2024**, *35*, 2345–2366. [CrossRef]

land

MDPI

Article

An Inquiry into the Characteristics of Carbon Emissions in Inter-Provincial Transportation in China: Aiming to Typological Strategies for Carbon Reduction in Regional Transportation

Yuhao Yang and Fengying Yan *

School of Architecture, Tianjin University, Tianjin 300072, China; yangyuhao@tju.edu.cn
* Correspondence: fengying@tju.edu.cn

Abstract: The low-carbon development of the transportation sector is crucial for China to achieve its national goals of carbon peaking and carbon neutrality. Since China is a vast country with unbalanced regional development, there are considerable differences in the levels of carbon dioxide emissions from the transportation sector across regions. Therefore, revealing the influencing factors that shape the characteristics of transportation carbon dioxide emissions (TCO_2) can inform tailored sub-national carbon reduction strategies based on local conditions, which is an important technical approach for achieving national goals. Based on an extended Kaya identity, we derived indicators of the impacts on provincial TCO_2 from factors such as economic development, population density, energy structure, transportation efficiency, technology research and development (R&D), infrastructure construction, transportation operation conditions, and residents' transportation behavior. Using a multi-indicator joint characterization method, we explored the characteristics of provincial TCO_2 in China in 2019. By applying Ward's method to hierarchical clustering, the thirty provinces of China were classified into six characteristic types (Types I to VI). Based on the total TCO_2 (TC), the intensity of TCO_2 (TI), and the per capita TCO_2 (TP) calculated for each province in 2019, the priority control directions and indicators for carbon reduction in each type were obtained through relative relationships with provincial averages and correlation analysis with the indicators. Specifically, Type I and Type IV can be categorized as TP-controlled, Type II and Type III as TC-controlled, and Type V and Type VI as TI-controlled. Finally, we provided typological strategies and key performance indicators (KPIs) relevant to local governments to better achieve carbon reduction goals in each provincial type. It can promote cooperative development and collaborative governance in carbon reduction across regions and the unified implementation of China's dual-carbon goals.

Keywords: transportation carbon dioxide emissions; extended kaya identity; carbon emissions characteristics; inter-provincial difference; low-carbon development; influencing factors; typological strategies

Citation: Yang, Y.; Yan, F. An Inquiry into the Characteristics of Carbon Emissions in Inter-Provincial Transportation in China: Aiming to Typological Strategies for Carbon Reduction in Regional Transportation. *Land* **2024**, *13*, 15. https://doi.org/10.3390/land13010015

Academic Editors: Jinyan Zhan, Chao Wang and Xueting Zeng

Received: 1 December 2023
Revised: 14 December 2023
Accepted: 18 December 2023
Published: 20 December 2023

1. Introduction

Practicing low-carbon development to mitigate increasingly severe global climate change has become an important international consensus. The transportation sector is a major contributor to global CO_2 emissions. In 2021, CO_2 emissions from the transportation sector reached 7.7 billion metric tons, which accounted for 25% of the total global CO_2 emissions [1]. Therefore, the transportation sector is a key industry for achieving global carbon reduction goals [2–5]. As the world's largest greenhouse gas emitting country [5–7], China's transportation carbon dioxide emissions (TCO_2) rank third nationally across all sectors [7–10]. According to International Energy Agency predictions, China's TCO_2 is predicted to account for more than one-third of global transportation emissions by 2035 [11]. Meanwhile, as the largest developing country, China's TCO_2 is expected to continue growing rapidly, making it a key sector for achieving the goals of carbon peaking and carbon neutrality [5,7].

As subordinate units tasked with achieving China's national low-carbon goals, provincial administrations play an overarching institutional role in planning and coordination. China's vast geographic expanse has resulted in significant objective differences across provinces in factors like economic development, population distribution, resource endowments, and urbanization levels. This has led to considerable variability in CO_2 emission levels across provincial transportation sectors [12]. Therefore, an in-depth analysis of inter-provincial differences in the transportation sector, using scientific and rational methods to reveal characteristics of provincial TCO_2, followed by tailored carbon reduction strategies for different characteristic regions, is the basic premise and important guarantee for effectively achieving low-carbon transportation development goals.

The provincial TCO_2 characteristics described in this study refer to the combination of multiple influencing factors affecting the direct quantity of TCO_2, including influencing factors affecting the total TCO_2 (TC), the intensity of TCO_2 (TI), the per capita TCO_2 (TP), etc., which can effectively reflect the systematic characteristics of inter-provincial transportation sectors in aspects such as economy, energy, efficiency, technology, infrastructure, operation, and so on. Due to the necessity and urgency of understanding inter-provincial TCO_2 characteristics, scholars have conducted extensive research on this topic in recent years, which can be summarized into three aspects: direct quantity characteristics, correlated quantity characteristics, and influencing factor characteristics. (1) Direct quantity characteristics refer to revealing spatial distribution characteristics of the direct quantity of TCO_2 [13–15], spatial correlation characteristics [16], and their evolutionary patterns [17], based on provincial TCO_2 accounting. (2) Correlated quantity characteristics refer to characteristics reflecting specific aspects that influence the direct quantity of TCO_2, such as transportation CO_2 emission efficiency [18–21], TCO_2 reduction potential [7], inter-provincial intelligent transportation characteristics [22], and carbon reduction effects of transportation structure adjustments [23]. (3) Influencing factor characteristics involve a more comprehensive and detailed description of inter-provincial TCO_2 characteristics by exploring the factors that influence the direct quantity of TCO_2. Existing studies mainly adopt econometric models like multivariate regression, panel data models, and extended models based on factors such as Kaya identity, IPAT, and STIRPAT to reveal the influencing factors of the direct quantity of TCO_2. Furthermore, factor decomposition models (e.g., Laspeyres index decomposition, Divisia index decomposition, LMDI, generalized fisher index decomposition) are also applied to study the impacts of influencing factors on the direct quantity of TCO_2.

Existing studies have explored the macro-level influencing factors of TCO_2 characteristics, including economic development level, population size, transportation energy intensity, transportation energy structure, transportation intensity, and industrial structure [5,24–26]. Additionally, studies have examined the impacts of transportation infrastructure development, such as urbanization rate, fixed asset investment in the transportation industry [27,28], length of road network [29–31], level of public transportation development [32,33], per capita private car ownership, passenger and freight turnover [34,35], average transportation distance [36], logistics scale, and express delivery industry development [37,38]. Furthermore, the impacts of transportation technology level and new energy industry planning have been investigated, such as R&D investment [39,40], level of digital innovation [41], and new energy vehicle industry [42], etc.

In summary, although existing studies on inter-provincial TCO_2 characteristics have gradually become more comprehensive in coverage, more detailed in evaluation indicators, and clearer in understanding the relationships, this study of CO_2 emissions in the transportation sector is a complex system with numerous influencing factors. The selection of evaluation indicators needs to balance comprehensiveness and feasibility, and the classification of characteristics needs to assist in coordinating the advantages and disadvantages of provinces in low-carbon transportation development. Otherwise, only broad and general conclusions can be drawn, which is not conducive to the implementation of carbon reduction actions by provinces or regional cooperation and coordinated governance. Moreover, macro-level indicators used in existing research, in order to have a strong mathe-

matical relationship with TCO_2, tend to be broader and more general in terms of coverage (i.e., evaluation indicators have macroscopic and comprehensive characteristics), which correspondingly may sacrifice the coverage of indicator content and the directedness of regulatory mechanisms.

Compared to existing research, this study makes the following contributions: (1) A multi-indicator joint characterization method is proposed to reveal provincial TCO_2 characteristics comprehensively. (2) The coverage of provincial TCO_2 characteristics is expanded by adding indicators for urban and county population density levels (UPL), transportation operation pressure (TOP), and resident living consumption levels (RLC). (3) The hierarchical clustering categorization effectively reveals provincial advantages and disadvantages in TCO_2 characteristics, which facilitates cooperation and coordinated governance across Chinese regions. (4) Characteristic indicators have an important integrating function, combining to reflect the inter-provincial TCO_2 characteristics, the evaluation criteria for the classification of characteristic types, and directly corresponding to typological carbon reduction measures and key performance indicators (KPIs).

2. Materials and Methods

This study proposes a multi-indicator joint characterization method to construct evaluation indicators and typological categorization of inter-provincial TCO_2 characteristics in China, aiming to establish carbon reduction strategies supporting provincial differentiation and regional collaboration. The methods used in this study can be divided into five steps: (1) a multi-indicator joint characterization method; (2) hierarchical cluster analysis following Ward's method; (3) analysis of provincial type characteristics; (4) TCO_2 accounting and their correlation analysis with indicators; (5) carbon reduction strategies and KPIs for provincial types. Figure 1 illustrates the procedures, methods, and contents for achieving the research objectives. The overall research framework adopted this approach to measure sub-national TCO_2 characteristics, categorize types, and formulate carbon reduction strategies, which is applicable to studies of other countries and regions with similar needs and data sources for carbon reduction.

2.1. Data Sources

As China was affected by the COVID pandemic, the data from 2020 to 2022 are expected to be less representative, so this study uses the data from 2019 for the calculation of the indicators. Among them, TES, TEE, and RDL are from the *China Transport Statistical Yearbook 2019* and *China Energy Statistical Yearbook 2020*. The other six indicators are from the *China Statistical Yearbook 2020*. Due to missing energy data or statistical calibration differences, Tibet, Hong Kong, Macau, and Taiwan are excluded from the study sample.

It is worth noting that in China, the transportation, storage, and postal sectors are commonly perceived as a unified industrial entity due to historical continuity, functional interconnections, management efficiency, and industry characteristics. This integration is aimed at enhancing regulatory oversight and operational coordination. Therefore, in this study, when referring to the transportation sector, we specifically denote transportation, storage, and postal services. This approach is adopted to comprehensively consider the impact and role of these sectors in carbon emissions.

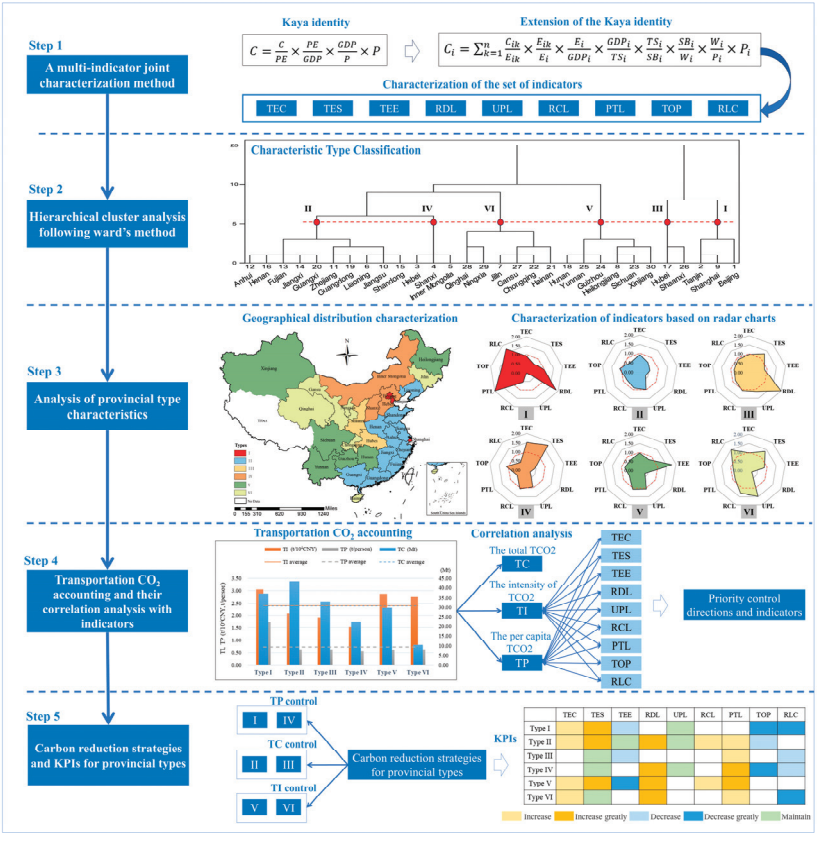

Figure 1. Framework of the research process workflow.

2.2. Multi-Indicator Joint Characterization Method for Provincial TCO_2 Characteristics

2.2.1. Construction Process of Characteristic Indicators

The Kaya identity establishes mathematical relationships among factors like population, energy, economy, and CO_2 emissions [43]. Due to its simple structure and convenient operation, it can fully decompose CO_2 emissions structurally and is often used to build relationships between CO_2 emissions and influencing factors. The equation can be expressed as follows:

$$C = \frac{C}{PE} \times \frac{PE}{GDP} \times \frac{GDP}{P} \times P \tag{1}$$

where C represents total CO_2 emissions, PE represents total energy consumption, GDP represents gross domestic product, and P represents total population. In this study, CO_2 emissions from transportation sector energy consumption are determined by extending the Kaya equation to identify influencing factors. Then Formula (1) can be expanded as:

$$C_i = \sum_{k=1}^{n} \frac{C_{ik}}{E_{ik}} \times \frac{E_{ik}}{E_i} \times \frac{E_i}{GDP_i} \times \frac{GDP_i}{TS_i} \times \frac{TS_i}{SB_i} \times \frac{SB_i}{W_i} \times \frac{W_i}{P_i} \times P_i \tag{2}$$

where i represents the thirty provinces in China, k represents the n types of energy consumed in the transportation sector, C_{ik} represents the CO_2 emissions of energy type k in province i, E_{ik} represents the consumption of energy type k in province i, C_{ik}/E_{ik} represents the CO_2 emission coefficient of energy type k, E_i represents the total energy consumption of the transportation sector in province i, E_{ik}/E_i represents the energy structure of the trans-

portation sector in province i, GDP_i represents the added value of transportation, storage and post in province i, E_i/GDP_i represents the energy consumption per unit added value of the transportation sector in province i (i.e., transportation energy intensity), TS_i represents the area of transportation infrastructure in province i, GDP_i/TS_i represents the economic returns per unit area of transportation infrastructure (i.e., transportation economic output intensity), SB_i represents the built-up area in province i, TS_i/SB_i is the proportion of transportation infrastructure area to built-up area, representing the level of transportation infrastructure construction in province i, W_i represents the total transportation pollutants in province i, SB_i/W_i is the reciprocal of built-up area per unit transportation pollutants, with the ratio relationship reflecting transportation pollution intensity in province i, and P_i represents the year-end population in province i, W_i/P_i represents per capita transportation pollutants, indicating the pollution intensity of resident transportation behaviors in province i.

2.2.2. Definition of Characteristic Indicators

Based on the identified influencing factors of TCO_2 described above and referring to evaluation indicators corresponding to influencing factors in existing studies [5,9,17,24–27,32,33,39,44,45], this study adopts a multi-indicator joint characterization method and constructs nine characteristic indicators to reveal provincial TCO_2 characteristics (Table 1).

Table 1. Expressions and parameter definitions of characteristic indicators.

Influence Factors	Indicator Name and Abbreviation	Indicator Description	Indicator Expression and Parameter Definition
Transportation economic output intensity	Transportation economic structure (TEC)	Reflects the level of economic structure share of the transportation sector in province i compared to the provincial average.	$\mathrm{TEC} = \frac{\mathrm{EC}_i/\mathrm{GDP}_i}{\overline{TEC'}}$ EC_i is the added value of the transportation sector in province i, GDP_i is the gross domestic product of province i, $\overline{TEC'}$ is the provincial average value of the numerator.
Transportation energy structure	Transportation energy structure (TES)	Reflects the level of clean energy structure share in the transportation energy consumption of province i compared to the provincial average.	$\mathrm{TES} = \frac{\mathrm{RE}_i/\mathrm{TE}_i+\mathrm{HE}_i}{\overline{TES'}}$ RE_i is the consumption of clean energies such as electricity and natural gas in the transportation sector of province i, TE_i is the total energy consumption of transportation in province i, HE_i is the consumption of "gasoline" and "diesel oil" in "residential life" of province i, $\overline{TES'}$ is the provincial average value of the numerator.
transportation energy intensity	Transportation energy consumption efficiency (TEE)	Reflects the level of energy consumption per unit of transportation turnover in province i compared to the provincial average.	$\mathrm{TEF} = \frac{(\mathrm{TE}_i+\mathrm{HE}_i)/\mathrm{TT}_i}{\overline{TEF'}}$ TT_i is the total transportation turnover (including passenger and freight turnover), $\overline{TEF'}$ is the provincial average value of the numerator.
	R&D level of transportation technology (RDL)	Reflects the level of technological R&D capability in the transportation sector of province i compared to the provincial average.	$\mathrm{RDL} = \frac{\mathrm{RD}_i/\mathrm{PO}_i}{\overline{RDL'}}$ RD_i is the internal expenditure on R&D funds for the transportation sector in province i, PO_i is the year-end population of province i, $\overline{RDL'}$ is the provincial average value of the numerator.
Population factor	Urban population density level (UPL)	Reflects the level of the gap between the population density of urban and county in province i compared to the provincial average (lower values indicate higher urban population density).	$\mathrm{UPL} = \frac{\mathrm{CP}_i/\mathrm{UP}_i}{\overline{UPL'}}$ CP_i is the county population density of province i, UP_i is the urban population density of province i, $\overline{UPL'}$ is the provincial average value of the numerator.

Table 1. *Cont.*

Influence Factors	Indicator Name and Abbreviation	Indicator Description	Indicator Expression and Parameter Definition
Transportation infrastructure construction	Road construction level (RCL)	Reflects the level of intensity of urban road and highway construction in province i compared to the provincial average.	$RCL = 0.5 \times \frac{UR_i/UP_i}{\overline{R1'}} + 0.5 \times \frac{HM_i/PO_i}{\overline{R2'}}$ UR_i is the actual urban road length by year-end of province i, UP_i is the urban population by year-end of province i, HM_i is the highway mileage of province i, $\overline{R1'}$ and $\overline{R2'}$ are the provincial average values of each numerator.
	Public transportation construction level (PTL)	Reflects the level of intensity of urban public transportation construction in province i compared to the provincial average.	$PTL = 0.5 \times \frac{BT_i/UP_i}{\overline{P1'}} + 0.3 \times \frac{RT_i/UP_i}{\overline{P2'}} + 0.2 \times \frac{TX_i/UP_i}{\overline{P3'}}$ BT_i is the number of operating buses and trolley buses in cities of province i, RT_i is the number of rail transit vehicles assigned in province i, TX_i is the number of taxis in province i, $\overline{P1'}$, $\overline{P2'}$, and $\overline{P3'}$ are the provincial average values of each numerator.
Transportation pollution intensity	Traffic operation pressure (TOP)	Reflects the level of potential and current pressure from road traffic operation in province i compared to the provincial average.	$TOP = 0.5 \times \frac{PC_i/PO_i}{\overline{T1'}} + 0.5 \times \frac{TC_i}{\overline{T2'}}$ PC_i is the private car ownership in province i, TC_i is the sum of road traffic congestion in province i. $\overline{T1'}$, and $\overline{T2'}$ are the provincial average values of each numerator.
Pollution intensity of resident transportation behaviors	Residents' living consumption level (RLC)	Reflects the level of consumption and travel frequency of residents in province i compared to the provincial average.	$RLC = 0.5 \times \frac{TR_i/PO_i}{\overline{C1'}} + 0.5 \times \frac{TP_i/PO_i}{\overline{C2'}}$ TR_i is the total resident consumption expenditure of province i, TP_i is the passenger volume of province i. $\overline{C1'}$, and $\overline{C2'}$ are the provincial average values of each numerator.

Note: (1) The indicators are dimensionless, and no unit description is provided. (2) The total transportation turnover in the TEE indicator includes both passenger turnover and freight turnover. Following existing research [46], passenger turnover was converted to freight turnover using a conversion coefficient of 1 t·km = 7.1 person·km, and then summed up. (3) For UPL, since Beijing, Shanghai, and Tianjin are cities in the later stages of urbanization, county population statistics are not available (values are 0) in the *China Statistical Yearbook 2020*. Therefore, county population was used as the numerator for calculation.

To eliminate unfairness caused by inter-provincial differences as well as dimensional and quantitative differences among indicators, indicator values are quantified by the ratio of provincial value to provincial average. Indicator values less than or equal to 1 indicate the provincial characteristic is below or equal to the national average, and vice versa. This method of index construction enables the monitoring of current deficiencies in governmental low-carbon actions and the identification of existing measures with poor implementation effectiveness.

For indicators involving multiple sub-contents, weights are assigned for definition. The two sub-contents of RCL, TOP, and RLC are assigned equal importance weights of 0.5. For the three sub-contents of PTL, weights are assigned based on generality and relative importance (Table 1).

2.3. Hierarchical Cluster Analysis following Ward's Method

Cluster analysis provides means of data dimensionality reduction and visualization, representative sample screening, and enables scientific classification and grouping of data, thus revealing similarities and differences among provinces and promoting cooperation and coordinated governance across regions. Before cluster analysis, this study standardized the indicators. The value range of the constructed characteristic indicators is [0, ∞]. To eliminate the negative effects of excessive outliers and facilitate effective interpretation of indicator meanings, this study assigned a value of 2 to all indicators greater than 2. Thus, the indicator value range is [0, 2]. An indicator value of 2 indicates the provincial

characteristic is far above the provincial average level. Based on validation with our existing study [47], the maximum value control approach has good effects on the stability of type division and eliminates potential unfairness in inter-provincial policy allocation.

Hierarchical clustering is the most widely used clustering method [48]. Each sample starts as its own cluster, and at each iteration of the algorithm, clusters with high similarity are merged. This process repeats until a preset number of clusters is reached or only one cluster remains. Since this method does not require pre-classification, it is suitable for classification decisions combining subjective and objective factors. In hierarchical cluster analysis, Ward's method [49] uses squared Euclidean distance as the distance between categories, emphasizing smaller internal differences within the same category and greater differences between different categories. Therefore, this study applies Ward's method to the nine characteristic indicators across thirty Chinese provinces, which can effectively reveal similarities and differences in provincial TCO_2 characteristics.

2.4. Transportation CO_2 Emissions Calculation Methods

To ensure the convenience and accuracy of calculations, this study is based on the IPCC guidelines [50] and the research of Shan et al. [51] for TCO_2 calculations. TC from the transportation sector is the sum of direct CO_2 emissions from fossil energy consumption in the transportation sector (not including indirect emissions from electricity consumption) and CO_2 emissions from gasoline and diesel consumption related to residential life. TI is the ratio of TC to the value-added of the transportation sector. TP is the ratio of TC to the year-end population of the province.

Total CO_2 emissions from the transportation sector are calculated as follows:

$$C = CF_{tr} + CF_{li} \tag{3}$$

where C represents total CO_2 emissions from the transportation sector, CF_{tr} represents CO_2 emissions from fossil fuel consumption in the transportation sector, and CF_{li} represents CO_2 emissions from fossil fuel consumption in transportation activities in residential life.

The CO_2 emissions from fossil energy consumption in the transportation sector are calculated as follows:

$$CF = \sum_{j}^{n} E_j \times NCV_j \times CC_j \times O_j \tag{4}$$

In the CF_{tr} CO_2 emission calculations, E_j represents the total consumption of fossil fuel type j, involving raw coal, cleaned coal, other washed coal, briquettes, coke oven gas, gasoline, kerosene, diesel oil, fuel oil, lubricants, liquefied petroleum gas, natural gas, and other energy sources. NCV_j represents the net calorific value of different energy types, i.e., the heat value generated per physical unit of fuel combusted. CC_j (carbon content) is the CO_2 emissions per unit of net calorific value generated by fuel j. O_j represents the oxidation rate during fuel combustion. For CF_{li}, only CO_2 emissions from transportation-related gasoline and diesel oil consumption are calculated for urban and rural residents.

2.5. Correlation Analysis between Characterization Indicators and the Direct Quantity of TCO_2

Correlation analysis is a commonly used method for discovering associations between things. Among them, the Pearson correlation coefficient method [52] can examine the linear correlation between variables, measured on a scale from -1 to +1. It reflects both the directionality of the co-variation between two variables as well as the extent of it. A value of 0 indicates no correlation; positive values denote positive correlation; and negative values mean negative correlation. The larger the absolute value, the stronger the correlation. This method has been widely applied across numerous fields and disciplines. In this study, the Pearson correlation coefficient method was used to analyze the correlations between the direct quantity of TCO_2 (TI and TP) in thirty provinces of China and the original values of nine selected feature indicators (i.e., values greater than two were retained). The aim

was to determine the degree of correlation between variables and provide more accurate references for implementing carbon reduction measures.

3. Results and Discussion

3.1. Results of Characteristic Indicator Calculation and Cluster Analysis

After calculating the nine characteristic indicators across thirty Chinese provinces in 2019, this study conducted standardization processing on the indicator values (i.e., defining maximum indicator values), so the value range of the characteristic indicators is [0, 2]. See Appendix A, Table A1. This study performed hierarchical cluster analysis with Ward's method on the characteristic indicators across thirty provinces using SPSS Statistics 25 software to obtain the classification dendrogram of provinces and divided the thirty Chinese provinces into six types by the vertical line segmentation method (Figure 2).

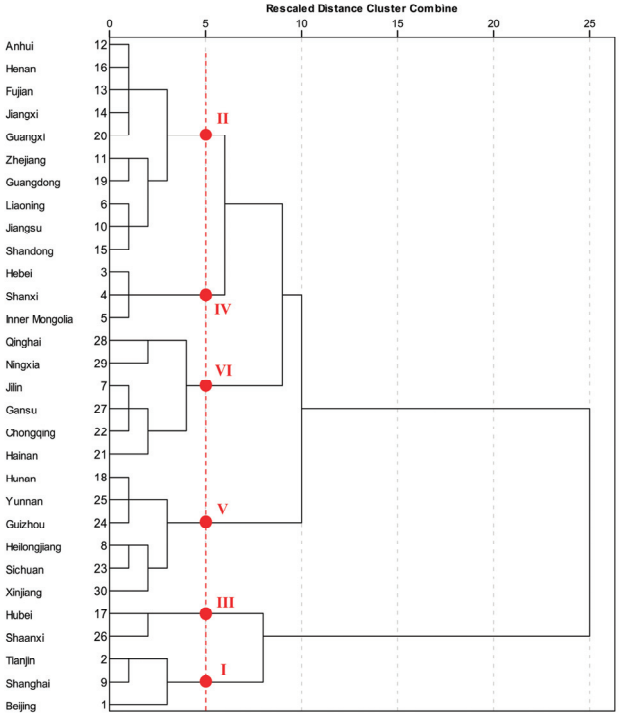

Figure 2. Type division based on hierarchical cluster analysis with Ward's method.

3.2. Analysis of Provincial Type Characteristics

The geographic distribution and TCO_2 characteristics of the six types and their member provinces are shown in Figure 3. Except for a few individual provinces, the member provinces of each type generally have distinct geographical adjacencies. The average value of each indicator across the member provinces in each type was used as the characteristic indicator for types I to VI (Table 2). Comparing with the provincial average (i.e., average value of 1) helps identify the advantageous and disadvantageous characteristics of each type for more effective indicator feature analysis.

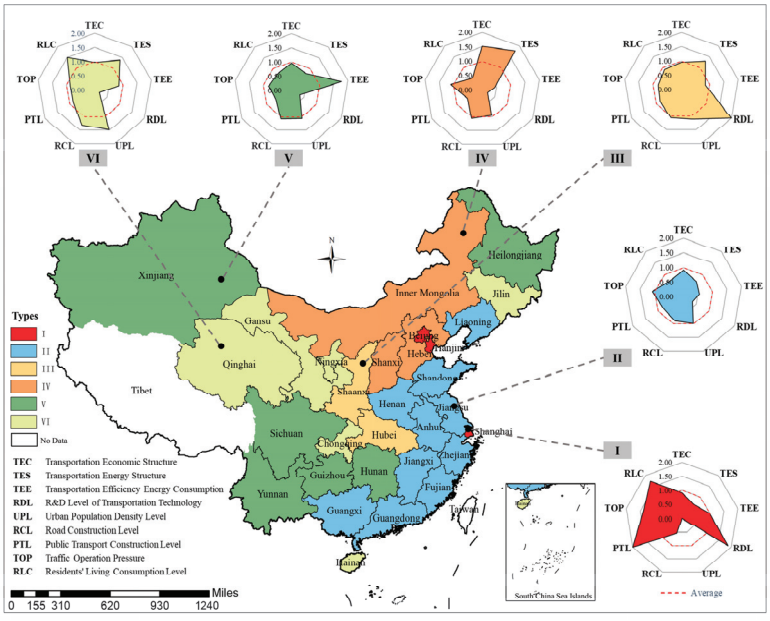

Figure 3. The geographic distribution and TCO_2 characteristics of types I–VI.

Table 2. Numerical values of characteristic indicators for Types I–VI.

Type	TEC	TES	TEE	RDL	UPL	RCL	PTL	TOP	RLC
Type I	0.91	0.65	0.99	1.87	0.00	0.54	2.00	1.39	1.73
Type II	0.91	0.68	0.55	0.35	0.97	0.88	0.80	1.08	0.72
Type III	0.96	1.29	0.86	2.00	1.11	1.05	0.85	0.82	0.92
Type IV	1.51	1.77	0.45	0.21	0.94	1.05	0.59	1.10	0.53
Type V	0.96	0.78	1.77	0.34	1.06	1.08	0.64	0.81	0.76
Type VI	0.98	1.38	0.86	0.18	1.47	1.30	0.86	0.87	1.50

For indicator value interpretation, this study divided the [0, 2] interval of the indicator range into different levels: [0, 0.5] indicates a low level, (0.5, 0.95) indicates a relatively low level, [0.95, 1.05] indicates reaching the provincial average level, (1.05, 1.5) indicates a relatively high level, [1.5, 2) indicates a high level, and 2 represents far above the provincial average and is the maximum value in the indicators. What is worth noting is that due to the special construction of the UPL, its values exhibit the opposite levels, i.e., lower values indicate higher urban population density. The TES is similar, with higher values indicating lighter energy structures characterized by degrees of light and heavy.

(1) Type I includes Beijing, Tianjin, and Shanghai, which are municipalities directly under the central government in China. They have high levels of economic development and urbanization, comprehensive infrastructure construction, and are the most densely populated areas in China. As shown in Figure 4, the advantageous characteristics of Type I are as follows: a high level of transportation technology R&D (RDL), which ranks the second highest among all types; the highest level of public transportation construction (PTL) among all types; and transportation energy consumption efficiency (TEE) reaching the provincial average. The disadvantageous characteristics are as follows: a relatively heavy transportation energy structure (TES), characterized by a lower share of clean transportation energy (ranked lowest among all types); high urban population density level (UPL), which is the highest among all types; high traffic operation pressure (TOP), which refers to the number of private cars and the degree of road congestion (ranked the highest among the

types); high residents' living consumption level (RLC), which is the highest among the types; relatively low road construction level (RCL), which is the lowest among the types; and low transportation economic structure (TEC), which ranks lowest among the types.

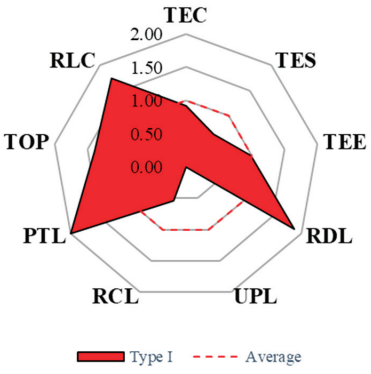

Figure 4. Radar chart of characteristic indicators for Type I.

(2) Type II includes Liaoning, Jiangsu, Zhejiang, Anhui, Fujian, Jiangxi, Shandong, Henan, Guangdong, and Guangxi, mostly located in economically vibrant eastern coastal regions and adjacent coastal provinces in central China, with good geographical adjacency, high economic development, high urbanization levels, high population density, and complex and developed transportation networks. As shown in Figure 5, the advantageous characteristics are as follows: relatively low TEE indicator (2nd lowest among the types), UPL indicator reaching provincial average, and relatively low RLC indicator (2nd lowest among the types). The disadvantageous characteristics are as follows: low RDL indicator, relatively heavy TES indicator (2nd highest among the types), relatively low PTL indicator, high TOP indicator, relatively low RCL indicator (2nd lowest among the types), and the lowest TEC indicator among the types.

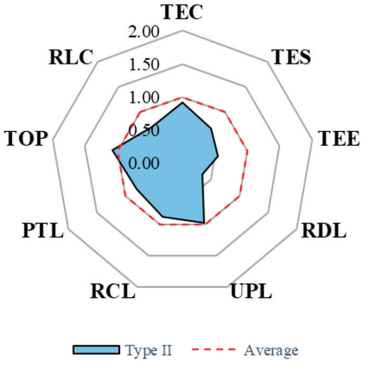

Figure 5. Radar chart of characteristic indicators for Type II.

(3) Type III includes Hubei and Shaanxi, adjacent provinces in central China with medium levels of economic development and urbanization. They are important industrial bases with relatively complete industrial systems and also play important transportation hub roles in their regions. As shown in Figure 6, the advantageous characteristics are as follows: relatively low UPL and TOP indicators (2nd lowest among the types), relatively low TEE and RLC indicators, relatively light TES indicators, and the highest RDL indicators among the types. Additionally, the RCL indicator and TEC indicators reach provincial averages. The disadvantageous characteristic is the relatively low PTL indicator. Type III is

the type with the most advantages for low-carbon transportation development among the six types.

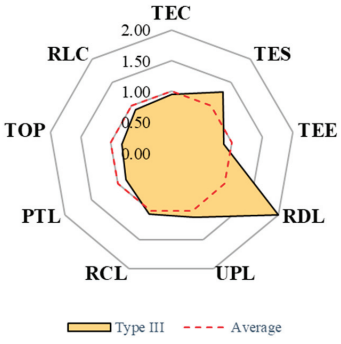

Figure 6. Radar chart of characteristic indicators for Type III.

(4) Type IV includes Hebei, Shanxi, and Inner Mongolia, all located in northern China with good geographical adjacency. They are focused on heavy industry and energy production, have relatively lower economic development, abundant natural mineral resources, and are important coal production bases in China. As shown in Figure 7, the advantageous characteristics are as follows: the highest TEC indicator, the lightest TES indicator, and the lowest TEE indicator among the types. Additionally, there is a relatively low RLC indicator (ranked 1st among the types), and the RCL indicator reaches the provincial average. The disadvantageous characteristics are as follows: relatively low PTL indicator (ranked the lowest among the types), low RDL indicator (2nd lowest among the types), relatively high TOP and UPL indicators (2nd highest among the types).

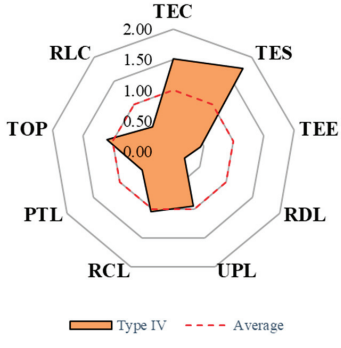

Figure 7. Radar chart of characteristic indicators for Type IV.

(5) Type V includes Heilongjiang, Hunan, Sichuan, Guizhou, Yunnan, and Xinjiang, mainly located in northern and southwestern China. Their economic development levels vary, but they are overall relatively low. They are undergoing rapid urbanization, possess abundant natural resources, and are important energy bases in China, with vast territories and complex terrains. As shown in Figure 8, the advantageous characteristics are as follows: relatively high RCL indicator (2nd highest among the types), relatively low RLC and UPL indicators, relatively light TES indicator, TEC indicator reaching provincial average, and the lowest TOP indicator among the types. The disadvantageous characteristics are as follows: the highest TEE indicator among the types, a low RDL indicator, and a relatively low PTL indicator (2nd lowest among the types).

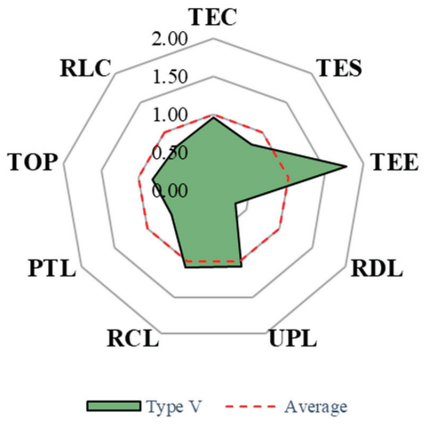

Figure 8. Radar chart of characteristic indicators for Type V.

(6) Type VI includes Jilin, Hainan, Chongqing, Gansu, Qinghai, and Ningxia, primarily located in the western region of China, with the inclusion of provinces situated in specific geographical locations in the northeastern region (e.g., Jilin) and the eastern region (e.g., Hainan). These provinces have a large spatial span and poor geographical adjacency, varying levels of economic development and urbanization, relatively low economic output and growth rate, and are in the stage of actively promoting new urbanization. They possess abundant natural and cultural tourism resources, with Gansu and Qinghai being important new energy bases in China. As shown in Figure 9, the advantageous characteristics are as follows: the highest RCL indicator and the lowest UPL indicators among the types; the TEC indicator reaches the provincial average, ranking as the second highest among the types. Additionally, it exhibits a relatively light TES indicator, which is also the second highest among the types. Moreover, this type shows relatively low TEE and TOP indicators. The disadvantageous characteristics are as follows: the lowest RDL indicator among the types, a relatively low PTL indicator, and a high RLC indicator (2nd highest among the types).

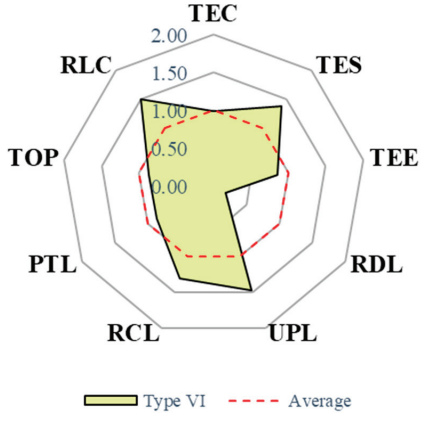

Figure 9. Radar chart of characteristic indicators for Type VI.

3.3. Calculation Results of Provincial TCO_2

By applying Formulas (3) and (4) to calculate the TCO_2 for each province, TC, TI, and TP for each province and Types I–VI are obtained, as shown in Appendix A, Table A2. For the TC of provinces in China, regions with relatively high TC ($\geq$24.29 Mt, where Mt represents 10^6 tons), excepting Jiangxi Province, are mainly eastern coastal provinces

and adjacent provinces, while western regions are mainly the two adjacent provinces of Sichuan and Yunnan. The provinces with the highest TC are Guangdong (93.34 Mt), Jiangsu (60.4 Mt), Shanghai (58.56 Mt), and Shandong (56.77 Mt), all located in eastern coastal regions. Furthermore, provinces with relatively low TC (<24.8 Mt) exhibit an approximately "Y-shaped" spatial distribution pattern. For the TI of provinces in China, regions with relatively high TI ($\geq$2.44 t/10^4 CNY) are mainly clustered in western regions, with sporadic distributions in central, eastern, and northeastern regions. The provinces with the highest TI are Qinghai (4.56 t/10^4 CNY), Heilongjiang (3.82 t/10^4 CNY), Beijing (3.69 t/10^4 CNY), Liaoning (3.62 t/10^4 CNY), and Shanghai (3.55 t/10^4 CNY). For the TP of provinces in China, areas with relatively high TP ($\geq$0.65 t/person) mainly exhibit sporadic spatial distributions, with Shanghai (2.41 t/person) and Beijing (1.76 t/person) having the highest values. See Figures 10 and 11, and Table 3 for details.

Table 3. Numerical values of TC, TI, and TP for Types I–VI.

Type	TC (Mt)	TI (t/10^4 CNY)	TP (t/Person)
Type I	37.15	3.05	1.71
Type II	43.47	2.07	0.63
Type III	33.06	1.91	0.64
Type IV	22.41	1.53	0.56
Type V	29.89	2.88	0.63
Type VI	10.49	2.76	0.64
Provincial average	30.73	2.40	0.73

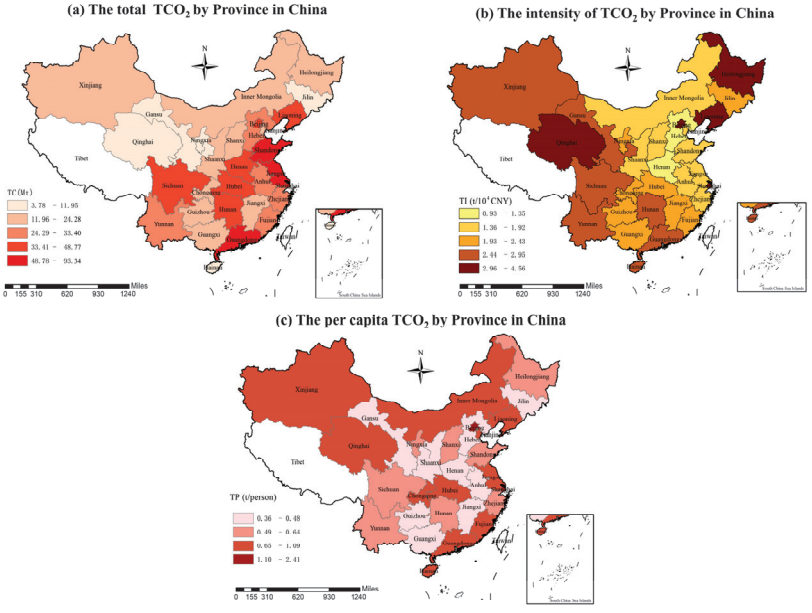

Figure 10. The geographic distribution of TC, TI, and TP across Chinese provinces.

For TC of the types, Type I accounted for 37.15 Mt, Type II accounted for 43.47 Mt, Type III accounted for 33.06 Mt, Type IV accounted for 22.41 Mt, Type V accounted for 29.89 Mt, and Type VI accounted for 10.49 Mt, with a provincial average of 30.73 Mt. For TI of the types, Type I accounted for 3.05 t/10^4 CNY, Type II accounted for 2.07 t/10^4 CNY, Type III accounted for 1.91 t/10^4 CNY, Type IV accounted for 1.53 t/10^4 CNY, Type V accounted for 2.88 t/10^4 CNY, and Type VI accounted for 2.76 t/10^4 CNY, with a provincial average of 2.41 t/10^4 CNY. For TP of the types, Type I accounted for 1.71 t/person, Type

II accounted for 0.63 t/person, Type III accounted for 0.64 t/person, Type IV accounted for 0.56 t/person, Type V accounted for 0.63 t/person, and Type VI accounted for 0.64 t/person, with a provincial average of 0.73 t/person. See Figures 10 and 11 and Table 3 for details.

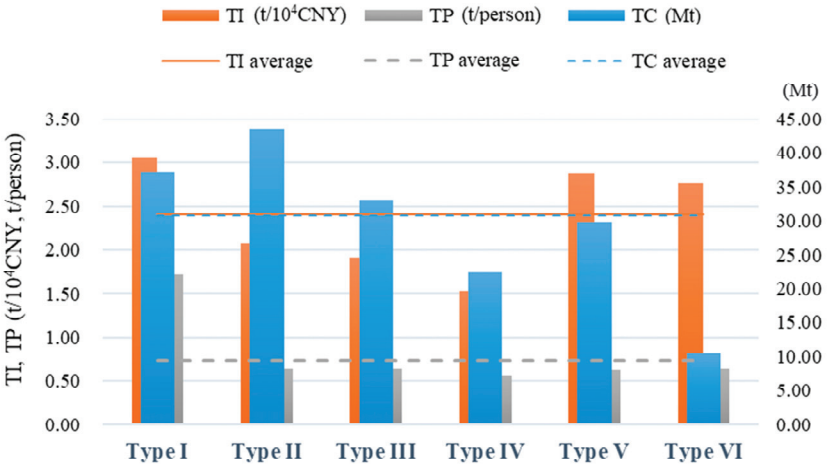

Figure 11. Comparison of the numerical values of TC, TI, and TP among the six feature types.

We further determined the priority control directions for carbon reduction in each type based on the ratio relationships of TC, TI, and TP with provincial averages (Table 4). Types I and VI were determined as per capita transportation CO_2 control (i.e., TP control). Types II and III were determined as total transportation CO_2 control (i.e., TC control). Types V and VI were determined as transportation CO_2 intensity control (i.e., TI control).

Table 4. The ratios of TC, TI, and TP values to their averages and directions of priority control for carbon reduction for Types I–VI.

Province	TC/TC Average	TI/TI Average	TP/TP Average	Priority Control Directions for Carbon Reduction
Type I	1.21	1.27	2.33	TP control
Type II	1.41	0.86	0.86	TC control
Type III	1.08	0.79	0.87	TC control
Type IV	0.73	0.63	0.77	TP control
Type V	0.97	1.20	0.85	TI control
Type VI	0.34	1.15	0.87	TI control

3.4. Correlation Analysis Results of Characterization Indicators with the per Capita TCO_2 and the Intensity of TCO_2

To identify priority control indicators for carbon reduction in the six types, this study further conducted correlation analysis between TI and TP and the original values of the nine characteristic indicators. Since the nine characteristic indicators are derived from TC through the extended Kaya identity, we believe these indicators can indirectly reflect the impacts on TC. Further correlation analysis with TC may cause redundant information or repeated analysis. Therefore, TC id not included in the correlation analysis.

3.4.1. The Correlation Analysis Results between TP and Characteristic Indicators

The correlation analysis results between TP and characteristic indicators show that TP is extremely strongly correlated with RDL (r = 0.857) and PTL (r = 0.842), moderately negatively correlated with UPL (r = −0.567), and moderately positively correlated with RLC

(r = 0.498) and TOP (r = 0.485) at the 1% significant level (Table 5). Among them, the impacts of road congestion in TOP and travel frequency in RLC on generating TC are obvious conclusions. (1) The number of private cars corresponding to TOP and the consumption level of residents (which can also reflect income level to some extent) corresponding to RLC can directly or indirectly generate additional TCO_2 through resident behaviors, which is consistent with the research conclusions [24,25,34,35,53]. (2) The extremely strong correlation between PTL and TP indicates that improving public transportation construction can attract more resident trips, thus causing more TCO_2. However, Yang et al. (2015, 2019) [30,53] found PTL has significantly negative impacts on TP, suggesting a non-linear relationship between the two. This is consistent with the "inverted U-shaped" relationship between public transportation and CO_2 emissions [32,33]. Public transportation can increase TCO_2 during initial construction, but complete systems can reduce TCO_2 in the long run. Moreover, it should be noted that the carbon reduction effect of public transportation infrastructure reaches a certain threshold level, beyond which its impact gradually decreases [33]. (3) The moderately negative correlation between the UPL (lower values indicate higher urban population density) and TP shows that higher urban population density significantly increases TCO_2 [5,24,26,34,54,55]. However, Kenworthy and Laube (1996) [56], Ewing (1997) [57], and Newman (2006) [58] proposed that TCO_2 is negatively correlated with population density and that compact, high-density urban forms result in lower TCO_2. This again suggests a non-linear relationship between UPL and TCO_2. Since urban population density in China is already very high, overly high density may not effectively decrease TCO_2 [30,53,59]. Therefore, population scales should be reasonably controlled for different cities based on specific urbanization conditions.

Table 5. Correlation analysis results of TP with RDL, UPL, PTL, TOP, and RLC.

		RDL	UPL	PTL	TOP	RLC
TP	Pearson correlation	0.857 **	−0.567 **	0.842 **	0.485 **	0.498 **
	Sig. (2-tailed)	0.000	0.001	0.000	0.007	0.005
	N	30	30	30	30	30

Note: ** indicates a significant level of correlation of 1%.

(4) Technological progress can effectively reduce transportation energy consumption efficiency through indigenous innovation and technology spillover, thus reducing TCO_2 [27,44,60]. Typically, RDL should show a negative correlation with TP; however, our results show an extremely strong positive correlation, consistent with Shao et al. (2021) [4] and Yang et al. (2021) [39]. This indicates that RDL and TP do not exhibit a simple linear relationship, with RDL having both positive and negative externalities [40]. Shi et al. (2021) [27] pointed out an "inverted U-shaped" relationship between RDL and TCO_2, suggesting long-term research investment is needed to overcome the slow initial impact of transportation technology development on TCO_2 [61] or introduce advanced energy conservation and carbon reduction technologies [62]. Further analysis in Table 6 shows RDL has an extremely strong positive correlation between PTL (r = 0.880), moderately positive correlation with TOP (r = 0.498), and moderately negative correlation with UPL (r = −0.569) at the 1% significant level, and moderately positive correlation with RLC (r = 0.437) at the 5% significant level. This indicates that the R&D direction of transportation technology may primarily revolve around the planning and construction of transportation infrastructure. There is a certain degree of inadequacy in the development of carbon reduction technologies, as well as shortcomings in practical application and technology transfer in the transformation of scientific achievements in transportation technology. Furthermore, RDL mainly reflects the potential magnitude of technological carbon reduction rather than its practical implementation. Based on the above analysis, RDL, PTL, UPL, RLC, and TOP are important indicators for priority control of TP.

Table 6. Correlation analysis results of RDL with UPL, PTL, TOP, and RLC.

		UPL	PTL	TOP	RLC
RDL	Pearson correlation	−0.569 **	0.880 **	0.498 **	0.437 *
	Sig. (2-tailed)	0.001	0.000	0.005	0.016
	N	30	30	30	30

Note: ** indicates a significant level of correlation of 1%, and * indicates a significant level of correlation of 5%.

3.4.2. The Correlation Analysis Results between TI and Characteristic Indicators

The correlation analysis results between TI and characteristic indicators reveal that TI has a moderately positive correlation with TEE (r = 0.528) and RLC (r = 0.501) at the 1% significant level, a moderately negative correlation with TEC (r = −0.415), and a slight positive correlation with PTL (r = 0.386) at the 5% significant level (Table 7). Among them, the quantity and efficiency of passenger and freight turnover corresponding to TEE are key factors causing TCO_2, consistent with previous studies [24,34,35]. Furthermore, Xie et al. (2017) [54], Yang et al. (2019) [30], and Wang (2021) [29] also found RLC promotes both TC and TI. The moderately negative correlation between TEC and TI indicates that increasing transportation economic share in provincial GDP facilitates accelerated commodity and population flow, improving transportation efficiency, and thus reducing TI. With regard to the slight positive correlation between PTL and TI, as mentioned previously, PTL exhibits a non-linear relationship with TCO_2 and TP. Further correlation analysis reveals that PTL has a moderately negative correlation between UPL (r = −0.625) and positive correlations with TOP (r = 0.607) and RLC (r = 0.573) at the 1% significant level. Additionally, PTL exhibits a moderately positive correlation with TEE (r = 0.439) and a slight negative correlation with RCL (r = −0.384) at the 5% significant level (Table 8). These findings highlight the existence of certain negative impacts associated with public transportation construction, including increased energy consumption in transportation efficiency, exacerbated road congestion, and an increased frequency of resident travel. Moreover, these results validate the threshold effect and negative consequences of PTL and TCO_2 [33]. This suggests that in densely populated areas, excessive allocation of public transportation resources can, to some extent, increase residents' frequency of consumption and travel, exacerbate traffic congestion pressure, and lead to an unreasonable growth in TI. Based on the above analysis, TEE, RLC, TEC, and PTL can be identified as important indicators for prioritizing TI control.

Table 7. Correlation analysis results of TI with TEC, TEE, PTL, and RLC.

		TEC	TEE	PTL	RLC
TI	Pearson correlation	−0.415 *	0.528 **	0.386 *	0.501 **
	Sig. (2-tailed)	0.023	0.003	0.035	0.005
	N	30	30	30	30

Note: ** indicates a significant level of correlation of 1%, and * indicates a significant level of correlation of 5%.

Table 8. Correlation analysis results of PTL with TEE, UPL, RCL, TOP, and RLC.

		TEE	UPL	RCL	TOP	RLC
PTL	Pearson correlation	0.439 *	−0.625 **	−0.384 *	0.607 **	0.573 **
	Sig. (2-tailed)	0.015	0.000	0.036	0.000	0.001
	N	30	30	30	30	30

Note: ** indicates a significant level of correlation of 1%, and * indicates a significant level of correlation of 5%.

3.5. Carbon Reduction Strategies and KPIs for Provincial Types

3.5.1. Carbon Reduction Strategies for Provincial Types

(1) Types I and IV are the TP control and the direction for carbon reduction. Based on the above analysis, the strategies for Type I should focus on: strengthening R&D investment and application of technological achievements in carbon reductions; strictly controlling urban population scales and effectively guiding spatial layout adjustments

for over-concentrated urban areas; paying attention to the problem of excessive configuration of urban public transportation; effectively alleviating road congestion and strictly controlling the number of fuel-powered private vehicles; significantly promoting effective guidance of low-carbon residents' behaviors, including consumption and travel. Secondary focus should be placed on: rationally increasing the share of transportation economy and promoting low-carbon transformation of transportation economic structure; significantly increasing the utilization of renewable energy in transportation energy structure, such as strictly requiring motor vehicle emission standards, promoting new energy transportation tools, and rationally deploying new energy transportation infrastructure; further reducing transportation energy consumption efficiency by promoting combined transportation modes and intelligent transportation to improve efficiency; significantly improving road construction by promoting sustainable urban-rural planning to optimize existing road networks and expanding high-quality highways and rapid urban road systems.

Strategies for Type IV should be focused on: strengthening R&D investment in carbon reductions and introducing advanced energy conservation and carbon reduction technologies; promoting urban-rural integrated development to prevent excessive urban concentration; significantly improving public transportation service level and quality; effectively alleviating road congestion; and strictly controlling the number of fuel-powered private vehicles. A secondary focus should be placed on maintaining the level of renewable energy utilization in the transportation sector.

(2) Type II and Type III use TC control as the direction for carbon reduction. Based on the above analysis, strategies for Type II should focus on: leveraging locational and industrial advantages to drive economic development in surrounding provinces, thus promoting low-carbon transformation of the transportation economic structure; significantly increasing renewable energy utilization in the transportation energy structure (same measures as Type I); maintaining transportation energy consumption efficiency; strengthening R&D investment in carbon reductions and introducing advanced energy conservation and carbon reduction technologies; promoting urban-rural integrated development and reasonably controlling urban population scales; effectively improving road construction (same measures as Type I); reasonably improving the level and quality of public transportation services; effectively alleviating road congestion and reasonably controlling the number of fuel-powered private vehicles.

Strategies for Type III should be focused on: maintaining the utilization of renewable energy; effectively reducing transportation energy consumption efficiency; strengthening R&D investment and application of technological achievements in carbon reduction; reasonably improving the level and quality of public transportation services; effectively guiding low-carbon residents' behaviors, including consumption and travel.

(3) Type V and Type VI are TI-controlled in the direction of carbon reduction. Based on the above analysis, strategies for Type V should focus on: maintaining the transportation economic structure and further promoting its low-carbon transformation; significantly reducing transportation energy consumption efficiency; further improving road construction effectively; and significantly improving public transportation service level and quality. Secondary focus should be placed on: significantly increasing renewable energy utilization in the transportation energy structure (same measures as Type I); strengthening R&D investment in carbon reductions; and introducing advanced energy conservation and carbon reduction technologies.

Strategies for Type VI should be focused on: maintaining the transportation economic structure and further promoting its low-carbon transformation; reasonably improving the level and quality of public transportation services. Secondary focus should be placed on: maintaining the utilization of renewable energy; strengthening R&D investment in carbon reductions and introducing advanced energy conservation and carbon reduction technologies; and significantly promoting effective guidance of low-carbon residents' behaviors, including consumption and travel.

3.5.2. Carbon Reduction KPIs for Provincial Types

Based on the above-proposed carbon reduction measures for each type, this study further developed different KPIs related to local government for better achieving carbon reduction goals in each of the six types, aiming to promote effective implementation and supervision of the carbon reduction measures.

Figure 12 provides the corresponding KPIs for each type, respectively. Specifically, (1) For Type I, the primary focus should be on: increasing the TEC indicator, greatly increasing the TES indicator, decreasing the TEE indicator, maintaining the UPL indicator, and greatly decreasing both the TOP and RLC indicators. (2) For Type II, particular attention needs to be paid to: increasing the TEC, RCL, and PTL indicators, greatly increasing the TES and RDL indicators, maintaining the TEE and UPL indicators, and decreasing the TOP indicator. (3) For Type III, the primary focus should be on maintaining the TES indicator, decreasing the TEE and RLC indicators, and increasing the PTL indicator. (4) For Type IV, particular attention needs to be paid to: maintaining the TES and UPL indicators, greatly increasing the RDL and PTL indicators, greatly decreasing the TOP indicator, and decreasing the RLC indicator. (5) In the context of Type V, emphasis should be placed on increasing the TEC and RCL indicators, greatly increasing the TES, RDL, and PTL indicators, and greatly decreasing the TEE indicator. (6) Lastly, for Type VI, the primary focus should be on increasing the TEC and PTL indicators, maintaining the TES indicator, greatly increasing the RDL indicator, and greatly decreasing the RLC indicator.

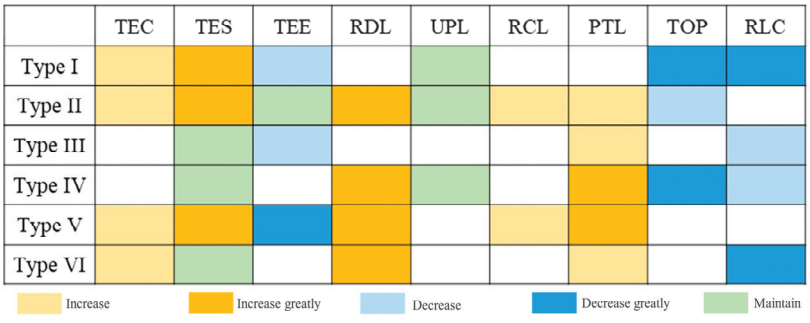

Figure 12. KPIs related to the local government's efforts to reduce TCO_2 in six types of China.

4. Conclusions and Policy Implications

The exploration of similarities and differences in provincial TCO_2 characteristics in China using the multi-indicator joint characterization method and type categorization through clustering analysis is novel in our research. Firstly, influencing factors such as economic development, population density, energy structure, transportation efficiency, R&D, infrastructure construction, transportation operation conditions, and residents' transportation behavior were derived by effectively extending the Kaya identity, based on which a joint characterization method using nine evaluation indicators (TEC, TES, TEE, RDL, UPL, RCL, PTL, TOP, and RLC) was constructed. Secondly, Ward's method was used in the hierarchical clustering of the characteristic indicators to categorize thirty Chinese provinces in 2019 into six types (types I to VI). Thirdly, based on the calculation of TC, TI, and TP for each province, the priority control directions and indicators for carbon reduction were obtained through relative relationships with provincial averages and correlation analysis with the indicators, i.e., Type I and Type IV can be categorized as TP-controlled, Type II and Type III as TC-controlled, and Type V and Type VI as TI-controlled. The priority control indicators were RDL, PTL, UPL, RLC, and TOP for TP, and TEE, RCL, TEC, and PTL for TI. Furthermore, UPL, RDL, and PTL have non-linear effects and threshold effects on TP, and PTL exhibits threshold effects and a certain degree of negative impacts on TCO_2. Finally, typological carbon reduction strategies and KPIs related to carbon reduction

efforts by local governments were provided for each provincial type. When it comes to carbon emission reduction measures, special attention should be given to the importance of R&D in transportation technologies, transitioning from the planning and construction of transportation infrastructure to the development of carbon reduction technologies. Additionally, in densely populated cities, it is crucial to address issues related to excessive population density and overallocation of public transportation resources in order to curb the unreasonable increase in transportation carbon emissions.

Policy makers should pay special attention to:

(1) Optimizing traffic congestion, controlling the number of fuel-powered private vehicles, and advocating low-carbon residents' behaviors are important measures to effectively control the direct quantity of TCO_2 (TC, TI, and TP). Provinces categorized as Type I, Type II, and Type IV should primarily optimize urban vehicle restriction policies and conduct reasonable adjustments in urban spatial planning (such as industrial layout, development of industrial parks, establishment of employment centers, educational layout, and planning multifunctional community areas) to fundamentally address urban traffic congestion issues. Provinces identified as Type IV and Type V should enhance the coverage and service efficiency of public transportation systems (such as bus rapid transit and dedicated bus lanes). Provinces classified as Type I and Type II, benefiting from comprehensive road monitoring facilities, need to reinforce the sharing of information on road traffic operations to alleviate traffic congestion. Provinces in China should continue to strengthen promotion efforts and policy support for new energy vehicles, expanding the deployment of new energy transportation infrastructure (e.g., charging stations, wireless charging, etc.). They should encourage low-carbon lifestyles, advocate for energy conservation and emissions reduction through various channels, and incentivize the use of public transportation and shared mobility practices (particularly among Type I, Type III, and Type IV provinces).

(2) Improving transportation energy efficiency and reducing passenger and freight turnover energy consumption through technology are necessary to reduce TC, TI, and TP. The government should fully recognize the initial slow impacts of carbon reduction technologies and persist in long-term support for domestic industry-academia-research cooperation in R&D and promotion of technologies related to carbon reduction in transportation, as well as introducing advanced international technologies. Provinces categorized as Type I and Type III should shift transportation R&D focus from infrastructure construction to carbon reduction technologies. The other types of provinces should increase investments in carbon reduction technologies for transportation or introduce advanced carbon reduction technologies. Provinces in China should promote transportation electrification and combined transportation modes to improve efficiency and achieve the goal of low-carbon development in transportation.

(3) For provinces with high levels of urbanization (such as Type I and Type II), attention should be given to the issues of excessive population density and over-configuration of public transportation in urban areas to curb the unreasonable increase in TCO_2. In contrast, for provinces with lower levels of urbanization (such as Types III to VI), the population aggregation effect should be fully utilized. It is important to focus on constructing intensive and efficient urban spatial patterns, improving the utilization and sharing rates of public transportation, and scientifically expanding urban road infrastructure to achieve long-term carbon reduction.

(4) Since provinces have different advantages and disadvantages in their TCO_2 characteristics for low-carbon development, the Chinese government should promote cooperative development and collaborative governance mechanisms across regions to achieve win-win carbon reduction and economic growth in provincial transportation sectors. Regarding regional energy-economy cooperation, resource-rich provinces (such as Type V and Type VI) can provide clean energy like natural gas and electricity to provinces with energy-intensification structures through national projects like "West-to-East Gas Transmission" and "West-to-East Power Transmission", trans-

forming regional resource advantages into economic benefits while also promoting low-carbon transitions in these energy-intensification provinces (such as Type I and Type II). For collaborative development of advanced technologies across regions, developed provinces (like eastern coastal type I and type II) should give full play to their advantages in transportation technology R&D funding, talent pool, and exemplary leadership, strengthening interactive exchanges of technological and economic ties across regions through spillover and learning effects, to achieve collaborative regional carbon reductions through technology. For collaborative governance across regions, differentiated carbon reduction policies and measures should be implemented with a collaborative assessment system incorporating rewards and punishments established to reinforce the responsibilities and consciousness of all parties, thus achieving collaborative governance on carbon reduction in provincial transportation sectors.

Author Contributions: Y.Y. conceived and designed the study, conducted data processing and analysis, and drafted the manuscript. Y.Y. and F.Y. performed software analysis and mapping. F.Y. revised the paper and performed project management and funding acquisition. All authors have read and agreed to the published version of the manuscript.

Funding: This research was funded by the "Special project of National Natural Science Foundation of China", grant numbers "42341207".

Data Availability Statement: Data is contained within the article.

Acknowledgments: The authors would like to thank the anonymous reviewers for their comments and suggestions.

Conflicts of Interest: The authors declare no conflict of interest.

Appendix A

Table A1. Characteristic indicator values of provinces in each type.

Type	Province	TEC	TES	TEE	RDL	UPL	RCL	PTL	TOP	RLC
I	Beijing	0.62	0.63	2.00	2.00	0.00	0.55	2.00	1.47	2.00
	Tianjin	1.19	1.07	0.73	1.62	0.00	0.77	2.00	1.25	1.74
	Shanghai	0.92	0.24	0.23	2.00	0.00	0.31	2.00	1.45	1.45
	Type average	0.91	0.65	0.99	1.87	0.00	0.54	2.00	1.39	1.73
II	Liaoning	1.13	0.62	0.65	0.39	1.11	0.97	1.20	0.98	0.97
	Jiangsu	0.68	1.03	0.75	0.49	1.15	1.05	1.14	1.27	0.80
	Zhejiang	0.67	0.49	0.34	0.54	0.54	0.84	1.09	1.52	1.04
	Anhui	1.14	0.75	0.36	0.08	0.80	0.85	0.53	0.95	0.56
	Fujian	0.75	0.45	0.44	0.14	0.94	0.83	0.78	0.80	0.86
	Jiangxi	0.93	0.47	0.70	0.20	1.49	0.96	0.38	0.69	0.74
	Shandong	1.09	0.72	0.69	0.39	1.00	1.07	0.82	1.36	0.40
	Henan	1.17	0.89	0.57	0.24	0.68	0.63	0.50	1.00	0.56
	Guangdong	0.69	0.36	0.41	0.74	0.51	0.80	1.16	1.31	0.65
	Guangxi	0.91	1.03	0.62	0.28	1.53	0.79	0.39	0.90	0.59
	Type average	0.91	0.68	0.55	0.35	0.97	0.88	0.80	1.08	0.72
III	Hubei	1.04	0.59	0.95	2.00	1.31	1.16	0.87	0.86	0.82
	Shaanxi	0.88	2.00	0.76	2.00	0.91	0.94	0.83	0.79	1.01
	Type average	0.96	1.29	0.86	2.00	1.11	1.05	0.85	0.82	0.92

Table A1. *Cont.*

Type	Province	TEC	TES	TEE	RDL	UPL	RCL	PTL	TOP	RLC
IV	Hebei	1.77	1.73	0.27	0.11	1.11	0.70	0.51	1.25	0.39
	Shanxi	1.26	1.77	0.48	0.25	1.10	0.86	0.52	1.07	0.51
	Inner Mongolia	1.49	1.81	0.59	0.26	0.61	1.58	0.75	0.98	0.71
	Type average	1.51	1.77	0.45	0.21	0.94	1.05	0.59	1.10	0.53
V	Heilongjiang	0.84	0.76	1.57	0.27	0.63	1.10	0.90	0.67	0.62
	Hunan	0.84	0.46	1.94	0.35	1.30	0.73	0.55	0.82	0.77
	Sichuan	0.67	0.99	2.00	0.78	0.45	0.92	0.76	0.98	0.58
	Guizhou	0.90	0.92	1.60	0.38	1.28	0.97	0.43	0.82	1.29
	Yunnan	1.02	0.28	2.00	0.18	1.63	0.97	0.45	0.74	0.52
	Xinjiang	1.50	1.28	1.52	0.06	1.08	1.79	0.73	0.85	0.76
	Type average	0.96	0.78	1.77	0.34	1.06	1.08	0.64	0.81	0.76
VI	Jilin	1.05	1.52	0.86	0.07	1.75	1.05	1.16	0.81	0.89
	Hainan	0.99	0.52	0.51	0.00	1.51	1.26	0.64	0.91	1.90
	Chongqing	0.88	1.04	0.78	0.49	1.69	1.13	1.19	0.87	1.19
	Gansu	1.07	1.69	0.61	0.08	1.83	1.10	0.55	0.78	1.01
	Qinghai	0.89	1.53	1.68	0.21	0.79	2.00	0.74	0.87	2.00
	Ningxia	1.02	2.00	0.73	0.23	1.27	1.24	0.87	0.97	1.99
	Type average	0.98	1.38	0.86	0.18	1.47	1.30	0.86	0.87	1.50

Table A2. The total TCO_2 (TC), the intensity of TCO_2 (TI) and the per capita TCO_2 (TP) of the provinces in each type.

Type	Province	TC (Mt)	TI (t/10^4 CNY)	TP (t/person)
I	Beijing	37.84	3.69	1.76
	Tianjin	15.06	1.91	0.96
	Shanghai	58.56	3.55	2.41
	Type average	37.15	3.05	1.71
II	Liaoning	47.57	3.62	1.09
	Jiangsu	60.40	1.91	0.75
	Zhejiang	33.40	1.70	0.57
	Anhui	30.68	1.55	0.48
	Fujian	29.85	2.01	0.75
	Jiangxi	22.49	2.08	0.48
	Shandong	56.77	1.56	0.56
	Henan	40.15	1.35	0.42
	Guangdong	93.34	2.69	0.81
	Guangxi	20.07	2.22	0.40
	Type average	43.47	2.07	0.63
III	Hubei	48.77	2.18	0.82
	Shaanxi	17.36	1.64	0.45
	Type average	33.06	1.91	0.64
IV	Hebei	27.20	0.93	0.36
	Shanxi	19.37	1.92	0.52
	Inner Mongolia	20.66	1.72	0.81
	Type average	22.41	1.53	0.56

Table A2. *Cont.*

Type	Province	TC (Mt)	TI (t/10^4 CNY)	TP (t/person)
V	Heilongjiang	20.38	3.82	0.54
	Hunan	43.06	2.77	0.62
	Sichuan	43.27	2.95	0.52
	Guizhou	17.24	2.43	0.48
	Yunnan	31.12	2.80	0.64
	Xinjiang	24.28	2.55	0.96
	Type average	29.89	2.88	0.63
VI	Jilin	11.95	2.08	0.44
	Hainan	6.97	2.82	0.74
	Chongqing	23.11	2.37	0.74
	Gansu	11.50	2.62	0.43
	Qinghai	5.62	4.56	0.92
	Ningxia	3.78	2.12	0.54
	Type average	10.49	2.76	0.64
Provincial average		30.73	2.40	0.73

References

1. IEA. *World Energy Outlook 2022*; International Energy Agency: Paris, France, 2022. Available online: https://www.iea.org/reports/world-energy-outlook-2022 (accessed on 11 November 2023).
2. Cohan, D.S.; Sengupta, S. Net Greenhouse Gas Emissions Savings from Natural Gas Substitutions in Vehicles, Furnaces, and Power Plants. *Int. J. Glob. Warm.* **2016**, *9*, 254–273. [CrossRef]
3. IEA. *CO_2 Emissions from Fuel Combustion 2018*; International Energy Agency: Paris, France, 2018. [CrossRef]
4. Shao, H.; Wang, Z. Spatial Network Structure of Transportation Carbon Emission Efficiency in China and Its Influencing Factors. *Chin. J. Popul. Resour. Environ.* **2021**, *19*, 295–303. [CrossRef]
5. Cai, J.; Ma, S.; Ji, H.; Jiang, W.; Bai, Z. Spatial–Temporal Characteristics and Decoupling Effects of China's Transportation CO_2 Emissions. *Environ. Sci. Pollut. Res.* **2023**, *30*, 32614–32627. [CrossRef]
6. Ortega-Ruiz, G.; Mena-Nieto, A.; Golpe, A.A.; García-Ramos, J.E. CO_2 Emissions and Causal Relationships in the Six Largest World Emitters. *Renew. Sustain. Energy Rev.* **2022**, *162*, 112435. [CrossRef]
7. Bai, C.; Chen, Z.; Wang, D. Transportation Carbon Emission Reduction Potential and Mitigation Strategy in China. *Sci. Total Environ.* **2023**, *873*, 162074. [CrossRef]
8. IEA. *CO2 Emissions from Fuel Combustion 2019*; International Energy Agency: Paris, France, 2019. [CrossRef]
9. Lin, D.; Zhang, L.; Chen, C.; Lin, Y.; Wang, J.; Qiu, R.; Hu, X. Understanding Driving Patterns of Carbon Emissions from the Transport Sector in China: Evidence from an Analysis of Panel Models. *Clean. Technpl. Environ. Policy* **2019**, *21*, 1307–1322. [CrossRef]
10. Xu, H.; Li, Y.; Zheng, Y.; Xu, X. Analysis of Spatial Associations in the Energy–Carbon Emission Efficiency of the Transportation Industry and Its Influencing Factors: Evidence from China. *Environ. Impact Assess. Rev.* **2022**, *97*, 106905. [CrossRef]
11. IEA. *Energy and Climate Change: World Energy Outlook Special Report 2015*; International Energy Agency: Paris, France, 2015. Available online: https://www.iea.org/reports/energy-and-climate-change (accessed on 11 November 2023).
12. Zeng, X.; Qiu, R.; Lin, D.; Hou, X.; Zhang, L.; Hu, X. Spatio-temporal heterogeneity of transportation carbon emissions and its influencing factors in China. *China Environ. Sci.* **2020**, *40*, 4304–4313. (In Chinese) [CrossRef]
13. Ma, F.; Wang, Y.; Yuen, K.F.; Wang, W.; Li, X.; Liang, Y. The Evolution of the Spatial Association Effect of Carbon Emissions in Transportation: A Social Network Perspective. *Int. J. Environ. Res. Public Health* **2019**, *16*, 2154. [CrossRef]
14. Bai, C.; Mao, Y.; Gong, Y.; Feng, C. Club Convergence and Factors of Per Capita Transportation Carbon Emissions in China. *Sustainability* **2019**, *11*, 539. [CrossRef]
15. Wang, L.; Fan, J.; Wang, J.; Zhao, Y.; Li, Z.; Guo, R. Spatio-Temporal Characteristics of the Relationship between Carbon Emissions and Economic Growth in China's Transportation Industry. *Environ. Sci. Pollut. Res.* **2020**, *27*, 32962–32979. [CrossRef]
16. Bai, C.; Zhou, L.; Xia, M.; Feng, C. Analysis of the Spatial Association Network Structure of China's Transportation Carbon Emissions and Its Driving Factors. *J. Environ. Manag.* **2020**, *253*, 109765. [CrossRef]
17. Liu, J.; Li, S.; Ji, Q. Regional Differences and Driving Factors Analysis of Carbon Emission Intensity from Transport Sector in China. *Energy* **2021**, *224*, 120178. [CrossRef]
18. Peng, Z.; Wu, Q.; Wang, D.; Li, M. Temporal-Spatial Pattern and Influencing Factors of China's Province-Level Transport Sector Carbon Emissions Efficiency. *Pol. J. Environ. Stud.* **2019**, *29*, 233–247. [CrossRef]
19. Jiang, M.; Li, J. Study on the Change in the Total Factor Carbon Emission Efficiency of China's Transportation Industry and Its Influencing Factors. *Energies* **2022**, *15*, 8502. [CrossRef]

20. Xu, G.; Zhao, T.; Wang, R. Research on Carbon Emission Efficiency Measurement and Regional Difference Evaluation of China's Regional Transportation Industry. *Energies* **2022**, *15*, 6502. [CrossRef]
21. Zhao, P.; Zeng, L.; Li, P.; Lu, H.; Hu, H.; Li, C.; Zheng, M.; Li, H.; Yu, Z.; Yuan, D.; et al. China's Transportation Sector Carbon Dioxide Emissions Efficiency and Its Influencing Factors Based on the EBM DEA Model with Undesirable Outputs and Spatial Durbin Model. *Energy* **2022**, *238*, 121934. [CrossRef]
22. Zhao, C.; Wang, K.; Dong, X.; Dong, K. Is Smart Transportation Associated with Reduced Carbon Emissions? The Case of China. *Energy Econ.* **2022**, *105*, 105715. [CrossRef]
23. Lin, S.; Wang, J. Carbon Emission Reduction Effect of Transportation Structure Adjustment in China: An Approach on Mul-ti-Objective Optimization Model. *Environ. Sci. Pollut. Res.* **2022**, *29*, 6166–6183. [CrossRef]
24. Liang, Y.; Niu, D.; Wang, H.; Li, Y. Factors Affecting Transportation Sector CO_2 Emissions Growth in China: An LMDI Decomposition Analysis. *Sustainability* **2017**, *9*, 1730. [CrossRef]
25. Bai, C.; Chen, Y.; Yi, X.; Feng, C. Decoupling and Decomposition Analysis of Transportation Carbon Emissions at the Pro-vincial Level in China: Perspective from the 11th and 12th Five-Year Plan Periods. *Environ. Sci. Pollut. Res.* **2019**, *26*, 15039–15056. [CrossRef]
26. Zhu, C.; Wang, M.; Yang, Y. Analysis of the Influencing Factors of Regional Carbon Emissions in the Chinese Transportation Industry. *Energies* **2020**, *13*, 1100. [CrossRef]
27. Shi, T.; Si, S.; Chan, J.; Zhou, L. The Carbon Emission Reduction Effect of Technological Innovation on the Transportation Industry and Its Spatial Heterogeneity: Evidence from China. *Atmosphere* **2021**, *12*, 1169. [CrossRef]
28. Chen, Q.; Wang, Q.; Zhou, D.; Wang, H. Drivers and Evolution of Low-Carbon Development in China's Transportation In-dustry: An Integrated Analytical Approach. *Energy* **2023**, *262*, 125614. [CrossRef]
29. Wang, J.; Ma, X. Influencing Factors of Carbon Emissions from Transportation in China: Empirical Analysis Based on Two-level Econometrics Method. *Acta Sci. Nat. Univ. Pekin.* **2021**, *57*, 1133–1142. (In Chinese) [CrossRef]
30. Yang, W.; Wang, W.; Ouyang, S. The Influencing Factors and Spatial Spillover Effects of CO_2 Emissions from Transportation in China. *Sci. Total Environ.* **2019**, *696*, 133900. [CrossRef]
31. Chen, Z.; Antunes, J.; Wanke, P.; Zhou, M. Sustainability Drivers in Road Transportation System: Evidence from China. *Sci. Total Environ.* **2021**, *798*, 149259. [CrossRef]
32. Jiang, Y.; Zhou, Z.; Liu, C. The Impact of Public Transportation on Carbon Emissions: A Panel Quantile Analysis Based on Chinese Provincial Data. *Environ. Sci. Pollut. Res.* **2019**, *26*, 4000–4012. [CrossRef]
33. Jing, Q.-L.; Liu, H.-Z.; Yu, W.-Q.; He, X. The Impact of Public Transportation on Carbon Emissions—From the Perspective of Energy Consumption. *Sustainability* **2022**, *14*, 6248. [CrossRef]
34. Sun, H.; Hu, L.; Geng, Y.; Yang, G. Uncovering Impact Factors of Carbon Emissions from Transportation Sector: Evidence from China's Yangtze River Delta Area. *Mitig. Adapt. Strateg. Glob. Chang.* **2020**, *25*, 1423–1437. [CrossRef]
35. Li, R.; Li, L.; Wang, Q. The Impact of Energy Efficiency on Carbon Emissions: Evidence from the Transportation Sector in Chinese 30 Provinces. *Sustain. Cities Soc.* **2022**, *82*, 103880. [CrossRef]
36. Meng, M.; Li, M. Decomposition Analysis and Trend Prediction of CO_2 Emissions in China's Transportation Industry. *Sustainability* **2020**, *12*, 2596. [CrossRef]
37. Zhao, C.; Zhou, B. Impact of Express Delivery Industry's Development on Transportation Sector's Carbon Emissions: An Empirical Analysis from China. *Sustainability* **2021**, *13*, 8908. [CrossRef]
38. Sun, Y.; Liu, S.; Li, L. Grey Correlation Analysis of Transportation Carbon Emissions under the Background of Carbon Peak and Carbon Neutrality. *Energies* **2022**, *15*, 3064. [CrossRef]
39. Yang, X.; Jia, Z.; Yang, Z.; Yuan, X. The Effects of Technological Factors on Carbon Emissions from Various Sectors in China—A Spatial Perspective. *J. Clean. Prod.* **2021**, *301*, 126949. [CrossRef]
40. Liu, Y.; Chen, L.; Huang, C. Study on the Carbon Emission Spillover Effects of Transportation under Technological Ad-vancements. *Sustainability* **2022**, *14*, 10608. [CrossRef]
41. Chen, X.; Mao, S.; Lv, S.; Fang, Z. A Study on the Non-Linear Impact of Digital Technology Innovation on Carbon Emissions in the Transportation Industry. *Int. J. Environ. Res. Public. Health* **2022**, *19*, 12432. [CrossRef]
42. Zhao, M.; Sun, T. Dynamic Spatial Spillover Effect of New Energy Vehicle Industry Policies on Carbon Emission of Trans-portation Sector in China. *Energy Policy* **2022**, *165*, 112991. [CrossRef]
43. Kaya, Y. *Impact of Carbon Dioxide Emission Control on GNP Growth: Interpretation of Proposed Scenarios*; IPCC Energy and Industry Subgroup, Response Strategies Working Group: Paris, France, 1990.
44. Liu, M.; Zhang, X.; Zhang, M.; Feng, Y.; Liu, Y.; Wen, J.; Liu, L. Influencing Factors of Carbon Emissions in Transportation Industry Based on CD Function and LMDI Decomposition Model: China as an Example. *Environ. Impact Assess. Rev.* **2021**, *90*, 106623. [CrossRef]
45. Yu, Y.; Li, S.; Sun, H.; Taghizadeh-Hesary, F. Energy Carbon Emission Reduction of China's Transportation Sector: An Input–Output Approach. *Econ. Anal. Policy* **2021**, *69*, 378–393. [CrossRef]
46. Wang, J.; Wang, Z.; Zhao, Y. Determination of the Conversion Factor of Highway Passenger Turnover in the Perspective of Energy. *J. Transp. Eng.* **2016**, *16*, 31–34. (In Chinese) [CrossRef]
47. Yang, Y.; Yan, F.; Yang, Y.; Chen, Y. Evaluating Provincial Carbon Emission Characteristics under China's Carbon Peaking and Carbon Neutrality Goals. *Ecol. Indic.* **2023**, *156*, 111146. [CrossRef]

48. Bai, H.; Qiao, S.; Liu, T.; Zhang, Y.; Xu, H. An Inquiry into Inter-Provincial Carbon Emission Difference in China: Aiming to Differentiated KPIs for Provincial Low Carbon Development. *Ecol. Indic.* **2016**, *60*, 754–765. [CrossRef]
49. Ward, J.H. Hierarchical Grouping to Optimize an Objective Function. *J. Am. Stat. Assoc.* **1963**, *58*, 236–244. [CrossRef]
50. Eggleston, H.S.; Buendia, L.; Miwa, K.; Ngara, T.; Tanabe, K. 2006 IPCC Guidelines for National Greenhouse Gas Inventories. Japan. 2006. Available online: https://www.ipcc-nggip.iges.or.jp/public/2006gl/index.html (accessed on 12 November 2023).
51. Shan, Y.; Huang, Q.; Guan, D.; Hubacek, K. China CO_2 Emission Accounts 2016–2017. *Sci. Data* **2020**, *7*, 54. [CrossRef]
52. Benesty, J.; Chen, J.; Huang, Y. On the Importance of the Pearson Correlation Coefficient in Noise Reduction. *IEEE Trans. Audio Speech Lang. Process.* **2008**, *16*, 757–765. [CrossRef]
53. Yang, W.; Li, T.; Cao, X. Examining the Impacts of Socio-Economic Factors, Urban Form and Transportation Development on CO_2 Emissions from Transportation in China: A Panel Data Analysis of China's Provinces. *Habitat. Int.* **2015**, *49*, 212–220. [CrossRef]
54. Xie, R.; Fang, J.; Liu, C. The Effects of Transportation Infrastructure on Urban Carbon Emissions. *Appl. Energy* **2017**, *196*, 199–207. [CrossRef]
55. Wang, B.; Sun, Y.; Chen, Q.; Wang, Z. Determinants Analysis of Carbon Dioxide Emissions in Passenger and Freight Transportation Sectors in China. *Struct. Chang. Econ. Dyn.* **2018**, *47*, 127–132. [CrossRef]
56. Kenworthy, J.R.; Laube, F.B. Automobile Dependence in Cities: An International Comparison of Urban Transport and Land Use Patterns with Implications for Sustainability. *Environ. Impact Assess. Rev.* **1996**, *16*, 279–308. [CrossRef]
57. Ewing, R. Is Los Angeles-Style Sprawl Desirable? *J. Am. Plan. Assoc.* **1997**, *63*, 107–126. [CrossRef]
58. Newman, P. The Environmental Impact of Cities. *Environ. Urban.* **2006**, *18*, 275–295. [CrossRef]
59. Reichert, A.; Holz-Rau, C.; Scheiner, J. GHG Emissions in Daily Travel and Long-Distance Travel in Germany—Social and Spatial Correlates. *Transp. Res. Part D Transp. Environ.* **2016**, *49*, 25–43. [CrossRef]
60. Zhang, Y.-J.; Jiang, L.; Shi, W. Exploring the Growth-Adjusted Energy-Emission Efficiency of Transportation Industry in China. *Energy Econ.* **2020**, *90*, 104873. [CrossRef]
61. Li, W.; Elheddad, M.; Doytch, N. The Impact of Innovation on Environmental Quality: Evidence for the Non-Linear Relationship of Patents and CO_2 Emissions in China. *J. Environ. Manag.* **2021**, *292*, 112781. [CrossRef]
62. Godil, D.I.; Yu, Z.; Sharif, A.; Usman, R.; Khan, S.A.R. Investigate the Role of Technology Innovation and Renewable Energy in Reducing Transport Sector CO_2 Emission in China: A Path toward Sustainable Development. *Sustain. Dev.* **2021**, *29*, 694–707. [CrossRef]

land

MDPI

Article

Spatiotemporal Variation and Development Stage of CO_2 Emissions of Urban Agglomerations in the Yangtze River Economic Belt, China

Qikai Lu [1,2,3], Tiance Lv [1,4], Sirui Wang [4,5] and Lifei Wei [1,3,*]

1 Faculty of Resources and Environmental Science, Hubei University, Wuhan 430062, China; qikai_lu@hotmail.com (Q.L.); lvtiance2002@163.com (T.L.)
2 Key Laboratory of Digital Mapping and Land Information Application, Ministry of Natural Resources, Wuhan University, Wuhan 430079, China
3 Hubei Key Laboratory of Regional Development and Environmental Response, Hubei University, Wuhan 430062, China
4 Chucai Honors College, Hubei University, Wuhan 430062, China; wangsirui200207@163.com
5 School of Public Administration, Hubei University, Wuhan 430062, China
* Correspondence: weilifei2508@hubu.edu.cn

Abstract: As the world's largest developing country, China has played an important role in the achievement of the global CO_2 emissions mitigation goal. The monitoring and analysis of CO_2 emissions in the Yangtze River Economic Belt (YREB) urban agglomerations is strategic to the carbon peak and carbon neutrality in China. In this paper, we revealed the spatial and temporal variations of CO_2 emissions in Cheng-Yu urban agglomeration (CY-UA), Yangtze River Middle-Reach urban agglomeration (YRMR-UA), and Yangtze River Delta urban agglomeration (YRD-UA) in YREB and investigated the carbon emission development stage of YREB urban agglomerations. Particularly, a carbon emission development stage framework that considered the relationship between economic growth and carbon emissions was built based on Environmental Kuznets Curves (EKCs). Meanwhile, multiscale geographically weighted regression (MGWR) was used to analyze the impact of different influencing factors, including population (POP), GDP per capita (GDPPC), the proportion of secondary industry (SI), carbon emission intensity (CI), and urbanization (UR), on the CO_2 emissions of three urban agglomerations. The results illustrate the following: (1) The CO_2 emissions of YREB urban agglomerations decreased, with YRD-UA having the highest CO_2 emissions among the three urban agglomerations and contributing 41.87% of YREB CO_2 emissions in 2017. (2) CY-UA, YRMR-UA, and YRD-UA reached the CO_2 emissions peak in 2012, 2011, and 2020, respectively, all of which are at the low-carbon stage. (3) POP and GDPPC show the greatest impact on the CO_2 emissions of the three YREB urban agglomerations.

Keywords: carbon emission; Yangtze River Economic Belt; urban agglomeration; influencing factor; multiscale geographically weighted regression

Citation: Lu, Q.; Lv, T.; Wang, S.; Wei, L. Spatiotemporal Variation and Development Stage of CO_2 Emissions of Urban Agglomerations in the Yangtze River Economic Belt, China. *Land* **2023**, *12*, 1678. https://doi.org/10.3390/land12091678

Academic Editors: Jinyan Zhan, Chao Wang and Xueting Zeng

Received: 28 July 2023
Revised: 23 August 2023
Accepted: 24 August 2023
Published: 28 August 2023

1. Introduction

The 21st century is the fastest-growing period of CO_2 emissions in human history [1]. CO_2 accounts for more than 70% of greenhouse gases, which enhance the trend of global warming [2]. The current global temperature has increased by 0.86 °C compared to the average temperature of the 20th century, which was 13.9 °C [3]. According to the Intergovernmental Panel on Climate Change (IPCC) projections, CO_2 emissions in 2030 will be 30% higher than those in 2010 [4]. Global sustainable development will be threatened by increasing temperatures and unstable climate change. Global warming has become an important environmental issue around the world [5], which has caused widespread and rapid changes in human society. Over the past decades, the international community has signed the United Nations Framework Convention on Climate Change, the Kyoto Protocol,

the Copenhagen Accord, the Glasgow Climate Agreement, etc., to enable global sustainable development [6]. Nowadays, more than 130 countries have proposed carbon neutrality targets, which is one of the most important issues in the world [7].

To achieve the carbon neutrality target, it is necessary to monitor and analyze the spatial distribution and temporal patterns of CO_2 emissions. In recent years, numerous studies have been proposed to investigate the spatiotemporal variation of CO_2 emissions as well as the influencing factors. Xiao et al. examined the spatiotemporal characteristics of carbon emission efficiency in 136 countries and analyzed the influencing factors of carbon emission efficiency using the Tobit model [8]. Andreoni et al. conducted a decomposition analysis of energy-related CO_2 emissions in 33 countries worldwide using the index decomposition method in order to explore the drivers of CO_2 emissions variation [9]. Grodzicki et al. assessed the impact of renewable energy usage and urbanization levels on CO_2 emissions in Europe from 1995 to 2018 using a spatiotemporal approach [10]. Namahoro et al. analyzed the long-term impacts of energy intensity, renewable energy consumption, and economic growth on CO_2 emissions across regions and income levels in over 50 African countries [11]. Fragkias examined the relationship between urban scale and CO_2 emissions for metropolitan and micropolitan areas in the United States [12]. Wen and Shao used a nonparametric additive regression approach to explore the spatial and temporal variations of CO_2 emissions in China and analyze the main influencing factors [13].

As a developing country, China has set a goal and committed to achieving a carbon peak in 2030 and carbon neutrality in 2060 [14,15]. The Chinese government has allocated emission reduction targets to different regions [16]. YREB in China is a globally influential inland economic region and a pioneering demonstration belt for the construction of ecological civilization [17]. Together with the Belt and Road and the coordinated development of the Beijing–Tianjin–Hebei region, YREB is one of China's major regional economic development strategies [18]. With the rapid economic growth of cities in YREB, a large number of major projects have been concentrated, which are the main sources of CO_2 emissions [19]. In 2017, YREB contributed 40.8% of China's GDP and 43.6% of China's CO_2 emissions [20]. Specifically, there are three national urban agglomerations in YREB, namely, the Cheng-Yu urban agglomeration (CY-UA), the Yangtze River Middle-Reach urban agglomeration (YRMR-UA), and the Yangtze River Delta urban agglomeration (YRD-UA). Urban agglomeration is the manifestation of urban spatial clustering [21], and its development is always guided by regional integration policies [22]. As an important part of the national economy as well as the most concentrated areas of industrialization and urbanization [23], urban agglomerations are important areas for achieving carbon neutrality in China [24]. In the YREB urban agglomerations, a lot of heavy industrial projects are concentrated, and the massive consumption of fossil energy contributed to the high CO_2 emissions [25]. In 2017, the three urban agglomerations contributed 65.31% of the GDP as well as 78.39% of the CO_2 emissions of YREB. Particularly, the resource endowment and economic development of the upper, middle, and lower reaches of YREB are unbalanced where the cities show different CO_2 emissions patterns [26].

As a pivotal economic region, YREB plays an important role in implementing a carbon neutrality strategy. Hence, studying the CO_2 emissions of YREB urban agglomerations is conducive to revealing the interaction between economic development and carbon emissions, which provides insights for urban planning and regional sustainable development. The goal of this study was to explore the spatiotemporal variation and development stage of CO_2 emissions in YREB urban agglomerations. Specifically, this study focused on the CO_2 emissions patterns of urban agglomerations in YREB, China, and developed a carbon emission development stage framework that takes economic development and carbon emissions into account. The main contributions are summarized as follows: (1) The spatial and temporal variations of CO_2 emissions in urban agglomerations in YREB were revealed. (2) The carbon emission development stages of CY-UA, YRMR-UA, and YRD-UA were analyzed on the basis of EKCs. (3) The influencing factors of CO_2 emissions in three ur-

ban agglomerations were discussed using the multiscale geographic weighted regression (MGWR) model.

The rest of this paper is as follows: In Section 2, the datasets and methods are introduced. Section 3 shows the results. In Section 4, the discussions are presented. In Section 5, the conclusion is presented.

2. Datasets and Methods

2.1. Study Area

YREB covers an area of about 205.23 × 10^4 km^2 with 11 provinces and municipalities, with the population and GDP accounting for over 40% of China [27]. Since the release of the Outline of the Yangtze River Economic Belt Development Plan in September 2016, YREB has formed a development pattern of "one axis, two wings, three poles, and multiple points". As shown in Figure 1, CY-UA, YRMR-UA, and YRD-UA are the three poles of YREB. The administrative boundary data were obtained from the Resource and Environment Science and Data Center (https://www.resdc.cn/, accessed on 2 January 2023). Table 1 lists the cities contained in three urban agglomerations.

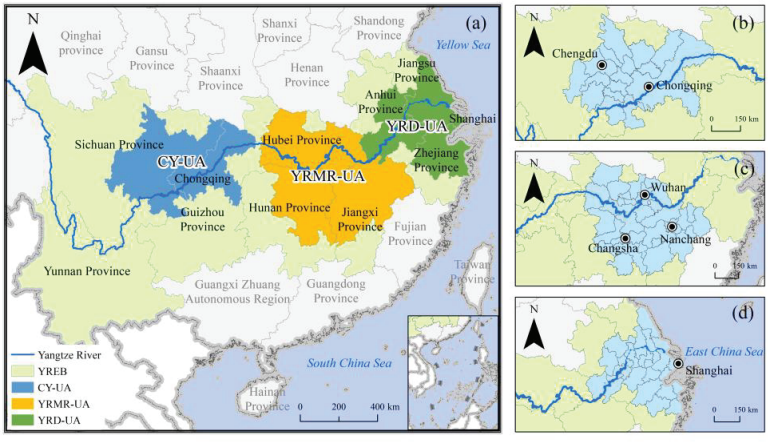

Figure 1. Locations of (**a**) YREB, (**b**) CY-UA, (**c**) YRMR-UA, and (**d**) YRD-UA.

Table 1. Cities in three YREB urban agglomerations.

	Cities
CY-UA	Chongqing, Chengdu, Dazhou, Deyang, Guangan, Leshan, Luzhou, Meishan, Mianyang, Nanchong, Neijiang, Suining, Yaan, Yibin, Ziyang, Zigong
YRMR-UA	Wuhan, Changsha, Nanchang, Changde, Ezhou, Fuzhou, Hengyang, Huanggang, Huangshi, Ji'an, Jingdezhen, Jingmen, Jingzhou, Jiujiang, Loudi, Pingxiang, Qianjiang, Shangrao, Tianmen, Xiantao, Xianning, Xiangtan, Xiangyang, Xiaogan, Xinyu, Yichang, Yichun, Yingtan, Yiyang, Yueyang, Zhuzhou
YRD-UA	Shanghai, Nanjing, Hangzhou, Anqing, Changzhou, Chizhou, Chuzhou, Hefei, Huzhou, Jiaxing, Jinhua, Ma'anshan, Nantong, Ningbo, Shaoxing, Suzhou, Taizhou, Taizhou, Tongling, Wuhu, Wuxi, Xuancheng, Yancheng, Yangzhou, Zhenjiang, Zhoushan

2.2. Datasets

2.2.1. CO_2 Emissions Data

CO_2 emissions data were obtained from the Multi-resolution Emission Inventory model for Climate and air pollution research (MEIC), which is a bottom-up multi-scale

emission inventory model developed by Tsinghua University [28,29]. MEIC aims to build a high-resolution global-scale, multi-scale anthropogenic source greenhouse gas and air pollutant emission inventory model. The MEIC CO_2 emissions data at a 0.25-degree grid resolution contains industry sources, power sources, residential sources, and transportation sources (http://meicmodel.org.cn/, accessed on 29 May 2023). Based on China's measured emission factors, MEIC is more suitable than the IPCC method for the assessment of China's CO_2 emissions [30]. Meanwhile, MEIC has the advantages of objectivity, stability, high precision, and wide coverage and provides multi-year, different spatial scales, dynamic, and continuous CO_2 emissions monitoring information.

2.2.2. Socio-Economic Data

Based on numerous previous studies on CO_2 emissions from urban agglomerations [31–33], population (POP), GDP per capita (GDPPC), the proportion of secondary industry (SI), carbon emission intensity (CI), and urbanization (UR) were selected as the influencing factors of CO_2 emissions in this study. All data were derived from the China City Statistical Yearbook (2009–2018 editions).

Table 2 reports the influencing factors used in this study. POP represents the size of the population. GDPPC is the ratio of GDP to total population, which represents the regional economic development level. SI is the ratio of the value added of the secondary industry's GDP to total GDP, which represents the industrial structure. The resource endowments in the upper, middle, and lower reaches of YREB are unbalanced, and the industrial structure differs greatly [34]. CI is the ratio of total CO_2 emissions to GDP, which represents the technology level. UR represents the urbanization level.

Table 2. Brief description of influencing factors.

Factor	Abbreviation	Description	Unit
CO_2 emissions	CE	Total anthropogenic CO_2 emissions	10^4 tons
Population	POP	Total resident population	person
GDP per capita	GDPPC	GDP/Population	10^4 yuan/person
Proportion of secondary industry	SI	Added value of the secondary industry/GDP	%
Carbon emission intensity	CI	CO_2 emissions/GDP	ton/10^4 yuan
Urbanization	UR	Non-agricultural population/Population	%

POP, GDPPC, SI, CI, and UR were used to construct the MGWR model to analyze the influencing factors of CO_2 emissions in YREB urban agglomerations. Moreover, GDPPC was used in EKCs to depict economic growth.

2.3. Spatial Autocorrelation

2.3.1. Global Autocorrelation

Global Moran's I is a typical spatial autocorrelation index that measures the degree of spatial autocorrelation of CO_2 emissions in each urban agglomeration [35]. It determines whether the geographic phenomenon is aggregated. The calculation formula is as follows:

$$I = \frac{n\sum_{i=1}^{n}\sum_{j=1}^{n} W_{ij}(x_i - \overline{y})(x_j - \overline{x})}{\left(\sum_{i=1}^{n}\sum_{j=1}^{n} W_{ij}\right)\sum_{j=1}^{n}(x_i - \overline{x})^2} \quad (1)$$

where n is the number of units in each urban agglomeration, x_i and x_j denote the CO_2 emissions of spatial units i and j, respectively, $\overline{x}$ denotes the average CO_2 emissions of each urban agglomeration, and W_{ij} denotes the spatial weight matrix.

The value of I ranges from -1 to 1. $I > 0$ indicates positive spatial autocorrelation, and the observations tend to be spatially clustered. The closer I is to 1, the stronger the aggregation. $I < 0$ indicates negative spatial autocorrelation, and the observations tend to

be dispersed. The closer I is to -1, the more dispersed it is. $I = 0$ indicates that there is no spatial autocorrelation, and the observations are randomly distributed.

2.3.2. Local Autocorrelation

The local indicators of spatial association (LISA) are used to describe the correlation between a spatial unit and its neighboring unit [36], and the formula is as follows:

$$I_i = \frac{(x_i - \overline{x})}{S^2} \sum_{j=1}^{m} W_{ij}(x_j - \overline{x}), S^2 = \frac{1}{n} \sum_{i=1}^{n} (x_i - \overline{x}_i)^2 \quad (2)$$

where x_i and x_j denote the CO_2 emissions of spatial units i and j, respectively, $\overline{x}$ denotes the average CO_2 emissions of the urban agglomeration, S^2 denotes the variance of CO_2 emissions of spatial units, W_{ij} denotes the spatial weight matrix, n denotes the number of spatial units in the urban agglomeration, and m denotes the number of neighboring units of unit i.

$I_i > 0$ means that the observations of this spatial unit and its neighboring units show a positive correlation, as high values are surrounded by high values (H-H), or low values are surrounded by low values (L-L). $I_i < 0$ shows a negative correlation, as high values are surrounded by low values (H-L), or low values are surrounded by high values (L-H).

2.4. Carbon Emission Development Stage

2.4.1. Environmental Kuznets Curve (EKC)

EKC depicts the inverted U-shaped relationship between economic growth and carbon emissions [37]. In this paper, CI, CO_2 emissions per capita (CEPC), and CE are selected as indicators of carbon emissions. Meanwhile, GDPPC is used as an economic growth indicator. In this study, the quadratic polynomial is used to represent EKC, and if the coefficients of the cubic term were not significant, the quadratic polynomial is used to represent EKC [38].

$$\ln(E) = \beta_0 + \beta_1(\ln G) + \beta_2(\ln G)^2 + \beta_3(\ln G)^3 + \varepsilon \quad (3)$$

where E denotes carbon emission index, β_0 is a constant term, $\ln G$ denotes the natural logarithm of GDPPC, β_1, β_2, and β_3 are the primary, secondary, and tertiary coefficients, respectively, and ε is the error term.

2.4.2. Carbon Emission Development Stage Division Based on EKCs

Urban agglomerations exhibit different carbon emission characteristics at different stages of economic development. It is necessary to consider the development stage of carbon emissions with the state of economic development. As shown in Figure 2, there are three types of EKCs that present a relationship between carbon emissions and economic growth [39]: (1) EKC with CI, where GDPPC is the independent variable and CI is the dependent variable; (2) EKC with CE, where GDPPC is the independent variable and CE is the dependent variable; and (3) EKC with CEPC, where GDPPC is the independent variable and CEPC is the dependent variable. There is a turning point for each curve, namely TP_1, TP_2, and TP_3. The development stage of carbon emissions can be divided into four stages based on the three TPs of the EKCs. S_1 is the rapid growth stage, where the carbon emission index increases rapidly with economic growth; S_2 is the pre-peak stage, where the carbon emission index continues to grow but at a slower rate and decreases until it reaches the peak; and S_3 is the over-peak stage, in which the carbon emission index starts to decrease. S_4 is the low-carbon stage, in which the carbon emission index gradually decreases to a lower level.

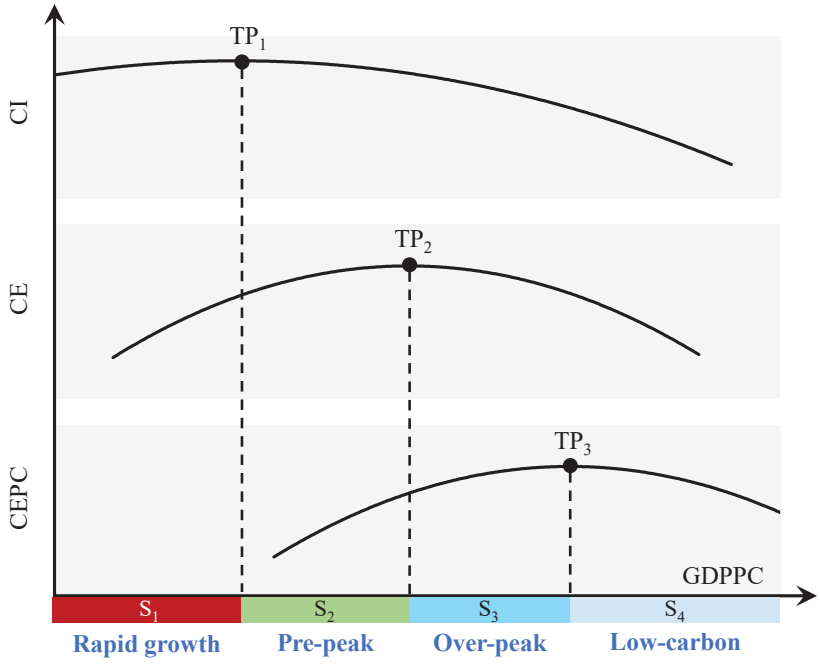

Figure 2. Carbon emission development stage based on EKCs.

2.5. MGWR Model

MGWR is an extension of geographic weighted regression (GWR) and has been widely used in the analysis of spatial relationships of explanatory variables. GWR is a model for geographic analysis that allows the model parameters to be verified based on a specific location [40]. The GWR model is formulated as follows:

$$y_i = \beta_0(u_i, v_i) + \sum_{j=1}^{n} \beta_j(u_i, v_i) x_{ij} + \varepsilon_i \quad (4)$$

where i represents the i-th unit, (u_i, v_i) are the latitude and longitude coordinates of city i, y_i is the CO_2 emissions of unit i, $\beta_0(u_i, v_i)$ is the intercept at i, $\beta_j(u_i, v_i)$ is the regression coefficient of the j-th variable of unit i, j denotes the uniform bandwidth of the regression coefficient, x_{ij} is the j-th influencing factor for unit i, and ε is the error term of i. When $\beta_j(u_i, v_i)$ is a constant, GWR is equal to the ordinary least squares (OLS) model.

However, the bandwidth of GWR is constant, and it cannot explain the phenomena, which involve numerous spatial processes with various [41]. Therefore, Fotheringham et al. (2017) proposed a multiscale geographically weighted regression (MGWR) model [42]. MGWR allows an optimal bandwidth for the explanatory variables based on local regression. MGWR is formulated as follows:

$$y_i = \beta_{bw0}(u_i, v_i) + \sum_{j=1}^{n} \beta_{bwj}(u_i, v_i) x_{ij} + \varepsilon_i \quad (5)$$

where $bw0$ denotes the bandwidth used for the regression coefficient of the global variable, bwj denotes the bandwidth used for the regression coefficient of the j-th variable, and the other variables have the same meaning as in the GWR model.

3. Results

3.1. Spatiotemporal Variation of CO_2 Emissions

3.1.1. Temporal Variation of CO_2 Emissions

Figure 3 shows the CO_2 emissions of three urban agglomerations in YREB during 2008–2017. The CO_2 emissions of three urban agglomerations reached their peak around 2012–2013 and then began to decrease, with the lowest emissions of the three urban agglomerations in 2017. Moreover, the CO_2 emissions of YRD-UA were much higher than those of CY-UA and YRMR-UA, where 41.87% of the CO_2 emissions in YREB were contributed by YRD-UA. YRD-UA had entered the middle and late stages of urban agglomeration development with a higher level of regional integration and stronger comprehensive strength [43]. The CO_2 emissions of CY-UA were the lowest among the urban agglomerations since CY-UA was at the initial stage of urban agglomeration development with fewer megacities [44].

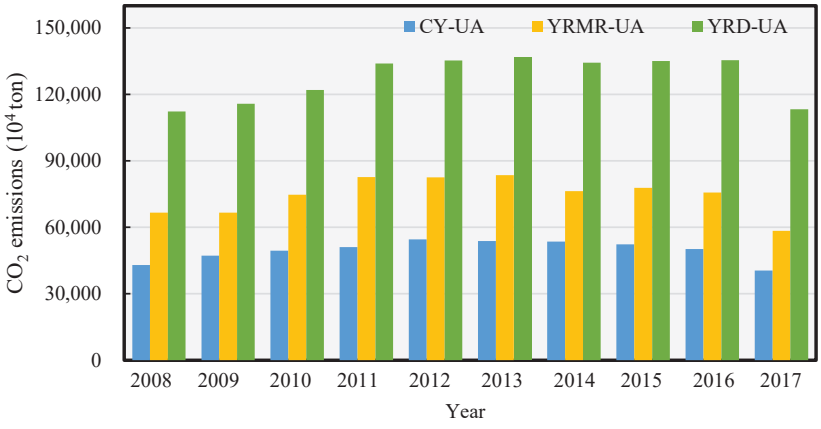

Figure 3. The CO_2 emissions of the three urban agglomerations from 2008 to 2017.

Since 2013, the CO_2 emissions of three YREB urban agglomerations have shown a decreasing trend; CY-UA reached its peak around 2012, while YRMR-UA and YRD-UA reached their peaks around 2013. Specifically, the CO_2 emissions in YRMR-UA declined most significantly, while the CO_2 emissions decline in YRD-UA was relatively stable. In 2016, a symposium on comprehensively advancing the development of the sustainable development of YREB was held for the first time, highlighting the importance of ecological conservation and environmental management [45]. The significant reduction of CO_2 emissions in 2017 illustrated the effectiveness of government policies.

3.1.2. Spatial Variation of CO_2 Emissions

Figure 4 shows the CO_2 emissions in 2008 and 2017. The 10-year average CO_2 emissions of CY-UA was 49,553 $\times$ 10^4 tons, with the low-value area distributed in the western mountainous area and northern mountainous areas, and the high-value area distributed in the urban areas around Chongqing and Chengdu. The 10-year average CO_2 emissions of YRMR-UA was 74,461 $\times$ 10^4 tons, with the low-value area distributed in the southern mountainous area and the border of Jiangxi and Hubei provinces, and the high-value area distributed in Wuhan, Changsha, and Nanchang. For YRD-UA, the 10-year average CO_2 emissions was 127,413 $\times$ 10^4 tons, with the low-value areas distributed in the southwestern mountains and western and northern plains, and the high-value areas distributed in Shanghai, Hangzhou, Nanjing, and the surrounding areas. Notably, the CO_2 emissions of several large cities, such as Chengdu in the CY-UA and Wuhan in the YRMR-UA, decreased in 2017 compared to 2008.

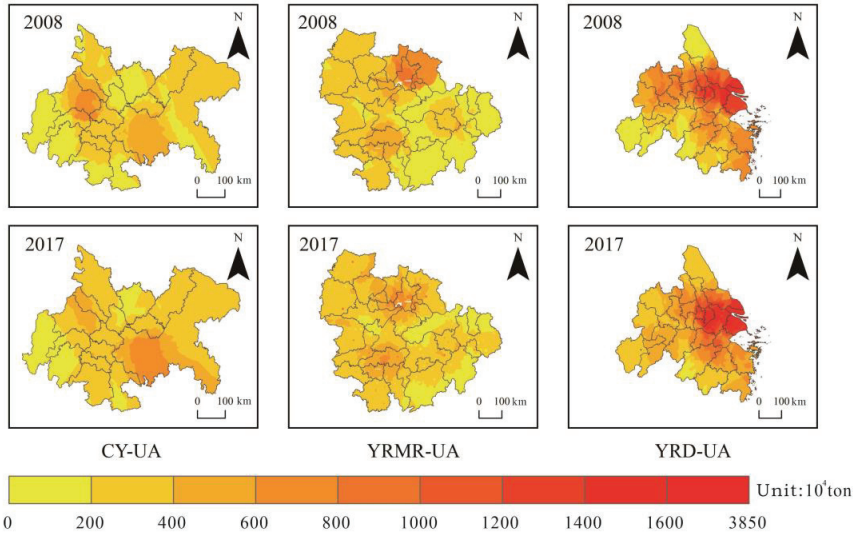

Figure 4. Spatial variation of CO_2 emissions in the three urban agglomerations in 2008 and 2017.

3.1.3. Spatial Aggregation of CO_2 Emissions

Table 3 shows the global autocorrelation performance. The *Z* score is a multiple of the standard deviation, and the *p* value indicates probability. *Z* is correlated with *p*, where $p < 0.05$ indicates that the confidence level is greater than 95% [46]. CY-UA and YRD-UA presented significant spatial aggregation characteristics. The Moran's *I* of CY-UA in 2008 and 2017 were 0.146 and 0.173, respectively, where the spatial autocorrelation of CO_2 emissions increased. The Moran's *I* of YRMR-UA in 2008 and 2017 was 0.034 and 0.045, respectively. As for YRD-UA, the Moran's *I* was 0.180 and 0.135 in 2008 and 2017, respectively.

Table 3. Global spatial autocorrelation of CO_2 emissions in three urban agglomerations.

2008	CY-UA	YRMR-UA	YRD-UA	2017	CY-UA	YRMR-UA	YRD-UA
Moran's *I*	0.146	0.034	0.180	Moran's *I*	0.173	0.045	0.135
Z score	4.260	0.969	3.257	*Z* score	5.463	1.105	2.427
p value	0.000	0.333	0.001	*p* value	0.000	0.269	0.015

Figure 5 shows the spatial aggregation characteristics of the CO_2 emissions of three urban agglomerations. For CY-UA, the H-H clusters and L-H clusters were distributed around Chongqing and Chengdu, and the L-L clusters were distributed in the western mountainous areas and scattered in the south and east. The cluster pattern of CO_2 emissions in CY-UA can be described as high in the middle and low around, and the overall pattern has not changed in the decade. For YRMR-UA, the H-H clusters mainly appeared in the north area, the L-H clusters mainly appeared around Wuhan, Changsha, and Nanchang, and the L-L clusters appeared in the southeast area. The cluster pattern of CO_2 emissions in YRMR-UA was high in the north and low in the south. For YRD-UA, the H-H clusters and L-H clusters were mainly distributed in the eastern coastal area, including Shanghai and Nanjing, while the L-L clusters were scattered in the south and southwest areas. The cluster pattern of CO_2 emissions in YRD-UA was high along the coast and low in the southwest.

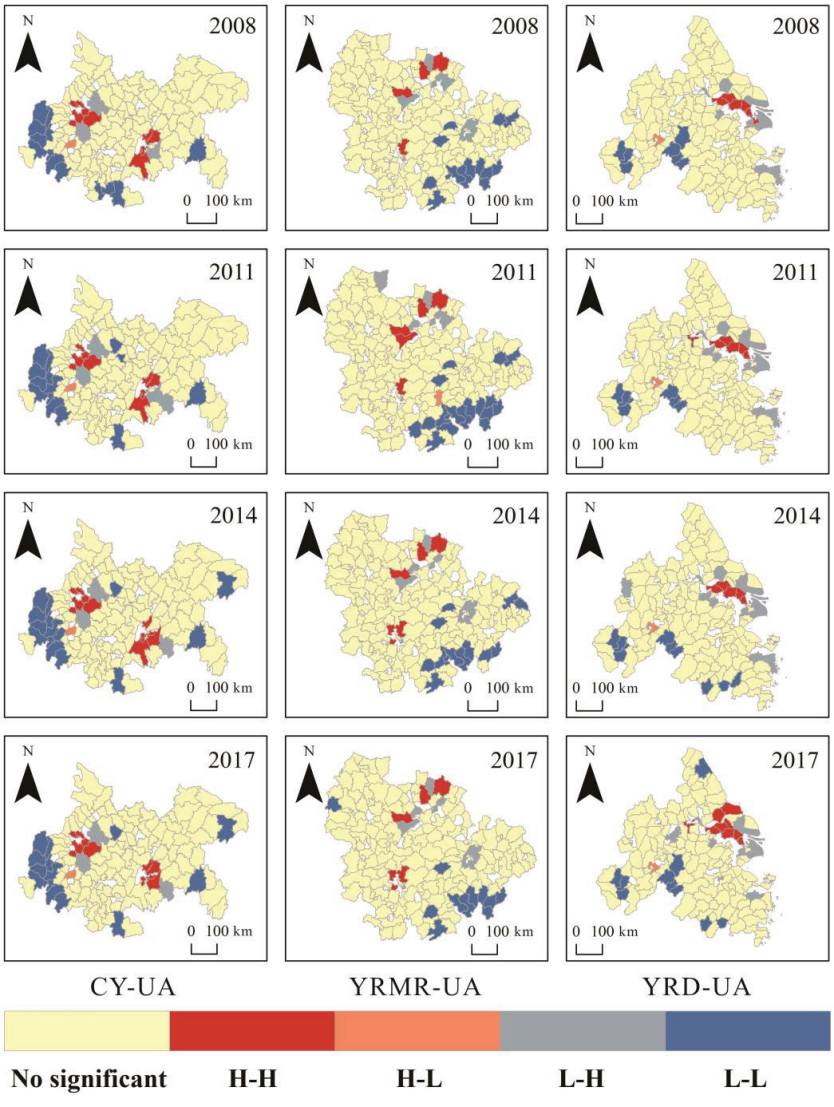

Figure 5. Spatial autocorrelation of CO_2 emissions in the three urban agglomerations.

3.2. Carbon Emission Development Stage Analysis

Figure 6 shows the relationship between carbon emissions and GDPPC for CY-UA. The carbon emission development stage of CY-UA could be divided into three stages: S_1 (–2005), S_2 (2005–2012), and S_4 (2012–). S_3 and S_4 of CY-UA largely overlapped and could be combined into one stage. The peak time of CO_2 emissions in CY-UA was around 2011, and CY-UA is at the low-carbon stage.

Figure 7 shows the relationship between carbon emissions and GDPPC for YRMR-UA. Similar to CY-UA, the S_3 and S_4 stages of YRMR-UA were combined. The YRMR-UA CO_2 emissions could be divided into three stages: S_1 (–2008), S_2 (2008–2011), and S_4 (2011–). The peak time of CO_2 emissions in YRMR-UA was around 2011, and YRMR-UA is at the low-carbon stage.

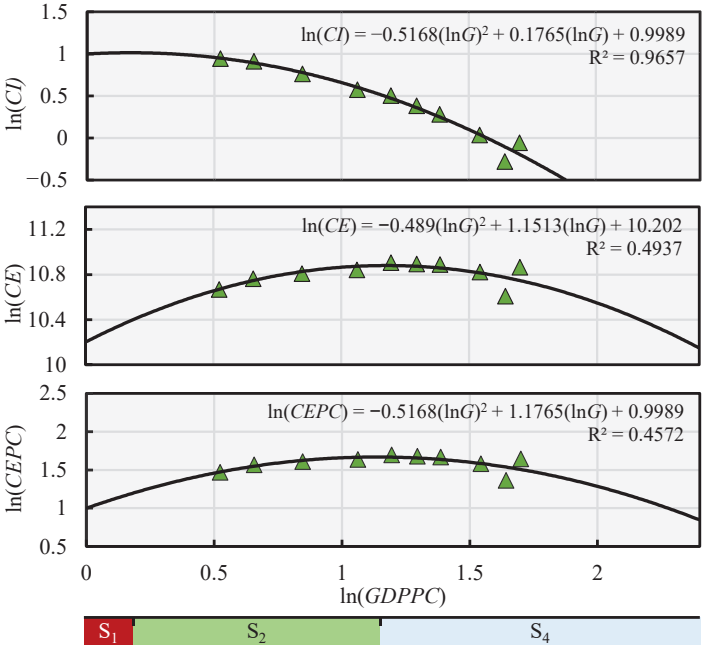

Figure 6. Carbon emission development stage of CY-UA.

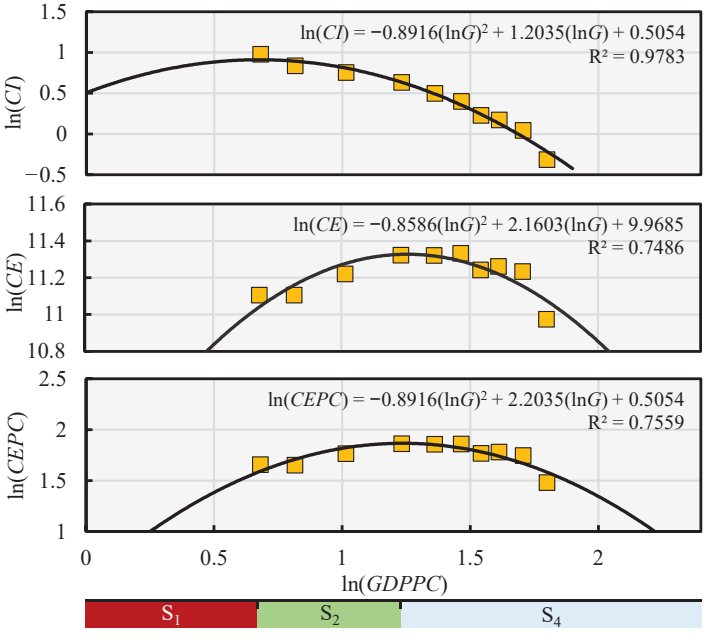

Figure 7. Carbon emission development stage of YRMR-UA.

Figure 8 shows the relationship between carbon emissions and GDPPC for YRD-UA. The emissions of YRD-UA could be divided into four stages: S_1 (–2005), S_2 (2005–2020), S_3 (2020–2022), and S_4 (2022–). The CO_2 emissions of YRD-UA reached the peak around 2020, and YRD-UA was at S_4 stage. Obviously, the actual CO_2 emissions peaked earlier than the

carbon emission development stage. It could be concluded that the Yangtze River Delta integration policy strongly deepened the industrial division of labor and industrial transfer among cities, which contribute to the reduction of CO_2 emissions.

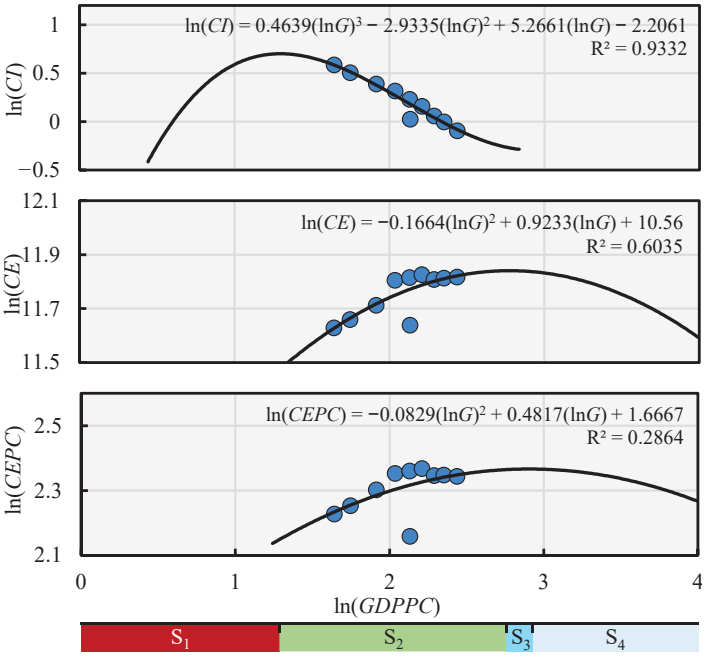

Figure 8. Carbon emission development stage of YRD-UA.

3.3. Model Comparison

3.3.1. Comparison of Model Performance

Table 4 shows the statistical results of OLS, GWR, and MGWR. R^2 is the coefficient of determination. Adjusted R^2 excludes the effect of the number of independent variables on R^2. AICc denotes the corrected Akaike information criterion, which is a relative measure of the goodness of fit [47]. RSS is the sum of squared errors. The effective number of parties (ENP) is a trade-off between the variance of the fitted values and the deviation of the coefficient estimates to measure the value of the equilibrium point.

Table 4. Comparison of OLS, GWR, and MGWR indicators from 2008–2017.

Year	Model	R^2	Adjusted R^2	AICc	RSS	ENP
2008	MGWR	0.96	0.95	5.38	2.85	11.42
	GWR	0.96	0.95	7.40	2.80	12.52
	OLS	0.93	0.92	1159.39	/	/
2011	MGWR	0.95	0.94	13.24	3.33	10.42
	GWR	0.95	0.94	17.48	3.81	8.61
	OLS	0.93	0.92	1177.63	/	/
2014	MGWR	0.95	0.94	12.45	3.35	10.01
	GWR	0.95	0.94	13.92	3.59	8.83
	OLS	0.93	0.93	1165.29	/	/
2017	MGWR	0.88	0.87	74.08	8.12	9.88
	GWR	0.87	0.86	75.64	8.80	8.43
	OLS	0.86	0.85	1204.20	/	/

As shown in Table 4, compared to GWR and OLS, MGWR gave higher R^2, adjusted R^2, and ENP, with lower AICc and RSS, indicating that MGWR had a better local fit and less information loss. Meanwhile, the spatial distribution of R^2 for GWR and MGWR is presented in Figure 9. CY-UA shows a higher R^2 than the other urban agglomerations.

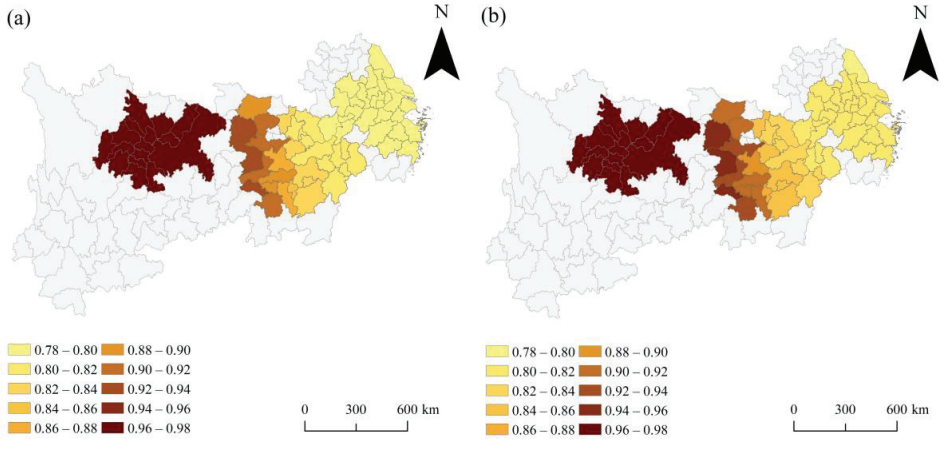

Figure 9. Distribution of the local R^2 for (**a**) GWR and (**b**) MGWR in 2017.

3.3.2. Comparison of Model Bandwidth

Table 5 presents the bandwidths of each influencing factor for GWR and MGWR in different years. In GWR, the factors shared the same bandwidth, while they were assigned to different bandwidths in MGWR. The different values of bandwidth demonstrated the spatial heterogeneity of factors, by which the diversity of influencing factors can be better represented [48].

Table 5. Bandwidths of different influencing factors in MGWR and GWR.

Factors	2008		2011		2014		2017	
	MGWR	GWR	MGWR	GWR	MGWR	GWR	MGWR	GWR
POP	66	51	68	67	68	66	68	69
GDPPC	48	51	59	67	53	66	68	69
SI	68	51	68	67	68	66	68	69
CI	44	51	48	67	68	66	52	69
UR	46	51	46	67	46	66	44	69

3.4. Influencing Factors for CO_2 Emissions

Table 6 shows the descriptive statistics of the regression coefficients of influencing factors in MGWR. It can be seen that the rank of the generated regression coefficients was POP > GDPPC > CI > UR > SI. Obviously, POP and GDPPC presented the highest regression coefficients. The coefficient of POP is positive, indicating that the rise of population will promote the CO_2 emissions of urban agglomerations in YREB. GDPPC presented the second highest regression coefficient, indicating that GDPPC had a facilitating effect on CO_2 emissions. The coefficients of UR and SI were much lower, and their impact on CO_2 emissions was not significant.

Table 6. Statistics of regression coefficients for different influencing factors in MGWR.

Factors	Year	Min	Median	Max	Mean	STD
POP	2008	0.637	0.818	0.992	0.814	0.134
	2011	0.664	0.814	0.89	0.79	0.089
	2014	0.705	0.805	0.961	0.821	0.102
	2017	0.719	0.732	0.743	0.733	0.007
GDPPC	2008	0.594	0.659	0.678	0.647	0.03
	2011	0.591	0.63	0.647	0.625	0.019
	2014	0.635	0.647	0.66	0.65	0.007
	2017	0.183	0.192	0.234	0.201	0.018
SI	2008	−0.034	−0.017	0.106	0.011	0.052
	2011	−0.035	−0.027	0.011	−0.019	0.017
	2014	0.016	0.022	0.047	0.028	0.012
	2017	0.037	0.065	0.083	0.063	0.015
CI	2008	0.098	0.184	0.285	0.202	0.066
	2011	0.105	0.171	0.3	0.195	0.066
	2014	0.082	0.16	0.269	0.177	0.063
	2017	0.157	0.236	0.509	0.262	0.091
UR	2008	−0.068	0.075	0.161	0.041	0.07
	2011	−0.038	0.038	0.111	0.027	0.038
	2014	−0.048	−0.044	−0.004	−0.033	0.017
	2017	0.132	0.214	0.408	0.255	0.108

Figure 10 shows the spatial distribution of the regression coefficients of POP. There was a significant positive correlation between POP and CE, where an increase in population will increase energy consumption and thus produce more CO_2 emissions [49]. The impact of POP on CE was significant in YRD-UA. YRD-UA was an important economic center in China, which provided sufficient jobs and attracted a large number of migrants [50]. Traffic congestion caused by population concentration was not conducive to adequate combustion of fuels [51], leading to an increase in transportation CO_2 emissions. The transportation CO_2 emissions in YRD-UA amounted to 9971.78×10^4 tons in 2017, which is approximately equal to the sum of CY-UA and YRMR-UA.

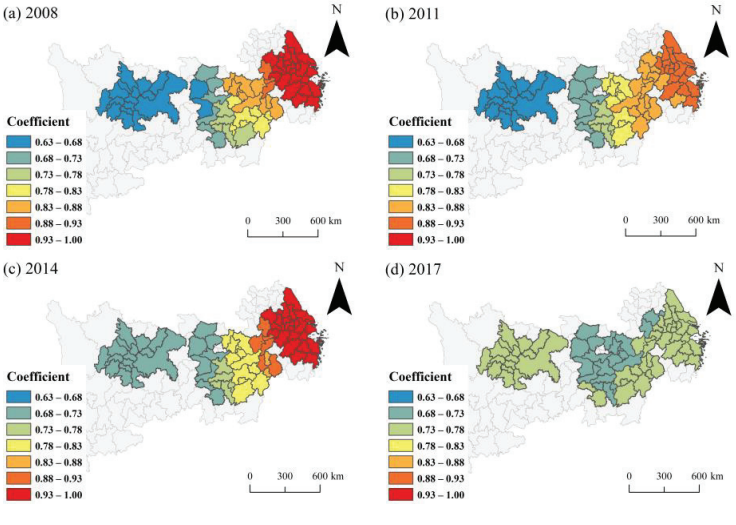

Figure 10. Spatial distribution of regression coefficients of POP.

Figure 11 shows the spatial distribution of regression coefficients for GDPPC. The positive correlation between GDPPC and CE indicates that the growth of GDPPC promoted CO_2 emissions in YREB urban agglomerations. The influence of GDPPC on CE was significant in YRD-UA, and the regression coefficient decreased from east to west in 2008, 2011, and 2014. Economically developed regions responded better to the policy. The government improves local competitiveness in response to economic conditions [52]. More attention should be paid to the change in people's awareness and environmental management caused by the economic improvement.

Figure 12 shows the spatial distribution of the regression coefficients of CI. The positive correlation between CI and CE indicates that the adoption of technological innovations and the improvement of energy use efficiency reduced CO_2 emissions [53]. The impact of CI on CE was significant in YRD-UA. Technological advances promoted the harmonization of economic and environmental development [54]. Companies were more inclined to use environmentally friendly technologies [55].

Figure 13 shows the spatial distribution of regression coefficients for UR. The impact of UR on CE was insignificant, and the value of the regression coefficient varied between −0.07 and 0.41. The reason was that urbanization led to an increase in people's demand for employment, housing, transportation, commodities, and energy dependence [56], and urban construction increased society's demand for high-emitting industries such as steel and cement [57].

Figure 14 shows the spatial distribution of regression coefficients for SI. SI presented a negative correlation with CE in 2008 and 2011, while SI positively correlated with CE in 2014 and 2017. The reason may be that some cities in YREB were at the stage of industrial start-up and development. YRD-UA was dominated by light industry and high-tech industry with low CO_2 emissions [58]. YRMR-UA was at the initial stage of the Rise of Central China Plan, and CY-UA was vital to China's western development [59]. The industrial layout and energy structure of YREB are gradually maturing.

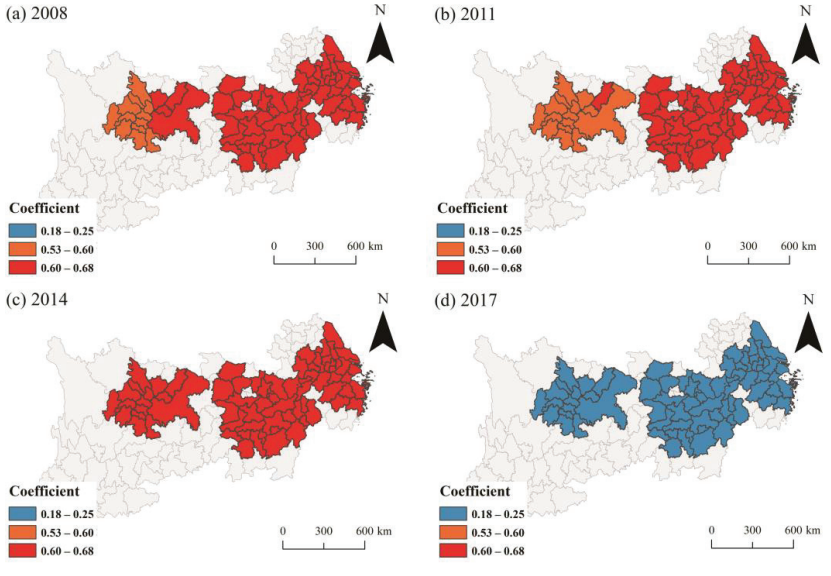

Figure 11. Spatial distribution of regression coefficients of GDPPC.

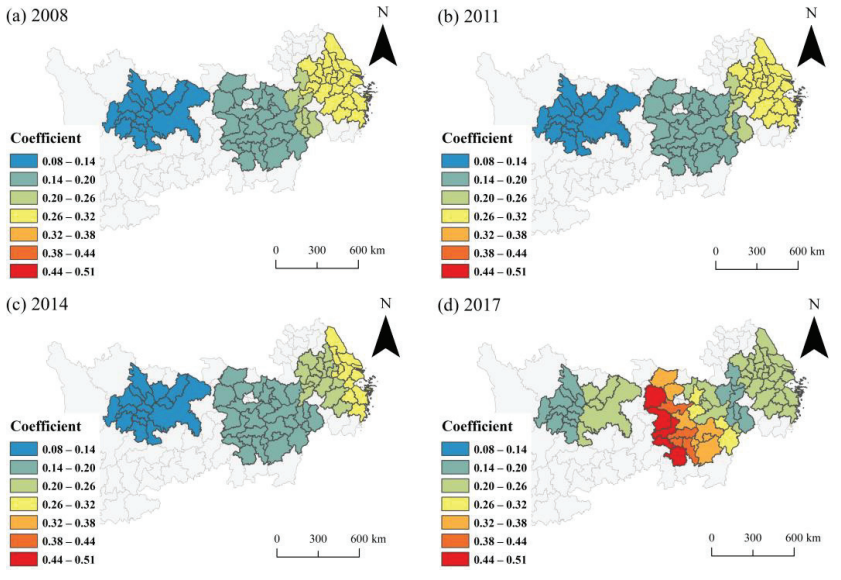

Figure 12. Spatial distribution of regression coefficients of CI.

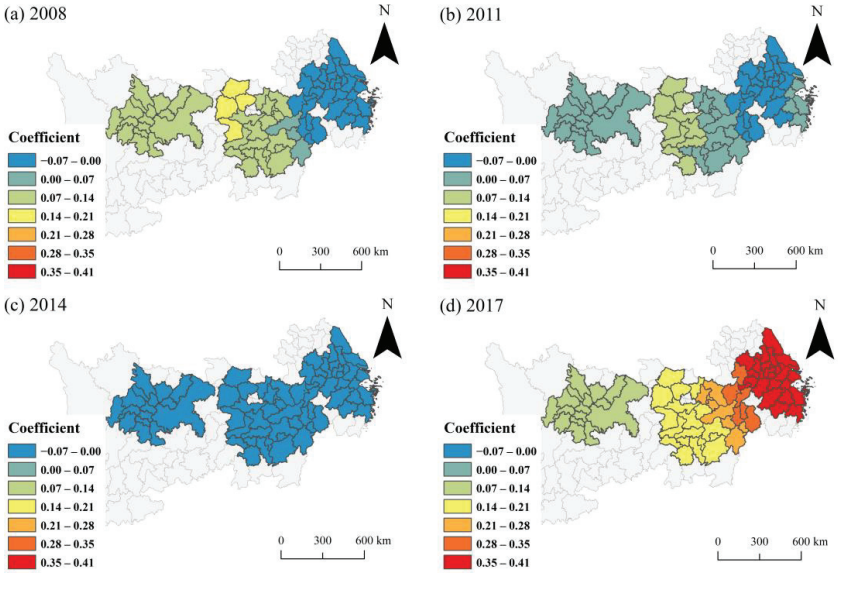

Figure 13. Spatial distribution of regression coefficients of UR.

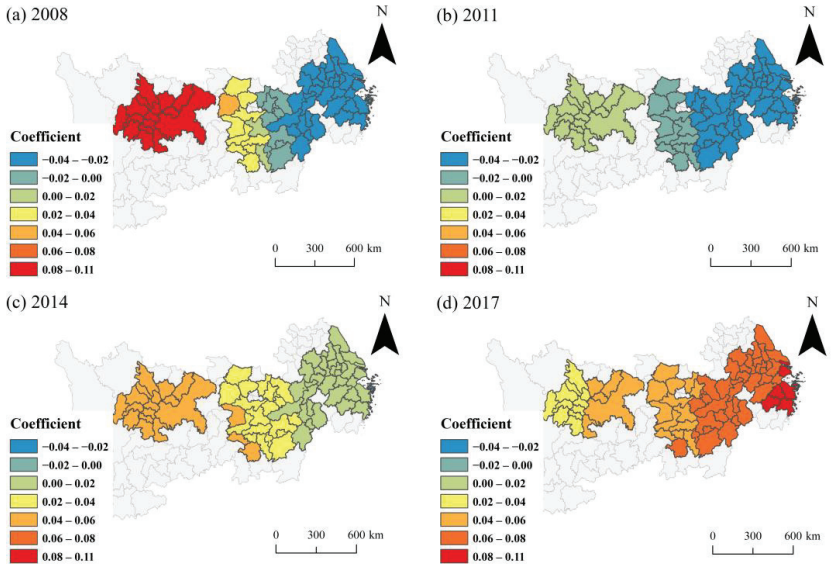

Figure 14. Spatial distribution of regression coefficients of SI.

It is noteworthy that the spatial distribution of five influencing factors changed significantly in 2017. The spatial heterogeneity of POP decreased, the impact of GDPPC decreased, the spatial heterogeneity of CI increased, and the spatial heterogeneity of UR increased. It may be due to the convening of the symposium on comprehensively advancing the development of sustainable development in YREB held in 2016. The difference in the sensitivities of inland and coastal cities to policies resulted in changes in the regression coefficients of the influencing factors in 2017.

4. Discussion

4.1. Insights into the CO_2 Emissions of YREB Urban Agglomerations

As a pioneer demonstration belt for the construction of ecological civilization in China, YREB is of great significance to China and the world in achieving emission reduction and sustainable development. Different urban agglomerations present different carbon emission characteristics at different stages of economic development, making it important to develop targeted emission reduction measures. China is in the process of rapid urbanization and industrialization [60]. In 2017, the proportion of tertiary industry in YRD-UA was 2.84% higher than the proportion of secondary industry [53]. Several cities in the southeast coastal region had already crossed the industrialization stage and entered the post-industrialization period [61], which was confirmed by the low proportion of industrial CO_2 emissions in YRD-UA and the significant growth of electricity CO_2 emissions. However, most cities in central and western China were in the process of industrialization, and the proportion of tertiary industry was lower than the proportion of secondary industry [62], which led to a higher proportion of industrial CO_2 emissions in CY-UA and YRMR-UA than that in YRD-UA.

The optimization and upgrading of industrial structures could promote carbon mitigation in CY-UA and YRMR-UA. Specifically, attention can be paid to industries such as electronic information, engineering machinery, rail transportation equipment, automobiles, aerospace, biomedicine, and new materials. In addition, CY-UA and YRMR-UA could undertake the transfer of high-tech industries from the developed coastal regions. With the deepening of the 14th Five-Year Plan and the vigorous development of wind, hydro, and photovoltaic power generation [63], renewable energy will be the mainstream of the future energy structure in YREB. The west-east gas pipeline project has provided cleaner energy

and reduced fossil fuel consumption [64]. More attention should be paid to taking measures to reduce CO_2 emissions from production and life while increasing the share of the service industry in the regional economy. Meanwhile, YRD-UA should focus on reducing the facilitating effects of population on CO_2 emissions by considering human capital agglomeration in the process of urbanization [65]. The investigation of spatiotemporal variations in CO_2 emissions contributes to timely policy adjustments for carbon emission mitigation in YREB urban agglomerations. Meanwhile, EKCs revealed the relationship between CO_2 emissions and economic development, providing a strategy that can be applied to analyze the carbon emission development stage of more regions. Furthermore, the importance of different influencing factors for CO_2 emissions was generated and discussed, which can be conducive to promoting regional sustainable development.

4.2. Limitations

This study investigated the CO_2 emissions of YREB urban agglomerations, but there is still room for further research. The MEIC CO_2 emissions data is from 2008 to 2017, and the spatiotemporal patterns of CO_2 emissions after 2017 were not explored in this study. Therefore, expanded CO_2 emissions datasets with more recent years will be considered in the future. Meanwhile, five influencing factors that reveal economic and social characteristics were selected in this study, and future studies will focus on the selection of representative and comprehensive influencing factors of CO_2 emissions in urban agglomerations.

5. Conclusions

This paper revealed the spatial and temporal variations of CO_2 emissions in three urban agglomerations in YREB. Meanwhile, the carbon emission development stage of the YREB urban agglomerations was explored based on EKCs that take economic growth and carbon emissions into account. In addition, the influencing factors of CO_2 emissions were analyzed using MGWR. The main conclusions are as follows:

(1) The CO_2 emissions in the three urban agglomerations first increased and then decreased from 2008 to 2017. YRD-UA contributed 41.87% of the CO_2 emissions of YREB, with the highest CO_2 emissions among the three urban agglomerations. A symposium on comprehensively advancing the development of the sustainable development of YREB was held in 2016, and the CO_2 emissions in three urban agglomerations decreased significantly in 2017.

(2) The carbon emission development stage of urban agglomeration was analyzed based on the relationship between carbon emissions and economic growth. According to the EKCs, CY-UA, YRMR-UA, and YRD-UA reached the CO_2 emissions peaks around 2012, 2011, and 2020, respectively. Nowadays, the urban agglomerations in YREB are at the low-carbon stage.

(3) The CO_2 emissions of YREB urban agglomerations were significantly affected by POP and GDPPC, while the impacts of UR and SI were not significant. The spatial distribution of influencing factors changed significantly in 2017. To reduce CO_2 emissions, human capital agglomeration and clean energy should be considered in the process of urbanization.

Moreover, future work will focus on the long-term carbon emission development stage analysis of typical urban agglomerations, where more comprehensive CO_2 emissions data and influencing factors will be taken into account.

Author Contributions: Conceptualization, Q.L.; methodology, Q.L. and T.L.; software, T.L.; validation, Q.L. and T.L.; formal analysis, Q.L. and T.L.; investigation, T.L. and S.W.; resources, T.L. and S.W.; data curation, T.L.; writing—original draft preparation, T.L. and S.W.; writing—review and editing, Q.L., T.L. and L.W.; visualization, T.L.; supervision, Q.L.; project administration, Q.L. and L.W.; funding acquisition, Q.L. and L.W. All authors have read and agreed to the published version of the manuscript.

Funding: This work was supported by the Natural Science Foundation of Hubei Province (2021CFB116), the Hubei Key Research and Development Program (2021BID002), and the Open Research Fund Program of the Key Laboratory of Digital Mapping and Land Information Application, Ministry of Natural Resources (ZRZYBWD202208).

Data Availability Statement: Not applicable.

Acknowledgments: We are grateful to the MGWR 2.2 software from the School of Geographical Sciences and Urban Planning at Arizona State University for providing the basis for data processing in this paper and to the MEIC team at Tsinghua University for publishing the inventory of anthropogenic CO_2 emissions. We thank the Resource and Environment Science and Data Center of the Institute of Geographic Science and Natural Resources Research, CAS, for providing administrative boundary data. We appreciate the editors and reviewers for their valuable suggestions and comments.

Conflicts of Interest: The authors declare no conflict of interest.

References

1. Clark, P.U.; Shakun, J.D.; Marcott, S.A.; Mix, A.C.; Eby, M.; Kulp, S.; Levermann, A.; Milne, G.A.; Pfister, P.L.; Santer, B.D.; et al. Consequences of twenty-first-century policy for multi-millennial climate and sea-level change. *Nat. Clim. Change* **2016**, *6*, 360–369. [CrossRef]
2. Wang, S.; Wang, J.; Li, S.; Fang, C.; Feng, K. Socioeconomic driving forces and scenario simulation of CO_2 emissions for a fast-developing region in China. *J. Clean. Prod.* **2019**, *216*, 217–229. [CrossRef]
3. Lindsey, R.; Dahlman, L. Climate Change: Global Temperature. 2020. Available online: https://www.climate.gov/news-features/understanding-climate/climate-change-global-temperature (accessed on 1 January 2023).
4. Frame, D.J.; Held, H.; Kriegler, E.; Mach, K.J.; Matschoss, P.R.; Plattner, G.-K.; Zwiers, F.W.; Matschoss, P.R. Guidance Note for Lead Authors of the IPCC Fifth Assessment Report on Consistent Treatment of Uncertainties. Intergovernmental Panel on Climate Change (IPCC). Available online: http://www.ipcc.ch (accessed on 30 March 2023).
5. Qian, Y.; Wang, H.; Wu, J. Spatiotemporal association of carbon dioxide emissions in China's urban agglomerations. *J. Environ. Manage.* **2022**, *323*, 116109. [CrossRef]
6. Wang, F.; Harindintwali, J.D.; Yuan, Z.; Wang, M.; Wang, F.; Li, S.; Yin, Z.; Huang, L.; Fu, Y.; Li, L.; et al. Technologies and perspectives for achieving carbon neutrality. *Innovation* **2021**, *2*, 100180. [CrossRef] [PubMed]
7. Dong, F.; Li, Y.; Gao, Y.; Zhu, J.; Qin, C.; Zhang, X. Energy transition and carbon neutrality: Exploring the non-linear impact of renewable energy development on carbon emission efficiency in developed countries. *Resour. Conserv. Recycl.* **2022**, *177*, 106002. [CrossRef]
8. Xiao, Y.; Ma, D.; Zhang, F.; Zhao, N.; Wang, L.; Guo, Z.; Zhang, J.; An, B.; Xiao, Y. Spatiotemporal differentiation of carbon emission efficiency and influencing factors: From the perspective of 136 countries. *Sci. Total Environ.* **2023**, *879*, 163032. [CrossRef]
9. Andreoni, V.; Galmarini, S. Drivers in CO_2 emissions variation: A decomposition analysis for 33 world countries. *Energy* **2016**, *103*, 27–37. [CrossRef]
10. Grodzicki, T.; Jankiewicz, M. The impact of renewable energy and urbanization on CO_2 emissions in Europe—Spatio-temporal approach. *Environ. Dev.* **2022**, *44*, 100755. [CrossRef]
11. Namahoro, J.; Wu, Q.; Zhou, N.; Xue, S. Impact of energy intensity, renewable energy, and economic growth on CO_2 emissions: Evidence from Africa across regions and income levels. *Renew. Sustain. Energy Rev.* **2021**, *147*, 111233. [CrossRef]
12. Fragkias, M.; Lobo, J.; Strumsky, D.; Seto, K.C. Does size matter? Scaling of CO_2 emissions and US urban areas. *PLoS ONE* **2013**, *8*, e64727. [CrossRef]
13. Wen, L.; Shao, H. Analysis of influencing factors of the CO_2 emissions in China: Nonparametric additive regression approach. *Sci. Total Environ.* **2019**, *694*, 133724. [CrossRef]
14. Liu, Z.; Deng, Z.; He, G.; Wang, H.; Zhang, X.; Lin, J.; Qi, Y.; Liang, X. Challenges and opportunities for carbon neutrality in China. *Nat. Rev. Earth Environ.* **2021**, *3*, 141–155. [CrossRef]
15. Zeng, N.; Jiang, K.; Han, P.; Hausfather, Z.; Cao, J.; Kirk-Davidoff, D.; Ali, S.; Zhou, S. The Chinese carbon-neutral goal: Challenges and prospects. *Adv. Atmos. Sci.* **2022**, *39*, 1229–1238. [CrossRef] [PubMed]
16. Wang, K.; Zhang, X.; Wei, Y.-M.; Yu, S. Regional allocation of CO_2 emissions allowance over provinces in China by 2020. *Energy Policy* **2013**, *54*, 214–229. [CrossRef]
17. Liu, J.; Tian, Y.; Huang, K.; Yi, T. Spatial-temporal differentiation of the coupling coordinated development of regional energy-economy-ecology system: A case study of the Yangtze River Economic Belt. *Ecol. Indic.* **2021**, *124*, 107394. [CrossRef]
18. Yuan, L.; Li, R.; Wu, X.; He, W.; Kong, Y.; Ramsey, T.S.; Degefu, D.M. Decoupling of economic growth and resources-environmental pressure in the Yangtze River Economic Belt, China. *Ecol. Indic.* **2023**, *153*, 110399. [CrossRef]
19. Liu, Q.; Hao, J. Regional Differences and Influencing Factors of Carbon Emission Efficiency in the Yangtze River Economic Belt. *Sustainability* **2022**, *14*, 4814. [CrossRef]
20. Li, K.; Zhou, Y.; Xiao, H.; Li, Z.; Shan, Y. Decoupling of economic growth from CO_2 emissions in Yangtze River Economic Belt cities. *Sci. Total Environ.* **2021**, *775*, 145927. [CrossRef]

21. Fang, C.; Yu, D. Urban agglomeration: An evolving concept of an emerging phenomenon. *Landsc. Urban Plan.* **2017**, *162*, 126–136. [CrossRef]
22. Li, L.; Ma, S.; Zheng, Y.; Xiao, X. Integrated regional development: Comparison of urban agglomeration policies in China. *Land Use Policy* **2022**, *114*, 105939. [CrossRef]
23. Yu, X.; Wu, Z.; Zheng, H.; Li, M.; Tan, T. How urban agglomeration improve the emission efficiency? A spatial econometric analysis of the Yangtze River Delta urban agglomeration in China. *J. Environ. Manage.* **2020**, *260*, 110061. [CrossRef] [PubMed]
24. Tan, J.; Wang, R. Research on evaluation and influencing factors of regional ecological efficiency from the perspective of carbon neutrality. *J. Environ. Manage.* **2021**, *294*, 113030. [CrossRef] [PubMed]
25. Rao, G.; Liao, J.; Zhu, Y.; Guo, L. Decoupling of economic growth from CO_2 emissions in Yangtze River Economic Belt sectors: A sectoral correlation effects perspective. *Appl. Energy* **2022**, *307*, 118223. [CrossRef]
26. Wang, P.; Wu, J. Impact of environmental investment and resource endowment on regional energy efficiency: Evidence from the Yangtze River Economic Belt, China. *Environ. Sci. Pollut. Res.* **2022**, *29*, 5445–5453. [CrossRef]
27. Chen, Y.; Zhang, S.; Huang, D.; Li, B.-L.; Liu, J.; Liu, W.; Ma, J.; Wang, F.; Wang, Y.; Wu, S.; et al. The development of China's Yangtze River Economic Belt: How to make it in a green way? *Sci. Bull.* **2017**, *62*, 648–651. [CrossRef] [PubMed]
28. Li, M.; Liu, H.; Geng, G.; Hong, C.; Liu, F.; Song, Y.; Tong, D.; Zheng, B.; Cui, H.; Man, H.; et al. Anthropogenic emission inventories in China: A review. *Natl. Sci. Rev.* **2017**, *4*, 834–866. [CrossRef]
29. Zheng, B.; Tong, D.; Li, M.; Liu, F.; Hong, C.; Geng, G.; Li, H.; Li, X.; Peng, L.; Qi, J.; et al. Trends in China's anthropogenic emissions since 2010 as the consequence of clean air actions. *Atmos. Chem. Phys.* **2018**, *18*, 14095–14111. [CrossRef]
30. Liu, F.; Zhang, Q.; Tong, D.; Zheng, B.; Li, M.; Huo, H.; He, K.B. High-resolution inventory of technologies, activities, and emissions of coal-fired power plants in China from 1990 to 2010. *Atmos. Chem. Phys.* **2015**, *15*, 13299–13317. [CrossRef]
31. Liu, Q.; Wu, S.; Lei, Y.; Li, S.; Li, L. Exploring spatial characteristics of city-level CO_2 emissions in China and their influencing factors from global and local perspectives. *Sci. Total Environ.* **2021**, *754*, 142206. [CrossRef]
32. Cui, E.; Ren, L.; Sun, H. Analysis on the regional difference and impact factors of CO_2 emissions in China. *Environ. Prog. Sustain. Energy* **2017**, *36*, 1282–1289. [CrossRef]
33. Zhao, Y.; Chen, R.; Sun, T.; Yang, Y.; Ma, S.; Xie, D.; Zhang, X.; Cai, Y. Urbanization Influences CO_2 Emissions in the Pearl River Delta: A Perspective of the "Space of Flows". *Land* **2022**, *11*, 1373. [CrossRef]
34. Liu, Y.; Zhang, X.; Pan, X.; Ma, X.; Tang, M. The spatial integration and coordinated industrial development of urban agglomerations in the Yangtze River Economic Belt, China. *Cities* **2020**, *104*, 102801. [CrossRef]
35. Dong, L.; Liang, H. Spatial analysis on China's regional air pollutants and CO_2 emissions: Emission pattern and regional disparity. *Atmos. Environ.* **2014**, *92*, 280–291. [CrossRef]
36. Anselin, L. Local Indicators of Spatial Association-LISA. *Geogr. Anal.* **2010**, *27*, 93–115. [CrossRef]
37. Stern, D.I. The Rise and Fall of the Environmental Kuznets Curve. *World Dev.* **2004**, *32*, 1419–1439. [CrossRef]
38. Carson, R.T. The Environmental Kuznets Curve: Seeking Empirical Regularity and Theoretical Structure. *Rev. Environ. Econ. Policy* **2010**, *4*, 3–23. [CrossRef]
39. Shen, L.; Wu, Y.; Lou, Y.; Zeng, D.; Shuai, C.; Song, X. What drives the carbon emission in the Chinese cities?—A case of pilot low carbon city of Beijing. *J. Clean. Prod.* **2018**, *174*, 343–354. [CrossRef]
40. Brunsdon, C.; Fotheringham, A.S.; Charlton, M.E. Geographically Weighted Regression: A Method for Exploring Spatial Nonstationarity. *Geogr. Anal.* **2010**, *28*, 281–298. [CrossRef]
41. Mansour, S.; Al Kindi, A.; Al-Said, A.; Al-Said, A.; Atkinson, P. Sociodemographic determinants of COVID-19 incidence rates in Oman: Geospatial modelling using multiscale geographically weighted regression (MGWR). *Sustain. Cities Soc.* **2021**, *65*, 102627. [CrossRef]
42. Fotheringham, A.S.; Yang, W.; Kang, W. Multiscale Geographically Weighted Regression (MGWR). *Ann. Am. Assoc. Geogr.* **2017**, *107*, 1247–1265. [CrossRef]
43. Wu, J.; Sun, W. Regional Integration and Sustainable Development in the Yangtze River Delta, China: Towards a Conceptual Framework and Research Agenda. *Land* **2023**, *12*, 470. [CrossRef]
44. Shen, W.; Liang, H.; Dong, L.; Ren, J.; Wang, G. Synergistic CO_2 reduction effects in Chinese urban agglomerations: Perspectives from social network analysis. *Sci. Total Environ.* **2021**, *798*, 149352. [CrossRef] [PubMed]
45. Zhou, B.; Zhou, F.; Zhou, D.; Qiao, J.; Xue, B. Improvement of environmental performance and optimization of industrial structure of the Yangtze River economic belt in China: Going forward together or restraining each other? *J. Chin. Gov.* **2021**, *6*, 435–455. [CrossRef]
46. Greenland, S.; Senn, S.J.; Rothman, K.J.; Carlin, J.B.; Poole, C.; Goodman, S.N.; Altman, D.G. Statistical tests, P values, confidence intervals, and power: A guide to misinterpretations. *Eur. J. Epidemiol.* **2016**, *31*, 337–350. [CrossRef]
47. Bivand, R.; Pebesma, E.J.; Gómez-Rubio, V. *Applied Spatial Data Analysis with R*; Use R! Springer: New York, NY, USA, 2008; ISBN 978-0-387-78170-9.
48. Li, Z.; Wang, F.; Kang, T.; Wang, C.; Chen, X.; Miao, Z.; Zhang, L.; Ye, Y.; Zhang, H. Exploring differentiated impacts of socioeconomic factors and urban forms on city-level CO_2 emissions in China: Spatial heterogeneity and varying importance levels. *Sustain. Cities Soc.* **2022**, *84*, 104028. [CrossRef]
49. Solarin, S.A.; Al-Mulali, U.; Gan, G.G.G.; Shahbaz, M. The impact of biomass energy consumption on pollution: Evidence from 80 developed and developing countries. *Environ. Sci. Pollut. Res.* **2018**, *25*, 22641–22657. [CrossRef]

50. Wang, L.; Zhao, P. From dispersed to clustered: New trend of spatial restructuring in China's metropolitan region of Yangtze River Delta. *Habitat Int.* **2018**, *80*, 70–80. [CrossRef]
51. Lu, J.; Li, B.; Li, H.; Al-Barakani, A. Expansion of city scale, traffic modes, traffic congestion, and air pollution. *Cities* **2021**, *108*, 102974. [CrossRef]
52. Wolfson, J.; Frisken, F. Local Response to the Global Challenge: Comparing Local Economic Development Policies in a Regional Context. *J. Urban Aff.* **2000**, *22*, 361–384. [CrossRef]
53. Wang, X.; Song, J.; Duan, H.; Wang, X. Coupling between energy efficiency and industrial structure: An urban agglomeration case. *Energy* **2021**, *234*, 121304. [CrossRef]
54. Andersen, M.S.; Massa, I. Ecological modernization—Origins, dilemmas and future directions. *J. Environ. Policy Plan.* **2000**, *2*, 337–345. [CrossRef]
55. Heidenreich, S.; Spieth, P.; Petschnig, M. Ready, steady, green: Examining the effectiveness of external policies to enhance the adoption of eco-friendly innovations. *J. Prod. Innov. Manag.* **2017**, *34*, 343–359. [CrossRef]
56. Bai, Y.; Deng, X.; Gibson, J.; Zhao, Z.; Xu, H. How does urbanization affect residential CO_2 emissions? An analysis on urban agglomerations of China. *J. Clean. Prod.* **2019**, *209*, 876–885. [CrossRef]
57. Yang, Z.; Gao, W.; Han, Q.; Qi, L.; Cui, Y.; Chen, Y. Digitalization and carbon emissions: How does digital city construction affect china's carbon emission reduction? *Sustain. Cities Soc.* **2022**, *87*, 104201. [CrossRef]
58. Cui, W.; Lin, X.; Wang, D.; Mi, Y. Urban Industrial Carbon Efficiency Measurement and Influencing Factors Analysis in China. *Land* **2022**, *12*, 26. [CrossRef]
59. Tian, P.; Liu, Y.; Li, J.; Pu, R.; Cao, L.; Zhang, H. Spatiotemporal patterns of urban expansion and trade-offs and synergies among ecosystem services in urban agglomerations of China. *Ecol. Indic.* **2023**, *148*, 110057. [CrossRef]
60. Xu, S.-C.; He, Z.-X.; Long, R.-Y. Factors that influence carbon emissions due to energy consumption in China: Decomposition analysis using LMDI. *Appl. Energy* **2014**, *127*, 182–193. [CrossRef]
61. Wei, L.; Wang, Z. Differentiation Analysis on Carbon Emission Efficiency and Its Factors at Different Industrialization Stages: Evidence from Mainland China. *Int. J. Environ. Res. Public. Health* **2022**, *19*, 16650. [CrossRef]
62. Xu, R.; Lin, B. Why are there large regional differences in CO_2 emissions? Evidence from China's manufacturing industry. *J. Clean. Prod.* **2017**, *140*, 1330–1343. [CrossRef]
63. Stern, N.; Xie, C. China's new growth story: Linking the 14th Five-Year Plan with the 2060 carbon neutrality pledge. *J. Chin. Econ. Bus. Stud.* **2023**, *21*, 5–25. [CrossRef]
64. Gao, C.; Su, B.; Sun, M.; Zhang, X.; Zhang, Z. Interprovincial transfer of embodied primary energy in China: A complex network approach. *Appl. Energy* **2018**, *215*, 792–807. [CrossRef]
65. Zhu, Z.; Yu, J.; Luo, J.; Zhang, H.; Wu, Q.; Chen, Y. A GDM-GTWR-Coupled Model for Spatiotemporal Heterogeneity Quantification of CO_2 Emissions: A Case of the Yangtze River Delta Urban Agglomeration from 2000 to 2017. *Atmosphere* **2022**, *13*, 1195. [CrossRef]

land

MDPI

Article

Spatiotemporal Evolution and Correlation Analysis of Carbon Emissions in the Nine Provinces along the Yellow River since the 21st Century Using Nighttime Light Data

Yaohui Liu [1,2], Wenyi Liu [1], Peiyuan Qiu [1,*], Jie Zhou [3,4] and Linke Pang [1]

[1] School of Surveying and Geo-Informatics, Shandong Jianzhu University, Jinan 250101, China
[2] College of Geodesy and Geomatics, Shandong University of Science and Technology, Qingdao 266590, China
[3] Institute of Geology, China Earthquake Administration, Beijing 100029, China
[4] Key Laboratory of Seismic and Volcanic Hazards, China Earthquake Administration, Beijing 100029, China
* Correspondence: qiupeiyuan20@sdjzu.edu.cn

Abstract: Monitoring carbon emissions is crucial for assessing and addressing economic development and climate change, particularly in regions like the nine provinces along the Yellow River in China, which experiences significant urbanization and development. However, to the best of our knowledge, existing studies mainly focus on national and provincial scales, with fewer studies on municipal and county scales. To address this issue, we established a carbon emission assessment model based on the "NPP-VIIRS-like" nighttime light data, aiming to analyze the spatiotemporal variation of carbon emissions in three different levels of nine provinces along the Yellow River since the 21st century. Further, the spatial correlation of carbon emissions at the county level was explored using the Moran's *I* spatial analysis method. Results show that, from 2000 to 2021, carbon emissions in this region continued to rise, but the growth rate declined, showing an overall convergence trend. Per capita carbon emission intensity showed an overall upward trend, while carbon emission intensity per unit of GDP showed an overall downward trend. Its spatial distribution generally showed high carbon emissions in the eastern region and low carbon emissions in the western region. The carbon emissions of each city mainly showed a trend of "several"; that is, the urban area around the Yellow River has higher carbon emissions. Meanwhile, there is a trend of higher carbon emissions in provincial capitals. Moran's *I* showed a trend of decreasing first and then increasing and gradually tended to a stable state in the later stage, and the pattern of spatial agglomeration was relatively fixed. "High–High" and "Low–Low" were the main types of local spatial autocorrelation, and the number of counties with "High–High" agglomeration increased significantly, while the number of counties with "Low–Low" agglomeration gradually decreased. The findings of this study provide valuable insights into the carbon emission trends of the study area, as well as the references that help to achieve carbon peaking and carbon neutrality goals proposed by China.

Keywords: carbon emissions; nighttime lights; spatiotemporal variation; spatial correlation; nine provinces along the Yellow River

Citation: Liu, Y.; Liu, W.; Qiu, P.; Zhou, J.; Pang, L. Spatiotemporal Evolution and Correlation Analysis of Carbon Emissions in the Nine Provinces along the Yellow River since the 21st Century Using Nighttime Light Data. *Land* **2023**, *12*, 1469. https://doi.org/10.3390/land12071469

Academic Editors: Chao Wang, Jinyan Zhan and Xueting Zeng

Received: 27 June 2023
Revised: 17 July 2023
Accepted: 21 July 2023
Published: 23 July 2023

1. Introduction

Since the Industrial Revolution, increasing carbon emissions from human activities have become a major contributor to global climate change. As a result, climate change has become a pressing global issue, garnering attention from the international community [1–3]. To develop and implement climate change mitigation and adaptation policies and plans, there is an urgent need for accurate, reliable, and real-time carbon emission data [4,5]. Consequently, monitoring and evaluating carbon emissions has become a critical priority and research hotspot, which helps ecological environment protection and prompts high-quality development.

In recent years, a growing amount of research has been conducted on studying the spatiotemporal characteristics, and monitoring and evaluation of carbon emissions [6–9]. Researchers have investigated various factors that influence carbon emissions in different regions and proposed predictive models to forecast carbon emissions in specific areas. For instance, Huang et al. [10] analyzed the carbon peak and carbon emission information of the Yangtze River Economic Belt, and proposed a support vector regression (SVR) machine prediction model to predict the carbon emission information in the region. Du et al. [11] established a China Carbon Watch (CCW) system, enabling the monthly calculation of carbon emissions from provincial-level urban and rural households between January and May 2020. Liu et al. [12] used the Lasso regression model to screen out eight significant factors affecting carbon emissions based on the data of Jiangsu province from 2001 to 2018 and used the BP neural network model to predict the carbon emissions of Jiangsu province from 2019 to 2030. Ning et al. [13] established a prediction model for carbon emissions in four representative provinces and cities in Beijing, Henan, Guangdong, and Zhejiang from 1997 to 2017. However, the abovementioned research lacks the capability of achieving small-scale refined monitoring, such as at the county level, and cannot provide real-time monitoring and assessment of carbon emissions. Therefore, new methods and technologies are highly needed to enable more granular, comprehensive, and real-time monitoring and assessment of carbon emissions.

Nighttime light remote sensing is an optical remote sensing technology that detects and obtains information on nighttime lights, providing a quick, accurate, and objective view of the surface and human activities [14–16]. Unlike daytime remote sensing, nighttime light remote sensing can reveal information that is not visible during the day [17,18]. Since most of the stable light at night comes from artificial sources in urban areas, remote sensing images of nighttime lights can more intuitively reflect differences in human activity at night [19–22]. Nighttime light data has become a new monitoring method with the advantages of large coverage, fast timeliness, and convenient access, making it suitable for multi-scale and long-term research on urban issues [23]. Nighttime light data has been used in many studies related to disaster monitoring, urban sprawl, and human activity [24–28]. For instance, Fan et al. [29] used NPP-VIIRS nighttime light data to monitor recovery after earthquakes and quickly assess earthquake damage. Li et al. [30] researched the variation of nighttime illumination in different seismic regions and the influence of human activities on nighttime illumination. Liu et al. [31] used NPP-VIIRS nighttime light data to explore the resilience and post-disaster recovery of Zhengzhou City, using the extremely heavy rainstorm in Zhengzhou City on July 20, 2021 as an example. Chen et al. [32] constructed a new nighttime light landscape indicator, taking various townships in Fujian Province as examples to reveal rural and urban economic development, and their differences and economic expansion from multiple perspectives.

Nighttime light data has also been used to explore carbon emissions [33–37]. Doll et al. [38] produced the world's first 1×1 resolution carbon emission distribution map, revealing the difference in carbon emission levels of countries at different stages of development based on the correlation between DMSP-OLS nighttime light data and carbon emissions. Sun et al. [39] monitored the variation in China's city-level carbon emissions from 2000 to 2017 based on nighttime light data, and found that low-carbon cities are concentrated in western and central China, while high-carbon-emission cities are mainly distributed in the Beijing–Tianjin–Hebei and Yangtze River Delta regions. Yang et al. [40] established a regional Chinese building carbon emission calculation model based on the nighttime light data and building carbon emission data in the eastern, central, and western regions of China. Guo et al. [41] analyzed the spatiotemporal variation patterns, correlations, and heterogeneity of carbon emissions of three different administrative units from 2012 to 2019 based on nighttime light data and normalized difference vegetation index. Overall, nighttime light remote sensing is an effective tool for monitoring human activity and carbon emissions, providing valuable information for urban and environmental studies,

and has the potential to contribute significantly to the development of urban planning and environmental management policies.

Located in the central and western regions of China, the nine provinces along the Yellow River are important areas for achieving coordinated regional development. This region is China's main energy and heavy chemical industry base, containing high-carbon industries such as coal, oil, steel, and chemicals, resulting in the issues of carbon emissions of this region being more prominent [42–44]. The development of this region can promote the economic development of the western region, narrow the development gap between the eastern and western regions, and achieve a balanced and coordinated national economy. In addition, the development of this region also has a significant impact on the development of the global economy, which can promote the vitality of global trade and investment. To achieve the coordinated development of economic development and environmental protection, the Chinese government has adopted a series of policies and measures to promote the construction of ecological civilization and energy conservation, and emission reduction, and strive to achieve the goals of carbon peak and carbon neutrality. However, to the best of our knowledge, existing studies mainly focus on the national and provincial scales and fewer studies are conducted at the municipal and county scales. This inevitably ignores the development stage and regional differences, which is not conducive to the national level and all levels of government developing practical carbon reduction and pollution reduction programs based on local conditions while improving the quality of economic development and steadily promoting the urbanization process. Therefore, the monitoring and analysis of carbon emissions at the municipal and county levels in the region will help the government adjust its policies on time, optimize the industrial and energy structures, accelerate green and low-carbon development, promote economic transformation and upgrading, and achieve sustainable economic development.

This study aims to investigate the spatiotemporal variation, per capita carbon emission intensity, and carbon emission intensity per unit of GDP in the nine provinces along the Yellow River since the 21st century. We first build a fitting model for carbon emission monitoring and evaluation using "NPP-VIIRS-like" nighttime light data and other multi-source data. The spatiotemporal evolution characteristics of carbon emissions at municipal and county levels are monitored and assessed. Furthermore, Moran's I is employed to investigate the spatial correlations of carbon emissions at county levels in the region. This study provides important reference information for decision-making departments to formulate more reasonable and effective carbon emission reduction policies to optimize the industrial structure of this region and reduce carbon emissions.

This study has the following three main objectives:

1. Construct a fitting model of the nighttime lighting index and carbon emissions for the timely and accurate prediction of carbon emissions;
2. Investigate the spatiotemporal characteristics and trends of carbon emissions in the nine provinces along the Yellow River of China since the 21st century;
3. Explore the spatial correlation of carbon emissions at the county level using Moran's I statistical method.

The rest of this study is organized as follows: Section 2 describes the study area and data. Section 3 introduces the calculation method of carbon emissions, the processing method of nighttime lighting data, the fitting model construction, and the spatial correlation analysis method. Section 4 introduces the spatiotemporal variation of carbon emissions and the fitting model of the nine provinces along the Yellow River. The discussion and conclusion are presented in Sections 5 and 6, respectively.

2. Study Area and Data

2.1. Study Area

The Yellow River is considered the "mother river" of China. This massive river, one of the longest in the world and the second longest in China, is located in the northern part of the country. The Yellow River basin encompasses a vast area that includes nine

provinces: Shanxi, Inner Mongolia, Shandong, Henan, Sichuan, Shaanxi, Gansu, Qinghai, and Ningxia, as depicted in Figure 1. This region covers a staggering 3,569,000 km^2, which constitutes around 37.2% of China's entire territory. As of 2022, the population of this region is approximately 420 million people, accounting for 29.8% of China's total population. Additionally, the GDP of this region is estimated at 28.7 trillion yuan, which is equivalent to 25.1% of China's overall GDP. The Yellow River basin is a crucial area for China's economy and culture, with a rich history and a vibrant present. Moreover, this region is rich in biodiversity and ecosystems, including wetlands, forests, grasslands, and rivers. These ecosystems are vital to maintaining the ecological balance of the region, protecting rare species, and preserving natural ecological functions. Protecting the ecosystems along the nine Yellow Provinces will help maintain the stability of the global ecosystem.

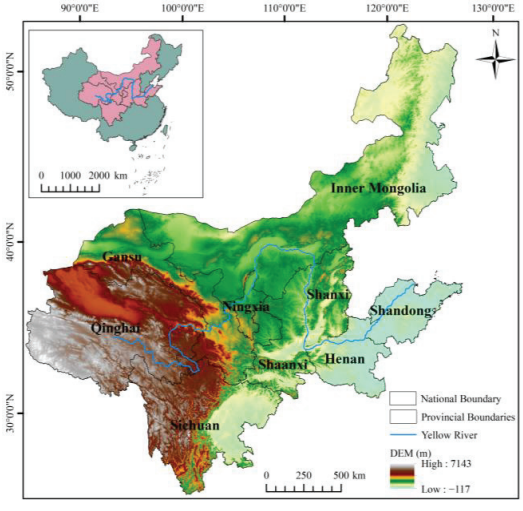

Figure 1. Geographical location of the study area.

2.2. Data

To conduct a comprehensive analysis of carbon emissions in the study area, various energy data, including raw coal, coke, crude oil, gasoline, kerosene, diesel, fuel oil, natural gas, heat, and electricity, were selected. The energy statistics were obtained from the Statistical Yearbook, China Energy Statistical Yearbook, and Urban Greenhouse Gas Inventory Research of nine provinces and cities from 2000 to 2021. To estimate carbon emissions in the study area, "NPP-VIIRS-like" nighttime light data from 2000 to 2021 were obtained from the AI-Earth Earth Science Cloud Platform (https://engine-aiearth.aliyun.com, accessed on 15 March 2023). The spatial resolution of this data is 500 m, which has the advantages of high spatial resolution, global coverage, long-term continuous observation, and strong data consistency and comparability, and provides a powerful tool for researchers to analyze and understand the distribution and changes of nighttime lights on the Earth's surface, and can be used to construct a reliable model for monitoring and evaluating carbon emissions [45–47]. Population and GDP data were also collected from the Statistical Yearbooks of nine provinces and cities from 2000 to 2021. Table 1 shows the data-related information, including data name, time range, and sources of data.

Table 1. Data sources in this study.

Data	Time Range	Data Sources
Energy statistics	2000–2021	Statistical Yearbook, China Energy Statistical Yearbook, Urban Greenhouse Gas Inventory Research of nine provinces and cities
"NPP-VIIRS-like" nighttime light data	2000–2021	AI-Earth Earth Science Cloud Platform (https://engine-aiearth.aliyun.com)
Population and GDP data	2000–2021	Statistical Yearbooks of nine provinces and cities

3. Methodology

In this study, we focused on assessing the spatiotemporal variation of the carbon emissions in the nine provinces along the Yellow River since the 21st century based on nighttime light remote sensing and multisource data. The overall workflow of this study is presented in Figure 2.

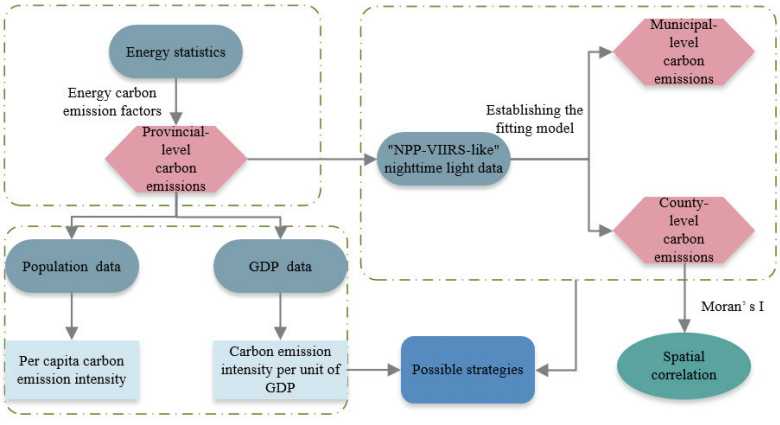

Figure 2. The workflow of this study.

3.1. Calculation of Carbon Emissions

To estimate the carbon emissions of each province in the study area, this study uses the 2006 Greenhouse Gas Emissions Inventory published by the IPCC (Intergovernmental Panel on Climate Change) [48]. The carbon emissions are calculated using the following equation:

$$CO_2 = \frac{44}{12} \times \sum_{i=1}^{10} K_i E_i \quad (1)$$

where i is 10 energy types; E_i is the consumption of energy i in terms of standard coal (10,000 tons); and K_i is the carbon emission factor of energy i (10,000 carbon)/(10,000 standard coal), from the default value of IPCC carbon emission calculation guidelines, where the original data unit is J. To be consistent with the statistical data unit, it is converted into standard coal with a conversion factor of 1×10^4 tons of standard coal equal to 2.93×10^5 GJ. The carbon emission factors for each type of energy are presented in Table 2 [49].

Table 2. Energy carbon emission factors.

Energy Type	Raw Coal	Coke	Crude Oil	Gasoline	Kerosene	Diesel	Fuel Oil	Natural Gas	Heat	Electricity
Converted to standard coal (tons of standard coal/ton)	0.7143	0.9714	1.4286	1.4714	1.4714	1.4751	1.4286	1.33	34.12	0.345
Carbon emission factor (10^4 tons carbon/10^4 tons standard coal)	0.7559	0.855	0.5857	0.5538	0.5714	0.5921	0.6185	0.4483	0.67	0.272

3.2. Per Capita Carbon Emission Intensity and Carbon Emission Intensity Per Unit of GDP

To obtain a comprehensive understanding of carbon emission patterns and mechanisms, this study integrates the demographic and economic statistics of each province. The aim is to investigate the spatiotemporal distribution characteristics and influence factors of per capita carbon emission intensity and carbon emission intensity per unit of GDP in each province, with the following equations:

$$\text{Per capita carbon emission intensity} = CO_2/p \tag{2}$$

$$\text{Carbon emission intensity per unit of GDP} = CO_2/GDP \tag{3}$$

where CO_2 is total carbon emissions (10,000 tons); p is the year-end resident population data (10,000 people); and GDP is gross regional product (10,000 yuan).

3.3. Nighttime Light Index Calculation

For this study, the total nighttime light index ($TNLI$) is selected as the index for calculation and analysis. $TNLI$ is calculated as the sum of the light digital number (DN) values of administrative units, as presented by the following equation:

$$TNLI = \sum_{i=1}^{n} DN_i \tag{4}$$

where n is the number of rasters and DN_i is the radiation value of the image element corresponding to each raster.

3.4. Establishing the Fitting Model

Given the significant correlation between $TNLI$ and carbon emissions, we used a linear regression model to fit the $TNLI$ and total carbon emissions of the study area. In this model, the intercept was set to 0, reflecting the absence of energy-related carbon emissions in unlit regions. The equation for the linear regression model is as follows:

$$CO_2 = a \times TNLI \tag{5}$$

where CO_2 is the total carbon emission, $TNLI$ is the total nighttime light index, and a is the fitting factor.

From 2000 to 2021, the TNLI and carbon emissions of nine provinces showed an approximate linear growth in the early years, and then reached the inflection point and gradually slowed down. Moreover, carbon emissions were affected by the phased emission reduction targets and tasks proposed by China's government in 2009 and 2015, and the growth rate had shown a rapid downward trend. Therefore, considering the inherent attributes of the data in conjunction with the temporal milestones associated with carbon emission mitigation policies, it has been delineated into seven distinct temporal intervals to conduct a comprehensive fitting analysis. The outcomes of this analysis are presented in Table 3, where a denotes the fitting coefficient of carbon emissions and TNLI, and R^2 denotes the correlation coefficient of carbon emissions and TNLI: the larger this value, the stronger the correlation.

Table 3. Parameters of the quadratic polynomial model of carbon emissions from 2000 to 2021.

Year	*a*	R^2
2000–2004	0.1465	0.9208
2005–2008	0.1763	0.9483
2009–2012	0.2079	0.9602
2013–2014	0.1410	0.9016
2015–2016	0.1439	0.9007
2017–2018	0.1059	0.8485
2019–2021	0.0858	0.7813

3.5. Spatial Correlation

To investigate the spatiotemporal dynamics of carbon emissions, we employ global Moran's *I* and local indicators of spatial association (LISA). Global Moran's *I* is calculated using Equation (6), with values ranging from −1 to 1. Values closer to 1 indicate a stronger positive correlation, while values closer to −1 indicate a stronger negative correlation. Values close to 0 indicate a lack of significant correlation. Local Moran's *I* is calculated using Equation (7). LISA analysis is used to describe the correlation of spatial units based on five attributes: "High–High", "Low–Low", "High–Low", "Low–High", and "Not Significant".

$$I = \frac{\sum_{i=1}^{n}\sum_{j=1}^{n}\omega_{ij}(x_i-\overline{x})(x_j-\overline{x})}{\frac{1}{n}\sum_{i=1}^{n}(x_i-\overline{x})^2\cdot\sum_{i=1}^{n}\sum_{j=1}^{n}\omega_{ij}} \quad (6)$$

$$I_i = \frac{x_i-\overline{x}}{\frac{1}{n}\sum_{i=1}^{n}(x_i-\overline{x})^2}\sum_{j=1,j\neq i}^{n}\omega_{ij}(x_j-\overline{x}) \quad (7)$$

where n is the number of regions, x_i is the carbon emissions of the ith region, the upper horizontal line represents the mean value, and ω_{ij} is the spatial symmetric weight.

4. Results

4.1. Temporal Characteristics of Provincial-Level Carbon Emissions

The carbon emissions of the study area from 2000 to 2021 are presented in Figure 3. Since the 21st century, the total carbon emissions of this region have continued to rise, but the growth rate has gradually decreased, showing an overall trend of convergence. It is worth noting that, despite this convergence, the region has not yet reached peak carbon. In 2000, the total carbon emissions were 890.849 million tons; in 2012, they reached 3440.83 million tons; and, in 2021, they increased to 3787.586 million tons. The total carbon emissions continued to rise, but the average annual growth rate showed a downward trend: the average annual growth rate of carbon emissions from 2000 to 2012 was 12.01%, and it fell rapidly to 1.10% from 2012 to 2021. This demonstrates that the emission reduction targets and tasks established by China at the Copenhagen Conference in 2009 and the 75th session of the United Nations General Assembly in 2020 [50] have an important impact on carbon emission reduction in the Yellow River Basin. Figure 4 shows the share of carbon emissions upstream of the Yellow River (including Qinghai, Inner Mongolia, Sichuan, Gansu, and Ningxia), the midstream (including Shaanxi and Shanxi), and the downstream (including Henan and Shandong). From 2000 to 2021, the difference between upstream and downstream carbon emission levels was small, accounting for about 80% of the carbon emissions of the nine Yellow River provinces, while the midstream carbon emissions accounted for a relatively small amount, about 20%. The proportion of upstream and midstream carbon emissions has gradually increased, from 31.41% in 2001 to 41.07% in 2021, and from 20.96% in 2005 to 22.14% in 2021. The upstream and midstream have been in pursuit of rapid economic development, and the resulting energy consumption has led to an increase in carbon emissions. The proportion of downstream carbon emissions showed a trend of first rising and then decreasing, rising from 43.88% in 2001 to 48.75% in 2005 and 36.79% in 2021. This is closely related to the shift of the focus of its economic development

from the early pursuit of rapid economic development to improving the high-quality and efficiency of economic development and optimizing the economic structure.

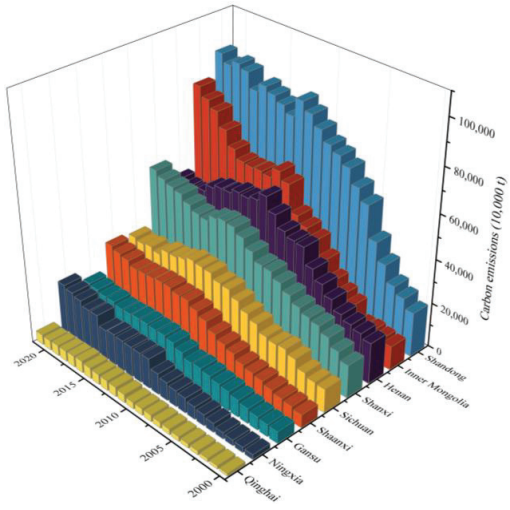

Figure 3. Temporal characteristics of provincial-level carbon emissions in the study area from 2000 to 2021.

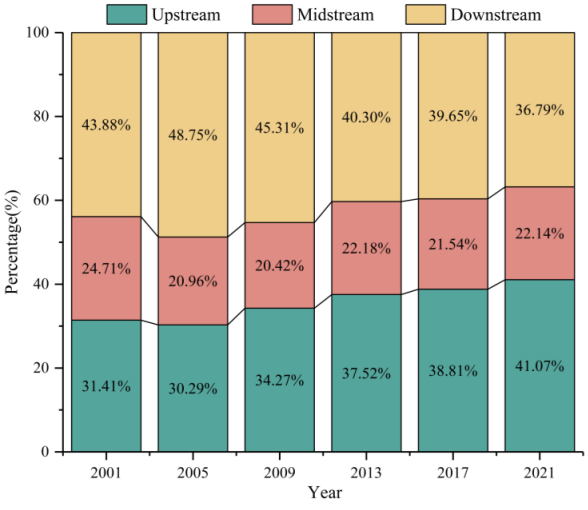

Figure 4. Percentage of carbon emissions in the study area from 2000 to 2021.

4.2. Spatial Characteristics of Provincial-Level Carbon Emissions

The spatial trends of carbon emissions of the study area from 2000 to 2021 are displayed in Figure 5. To investigate the spatial variation of carbon emissions across different regions and years, we employed the natural interruption point method to categorize the carbon emission data. Overall, carbon emissions from the nine Yellow River provinces show a trend of high in the east and low in the west. Specifically, the total carbon emissions of nine provinces along the Yellow River in 2001 were relatively low. In 2005, carbon emissions from Shandong, Shanxi, Henan, Inner Mongolia, Sichuan, and Gansu increased significantly, with Shandong's emissions exceeding 50 million tons. In 2013, carbon emissions in all four eastern provinces were at high levels. Shanxi's carbon emissions fell in 2017. This reduction

can be attributed to the successful implementation of an innovative initiative in Taiyuan, the provincial capital, wherein all taxis were electrified in 2016. However, carbon emissions in Shanxi and Shaanxi gradually increased in 2021, while those in Henan declined. This divergence can be attributed to the implementation of the "Notice on the Implementation of the Three-Year Action Plan for Energy Conservation and Carbon Reduction Transformation of Key Energy-using Units" by Henan province in 2021. The notice pointed out that, by 2023, key energy-using units will achieve an energy-saving capacity of more than 6 million tons of standard coal/year, and achieve maximum improvement in energy efficiency.

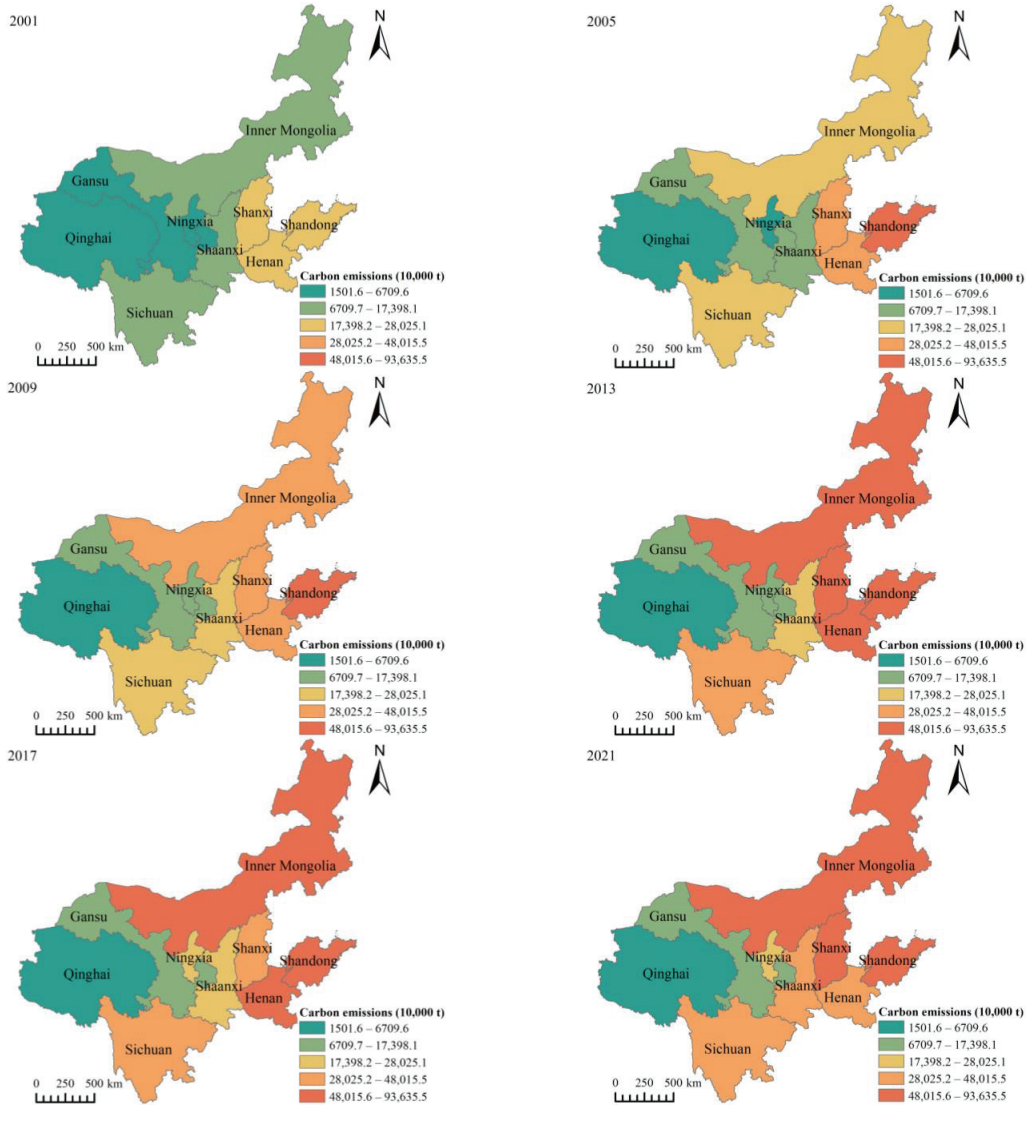

Figure 5. Spatial characteristics of provincial-level carbon emissions in the study area from 2000 to 2021.

4.3. Temporal Characteristics of Per Capita Carbon Emission Intensity and Carbon Emission Intensity Per Unit of GDP

The per capita carbon emission intensity is a crucial indicator of carbon emission levels and is the central critical issue in climate negotiations. It is important for developing effective carbon reduction strategies and for ensuring a sustainable future. The temporal characteristics of per capita carbon emission intensity in the study area from 2000 to 2021 are presented in Figure 6. From 2000 to 2021, the per capita carbon emission intensity of nine provinces along the Yellow River showed an overall upward trend. Among them, Inner Mongolia has the highest per capita carbon emission intensity, reaching 34.7 tons in 2021. Its growth trend is the largest, with an average annual growth rate of 10.94%. This is mainly due to its development mode of "relying on energy and relying on heavy energy", the characteristics of heavy industrial structure and high carbonization of energy structure, large stock and a high proportion of energy and raw material industries, and high energy consumption and high emission industries; renewable energy has become the main basic energy still to be developed, and the role of carbon emission reduction is not sufficient. Moreover, Ningxia's per capita carbon emission intensity is just below Inner Mongolia's, with a faster growth rate. Shanxi's per capita carbon emission intensity is in the middle of the range until it exceeds 15 tons in 2021. In contrast, Sichuan has the lowest per capita carbon emission intensity, at 3.4 tons. Its growth trend is also the smallest, with an average annual growth rate of 5.04%. This may be related to Sichuan's relatively clean industrial structure and relatively diversified energy structure, while Sichuan's vigorous development of renewable energy, such as hydropower and wind power, has also played a positive role in reducing carbon emissions. The per capita carbon emission intensity of the other provinces varies little, and they are all relatively low, located below 10 tons.

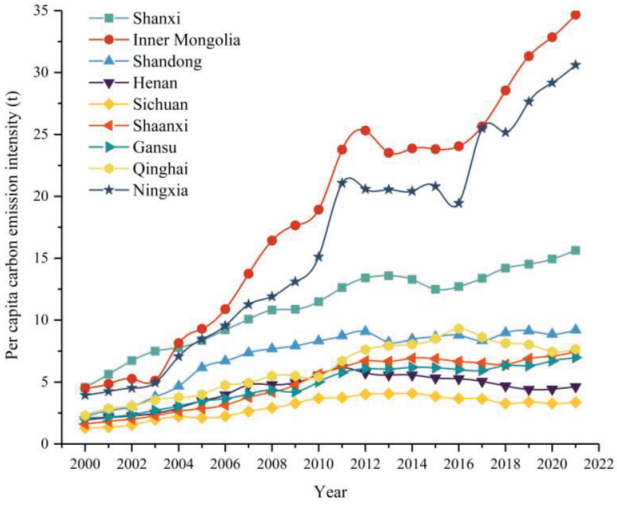

Figure 6. Temporal characteristics of per capita carbon emission intensity in the study area from 2000 to 2021.

The carbon emission intensity per unit of GDP is an internationally recognized indicator for measuring the effectiveness of emission reduction. The temporal characteristics of the carbon emission intensity per unit of GDP in the study area from 2000 to 2021 are presented in Figure 7. From 2000 to 2021, the carbon emission intensity per unit of GDP in the study area showed an overall downward trend. Ningxia has the highest carbon emission intensity per unit of GDP, reaching 4.9 tons/10,000 yuan in 2021. This is mainly because the energy structure of Ningxia is mainly based on coal, which accounts for a relatively high proportion of energy consumption. Moreover, Ningxia is a relatively underdeveloped

economic region, and, to catch up with the development speed of other regions, it may have neglected the importance of environmental protection in the process of economic development. There may be some lag in the utilization of resources and transformation of industrial structure, resulting in a high carbon emission intensity per unit GDP. Sichuan, on the other hand, has the smallest carbon emission intensity per unit of GDP, as low as 0.5 tons/10,000 yuan in 2021. This is due to Sichuan's active development of other new energy sources, and the utilization of these clean energy sources has helped to reduce its dependence on traditional high-carbon energy sources, further reducing the carbon emission intensity per unit of GDP. Moreover, Sichuan's economic structure is relatively lightweight. Lightweight industries usually have a relatively low energy demand, thus reducing the carbon emission intensity per unit of GDP. Henan has been actively restructuring and transforming its energy mix over the past few years. Consequently, Henan has the largest downward trend in carbon emission intensity per unit of GDP, with an average annual reduction rate of 6.97%. By contrast, due to Ningxia's relatively homogenous energy structure, the energy transition and emission reduction efforts face greater challenges. Consequently, Ningxia has the smallest downward trend in carbon emission intensity per unit of GDP, with an average annual reduction rate of 1.48%.

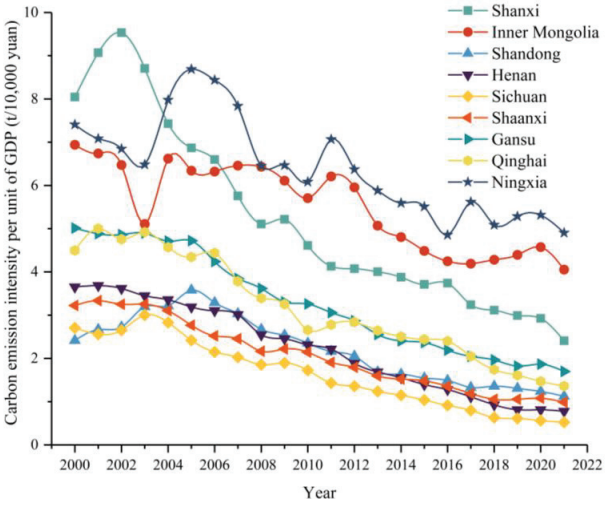

Figure 7. Temporal characteristics of carbon emission intensity per unit GDP in the study area from 2000 to 2021.

4.4. Spatial Characteristics of Municipal-Level Carbon Emissions

Based on the fitting model proposed above and the nighttime light index at the municipal scale, the inversion obtained the spatial characteristics of municipal-level carbon emissions in the study area from 2000 to 2021 (as presented in Figure 8). From 2000 to 2021, the carbon emissions of this region mainly showed a trend of "several"; that is, the carbon emissions of urban areas around the Yellow River were higher, and the carbon emissions of provincial capitals were higher. From 2000 to 2009, carbon emissions increased rapidly, and the proportion of cities with high carbon emissions increased from 4.35% in 2001 to 32.17% in 2021. In 2001, only Jinan, Qingdao, Yantai, Zhengzhou, and Taiyuan had high levels of carbon emissions. In 2021, only the eastern and northern cities had faster carbon emission growth, while the southwestern cities had a slower growth rate. Shandong is a province with a large population and rapid economic development, accounting for about 9% of the country's carbon emissions in 2020, making it the largest carbon emitter province in China. Moreover, Shandong is also the largest coal power province in China, accounting for 9.5% of the country's installed capacity. More than 99% of its heat demand is met by coal, with

the rest coming from oil and gas. Therefore, in 2021, only Rizhao in Shandong had carbon emissions of less than 30 million tons.

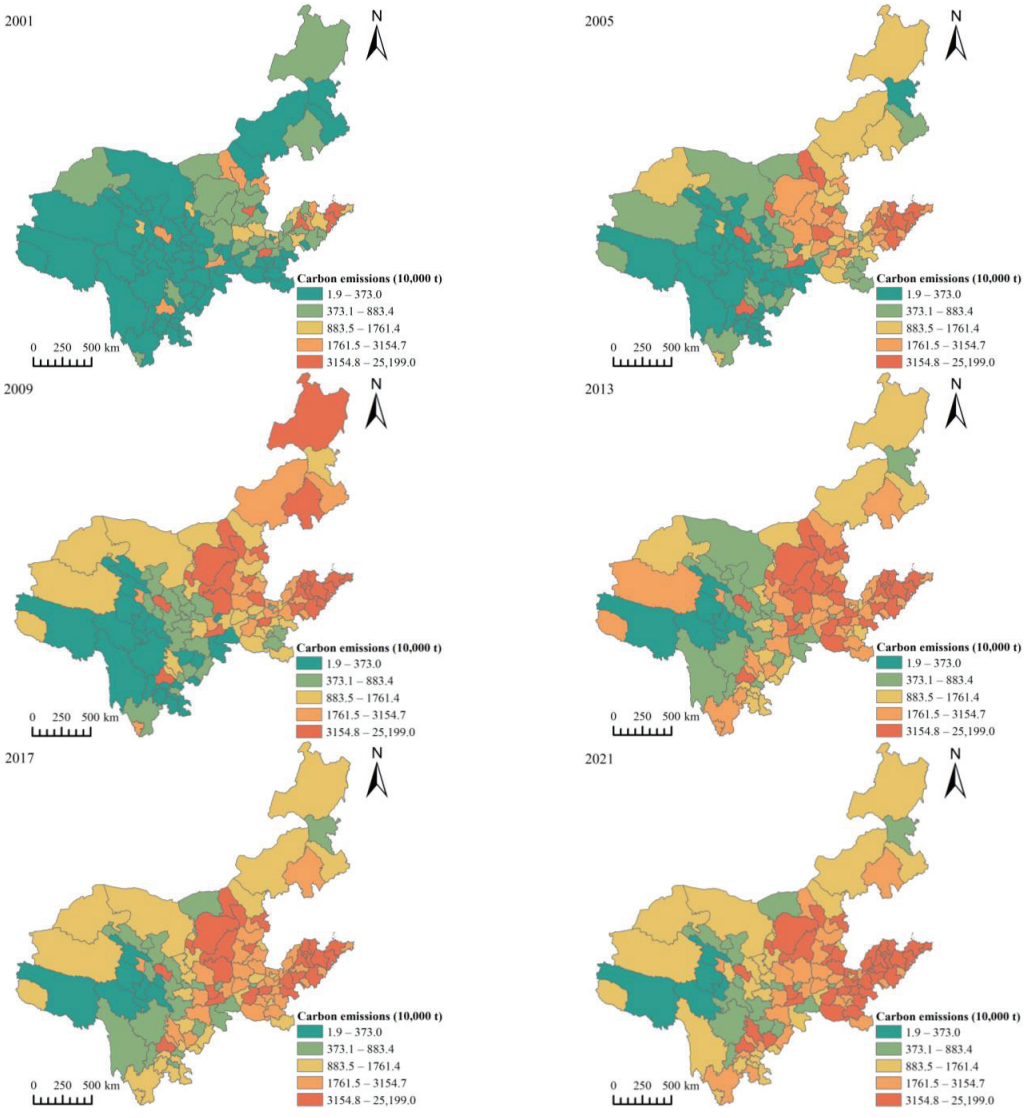

Figure 8. Spatial characteristics of municipal-level carbon emissions in the study area from 2000 to 2021.

4.5. Spatial Characteristics of County-Level Carbon Emissions

The spatial characteristics of county-level carbon emissions in the study area from 2000 to 2021 are presented in Figure 9. From 2000 to 2021, the carbon emissions of all districts and counties along this region increased significantly, showing a spatial distribution pattern of "southeast high and northwest low". Among them, counties in Shandong and Henan have higher carbon emissions, accounting for 91.97% and 81.65% of the high-carbon-emission counties in the two provinces in 2021. The growth rate of carbon emissions in each county and district showed a trend of "first urgent and then slow", with 2009 as the cut-off point.

The proportion of counties with high carbon emissions increased from 12.72% in 2001 to 40.56% in 2009 and 55.68% in 2021.

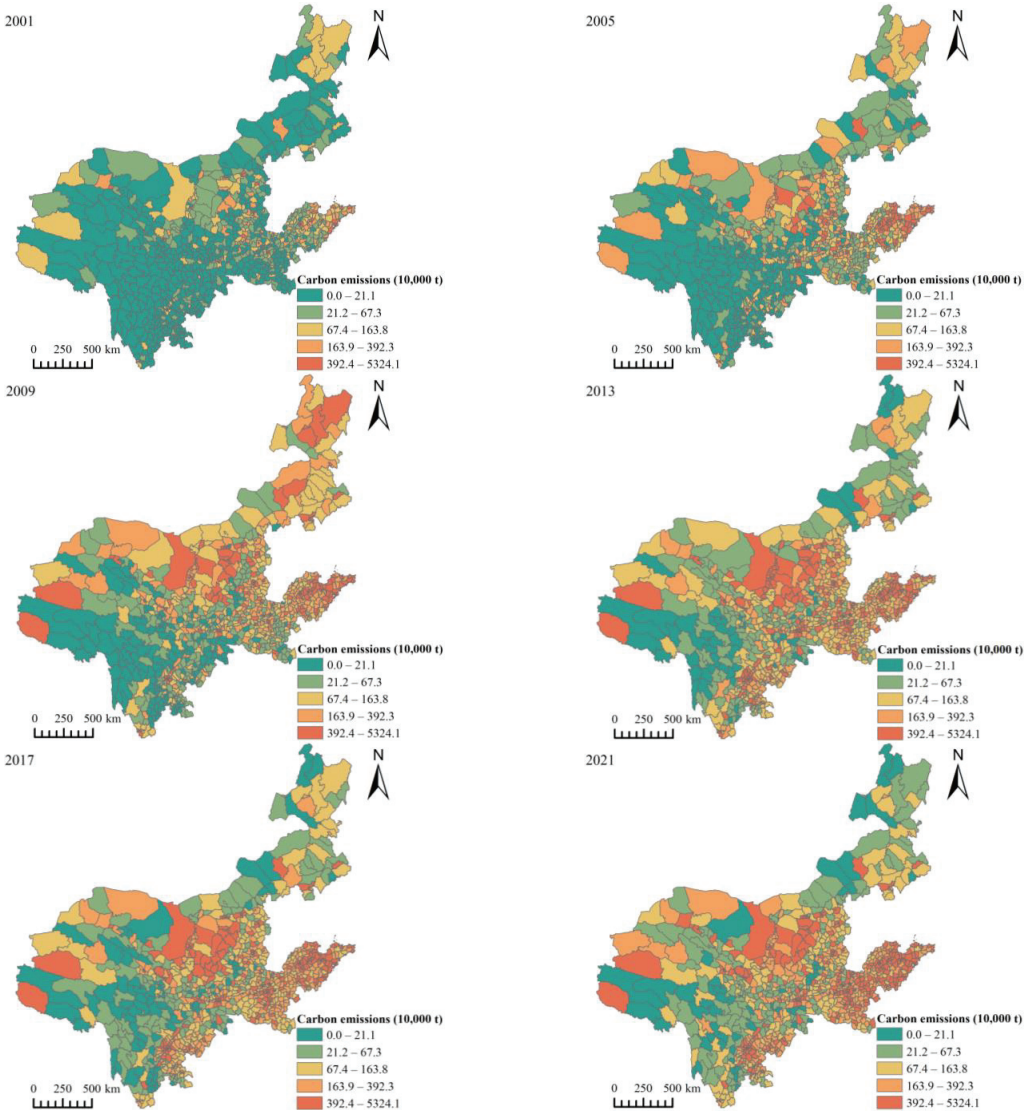

Figure 9. Spatial characteristics of county-level carbon emissions in the study area from 2000 to 2021.

5. Discussion

5.1. Global Spatial Correlation

GeoDa software was utilized to establish the spatial weights, and the global spatial correlation index (Moran's *I*) of county-level carbon emissions in the study area from 2000 to 2021 was calculated. The results are presented in Table 4. All the Moran's *I* of this region is positive, and the *p*-values are all zero, indicating a significant spatial correlation of county-level carbon emissions in the region. Moran's *I* shows a trend of decreasing first and then increasing and gradually tends to a stable state in the later stage, and the pattern of spatial agglomeration is relatively fixed. Before 2013, there was an overall downward

trend, from 0.314 in 2001 to 0.223 in 2013, indicating that counties with similar carbon emissions are more likely to be dispersed. This is because, since the beginning of the 21st century, all regions have made great efforts to build and develop, but the development has been uneven, resulting in different carbon emission levels. After 2013, the overall trend increased, from 0.223 in 2013 to 0.287 in 2021, and eventually stabilized, indicating that counties with similar carbon emissions are more inclined to agglomerate.

Table 4. Moran's *I* of county-level carbon emissions in the study area from 2000 to 2021.

Year	Moran's *I*	*p*
2001	0.314	0
2005	0.351	0
2009	0.313	0
2013	0.223	0
2017	0.270	0
2021	0.287	0

5.2. Local Spatial Correlation

The LISA clustering maps of county-level carbon emissions in the study area are presented in Figure 10. In general, the spatial agglomeration mode of county-level carbon emissions was relatively fixed, "High–High" and "Low–Low" were the main types of local spatial autocorrelation, and the number of counties and districts where "High–High" agglomeration increased significantly, while the number of counties and districts where "Low–Low" agglomeration gradually decreased. From 2000 to 2013, the "High–High" and "Low–High" types of counties and districts were mainly distributed along the Yellow River, and the number of "Low–High" types of districts and counties gradually increased, mainly because the counties along the Yellow River developed rapidly, but, due to uneven development caused by regional differences, most of the counties and districts along the coast had a "radiation effect" on surrounding cities, and carbon emissions formed the "High–High" type. Meanwhile, some counties and districts have a "siphon effect" on surrounding cities, and carbon emissions with a "Low–High" type. The "Low–Low" type is mainly distributed in Sichuan, which is because Sichuan's clean energy accounts for more than 80% to 90%, which is much higher than the national level, and the carbon emissions of each county are low. From 2013 to 2021, Shanxi's "High–High" and "Low–Low" gradually disappeared. The Sichuan Basin gradually formed the "High–High" type centered on Chengdu, and the number gradually increased. The "Low–Low" type in eastern Inner Mongolia and Yan'an and Linfen in Shaanxi is gradually increasing.

5.3. Possible Strategies

To prompt the ecological protection and high-quality development of the Yellow River Basin, the following strategies may be implemented:

(1) The upstream of the Yellow River should develop clean energy. The upstream of the Yellow River is rich in hydropower and wind energy resources, and vigorously develops hydropower and wind power to reduce the use of fossil energy and carbon emissions.

(2) The midstream of the Yellow River should promote industrial transformation and upgrading. The midstream of the Yellow River has a high degree of industrialization and should promote industrial transformation and upgrading, promote clean production technologies and circular economy models, reduce the use of fossil fuels, and reduce carbon emissions.

(3) The downstream of the Yellow River should promote green development. The downstream of the Yellow River comprises China's economic centers and urban agglomerations and should promote green development, encourage low-carbon consumption and lifestyles, and promote renewable energy and clean transportation.

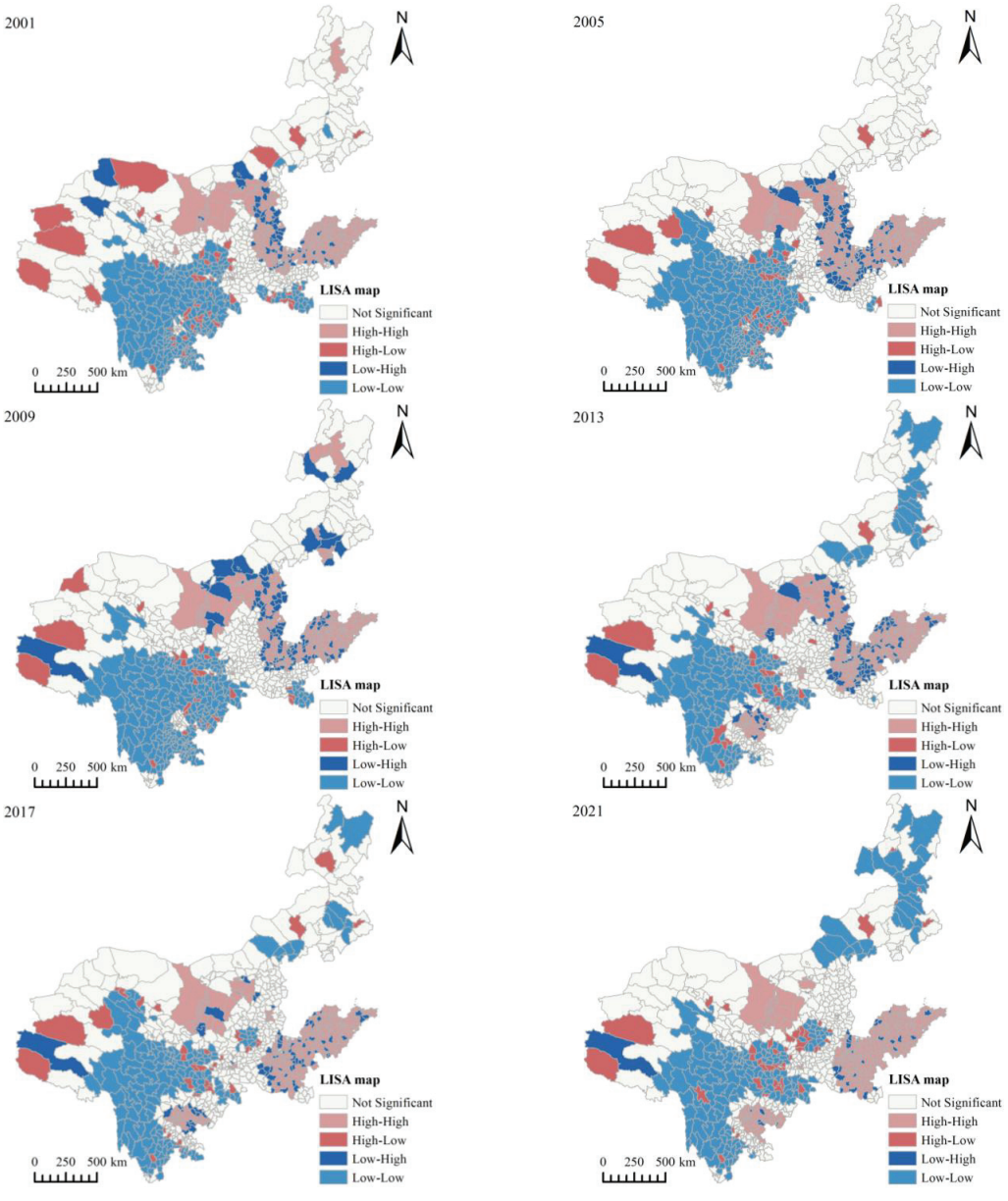

Figure 10. LISA map of county-level carbon emissions in the study area from 2000 to 2021.

6. Conclusions

This study establishes a carbon emission assessment model based on the "NPP-VIIRS-like" nighttime light data, investigating the spatiotemporal characteristics and trends of carbon emissions, per capita carbon emission intensity, and carbon emission intensity per unit of GDP in the study area since the 21st century. Further, the spatial correlation of carbon emissions at the county level is explored using the Moran's *I* spatial analysis method. This comprehensive method overcomes the limitations of incomplete traditional

statistics and differing statistical calibers, providing a reliable new tool for monitoring carbon emissions. The main conclusions drawn from this study are as follows:

(1) TNLI and carbon emission models of the study area were constructed according to different years. The model exhibited high accuracy with an average correlation coefficient R2 of 0.8945. The model has proven effective in estimating carbon emissions at the city and county levels, enabling the timely monitoring and assessment of carbon emissions in small-scale areas.

(2) In terms of temporal variation, from 2000 to 2021, carbon emissions in the study area continued to rise but the growth rate declined, showing an overall convergence trend, but not yet reaching a carbon peak. The proportion of upstream and midstream carbon emissions has gradually increased, while the proportion of downstream carbon emissions has gradually decreased. Per capita carbon emission intensity is generally on the rise, with Inner Mongolia having the largest per capita carbon intensity and Sichuan having the smallest. The carbon emission intensity per unit of GDP is generally declining. Ningxia has the highest carbon intensity per unit of GDP, while Sichuan has the lowest carbon intensity per unit of GDP.

(3) In terms of spatial variation, the carbon emissions of the study area generally show high carbon emissions in the eastern region and low carbon emissions in the western region. The carbon emissions of each city mainly show a trend of "several"; that is, the urban area around the Yellow River has higher carbon emissions. Meanwhile, there is a trend of higher carbon emissions in provincial capitals. The proportion of cities with high carbon emissions increased from 4.35% in 2001 to 32.17% in 2021. Counties in Shandong and Henan have higher carbon emissions, accounting for 91.97% and 81.65% of the two provinces in 2021, respectively.

(4) In terms of spatial relationship, Moran's *I* shows a trend of first decreasing and then increasing and gradually tends to a stable state in the later stage, and the pattern of spatial agglomeration is relatively fixed. "High–High" and "Low–Low" are the main types of local spatial autocorrelation, and the number of counties with "High–High" agglomeration increases significantly, while the number of counties with "Low–Low" agglomeration gradually decreases. From 2000 to 2013, counties of the "High–High" and "Low–High" types were mainly distributed along the Yellow River, and the "Low–Low" type was mainly distributed in Sichuan. From 2013 to 2021, Shanxi's "High–High" and "Low–Low" gradually disappeared. The Sichuan Basin gradually formed the "High–High" type centered on Chengdu, and the number gradually increased.

The spatial and temporal variations in carbon emissions show a converging trend of decreasing growth rates. While emissions continue to rise, the declining rate of growth suggests potential improvements in emission management and control measures. The rise in the per capita carbon emission intensity indicates the need for more sustainable and efficient use of resources. The decline in carbon emission intensity per unit of GDP indicates progress in decoupling economic growth from carbon emissions. Spatial differences in carbon emissions can be attributed to changes in economic activity, population density, and energy sources. Understanding these spatial differences can help target emission reduction strategies where they are most needed. Understanding the spatial relationships and patterns of carbon emissions can help policymakers to identify areas where targeted interventions are needed and to work together towards effective mitigation strategies. Taken together, these findings can guide policymakers in developing strategies and policies to mitigate carbon emissions, promote sustainable development, and achieve emission reduction targets.

This study presents a unique perspective on carbon emissions monitoring, providing valuable data references and decision-making support for governmental entities and businesses aiming to advance sustainable economic development and foster the establishment of ecological civilization. In our future research endeavors, we intend to delve deeper into the analysis of influencing factors and mechanisms associated with carbon

emissions, while also exploring effective monitoring technologies for carbon emissions based on heterogeneous data from multiple sources.

Author Contributions: Conceptualization, Y.L. and W.L.; methodology, W.L.; software, W.L.; validation, P.Q. and L.P.; formal analysis, Y.L.; investigation, J.Z.; resources, Y.L.; data curation, W.L.; writing—original draft preparation, W.L.; writing—review and editing, Y.L.; visualization, P.Q., J.Z. and L.P.; supervision, P.Q.; project administration, Y.L. and J.Z.; funding acquisition, Y.L. and P.Q. All authors have read and agreed to the published version of the manuscript.

Funding: This research was supported in part by the Natural Science Foundation of China, grant numbers 42001341, 42201077, and 42177453; the Natural Science Foundation of Shandong Province, grant number ZR2021QD074; and the China Postdoctoral Science Foundation, grant number 2023M732105.

Data Availability Statement: Data will be made available upon request.

Conflicts of Interest: The authors declare no conflict of interest.

References

1. Liu, Z.; Deng, Z.; Davis, S.J.; Giron, C.; Ciais, P. Monitoring global carbon emissions in 2021. *Nat. Rev. Earth Environ.* **2022**, *3*, 217–219. [CrossRef]
2. Wang, Y.; Guo, C.-H.; Du, C.; Chen, X.-J.; Jia, L.-Q.; Guo, X.-N.; Chen, R.-S.; Zhang, M.-S.; Chen, Z.-Y.; Wang, H.-D. Carbon peak and carbon neutrality in China: Goals, implementation path, and prospects. *China Geol.* **2021**, *4*, 720–746. [CrossRef]
3. Rising, J.A.; Taylor, C.; Ives, M.C.; Ward, R.E. Challenges and innovations in the economic evaluation of the risks of climate change. *Ecol. Econ.* **2022**, *197*, 107437. [CrossRef]
4. Khan, M.K.; Trinh, H.H.; Khan, I.U.; Ullah, S. Sustainable economic activities, climate change, and carbon risk: An international evidence. *Environ. Dev. Sustain.* **2022**, *24*, 9642–9664. [CrossRef]
5. Chen, L.; Msigwa, G.; Yang, M.; Osman, A.I.; Fawzy, S.; Rooney, D.W.; Yap, P.-S. Strategies to achieve a carbon neutral society: A review. *Environ. Chem. Lett.* **2022**, *20*, 2277–2310. [CrossRef] [PubMed]
6. Chuai, X.; Feng, J. High resolution carbon emissions simulation and spatial heterogeneity analysis based on big data in Nanjing City, China. *Sci. Total Environ.* **2019**, *686*, 828–837. [CrossRef]
7. Han, P.; Cai, Q.; Oda, T.; Zeng, N.; Shan, Y.; Lin, X.; Liu, D. Assessing the recent impact of COVID-19 on carbon emissions from China using domestic economic data. *Sci. Total Environ.* **2021**, *750*, 141688. [CrossRef]
8. Sun, S.; Xie, Y.; Li, Y.; Yuan, K.; Hu, L. Analysis of Dynamic Evolution and Spatial-Temporal Heterogeneity of Carbon Emissions at County Level along "The Belt and Road"—A Case Study of Northwest China. *Int. J. Environ. Res. Public Health* **2022**, *19*, 13405. [CrossRef]
9. Li, H.; Mu, H.; Zhang, M.; Gui, S. Analysis of regional difference on impact factors of China's energy–Related CO_2 emissions. *Energy* **2012**, *39*, 319–326. [CrossRef]
10. Huang, H.; Wu, X.; Cheng, X. The Prediction of Carbon Emission Information in Yangtze River Economic Zone by Deep Learning. *Land* **2021**, *10*, 1380. [CrossRef]
11. Du, M.; Zhang, X.; Xia, L.; Cao, L.; Zhang, Z.; Zhang, L.; Zheng, H.; Cai, B. The China Carbon Watch (CCW) system: A rapid accounting of household carbon emissions in China at the provincial level. *Renew. Sustain. Energy Rev.* **2022**, *155*, 111825. [CrossRef]
12. Liu, X.; Meng, X.; Wang, X. Carbon Emissions Prediction of Jiangsu Province Based on Lasso-BP Neural Network Combined Model. *IOP Conf. Ser. Earth Environ. Sci.* **2021**, *769*, 022017. [CrossRef]
13. Ning, L.; Pei, L.; Li, F. Forecast of China's Carbon Emissions Based on ARIMA Method. *Discret. Dyn. Nat. Soc.* **2021**, *2021*, 1441942. [CrossRef]
14. Liu, Y.; Liu, W.; Zhang, X.; Lin, Y.; Zheng, G.; Zhao, Z.; Cheng, H.; Gross, L.; Li, X.; Wei, B.; et al. Nighttime light perspective in urban resilience assessment and spatiotemporal impact of COVID-19 from January to June 2022 in mainland China. *Urban Clim.* **2023**, *50*, 101591. [CrossRef]
15. Shen, Y.; Chen, X.; Yao, Q.; Ding, J.; Lai, Y.; Rao, Y. Examining the Impact of China's Poverty Alleviation on Nighttime Lighting in 831 State-Level Impoverished Counties. *Land* **2023**, *12*, 1128. [CrossRef]
16. Wang, J.; Qiu, S.; Du, J.; Meng, S.; Wang, C.; Teng, F.; Liu, Y. Spatial and Temporal Changes of Urban Built-Up Area in the Yellow River Basin from Nighttime Light Data. *Land* **2022**, *11*, 1067. [CrossRef]
17. Kyba, C.C.M.; Aubé, M.; Bará, S.; Bertolo, A.; Bouroussis, C.A.; Cavazzani, S.; Espey, B.R.; Falchi, F.; Gyuk, G.; Jechow, A.; et al. Multiple Angle Observations Would Benefit Visible Band Remote Sensing Using Night Lights. *J. Geophys. Res. Atmos.* **2022**, *127*, e2021JD036382. [CrossRef]
18. Zheng, Q.; Seto, K.C.; Zhou, Y.; You, S.; Weng, Q. Nighttime light remote sensing for urban applications: Progress, challenges, and prospects. *ISPRS J. Photogramm. Remote Sens.* **2023**, *202*, 125–141. [CrossRef]
19. Zhao, X.; Yu, B.; Liu, Y.; Yao, S.; Lian, T.; Chen, L.; Yang, C.; Chen, Z.; Wu, J. NPP-VIIRS DNB Daily Data in Natural Disaster Assessment: Evidence from Selected Case Studies. *Remote Sens.* **2018**, *10*, 1526. [CrossRef]

20. He, L.; Lv, M.; Zhu, T. Integration of DMSP-OLS and NPP-VIIRS nighttime light remote sensing images. *Bull. Surv. Mapp.* **2023**, *1*, 31–38. [CrossRef]
21. Yuan, Y.; Wang, C.; Liu, S.; Chen, Z.; Ma, X.; Li, W.; Zhang, L.; Yu, B. The Changes in Nighttime Lights Caused by the Turkey–Syria Earthquake Using NOAA-20 VIIRS Day/Night Band Data. *Remote Sens.* **2023**, *15*, 3438. [CrossRef]
22. Yuan, Y.; Chen, Z. The impacts of land cover spatial combination on nighttime light intensity in 2010 and 2020: A case study of Fuzhou, China. *Comput. Urban Sci.* **2023**, *3*, 5. [CrossRef]
23. Zhao, F.; Ding, J.; Zhang, S.; Luan, G.; Song, L.; Peng, Z.; Du, Q.; Xie, Z. Estimating Rural Electric Power Consumption Using NPP-VIIRS Night-Time Light, Toponym and POI Data in Ethnic Minority Areas of China. *Remote Sens.* **2020**, *12*, 2836. [CrossRef]
24. Shi, K.; Chen, Z.; Cui, Y.; Wu, J.; Yu, B. NPP-VIIRS Nighttime Light Data Have Different Correlated Relationships with Fossil Fuel Combustion Carbon Emissions from Different Sectors. *IEEE Geosci. Remote Sens. Lett.* **2020**, *18*, 2062–2066. [CrossRef]
25. Wu, B.; Yang, C.; Wu, Q.; Wang, C.; Wu, J.; Yu, B. A building volume adjusted nighttime light index for characterizing the relationship between urban population and nighttime light intensity. *Comput. Environ. Urban Syst.* **2023**, *99*, 101911. [CrossRef]
26. Yu, B.; Shi, K.; Hu, Y.; Huang, C.; Chen, Z.; Wu, J. Poverty Evaluation Using NPP-VIIRS Nighttime Light Composite Data at the County Level in China. *IEEE J. Sel. Top. Appl. Earth Obs. Remote Sens.* **2015**, *8*, 1217–1229. [CrossRef]
27. Zhang, Z.; Wang, J.; Xiong, N.; Liang, B.; Wang, Z. Air Pollution Exposure Based on Nighttime Light Remote Sensing and Multi-source Geographic Data in Beijing. *Chin. Geogr. Sci.* **2023**, *33*, 320–332. [CrossRef]
28. Xie, Z.; Yuan, M.; Zhang, F.; Chen, M.; Tian, M.; Sun, L.; Su, G.; Liu, R. A Structure Identification Method for Urban Agglomeration Based on Nighttime Light Data and Railway Data. *Remote Sens.* **2023**, *15*, 216. [CrossRef]
29. Fan, X.; Nie, G.; Deng, Y.; An, J.; Zhou, J.; Li, H. Rapid detection of earthquake damage areas using VIIRS nearly constant contrast night-time light data. *Int. J. Remote Sens.* **2019**, *40*, 2386–2409. [CrossRef]
30. Li, X.; Zhan, C.; Tao, J.; Li, L. Long-Term Monitoring of the Impacts of Disaster on Human Activity Using DMSP/OLS Nighttime Light Data: A Case Study of the 2008 Wenchuan, China Earthquake. *Remote Sens.* **2018**, *10*, 588. [CrossRef]
31. Liu, Y.; Liu, W.; Lin, Y.; Zhang, X.; Zhou, J.; Wei, B.; Nie, G.; Gross, L. Urban waterlogging resilience assessment and postdisaster recovery monitoring using NPP-VIIRS nighttime light data: A case study of the 'July 20, 2021' heavy rainstorm in Zhengzhou City, China. *Int. J. Disaster Risk Reduct.* **2023**, *90*, 103649. [CrossRef]
32. Chen, Z.; Yu, S.; You, X.; Yang, C.; Wang, C.; Lin, J.; Wu, W.; Yu, B. New nighttime light landscape metrics for analyzing urban-rural differentiation in economic development at township: A case study of Fujian province, China. *Appl. Geogr.* **2023**, *150*, 102841. [CrossRef]
33. Yang, J.; Li, W.; Chen, J.; Sun, C. Refined Carbon Emission Measurement Based on NPP-VIIRS Nighttime Light Data: A Case Study of the Pearl River Delta Region, China. *Sensors* **2023**, *23*, 191. [CrossRef]
34. Xu, G.; Zeng, T.; Jin, H.; Xu, C.; Zhang, Z. Spatio-Temporal Variations and Influencing Factors of Country-Level Carbon Emissions for Northeast China Based on VIIRS Nighttime Lighting Data. *Int. J. Environ. Res. Public Health* **2023**, *20*, 829. [CrossRef]
35. Wu, S.; Hu, S.; Frazier, A.E.; Hu, Z. China's urban and rural residential carbon emissions: Past and future scenarios. *Resour. Conserv. Recycl.* **2023**, *190*, 106802. [CrossRef]
36. Guo, R.; Leng, H.; Yuan, Q.; Song, S. Impact of Urban Form on CO_2 Emissions under Different Socioeconomic Factors: Evidence from 132 Small and Medium-Sized Cities in China. *Land* **2022**, *11*, 713. [CrossRef]
37. Fang, G.; Gao, Z.; Tian, L.; Fu, M. What drives urban carbon emission efficiency? Spatial analysis based on nighttime light data. *Appl. Energy* **2022**, *312*, 118772. [CrossRef]
38. Doll, C.H.; Muller, J.-P.; Elvidge, C.D. Night-time imagery as a tool for global mapping of socioeconomic parameters and greenhouse gas emissions. *AMBIO J. Hum. Environ.* **2000**, *29*, 157–162. [CrossRef]
39. Sun, Y.; Zheng, S.; Wu, Y.; Schlink, U.; Singh, R.P. Spatiotemporal Variations of City-Level Carbon Emissions in China during 2000–2017 Using Nighttime Light Data. *Remote Sens.* **2020**, *12*, 2916. [CrossRef]
40. Yang, T.; Liu, J.; Mi, H.; Cao, Z.; Wang, Y.; Han, H.; Luan, J.; Wang, Z. An Estimating Method for Carbon Emissions of China Based on Nighttime Lights Remote Sensing Satellite Images. *Sustainability* **2022**, *14*, 2269. [CrossRef]
41. Guo, W.; Li, Y.; Li, P.; Zhao, X.; Zhang, J. Using a combination of nighttime light and MODIS data to estimate spatiotemporal patterns of CO_2 emissions at multiple scales. *Sci. Total Environ.* **2022**, *848*, 157630. [CrossRef] [PubMed]
42. Zhang, Y.; Xu, X. Carbon emission efficiency measurement and influencing factor analysis of nine provinces in the Yellow River basin: Based on SBM-DDF model and Tobit-CCD model. *Environ. Sci. Pollut. Res.* **2022**, *29*, 33263–33280. [CrossRef] [PubMed]
43. Zhang, Y.; Yu, Z. Spatiotemporal evolution characteristics and dynamic efficiency decomposition of carbon emission efficiency in the Yellow River Basin. *PLoS ONE* **2022**, *17*, e0264274. [CrossRef] [PubMed]
44. Zhao, J.; Kou, L.; Wang, H.; He, X.; Xiong, Z.; Liu, C.; Cui, H. Carbon Emission Prediction Model and Analysis in the Yellow River Basin Based on a Machine Learning Method. *Sustainability* **2022**, *14*, 6153. [CrossRef]
45. Shi, K.; Wu, Y.; Liu, S.; Chen, Z.; Huang, C.; Cui, Y. Mapping and evaluating global urban entities (2000–2020): A novel perspective to delineate urban entities based on consistent nighttime light data. *GISci. Remote Sens.* **2023**, *60*, 2161199. [CrossRef]
46. Yin, J.; Yao, M.; Yuan, Z.; Yu, G.; Li, X.; Qi, L. Spatial-temporal variations in vegetation and their responses to climatic and anthropogenic factors in upper reaches of the Yangtze River during 2000 to 2019. *Watershed Ecol. Environ.* **2023**, *5*, 114–124. [CrossRef]
47. Chen, Z.; Yu, B.; Yang, C.; Zhou, Y.; Yao, S.; Qian, X.; Wang, C.; Wu, B.; Wu, J. An extended time series (2000–2018) of global NPP-VIIRS-like nighttime light data from a cross-sensor calibration. *Earth Syst. Sci. Data* **2021**, *13*, 889–906. [CrossRef]

48. Solomon, B.D. Intergovernmental Panel on Climate Change (IPCC). In *Dictionary of Ecological Economics*; Edward Elgar Publishing: Cheltenham, UK, 2023; p. 302.
49. Eggleston, H.S.; Buendia, L.; Miwa, K.; Ngara, T.; Tanabe, K. *2006 IPCC Guidelines for National Greenhouse Gas Inventories*; IPCC: Geneva, Switzerland, 2006.
50. Qiu, S.; Lei, T.; Wu, J.; Bi, S. Energy demand and supply planning of China through 2060. *Energy* **2021**, *234*, 121193. [CrossRef]

land

MDPI

Article

Differentiation of Carbon Sink Enhancement Potential in the Beijing–Tianjin–Hebei Region of China

Huicai Yang [1,2,3], Shuqin Zhao [4,*], Zhanfei Qin [2,3], Zhiguo Qi [2,3], Xinying Jiao [2,3] and Zhen Li [2,3]

[1] Academy of Eco-Civilization Development for Jing-Jin-Ji Megalopolis, Tianjin Normal University, Tianjin 300387, China
[2] Hebei International Joint Research Center for Remote Sensing of Agricultural Drought Monitoring, Hebei GEO University, Shijiazhuang 050031, China; qinzhanfei@nwafu.edu.cn (Zhanfei Qin)
[3] College of Land Science and Spatial Planning, Hebei GEO University, Shijiazhuang 050031, China
[4] Graduate School, Hebei GEO University, Shijiazhuang 050031, China
* Correspondence: zhaoshuqin1@hgu.edu.cn

Abstract: Carbon sink enhancement is of great significance to achieving carbon peak and carbon neutrality. This study firstly estimated the carbon sink in the Beijing–Tianjin–Hebei Region using the carbon absorption coefficient method. Then, this study explored the differentiation of carbon sink enhancement potential with a carbon sink–economic carrying capacity index matrix based on carbon sink carrying capacity and economic carrying capacity under the baseline scenario and target scenario of land use. The results suggested there was a remarkable differentiation in total carbon sink in the study area, reaching 2,056,400 and 1,528,300 tons in Chengde and Zhangjiakou and being below 500,000 tons in Langfang and Hengshui, while carbon sink per unit land area reached 0.66 ton/ha in Qinhuangdao and only 0.28 t/ha in Tianjin under the baseline scenario. Increasing area and optimizing spatial distribution of arable land, garden land, and forest, which made the greatest contribution to total carbon sinks, is an important way of enhancing regional carbon sinks. A hypothetical benchmark city can be constructed according to Qinhuangdao and Beijing, in comparison with which there is potential for carbon sink enhancement by improving carbon sink capacity in Beijing, promoting economic carrying capacity in Qinhuangdao, and improving both in the other cities in the study area.

Keywords: Beijing–Tianjin–Hebei; carbon sink; arable land; land use; carbon sink–economic carrying capacity

Citation: Yang, H.; Zhao, S.; Qin, Z.; Qi, Z.; Jiao, X.; Li, Z. Differentiation of Carbon Sink Enhancement Potential in the Beijing–Tianjin–Hebei Region of China. *Land* **2024**, *13*, 375. https://doi.org/10.3390/land13030375

Academic Editor: Marko Scholze

Received: 4 February 2024
Revised: 12 March 2024
Accepted: 13 March 2024
Published: 16 March 2024

1. Introduction

The drastic increase in carbon emitted into the atmosphere since the industrial revolution has made a great contribution to climate change, and enhancing carbon sink while promoting economic growth is an important way to achieve the strategic goals of carbon peak by 2030 and carbon neutrality by 2060 for alleviating climate change [1]. Carbon sink refers to the natural or anthropogenic banks of greenhouse gases, including soils, plants and oceans, which can reduce the greenhouse gas concentration in the atmosphere through vegetation restoration and so on [2]. Specifically, land carbon stocks primarily include vegetation and soil carbon stocks in the forest, grassland, deserts, arable land, and wetland [3]. Terrestrial vegetation and soils have currently absorbed approximately 40% of CO_2 emissions from human activities, and there is considerable potential to further increase their uptake and storage of CO_2 and increase carbon sinks with various management policies and measures [2] The Kyoto Protocol (1997), Copenhagen Accord (2009), and the Glasgow Climate Convention (2021) also suggested that carbon sink enhancement of the terrestrial ecosystem is the most economical and effective technological pathway to improving carbon sinks [3]. The "carbon sink–economic carrying capacity", as an integration of carbon sink and economic carrying capacity, generally refers to the maximum amount

of carbon emissions that an economic system can absorb or offset without causing detrimental environmental impacts [4,5]. Research on carbon sink–economic carrying capacity can provide a valuable reference for understanding and managing the balance between economic growth and sustainable development in different regions of the world, especially in the context of climate change [6–8].

Carbon sinks are generally estimated with the land area and carbon emission coefficient, since the carbon sequestration rates and status quo carbon sink capacities vary significantly among different land carbon sinks [9]. For example, the spatial and temporal differentiation patterns of carbon emission and compensation in China have been revealed at the provincial scale with the carbon emission coefficient method [10]. In fact, construction land, e.g., urban villages, industrial and mining land, transportation land, and water conservancy land, may serve as both a carbon source and sink, but its carbon source intensity is generally much higher than its carbon sink intensity [2]. By contrast, arable land, garden land, forest land, grassland, wetland, and watershed are both carbon sinks and carbon sources, but their carbon sink intensity is generally much higher than their carbon source intensity [11].

The core of carbon sink enhancement is to improve the carbon sequestration capacity of terrestrial ecosystems through "optimal ecosystem layout, species allocation and ecosystem management" [12], and territorial spatial planning is widely recognized as an effective way of controlling greenhouse gas emissions from the macro perspective [2,13]. For example, the central government of China has issued the National Outline of Territorial Spatial Planning (2021–2035), which provides an important basis for guiding the planning of national carbon sink function areas and lays an important foundation for macro decision making on the upgrading of ecological carbon sinks [14]. The central government of China has also proposed to implement this planning by adhering to planning and coordination, focusing on constructing a spatial pattern of ecological protection and restoration, with the goal of constructing a national ecological security barrier system [14,15]. However, land and urban–rural planning in the past has primarily focused more on carbon reduction by balancing ecological, agricultural, and urban spaces, rather than the enhancement of carbon sinks by improving land management [16]. Carbon sequestration and sink enhancement have been mentioned in a lot of local planning from the perspective of current territorial planning, but generally with only some ideas and entries [17]. In particular, the current technical framework of territorial spatial planning lacks both clear quantitative coupling methods for carbon emissions and sinks and carbon sink target constraints on the whole [18]. Nevertheless, previous studies have indicated that there is a finite size and duration for carbon sink enhancement potential through changes in land management practices, and it is necessary to explore the potential role of land management and other measures in increasing the global land carbon sink [19].

China has made considerable efforts to enhance land carbon sinks, as deforestation as well as grassland and lake reclamation have been effectively curbed [5]. In fact, China has sequestered approximately 600 million tons of carbon annually through ecosystem management in recent decades [20,21]. In particular, the continuous improvement from main function zoning to integrated ecological protection and restoration, to the realization of Beautiful China has not only led to an increase in carbon sinks but also provided outstanding ecological benefits [20]. In particular, the panel data of carbon emission and sequestration of prefecture-level and above cities in China provided an important foundation for the relevant research of carbon sink enhancement and policy formulation for improving carbon sinks [22,23]. However, the constraints of human activities such as accelerated urbanization have greatly affected vegetation carbon sequestration and resulted in significant uncertainties in understanding future land carbon sink enhancement potential [24].

The Beijing–Tianjin–Hebei Region is an important ecosystem sink project region with high carbon sink potential in China, which is also an important zone for ecological conservation [2]. This region falls under the planning scope of ecological protection and restoration in the northern sand-proof belt and the coastal zone in the "Three Zones and Four Belts" project under the "Overall Planning for The National Important Ecosystem Protection and Restoration " and the "Two Screens and Three Belts" project under the "National Main Functional Areas Planning" [25]. The continuous improvement from main function zoning to integrated ecological protection and restoration to the realization of a beautiful China not only means that the Beijing–Tianjin–Hebei Region plays an outstanding role in providing ecological benefits, but has also significantly increased the regional carbon sinks [26]. However, there is a significant spatial imbalance of carbon sinks in the Beijing–Tianjin–Hebei Region, and there is still an urgent need for a large amount of spatial resource inputs to improve the carbon sinks and meet economic and social development in this region in the future according to the Beijing–Tianjin–Hebei Synergistic Development Plan Outline [27,28]. It is necessary to reveal the current spatial patterns of carbon sink distribution within the Beijing–Tianjin–Hebei Region. Meanwhile, there is an urgent need to explore the contributions of different ecosystems within this region to the regional carbon sink and their potentials for enhancing the regional carbon sink. This study has therefore aimed to estimate the regional carbon sinks and reveal the differentiation in the carbon sink enhancement potential of the Beijing–Tianjin–Hebei Region for identifying strategies to enhance regional carbon sinks and thereby promote ecological civilization construction and synergistic development in this region.

2. Materials and Methods

2.1. Study Area

The Beijing–Tianjin–Hebei Region consists of Beijing City, Tianjin City, and 11 municipalities in Hebei Province (113°05′–119°50′ E, 36°05′–42°39′ N), covering an area of 218,000 km^2 (Figure 1). It is one of the three major urban agglomerations in China, which has undergone the most rapid urbanization in northern China. It is also one of the most densely populated urban agglomerations in China, with a total resident population of 113.07 million by the end of 2019, among which 21.54 million, 15.62 million, and 75.92 million lived in Beijing, Tianjin, and Hebei Province, respectively. The Beijing–Tianjin–Hebei Region as a whole achieved a gross regional Gross Domestic Product (GDP) of CNY 8458 billion, accounting for 8.53% of the national total GDP in 2020 [29]. Meanwhile, it is one of the agglomeration areas of energy consumption and carbon emissions in China, accounting for approximately 11% of the national total carbon emissions, where the carbon emission intensity is about 40% higher than the national average level, making it a key area for carbon emission control and carbon sink enhancement in 2020 [30]. The large amount of carbon dioxide emissions in the Beijing–Tianjin–Hebei Region primarily result from the energy structure, which is dominated by coal, and the industrial structure, which is dominated by high-energy-consuming industries [31]. It is notable that different parts of the Beijing–Tianjin–Hebei Region are at different stages of development and face different challenges of carbon sink enhancement. Although the energy consumption per unit of GDP in Hebei Province has continuously declined during 2013–2020, it is still 1.2 times the national average level. Nevertheless, the Beijing–Tianjin–Hebei Region has continuously enhanced synergistic linkages since the implementation of the Beijing–Tianjin–Hebei Cooperative Development Strategy in 2014, and carbon peak and carbon neutrality policies have been put into practice step by step.

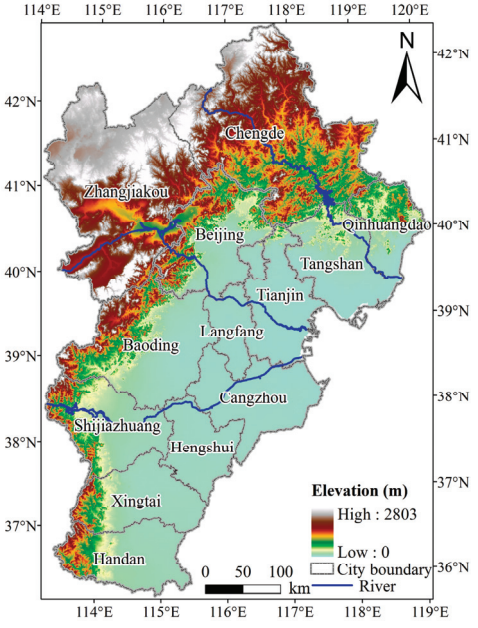

Figure 1. Location of the Beijing–Tianjin–Hebei Region.

2.2. Data Sources and Processing

The data used in this study mainly include the socio-economic data, land use data, and other data (Table 1). Specifically, the socio-economic data such as the Gross Domestic Product (GDP) were mainly derived from the China Urban Statistical Yearbook (2001–2020), Hebei Economic Yearbook (2001–2020), and Statistical Yearbook of Municipalities (2001–2020). The land use data were all derived from the dataset of the Third National Land Survey, which was carried out during 2017–2020, with 31 December 2019 as the standard time point for summarizing data. In addition, the administrative boundary data and Digital Elevation Model (DEM) were downloaded from the Resources and Environmental Science Data Center, Chinese Academy of Sciences (https://www.resdc.cn/, accessed on 20 May 2022). All these data were processed with ArcGIS 10.8.1.

Table 1. Socio-economic data and land area of the Beijing–Tianjin–Hebei Region in 2019.

Cities	GDP (CNY 100 Million)	Land Area (Ten Thousand Hectares)	GDP/LD (CNY Ten Thousand Per Hectare)
Beijing	35,371.3	162.96	217.06
Tianjin	14,104.3	117.73	119.80
Shijiazhuang	3546.6	138.2	25.66
Tangshan	3552.6	140.03	25.37
Qinhuangdao	772.7	76.81	10.06
Handan	1435.0	119	12.06
Xingtai	379.6	122.96	3.09
Baoding	1490.3	219.02	6.80
Zhangjiakou	760.0	364.74	2.08
Chengde	383.0	390.11	0.98
Cangzhou	984.7	141.27	6.97
Langfang	726.5	63.78	11.39
Hengshui	514.3	87.75	5.86

The land types were classified into arable land; garden land; forest land; grassland; wetland; land for towns, villages, industry, and mines; land for transportation; and land for watersheds and water conservancy facilities in this study. It is notable that the land use data in rural areas were comprehensively retrieved with remote sensing images with a resolution higher than 1 m from satellites such as Gaofen-2 and Beijing-2, WorldView-1 and WorldView-2, while the land data within towns and villages were retrieved with aerial remote sensing data with a resolution higher than 0.2 m. The Third National Land Survey widely used new technologies and strict quality control throughout the entire process, providing an important data basis for grasping a detailed and accurate view of the current situation of land use and changes in natural resources in the Beijing–Tianjin–Hebei Region and the whole country.

2.3. Methods

This study firstly analyzed the carbon source and sink process and then estimated the carbon sink in the study area using the carbon absorption coefficient method. This study thereafter constructed the carbon sink–economic carrying capacity index matrix based on the carbon sink carrying capacity and the economic carrying capacity under the baseline scenario and target scenario of land use to reveal the differentiation of carbon sink enhancement potential in the study area.

(1) Estimation of carbon sinks. Carbon sinks mainly originate from arable land, garden land, forest land, grassland, wetland, and waters (except land for water conservancy facilities), which was calculated using the carbon absorption coefficient method as follows.

$$C_i = G_i \times f_i \quad (1)$$

where C_i and G_i and are the carbon sink and the area of the ith land type, respectively; and f_i is the carbon sink coefficient of the ith land type, the data of which were mainly extracted from previous studies (Table 2) [2,28,29].

Table 2. Carbon sink coefficients of different land use types.

Land Use Types	Carbon Sink Coefficients (ton/ha·a)
Arable land	0.422–1.16
Wetland	0.67–2.36
Garden land	2.10
Forest	0.58–0.87
Grassland	0.02
Water bodies	0.30–0.67

(2) Exploration of differentiation of carbon sink enhancement potential. This study explored the differentiation in carbon sink enhancement potential based on the carbon sink carrying capacity and the economic carrying capacity under the baseline scenario and target scenario of land use. This study established the baseline scenario and target scenario of land use according to the specific situation of the study area. The baseline scenario refers to the conditions in which the land use mode and management measures maintain the current development trend and do not aim for a high carbon sink trend in the Beijing–Tianjin–Hebei Region, which can reveal the lower limit of carbon sink under the existing policies. Specifically, the existing economic development and ecological conservation policies will continue as usual under the baseline scenario, without additional measures for improving carbon sink. The target scenario indicates that more positive policies will be carried out to promote the coordination of economic development and ecological conservation, which can more effectively improve carbon sink. Under the target scenario, the carbon sink capacity and soil carbon sequestration capacity will be further effectively improved with various measures such as carbon sink space optimization and governance and integrated protection and ecological restoration projects for mountains, water, forests, arable land, lakes, grasses,

and sand land. The carbon sink coefficients under the baseline scenario and target scenario of land use were set as the lower and higher limits of the carbon sink coefficient in Table 2, respectively. For example, the carbon sink coefficients of arable land under the target scenario and the baseline scenario are 1.16 and 0.422, respectively.

The carbon sink carrying capacity (CA_n/LD) reflects the carbon sink capacity per unit land area, and the economic carrying capacity (GDP/LD) is the ratio of GDP per unit land area. The carbon sink–economic carrying capacity index is the ratio of carbon sink carrying capacity to the economic carrying capacity, which was estimated as follows:

$$THD = \frac{CA_n/LD}{GDP/LD} = CA_n/GDP \quad (2)$$

where THD is the carbon sink–economic carrying capacity index, and CA_n, GDP, and LD refer to the carbon sink, gross domestic product, and land area of the nth city of the study area, respectively.

This study constructed the carbon sink–economic carrying capacity index matrix, using CA_n/GDP and GDP/LD as the horizontal and vertical coordinate axes, respectively, and their deviation values formed the quadrant diagram. The four quadrants represent "high carbon sink–high GDP", "low carbon sink–high GDP", "high carbon sink–low GDP", and "low carbon sink–low GDP", respectively, which were used to judge the matching degree of the land carbon sink and economic carrying degree of each city in the study area. Specifically, the "high carbon sink–high GDP" quadrant belongs to the "high matching degree" scenario, the "low carbon sink–low GDP" quadrant belongs to the "low matching degree" scenario, and the other conditions belong to the "poor matching degree" scenario, according to which the differentiation in carbon sink enhancement potential was explored.

3. Results and Discussion

3.1. Carbon Sink Carrying Capacity

3.1.1. Total Carbon Sink

There was remarkable differentiation of total carbon sink (CA_n) among different cities under the baseline scenario (Figure 2). Specifically, the total carbon sinks exceeded one million tons in only two cities under the baseline scenario, i.e., Chengde and Zhangjiakou, reaching 2,056,400 and 1,528,300 tons, respectively. It is notable that Chengde and Zhangjiakou had the largest carbon sinks under the baseline scenario, accounting for 38% of the total carbon sink of the study area, while this ranged between 500,000 and 1,000,000 tons in seven cities under the baseline scenario, i.e., Baoding, Beijing, Shijiazhuang, Tangshan, Xingtai, Cangzhou, and Qinhuangdao, reaching 895,400, 870,000, 672,500, 661,900, 594,700, 547,000, and 504,200 tons, respectively. Meanwhile, it was below 500,000 tons in four cities, reaching only 458,900, 367,100, 331,500, and 248,900 tons in Handan, Hengshui, Tianjin, and Langfang, respectively, and the latter two cities had the smallest carbon sinks, accounting for only 7% of the total carbon sink of the study area.

The carbon sink under the target scenario differed significantly from that under the baseline scenario (Figure 2). Specifically, the carbon sink exceeded one million tons in eight cities under the target scenario, i.e., Chengde, Zhangjiakou, Baoding, Beijing, Cangzhou, Tangshan, Shijiazhuang, and Xingtai, reaching 3.216, 2.794, 1.6615, 1.260, 1.2563, 1.228, 1.1806, and 1.1354 million tons, respectively. Meanwhile, it exceeded 500,000 tons in all other cities, reaching 9,960,000 tons, 824,000, 816,100, 736,100, and 507,200 tons in Handan, Hengshui, Tianjin, Qinhuangdao, and Langfang, respectively. In particular, Chengde and Zhangjiakou had the largest amount of carbon sink, accounting for 33.7% of the total regional carbon sink of the study area, which is consistent with that under the baseline scenario, while Langfang and Qinhuangdao had the smallest amount of carbon sink, accounting for only 7% of the total carbon sink of the study area, which is slightly different from that under the baseline scenario.

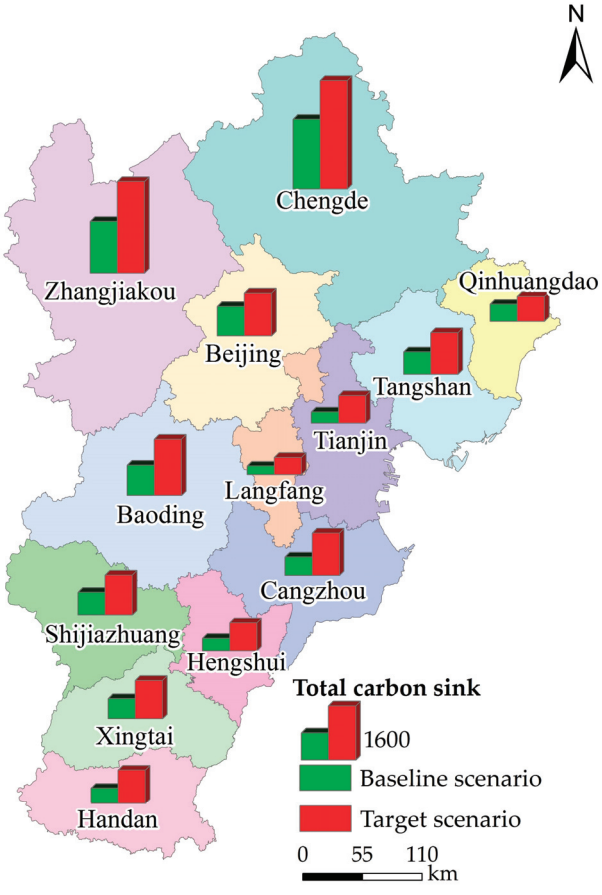

Figure 2. Total carbon sink under the baseline scenario and target scenario (tons).

3.1.2. Carbon Sink Per Unit Land Area (CA_n/LD)

There was remarkable differentiation in the carbon sink per unit land area under the baseline scenario and target scenario (Figure 3). The carbon sink per unit land area was the highest in Qinhuangdao under the baseline scenario, reaching 0.66 ton/ha, and it reached 0.53 tons/ha in Beijing and Chengde. Meanwhile, it ranged between 0.40 and 0.50 ton/ha in six cities, including Shijiazhuang, Xingtai, Tangshan, Zhangjiakou, Hengshui, and Baoding. In particular, it reached 0.39 t/ha in Handan, Langfang, and Cangzhou; however, it was the least in Tianjin, reaching only 0.28 t/ha. By contrast, the carbon sink per unit land area under the target scenario was still the highest in Qinhuangdao, reaching 1.61 ton/ha. Meanwhile, it reached between 1.2 and 1.5 tons/ha in eight cities, including Xingtai, Hengshui, Shijiazhuang, Tangshan, Chengde, Beijing, Cangzhou, and Handan. The carbon sink per unit land in Cangzhou and Hengshui improved significantly under the target scenario compared to that under the baseline scenario. In particular, it was between 1 and 1.2 tons/ha in Langfang, Baoding, and Zhangjiakou, and it remained the least in Tianjin, reaching only 0.97 tons/ha.

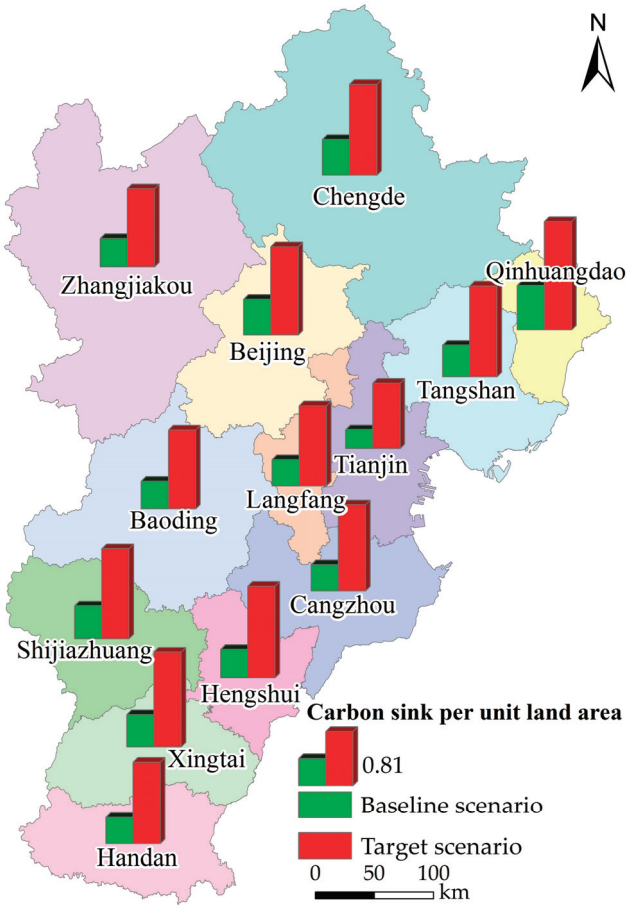

Figure 3. Carbon sink per unit land area under the baseline scenario and target scenario (tons/ha).

3.1.3. Carbon Sink Component

There was a very significant differentiation in the major components of land carbon sink among cities in the study area under the baseline and target scenarios. The major components of land carbon sink consisted of forest in Beijing, Baoding, Zhangjiakou, and Chengde, while it primarily included arable land and garden land in Shijiazhuang and Tangshan, and it mainly included arable land in Tianjin, Handan, Xingtai, Cangzhou, Langfang, and Hengshui. The carbon sink in the study area was therefore dominated by three land use types, namely forest, arable land, and garden land, which accounted for 94.2% and 98% of the total carbon sink of the study area under the baseline scenario and target scenario, respectively. There was also remarkable differentiation in the land use types that made major contributions to the upgrading process of the carbon sink per unit land area from the baseline scenario to the target scenario among these cities in the study area. Specifically, the main contributors were arable land, water bodies, wetland, and forest in most parts of the study area, including Tianjin, Qinhuangdao, Xingtai, Baoding, Chengde, Tangshan, and Cangzhou, while the main contributors in Qinhuangdao, Handan, and Hengshui were arable land, forest, and water bodies, respectively. Meanwhile, the main contributors were primarily arable land, water bodies, and wetland in Shijiazhuang and forest and arable land in Beijing.

3.2. Carbon Sink–Economic Carrying Capacity Index

There was remarkable differentiation in the carbon sink–economic carrying capacity index under the baseline scenario (Figure 4). The origin was (0.45, 34.4) and the quadrant positions of all other cities were determined according to their deviation from the origin. There was significant differentiation in the carbon sink–economic carrying capacity of these 13 cities in the study area, which were unevenly distributed in four quadrants. The results suggested most cities were distributed in the "III-low carbon sink-high GDP" zone, including Shijiazhuang, Tangshan, Chengde, Zhangjiakou, Qinhuangdao, and Xingtai, while only Beijing (0.53, 217.06) was distributed in the "I-high carbon sink-high GDP" zone, and only Tianjin (0.28, 119.8) was distributed in the "II-low carbon sink-high GDP" zone. By contrast, other cities were in the "IV-low carbon sink-low GDP" zone, including Handan, Langfang, Cangzhou, and Hengshui.

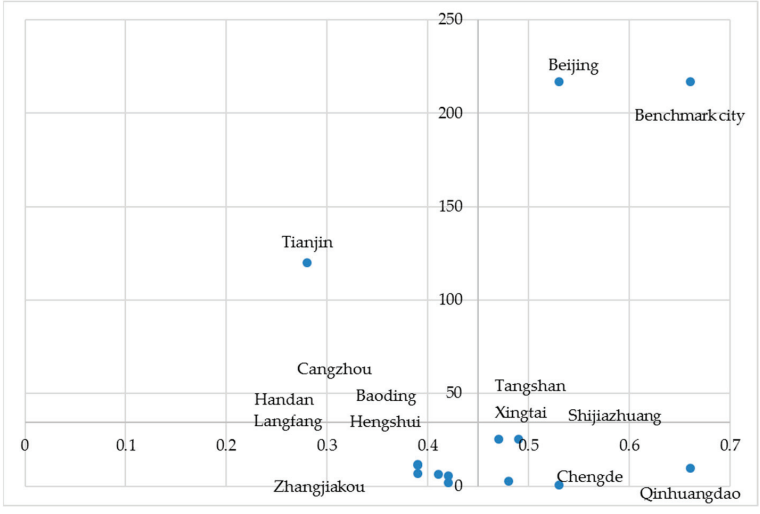

Figure 4. Carbon sink–economic carrying capacity index under the baseline scenario: the horizontal coordinate is the carbon sink carrying capacity (CA_n/LD) (unit: tons/ha), and the vertical coordinate is the economic carrying capacity (GDP/LD) (unit: ten thousand CNY/ha).

There was also remarkable differentiation in the carbon sink–economic carrying capacity under the target scenario (Figure 5), where the origin was (1.29, 34.4), and the results suggested the 13 cities in the study area were still distributed in the four quadrants under the target scenario. Specifically, most cities were also still distributed in the "III-high carbon sink-low GDP" zone, including Shijiazhuang, Tangshan, Chengde, Zhangjiakou, Qinhuangdao, Xingtai, and Hengshui. Beijing (1.31, 217.06) was still distributed in the "I-high carbon sink-high GDP" zone, and Tianjin (0.97, 119.06) was still distributed in the "II-low carbon sink-high GDP" zone, while Handan, Langfang, and Cangzhou were in the "IV-low carbon sink-low GDP" zone. It is notable that Hengshui was upgraded from the IV zone to the III zone under the target scenario compared to that under the baseline scenario, while the other zones remained in the same zone. The improvement of the carbon sink–economic carrying capacity in Hengshui primarily resulted from the enhancement of the carbon sink carrying capacity, while the latter was mainly due to the increase in the carbon sink of arable land.

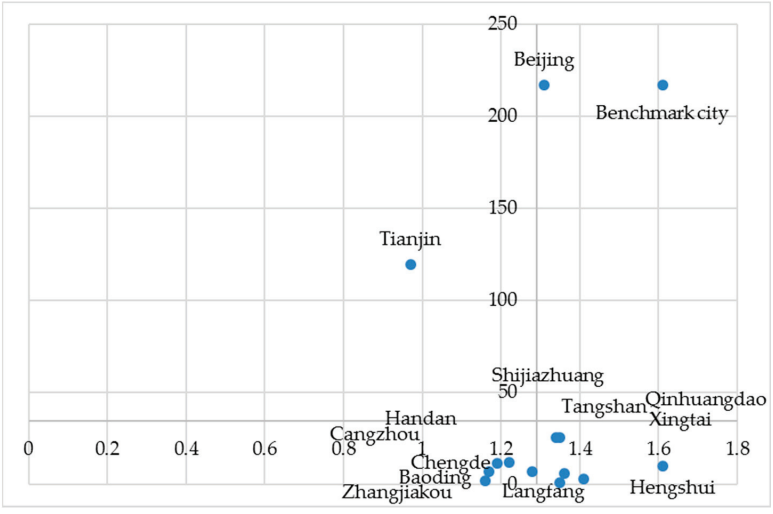

Figure 5. Carbon sink–economic carrying capacity index under the target scenario: the horizontal coordinate is the carbon sink carrying capacity (CA_n/LD) (unit: ton/ha), and the vertical coordinate is the economic carrying capacity (GDP/LD) (unit: ten thousand CNY/ha).

The results suggested various enhancement potentials for the carbon sink per unit land area in most cities of the study area, with Qinhuangdao serving as the benchmark city (1.61 ton/ha) (Table 3). The carbon sink per unit area of these cities can be enhanced in approximately two steps. Specifically, the first step is to upgrade from the carbon sink under the baseline scenario to that under the target scenario, and the second step is to upgrade from the latter to the level of the benchmark city. For example, the first step for Beijing is to upgrade the carbon sink per unit land area from 0.53 ton/ha under the baseline scenario to 1.31 ton/ha under the target scenario, and the second step is to further upgrade it to the level of the benchmark city, i.e., 1.61 ton/ha.

Table 3. Carbon sink per unit land area of each city under the baseline scenario and target scenario in 2019 (unit: ton/ha).

Cities	Carbon Sink per Unit Land Area under the Baseline Scenario	Carbon Sink per Unit Land Area under the Target Scenario	Difference between the Baseline Scenario and Target Scenario	Difference from the Level of the Benchmark City
Beijing	0.53	1.31	0.78	0.30
Tianjin	0.28	0.97	0.69	0.64
Shijiazhuang	0.49	1.34	0.85	0.27
Tangshan	0.47	1.35	0.88	0.26
Qinhuangdao	0.66	1.61	0.95	0.00
Handan	0.39	1.22	0.83	0.39
Xingtai	0.48	1.41	0.93	0.20
Baoding	0.41	1.17	0.76	0.44
Zhangjiakou	0.42	1.16	0.74	0.45
Chengde	0.53	1.35	0.82	0.26
Cangzhou	0.39	1.28	0.89	0.33
Langfang	0.39	1.19	0.80	0.42
Hengshui	0.42	1.36	0.94	0.25

A hypothetical benchmark city of the carbon sink–economic carrying capacity in the study area can be established by taking the carbon sink per unit land area of Qinhuangdao as the horizontal coordinate and the GDP per unit land area of Beijing as the vertical coordinate

under the baseline scenario (0.66, 217.06) and the target scenario (1.61, 217.06). Aiming at this hypothetical benchmark city, it is necessary to further improve the carbon sink capacity in Beijing and further improve the economic carrying capacity in Qinhuangdao, while it is necessary to further improve both the carbon sink capacity and economic carrying capacity in other cities.

3.3. Discussion

The land carbon sink estimated in this study is generally consistent with that in previous studies. For example, the carbon sink per unit land area in Chengde and Qinhuangdao with widespread forest under the baseline scenario reached 0.53 and 0.66 ton/ha, respectively, which is approximately consistent with the results of previous studies in China and around the world (e.g., 0.3–0.8 and 0.66 ton/ha) [32,33]. Additionally, the spatial distribution of the total carbon sink in this study is also generally consistent with the results in previous studies [34,35]. Specifically, the total carbon sink was higher in the northern and northwest parts of the study area and lower in the middle and southern parts of the study area, showing remarkable spatial differentiation. In fact, there is generally widespread forest and grassland with high vegetation coverage and higher carbon sink per unit land area in these mountainous areas, with complex terrain in the northern and northwest parts of the study area, e.g., the Bashang Plateau, the Northern Hebei Mountains, and the Taihang Mountains in Zangjiakou and Chengde [34], while there is widespread arable land with relatively lower carbon sink per unit land area in the middle and southern parts of the study area [34]. In particular, there is widespread construction land in these areas, such as Beijing, Tianjin, and coastal areas, the carbon emission per unit land area of which is far higher than the carbon sink per unit land area of the arable land, leading to a core–periphery spatial pattern of carbon emission centering in Beijing–Tianjin–Tangshan [35,36].

There are also some differences between the results of this study and previous studies, which may be primarily due to the differences in the data sources and parameter settings. For example, most previous studies generally used land use data with a spatial resolution of 1 km, which were generally provided by the Data Center for Resources and Environmental Sciences (http://www.resdc.cn, accessed on 28 May 2023) [2,34,36]. By contrast, this study used the land use data derived from the dataset of the Third National Land Survey, with the spatial resolutions of 1 m and even 0.2 m, which are much higher than that of previous studies. Additionally, there are also some differences in the carbon sink settings of the same land use types between this study and some previous studies. For example, some previous study considered arable land as a carbon source [36], while this study took arable land as a carbon sink, which is consistent with the fact that arable land is generally a weak carbon sink [24,37]. Meanwhile, this study took water bodies into account, which were not involved in some previous studies [36]. In addition, this study used the carbon absorption coefficient method, which is consistent with most previous studies, but there is inevitably some limitation of this method. For example, the carbon sink coefficients were set across different land use types, without consideration of the difference of the carbon sink intensity within the same land use types with different vegetation composition [34]. In fact, it is notable that the carbon sink coefficients of the same land use type may vary greatly in different regions, and it is necessary to carry out relevant research on the carbon sink coefficients according to the specific conditions of different regions [38]. Meanwhile, this study also ignored the variations in the carbon sink per unit land area across time, which can generally remain approximately stable during a long-term period but may vary greatly in a short-term period during some short-term disturbances, e.g., extreme climate change [39]. In fact, there was a risk of instability in the land carbon sink due to the impacts of climate change in a number of regions in the world, e.g., eastern Africa, India, and Southeast Asia [40]. In particular, there is strong wind and frequent drought in the spring in the northwest and northern parts of the study area, which can severely limit vegetation growth and consequently lead to the instability of the land carbon sinks [41]. Additionally, the carbon sink per unit land area of the forest varied along with the change

in the age of stand [42], which was not considered in this study. In particular, there is a large amount of planted or secondary forest with considerable carbon sink potential after decades of reforestation in the northwest and northern parts of the study area [43,44], but there has been limited research on the carbon sink potential concerning tree growth relationships at fine spatial scales [45]. It is therefore necessary to carry out more in-depth research on changes in carbon sink per unit land area over time based on dynamic carbon sink coefficients and accurate vegetation types by integrating the data of vegetation types, crop types, and forest growth data so as to provide a better understanding of carbon sink enhancement potential in the future [34].

3.4. Management Implications

The urgency of increasing carbon sink varied among different cities in the study area, and proper measures should be taken according to the specific situation to increase carbon sink and ease the pressure of emission reductions so as to realize the strategic goal of "carbon neutrality".

(1) There is a more urgent need for increasing the carbon sinks in Tianjin and Beijing, which may be met in three ways. First, carbon sinks can be increased through optimizing their structure and spatial layout. For example, it is helpful to increase carbon sinks by increasing the area proportion of garden land, forest, and wetland and controlling the expansion of construction land. The government should strengthen the spatial planning and use control of the national territory, and strictly abide by the red line of ecological protection, strictly control the occupation of ecological space, and stabilize the role of carbon sequestration in existing forest, grassland, wetland, soils, and so on [46]. Second, improving the carbon sink capacity can make some contributions to increasing the carbon sink. For example, adjustment of the planting structure and the multiple cropping index can effectively enhance the carbon sink coefficient of arable land and subsequently increase carbon sinks. Third, ecological restoration projects also provide an important way to increase carbon sinks, and expansion of the green space in urban construction land can play an important role in increasing carbon sinks. For example, the carbon sink coefficients of various land types can be increased through carrying out ecological restoration, thereafter leading to the increase in the total carbon sink.

(2) Some cities, including Shijiazhuang, Tangshan, Chengde, Qinhuangdao, and Xingtai in Hebei Province, should enhance their economic development without reducing their carbon sinks. These cities may achieve proper economic development and meanwhile enhance the carbon sink by optimizing the land carbon sink space and improving the carbon sink capacity. For example, although the carbon sink capacity of forest is higher than that of arable land, the latter lays an important foundation for guaranteeing food security, which is of great significance to the sustainable development of the whole study area. For example, arable land is the main source of carbon sinks for these cities in Hebei Province, which is conducive to realizing the goal of arable land protection. Only by steadily expanding agricultural production space and making every effort to improve the quality of arable land can the study area improve food production and increase carbon sinks at the same time. Additionally, these cities can also improve fruit production and forestry output value by combining the carbon sink improvement with the supply of ecosystem services such as soil and water conservation, headwater conservation, pollution purification. This can contribute to realizing the win–win situation of the carbon sink and ecosystem service development and subsequently improving the economic carrying capacity per unit land.

(3) Other cities, including Handan, Langfang, Cangzhou, Hengshui, Baoding, and Zhangjiakou in Hebei Province, can synchronize their carbon sink improvement with their economic development by improving their carbon sink capacity. In addition to improving the carbon sink capacity and economic output per unit land area, these cities should further improve the economic output capacity per unit land area in the existing construction land. In particular, Zhangjiakou is an essential ecological barrier of the Beijing–Tianjin–Hebei Region, and the government should further implement major ecological protection and

restoration projects for the integrated protection and restoration of mountain, water, forest, field, lake, grassland, and sand land [46,47]. The government should also implement forest quality improvement projects to continuously increase the area and volume of forests, and carry out arable land quality improvement actions to enhance the carbon sinks of ecological agriculture [48].

4. Conclusions

There is an urgent need for revealing the differentiation of carbon sink enhancement potential in the Beijing–Tianjin–Hebei Region, which is an important ecosystem sink project region in China. This study has focused on estimating the regional carbon sink and revealing the differentiation of carbon sink enhancement potential in this region based on the carbon sink–economic carrying capacity index matrix. The results of this study can lay a firm foundation for enhancing regional carbon sink and promoting ecological civilization construction and synergistic development of this region. The major conclusions of this study were as follows: (1) There was significant differentiation in the carbon sinks of different cities in the Beijing–Tianjin–Hebei Region. Chengde and Zhangjiakou had the highest total carbon sinks under the baseline scenario, reaching 2,056,400 and 1,528,300 tons, respectively, while Langfang and Hengshui had the least, which were below 500,000 tons. The largest contributions to carbon sinks in the study area were mainly from arable land, garden land, and forest, accounting for 94.2% and 98% of the total carbon sink of the study area under the baseline scenario and target scenario, respectively. (2) There was also remarkable differentiation in the carbon sink per unit land area among different cities in the study area. Qinhuangdao had the highest carbon sink per unit land area, reaching 0.66 ton/ha under the baseline scenario, while Tianjin had the lowest one, reaching only 0.28 t/ha. Optimizing the spatial distribution of land carbon sink is an important way to improve regional carbon sink. (3) A hypothetical benchmark city of the carbon sink–economic carrying capacity can be constructed according to the carbon sink per unit land area of Qinhuangdao and the GDP per unit land area of Beijing. In comparison with this benchmark city, there is potential for carbon sink enhancement by improving the carbon sink capacity in Beijing, promoting the economic carrying capacity in Qinhuangdao, and improving both their carbon sink capacity and their economic carrying capacity in the other cities of the study area.

Author Contributions: Conceptualization, H.Y.; Methodology, X.J.; Software, Z.L.; Validation, Z.Q. (Zhiguo Qi); Formal analysis, Z.Q. (Zhiguo Qi) and X.J.; Resources, Z.L.; Writing—original draft, H.Y.; Writing—review & editing, S.Z. and Z.Q. (Zhanfei Qin); Visualization, Z.Q. (Zhanfei Qin); Project administration, S.Z. All authors have read and agreed to the published version of the manuscript.

Funding: This study was funded by the 333 Talent Project of Hebei Province (C20221028), Youth Top Talent Program of Hebei Education Department (BJ2019045), Natural Science Foundation of Hebei Province (G2023403002, D2020403067), Major Project of Humanities and Social Science Research of Hebei Education Department (ZD201907), and Hebei Province Key Research and Development Program of China (21374201D).

Institutional Review Board Statement: Not applicable.

Informed Consent Statement: Not applicable.

Data Availability Statement: The original contributions presented in the study are included in the article, further inquiries can be directed to the corresponding author.

Conflicts of Interest: The authors declare no conflicts of interest.

References

1. Sun, L.-L.; Cui, H.-J.; Ge, Q.-S. Will China achieve its 2060 carbon neutral commitment from the provincial perspective? *Adv. Clim. Chang. Res.* **2022**, *13*, 169–178. [CrossRef]
2. Huang, Y.; Li, Z.; Shi, M. Prediction of plant carbon sink potential in Beijing-Tianjin-Hebei region of China. *Environ. Dev. Sustain.* **2022**, *26*, 3529–3556. [CrossRef]

3. Qiu, S.; Fang, M.; Yu, Q.; Niu, T.; Liu, H.; Wang, F.; Xu, C.; Ai, M.; Zhang, J. Study of spatialtemporal changes in Chinese forest eco-space and optimization strategies for enhancing carbon sequestration capacity through ecological spatial network theory. *Sci. Total Environ.* **2022**, *859*, 160035. [CrossRef] [PubMed]
4. Liang, S.; Hurteau, M.D.; Westerling, A.L. Potential decline in carbon carrying capacity under projected climate-wildfire interactions in the Sierra Nevada. *Sci. Rep.* **2017**, *7*, 2420. [CrossRef] [PubMed]
5. Yu, Z.; Lin, Q.; Huang, C. Re-measurement of agriculture green total factor productivity in China from a carbon sink perspective. *Agriculture* **2022**, *12*, 2025. [CrossRef]
6. Ye, M.; Deng, F.; Yang, L.; Liang, X. Evaluation of regional low-carbon circular economy development: A case study in Sichuan province, China. *Int. J. Clim. Chang. Strateg. Manag.* **2022**, *14*, 54–77. [CrossRef]
7. Roxburgh, S.; Wood, S.; Mackey, B.; Woldendorp, G.; Gibbons, P. Assessing the carbon sequestration potential of managed forests: A case study from temperate Australia. *J. Appl. Ecol.* **2006**, *43*, 1149–1159. [CrossRef]
8. Zhang, X.; Brandt, M.; Yue, Y.; Tong, X.; Wang, K.; Fensholt, R. The carbon sink potential of southern China after two decades of afforestation. *Earth's Future* **2022**, *10*, e2022EF002674. [CrossRef]
9. Wu, H.; Guo, S.; Guo, P.; Shan, B.; Zhang, Y. Agricultural water and land resources allocation considering carbon sink/source and water scarcity/degradation footprint. *Sci. Total Environ.* **2022**, *819*, 152058. [CrossRef]
10. Xiang, S.; Wang, Y.; Deng, H.; Yang, C.; Wang, Z.; Gao, M. Response and multi-scenario prediction of carbon storage to land use/cover change in the main urban area of Chongqing, China. *Ecol. Indic.* **2022**, *142*, 109205. [CrossRef]
11. Zhang, C.-Y.; Zhao, L.; Zhang, H.; Chen, M.-N.; Fang, R.-Y.; Yao, Y.; Zhang, Q.-P.; Wang, Q. Spatial-temporal characteristics of carbon emissions from land use change in Yellow River Delta region, China. *Ecol. Indic.* **2022**, *136*, 108623. [CrossRef]
12. Yan, H.; Guo, X.; Zhao, S.; Yang, H. Variation of net carbon emissions from land use change in the Beijing-Tianjin-Hebei region during 1990–2020. *Land* **2022**, *11*, 997. [CrossRef]
13. Read, D.; Beerling, D.; Cannell, M.; Cox, P.; Curran, P.; Grace, J.; Ineson, P.; Jarvis, P.; Malhi, Y.; Powlson, D.; et al. *The Role of Land Carbon Sinks in Mitigating Global Climate Change*; Royal Society: London, UK, 2001; pp. 1–27.
14. Zhang, H.; Yang, Q.; Zhang, H.; Zhou, L.; Chen, H. Optimization of land use based on the source and sink landscape of ecosystem services: A case study of fengdu county in the three gorges reservoir area, China. *Land* **2021**, *10*, 1242. [CrossRef]
15. Liu, Y.; Zhou, Y. Territory spatial planning and national governance system in China. *Land Use Policy* **2021**, *102*, 105288. [CrossRef]
16. Hurlimann, A.; Moosavi, S.; Browne, G.R. Urban planning policy must do more to integrate climate change adaptation and mitigation actions. *Land Use Policy* **2021**, *101*, 105188. [CrossRef]
17. Yue, W.; Hou, B.; Ye, G.; Wang, Z. China's land-sea coordination practice in territorial spatial planning. *Ocean Coast. Manag.* **2023**, *237*, 106545. [CrossRef]
18. Wu, J.; Li, B. Spatio-temporal evolutionary characteristics of carbon emissions and carbon sinks of marine industry in China and their time-dependent models. *Mar. Policy* **2022**, *135*, 104879. [CrossRef]
19. Ying, J.; Jiang, J.; Wang, H.; Liu, Y.; Gong, W.; Liu, B.; Han, G. Analysis of the income enhancement potential of the terrestrial carbon sink in China based on remotely sensed data. *Remote Sens.* **2023**, *15*, 3849. [CrossRef]
20. Fu, B.; Liu, Y.; Meadows, M.E. Ecological restoration for sustainable development in China. *Natl. Sci. Rev.* **2023**, *10*, nwad033. [CrossRef] [PubMed]
21. Liu, G.; Cai, B.; Li, Q.; Zhang, X.; Ouyang, T. China's pathways of CO_2 capture, utilization and storage under carbon neutrality vision 2060. *Carbon Manag.* **2022**, *13*, 435–449. [CrossRef]
22. Meng, Z.; Li, W.-B.; Chen, C.; Guan, C. Carbon Emission Reduction Effects of the Digital Economy: Mechanisms and Evidence from 282 Cities in China. *Land* **2023**, *12*, 773. [CrossRef]
23. Chen, J.; Gao, M.; Cheng, S.; Hou, W.; Song, M.; Liu, X.; Liu, Y.; Shan, Y. County-level CO_2 emissions and sequestration in China. *Sci. Data* **2020**, *7*, 391. [CrossRef]
24. Wu, L.; Zhang, Y.; Luo, G.; Chen, D.; Yang, D.; Yang, Y.; Tian, F. Characteristics of vegetation carbon sink carrying capacity and restoration potential of China in recent 40 years. *Front. For. Glob. Chang.* **2023**, *6*, 1266688. [CrossRef]
25. Hou, W.; Zhai, L.; Walz, U. Identification of spatial conservation and restoration priorities for ecological networks planning in a highly urbanized region: A case study in Beijing-Tianjin-Hebei, China. *Ecol. Eng.* **2023**, *187*, 106859. [CrossRef]
26. Wang, C.; Zhan, J.; Chu, X.; Liu, W.; Zhang, F. Variation in ecosystem services with rapid urbanization: A study of carbon sequestration in the Beijing–Tianjin–Hebei region, China. *Phys. Chem. Earth Parts A/B/C* **2019**, *110*, 195–202. [CrossRef]
27. Fu, H.; Zhao, S.; Liao, C. Spatial governance of Beijing-Tianjin-Hebei urban agglomeration towards low-carbon transition. *China Agric. Econ. Rev.* **2022**, *14*, 774–798. [CrossRef]
28. Ding, H.; Wang, Z.; Huang, C.; Liu, L.; Bedra, K.B. Carbon pressure and economic growth in the urban agglomeration in the Middle Reaches of the Yangtze River: A study on decoupling effect and driving factors. *Sustainability* **2023**, *15*, 7862. [CrossRef]
29. Wang, S.; Wang, Y.; Zhou, C.; Wang, X. Projections in Various Scenarios and the Impact of Economy, Population, and Technology for Regional Emission Peak and Carbon Neutrality in China. *Int. J. Environ. Res. Public Health* **2022**, *19*, 12126. [CrossRef] [PubMed]
30. Wang, X.; Wang, K.; Zhang, Y.; Gao, J.; Xiong, Y. Impact of Climate on the Carbon Sink Capacity of Ecological Spaces: A Case Study from the Beijing–Tianjin–Hebei Urban Agglomeration. *Land* **2023**, *12*, 1619. [CrossRef]
31. Guo, M.; Meng, J. Exploring the driving factors of carbon dioxide emission from transport sector in Beijing-Tianjin-Hebei region. *J. Clean. Prod.* **2019**, *226*, 692–705. [CrossRef]

32. Hubau, W.; Lewis, S.L.; Phillips, O.L.; Affum-Baffoe, K.; Beeckman, H.; Cuní-Sanchez, A.; Daniels, A.K.; Ewango, C.E.; Fauset, S.; Mukinzi, J.M. Asynchronous carbon sink saturation in African and Amazonian tropical forests. *Nature* **2020**, *579*, 80–87. [CrossRef]
33. Yang, Y.; Shi, Y.; Sun, W.; Chang, J.; Zhu, J.; Chen, L.; Wang, X.; Guo, Y.; Zhang, H.; Yu, L. Terrestrial carbon sinks in China and around the world and their contribution to carbon neutrality. *Sci. China Life Sci.* **2022**, *65*, 861–895. [CrossRef]
34. Yu, Y.; Guo, B.; Wang, C.; Zang, W.; Huang, X.; Wu, Z.; Xu, M.; Zhou, K.; Li, J.; Yang, Y. Carbon storage simulation and analysis in Beijing-Tianjin-Hebei region based on CA-plus model under dual-carbon background. *Geomat. Nat. Hazards Risk* **2023**, *14*, 2173661. [CrossRef]
35. Xia, S.; Yang, Y. Examining spatio-temporal variations in carbon budget and carbon compensation zoning in Beijing-Tianjin-Hebei urban agglomeration based on major functional zones. *J. Geogr. Sci.* **2022**, *32*, 1911–1934. [CrossRef]
36. Wang, C.; Zhan, J.; Zhang, F.; Liu, W.; Twumasi-Ankrah, M.J. Analysis of urban carbon balance based on land use dynamics in the Beijing-Tianjin-Hebei region, China. *J. Clean. Prod.* **2021**, *281*, 125138. [CrossRef]
37. Fang, J.; Guo, Z.; Piao, S.; Chen, A. Terrestrial vegetation carbon sinks in China, 1981–2000. *Sci. China Ser. D Earth Sci.* **2007**, *50*, 1341–1350. [CrossRef]
38. Li, M.; Liu, H.; Yu, S.; Wang, J.; Miao, Y.; Wang, C. Estimating the decoupling between net carbon emissions and construction land and its driving factors: Evidence from Shandong province, China. *Int. J. Environ. Res. Public Health* **2022**, *19*, 8910. [CrossRef] [PubMed]
39. Ruehr, S.; Keenan, T.F.; Williams, C.; Zhou, Y.; Lu, X.; Bastos, A.; Canadell, J.G.; Prentice, I.C.; Sitch, S.; Terrer, C. Evidence and attribution of the enhanced land carbon sink. *Nat. Rev. Earth Environ.* **2023**, *4*, 518–534. [CrossRef]
40. Fernández-Martínez, M.; Peñuelas, J.; Chevallier, F.; Ciais, P.; Obersteiner, M.; Rödenbeck, C.; Sardans, J.; Vicca, S.; Yang, H.; Sitch, S. Diagnosing destabilization risk in global land carbon sinks. *Nature* **2023**, *615*, 848–853. [CrossRef] [PubMed]
41. Reichstein, M.; Bahn, M.; Ciais, P.; Frank, D.; Mahecha, M.D.; Seneviratne, S.I.; Zscheischler, J.; Beer, C.; Buchmann, N.; Frank, D.C. Climate extremes and the carbon cycle. *Nature* **2013**, *500*, 287–295. [CrossRef]
42. Heinrich, V.H.; Dalagnol, R.; Cassol, H.L.; Rosan, T.M.; de Almeida, C.T.; Silva Junior, C.H.; Campanharo, W.A.; House, J.I.; Sitch, S.; Hales, T.C. Large carbon sink potential of secondary forests in the Brazilian Amazon to mitigate climate change. *Nat. Commun.* **2021**, *12*, 1785. [CrossRef]
43. Tong, X.; Brandt, M.; Yue, Y.; Ciais, P.; Rudbeck Jepsen, M.; Penuelas, J.; Wigneron, J.-P.; Xiao, X.; Song, X.-P.; Horion, S. Forest management in southern China generates short term extensive carbon sequestration. *Nat. Commun.* **2020**, *11*, 129. [CrossRef]
44. Qubaja, R.; Grünzweig, J.M.; Rotenberg, E.; Yakir, D. Evidence for large carbon sink and long residence time in semiarid forests based on 15 year flux and inventory records. *Glob. Chang. Biol.* **2020**, *26*, 1626–1637. [CrossRef]
45. He, G.; Zhang, Z.; Zhu, Q.; Wang, W.; Peng, W.; Cai, Y. Estimating carbon sequestration potential of forest and its influencing factors at fine spatial-scales: A case study of Lushan City in Southern China. *Int. J. Environ. Res. Public Health* **2022**, *19*, 9184. [CrossRef]
46. Lin, J.; Nie, J.; Wang, T.; Yue, X.; Cai, W.; Liu, Y.; Zhang, Q. Towards carbon-neutral sustainable development of China. *Environ. Res. Lett.* **2023**, *18*, 060201. [CrossRef]
47. Liu, Z.; Deng, Z.; He, G.; Wang, H.; Zhang, X.; Lin, J.; Qi, Y.; Liang, X. Challenges and opportunities for carbon neutrality in China. *Nat. Rev. Earth Environ.* **2022**, *3*, 141–155. [CrossRef]
48. Qiu, S.; Yu, Q.; Niu, T.; Fang, M.; Guo, H.; Liu, H.; Li, S.; Zhang, J. Restoration and renewal of ecological spatial network in mining cities for the purpose of enhancing carbon sinks: The case of Xuzhou, China. *Ecol. Indic.* **2022**, *143*, 109313. [CrossRef]

land

MDPI

Article

Spatial-Temporal Dynamics of Carbon Budgets and Carbon Balance Zoning: A Case Study of the Middle Reaches of the Yangtze River Urban Agglomerations, China

Yiqi Fan [1,2], Ying Wang [1,2,*], Rumei Han [1] and Xiaoqin Li [1]

[1] School of Public Administration, China University of Geosciences, Wuhan 430074, China; fanyiqi@cug.edu.cn (Y.F.); 1202311030@cug.edu.cn (R.H.); lxq2024@cug.edu.cn (X.L.)
[2] Key Laboratory of Law and Government, Ministry of Natural Resources of China, Wuhan 430074, China
* Correspondence: yingwang@cug.edu.cn

Abstract: Analysis of the spatial variation characteristics of regional carbon sources/sinks is a prerequisite for clarifying the position of carbon balance zones and formulating measures to reduce emissions and increase sinks. Studies of carbon sinks have often used the coefficient method, which is limited by sample size, measurement error, and low spatial resolution. In this study, 31 cities in the middle reaches of the Yangtze River urban agglomerations (MRYRUA) were studied with the improved CASA (Carnegie Ames Stanford Approach) model to estimate the grid-scale net ecosystem productivity (NEP) and explore the spatial-temporal evolution of carbon budgets from 2005 to 2020. By calculating the carbon balance index (CBI), economic contribution coefficient (ECC), and ecological support coefficient (ESC), carbon balance zoning was conducted. Corresponding suggestions are based on the carbon balance zoning results. From 2005 to 2020, carbon budgets increased and were high in the north-central region and low in the south. In addition, carbon sink functional zones were distributed in cities with rich ecological resources. Low-carbon economic zones shifted from the Poyang Lake Urban Agglomeration to the Wuhan City Circle; low-carbon optimization zones occurred from the Wuhan City Circle to the Poyang Lake Urban Agglomeration. Carbon intensity control and high-carbon optimization zones were distributed in cities with rapid economic development. Our results support the MRYRUA in achieving "double carbon" targets and formulating regional collaborative emissions reduction policies.

Keywords: CASA (Carnegie Ames Stanford Approach); NEP; carbon budgets; carbon balance zoning; middle reaches of the Yangtze River urban agglomerations (MRYRUA)

Citation: Fan, Y.; Wang, Y.; Han, R.; Li, X. Spatial-Temporal Dynamics of Carbon Budgets and Carbon Balance Zoning: A Case Study of the Middle Reaches of the Yangtze River Urban Agglomerations, China. *Land* **2024**, *13*, 297. https://doi.org/10.3390/land13030297

Academic Editors: Chao Wang, Jinyan Zhan and Xueting Zeng

Received: 25 January 2024
Revised: 18 February 2024
Accepted: 23 February 2024
Published: 27 February 2024

1. Introduction

Since the industrial revolution, humans have produced carbon emissions from the use of fossil fuels [1], leading to the greenhouse effect and gradual warming of the climate [2]. Recently, the 28th Conference of the Parties to the United Nations Framework Convention on Climate Change (UNFCCC) upheld the objectives, principles, and institutional arrangements of the UNFCCC and the Paris Agreement, demonstrating that climate change is a global challenge that requires concerted international cooperation. As the world's largest carbon emitter and energy consumer [3], China has taken the international responsibility of addressing climate change and made unremitting efforts to promote domestic energy conservation, emissions reduction, and ecological civilization [4–6]. However, achieving a carbon balance and further "carbon neutrality" is still a serious challenge for China.

Cities account for only 2% of the global land area but generate approximately 75% of global carbon emissions [7]. Urban agglomerations are important population and economic centers in China [8] and are strategic spaces that drive overall improvements in the national economy and support high-quality development [9]. Huge urban agglomerations have become areas of high energy consumption and carbon emissions. In China,

urban agglomerations (mega metropolitan areas) contribute nearly 70% of carbon emissions [10]. Coordinated regional development [11] and collaborative emissions reduction by urban agglomerations are key areas for energy conservation and emissions reduction in China. Therefore, there is an urgent need to analyze the spatial-temporal changes in the carbon budgets of urban agglomerations and promote synergistic transitions. At the same time, the division of functional zones according to different carbon balances and the creation of carbon balance zoning are critical to low-carbon development in each functional zone and in promoting the synergistic management of the environment in urban agglomerations [12].

Achieving carbon neutrality requires the comprehensive consideration of "emission reduction" and "sequestration enhancement". Accurately estimating carbon emissions and improving carbon sequestration calculations and spatial location accuracy will help clarify regional carbon emission reduction pressures and the carbon sequestration potential. Currently, the methods for estimating carbon emissions include field surveys [13], empirical modeling [14], and the IPCC inventory method [15,16]. For example, Shan et al. developed a methodology for constructing CO_2 emission inventories for Chinese cities based on energy balance sheets [17]. To date, most studies have estimated carbon emissions based on these methods at the national [18], provincial [19], and municipal scales [20] using statistical data, but there is often uncertainty in the results from areas with a lack of information or poor data. Moreover, most scholars focus on carbon emissions. There has been less research on carbon sequestration, which must be improved to realize "carbon neutrality" [21,22].

Methods for calculating carbon sequestration include the sample plot inventory method, the IPCC parameter method, and the model simulation method. The sample plot inventory method can obtain point source data with higher accuracy [23], but it relies on sampling methods for overall accuracy and is time consuming, has a large error, and is generally used as a method for estimating carbon sequestration in small-scale regions [24]. The IPCC parameter method is commonly used for direct accounting of carbon sequestration [25]. Mohareb et al. calculated carbon sequestration for Toronto for 2005, using the IPCC parameter method (for direct sequestration) and peer-reviewed literature (for implicit sequestration), as a direct sequestration of 317,000 tons and an implicit sequestration of 234,000 tons [26]. However, the parameters of the IPCC coefficient method lack specific regional characteristics and are prone to errors. El Mderssio et al. compared the results of the direct field survey with results obtained using the IPCC parameters for the Central Atlas region and found that the directly calculated amount of carbon was 858,387 tons of dry matter, whereas the IPCC parameters estimated 1,201,789 tons [27]. Moreover, integrating carbon sequestration calculations into economic assessments and investigating the economic significance of carbon sequestration can aid in attaining regional carbon neutrality. Luo et al. investigated how local communities perceived the overall effects of carbon capture, utilization, and storage (CCUS) projects and quantified the influence of proximity to CCUS projects on neighboring housing prices [28]. Kazak et al. considered carbon sequestration in the valuation of forest properties using the income approach [29].

The development of Remote Sensing and Geographic Information System technology has provided basic support for carbon sequestration accounting and monitoring [30]. Net ecosystem productivity (NEP) is a key indicator that directly describes the carbon sources/sequestration capacity of terrestrial ecosystems [21,31,32] and is widely used in regional carbon sequestration assessments [33,34]. The CASA (Carnegie Ames Stanford Approach) model is a representative model based on light use efficiency [35], and it can effectively support accounting for long time periods and a large regional NEP because of its data availability, its ability to reflect the distribution of carbon sequestration in large-scale regions, and the ease with which it can be used for long-term monitoring and estimation of carbon sequestration. The CASA method accounts for the mechanism of the carbon cycle, which makes simulation results more accurate and reliable [36,37], and it

requires a small number of physical parameters, which makes the error correspondingly small [35,38–40].

Carbon balance analysis and zoning has become an important research field in the context of global climate warming [41] and China's "double carbon" targets [42]. Most studies rely on indicators affecting the regional carbon balance to establish functional zoning and make low-carbon policy recommendations [43,44]. Vaccari et al. conducted a carbon balance study for the city of Florence and found that green spaces offset 6.2% of direct carbon emissions, which informed subsequent development planning in the city [45]. Ainsworth et al. analyzed the carbon balance of European grassland ecosystems and found that reducing the intensity of grassland management increased grassland ecosystem carbon sequestration [46]. Zamolodchikov et al. investigated the carbon balance of the Russian tundra using seasonal and geographical extrapolations and mathematical simulations [47]. Scholars have also started to study China's carbon balance and carbon sequestration potential. Zhang et al. took Suzhou as an example and used the spatial pattern of carbon emissions to construct a carbon balance zoning method and achieved carbon balance zoning at a micro-scale in the city [48]. Li et al. re-examined the carbon balance of China's terrestrial ecosystems under land use and climate change to guide low-carbon spatial planning policies in various regions [32]. Zhao et al. divided the Central Plains Economic Zone into a carbon intensity control zone, carbon balance zone, carbon sequestration functional zone, total carbon control zone, and low-carbon optimization zone based on the carbon balance zoning theory [49]. However, at the level of carbon balance analysis, the existing indicator system is difficult to implement and lacks accurate and practical standards for evaluating carbon functional zoning. Most studies have focused on provincial and county areas, ignoring the significance of urban agglomerations in China's carbon balance. Therefore, it is necessary to study the differences in ecological and carbon sequestration resource endowment and socio-economic development within urban agglomerations, analyze the spatial-temporal characteristics of carbon balance, and explore carbon balance zoning in urban agglomerations.

As the largest inter-regional urban agglomeration in China by land area, the middle reaches of the Yangtze River urban agglomerations (MRYRUA) is important in China's economic and social development. The MRYRUA is dominated by heavy industries, which requires high energy consumption and has caused rapid growth in carbon emissions in the region. At the same time, the MRYRUA has a large, heavily aggregated population with a correspondingly large demand for energy, and there is pressure to reduce emissions. Therefore, from the perspectives of industrial development and ecological improvement, the zoning of carbon balance is of great significance for realizing the "double carbon" goal.

In this study, we used 31 cities to analyze the spatial-temporal changes in the carbon balance in the MRYRUA from 2005 to 2020, based on carbon emission data from the Carbon Emission Accounts and Datasets (CEADs) and carbon sequestration data estimated with the CASA model. We adopted the carbon balance index (CBI), economic contribution coefficient (ECC), and ecological support coefficient (ESC) to carry out carbon balance zoning that enabled us to assess differences in the regional carbon balance, put forward corresponding strategies for reducing emissions, and formulate carbon-neutral development strategies in line with the actual development strategies for the MRYRUA (Figure 1).

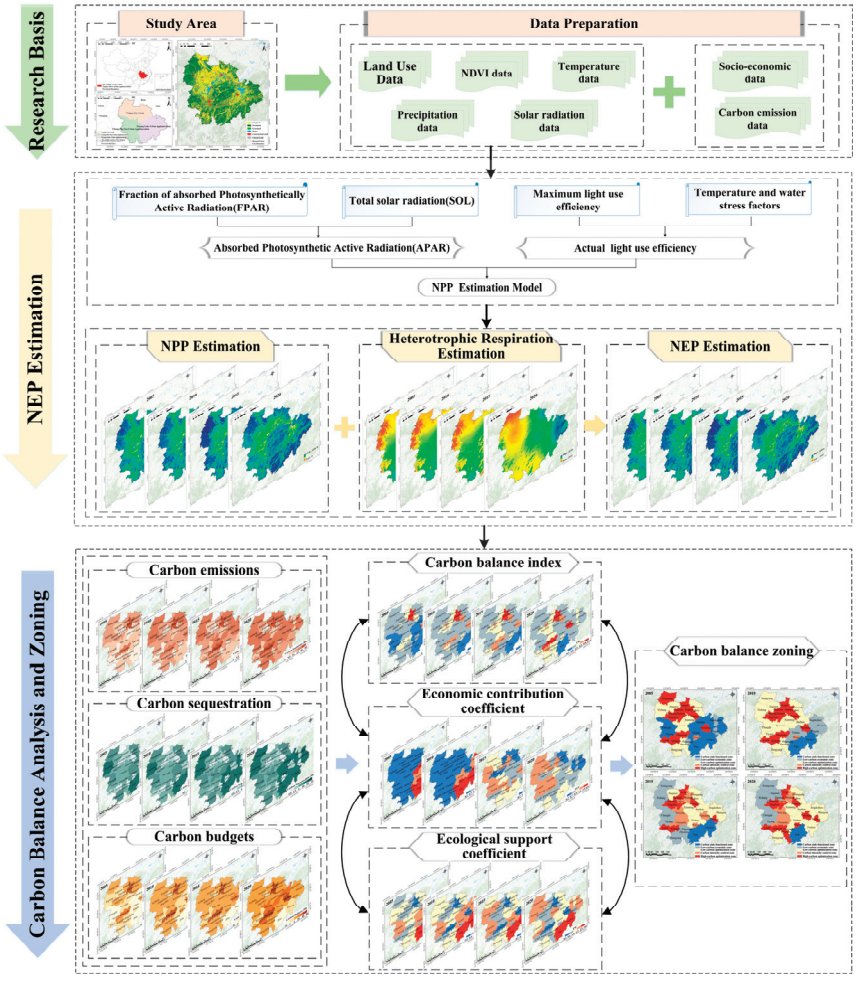

Figure 1. Research framework diagram.

2. Study Area and Data Sources

2.1. Study Area

The MRYRUA is located at 26°03′–32°38′ N, 110°45′–118°21′ E in the middle part of the Yangtze River Basin and covers an area of approximately 326,100 km^2. The MRYRUA is centered on Wuhan and dominated by the Wuhan City Circle in Hubei province, the Chang-Zhu-Tan Urban Agglomeration in Hunan province, and the Poyang Lake Urban Agglomeration in Jiangxi province. The MRYRUA spans Hubei, Hunan, and Jiangxi provinces (Figure 2). The MRYRUA has a subtropical monsoon climate, with an average annual precipitation of 800–1943 mm. The terrain is dominated by plains, with a small number of hills and mountains, and has an average altitude of 20–3105 m. The MRYRUA has a favorable natural geographic location and is bounded on the east and the west and connected to the south and the north.

By the end of 2020, the region had a resident population of 130 million, with an urbanization rate of 63.3%. The gross domestic product (GDP) of the MRYRUA in 2020 was 11.1 trillion yuan, of which primary industry accounted for 8.75%, secondary industry accounted for 40.81%, and tertiary industry accounted for 50.44%. From 2005 to 2020, the GDP

of the MRYRUA grew from 4.2 trillion yuan to 11.1 trillion yuan, with an average annual growth rate of 11.0%, demonstrating great potential for development in the MRYRUA.

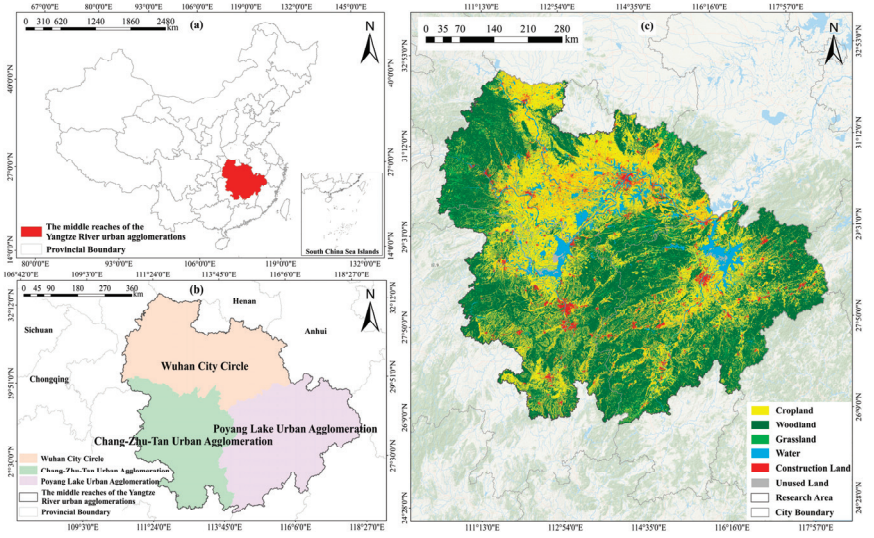

Figure 2. (**a**) The geographical location of the MRYRUA in China. (**b**) The location of the Wuhan City Circle, the Chang-Zhu-Tan Urban Agglomeration, and the Poyang Lake Urban Agglomeration in the MRYRUA. (**c**) Land use data for the MRYRUA in 2020.

2.2. Data Sources

The data in this study include land use data, carbon emission data, and GDP data. The CASA model also requires temperature data, precipitation data, normalized difference vegetation index (NDVI), and surface solar radiation data (Table 1).

Table 1. Data used in this study.

Data Name	Data Type	Year	Source
Land use data	30 m × 30 m Raster data	2005, 2010, 2015, 2020	Resource and Environmental Science Data Center of the Chinese Academy of Sciences (https://www.resdc.cn/ accessed on 8 August 2023)
Carbon emission data	Text data	2005, 2010, 2015, 2020 *	Carbon Emission Accounts and Datasets (CEADs) (https://www.ceads.net.cn accessed on 12 August 2023)
Gross domestic product	Text data	2005, 2010, 2015, 2020	Statistical yearbook of CNKI (https://data.cnki.net/Yearbook accessed on 6 August 2023)
Temperature data	1 km × 1 km Raster data	2005, 2010, 2015, 2020	Resource and Environmental Science Data Center of the Chinese Academy of Sciences (https://www.resdc.cn/ accessed on 10 August 2023)
Precipitation data	1 km × 1 km Raster data	2005, 2010, 2015, 2020	Resource and Environmental Science Data Center of the Chinese Academy of Sciences (https://www.resdc.cn/ accessed on 11 August 2023)
Normalized difference vegetation index	1 km × 1 km Raster data	2005, 2010, 2015, 2020	National Aeronautics and Space Administration (https://ladsweb.modaps.eosdis.nasa.gov/search/ accessed on 12 August 2023)
Surface solar radiation data	10 km × 10 km Raster data	2005, 2010, 2015, 2020 *	National Tibetan Plateau Data Center (https://data.tpdc.ac.cn accessed on 9 August 2023)

*: As the county-level data from CEADs are only available up to 2017, the carbon emission data from 2018 to 2020 were estimated using the Autoregressive Integrated Moving Average (ARIMA) model utilizing these existing county-level data from CEADs [50]. Additionally, the surface solar radiation data for 2020 were spatially interpolated using site data obtained from the Climatic Data Center, National Meteorological Information Center, and China Meteorological Administration (https://data.cma.cn accessed on 10 August 2023).

3. Methods

3.1. NEP Estimation by CASA Model

In this paper, NEP is an important contributor to regional carbon balance estimation and is often used as a measure of carbon sequestration. Without considering the influence of other natural and anthropogenic conditions, the net ecosystem productivity (*NEP*) of vegetation is expressed as the difference between net primary productivity (*NPP*) of vegetation in the ecosystem and carbon emission from heterotrophic respiration (R_H). The specific formula is as follows:

$$NEP = NPP - R_H \tag{1}$$

where *NEP* is net ecosystem productivity of vegetation, *NPP* is net primary productivity of vegetation, and R_H is heterotrophic respiration.

(1) NPP estimation

An improved CASA model [51] was used to estimate *NPP* in the MRYRUA, which combined with heterotrophic respiration can be used to derive the amount of carbon sequestered by vegetation in the urban agglomerations. The main parameters of the CASA model are absorbed photosynthetic active radiation (*APAR*), which can be absorbed by the plants, and actual light use efficiency (ε). The specific formula is as follows:

$$NPP(x,t) = APAR(x,t) \times \varepsilon(x,t) \tag{2}$$

where *APAR*(*x*,*t*) represents absorbed photosynthetic active radiation (g C·m^{-2}·month^{-1}) by image element *x* in month *t*, and ε(*x*,*t*) represents light use efficiency (g C·MJ^{-1}) of image *x* in month *t*.

APAR represents the absorbed photosynthetic active radiation that directly irradiates the vegetation canopy, and the light use efficiency (ε) represents the efficiency of the conversion of *APAR* into organic carbon. We followed "Sense-by-Sense Estimation of Net Primary Productivity of Terrestrial Vegetation in China" and calculated *APAR* and ε by using solar radiation, precipitation, temperature, vegetation type, and MODIS data, using the following formulas:

$$APAR(x,t) = SOL(x,t) \times FRAR(x,t) \times 0.5 \tag{3}$$

$$FPAR(x,t) = \alpha FPAR_{NDVI} + (1-\alpha) FPAR_{SR} \tag{4}$$

$$FPAR_{NDVI} = \frac{(NDVI_{(x,t)} - NDVI_{(i,\min)})}{(NDVI_{(i,\max)} - NDVI_{(i,\min)})} \times (FPAR_{\max} - FPAR_{\min}) + FPAR_{\min} \tag{5}$$

$$FPAR_{SR} = \frac{(SR_{(x,t)} - SR_{(i,\min)})}{(SR_{(i,\max)} - SR_{(i,\min)})} \times (FPAR_{\max} - FPAR_{\min}) + FPAR_{\min} \tag{6}$$

$$SR(x,t) = \frac{(1 + NDVI_{(x,t)})}{(1 - NDVI_{(x,t)})} \tag{7}$$

$$\varepsilon(x,t) = T_{\varepsilon 1}(x,t) \times T_{\varepsilon 2}(x,t) \times W_{\varepsilon}(x,t) \times \varepsilon_{\max} \tag{8}$$

where *SOL*(*x*,*t*) denotes total solar radiation at image element *x* in month *t* (MJ·m^{-2}·month^{-1}), *FPAR* is the fraction of photosynthetically active radiation absorbed by the canopy, and 0.5 is the ratio of the effective radiation of the sun utilized by the vegetation relative to total radiation. $NDVI_{(i,max)}$ and $NDVI_{(i,min)}$ represent, respectively, the maximum and minimum NDVI in plant type *i*. $FPAR_{min}$ and $FPAR_{max}$ are 0.001 and 0.95, respectively. $SR_{(i,min)}$ and $SR_{(i,max)}$ correspond to the 5% and 95% percentile of NDVI in plant type *i*, respectively, and a value of 0.5 was used for α. $T_{\varepsilon 1}(x,t)$ and $T_{\varepsilon 2}(x,t)$ are the stress effects of low and high

temperatures on the light use efficiency. $W_\varepsilon(x,t)$ is the coefficient of water stress, and ε_{max} is the maximum light use efficiency.

(2) Heterotrophic respiration estimation

Based on previous studies, we used the model for heterotrophic respiration established by Zhuang et al. based on measured data [52]. Zhuang et al. investigated the relationship between carbon emissions and environmental factors and established a regression equation between temperature, precipitation, and carbon emissions to estimate heterotrophic respiration. The specific formula is as follows:

$$R_H = 0.22 \times (Exp(0.0913T) + Ln(0.3145R + 1)) \times 30 \times 46.5\% \quad (9)$$

where R_H denotes heterotrophic respiration (g C·m^{-2}·a^{-1}), T is temperature (°C), and R is precipitation (mm).

3.2. Carbon Budgets

The carbon budgets is a measure of the relationship between carbon emissions and carbon sequestration caused by natural factors and human activities in a certain area. It is specifically expressed as the difference between carbon emissions and carbon sequestration in the following formula:

$$CB_i = CE_i - NEP_i \quad (10)$$

where CB_i is the carbon budgets (t) of city cluster i in the MRYRUA, CE_i is the carbon emissions (t) of city cluster i in the MRYRUA, and NEP_i is the carbon sequestration (t) of city cluster i in the MRYRUA (Table 2).

Table 2. Regional carbon budget conditions.

	Condition of CE_i	**Condition of NEP_i**	**Relationship between CE_i and NEP_i**	**Result of CB_i**
Balance point	$CE_i \geq 0$	$NEP_i \geq 0$	$\lvert CE_i \rvert = \lvert NEP_i \rvert$	$CB_i = 0$
Carbon surplus	$CE_i \geq 0$	$NEP_i > 0$	$\lvert CE_i \rvert < \lvert NEP_i \rvert$	$CB_i < 0$
Carbon deficit	$CE_i \geq 0$	$NEP_i > 0$	$\lvert CE_i \rvert > \lvert NEP_i \rvert$	$CB_i > 0$
	$CE_i \geq 0$	$NEP_i < 0$	$\lvert CE_i \rvert > \lvert NEP_i \rvert$	$CB_i > 0$

3.3. CBI

Vegetation can effectively absorb CO_2 emissions from fossil fuel combustion through photosynthesis, thus maintaining the stability of carbon and oxygen in the biosphere and slowing the greenhouse effect. We quantified the relationship between energy carbon emissions and vegetation carbon sequestration based on the CBI, which reflects the impact of regional carbon emissions on ecological stress [53]. The formula is as follows:

$$CBI = CE_i / CS_i \quad (11)$$

where CBI is the carbon balance index, CE_i is the carbon emissions (t) in a given year in city region i, and CS_i is the carbon sequestration (t) in a given year in city area i, which represents NEP_i.

3.4. ECC

The ECC of carbon emissions is a measure of the variability of regional carbon emissions from the perspective of economic efficiency [54], which reflects the magnitude of regional carbon productivity and the degree of matching between regional carbon emissions and their economic contribution. The formula is as follows:

$$ECC = \frac{G_i}{G} / \frac{CE_i}{CE} \quad (12)$$

where *ECC* is the economic contribution coefficient of carbon emission; G_i is the GDP (yuan) of city unit *i* in the MRYRUA; CE_i is the carbon emissions (*t*) of city unit *i*; and *CE* is the total carbon emissions (*t*) of the MRYRUA.

3.5. ESC

The ESC is the quotient of the ratio of carbon absorption of a certain unit to carbon absorption of the whole region and the ratio of carbon emission of the unit to carbon emission of the whole region [44]. It reflects the strength of regional carbon sequestration capacity from the perspective of carbon balance. The formula is as follows:

$$ESC = \frac{CS_i}{CS} / \frac{CE_i}{CE} \tag{13}$$

where *ESC* is the ecological support coefficient of carbon sequestration; CS_i is the carbon sequestration (*t*) of city unit *i*; *CS* is the total carbon sequestration (*t*) in the MRYRUA; CE_i is the carbon emissions (*t*) of city unit *i*; and *CE* is the total carbon emissions (*t*) in the MRYRUA.

3.6. Carbon Balance Zoning

To alleviate the imbalance between "carbon emission and carbon sequestration" in the MRYRUA, which is caused by regional economic development, energy consumption, and land use, we based our study on the perspective of carbon budget balance and regional low-carbon coordinated development, using the CBI, ECC, and ESC as the basis for carbon balance zoning. When the CBI is greater than 1, an area is a carbon source, and when the CBI is less than 1, an area is a carbon sink. A zoning threshold of 1 was used for the CBI. When the ECC is greater than 1, regional energy utilization efficiency is high; on the contrary, this implies that the regional carbon productivity is relatively low. To reflect the energy utilization efficiency and carbon productivity of the region, 1 was used as the zoning threshold for the ECC. When the ESC is greater than 1, a region has higher carbon sequestration capacity; When the ESC is less than 1, this means that the carbon sequestration capacity is weak. Therefore, 1 was used as the zoning threshold for the ESC [48,55]. Based on previous research [56], we divided the urban units of the MRYRUA into five functional zones: carbon sink functional zones, low-carbon economic zones, low-carbon optimization zones, carbon intensity control zones, and high-carbon optimization zones (Table 3). Zoning provides a basis for carbon emission reduction policies, development targets for achieving carbon neutrality, and regional development in the MRYRUA.

Table 3. Basis for carbon balance zoning.

Zoning	Basis	Features
Carbon sink functional zones	$CS_i > CE_i$, ESC > 1	Carbon sequestration is higher than carbon emissions, with a higher ecological support coefficient, overall carbon sink function, and strong carbon sequestration capacity
Low-carbon economic zones	$CS_i < CE_i$, ESC > 1, ECC > 1	Carbon sequestration is lower than carbon emissions, but the ecological support coefficient and economic contribution coefficient are higher, and total net carbon emissions is slightly lower
Low-carbon optimization zones	$CS_i < CE_i$, ESC > 1, ECC < 1	Carbon sequestration is lower than carbon emissions, and the ecological support coefficient is high, but the economic contribution coefficient is low
Carbon intensity control zones	$CS_i < CE_i$, ESC < 1, ECC > 1	Carbon sequestration is lower than carbon emissions; ecological support coefficient is low, but the economic contribution coefficient is high, and net carbon emissions is high
High-carbon optimization zones	$CS_i < CE_i$, ESC < 1, ECC < 1	Total net carbon emissions is high and both ecological support coefficient and economic contribution coefficient are low

4. Results

4.1. Spatial-Temporal Variation of Carbon Budgets

4.1.1. Temporal Trends of Carbon Budgets

Based on estimated carbon emissions and carbon sequestration, carbon budgets were analyzed in the MRYRUA (Wuhan City Circle, Chang-Zhu-Tan Urban Agglomeration, and Poyang Lake Urban Agglomeration around Poyang Lake) from 2005 to 2020 (Figure 3).

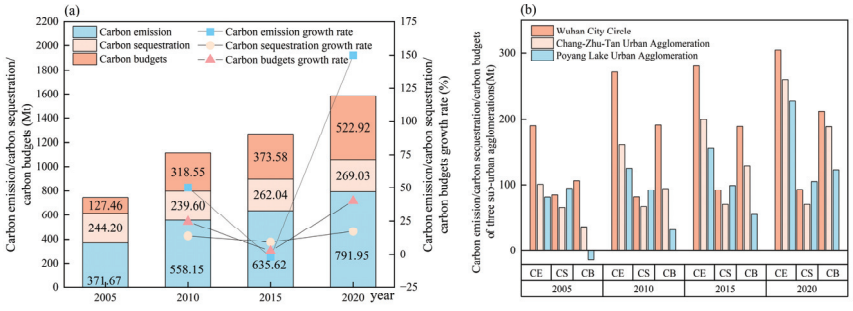

Figure 3. (**a**) Changes in carbon emissions, carbon sequestration, and carbon budgets in the MRYRUA from 2005 to 2020. (**b**) Changes in carbon emissions, carbon sequestration, and carbon budgets in three urban agglomerations from 2005 to 2020. Note: CE denotes carbon emissions, CS denotes carbon sequestration, CB denotes carbon budgets.

From 2005 to 2020, total carbon emissions in the MRYRUA exceeded total carbon sequestration, and carbon budgets increased. Carbon emissions increased by 113.08%, carbon sequestration increased by 10.16%, and carbon budgets increased by 310.25%. Changes in the carbon budgets were reflected by changes in carbon emissions, potentially due to the expansion in urban construction and the acceleration of the industrial process. Many factories and enterprises went into production, resulting in an increase in energy consumption and carbon emissions. From 2005 to 2010, carbon budgets increased by 149.91%. From 2010 to 2015, carbon budgets increased by 17.27%. During the "12th Five-Year Plan" period, environmental pollution and consumption of resources attracted national attention. From 2015 to 2020, carbon budgets increased by 39.98%. The MRYRUA have achieved certain results and actively responded to the national emissions reduction strategies and policies. However, energy conservation and emissions reduction remain challenges.

From 2005 to 2020, carbon emissions, carbon sequestration, and carbon budgets of the Wuhan City Circle, the Chang-Zhu-Tan Urban Agglomeration, and the Poyang Lake Urban Agglomeration generally increased. The Wuhan City Circle had the largest proportion of carbon emissions in the MRYRUA. The Poyang Lake Urban Agglomeration had the most carbon sequestration in the MRYRUA. Growth in carbon emissions, carbon sequestration, and carbon budgets in the Wuhan City Circle was similar to that in the MRYRUA, because Wuhan is an important industrial base and science and education base in the country. It carries the carbon emission activities of various cities and accounts for an important position in carbon emissions of the Wuhan City Circle and the MRYRUA. Over the past fifteen years, carbon sequestration of the Chang-Zhu-Tan Urban Agglomeration has increased. Following ecological restoration in this area, the carbon sequestration capacity of vegetation improved and excessive growth of carbon budgets was avoided. Carbon sequestration by the Poyang Lake Urban Agglomeration was highest among the three urban agglomerations and carbon budgets were the smallest, because this area has rich vegetation that functions as a carbon sink.

4.1.2. Spatial Evolution of Carbon Budgets

The spatial evolution of carbon emissions, carbon sequestration, and carbon budget patterns was analyzed in different cities (Figure 4). Overall, from 2005 to 2020, carbon

emissions from the MRYRUA were high in the north-central region and low in the south. From 2005 to 2020, Wuhan experienced rapid economic development and was a high-value area of carbon emissions, followed by Changsha. Changsha transformed from the previous second-highest value area to a high-value area. Nanchang also changed from a middle-value area to the second-highest value area. The high-value areas of carbon emissions in the MRYRUA mainly increased along the periphery of provincial capital cities, which was reflected between 2010 and 2015 and became more obvious after 2015. These changes between 2010 and 2015 reflect the "13th Five-Year Plan", which implemented the overall regional development strategy and promoted common development among regions. The rapid development of inter-regional economies has led to an increase in carbon emissions.

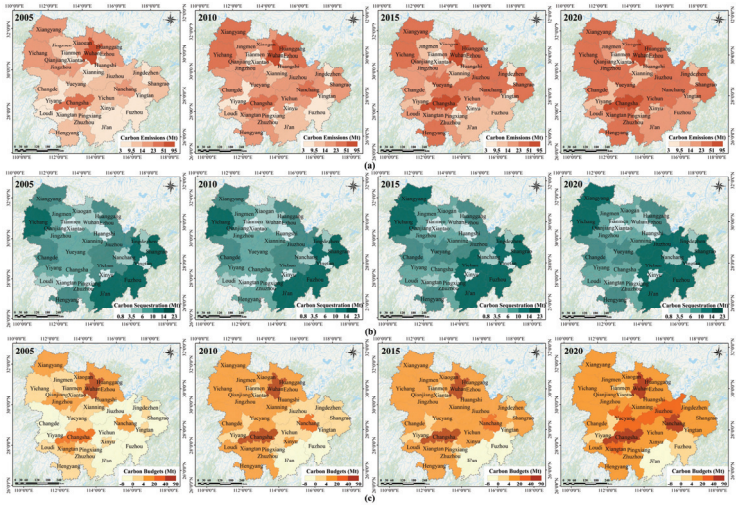

Figure 4. (**a**) Spatial-temporal evolution of carbon emissions in the MRYRUA from 2005 to 2020. (**b**) Spatial-temporal evolution of carbon sequestration in the MRYRUA from 2005 to 2020. (**c**) Spatial-temporal evolution of carbon budgets in the MRYRUA from 2005 to 2020.

Carbon sequestration in the MRYRUA was high on the periphery and low in the center. From 2005 to 2020, carbon sequestration was almost stable, reflecting the small impact of carbon sequestration on changes in carbon budgets. The spatial pattern of carbon budgets was similar to that of carbon emissions and was high in the central region, followed by the north, and lowest in the south. Carbon budgets increased the most from 2005 to 2010, and there was a trend in carbon budgets moving from low-value areas to high-value areas. From 2010 to 2015, carbon budgets moved from low-value areas to high-value areas in the Poyang Lake Urban Agglomeration. From 2015 to 2020, the highest value carbon budgets were in Wuhan and Changsha. Carbon budgets of the surrounding areas centered on Wuhan, Changsha, and Nanchang were relatively high. These cities are the economic centers of their respective urban agglomerations and have experienced rapid urban development and high carbon emissions. Generally, carbon emissions in the MRYRUA have exceeded carbon sequestration, and the pressure to reduce emissions is still high.

4.2. Carbon Balance Analysis

4.2.1. CBI

Based on the CBI, the relationship between carbon emissions and carbon sequestration in the MRYRUA can be further explored (Figure 5). The CBI of the MRYRUA increased 93.42% from 2005 to 2020. The CBI of Wuhan, Ezhou, and Nanchang increased, mainly due to an increase in urban population and energy consumption by industrial enterprises. From 2010 to 2015, the CBI of Wuhan, Ezhou, Xiaogan, Tianmen, and Xiangyang decreased.

From 2015 to 2020, the CBI of Xiangyang, Jingmen, and Tianmen decreased. This is because regions attach great importance to ecological and environmental protection and promote low-carbon, green, and sustainable urban development, which has inhibited the growth of the CBI.

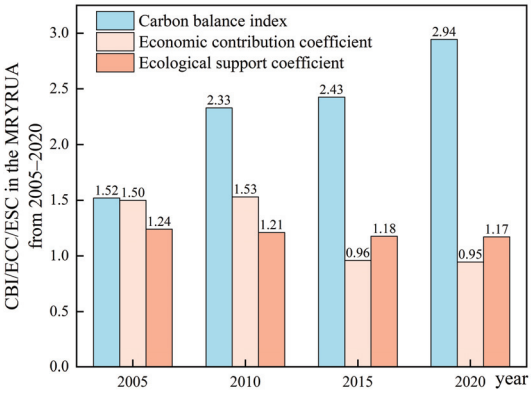

Figure 5. CBI, ECC, and ESC of the MRYRUA from 2005 to 2020.

The spatial patterns of the CBI in the MRYRUA from 2005 to 2020 are shown in Figure 6a. The CBI was high in the center and low in the periphery. The low-value areas of the CBI were in the southeastern Poyang Lake Urban Agglomeration and the northwest of the Chang-Zhu-Tan Urban Agglomeration. From 2005 to 2020, areas with a high CBI gradually shifted from Wuhan to the three provincial capitals. From 2010 to 2015, high-value areas of the CBI spread around Wuhan and Changsha. It may be due to rapid economic development that carbon emissions in construction areas have increased rapidly, while carbon sequestration has changed to a small extent, and the energy transition in some areas is slow. From 2015 to 2020, the CBI of the Chang-Zhu-Tan Urban Agglomeration was still lower than that of the other two urban agglomerations.

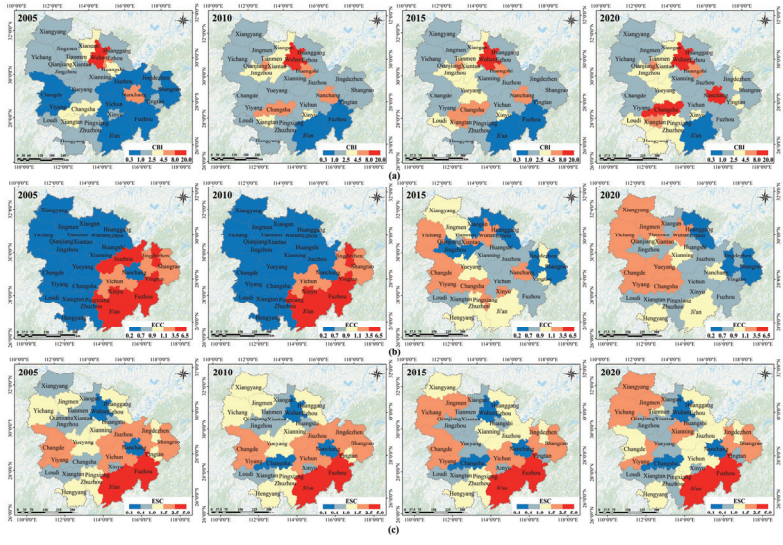

Figure 6. (**a**) Spatial distribution pattern of the CBI in the MRYRUA from 2005 to 2020. (**b**) Spatial distribution pattern of the ECC in the MRYRUA from 2005 to 2020. (**c**) Spatial distribution pattern of the ESC in the MRYRUA from 2005 to 2020.

4.2.2. ECC

From 2005 to 2020 (Figure 5), the ECC of the MRYRUA showed an overall decrease and the differences in the ECC of different cities gradually decreased. The ECC of the Wuhan City Circle and the Chang-Zhu-Tan Urban Agglomeration increased annually, while the ECC of the Poyang Lake Urban Agglomeration decreased. From 2005 to 2020, the ECC declined overall, indicating that the economic efficiency of carbon emissions decreased. In 2005, the ECC in the Wuhan City Circle and the Chang-Zhu-Tan Urban Agglomeration was smaller, ranging from 0.20 to 0.56. In 2015 and 2020, the ECC was mostly between 0.5 and 1.5, indicating that the ECC in each city was relatively balanced and regional differences were not obvious.

The ECC of the MRYRUA was low in the north-central location and high in the periphery (Figure 6b). From 2005 to 2020, the high-value area of the ECC changed from the Poyang Lake Urban Agglomeration to the other agglomerations. In 2005, the low-value areas of the ECC were distributed in Huanggang, Ezhou, and Xianning. They were affected by Wuhan's highly polluting industries and local economic development through extensive energy consumption. In 2015, the ECC in Fuzhou, Ji'an, and Yingtan was less than 1, indicating that the contribution rate of carbon emissions was greater than the economic contribution rate. Compared with 2015, change in the ECC was small. The ECC of the cities around Wuhan, Changsha, and Nanchang was larger than that of other regions. Overall, the economic efficiency of carbon emissions is relatively low.

4.2.3. ESC

From 2005 to 2020, the ESC of the MRYRUA decreased (Figure 5). The ESC in the Wuhan City Circle increased, while the ESC of most cities in the other two urban agglomerations decreased. Perhaps because of the concept that "Clear waters and green mountains are as valuable as mountains of gold and silver", China's ecological construction has accelerated, and regional carbon sink capabilities have become more significant. From 2005 to 2010, the maximum value of the ESC was 6.72% lower than in 2005. From 2010 to 2015, the ESC of the Wuhan City Circle increased, while the ESC of the Chang-Zhu-Tan Urban Agglomeration and the Poyang Lake Urban Agglomeration decreased. For fifteen years, Wuhan's ESC has been the smallest. Wuhan's extensive energy consumption creates more carbon emissions. At the same time, rapid industrialization and urbanization occupy more ecological space and reduce carbon sequestration levels. Thus, Wuhan has formulated total carbon emission control targets.

The spatial pattern of the ESC is similar to that of the ECC and is low in the center and high in the periphery of the MRYRUA (Figure 6c). From 2005 to 2020, the ESC in the central and northern regions was low, while the ESC in the southeastern and northeastern regions was high, with obvious differences between regions. From 2005 to 2010, the change was not significant in cities. From 2010 to 2015, the ESC of Yichang and Jingmen increased, indicating that this region had gradually attached importance to the protection of the environment. In the past fifteen years, the MRYRUA have vigorously promoted clean energy by balancing the relationship between economic development and ecological protection, reducing dependence on traditional energy sources, and improving energy utilization efficiency.

4.3. Carbon Balance Zoning

This study coupled the CBI, ECC, and ESC to divide the MRYRUA into five functional zones: carbon sink functional zones, low-carbon economic zones, low-carbon optimization zones, carbon intensity control zones, and high-carbon optimization zones (Figure 7). From 2005 to 2020, the number of carbon sink functional zones in the MRYRUA decreased significantly and were mainly distributed in the southern part of the Poyang Lake Urban Agglomeration. The number of low-carbon economic zones generally increased and the spatial distribution shifted from the Poyang Lake Urban Agglomeration to the Wuhan City Circle. The spatial distribution of low-carbon optimization zones shifted from the western

region to the eastern region. The number of carbon intensity control zones increased, mainly in the middle of the MRYRUA. The spatial distribution of high-carbon optimization zones demonstrated little change.

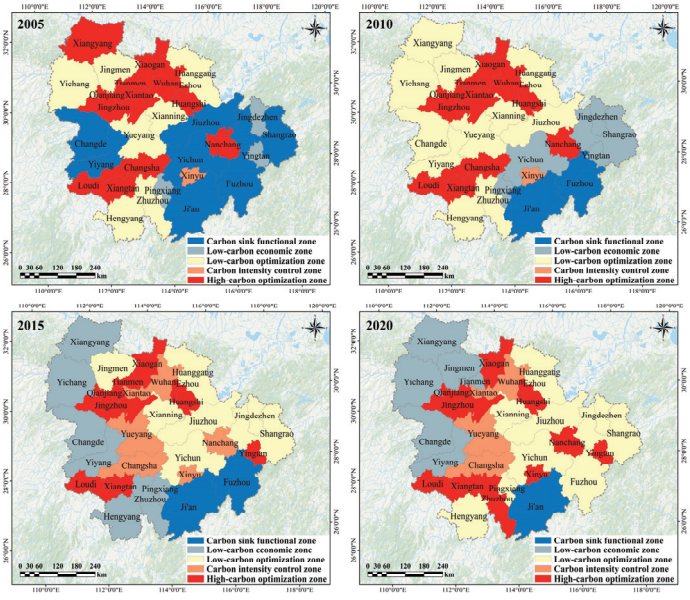

Figure 7. Carbon balance zoning in the MRYRUA from 2005 to 2020.

Carbon sink functional zones are mainly distributed in areas rich in ecological resources, such as woodland and grassland in the MRYRUA. Their spatial distribution is similar to areas with high carbon sequestration. From 2005 to 2020, the number of carbon sink functional zones decreased. In 2005, carbon sink functional zones accounted for 38.62% of the MRYRUA, accounting for the largest area. In 2010 and 2015, carbon sink functional zones accounted for 12.60% of the MRYRUA. In 2020, the area of carbon sink functional zones had decreased. The economic development of carbon sink functional zones is relatively low, carbon sequestration is higher than carbon emissions, environmental quality is high, and the carbon sequestration capacity is strong, all of which have a significant impact on ecological security. In the future, we should continue to improve the environment in this area, maintain the carbon sink function of the ecosystem, and develop the area while protecting regional ecological functions.

The spatial distribution of low-carbon economic zones changed significantly from 2005 to 2020, gradually moving from scattered distribution to agglomeration, and the number of low-carbon economic zones increased significantly. Low-carbon optimization zones were converted into low-carbon economic zones. In 2005 and 2010, low-carbon economic zones accounted for 3.62% and 15.46% of the MRYRUA, respectively. In 2015 and 2020, the area of low-carbon economic zones had increased, and they were mainly distributed in the Wuhan City Circle and the Chang-Zhu-Tan Urban Agglomeration. Carbon sequestration in these cities is less than carbon emissions, but the carbon sink capacity is also strong. Along with economic development, it is also necessary to control carbon emissions, prioritize ecological and environmental protection, avoid ecological degradation, and maintain regional carbon-balanced development. In the future, it will be necessary to stabilize the carbon sequestration capacity of regional vegetation, develop low-carbon industries, improve carbon emission efficiency, balance economic development and the environment, and pursue sustainable development.

From 2005 to 2020, low-carbon optimization zones gradually shifted from the Wuhan City Circle and the Chang-Zhu-Tan Urban Agglomeration to the Poyang Lake Urban Agglomeration. Some carbon sink functional zones were converted into low-carbon optimization zones. In 2005, compared with the other three years, the area accounted for the smallest proportion; in 2010 and 2015, low-carbon optimization zones were mainly distributed in the Wuhan City Circle and the Poyang Lake Urban Agglomeration. Low-carbon optimization zones clearly moved to the Poyang Lake Urban Agglomeration. In 2020, the low-carbon optimization zones were distributed in the central and eastern part of the MRYRUA. The economic development of these cities is average, and their carbon sink capacity is weak. Regional carbon emissions will affect the development of other surrounding areas. In the future, it will be necessary to protect the environment, promote green, low-carbon, and sustainable cities, and appropriately accelerate high-quality urban development.

Carbon intensity control zones were mainly distributed in urban areas with rapid economic development. From 2005 to 2020, the number of carbon intensity control zones gradually increased and distributed along and around the provincial capital center. Low-carbon optimization zones shifted to carbon intensity control zones. In 2005, the carbon intensity control zones accounted for 0.90% of the MRYRUA; in 2015, the area of the carbon intensity control zones was 13.76% and, in 2020, the area was 10.80%, mainly in Wuhan, Changsha, and Yueyang. Carbon sequestration in this region is less than carbon emissions. Wuhan, Changsha, and Nanchang have rapid economic development, high urbanization, increased carbon emissions, and a reduction in the amount of ecological land, and the carbon sequestration capacity of the ecosystem has weakened. In the future, this part of the region can reduce regional carbon emissions, develop low-carbon industries, improve technological innovation, and strengthen its cooperation with surrounding low-carbon areas to achieve a "win-win".

High-carbon optimization zones were spatially distributed in blocks and were relatively scattered. Some low-carbon optimization zones shifted to high-carbon optimization zones. In 2005 and 2010, high-carbon optimization zones accounted for 27.65% and 22.01% of the MRYRUA, respectively, and were mainly distributed in Ezhou and Huangshi. In 2015, high-carbon optimization zones accounted for 14.42% of the MRYRUA and were mainly distributed in Ezhou, Huangshi, and Xiaogan. In 2020, high-carbon optimization zones accounted for 19.85% of the MRYRUA. Carbon sequestration in this region is lower than carbon emissions, which is not conducive to the realization of regional carbon neutrality, and there is room for improvement between the economic development and environmental protection. In the future, it will be necessary to increase carbon sinks, implement ecological restoration projects, carry out integrated protection and management of natural resources (mountains, rivers, forests, fields, lakes, grass, and sand), enhance the carbon sequestration capacity of ecosystems, and strengthen the coupling and coordination capabilities between economic development and ecological protection.

5. Discussion

Our study differed from previous studies on land use carbon emissions and land use carbon balance zoning [57] by using the CASA model to calculate carbon sequestration on a more accurate grid scale [58], analyzing the spatial-temporal pattern of carbon budgets, and exploring carbon balance zoning. Compared with Zhang's analysis of the impact of carbon emissions from the cities of Wuhan, Changsha, and Nanchang, we analyzed spatial-temporal changes in 31 cities [59]. We found that carbon sequestration in the MRYRUA from 2005 to 2010 was slightly different from the results of previous studies. Carbon sequestration in 2005 and 2010 was smaller than previously determined, while carbon sequestration in 2015 and 2020 was closer to previous research results. This may be explained by our use of the CASA model to calculate the carbon sink of grid cells to obtain carbon sequestration for each city. These results are more accurate, while previous studies used cultivated land, grassland, water bodies, and unused areas. Carbon sequestration

is calculated based on individual plots as units, where each plot represents only one value. However, particular areas may exhibit uneven vegetation distribution. Using grid unit statistics helps minimize the error in estimating carbon sequestration, resulting in a closer approximation to the actual values. Compared with other urban agglomerations, the Wuhan City Circle had the largest carbon emissions from 2005 to 2020, potentially because the Wuhan City Circle is the economic center of the MRYRUA. Wuhan's economic development relies on industry, which results in extensive industrial carbon emissions. However, with adjustments to the industrial structure, carbon emissions in the Wuhan City Circle have moderated [60]. Carbon emissions in the Chang-Zhu-Tan Urban Agglomeration are relatively low. This may be because the development of heavy industry in the Chang-Zhu-Tan Urban Agglomeration has been relatively slow. The development of tertiary industry reduces energy consumption, and carbon emissions are relatively low. As carbon emissions increase in the Poyang Lake Urban Agglomeration, carbon sequestration is the highest in the MRYRUA. While the Poyang Lake Urban Agglomeration is developing, this area is also focused on improving carbon sinks.

Our results demonstrate that the degree of change in carbon emissions, carbon sequestration, and carbon budgets is different in the MRYRUA. The Wuhan City Circle plays an important role in the carbon budgets of the MRYRUA. Within fifteen years, due to expansion, carbon budgets within the Wuhan City Circle have increased from northwest to southeast. Carbon budgets of the Chang-Zhu-Tan Urban Agglomeration have also increased. This may be explained by the influence of "two-oriented" social construction and energy conservation and emissions reduction policies proposed by the country. The agglomeration continues to strengthen awareness of environmental protection and energy conservation. Compared with other urban agglomerations, the carbon budgets of the Poyang Lake Urban Agglomeration are smaller. Ji'an and Fuzhou have strong carbon sequestration capabilities, rich forest resources, and diverse ecosystems. However, cities in the northern part of the Poyang Lake Urban Agglomeration have experienced increased carbon emissions and larger carbon budgets. Perhaps due to the impact of the industrial transfer of Wuhan and Nanchang, industries may choose to set up their production bases in cities such as Jiujiang. From 2005 to 2020, growth in carbon emissions in the MRYRUA was obvious, but a goal of achieving carbon neutrality remains [61,62]. Therefore, measures to reduce emissions and increase sinks still require attention.

Based on the spatial-temporal dynamics of carbon budgets, the CBI, ECC, and ESC were calculated, and carbon balance zoning was conducted. Carbon sequestration remained relatively stable, and an increase in carbon emissions was the main reason for the increase in the CBI, which is consistent with Chen's calculation of the global CBI [63]. Although carbon balance zoning in this study was similar to that of Xiong's, it differed in the selection of zoning indicators. Xiong used the carbon productivity to measure regional carbon emissions from the perspective of economic benefits, while we used the ECC to characterize regional carbon productivity [44]. This indicator is more consistent with the energy utilization rate among cities within the MRYRUA. Compared with Wen's study on China's carbon balance zoning, our comparison of regional carbon emissions and carbon sequestration is conducive to the analysis of carbon balance characteristics and also makes the zoning results more detailed and reliable [55]. From 2005 to 2020, the number of carbon sink functional zones decreased, and most carbon sink functional zones were converted into low-carbon optimization zones. This may be because urbanization and industrialization were affected by the economic development of surrounding cities. As a result, land was used for industrial construction, causing the original carbon sink functional zones to be gradually occupied or destroyed. The carbon sequestration capacity of cities in the MRYRUA is inadequate to offset the total carbon emissions from energy consumption fully. Some low-carbon optimization zones shifted to carbon intensity control zones and high-carbon optimization zones. Limited land resources have caused construction to encroach on ecological land, resulting in an increase in carbon emissions and a reduction in carbon sequestration, which is consistent with Chuai's research on construction expansion and

carbon emissions [64]. Carbon intensity control zones and high-carbon optimization zones are important sources of carbon emissions. Limiting the massive expansion of construction is of great significance to regional carbon emissions reduction. In the future, it will be necessary to accelerate technological innovation, promote the transformation of high-carbon industries into low-carbon industries, optimize the energy structure, and improve energy utilization efficiency to achieve low-carbon development [65–67].

Our study has certain limitations. The smallest research unit was a city, and carbon balance policies do not take the county into consideration, which is not conducive to differentiation within a city. In the future, counties should be used as research units to achieve regional carbon balance goals and low-carbon development. Spatial elements were also ignored in carbon balance zoning, and spatial correlation was not analyzed. In the future, by building a spatial correlation network of carbon emissions and carbon sequestration between regions, using the CBI, ECC, and ESC, network spatial correlation characteristics and indicators related to economic development can be added to provide more accurate, multi-perspective zoning results and reference values for the formulation of low-carbon policies in different regions. In addition, the theory of comparative advantage can be introduced in the quantification of carbon balance zoning indicators, and regional carbon balance zoning can be carried out by calculating the standard comparative advantage index.

6. Conclusions and Policy Implications

6.1. Conclusions

In this study, we calculated carbon budgets and expenditures of 31 cities in the MRYRUA from 2005 to 2020, analyzed the spatial-temporal pattern of carbon budgets, and formulated carbon balance zoning. The main results are summarized below.

(1) From 2005 to 2020, carbon emissions and carbon budgets increased, the increase in carbon sequestration was relatively small, and changes in carbon budgets were reflected by changes in carbon emissions. Carbon emissions from the Wuhan City Circle accounted for the largest total carbon emissions in the MRYRUA. Carbon emissions and carbon sequestration by the Chang-Zhu-Tan Urban Agglomeration increased. The Poyang Lake Urban Agglomeration had the most carbon sequestration in the MRYRUA. Carbon emissions in the MRYRUA were high in the north-central region and low in the south. Carbon sequestration was high in the periphery and low in the center. Carbon budgets were high in the central region, followed by the north, and lowest in the south.

(2) From 2005 to 2020, the CBI of the MRYRUA increased. From 2005 to 2020, the CBI increased by 93.42% and was high in the center and low in the periphery. The low-value areas of carbon balance were distributed in the southeastern area of the Poyang Lake Urban Agglomeration and the northwest area of the Chang-Zhu-Tan Urban Agglomeration. The ECC decreased overall, and differences in the ECC of different cities gradually decreased. The ECC of each city of the Wuhan City Circle and the Chang-Zhu-Tan Urban Agglomeration increased annually. The ECC was low in the north-central region and high in the periphery. The area with a high ECC gradually shifted from the Poyang Lake Urban Agglomeration to the Wuhan City Circle. The ESC of all cities in the Wuhan City Circle increased, while the ESC of most cities in the other two urban agglomerations decreased. The spatial pattern of the ESC was similar to that of the ECC and was low in the center and high in the periphery. Obvious differences in the ESC occurred between regions.

(3) From 2005 to 2020, the number of carbon sink functional zones significantly decreased. These zones were distributed in areas with rich ecological resources. The number of low-carbon economic zones generally increased. The spatial distribution gradually shifted from the Poyang Lake Urban Agglomeration to the Wuhan City Circle, and the number of low-carbon optimization zones fluctuated greatly, mainly from the Wuhan City Circle and the Chang-Zhu-Tan Urban Agglomeration to the Poyang Lake Urban Agglomeration. The number of carbon intensity control zones increased and these

zones were mainly distributed in the provincial capital center and its surrounding cities. High-carbon optimization zones were spatially distributed in blocks and were relatively scattered.

6.2. Policy Implications

The spatial pattern of carbon budgets in the MRYRUA is unbalanced, and there are differences in the ECC and the ESC between cities. Based on a spatial-temporal analysis of carbon budgets and the results of carbon balance zoning, we put forward the following suggestions:

(1) Build a regional carbon balance adjustment mechanism oriented toward the goal of carbon neutrality. Based on the CBI, ECC, ESC, and carbon balance zoning results, carbon emissions reduction targets can be set. For Wuhan, Changsha, Nanchang, and surrounding cities, targets should formulate a carbon emission quota and monitoring system and set carbon emission caps for various industries. In addition, carbon sequestration in the southern part of the Poyang Lake Urban Agglomeration is relatively large. We should continue to strengthen carbon sink management, increase the carbon sequestration capacity, alleviate carbon emissions, and coordinate carbon emissions and carbon sequestration in the MRYRUA.

(2) Develop differentiated carbon emission reduction and carbon sink enhancement strategies based on regional characteristics. Carbon sink functional zones rich in ecological resources should continue to be maintained, ecological protection and restoration should be strengthened, carbon sink resources (such as forests, grasslands, and wetlands) should be increased, vegetation coverage should be increased, and the carbon sequestration capacity of the regional ecosystem should be improved. Carbon intensity control zones and high-carbon optimization zones should focus on carbon emissions reduction and continue to move toward low-carbon economic zones and low-carbon optimization zones. In addition, we should control the speed of urban expansion, guide regional development in a low-carbon direction, ensure the coordination of carbon balance and economic development, and improve regional economic-ecological-social benefits.

(3) Facilitate the exchange of technology among different regions. Urban agglomerations consistently promote collaborative efforts to reduce emissions. Carbon sink functional zones, carbon intensity control zones, and high-carbon optimization zones should enhance the dissemination of technologies. Carbon intensity control and high-carbon optimization zones experiencing rapid economic development can offer technical support to carbon sink functional zones. Similarly, carbon sink functional zones can mitigate carbon emissions generated by carbon intensity control and high-carbon optimization zones. Strengthening inter-regional cooperation and coordination can establish a carbon equilibrium mechanism that balances economic development with ecological protection.

Author Contributions: Conceptualization, Y.F. and Y.W.; methodology, Y.F. and R.H.; software, Y.F.; formal analysis, Y.F. and R.H.; resources, Y.F., R.H. and X.L.; data curation, Y.F. and X.L.; writing—original draft preparation, Y.F. and R.H.; writing—review and editing, Y.F. and Y.W.; visualization, Y.F. and R.H.; supervision, Y.W.; project administration, Y.W.; funding acquisition, Y.W. All authors have read and agreed to the published version of the manuscript.

Funding: This research was funded by the Youth Foundation of the School of Public Administration, China University of Geosciences (CUGGG--2301). The APC was funded by the "CUG Scholar" Scientific Research Funds at the China University of Geosciences (Wuhan) (2022128).

Data Availability Statement: The data presented in this study are available on request from the author. The data are not publicly available due to privacy restrictions.

Acknowledgments: We appreciate critical and constructive comments and suggestions from the reviewers that helped improve the quality of this manuscript.

Conflicts of Interest: The authors declare no conflicts of interest.

References

1. Piggot, G.; Erickson, P.; van Asselt, H.; Lazarus, M. Swimming upstream: Addressing fossil fuel supply under the UNFCCC. *Clim. Policy* **2018**, *18*, 1189–1202. [CrossRef]
2. Miao, Z.; Chen, X.D.; Balezentis, T.; Sun, C.W. Atmospheric environmental productivity across the provinces of China: Joint decomposition of range adjusted measure and Luenberger productivity indicator. *Energy Policy* **2019**, *132*, 665–677. [CrossRef]
3. Guan, D.B.; Liu, Z.; Geng, Y.; Lindner, S.; Hubacek, K. The gigatonne gap in China's carbon dioxide inventories. *Nat. Clim. Chang.* **2012**, *2*, 672–675. [CrossRef]
4. Wang, Y.; Chai, J.; Zhang, H.W.; Yang, B. Evaluating construction land use efficiency under carbon emission constraints: A comparative study of China and the USA. *Environ. Sci. Pollut. Res.* **2022**, *29*, 49998–50009. [CrossRef]
5. Wang, C.; Wang, X.; Wang, Y.F.; Zhan, J.Y.; Chu, X.; Teng, Y.M.; Liu, W.; Wang, H.H. Spatio-temporal analysis of human wellbeing and its coupling relationship with ecosystem services in Shandong province, China. *J. Geogr. Sci.* **2023**, *33*, 392–412. [CrossRef]
6. Yin, R.M.; Wang, Z.Q.; Chai, J.; Gao, Y.X.; Xu, F. The Evolution and Response of Space Utilization Efficiency and Carbon Emissions: A Comparative Analysis of Spaces and Regions. *Land* **2022**, *11*, 428. [CrossRef]
7. Churkina, G. The Role of Urbanization in the Global Carbon Cycle. *Front. Ecol. Evol.* **2016**, *3*, 9. [CrossRef]
8. Han, Z.; Deng, X.Z. Impacts of cross-regional population migration and agglomeration on carbon emissions in China. *Appl. Geogr.* **2023**, *159*, 13. [CrossRef]
9. Li, Z.J.; Zhang, W.J.; Sarwar, S.; Hu, M.J. The spatio-temporal interactive effects between ecological urbanization and industrial ecologization in the Yangtze River Delta region. *Sustain. Dev.* **2023**, *31*, 3254–3271. [CrossRef]
10. Wang, S.J.; Fang, C.L.; Sun, L.X.; Su, Y.X.; Chen, X.Z.; Zhou, C.S.; Feng, K.S.; Hubacek, K. Decarbonizing China's Urban Agglomerations. *Ann. Am. Assoc. Geogr.* **2019**, *109*, 266–285. [CrossRef]
11. Deng, X.Z.; Wang, Y.F.; Song, M.L. Development Geography for exploring solutions to promote regional development. *Geogr. Sustain.* **2023**, *4*, 49–57. [CrossRef]
12. Allen, M.R.; Frame, D.J.; Huntingford, C.; Jones, C.D.; Lowe, J.A.; Meinshausen, M.; Meinshausen, N. Warming caused by cumulative carbon emissions towards the trillionth tonne. *Nature* **2009**, *458*, 1163–1166. [CrossRef] [PubMed]
13. Sitch, S.; Huntingford, C.; Gedney, N.; Levy, P.E.; Lomas, M.; Piao, S.L.; Betts, R.; Ciais, P.; Cox, P.; Friedlingstein, P.; et al. Evaluation of the terrestrial carbon cycle, future plant geography and climate-carbon cycle feedbacks using five Dynamic Global Vegetation Models (DGVMs). *Glob. Chang. Biol.* **2008**, *14*, 2015–2039. [CrossRef]
14. Piao, S.L.; He, Y.; Wang, X.H.; Chen, F.H. Estimation of China's terrestrial ecosystem carbon sink: Methods, progress and prospects. *Sci. China-Earth Sci.* **2022**, *65*, 641–651. [CrossRef]
15. Zhou, Y.; Chen, M.X.; Tang, Z.P.; Mei, Z.A. Urbanization, land use change, and carbon emissions: Quantitative assessments for city-level carbon emissions in Beijing-Tianjin-Hebei region. *Sust. Cities Soc.* **2021**, *66*, 12. [CrossRef]
16. Chen, Q.L.; Cai, B.F.; Dhakal, S.; Pei, S.; Liu, C.L.; Shi, X.P.; Hu, F.F. CO_2 emission data for Chinese cities. *Resour. Conserv. Recycl.* **2017**, *126*, 198–208. [CrossRef]
17. Shan, Y.L.; Guan, D.B.; Liu, J.H.; Mi, Z.F.; Liu, Z.; Liu, J.R.; Schroeder, H.; Cai, B.F.; Chen, Y.; Shao, S.; et al. Methodology and applications of city level CO_2 emission accounts in China. *J. Clean. Prod.* **2017**, *161*, 1215–1225. [CrossRef]
18. Whitehead, D.; McNeill, S.J.E.; Mudge, P.L. Regional and national changes in soil carbon stocks with land-use change from 1990 to 2016 for New Zealand. *Reg. Environ. Chang.* **2021**, *21*, 13. [CrossRef]
19. Ye, B.; Jiang, J.L.; Li, C.S.; Miao, L.X.; Tang, J. Quantification and driving force analysis of provincial-level carbon emissions in China. *Appl. Energy* **2017**, *198*, 223–238. [CrossRef]
20. Long, Z.; Zhang, Z.L.; Liang, S.; Chen, X.P.; Ding, B.W.P.; Wang, B.; Chen, Y.B.; Sun, Y.Q.; Li, S.K.; Yang, T. Spatially explicit carbon emissions at the county scale. *Resour. Conserv. Recycl.* **2021**, *173*, 13. [CrossRef]
21. Zhang, D.N.; Zhao, Y.H.; Wu, J.S. Assessment of carbon balance attribution and carbon storage potential in China's terrestrial ecosystem. *Resour. Conserv. Recycl.* **2023**, *189*, 11. [CrossRef]
22. Piao, S.L.; Fang, J.Y.; Ciais, P.; Peylin, P.; Huang, Y.; Sitch, S.; Wang, T. The carbon balance of terrestrial ecosystems in China. *Nature* **2009**, *458*, 1009–1013. [CrossRef]
23. Damm, A.; Guanter, L.; Paul-Limoges, E.; van der Tol, C.; Hueni, A.; Buchmann, N.; Eugster, W.; Ammann, C.; Schaepman, M.E. Far-red sun-induced chlorophyll fluorescence shows ecosystem-specific relationships to gross primary production: An assessment based on observational and modeling approaches. *Remote Sens. Environ.* **2015**, *166*, 91–105. [CrossRef]
24. Zheng, D.; Prince, S.; Wright, R.J.G.C.B. Terrestrial net primary production estimates for 0.5° grid cells from field observations—A contribution to global biogeochemical modeling. *Glob. Chang. Biol.* **2003**, *9*, 46–64. [CrossRef]
25. Cui, X.L.; Wei, X.Q.; Liu, W.; Zhang, F.; Li, Z.H. Spatial and temporal analysis of carbon sources and sinks through land use/cover changes in the Beijing-Tianjin-Hebei urban agglomeration region. *Phys. Chem. Earth* **2019**, *110*, 61–70. [CrossRef]
26. Mohareb, E.; Kennedy, C. Gross Direct and Embodied Carbon Sinks for Urban Inventories. *J. Ind. Ecol.* **2012**, *16*, 302–316. [CrossRef]
27. El Mderssio, M.; Malki, F.; Ikraoun, H.; Ibijbijen, J.; Nassiri, L. Determining parameters to assess carbon stocks in forest ecosystems with Cedrus atlantica Manetti (Atlas Cedar) in Morocco: Specific and generic methods. *Bois For. Trop.* **2022**, *351*, 67–77.

28. Luo, K.; Qiu, Y.; Liu, P.; Mei, Y. *Estimation of Property Value Changes from Nearby Carbon Capture, Utilization, and Storage Projects in the United States*; Elsevier: Washington, DC, USA, 2023.
29. Kazak, J.; Malczyk, J.; Castro, D.G.; Szewrański, S. Carbon sequestration in forest valuation. *Real Estate Manag. Valuat.* **2016**, *24*, 76–86. [CrossRef]
30. Han, J.; Meng, X.; Liang, H.W.; Cao, Z.; Dong, L.; Huang, C. An improved nightlight-based method for modeling urban CO_2 emissions. *Environ. Modell. Softw.* **2018**, *107*, 307–320. [CrossRef]
31. Grant, R.F.; Barr, A.G.; Black, T.A.; Gaumont-Guay, D.; Iwashita, H.; Kidson, J.; McCaughey, H.; Morgenstern, K.; Murayama, S.; Nesic, Z.; et al. Net ecosystem productivity of boreal jack pine stands regenerating from clearcutting under current and future climates. *Glob. Chang. Biol.* **2007**, *13*, 1423–1440. [CrossRef]
32. Li, J.S.; Guo, X.M.; Chuai, X.W.; Xie, F.J.; Yang, F.; Gao, R.Y.; Ji, X.P. Reexamine China's terrestrial ecosystem carbon balance under land use-type and climate change. *Land Use Pol.* **2021**, *102*, 9. [CrossRef]
33. Liu, J.Y.; Yan, Q.Q.; Zhang, M.H. Ecosystem carbon storage considering combined environmental and land-use changes in the future and pathways to carbon neutrality in developed regions. *Sci. Total Environ.* **2023**, *903*, 16. [CrossRef]
34. Feng, H.P.; Kang, P.; Deng, Z.C.; Zhao, W.; Hua, M.; Zhu, X.Y.; Wang, Z. The impact of climate change and human activities to vegetation carbon sequestration variation in Sichuan and Chongqing. *Environ. Res.* **2023**, *238*, 11. [CrossRef]
35. Zhao, J.F.; Xie, H.F.; Ma, J.Y.; Wang, K.L. Integrated remote sensing and model approach for impact assessment of future climate change on the carbon budget of global forest ecosystems. *Glob. Planet. Chang.* **2021**, *203*, 7. [CrossRef]
36. Barrio-Anta, M.; Balboa-Murias, M.A.; Castedo-Dorado, F.; Diéguez-Aranda, U.; Alvarez-González, J.G. An ecoregional model for estimating volume, biomass and carbon pools in maritime pine stands in Galicia (northwestern Spain). *For. Ecol. Manag.* **2006**, *223*, 24–34. [CrossRef]
37. Sun, Z.Z.; Peng, S.S.; Li, X.R.; Guo, Z.D.; Piao, S.L. Changes in forest biomass over China during the 2000s and implications for management. *For. Ecol. Manag.* **2015**, *357*, 76–83. [CrossRef]
38. Yin, L.; Dai, E.F.; Zheng, D.; Wang, Y.H.; Ma, L.; Tong, M. What drives the vegetation dynamics in the Hengduan Mountain region, southwest China: Climate change or human activity? *Ecol. Indic.* **2020**, *112*, 12. [CrossRef]
39. Fetzel, T.; Niedertscheider, M.; Haberl, H.; Krausmann, F.; Erb, K.H. Patterns and changes of land use and land-use efficiency in Africa 1980-2005: An analysis based on the human appropriation of net primary production framework. *Reg. Environ. Chang.* **2016**, *16*, 1507–1520. [CrossRef]
40. Nanzad, L.; Zhang, J.H.; Batdelger, G.; Sharma, T.P.P.; Koju, U.A.; Wang, J.W.; Nabil, M. Analyzing NPP Response of Different Rangeland Types to Climatic Parameters over Mongolia. *Agronomy* **2021**, *11*, 647. [CrossRef]
41. Sanderman, J.; Hengl, T.; Fiske, G.J. Soil carbon debt of 12,000 years of human land use. *Proc. Natl. Acad. Sci. USA* **2017**, *114*, 9575–9580. [CrossRef] [PubMed]
42. Wang, W.X.; Wang, W.J.; Xie, P.C.; Zhao, D.Q. Spatial and temporal disparities of carbon emissions and interregional carbon compensation in major function-oriented zones: A case study of Guangdong province. *J. Clean. Prod.* **2020**, *245*, 13. [CrossRef]
43. Fu, H.Y.; Zhao, S.C.; Liao, C. Spatial governance of Beijing-Tianjin-Hebei urban agglomeration towards low-carbon transition. *China Agric. Econ. Rev.* **2022**, *14*, 774–798. [CrossRef]
44. Xiong, S.W.; Yang, F.; Li, J.Y.; Xu, Z.N.; Ou, J.G. Temporal-spatial variation and regulatory mechanism of carbon budgets in territorial space through the lens of carbon balance: A case of the middle reaches of the Yangtze River urban agglomerations, China. *Ecol. Indic.* **2023**, *154*, 18. [CrossRef]
45. Vaccari, F.P.; Gioli, B.; Toscano, P.; Perrone, C. Carbon dioxide balance assessment of the city of Florence (Italy), and implications for urban planning. *Landsc. Urban Plan.* **2013**, *120*, 138–146. [CrossRef]
46. Ainsworth, E.A.; Davey, P.A.; Hymus, G.J.; Osborne, C.P.; Rogers, A.; Blum, H.; Nösberger, J.; Long, S.P. Is stimulation of leaf photosynthesis by elevated carbon dioxide concentration maintained in the long term?: A test with Lolium perenne grown for 10 years at two nitrogen fertilization levels under Free Air CO_2 Enrichment (FACE). *Plant Cell Environ.* **2003**, *26*, 705–714. [CrossRef]
47. Zamolodchikov, D.G.; Karelin, D.V.; Zukert, N.V. Geoinformational model of the carbon budget of the Russian tundra zone. *Izv. Akad. Nauk Ser. Biol.* **2000**, 239–247.
48. Zhang, Z.L.; Yu, X.P.; Hou, Y.Z.; Chen, T.H.; Lu, Y.; Sun, H.H. Carbon Emission Patterns and Carbon Balance Zoning in Urban Territorial Spaces Based on Multisource Data: A Case Study of Suzhou City, China. *Isprs Int. J. Geo-Inf.* **2023**, *12*, 385. [CrossRef]
49. Zhao, R.Q.; Zhang, S.; Huang, X.J.; Qin, Y.C.; Liu, Y.; Ding, M.; Jiao, S. Spatial variation of carbon budget and carbon balance zoning of Central Plains Economic Region at county-level. *Acta Geogr. Sin.* **2014**, *69*, 1425–1437.
50. Guo, X.M.; Fang, C.L. How does urbanization affect energy carbon emissions under the background of carbon neutrality? *J. Environ. Manag.* **2023**, *327*, 10.
51. Zhu, W.Q.; Pan, Y.Z.; Hu, H.B.; Li, J.; Gong, P. Estimating net primary productivity of terrestrial vegetation based on remote sensing: A case study in Inner Mongolia, China. In Proceedings of the IEEE International Geoscience and Remote Sensing Symposium, Anchorage, AK, USA, 20–24 September 2004; pp. 528–531.
52. Zhuang, S.Y.; Wang, J.; Sun, X.; Wang, M.K. Effect of forest thinning on soil net nitrogen mineralization and nitrification in a Cryptomeria japonica plantation in Taiwan. *J. For. Res.* **2014**, *25*, 571–578. [CrossRef]
53. Ma, L.; Xiang, L.G.; Wang, C.; Chen, N.C.; Wang, W. Spatiotemporal evolution of urban carbon balance and its response to new-type urbanization: A case of the middle reaches of the Yangtze River Urban Agglomerations, China. *J. Clean. Prod.* **2022**, *380*, 14. [CrossRef]

54. Rong, T.Q.; Zhang, P.Y.; Jing, W.L.; Zhang, Y.; Li, Y.Y.; Yang, D.; Yang, J.X.; Chang, H.; Ge, L.N. Carbon Dioxide Emissions and Their Driving Forces of Land Use Change Based on Economic Contributive Coefficient (ECC) and Ecological Support Coefficient (ESC) in the Lower Yellow River Region (1995–2018). *Energies* **2020**, *13*, 2600. [CrossRef]
55. Wen, H.; Li, Y.; Li, Z.R.; Cai, X.X.; Wang, F.X. Spatial Differentiation of Carbon Budgets and Carbon Balance Zoning in China Based on the Land Use Perspective. *Sustainability* **2022**, *14*, 12962. [CrossRef]
56. Xue, H.; Shi, Z.Q.; Huo, J.G.; Zhu, W.B.; Wang, Z.Y. Spatial difference of carbon budget and carbon balance zoning based on land use change: A case study of Henan Province, China. *Environ. Sci. Pollut. Res.* **2023**, *30*, 109145–109161. [CrossRef]
57. Chuai, X.W.; Yuan, Y.; Zhang, X.Y.; Guo, X.M.; Zhang, X.L.; Xie, F.J.; Zhao, R.Q.; Li, J.B. Multiangle land use-linked carbon balance examination in Nanjing City, China. *Land Use Pol.* **2019**, *84*, 305–315. [CrossRef]
58. Liu, S.N.; Zhou, T.; Wei, L.Y.; Shu, Y. The spatial distribution of forest carbon sinks and sources in China. *Chin. Sci. Bull.* **2012**, *57*, 1699–1707. [CrossRef]
59. Zhang, D.; Wang, Z.Q.; Li, S.C.; Zhang, H.W. Impact of Land Urbanization on Carbon Emissions in Urban Agglomerations of the Middle Reaches of the Yangtze River. *Int. J. Environ. Res. Public Health* **2021**, *18*, 1403. [CrossRef] [PubMed]
60. Zhu, B.Z.; Zhang, M.F.; Zhou, Y.H.; Wang, P.; Sheng, J.C.; He, K.J.; Wei, Y.M.; Xie, R. Exploring the effect of industrial structure adjustment on interprovincial green development efficiency in China: A novel integrated approach. *Energy Policy* **2019**, *134*, 12. [CrossRef]
61. Zhao, Y.H.; Su, Q.; Li, B.K.; Zhang, Y.Y.; Wang, X.J.; Zhao, H.R.; Guo, S. Have those countries declaring "zero carbon" or "carbon neutral" climate goals achieved carbon emissions-economic growth decoupling? *J. Clean. Prod.* **2022**, *363*, 19. [CrossRef]
62. Zhan, J.Y.; Wang, C.; Wang, H.H.; Zhang, F.; Li, Z.H. Pathways to achieve carbon emission peak and carbon neutrality by 2060: A case study in the Beijing-Tianjin-Hebei region, China. *Renew. Sust. Energ. Rev.* **2024**, *189*, 15. [CrossRef]
63. Chen, J.D.; Li, Z.W.; Song, M.L.; Dong, Y.Z. Decomposing the global carbon balance pressure index: Evidence from 77 countries. *Environ. Sci. Pollut. Res.* **2021**, *28*, 7016–7031. [CrossRef]
64. Chuai, X.W.; Huang, X.J.; Lu, Q.L.; Zhang, M.; Zhao, R.Q.; Lu, J.Y. Spatiotemporal Changes of Built-Up Land Expansion and Carbon Emissions Caused by the Chinese Construction Industry. *Environ. Sci. Technol.* **2015**, *49*, 13021–13030. [CrossRef]
65. Zhu, W.W.; Zhu, Y.Q.; Lin, H.P.; Yu, Y. Technology progress bias, industrial structure adjustment, and regional industrial economic growth motivation—Research on regional industrial transformation and upgrading based on the effect of learning by doing. *Technol. Forecast. Soc. Chang.* **2021**, *170*, 12. [CrossRef]
66. Wang, Y.; Deng, X.Z.; Zhang, H.W.; Liu, Y.J.; Yue, T.X.; Liu, G. Energy endowment, environmental regulation, and energy efficiency: Evidence from China. *Technol. Forecast. Soc. Chang.* **2022**, *177*, 9. [CrossRef]
67. Zhang, F.; Deng, X.Z.; Phillips, F.; Fang, C.L.; Wang, C. Impacts of industrial structure and technical progress on carbon emission intensity: Evidence from 281 cities in China. *Technol. Forecast. Soc. Chang.* **2020**, *154*, 10. [CrossRef]

land

MDPI

Article

Rethinking Regional High-Quality Development Pathways from a Carbon Emission Efficiency Perspective

Chao Wang [1], Yuxiao Kong [2], Xingliang Lu [2], Hongyi Xie [3], Yanmin Teng [4] and Jinyan Zhan [2,*]

[1] School of Labor Economics, Capital University of Economics and Business, Beijing 100070, China; wangc@cueb.edu.cn
[2] State Key Laboratory of Water Environment Simulation, School of Environment, Beijing Normal University, Beijing 100875, China; 202111180038@mail.bnu.edu.cn (Y.K.); 202111180020@mail.bnu.edu.cn (X.L.)
[3] Department of Environmental Science and Engineering, Fudan University, Shanghai 200433, China; hyxie22@m.fudan.edu.cn
[4] Research Center for Eco-Environmental Engineering, Dongguan University of Technology, Dongguan 523808, China; tengym@dgut.edu.cn
* Correspondence: zhanjy@bnu.edu.cn

Abstract: Optimizing resource efficiency and mitigating climate change have become consensuses of human society. However, there is still a gap in assessing the carbon emission efficiency (CEE) and identifying the influence of various factors, especially in rapid urbanizing regions. In this paper, we built a stochastic frontier analysis model to assess CEE and conducted a case study in the Beijing–Tianjin–Hebei Urban Agglomeration (BTHUA), a typical area of collaborative development in China. A comprehensive influencing factor index was constructed to analyze and identify the key influencing factors of CEE. The results revealed that the average CEE among the 13 cities increased in volatility from 2000 to 2019. The average CEE in Langfang was lowest, while that in Tangshan was highest. The input-related factors had a negative effect on CEE, including carbon emissions per capita, employment per ten thousand people, total assets per capita, and energy intensity. GDP per capita, the urbanization level, and the proportion of the tertiary sector's GDP had positive impacts on CEE. Future policy formulation should focus on the transition from labor- and material-intensive industries to knowledge- and technology-intensive industries. All the results can contribute to achieving high-quality development and dual-carbon target of rapid-urbanizing areas.

Keywords: carbon emission efficiency; carbon reduction; influencing factor; stochastic frontier analysis; urban agglomeration; Beijing–Tianjin–Hebei

Citation: Wang, C.; Kong, Y.; Lu, X.; Xie, H.; Teng, Y.; Zhan, J. Rethinking Regional High-Quality Development Pathways from a Carbon Emission Efficiency Perspective. *Land* **2024**, *13*, 1441. https://doi.org/10.3390/land13091441

Academic Editor: Yan Li

Received: 25 July 2024
Revised: 3 September 2024
Accepted: 4 September 2024
Published: 5 September 2024

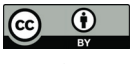

1. Introduction

Since the 20th century, global warming has made profound impacts on human society and has attracted increasing attention from all countries in the world. The IPCC report indicated that approximately 95% of the warming could be attributed to greenhouse gas (GHG) emissions over the past 50 years [1]. CO_2 is an important GHG causing the greenhouse effect. China is currently the global largest energy consumer and CO_2 emitter [2]. China's economic growth is predominantly driven by traditional industries, causing a large amount of fossil fuel consumption and infrastructure construction, which exert tremendous pressure on CO_2 emissions and climate change [3]. In order to control the carbon emissions and mitigate climate change, China pledged to peak carbon emissions by 2030 and achieve carbon neutrality by 2060, aiming to decouple economic development from carbon emissions. However, China's economic development and urbanization process continues to rapidly improve. Therefore, how to achieve greater economic development with fewer carbon emissions has become a problem that needs to be solved [4]. The concepts of high-quality and low-carbon developments have emerged to serve sustainable development. The key to achieving high-quality development lies in understanding the relationship

between economic development and the ecological environment. Improving ecological efficiency is key and urgent for regional development, in line with the requirement of green supply chain management (GSCM) [5]. The concept of carbon emission efficiency (CEE) has gained significant attention alongside the emergence of a low-carbon economy [6–8]. CEE serves as a crucial indicator that visually represents the relationship between regional economic development and carbon emissions, and it is essential for the estimation and monitoring of the ecological performance of a regional supply chain. Reducing carbon emissions and improving CEE have become global consensuses for the development of a low-carbon economy [9]. CEE assessments and analysis of its determinants have become research hot-spots.

The Beijing–Tianjin–Hebei Urban Agglomeration (BTHUA) is the largest economic zone in northern China and a vital part of China's supply chain, which has undergone rapid urbanization and industrialization. With the rapid development process, a greater number of problems have come into view and have attracted widespread attention, including those associated with the environment, population, resource utilization, and industrial structure. The burden of carbon emission reduction is huge for the BTHUA [10]. Meanwhile, the BTHUA is pursuing coordinated development and exploring valid pathways to optimize the energy structure and update and upgrade the industrial structure. Industrial restructuring and energy-structure optimization are urgent when pursuing sustainable and high-quality development [11]. Using the BTHUA as a representative study area when researching carbon emission reduction provides valuable insights for the formulation of carbon reduction strategies in other urban agglomerations with similar characteristics.

The purpose of this study was to evaluate the CEE of cities in the BTHUA and identify key influencing factors, supporting low-carbon and economic goals. The main objectives of this study were as follows: (1) to incorporate carbon emissions into traditional production functions and use the stochastic frontier function (SFA) method to build CEE estimation models; (2) to clarify the quantitative relationships between input and output factors and evaluate the CEE of prefecture-level cities in the BTHUA; (3) to construct an index system of the influencing factors of CEE and use the quantitative regression function to identify the key influencing factors of CEE and their characteristics; and (4) to propose specific policies to improve CEE, pursuing carbon emissions and economic development. All the findings contribute to the related policy formulation of industrial restructures, low-carbon transformations, and high-quality development for the BTHUA and other rapid-urbanizing areas.

2. Literature Review

In 1992, the United Nations Conference on Environment and Development introduced the concept of ecological efficiency, which represents the extent to which human needs are met per unit of resource used when using a unit of resource. Ecological efficiency can describe the input–output process of production activities, where inputs are the energy consumption or environmental losses of economic units and outputs are the products or services they provide [12]. Currently, ecological efficiency integrates the economy and ecosystems, becoming an increasingly crucial metric for policymakers and managers. In general, ecological efficiency focuses more on the relationship between macro-energy, macro-resources, and economic development but does not incorporate the role of carbon emissions in efficiency.

As sustainable development and decarbonization goals gain prominence, carbon emissions have gradually become an integral part of ecological efficiency research. Carbon emissions are the main GHG causing global warming. Enkvist et al. (2008) mentioned the concept of carbon productivity, also known as carbon intensity of GDP, which combines two expected goals in economic development, i.e., GDP growth and carbon emission control [13]. The concept of CEE has gradually become an important index to represent the greenness of a production process. At present, there is no clear and unified definition of CEE [14]. Most scholars define CEE as achieving higher economic growth with lower

carbon emissions. It is generally believed that when economic growth is certain, the fewer the carbon emissions and the higher the efficiency [15]. CEE combines economy, energy, and CO_2 in the production process, and can be expressed as a single-factor indicator such as carbon emissions per unit of GDP [16,17]. Similarly, energy efficiency was defined as the output per unit of energy consumption based on Pareto efficiency, considering energy to be an indispensable input factor in production processes [18]. Using this definition, metrics such as energy consumption or carbon emissions per unit of product or building area also can be developed. However, these single-factor indicators can only reflect certain aspects of ecological efficiency and overlook input factors and input–output relationships in production processes [19]. Energy efficiency represents the relationship between energy inputs and GDP outputs but does not consider carbon emissions and other input factors. Carbon productivity emphasizes the relationship between carbon emissions and economic added value but overlooks the influences of energy and other inputs.

Taking into account the input–output variables in the production process, more integrated models were developed. Total-factor productivity was also integrated into ecological efficiency. The total-factor carbon emission efficiency index can be defined as the ratio of target carbon emissions to actual carbon emissions [20]. Consequently, more comprehensive indicators and evaluation methods for CEE have been developed [21]. The methods widely used mainly include parametric methods (namely, data envelopment analysis (DEA)) and non-parametric methods (namely, SFA) [22,23]. Zhou et al. (2010) used DEA to evaluate the total-factor CEE of 18 high-carbon-emitting countries worldwide and found a 24% improvement in CEE from 1997 to 2004, suggesting that technology progress played a significant role in the improvement of CEE [24]. Meng et al. (2016) used DEA-type models to assess the energy efficiency and CEE of 30 Chinese provinces/regions during 2006–2015 and found that the east area had relative high efficiency values, while the central area had lower efficiency values [25]. Zhou et al. (2019) combined super-efficiency DEA and the global vector autoregressive (GVAR) model and discovered that there was a gradual decrease in the CEE of China's construction industry and that technology advancements and energy-structure adjustments were efficacious avenues for improvement [26]. DEA models have also been used to evaluate efficiency in various contexts such as technical efficiency [27], ecological efficiency in cities [28], environmental efficiency in industrial sectors [29], green economic growth levels [30], performance analyses of finance companies [31], and forestry efficiency [32]. In contrast, SFA is a parameterized method that provides a specific function to represent the relationship between input and output factors. Lin and Wang (2015) estimated the total-factor CEE of the steel industry in various Chinese provinces using the SFA method and further evaluated the carbon emission reduction potential [33]. Bai et al. (2017) quantitatively measured the environmental performance and carbon emission reduction potential of 39 industrial sectors in China using SFA [34]. Sun et al. (2019) evaluated the GHG emission efficiency of 26 industry sectors in China and analyzed the impacts of the determinants based on the SFA method [35]. Additionally, SFA has been employed to assess other forms of efficiency such as land use efficiency [36], energy efficiency [37], and agricultural production efficiency [38]. Therefore, both DEA and SFA can be used to assess the CEE of various decision units.

In contrast, SFA, as a parameter-based method to evaluate efficiency, employs fundamental theories like production functions and directional distance functions to assess efficiency. It precisely represents the functional relationship between input and output factors, with efficiency results ranging from 0 to 1, thereby addressing some of the limitations of DEA. Therefore, SFA was used to construct the CEE estimation model in this study. Furthermore, current research primarily focuses on the assessment of CEE, and there is a need for the further analysis of regional CEE and the development of a comprehensive indicator system for influencing factors to provide scientific guidance for regional productivity improvements.

3. Study Area and Data Sources

3.1. Study Area

The BTHUA includes Beijing (the capital of China), Tianjin (a municipality), and Hebei (a province) and is located on the North China Plain in the east of China (Figure 1). The elevation is high in the northwest and low in the southeast. There are thirteen prefecture-level cities in the BTHUA, including Beijing, Tianjin, Baoding, Shijiazhuang, Cangzhou, Chengde, Handan, Hengshui, Langfang, Qinhuangdao, Tangshan, Xingtai, and Zhangjiakou. The BTHUA is a highly representative region in China as well as globally, with typical characteristics of rapid economic development, urbanization, industrialization, and coordinated development. The GDP increased from CNY 9.4977×10^{12} in 2000 to CNY 8.4479×10^{13} in 2019. However, with the background of climate change and the requirements of SDGs and high-quality development, the BTHUA is urgently required to deal with the decoupling of carbon emissions and economic growth, contributing to the achievements of sustainable development and the dual-carbon target [39,40]. Therefore, taking the BTHUA as the study area, investigating the temporal and spatial characteristics of CEE and identifying its determinants are significant for the regional policy formulation of carbon reduction and economic regulations.

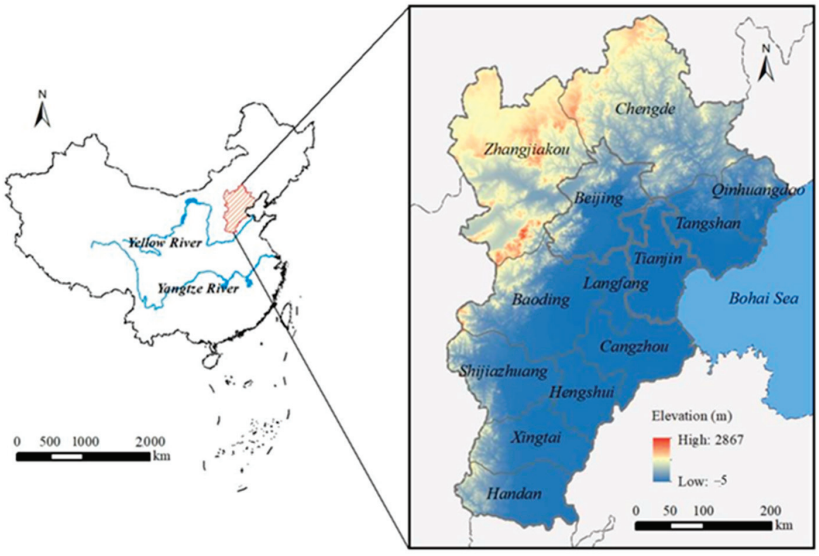

Figure 1. Location of the Beijing–Tianjin–Hebei Urban Agglomeration (BTHUA).

3.2. Data Sources

The original data used in this study mainly included carbon emission data and socio-economic data. Carbon emission data were calculated using the carbon emission factor method. We included energy-based carbon emissions, industrial-process-related carbon emissions, and other carbon emissions within the accounting scope of the carbon emissions [11]. The energy-based carbon emissions accounted for 17 types of energy, i.e., raw coal, washed coal, other washed coal, coal briquettes, coke, coke oven gas, other oven gas, other coking products, gasoline, crude oil, diesel, kerosene, fuel oil, other petroleum products, refinery dry gas, liquefied petroleum gas, and natural gas. The energy data were derived from local and national statistical yearbooks (2001–2020) and the CEDA database (https://www.ceads.net/, accessed on 1 July 2024). The industrial-process-related carbon emissions were derived from the CEDA database. The other carbon emissions included agricultural carbon emissions, animal husbandry carbon emissions, and human respiration. The statistical data related to agricultural activities (fertilizer, pesticides, crop planting areas,

agricultural machinery power, irrigation, and agricultural films), livestock (pigs, cattle, sheep, and poultry), and population were derived from statistical yearbooks (2001–2020). The socio-economic data primarily included the GDP, population, fixed investment, labor, foreign investment, and other relevant indicators. All the economic data were adjusted to the 2000 price level. The carbon emission coefficients referred to the IPCC (2006) [41] and related literature [42–44].

4. Methods

4.1. Carbon Emission Efficiency (CEE) Estimation Model

The production function is a prerequisite and the foundation when measuring production efficiency. The basic model is as follows:

$$y_i = f(x_i, \beta) exp(v_i - u_i) \tag{1}$$

where y_i represents the output of unit i; x_i represents the input elements; $f(*)$ represents the production function; β represents the vector of parameters to be estimated; v_i represents observation errors and other random factors, and is an independent random variable following a standard normal distribution; and μ_i represents technical inefficiency terms, which are non-negative variables and can be assumed to follow either a half-normal distribution or a truncated normal distribution. In addition, v_i and μ_i are independent of each other.

Based on the SFA method, technical efficiency (TE) in actual production can be expressed as the ratio of the expected value of a sample to the expected value of the stochastic frontier. In other words, the technical efficiency is equivalent to the ratio between the mean actual output and the mean theoretical maximum output.

$$TE_i = \frac{f(X_i, \beta) exp\lambda(v_i - u_i)}{f(X_i, \beta) exp\lambda(v_i)} = exp(-\mu_i) \tag{2}$$

where TE_i represents the technical efficiency of unit i.

In the CEE stimulation model, capital, labor, and carbon emissions were considered to be the input variables and economic growth was considered to be the output variable. The production function can be expressed as follows:

$$P^j(K, L, C) = \{(K, L, C, Y) : (K, L, C)\ can\ produce(Y)\}, j = 1 \ldots\ldots J \tag{3}$$

$$Input\ variable:\ x = (K,\ L, C) \in R_N^+ \tag{4}$$

$$Output\ variable:\ y \in R_M^+ \tag{5}$$

where K is the capital amount, L is the labor force, C is the carbon emission, and Y is the economic output. The decision making unit (DMU) was the prefecture-level city in this study.

Compared with traditional production functions, the trans-log production function offers greater flexibility and considers both the effects of variables on themselves and their interactions. This makes it well-suited for the study of the relationships between input and output variables. Additionally, the trans-log production function can effectively fit data [45]. Therefore, in this study, we chose the trans-log production function to establish a CEE estimation model. The specific form of the SFA model was as follows:

$$\begin{gathered} y_i = \beta_o + \beta_k k_{it} + \beta_l l_{it} + \beta_c c_{it} + \frac{1}{2}\beta_{kk}(k_{it})^2 + \frac{1}{2}\beta_{ll}(l_{it})^2 + \frac{1}{2}\beta_{cc}(c_{it})^2 + \beta_{kl} k_{it} l_{it} + \\ \beta_{kc} k_{it} c_{it} + \beta_{lc} l_{it} c_{it} + v_{it} - u_{it} \end{gathered} \tag{6}$$

$$v_{it} \sim N\left(0, \sigma_v^2\right) \tag{7}$$

$$u_{it} = exp\{-\eta(t - T_i)\}u_i \tag{8}$$

$$u_{it} \sim N\left(m_{it}, \sigma_u^2\right) \tag{9}$$

$$m_{it} = z_{it}\delta \tag{10}$$

$$k_{it} = lnK_{it} \tag{11}$$

$$l_{it} = lnL_{it} \tag{12}$$

$$c_{it} = lnC_{it} \tag{13}$$

$$y_{it} = lnY_{it} \tag{14}$$

where z_{it} represents other factors, except for technical efficiency; m_{it} represents an inefficiency term; and δ represents the estimated parameter. Capital input K, labor input L, carbon emissions C, and economic output Y were taken as a logarithm.

Furthermore, by subtracting c_{it} from both sides of the equation, we obtained new equations as follows:

$$\begin{gathered} y_i - c_{it} = \beta_o + \beta_k k_{it} + \beta_l l_{it} + (\beta_c - 1)c_{it} + \frac{1}{2}\beta_{kk}(k_{it})^2 + \frac{1}{2}\beta_{ll}(l_{it})^2 + \frac{1}{2}\beta_{cc}(c_{it})^2 + \\ \beta_{kl}k_{it}l_{it} + \beta_{kc}k_{it}c_{it} + \beta_{lc}l_{it}c_{it} + v_{it} - u_{it} \end{gathered} \tag{15}$$

$$\ln\left(\frac{Y_{it}}{C_{it}}\right) = y_i - c_{it} \tag{16}$$

The specific formula used to evaluate CEE in this paper was as follows:

$$CEE_{it} = \frac{E(Y_{it}/C_{it})}{E(Y_{it}/C_{it}|u_{it} = 0)} = \frac{exp(\beta_o + \ldots + v_{it} - \mu_i)}{exp(\beta_o + \ldots + v_{it})} = exp(-\mu_i) \tag{17}$$

According to the equation, $0 < CEE_{it} < 1$. When CP_{it} approached 0, CEE was low; when CP_{it} approached 1, CEE was high, revealing that the unit was close to the stochastic frontier.

4.2. Tobit Regression Model

A Tobit linear regression model was used to establish an explanatory relationship between the dependent variable (expenditure) and the independent variables for durable goods [46], as shown in the following equation:

$$y_i = \beta^T x_i + e_i;\ e_i \sim N(0, 1) \tag{18}$$

where y_i represents the dependent variable, x_i represents the independent variable, and β^T represents the regression parameter. Therefore, the specific formula for the influencing factor analysis of CEE was as follows:

$$\begin{gathered} CEE_{it} = \gamma_i + \beta_1 gdp_{it} + \beta_2 car_{it} + \beta_3 lab_{it} + \beta_4 cap_{it} + \beta_5 urb_{it} + \beta_6 pop_{it} + \beta_7 ind3_{it} + \\ \beta_8 ind3_{it} + \beta_9 ene_{it} + \beta_{10} ope_{it} + \beta_{11} gov_{it} + u_{it} \\ CEE_{it} = \begin{cases} CEE_{it}{}^*, if\ CEE \geq 0 \\ 0, \text{ other} \end{cases} \end{gathered} \tag{19}$$

where $CEE_{it}{}^{*}$ is *CEE* for the *i*-th city in the *t*-th year, as the dependent variable; $\beta_1-\beta_{11}$ are estimated parameters for the corresponding variables; γ_i represents the individual difference; and u_{it} represents the random error term. Four basic influencing factors, including gdp_{it} (GDP per capita), car_{it} (carbon emissions per capita), lab_{it} (employment per ten thousand people), and cap_{it} (total assets per capita), were considered to be the independent variables. urb_{it}, pop_{it}, $ind2_{it}$, $ind3_{it}$, ene_{it}, ope_{it}, and gov_{it} represented the proportions of urban population, population per unit land area, proportion of the secondary sector's GDP, proportion of the tertiary sector's GDP, energy consumption per unit of GDP, proportion of foreign direct investment in GDP, and proportion of local government fiscal expenditure in GDP, respectively. The meanings of the factors are explained in Table 1. Nine aspects, including economic level, technological level, input level, urbanization level, population density, industrial structure, energy intensity, level of opening up, and government intervention, were considered to analyze the impacts of the influencing factors of *CEE*.

Table 1. Influencing factor index of carbon emission efficiency (CEE).

Estimated Parameter	Variable	Influencing Factor	Aspect
β_1	gdp_{it}	GDP per capita	Economic level
β_2	car_{it}	Carbon emissions per capita	Technological level
β_3	lab_{it}	Employment per ten thousand people	Input level
β_4	cap_{it}	Total assets per capita	Input level
β_5	urb_{it}	Proportion of urban population	Urbanization level
β_6	pop_{it}	Population per unit land area	Population density
β_7	$ind2_{it}$	Proportion of the secondary sector's GDP	Industrial structure
β_8	$ind3_{it}$	Proportion of the tertiary sector's GDP	Industrial structure
β_9	ene_{it}	Energy consumption per unit of GDP	Energy intensity
β_{10}	ope_{it}	Proportion of foreign direct investment in GDP	Level of opening up
β_{11}	gov_{it}	Proportion of local government fiscal expenditure in GDP	Government intervention

5. Results

5.1. Variable Statistics and Model Testing

Panel data were used to estimate CEE for the 13 prefecture-level city levels in the BTHUA from 2000 to 2019. The statistics for the basic variables are shown in Table 2. Specifically, this analysis involved a total sample size of 260 observations. The CEE model employed the total assets, year-end employment, and total carbon emissions as proxies for the capital (K), labor (L), and carbon emissions (C), respectively, while GDP was used to represent the economic output (Y).

Table 2. Summary statistics of the variables for the CEE model.

Variable	Indicator	Obs	Unit	Mean	Maximum	Minimum	Standard Deviation
Capital (K)	Total assets	260	Billion CNY	1517.22	1807.05	33.84	9388.40
Labor (L)	Year-end employment	260	Ten thousand people	114.82	182.38	21.00	878.05
Carbon emissions (C)	Total carbon emissions	260	Ten thousand metric tons	4837.80	2922.93	224.29	11,685.87
Economic output (Y)	GDP	260	Billion CNY	2550.74	3829.57	163.03	24,591.17

Table 3 presents the coefficient values for the variables in the CEE estimation model. The overall model reliability was notably high, as indicated by a log-likelihood value of 128.844. Except for the non-significant coefficient estimates of capital (*lnK*) and labor (*lnL*) in the first-order terms, all the coefficients demonstrated significance at the 5% level or

higher. Carbon emissions exhibited a negative impact on CEE at a significance level of 1%, with a coefficient of −0.8865, indicating that a 1% increase in carbon emissions led to a 0.8865% reduction in CEE. This finding aligned with practical production processes, where higher carbon emissions tend to correspond with a lower CEE when other factors remain constant. Therefore, the CEE estimation model based on SFA and the CEE results were reliable and used to further analyze the spatiotemporal variations and influencing factors of CEE.

Table 3. The parameter assessment results for the SFA model.

Estimated Variable	Coef. Value	Std. Err.	z	*p*-Value
_cons	3.7777 **	1.5607	2.42	0.016
lnK	−0.0460	0.1370	−0.34	0.737
lnL	−0.4802	0.3276	−1.47	0.143
lnC	−0.8865 ***	0.2379	−3.73	0.000
$(lnK)^2$	0.1076 ***	0.0148	7.28	0.000
$(lnL)^2$	0.1117 ***	0.0237	4.71	0.000
$(lnC)^2$	0.3441 ***	0.0375	9.17	0.000
lnK×lnL	0.1147 ***	0.0280	4.09	0.000
lnK×lnC	−0.3339 ***	0.0379	−8.81	0.000
lnL×lnC	−0.2421 ***	0.0598	−4.05	0.000
Number of Obs = 260				Wald chi2 (9) = 4871.16
Log-likelihood = 128.844				Prob > chi2 = 0.000

*, **, and *** represent confidence at significance levels of 10%, 5%, and 1%, respectively.

5.2. Spatial and Temporal Variations in Carbon Emission Efficiency

Figure 2 shows the distribution of CEE across the 13 cities in the BTHUA from 2000 to 2019. The CEE distribution exhibited a left-skewed pattern, with a minimum value of 0.5065 (Langfang, in 2015) and a maximum value of 0.9810 (Beijing, in 2019). Of the 260 efficiency values, 70 fell within the range of 0.90 to 0.95, with a median of 0.8677 (Cangzhou, in 2019). Additionally, approximately 3.85% of the efficiency values were less than or equal to 0.60, while 64.62% were less than or equal to 0.90. This indicated that the overall CEE values in the BTHUA were relatively high, with a mean value of 0.8410. From a regionwide perspective, the mean value of CEE among the 13 cities fluctuated and increased during 2000–2019 (Figure 3). Specifically, the variations could be divided into four stages, i.e., a weak decrease from 2000 to 2005, a rapid increase from 2005 to 2008, a weak decrease from 2008 to 2015, and a rapid increase from 2015 to 2019.

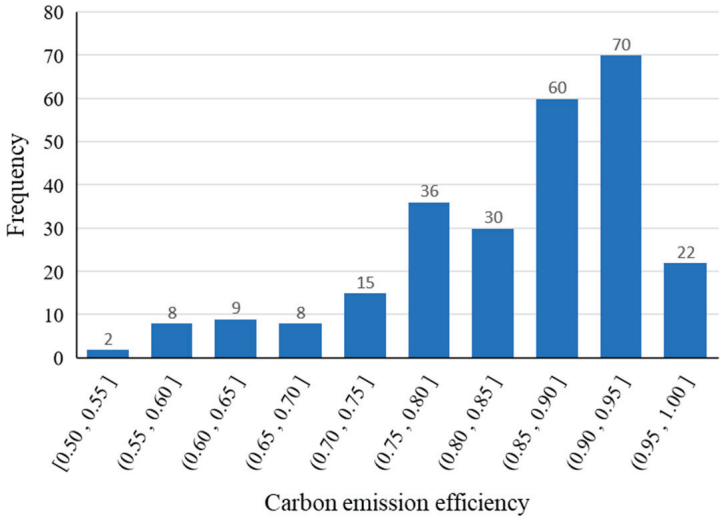

Figure 2. Frequency distribution of carbon emission efficiency in the BTHUA.

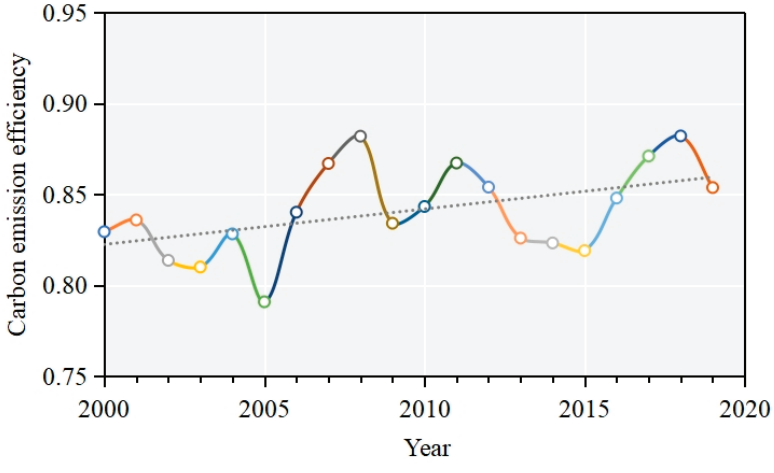

Figure 3. Variations in the average carbon emission efficiency of the BTHUA.

As shown in Figure 4, there were significant differences in the CEE levels among the 13 cities during 2000–2019. In terms of average CEE values, Langfang had the lowest CEE, with a mean value of 0.6799. In contrast, Tangshan and Hengshui exhibited high CEE levels, with mean values exceeding 0.9 (0.9475 and 0.9127, respectively). Beijing, Handan, and Zhangjiakou had moderately high average CEE values, slightly above 0.8 and below 0.9 (0.8172, 0.8090, and 0.8056, respectively). Tianjin and Baoding had lower average CEE values below 0.8 (0.7848 and 0.7853, respectively). Qinhuangdao, Shijiazhuang, and Xingtai had similar ranges in their CEE values, with small differences (0.8936, 0.8948, and 0.8694, respectively). In terms of the range in CEE variations, Hengshui and Tangshan consistently maintained higher efficiency levels compared with other cities, with very concentrated value distributions. Specifically, the minimum and maximum CEE values for Hengshui were 0.8569 (in 2014) and 0.9643 (in 2000), respectively, while for Tangshan, they were 0.9225 (in 2016) and 0.9660 (in 2011), respectively. Beijing, Tianjin, Baoding, and Handan had wider value distributions (greater variability), whereas Zhangjiakou had a narrower

value distribution (lower variability). Additionally, Cangzhou and Chengde had similar ranges in their CEE values but Cangzhou had a higher overall average CEE value than Chengde (0.8822 > 0.8507).

As observed in Figure 5, Beijing's CEE fluctuated and increased over the period, remaining below 0.8 before 2005 and rising above 0.85 after 2006.Tianjin's CEE followed an N-shaped trend, which indicated that CEE initially increased during 2000–2005, then decreased during 2005–2015, and finally increased during 2015–2019. Baoding's CEE initially fluctuated during 2000–2005 and then stabilized during 2005–2019. Cangzhou's CEE initially rapidly increased during 2000–2005 and then slightly declined during 2005–2019. Chengde's CEE exhibited significant fluctuations, with two distinct phases of continuous increase during 2001–2008 and continuous decrease from 2011 to 2017. Handan's CEE experienced an initial growth phase during 2000–2008, followed by a fluctuating decline after 2008, with a peak value of 0.9252 (the only CEE value above 0.9). Hengshui consistently maintained a relatively high CEE but showed a subtle declining trend. Langfang's CEE slightly declined during 2000–2015, followed by a rapid increase after 2015, reaching 0.9089 in 2019. Qinhuangdao's CEE showed no clear variation pattern and maintained relatively high levels. Shijiazhuang's CEE fluctuated and decreased from 0.9325 in 2000 to 0.7627 in 2019. Tangshan consistently maintained a high and stable CEE, with minimal overall variations. Xingtai's CEE fluctuated and decreased from 0.9060 in 2000 to 0.7666 in 2019. Zhangjiakou's CEE had an overall stable tendency and showed no clear variation pattern.

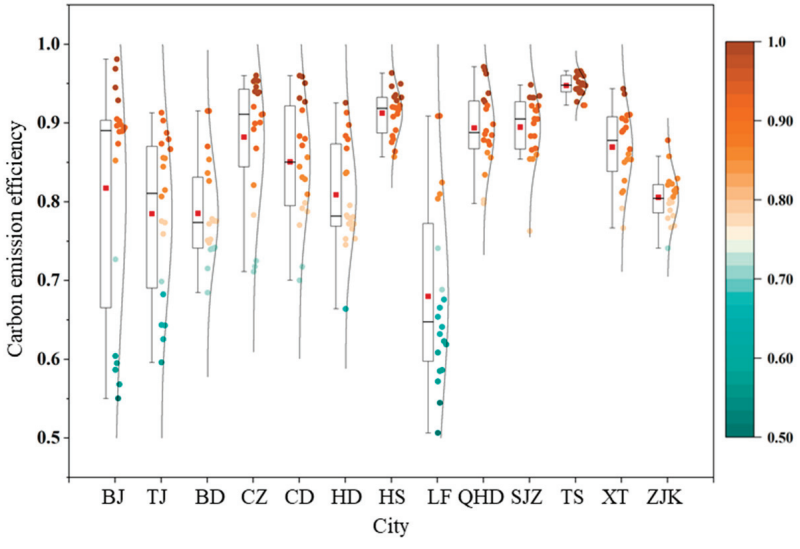

Figure 4. A box plot of carbon emission efficiency of 13 cities in the BTHUA. (BJ: Beijing; TJ: Tianjin; BD: Baoding; CZ: Cangzhou; CD: Chengde; HD: Handan; HS: Hengshui; LF: Langfang; QHD: Qinhuangdao; SJZ: Shijiazhuang; TS: Tangshan; XT: Xingtai; ZJK: Zhangjiakou).

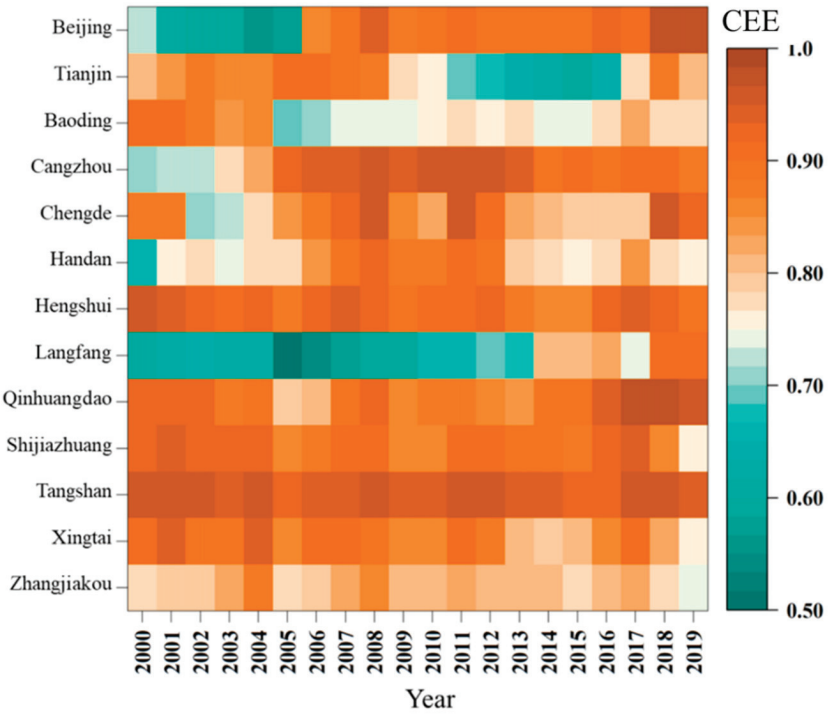

Figure 5. The changes in CEE of 13 cities in the BTHUA.

From 2000 to 2019, CEE in the BTHUA exhibited distinct spatial variations, as shown in Figure 6. The CEE values demonstrated clear spatial clustering, with noticeable clusters of low- and high-efficiency areas. In 2000, CEE in the region exhibited a spatial distribution characterized by two high-efficiency clusters in the southwest and northeast regions. In 2005, there were two prominent clusters emerging: a high-value area along the eastern Bohai Sea region and an extremely low-value area encompassing Beijing and Langfang. By 2010, the spatial distribution became relatively homogeneous, with a slightly lower CEE zone in the Baoding–Langfang–Tianjin region across the east–west axis, while Tangshan, Cangzhou, and Hengshui displayed higher efficiency values in the eastern zone. In 2015, Tianjin city exhibited extremely low CEE values, leading to an overall spatial distribution pattern characterized by lower efficiency in the northwest and higher efficiency in the southeast. By 2019, there was a clear spatial distribution pattern in the CEE values, with a gradual increase from the southwest to the northeast.

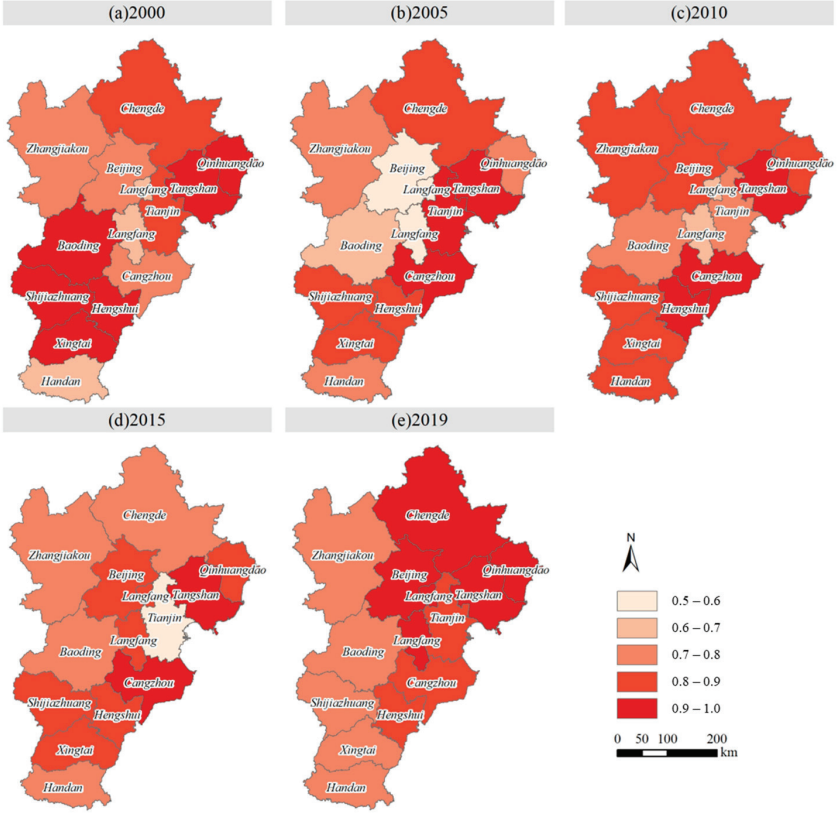

Figure 6. The spatial distribution of carbon emission efficiency.

5.3. Influencing Factors of Carbon Emission Efficiency

Based on the established influencing factor index shown in Table 4, the regression model provided the coefficients for the factors influencing CEE. GDP per capita had a significantly positive effect on CEE, with an estimated coefficient β_1 of 0.0633, indicating that higher economic development levels led to greater CEE. Carbon emissions per capita, employment per ten thousand people, and total assets per capita as basic input factors had significantly negative effects on CEE, with estimated coefficients (β_2, β_3, and β_4) of -0.0175, -1.3569, and -0.0540, respectively. This indicated that higher values of these input factors resulted in lower CEE.

The proportion of urban population significantly promoted CEE, with an estimated coefficient β_5 of 0.6732, which suggested that higher levels of urbanization led to greater CEE. Population density did not have a significant effect on CEE. The impact of industrial structures on CEE was relatively weak. The proportion of the tertiary sector's GDP had a positive effect on CEE at a 10% significance level, with an estimated coefficient β_8 of 0.0119, which indicated that a higher proportion of the tertiary sector's GDP led to greater CEE. This suggested that more advanced industrial structures resulted in higher CEE and that industrial updates could improve productivity efficiency. Energy consumption per unit of GDP, the proportion of foreign direct investment in GDP, and the proportion of local government fiscal expenditure in GDP had estimated coefficients (β_9, β_9, and β_{11}) of −0.0001, −0.5687, and −0.8530, respectively, all at a 1% significance level. This implied that an increase in energy intensity, the level of opening up, and government intervention all led to lower CEE. The impact characteristics of the influencing factors on CEE indicated that economic growth incurred a substantial carbon emission cost to the BTHUA in recent years. Therefore, the results highlighted the continued close relationship between economic development and carbon emissions in the region, suggesting that a decoupling of the two factors had not yet been achieved in the BTHUA.

Table 4. The regression results for the influencing factors of carbon emission efficiency.

Coefficient	Influencing Factor	Coef. Value	Std. Err.	t	P > |t|
β_1	gdp_{it}	0.0633 ***	0.0051	12.3100	0.0000
β_2	car_{it}	−0.0175 ***	0.0020	−8.8500	0.0000
β_3	lab_{it}	−1.3569 ***	0.1032	−13.1500	0.0000
β_4	cap_{it}	−0.0540 ***	0.0077	−7.0500	0.0000
β_5	urb_{it}	0.6732 ***	0.0782	8.6100	0.0000
β_6	pop_{it}	0.1717	0.2531	0.6800	0.4980
β_7	$ind2_{it}$	0.1530	0.2331	0.6600	0.5120
β_8	$ind3_{it}$	0.0119 *	0.0053	2.2600	0.0250
β_9	ene_{it}	−0.0001 ***	0.0000	−5.2300	0.0000
β_{10}	ope_{it}	−0.5687 ***	0.1622	−3.5100	0.0010
β_{11}	gov_{it}	−0.8530 ***	0.1249	−6.8300	0.0000
_cons	-	0.7686 ***	0.1960	3.9200	0.0000
		Log-likelihood = 335.8917			
		Prob > chi2 = 0.0000			
		LR chi2 (11) = 216.95			
		Pseudo R^2 = −0.477			

*, **, and *** represent significance levels at 10%, 5%, and 1%, respectively.

6. Discussions

6.1. Variations in Influencing Factors

To further analyze the changes in influencing factors affecting CEE, Figures 7 and 8 illustrate the variations in influencing factors from 2000 to 2019. All 13 cities experienced a rapid increase in GDP per capita, with Beijing and Tianjin consistently maintaining leading positions. Carbon emissions per capita in most cities initially increased and then slightly decreased or stabilized. Langfang and Tangshan had higher carbon emissions per capita, showing a trend of an initial increase followed by a decrease. Meanwhile, Beijing, Cangzhou, Handan, Langfang, and Tangshan exhibited a trend of an initial increase and then a decrease, while Tianjin, Qinhuangdao, and Shijiazhuang showed an initial increase followed by stabilization. Specifically, in Baoding, Chengde, Hengshui, Xingtai, and Zhangjiakou, the carbon emissions per capita fluctuated and increased during the study period. The changes in employment per ten thousand people were not highly pronounced, except in Beijing and Tianjin, which stood out with notably higher employment. Hebei, Tangshan, Qinhuangdao, and Shijiazhuang had relatively higher employment compared with the other cities, while Xingtai exhibited notably lower employment. Total assets per

capita rapidly increased in all 13 cities, with Tianjin, Shijiazhuang, Tangshan, and Langfang experiencing particularly fast growth, reaching high levels by 2019.

The urbanization level significantly increased during the period, with Beijing and Tianjin consistently maintaining high levels. Among the 11 cities in Hebei, there was a notable increase, with the urbanization levels of Shijiazhuang, Tangshan, Qinhuangdao, and Langfang all exceeding 60% by 2019. Significant differences in population density were observed among the 13 cities, with Beijing and Tianjin having higher population densities, while Chengde and Zhangjiakou had lower ones. The industrial structure in the BTHUA underwent notable changes. Beijing consistently maintained the lowest proportion of the secondary sector's GDP, which has fallen below 40% since 2000. In the other 12 cities, the proportion of the secondary sector's GDP generally slightly increased or stabilized and then significantly decreased. Correspondingly, the proportion of the tertiary sector's GDP in Beijing significantly increased, while in the other 12 cities, it slightly decreased or stabilized and then significantly increased. The level of openness was relatively high in Beijing and Tianjin, showing a trend of an initial decrease and then an increase. In contrast, a notable gap was observed in the other 11 cities compared with Beijing and Tianjin. Government intervention rapidly increased during the period. In 2019, Zhangjiakou, Xingtai, Hengshui, Chengde, Baoding, Tianjin, and Beijing had relatively high proportions of local government fiscal expenditure, whereas Tangshan had the lowest proportion.

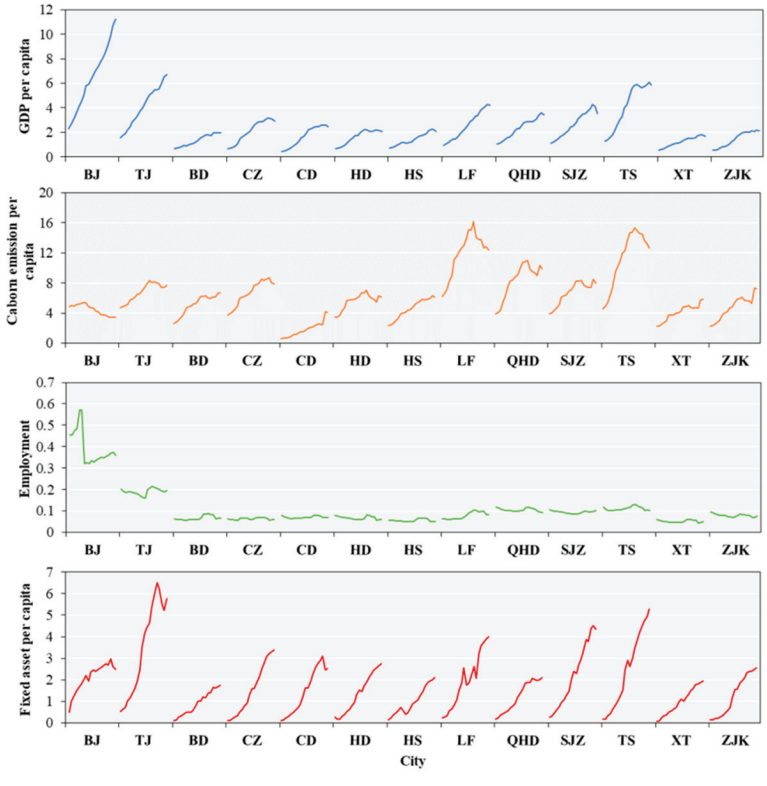

Figure 7. Changes in the fundamental influencing factors of CEE. (BJ: Beijing; TJ: Tianjin; BD: Baoding; CZ: Cangzhou; CD: Chengde; HD: Handan; HS: Hengshui; LF: Langfang; QHD: Qinhuangdao; SJZ: Shijiazhuang; TS: Tangshan; XT: Xingtai; ZJK: Zhangjiakou).

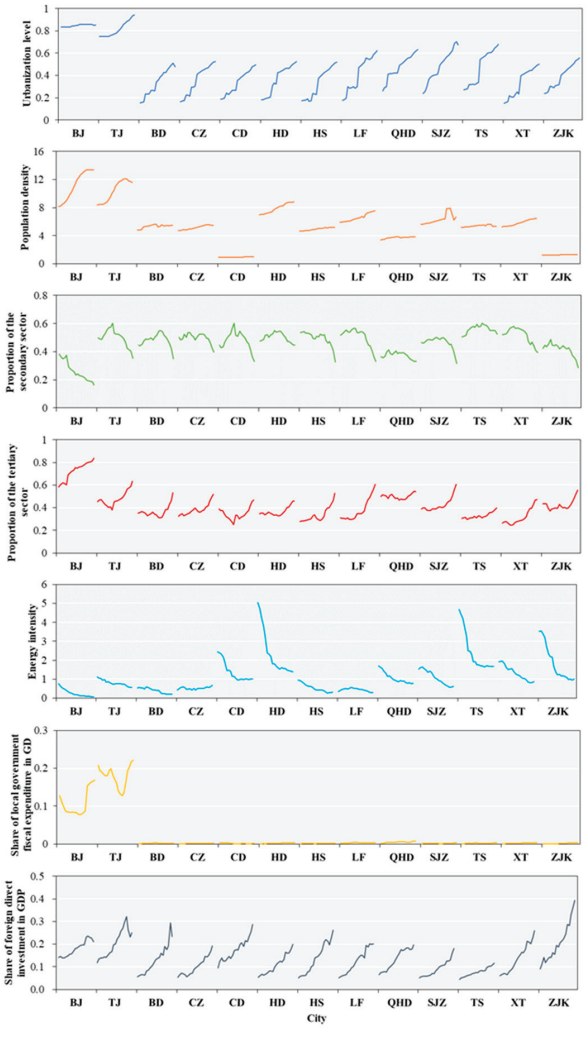

Figure 8. Changes in the influencing factors of carbon emission efficiency. (BJ: Beijing; TJ: Tianjin; BD: Baoding; CZ: Cangzhou; CD: Chengde; HD: Handan; HS: Hengshui; LF: Langfang; QHD: Qinhuangdao; SJZ: Shijiazhuang; TS: Tangshan; XT: Xingtai; ZJK: Zhangjiakou).

6.2. Impact of Influencing Factors

This paper analyzed the spatial and temporal characteristics of CEE and its influencing factors in the BTHUA from 2000 to 2019. The estimated CEE exhibited a fluctuating pattern, characterized by multiple stages of growth and decline. These results were influenced by the data from the input and output variables needed in the CEE estimation model. The overall weak increasing trend in CEE was consistent with the development of socio-economic conditions. Improvements in technology and science are expected to increase CEE. Therefore, the temporal variations in CEE were consistent with the general patterns of economic development. Similarly, other related studies also found overall increases in CEE in Shanxi, China [47], China's industrial sectors [48], and 59 countries worldwide [49]. In terms of spatial patterns, CEE showed an obvious spatial aggregation, which was consistent with the findings of Wang et al. (2019) [14] and Du et al. (2022) [7]. This indicated the presence of spatial spillover effects in CEE.

The influencing factors of CEE have been changing, without a fixed impact magnitude or direction. Sun and Huang (2020) found an inverted U-shaped relationship existing between urbanization and CEE [50]. Wang and Ma (2018) found the industrial structure and energy structure made obvious impacts on CEE [51]. Other studies have also explored the impacts of other factors on CEE, finding that digital investment [52], oil prices [53], and technology progress [49] all have positive impacts on CEE. Social progress, economic development, optimizing the energy structure, adjusting the industrial structure, and promoting technological progress are effective measures to achieve high-quality development.

6.3. Policy Recommendations

Based on the spatial and temporal characteristics of CEE and its influencing factors in the BTHUA, we propose the following suggestions to improve CEE and achieve high-quality development involving energy optimization, industry-structure upgrading, innovation, and technology promotion.

Firstly, reducing fossil fuel consumption can directly reduce carbon emissions and negatively impact CEE. Replacing fossil energy with clean and renewable sources is also a valid pathway to improve CEE. Reducing carbon emission sources can promote the decoupling of carbon emissions and high-density fossil energy from economic growth. Secondly, the proportion of the tertiary sector's GDP has a positive effect on CEE. Promoting industrial transformation and upgrading can increase the proportion of the tertiary sector [54]. Promoting the development of the service sector contributes to high-quality development and industrial structure optimization. Thirdly, it is important to fully leverage the power of knowledge and technology to promote high-quality development. The government should encourage the development of high and new technologies, gradually transitioning from labor- and material-intensive industries to the knowledge- and technology-intensive industries [55,56]. Fourthly, enhancing carbon sequestration can absorb carbon emissions emitted from product activities, contributing to carbon neutrality. Nature-based solutions can assist with ecological planning and address environmental problems [57]. All these policy recommendations contribute to regional high-quality development.

7. Conclusions

Against the backdrop of climate change and rapid economic development, we focused on CEE and its influencing factors in the BTHUA. A reliable CEE estimation model was constructed using SFA. The CEE of 13 cities from 2000 to 2019 was estimated. The influencing factors of CEE were further analyzed to incorporate comprehensive socio-economic factors, including the urbanization level, industrial structure, and population density.

The mean value of CEE among the 13 cities fluctuated and increased during 2000–2019. Significant differences were observed in the CEE levels among the 13 cities. Specifically, Beijing's CEE fluctuated and increased, Tianjin's CEE followed an N-shaped trend, Baoding's CEE initially decreased with fluctuations and then stabilized, Cangzhou's CEE initially increased and then stabilized, and the CEE of the other cities exhibited irregular changes. Moreover, CEE displayed significant spatial clustering characteristics across the BTHUA. Input-related influencing factors had significant effects on CEE, including the carbon emissions per capita, employment per ten thousand people, and total assets per capita. Moreover, the urbanization level had a significant positive effect on CEE. Industrial-structure upgrading could help to increase CEE. Energy intensity, the level of openness, and government intervention were all negative influencing factor parameters. All these results indicated that development is still at a stage of heavy reliance on a large amount of human and material resources in the BTHUA. In the future, the government should focus on the development of knowledge- and technology-intensive industries and pursue the decoupling of economic development and carbon emissions, thereby contributing to the achievement of regional high-quality development.

Author Contributions: Conceptualization, J.Z. and C.W.; methodology, C.W.; data curation, Y.K. and X.L.; writing—original draft preparation, C.W., Y.K. and X.L.; writing—review and editing, Y.T. and H.X.; supervision, C.W. and J.Z.; project administration, C.W. All authors have read and agreed to the published version of the manuscript.

Funding: This research was supported by research funds from the National Natural Science Foundation of China (No. 72304192), the Science Fund for Creative Research Groups of the National Natural Science Foundation of China (No. 72221002), and the Capital University of Economics and Business: The Fundamental Research Funds for Beijing Universities (No. XRZ2023066).

Data Availability Statement: The original contributions presented in the study are included in the article, further inquiries can be directed to the corresponding author.

Conflicts of Interest: The authors declare no conflict of interest.

References

1. Arora, N.K. Impact of climate change on agriculture production and its sustainable solutions. *Environ. Sustain.* **2019**, *2*, 95–96. [CrossRef]
2. Ahmed, K. Perspective on China's commitment to carbon neutrality under the innovation-energy-emissions nexus. *J. Clean. Prod.* **2023**, *390*, 136202. [CrossRef]
3. Zhang, R.; Tai, H.; Cheng, K.; Zhu, Y.; Hou, J. Carbon emission efficiency network formation mechanism and spatial correlation complexity analysis: Taking the Yangtze River Economic Belt as an example. *Sci. Total Environ.* **2022**, *841*, 156719. [CrossRef]
4. Wang, Q.; Li, L.; Li, R. Uncovering the impact of income inequality and population aging on carbon emission efficiency: An empirical analysis of 139 countries. *Sci. Total Environ.* **2023**, *857*, 159508. [CrossRef] [PubMed]
5. Das, M.; Das, A.; Pereira, P. Developing an integrated urban ecological efficiency framework for spatial ecological planning: A case on a tropical mega metropolitan area of the global south. *Geosci. Front.* **2023**, *14*, 101489. [CrossRef]
6. He, A.; Xue, Q.; Zhao, R.; Wang, D. Renewable energy technological innovation, market forces, and carbon emission efficiency. *Sci. Total Environ.* **2021**, *796*, 148908. [CrossRef]
7. Du, M.Z.; Feng, R.K.; Chen, Z.F. Blue sky defense in low-carbon pilot cities: A spatial spillover perspective of carbon emission efficiency. *Sci. Total Environ.* **2022**, *846*, 157509. [CrossRef]
8. Xiao, Y.; Ma, D.; Zhang, F.; Zhao, N.; Wang, L.; Guo, Z.; Zhang, J.; An, B.; Xiao, Y. Spatiotemporal differentiation of carbon emission efficiency and influencing factors: From the perspective of 136 countries. *Sci. Total Environ.* **2023**, *879*, 163032. [CrossRef] [PubMed]
9. Gao, M.; Chen, X.; Xu, Y.; Xia, T.; Wang, P.; Chen, B. A multi-dimensional analysis on potential drivers of China's city-level low-carbon economy from the perspective of spatial spillover effects. *J. Clean. Prod.* **2023**, *419*, 138300. [CrossRef]
10. Gu, R.; Li, C.; Yang, Y.; Zhang, J. The impact of industrial digital transformation on green development efficiency considering the threshold effect of regional collaborative innovation: Evidence from the Beijing-Tianjin-Hebei urban agglomeration in China. *J. Clean. Prod.* **2023**, *420*, 138345. [CrossRef]
11. Zhan, J.; Wang, C.; Wang, H.; Zhang, F.; Li, Z. Pathways to achieve carbon emission peak and carbon neutrality by 2060, a case study in the Beijing-Tianjin-Hebei region, China. *Renew. Sustain. Energy Rev.* **2024**, *189*, 113955. [CrossRef]
12. Caiado, R.G.G.; de Freitas Dias, R.; Mattos, L.V.; Quelhas, O.L.G.; Filho, W.L. Towards sustainable development through the perspective of eco-efficiency-A systematic literature review. *J. Clean. Prod.* **2017**, *165*, 890–904. [CrossRef]
13. Enkvist, P.; Nauclér, T.; Oppenheim, J.M. Business strategies for climate change. *McKinsey Q.* **2008**, *2*, 24.
14. Wang, C.; Zhan, J.; Bai, Y.; Chu, X.; Zhang, F. Measuring carbon emission performance of industrial sectors in the Beijing–Tianjin–Hebei region, China: A stochastic frontier approach. *Sci. Total Environ.* **2019**, *685*, 786–794. [CrossRef] [PubMed]
15. Wang, Q.W.; Zhou, P.; Shen, N.; Wang, S. Measuring carbon dioxide emission performance in Chinese provinces: A parametric approach. *Renew. Sustain. Energy Rev.* **2013**, *21*, 324–330. [CrossRef]
16. Fan, Y.; Liu, L.C.; Wu, G.; Tsai, H.-T.; Wei, Y.-M. Changes in carbon intensity in China: Empirical findings from 1980–2003. *Ecol. Econ.* **2007**, *62*, 683–691. [CrossRef]
17. Hu, X.; Liu, C. Carbon productivity: A case study in the Australian construction industry. *J. Clean. Prod.* **2016**, *112*, 2354–2362. [CrossRef]
18. Patterson, M.G. What is energy efficiency? Concepts, indicators and methodological issues. *Energy Policy* **1996**, *24*, 377–390. [CrossRef]
19. Du, K.; Li, J. Towards a green world: How do green technology innovations affect total factor carbon productivity. *Energy Policy* **2019**, *131*, 240–250. [CrossRef]
20. Hu, J.; Wang, S. Total-factor energy efficiency of regions in China. *Energy Policy* **2006**, *34*, 3206–3217. [CrossRef]
21. Fall, F.; Akim, A.; Wassongma, H. DEA and SFA research on the efficiency of microfinance institutions: A meta-analysis. *World Dev.* **2018**, *107*, 176–188. [CrossRef]
22. Zha, Y.; Zhao, L.; Bian, Y. Measuring regional efficiency of energy and carbon dioxide emissions in China: A chance constrained DEA approach. *Comput. Oper. Res.* **2016**, *66*, 351–361. [CrossRef]

23. Song, M.; Fisher, R.; Wang, J.; Cui, L.-B. Environmental performance evaluation with big data: Theories and methods. *Ann. Oper. Res.* **2018**, *270*, 459–472. [CrossRef]
24. Zhou, P.; Ang, B.W.; Han, J.Y. Total factor carbon emission performance: A Malmquist index analysis. *Energy Econ.* **2010**, *32*, 194–201. [CrossRef]
25. Meng, F.; Su, B.; Thomson, E.; Zhou, D.; Zhou, P. Measuring China's regional energy and carbon emission efficiency with DEA models: A survey. *Appl. Energy* **2016**, *183*, 1–21. [CrossRef]
26. Zhou, Y.; Liu, W.; Lv, X.; Chen, X.; Shen, M. Investigating interior driving factors and cross-industrial linkages of carbon emission efficiency in China's construction industry: Based on Super-SBM DEA and GVAR model. *J. Clean. Prod.* **2019**, *241*, 118322. [CrossRef]
27. Jradi, S.; Chameeva, T.B.; Delhomme, B.; Jaegler, A. Tracking carbon footprint in French vineyards: A DEA performance assessment. *J. Clean. Prod.* **2018**, *192*, 43–54. [CrossRef]
28. Bai, Y.; Deng, X.; Jiang, S.; Zhang, Q.; Wang, Z. Exploring the relationship between urbanization and urban eco-efficiency: Evidence from prefecture-level cities in China. *J. Clean. Prod.* **2018**, *195*, 1487–1496. [CrossRef]
29. Liu, W.; Zhan, J.; Wang, C.; Li, S.; Zhang, F. Environmentally sensitive productivity growth of industrial sectors in the Pearl River Delta. *Resour. Conserv. Recycl.* **2018**, *139*, 50–63. [CrossRef]
30. Zhao, X.; Ma, X.; Shang, Y.; Yang, Z.; Shahzad, U. Green economic growth and its inherent driving factors in Chinese cities: Based on the Metafrontier-global-SBM super-efficiency DEA model. *Gondwana Res.* **2022**, *106*, 315–328. [CrossRef]
31. Dutta, P.; Jain, A.; Gupta, A. Performance analysis of non-banking finance companies using two-stage data envelopment analysis. *Ann. Oper. Res.* **2020**, *295*, 91–116. [CrossRef]
32. Gutiérrez, E.; Lozano, S. Cross-country comparison of the efficiency of the European forest sector and second stage DEA approach. *Ann. Oper. Res.* **2022**, *314*, 471–496. [CrossRef]
33. Lin, B.; Wang, X. Carbon emissions from energy intensive industry in China: Evidence from the iron & steel industry. *Renew. Sustain. Energy Rev.* **2015**, *47*, 746–754.
34. Bai, Y.; Deng, X.; Zhang, Q.; Wang, Z. Measuring environmental performance of industrial sub-sectors in China: A stochastic metafrontier approach. *Phys. Chem. Earth Parts A/B/C* **2017**, *101*, 3–12. [CrossRef]
35. Sun, J.; Du, T.; Sun, W.; Na, H.; He, J.; Qiu, Z.; Yuan, Y.; Li, Y. An evaluation of greenhouse gas emission efficiency in China's industry based on SFA. *Sci. Total Environ.* **2019**, *690*, 1190–1202. [CrossRef] [PubMed]
36. Zhao, Z.; Bai, Y.; Wang, G.; Chen, J.; Yu, J.; Liu, W. Land eco-efficiency for new-type urbanization in the Beijing-Tianjin-Hebei Region. *Technol. Forecast. Soc. Change* **2018**, *137*, 19–26. [CrossRef]
37. Haider, S.; Mishra, P.P. Does innovative capability enhance the energy efficiency of Indian Iron and Steel firms? A Bayesian stochastic frontier analysis. *Energy Econ.* **2021**, *95*, 105128. [CrossRef]
38. Đokić, D.; Novaković, T.; Tekić, D.; Matkovski, B.; Zekić, S.; Milić, D. Technical efficiency of agriculture in the European Union and Western Balkans: SFA method. *Agriculture* **2022**, *12*, 1992. [CrossRef]
39. Sun, Y.; Wang, Y.; Zhang, Z. Economic environmental imbalance in China—Inter-city air pollutant emission linkage in Beijing–Tianjin–Hebei (BTH) urban agglomeration. *J. Environ. Manag.* **2022**, *308*, 114601. [CrossRef]
40. Zeng, Y.; Zhang, W.; Sun, J.; Sun, L.A.; Wu, J. Research on Regional Carbon Emission Reduction in the Beijing–Tianjin–Hebei Urban Agglomeration Based on System Dynamics: Key Factors and Policy Analysis. *Energies* **2023**, *16*, 6654. [CrossRef]
41. IPCC. National greenhouse gas inventories programme. In *2006 IPCC Guidelines for National Greenhouse Gas Inventories*; Eggleston, H.S., Buendia, L., Miwa, K., Ngara, T., Tanabe, K., Eds.; Institute for Global Environmental Strategies: Hayama, Japan, 2006.
42. West, T.O.; Marland, G. A synthesis of carbon sequestration, carbon emissions, and net carbon flux in agriculture: Comparing tillage practices in the United States. *Agric. Ecosyst. Environ.* **2002**, *91*, 217–232. [CrossRef]
43. Fang, J. *Carbon Cycle of Terrestrial Ecosystem in China and Its Global Meaning*; China Environmental Science Press: Beijing, China, 1996.
44. Kuang, Y.; Ouyang, T.; Zou, Y.; Liu, Y.; Li, C.; Wang, D. Present situation of carbon source and sink and potential for increase of carbon sink in Guangdong Province. *China Popul. Resour. Environ.* **2010**, *20*, 56–61.
45. Christensen, L.R.; Jorgenson, D.W.; Lau, L.J. Transcendental logarithmic production frontiers. *Rev. Econ. Stat.* **1973**, *55*, 28–45. [CrossRef]
46. Brown, J.E.; Dunn, P.K. Comparisons of Tobit, linear, and Poisson-gamma regression models: An application of time use data. *Sociol. Methods Res.* **2011**, *40*, 511–535. [CrossRef]
47. Guo, X.; Wang, X.; Wu, X.; Chen, X.; Li, Y. Carbon emission efficiency and low-carbon optimization in Shanxi Province under "Dual Carbon" background. *Energies* **2022**, *15*, 2369. [CrossRef]
48. Cheng, Z.; Li, L.; Liu, J.; Zhang, H. Total-factor carbon emission efficiency of China's provincial industrial sector and its dynamic evolution. *Renew. Sustain. Energy Rev.* **2018**, *94*, 330–339. [CrossRef]
49. Xie, Z.; Wu, R.; Wang, S. How technological progress affects the carbon emission efficiency? Evidence from national panel quantile regression. *J. Clean. Prod.* **2021**, *307*, 127133. [CrossRef]
50. Sun, W.; Huang, C. How does urbanization affect carbon emission efficiency? Evidence from China. *J. Clean. Prod.* **2020**, *272*, 122828. [CrossRef]
51. Wang, S.; Ma, Y. Influencing factors and regional discrepancies of the efficiency of carbon dioxide emissions in Jiangsu, China. *Ecol. Indic.* **2018**, *90*, 460–468. [CrossRef]

52. Xu, Q.; Zhong, M.; Cao, M. Does digital investment affect carbon efficiency? Spatial effect and mechanism discussion. *Sci. Total Environ.* **2022**, *827*, 154321. [CrossRef]
53. Liu, H.; Pata, U.K.; Zafar, M.W.; Kartal, M.T.; Karlilar, S.; Caglar, A.E. Do oil and natural gas prices affect carbon efficiency? Daily evidence from China by wavelet transform-based approaches. *Resour. Policy* **2023**, *85*, 104039. [CrossRef]
54. Jiang, H.; Yin, J.; Wei, D.; Luo, X.; Ding, Y.; Xia, R. Industrial carbon emission efficiency prediction and carbon emission reduction strategies based on multi-objective particle swarm optimization-backpropagation: A perspective from regional clustering. *Sci. Total Environ.* **2024**, *906*, 167692. [CrossRef]
55. Song, M.; Fisher, R.; Kwoh, Y. Technological challenges of green innovation and sustainable resource management with large scale data. *Technol. Forecast. Soc. Change* **2019**, *144*, 361–368. [CrossRef]
56. Wang, H.; Li, Y.; Lin, W.; Wei, W. How does digital technology promote carbon emission reduction? Empirical evidence based on e-commerce pilot city policy in China. *J. Environ. Manag.* **2023**, *325*, 116524. [CrossRef] [PubMed]
57. Seddon, N.; Smith, A.; Smith, P.; Key, I.; Chausson, A.; Girardin, C.; House, J.; Srivastava, S.; Turner, B. Getting the message right on nature-based solutions to climate change. *Glob. Change Biol.* **2021**, *27*, 1518–1546. [CrossRef]

land

MDPI

Article

Eco-Efficiency of the Urban Agglomerations: Spatiotemporal Characteristics and Determinations

Shuting Xue [1], Chao Wang [2,*], Shibin Zhang [1], Chuyao Weng [1] and Yuxi Zhang [1]

[1] School of Land Science and Technology, China University of Geosciences, Beijing 100083, China; xueshuting@cugb.edu.cn (S.X.); zhangshibin@cugb.edu.cn (S.Z.); wengcy@email.cugb.edu.cn (C.W.); 1012202103@cugb.edu.cn (Y.Z.)

[2] School of Labor Economics, Capital University of Economics and Business, Beijing 100070, China

* Correspondence: wangc@cueb.edu.cn

Abstract: Attaining optimal eco-efficiency is of paramount importance in promoting the sustainable and harmonious development of the economy and environment within urban agglomerations. Firstly, this paper utilizes the Super-SBM model with undesirable output to measure the eco-efficiency (*EE*) of 64 cities in the Beijing–Tianjin–Hebei metropolitan region (BTHMR), the Yangtze River Delta (YRD), the Pearl River Delta (PRD), and the Chengdu–Chongqing Economic Zone (CCEZ) from 2006 to 2019. Secondly, this study puts forth a novel and comprehensive index system aimed at evaluating the urbanization efficiency and sheds light on the spatiotemporal changes in *EE* and urbanization efficiency. Finally, the STIRPAT model is used to examine the influencing factors of *EE* and to investigate the correlation between *EE* and urbanization efficiency. The study found that the overall *EE* of the four typical urban agglomerations is high, but the trend varies with a decrease of about 12.9% from 2006 to 2019. The mean *EE* is in the order of CCEZ > PRD > BTHMR > YRD, with mean values of 0.941, 0.909, 0.842, and 0.732, respectively. The level of science and technology and the urbanization efficiency have a significant positive impact on *EE*, while population, industrial structure, *FDI*, and greening level have an inhibitory effect on urban eco-efficiency. Based on the results, policy suggestions such as paying attention to regional heterogeneity and giving full play to the government's macro-regulatory role in shaping the economic and industrial structure are proposed to serve as a guide for the coordinated development of urban agglomerations under the Dual Carbon Target.

Keywords: eco-efficiency; urbanization efficiency; US-SBM; STIRPAT; influencing factors; urban agglomerations

Citation: Xue, S.; Wang, C.; Zhang, S.; Weng, C.; Zhang, Y. Eco-Efficiency of the Urban Agglomerations: Spatiotemporal Characteristics and Determinations. *Land* **2023**, *12*, 1275. https://doi.org/10.3390/land12071275

Academic Editor: Rui Alexandre Castanho

Received: 30 May 2023
Revised: 20 June 2023
Accepted: 21 June 2023
Published: 23 June 2023

1. Introduction

Following China's reform and opening up, the nation's urbanization rate has experienced a rapid surge, with urban agglomerations emerging as the key regions driving China's economic development. As of 2019, 19 urban agglomerations in China accounted for 75% of the country's population and contributed 88% of its GDP [1]. The "people-oriented" new-type urbanization is more in line with the development law and meets people's aspirations for better living quality. In this context, the collaborative development of urban agglomerations has become an important trend and Chinese urbanization mainstream [2]. In particular, major regional strategies such as the coordinated development of the Beijing–Tianjin–Hebei region, integrated development of the Yangtze River Delta, and the construction of the Guangdong–Hong Kong–Macao Greater Bay Area have been further implemented. The construction of the Chengdu–Chongqing economic Zone in southwest China has been actively promoted. City agglomerations and urban areas have expanded, significantly enhancing economic and international influence. At the same time, rapid development has been accompanied by neglect of the urban population carrying

capacity, shortage of natural resources, and deterioration of the ecological environment. Extensive development, consuming high levels of energy, producing high levels of pollution, and operating with low efficiency, still exists. Urban agglomerations, the central focus of China's new urbanization, have become the key propellant of high-quality economic and social progress. They are entrusted with the dual responsibilities of promoting economic development and environmental protection through measures such as building a strong economic base, optimizing the industrial structure, and promoting coordinated regional development [3]. China's economic growth is shifting from the pursuit of 'high speed' to a focus on quality growth. The previous extensive development pattern is clearly inappropriate. How to encourage the urban agglomerations growth while effectively maximizing economic output, minimizing environmental degradation, and achieving sustainability, has become an important concern.

Eco-efficiency (*EE*), a tool for assessing the low carbon extent and the economic sustainability of a region [4], effectively gauges the correlation between economy, environment, resources, and development [5]. It is not only an inherent requirement for the coordinated development of new-type urbanization and ecology, moreover, it serves as a crucial foundation for evaluating the efficacy of the construction of urban ecological civilization [6]. Understanding *EE* has a practical significance in addressing and achieving socio-economic development, and further delving into its connection with urbanization can offer guidelines and policy suggestions for putting the "innovation, coordination, green, open and shared" concept into practice, thus promoting achievement of sustainability under the Dual Carbon Target.

In view of this, this paper takes typical urban agglomerations in China as case examples to scientifically measure eco-efficiency and urbanization efficiency and explore the spatiotemporal evolution in urban agglomerations. We further identify factors affecting eco-efficiency, delve into its relationship with urbanization, and provide guidance and policy recommendations for achieving sustainable development.

The remainder of this paper is structured as follows: Section 2 is a literature review. Section 3 outlines the research methodology and provides an overview of the data sources employed. Section 4 presents the findings pertaining to *EE* and the urbanization efficiency, and subsequently undertakes an analysis of their interrelationship. Section 5 constitutes a discussion of the research outcomes and offers recommendations for policy formulation. Finally, in Section 6, the paper concludes with a summary of main conclusions and policy implications.

2. Literature Review

Eco-efficiency was first proposed by Schaltegger and Sturm [7]. Subsequently, the strategy was further elaborated and promoted by the World Council for Sustainable Development and the Organization for Economic Development Cooperation. The crux of eco-efficiency lies in attaining optimal economic gains through minimal resource consumption and environmental expenses [8], existing research of which is mainly focused on the selection and measurement of indicators, spatial and temporal patterns, spatial convergence and spillover effects, evaluation, and optimization. Several researchers have discussed and analyzed the spatiotemporal evolution of *EE* at the national, provincial, and municipal scales, successfully applying the results to a wide range of fields, subjects, and sectors, such as industrial, agricultural, and eco-economic efficiency. Urbanization efficiency, as a crucial benchmark of high-quality urban development, is frequently assessed by comparing the output or efficacy of input resources. Scholars that explored urban [9], district, and county development efficiency as well as urban industrial efficiency [10], have conducted research on methods and models for measuring efficiency [11].

Research on assessing *EE* has attracted a great deal of academic attention. The indicator system approach [12], life cycle assessment [13], data envelopment analysis (DEA) [14], and stochastic frontier analysis (SFA) [15] are the key techniques for measuring *EE* and urbanization efficiency. Wursthorn et al. (2011) established an accounting framework

for evaluating eco-efficiency in European countries. This approach combines economic and ecological indicators to provide a comprehensive assessment [16]. Margarita et al. (2015) specified a new stochastic frontier model to evaluate the resource and environmental efficiency of European countries [17]. Compared to SFA models, DEA models and their extended versions based on linear programming, which do not require the specification of a specific form of production function, are more objective and widely used [18]. For example, Bai et al. (2018) employed a super-efficient DEA model to assess the correlation between urbanization and urban eco-efficiency in China between 2006 and 2013 [19]. Shi et al. (2023) used a two-stage DEA model to measure and analyze the eco-efficiency of urban agglomerations over the past 15 years, based on four major urban agglomerations along the eastern coast of China, to reveal the internal connections between integrated efficiency and sub-stage efficiency [20]. However, DEA is radial in nature and solely accounts for proportional transformations in input or output elements. As a result, it ignores non-radial slack variables and does not include non-desired output indicators, which can easily lead to high measured efficiency values. In this regard, Tone et al. (2001) proposed a non-radial, non-oriented SBM based on slack variables, which effectively solves the problems posed by slack variables [21]. However, the SBM cannot distinguish and rank multiple valid decision units. For this purpose, Tone et al. (2002) further presented the Super-SBM and constructed the undesirable slacks-based measurement (Undesirable SBM) to distinguish the attributes of outputs, this approach effectively addresses the challenge of comparing multiple decision-making units [22]. Using a panel dataset from 2005–2014, Zhou et al. (2018) assessed the eco-efficiency of 21 cities in Guangdong Province, China, which was achieved through the utilization of the Super-SBM that considers undesirable output and the Topsis [23]. Based on previous research, in this paper, we employ a Super-SBM model incorporating undesirable outputs to gauge the *EE* and urbanization efficiency.

Recently, the government of China works fixedly to achieve sustainable urban development, which aims to strike a balance between economic outputs and environmental protection. The analysis of influential factors of eco-efficiency assists positively in enhancing eco-efficiency and the achievement of sustainable regional development. Current research methods on influencing factors include spatial panel regression techniques [24], IPAT models, STIRPAT models [25,26], geodesic probes [27], Tobit regression models [28], quantile regression models [29], systematic GMM models, and spatial econometric models [30]. Fang and Wang (2013) performed a theoretical examination of the interactive coercive effects between urbanization and ecology [31]. Wang et al. (2014) presented a thorough system of indicators to assess urbanization and *EE* and analyze their correlation [32]. The IPAT was first proposed by Ehrlich and Holdren (1971), who attributed the effects of human activities on the surroundings to population, affluence, and technology level [33], and subsequent researchers developed an extend STIRPAT by introducing differential elasticity and random error terms [34]. In recent years, STIRPAT has become widespread in impact factor analysis. Scholars have extended the traditional STIRPAT from the perspectives of urbanization, trade, and investment, using a series of improved panel models to explore the interaction between urbanization and *EE* and the external influences on *EE*. Zhang et al. (2018) used STIRPAT to evaluate the influence of urbanization on CO_2 emissions in 141 countries [35]. Luo et al. (2013) utilized STIRPAT to investigate the correlation between urbanization and *EE* with empirical data at the provincial level [36]. Grossman further revealed the intrinsic "U" shaped pattern between urbanization and ecology (EKC) [37]. Moreover, the *EE*'s influential factors of different cities vary due to factors such as regional conditions, resource endowment, economic development patterns, and policy orientation [38]. Existing studies in the literature suggest that *EE* is influenced by environmental regulation, foreign direct investment, industrial infrastructure, urbanization efficiency, technological innovation, and economic agglomeration [39]. Chang et al. (2020) argued that foreign investment brought negative ecological benefits and that the Yangtze River Delta overall was in line with the "pollution paradise" hypothesis. Wu et al. (2016) found a high proportion of secondary sectors inhibited *EE* when studying its factors in Jiangsu Province [40]. In this paper, we

select the most appropriate influencing factors based on their frequency of occurrence and the availability of relevant data and use an extended STIRPAT model to analyze their relationship with eco-efficiency.

However, the majority of scholars have concentrated on analyzing eco-efficiency either on a macro level throughout China or in a particular geographical area, and there is a paucity of research conducted on several significant urban agglomerations in China. Moreover, few studies on the spatiotemporal evolution patterns among the four major urban agglomerations in China have covered recent years, and studies on the factors influencing urban eco-efficiency are relatively scarce. Some studies have even ignored assessing unexpected outputs. Therefore, based on the 2006–2019 panel dataset, the Super-SBM model incorporating undesirable outputs was developed to gauge the *EE* and urbanization efficiency of 64 cities located within the BTHMR, the YRD, the PRD, and the CCEZ. Furthermore, we applied an extended STIRPAT model combined with spatial panel Tobit analysis to explore the determinants of urban *EE*.

3. Methodology and Data

3.1. Study Area

Based on the relevant research results on urban agglomerations in China [41,42], and taking into account the defined scope and data availability of the planning documents of each urban agglomeration, 64 cities in four national urban agglomerations (Figure 1) were taken as the spatial scale research objects, namely the Beijing–Tianjin–Hebei metropolitan region (BTHMR), the Yangtze River Delta (YRD), the Pearl River Delta (PRD) and the Chengdu–Chongqing Economic Zone (CCEZ), which are key construction areas. The research samples covered four municipalities directly under the central government, namely Beijing, Tianjin, Shanghai, and Chongqing, as well as cities at the prefecture level and above in six provinces, namely Hebei, Jiangsu, Zhejiang, Anhui, Guangdong, and Sichuan.

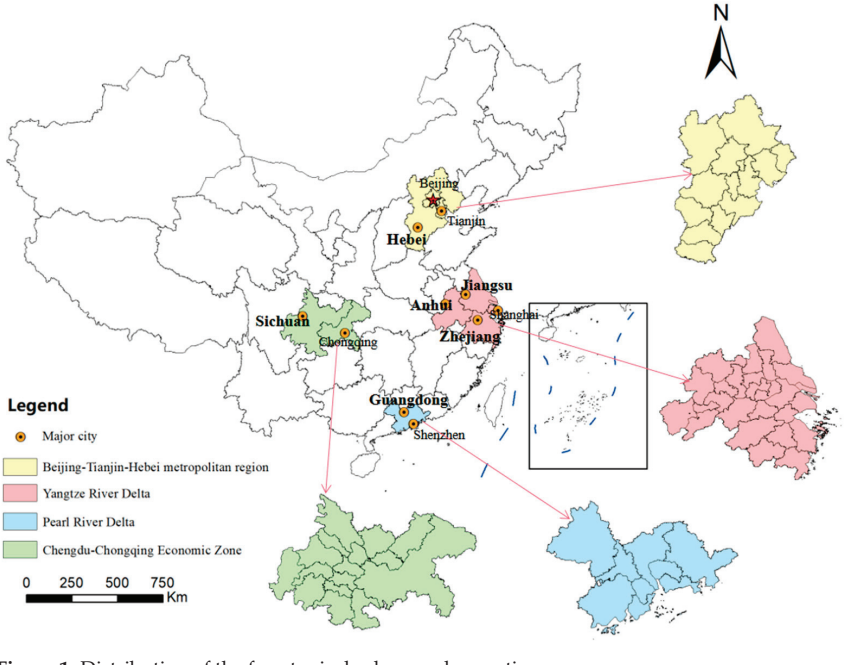

Figure 1. Distribution of the four typical urban agglomerations.

3.2. US-SBM Model

This study employs a US-SBM model that considers undesirable outputs and combines the advantages of the SBM and super-efficiency model. This model considers input relaxation and effectively measures the *EE* in the presence of undesirable outputs, enabling the comparison of multiple efficient DMUs and solving the issue of the inability to rank efficiency values. The super-SBM provides a more in-depth characterization of the cities' *EE* and sheds light on the characteristics and evolution process of green development in China's four national urban agglomerations. Specifically, this study constructs a Super-SBM with undesirable outputs (US-SBM) to measure the *EE* of 64 cities in the four national urban agglomerations and distinguishes efficient decision-making units at the boundary in the presence of undesirable outputs. Suppose there is n DMUs and each decision cell consists of m kinds of inputs (x), q_1 kinds of desired outputs (y^g) and q_2 kinds of undesirable outputs (y^b). The input variables x, the desired output variables y^g, and the undesirable output variables y^b are matrices, where $x = [x_1, x_2, \ldots, x_n]$, $y^g = \left[y_1^g, y_2^g, \ldots, y_n^g\right]$, $y^b = \left[y_1^b, y_2^b, \ldots, y_n^b\right]$, γ is the weight vector, and the set of production possibilities with variable payoffs to scale is $p = \left\{\left[\left(x, y^g, y^b\right) \middle| x \le x\gamma, y^g \le y^g\gamma, y^b \le y^b\gamma\right]\right\}$, the specific model is constructed as follows [43]:

$$\min\rho = \frac{1 + \frac{1}{m}\sum_{i=1}^{m} \frac{s_i^-}{x_{ik}}}{1 - \frac{1}{q_1+q_2}\left(\sum_{r=1}^{q_1} \frac{s_r^{g+}}{y_{rk}^g} + \sum_{t=1}^{q_2} \frac{s_t^{b-}}{y_{tk}^b}\right)} \tag{1}$$

$$s.t.\begin{cases} \sum\limits_{j=1,j\neq k}^{n} x_{ij}\gamma_j - s_i^- \le x_{ik} \\ \sum\limits_{j=1,j\neq k}^{n} y_{rj}\gamma_j + s_r^{g+} \ge y_{rk}^g \\ \sum\limits_{j=1,j\neq k}^{n} y_{tj}^b - s_t^{b-} \le y_{tk}^b \\ 1 - \frac{1}{q_1+q_2}\left(\sum\limits_{r=1}^{q_1} \frac{s_r^{g+}}{y_{rk}^g} + \sum\limits_{t=1}^{q_2} \frac{s_t^{b-}}{y_{tk}^b}\right) > 0 \\ s^- > 0, s^{b-} > 0, s^{g+} > 0, \gamma > 0 \\ i = 1, 2, \cdots, m; r = 1, 2, \cdots, q; j = 1, 2, \cdots, n(j \neq k) \end{cases} \tag{2}$$

where is the number of decision units, m, q_1, and q_2 represent the number of input indicators, desired outputs, and undesired outputs, respectively, k is the number of units being evaluated. i, r, t denotes the i-th input, the r-th desired output, the t-th undesired output, respectively. s^- is the number of input redundancies, s^{g+} denotes the desired output shortfall, and s^{b-} denotes the undesired output redundancies. x_{ij} denotes the i-th input of the j-th decision unit. y_{rj} is the r-th desired output of the j-th decision unit and y_{tj} is the t-th undesired output of the j-th unit. ρ is the efficiency value, when $\rho < 1$, the decision unit is in an inefficient state; when $\rho \geq 1$, the decision unit is in an efficient state.

3.3. STIRPAT Model

This study examines the factors influencing *EE* and explores the relationship between urbanization and *EE* by the STIRPAT model. The factors considered in the model include population, industrial structure, urbanization efficiency, openness to foreign trade, technological innovation, and green coverage level. The original form of the STIRPAT is as follows:

$$I_i = aP_i^b A_i^c T_i^d \tag{3}$$

where I, P, A, and T denote environmental pressure, population size, affluence, and technology level, respectively, a is the model coefficient, and e is the error term.

In practical applications, the two sides of the model are usually logarithmized for regression analysis, and model (3) becomes:

$$lnI_i = lna + blnP_i + clnA_i + dlnT_i + lne_i \quad (4)$$

Based on the literature review conducted earlier on the factors influencing eco-efficiency, this study categorized these factors based on their frequency of occurrence and the availability of relevant data, the total population (*POP*), the Share of secondary sector in GDP (*IS*), the urbanization efficiency (*URB*), the expenditure on science and technology (*TEC*), the actual amount of foreign capital used (*FDI*), and the greenery coverage of built-up area (*GRE*) are used as explanatory variables and eco-efficiency (*EE*) serves as the explained variable in 64 cities from 2006 to 2019. We extended the STIRPAT model to the following form:

$$ln(EE) = a_0 + bln(POP) + cln(IS) + dln(URB) + eln(FDI) + fln(TEC) + gln(GRE) + e_0 \quad (5)$$

where b, c, d, e, f, and g correspond to the model parameters, respectively, and the positive elasticity coefficient of the explanatory variable indicates a positive effect on the explained variable and vice versa. Moreover, the magnitude of the elasticity coefficient reflects the strength of the relationship between the explanatory variable and the dependent variable [32]. The significance of the elasticity coefficient is determined using p-values. When the p-value is less than 0.1, 0.05, or 0.01, the elasticity coefficient is significant at the 10%, 5%, and 1% levels, respectively, e_0 is the error value.

The appropriate econometric method can be used to estimate the parameters of the above model under the meeting of the corresponding hypotheses. However, there may be heteroscedasticity issues and interference terms may be correlated between different cities within the same province at the prefecture level due to the use of city-level data in this study. Additionally, the Super-SBM model is utilized to calculate the dependent variable and has a lower limit of 0 due to truncation of the data. If ordinary least squares (OLS) regression is directly used, there may be biased and inconsistent parameter estimation issues [44–46]. Therefore, through the F-test and Hausman test, the fixed-effects Tobit regression is chosen to investigate the factors affecting *EE*.

3.4. Index System Construction

The World Business Council for Sustainable Development (WBCSD) provides a range of input–output indicators as alternative indicators, among which labor, material resources, land, and capital are the primary input indicators [47]. In accordance with the principles of scientific rigor, objectivity, systematic analysis, and data availability, this study constructed separate evaluation index systems for eco-efficiency and urbanization efficiency by referring to relevant literature [43,48]. The evaluation index system for *EE* includes five input indicators: total fixed asset investment, year-end number of employees, total water supply, administrative land area, and urban electricity consumption. Total fixed asset investment represents the capital element, year-end number of employees represents the labor element, and total water supply, administrative land area, and urban electricity consumption represent the resource element. The index system also includes four output indicators: regional GDP representing the regional economic scale, sewage discharge, exhaust emission (SO_2), and dust emission as undesirable outputs representing urban ecological benefits level.

The urbanization efficiency evaluation index system includes four input indicators, i.e., built-up area, total fixed assets investment, fiscal expenditure, and year-end numbers of employees, where the input indicators include the land element represented by the built-up area, the capital element represented by the total fixed assets investment and fiscal expenditure, and human capital represented by year-end numbers of employees. Output indicators are residents' savings deposits and total retail sales of consumer goods, which represent economic scale and social consumption level, respectively. The evaluation indicator system is shown in Table 1.

Table 1. Evaluation index system of urbanization efficiency and eco-efficiency.

Purpose	Variables	Criteria	Indicators	Unit
Eco-efficiency	Input variables	Capital element input	Total fixed assets investment	10^4 Yuan
		Resource element input	Administrative land area	km^2
			Urban electricity consumption	10^4 kwh
			Total water supply	10^4 t
		Labor factors input	Year-end number of employees	10^4 person
	Output variables	Desirable output	Regional GDP	10^4 Yuan
		Undesirable output	Sewage discharge	10^4 t
			Exhaust emission (SO_2)	t
			Dust emission	t
Urbanization efficiency	Input variables	Human capital input	Year-end number of employees	10^4 person
		Capital element input	Total fixed assets investment	10^4 Yuan
			Fiscal expenditure	10^4 Yuan
		Land element input	Built-up area	km^2
	Output variables	Scale of the city's economy	Total retail sales of consumer goods	10^4 Yuan
			Residents' savings deposits	10^4 Yuan

To reflect the comprehensive influence of population, industrial structure, technology, greening level, degree of external openness, and urbanization efficiency, respectively, we selected the total population, the Share of secondary sector in GDP, the expenditure on science and technology, the greenery coverage of built-up area, the actual amount of foreign capital used, and the urbanization efficiency, as influencing factors in this paper (Table 2).

Table 2. STIRPAT variable names and descriptions.

Variable Type	Variables	Symbols	Indicators	Unit
Explained variables	Eco-efficiency	*EE*	Eco-efficiency values	%
Explanatory variables	Population	*POP*	Total population	10^4 person
	Industrial structure	*IS*	Share of secondary sector in GDP	%
	Technology input	*TEC*	Expenditure on science and technology	10^4 Yuan
	Greening level	*GRE*	Greenery coverage of built-up area	%
	Degree of external openness	*FDI*	Actual amount of foreign capital used	10^4 $
	Urbanization efficiency	*URB*	Urbanization efficiency values	%

3.5. Data Source

This study utilized panel data spanning from 2006 to 2019, which was primarily sourced from the China City Construction Statistical Yearbook (2007–2020) and statistical yearbooks and bulletins from various provinces. For variables with missing data, mean imputation and moving average methods were employed for estimation. The related price indices were used to adjust the data to a common baseline of 2006 in order to take into account indicators that may be impacted by price factors, such as GDP and fixed asset investment. Descriptive statistical data of variables in the US-SBM model are presented in Table 3. It is noteworthy that some variables exhibit maximum values tens of times greater than their corresponding minimum values, indicating significant differences between cities and considerable temporal variation in urban economic activities.

Table 3. Descriptive statistics of input and output variables.

Variable	Unit	Obs	Mean	Std. Dev.	Min	Max
Total fixed assets investment [a]	10^8 Yuan	896	1000	158	12.14	10,400
Administrative land area	km^2	896	2637.54	4381.70	115	43,263
Urban electricity consumption	10^4 kwh	896	2,172,687	2,846,518	49,826	15,714,000
Total water supply	10^4 t	896	31,066.36	54,248.76	23	349,481
Year-end number of employees	10^4 person	896	74.54	131.46	2	819
Regional GDP [a]	10^8 Yuan	896	2320	40,100	41.8741	27,800
Sewage discharge	10^4 t	896	11,986.30	13,162.75	232	91,260
Exhaust emission (SO_2)	t	896	60,370.82	77,906.86	978	682,922
Dust emission	t	896	34,735.23	85,485.82	162	1,859,866
Fiscal expenditure [a]	10^8 Yuan	896	261.33	567.02	3.09	4740
Built-up area	km^2	896	228.94	301.17	19	1515
Total retail sales of consumer goods [a]	10^8 Yuan	896	1130	14,700	45.54	9450
Residents' savings deposits [a]	10^8 Yuan	896	1880	3610	42.84	25,600

[a] At 2006 price.

4. Results

4.1. Analysis of the Evolution of Spatiotemporal Patterns of Eco-Efficiency

Based on US-SBM, this study measured the *EE* of 64 cities in China's four typical urban agglomerations from 2006 to 2019. The findings revealed average *EE* in the four areas was 0.866 during this period, indicating a moderately high level of *EE*, and their development trends exhibited variations. However, the overall *EE* level showed a downward trend (Figure 2), declining by approximately 12.9%. During the period between 2006 and 2019, the *EE* mean values of the four clusters in China were sorted in decreasing order as follows: CCEZ > PRD > BTHMR > YRD, with mean values of 0.981, 0.909, 0.842, and 0.732, respectively. Further examination of the eco-efficiency within each urban cluster revealed that, in 2006, a total of 36 cities had mean eco-efficiency values greater than 1, which accounted for 56.25%, 77.78%, 61.54%, and 46.15% of the cities in the CCEZ, the PRD, the BTHMR, and the YRD, respectively. These cities were Zhoushan, Tongling, Shanghai, and Wuxi in the YRD; Dazhou, Deyang, Guang'an, Suining, and Ziyang in the CCEZ; Shenzhen, Guangzhou, and Foshan in the PRD; and Beijing, Tianjin, Xingtai, Cangzhou, Langfang, and Hengshui in the BTHMR. By 2019, the number of cities that had reached the optimal frontier surface had decreased to 25, accounting for 38.46%, 55.56%, 53.85%, and 18.75% of the YRD, the PRD, the BTHMR, and the CCEZ, respectively. More importantly, both the PRD and the CCEZ experienced significant declines in the number of cities that had reached the optimal frontier. In 2013, the mean *EE* values of the four urban agglomerations were relatively low, primarily due to the slowing down of economic growth in 2012. In an effort to maintain economic increase, the urban agglomerations accelerated the development of high-polluting, high-energy-consuming, and high-emission industrial projects, which caused a decrease in *EE*. However, since the Chinese government proposed the concept of high-quality development in 2017, governments at all levels have begun to attach greater importance to ecological environmental protection and the promotion of resource utilization efficiency. Consequently, the downward and fluctuating trend in *EE* has gradually slowed down. Analyzing observations from three cross-sectional time points in 2006, 2013, and 2019, Shenzhen was consistently ranked first in eco-efficiency. As the window of China's reform and opening up, Shenzhen not only presents as a highly developed modern international city, but also has been awarded the dual honors of being a national ecological civilization construction demonstration area and a "Clear waters and green mountains are as valuable as mountains of gold and silver" practice innovation base in China. Shenzhen fully implemented the concept of ecological civilization, adhered to the synchronous development of park construction and special zone construction, and led the way in China. Conversely, cities such as Luzhou, Leshan, and Handan have relatively backward industrial development levels and economic levels, with low efficiency in factor

aggregation and allocation, resulting in less obvious production scale effects [49]. As a result, these cities have been consistently ranked at the bottom.

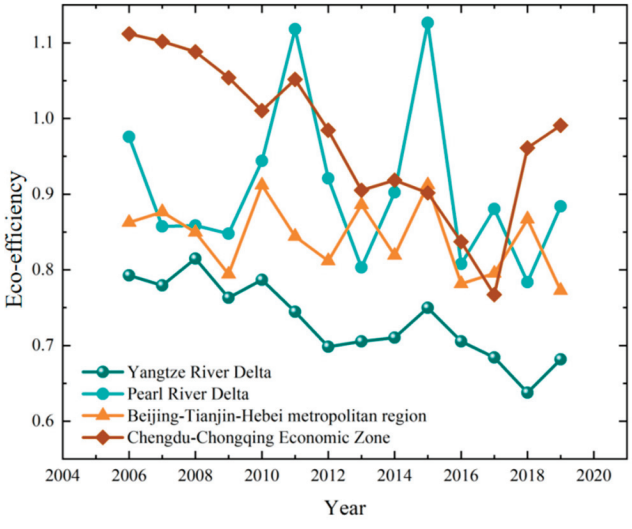

Figure 2. Changes of eco-efficiency in four urban agglomerations from 2006 to 2019.

EE values of the four urban agglomerations were classified into five levels using ArcGIS 10.3, according to the trend of changes observed. Level I ($EE > 1.4$) represents the highest *EE*, classified as a super-high level; Level II ($1.1 < EE < 1.4$) represents cities with high *EE*, classified as a high level; Level III ($0.8 < EE < 1.1$) represents cities with moderately high *EE*, classified as a moderately high level; Level IV ($0.4 < EE < 0.8$) represents cities with moderately low *EE*, classified as a moderately low level; and Level V ($EE < 0.4$) represents cities with low *EE* levels, classified as a low level. These five levels were used to classify urban efficiency into low, medium-low, moderately high, high, and super-high.

The overall mean *EE* of BTHMR is 0.842, ranking third among the four urban agglomerations. However, *EE* mean value fluctuated between 0.75 and 0.95, indicating an unstable development trend. The mean *EE* value in 2006 was 0.862, whereas in 2019, it decreased by approximately 10.3% to 0.773. The BTHMR demonstrated a mature cell-like structure [30], with Beijing, Tianjin, and the surrounding areas acting as the "cell nucleus" and the surrounding region of the capital economic belt serving as the "cell cytoplasm". From 2006 to 2019, *EE* of the BTHMR gradually illustrated a radial distribution pattern of moderately high in the middle and low in the periphery (Figure 3). Beijing and Tianjin have political advantages oriented toward resources, research advantages in knowledge innovation, quality advantages in environmental education, and tourism advantages in cultural history, which have less impact on the environment when promoting socio-economic development. In contrast, surrounding cities such as Shijiazhuang, Zhangjiakou, Tangshan, and Baoding mainly bear the upstream part of the regional industrial chain, which is dominated by resource-based industries in their development. They are affected by the pollution of industrial activities, which leads to a higher level of pollution discharge. Therefore, these cities play a significant role as the cornerstone among the urban clusters, while also posing threats to sustainability.

Figure 3. Spatial distribution of eco-efficiency in the typical urban agglomerations. (**a**–**c**) represent the EE of the BTHMR in 2006, 2013, 2019; (**d**–**f**) represent the EE of the YRD in 2006, 2013, 2019; (**g**–**i**) represent the EE of the PRD in 2006, 2013, 2019; (**j**–**l**) represent the EE of the CCEZ in 2006, 2013, 2019.

The overall average value of *EE* of the YRD is 0.732, and the average value remains around 0.7 in each year, with less fluctuation and more stable development. The average value of *EE* in 2006 is 0.793, while in 2019 it is 0.682, a decrease of around 14%. Cities like Shanghai, Zhoushan, Chizhou, and Tongling have been in the high-efficiency zone and are located on the optimal frontier surface (Figure 3). While vigorously developing their economies in recent years, the YRD has also been actively responding to and implementing policies related to ecological and environmental management, and strictly supervising and managing the pollution emission behavior of enterprises, making the development of *EE* more stable. Zhoushan and Tongling are national forest cities with relatively high *EE* by virtue of their reasonable industrial structure and lower resource consumption and environmental pollution. The spatial distribution structure of YRD is stable from 2006 to 2019, but local differences still exist. As the springboard for China's opening up to the world, Shanghai benefits from advantages of a platform for foreign exchanges, the transportation advantage of a port corridor, the resource advantage of natural landscape, and the industrial advantage of high technology; focusing on foreign trade and the information technology industry characterized by high profits and low consumption, its eco-efficiency is consistently at a high level. In recent years, the YRD, with its superior economic base and platform advantages, has seen the eastern coastal cities become the engine driving the region's development with high-tech, financial services, education, and healthcare, and the central and western cities become the cornerstone of regional development with

industrial manufacturing, logistics, and transportation. The YRD is seeking a high-quality development path with parallel economy and ecology.

The overall average *EE* value of the PRD is 0.908, ranking second among the four urban agglomerations. The average *EE* value in 2006 was 0.976, compared to 0.884 in 2019, approximately a 9.43% decrease. Among the urban cluster, there were seven high-efficiency cities and only one low-efficiency city, Jiangmen, in 2006, indicating a high level of *EE* for the entire urban agglomeration. However, the number of high-*EE* cities decreased in 2013, leading to a decline in overall eco-efficiency compared to 2006. In 2019, the number of low and moderately low *EE* cities significantly increased, accounting for 44.44%. The continuous strengthening of regional economic cooperation and the comprehensive implementation of the Guangdong–Hong Kong–Macao Greater Bay Area construction have brought economic benefits to the PRD. However, this has also led to new regional environmental problems. The spatial distribution of *EE* value in the PRD exhibits a radial pattern centered on Guangzhou and Shenzhen, as shown in Figure 3. Cities such as Shenzhen, Guangzhou, Zhongshan, and Foshan have a strong industrial foundation, high-quality human resources, and environmentally friendly industries, primarily focused on foreign trade, financial services, and information technology. However, small and medium-sized cities such as Huizhou, Zhaoqing, and Jiangmen have more high-pollution industries such as electroplating and printing, a weaker industrial foundation, and have not fully utilized the ecological environment resources to bring higher economic benefits.

The CCEZ demonstrates a high level of eco-efficiency, with an overall mean *EE* value of 0.981, despite its location in the western region and relatively weak economic foundation due to the support of the "Belt and Road" and western development strategy, which have increased government investment in environmental governance. However, the *EE* mean value has fluctuated between 0.8 and 1.2, with a decline from a mean *EE* value of 1.162 in 2006 to 0.991 in 2019, representing a decline of approximately 14.7%. In terms of time span, a declining-then-increasing trend has emerged, with the lowest point being 0.767 in 2017. In terms of spatial distribution, as shown in Figure 3, Chengdu serves as the core leading city of the region, primarily focusing on environmentally friendly industries such as the internet, electronic circuits, and new energy, resulting in relatively high eco-efficiency. However, surrounding cities such as Mianyang, Yibin, and Luzhou are more involved in the resource extraction, processing, manufacturing, and logistics industries, resulting in greater environmental pollution. The Chengdu–Chongqing Economic Zone is mainly characterized by "low input, low output and low pollution" and the adjustment of input and output in the context of low economic growth rates [50]. The publication of the "Development Plan for the Chengdu–Chongqing Urban Cluster" in 2016 officially initiated the process of modernizing western urban areas, accelerating the socio-economic development of the CCEZ, strengthening the flow of economic and industrial elements between cities, and gradually forming an industrial distribution along the Yangtze River economic belt. With the migration of people and the enhancement of scientific and innovative capabilities, although the balance between ecosystem protection and economic growth has not yet been established, the high-*EE* value zone along the Chengdu–Chongqing double-loop economic corridor is gradually becoming clearer.

4.2. Analysis of the Evolution of Spatiotemporal Patterns of Urbanization Efficiency

This study assesses the level of urbanization in the four urban agglomerations by constructing a novel comprehensive evaluation index system based on panel data from 64 cities between 2006 and 2019. US-SBM was employed for the evaluation, indicating the average urbanization efficiency demonstrating an upward trend from 2006 to 2019 (Figure 4). The overall urbanization efficiency of the four urban clusters during this period was 0.616, which falls within the medium to high range. Figure 5 displays the spatial distribution of *URB* in 2006, 2013, and 2019. The findings indicated that the urbanization efficiency was highest in eastern coastal cities such as Shenzhen, Guangzhou, and Shanghai. However, the spatial pattern of urbanization exhibited an uneven distribution, with urban-

ization efficiency gradually decreasing from east to west. Additionally, the number of cities with a relatively high degree of urbanization has increased, and the spatial pattern of cities with medium to high and medium urbanization efficiency has shown a trend of expanding from the east to the center. Overall, the spatial pattern of urbanization efficiency in the four urban clusters is consistent with China's strategic planning for urban transformation.

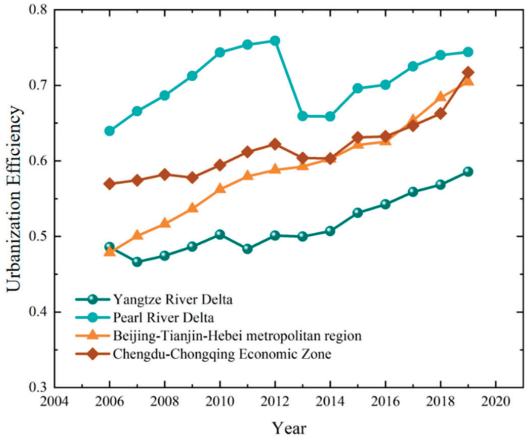

Figure 4. Changes of urbanization efficiency in the four urban agglomerations from 2006 to 2019.

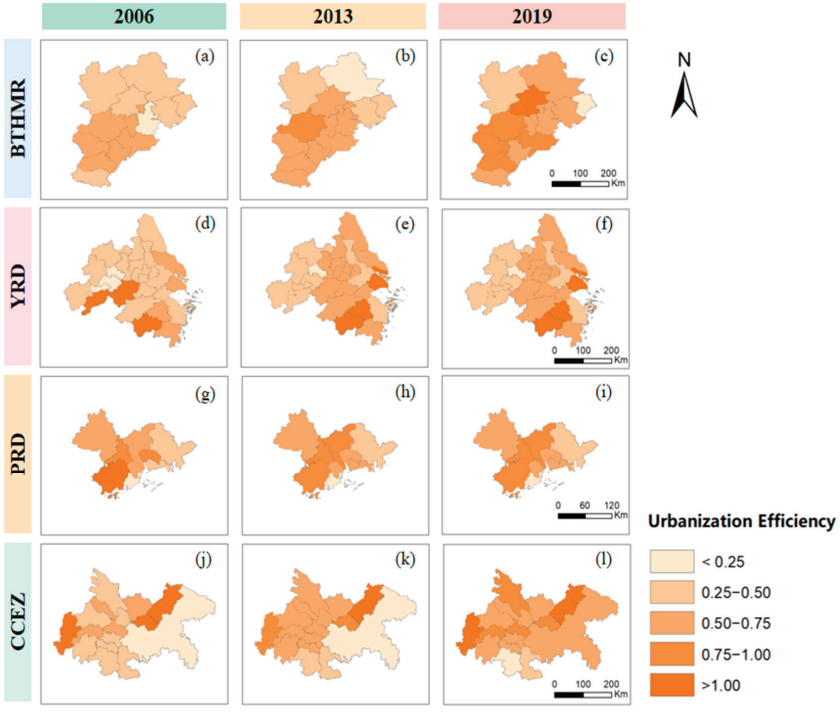

Figure 5. Spatial distribution of urbanization efficiency in the urban agglomerations. (**a**–**c**) represent the urbanization efficiency of the BTHMR in 2006, 2013, 2019; (**d**–**f**) represent the urbanization efficiency of the YRD in 2006, 2013, 2019; (**g**–**i**) represent the urbanization efficiency of the PRD in 2006, 2013, 2019; (**j**–**l**) represent the urbanization efficiency of the CCEZ in 2006, 2013, 2019.

4.3. Analysis of Factors Influencing Eco-Efficiency

Based on the aforementioned STIRPAT, an empirical analysis of the factors influencing EE in the four urban agglomerations was conducted using the STATA 16.0 software fixed-effects Tobit regression model, and the regression is shown in Table 4.

Table 4. Panel data regression results.

Explanatory Variable	Coefficient	Standard Error	*p*-Value
Cons	2.603565 ***	0.4538885	0.000
Population (ln*POP*)	−0.1036211 ***	0.0233198	0.000
Industrial structure (ln*IS*)	−0.3631796 ***	0.0827074	0.000
Urbanization (ln*URB*)	0.0760284 **	0.0358237	0.034
Foreign direct investment (ln*FDI*)	−0.0358348 ***	0.0133494	0.007
Technology input (ln*TEC*)	0.008113 *	0.0147322	0.082
Greenery (ln*GRE*)	−0.173352 **	0.0718395	0.016

Note: *, **, and *** represent coefficient significant at 10%, 5%, and 1%, respectively.

The effects of total population, industrial structure, *FDI*, and greenery on *EE* show significant negative correlation coefficients. Firstly, the total population has a significant negative impact on *EE* at the 1% level. A large population puts pressure on the economy, environment, and resources, which in turn leads to a reduction in *EE* and undermines sustainability of urban areas. Secondly, the analysis revealed that the coefficient of industrial structure on *EE* is significantly negative. Adjustments in this variable can cause changes in energy consumption and pollution emission intensity, which can have a significant impact on the environment. The study used the proportion of the secondary sector output to GDP to measure the industrial structure, and found heavy industries (fossil energy, machinery manufacturing, and assembly processing) account mainly for China's secondary industry and are characterized by high input and high pollution, which have a negative impact on *EE*. Thirdly, the results showed that *FDI* negatively affected *EE*, and the "pollution heaven" hypothesis is valid, which is consistent with the findings of Chang and others [51]. The study emphasized that regional competition leads to cities blindly introducing *FDI*, neglecting to examine the scale, direction, and quality of investment, resulting in a large proportion of foreign investment flowing into labor-intensive and low value-added traditional industries, which has an overall negative effect on the ecology. Additionally, the study found the short-term and long-term effects of *FDI* on the environment in China differ. In the short term, the structural and technological effects of foreign investment are greater than the scale effects, but as time increases, the scale effects of capacity expansion will gradually outweigh the technological spillover effects, with a corresponding increase in the scale of environmental pollution [52] and a consequent adverse impact on *EE*. Meanwhile, advanced production technologies can be introduced by way of *FDI* [53] to improve *EE*. Therefore, rational guidance in foreign direct investment is necessary. Lastly, this analysis revealed a negative correlation between the greening level and *EE* at a 5% significance level. The study highlighted that the main forms of greening in urban built-up areas, such as green belts and lawns, hardly constitute a complete ecosystem and to a large extent only serve to beautify the city. This is not conducive to improving environmental quality and instead reduces *EE* due to the high maintenance costs incurred later.

The technology inputs and urbanization have significant positive effects on *EE* at the 5% and 10% levels, respectively. Investing in science and technology has a significant catalytic impact on *EE*. "Innovation-driven" is a pivotal factor in economic transformation and a key driver of sustainable economic growth. Progress in science and technology can bring about technological and efficiency improvements in production and environmental protection, which are essential for establishing a favorable development environment for new urbanization. Technological progress can improve both factor utilization and resource utilization rates and can facilitate the formation of innovative and high-growth sectors, which can also increase the level of pollutant harmless treatment and effectively reduce

resource consumption and ecological environmental pressure, thus contributing to the improvement of *EE*. The coefficient of urbanization efficiency on *EE* is positive, indicating that *URB* can enhance eco-efficiency to a certain degree. This may be due to the fact that young laborers from medium and small cities and rural areas will flock to regional center cities in large numbers, bringing about the labor scale effects and industrial agglomeration effects. Further urban development will increasingly emphasize sustainable urban transformation, thus promoting low-carbon, green, and sustainable urban construction, transforming the traditional extensive economy into an intensive one, and fostering the recovery of urban eco-efficiency.

5. Discussion and Policy Suggestions

5.1. Discussion

Eco-efficiency is utilized as a metric for assessing the environmental performance of economic activities [7] and has become a crucial criterion in the formulation of economic and environmental advancement policies in regions and countries across the globe. Further deepening the investigation of eco-efficiency holds immense importance in promoting sustainable development. Therefore, this paper uses the period 2006–2019 as the examination period; based on the urban agglomeration perspective, the Super-SBM model with undesirable output is applied to measure the *EE* and urbanization efficiency of 64 cities within the BTHMR, the YRD, the PRD, and the CCEZ, revealing the spatiotemporal evolution patterns of eco-efficiency in the four major urban agglomerations, further identifying the factors influencing *EE* by constructing the STIRPAT model, and exploring the relationship between urbanization and *EE*.

Firstly, this paper distinguishes itself from prior research by conducting a comparative analysis of *EE* of typical urban agglomerations in China, rather than focusing on a single region. Simultaneously, it provides an in-depth analysis of spatiotemporal evolution patterns of eco-efficiency. The US-SBM model, which addresses the factor relaxation issue and accounts for undesirable output, is used to overcome the limitations of traditional DEA and SFA models to a certain extent and provides a more accurate measurement of *EE*. The findings indicate that the four major urban agglomerations possess high levels of eco-efficiency, yet exhibit divergent development trends, with a general downward trajectory. This trend can be attributed to a development paradigm that prioritizes GDP growth, resulting in suboptimal resource allocation, resource depletion, and environmental degradation. During the period of 2006−2019, the average *EE* value for the four major urban agglomerations was 0.865, indicating a moderately high level of *EE*. Among them, the BTHMR exhibited considerable fluctuations in *EE* with an unstable development trend, the mean *EE* value decreased by approximately 10.3% from 2006 to 2019. The YRD exhibited a relatively stable development trend in terms of *EE*, with a decline of 9.43% over the examined period. In contrast, the *EE* trend line of the PRD demonstrated an overall "M" shape, characterized by significant fluctuations and a rising-declining-rising-declining trajectory. The CCEZ showed a development trend of initially falling and then rising, reaching its lowest point in 2017 before a subsequent increase. From 2006 to 2019, the average *EE* of the four typical urban agglomerations, in descending order, are: CCEZ > PRD > BTHMR > YRD. There are structural differences in the *EE* of cities within urban agglomerations, and the polarization effect of central cities needs to be strengthened. The spatial distribution of the BTHMR presents a cellular structure with Beijing, Tianjin, and their surrounding areas as the "cell nucleus" and the surrounding Beijing–Tianjin economic belt as the "cytoplasm," gradually showing a radial distribution characteristic of high in the middle and low in the surrounding area. The spatial distribution structure of the YRD remains stable from 2006 to 2019, but local differences still exist. The distribution of eco-efficiency values of the PRD presents a radiation pattern centered on Guangzhou and Shenzhen. The *EE* distribution characteristics of the CCEZ are relatively stable, with Chengdu as the core city, showing a distribution feature of high in the middle and low in the periphery.

Furthermore, based on the extended STIRPAT model combined with fixed-effect Tobit regression, the factors influencing *EE* within the four primary urban agglomerations are identified and the correlation between urbanization and *EE* is explored. The results show the *TEC* and *URB* have significant positive effects on *EE*, while *POP*, *IS*, *FDI*, and *GRE* have a restraining effect on it. Among them, the effects of the level of science and technology as well as *FDI* on eco-efficiency are consistent with the results of Chang (2020) [51]. In other words, technological advances promote eco-friendly technology and *EE*. *FDI* leads to an increase in environmental pollution, indicating a current tendency that countries in less developed areas sacrifice resources for economic development and the lack of strict control of environmental protection regulations [54]. Provinces that are more open to the outside world may be more concerned about their city images. Major cities such as Shanghai and Shenzhen still manage to counteract the negative effects of *FDI* by improving technology, though this is not always effective. Moreover, the negative impact of industrial structure is contrary to the findings of Zhang (2021) [55], which may be attributed to the selection of indicators. This paper argues that China's current industrial structure presents developed third industries in developed cities such as Beijing, Shanghai, and Shenzhen. Even within the advanced economic urban agglomerations, it is still dominated by the export of labor-intensive products, heavy industry and heavy pollution. This industry structure limits industrial optimization and causes environmental pressures [56]. More notably, greening in urban built-up areas does not make a positive contribution to the *EE* of the four major urban agglomerations. It is likely that the chosen indicator only represents the amount of land allocated for greening. High greening rates on building sites can be low-quality vegetation cover or even barren land [57], and to some extent can also hinder the efficiency of building development resources. For example, the spacing of protective forest belts should be set at a reasonable scale to achieve the optimal effect of wind and sand control in a specific range of arrangement and prevent the resources waste with diminishing marginal benefits. In this regard, the General Office of the State Council has proposed guidelines for scientific greening.

5.2. Policy Suggestions

Through the analysis conducted in this paper, apparently, there is still room for improving the efficiency and balanced distribution of green development in China's four primary urban agglomerations. Additionally, it is essential for the green development of distinct urban agglomerations to align with their respective features to achieve a comprehensive and sustainable green transformation of China's economy and society. To this end, several targeted suggestions for green development in the four typical urban agglomerations are proposed for the future.

The growth of *EE* seeks the coordinated development of economy, society, and the environment, which requires structural adjustment, technical efficiency enhancement, and policy support. Firstly, it is essential to emphasize regional heterogeneity and facilitate coordinated development. For regions such as the YRD, the PRD, and the BTHMR, which are already relatively developed, the preeminent status of core cities should be reinforced, their diffusion effect amplified, and a virtuous competition mechanism of mutual support established. We should establish an integrated development consciousness, build a platform for information exchange and resource sharing, achieve functional complementarity through horizontal dislocation and vertical division of labor cooperation, promote the allocation of production factors in a reasonable and efficient manner, and achieve the transformation of the eco-efficiency of developed regions from "positive internalities" to "positive externalities" to low eco-efficiency cities in the surrounding areas. Specifically, the implementation of Beijing's capital function positioning should be carried out, and attention should be paid to the policy opportunities brought by the upgrading of energy strategies to neighboring cities. The YRD should maintain the green development momentum of two types of efficient cities with industrial and ecological advantages and promote the industrial optimization of inland cities in the Yangtze River Delta [58]. Consolidate the

growth pole status of cities such as Guangzhou and Shenzhen, pull the green development of the eastern and western ends of the PRD, and capitalize on the achievements of the construction of the Guangzhou–Shenzhen–Hong Kong–Macao Science and Technology Innovation Corridor to inject the momentum of science and technology innovation into green development. For the CCEZ, it should proactively capitalize on our strengths and undertake the transfer of industries from major cities, take the industrial transfer and innovation drive as an opportunity to promote the division of labor and upgrading of industries in each city, thus improving the layout of the industrial chain.

Secondly, in order to achieve green, circular, and low-carbon development, it is imperative for the government to assume a macro-regulatory role in the economy and industrial structure. Specifically, the government should incorporate the improvement of eco-efficiency as a fundamental criterion in the performance assessment system of local governments. Moreover, it is recommended that the government increase financial support for environmental protection and pollution control, while simultaneously encouraging enterprises to engage in research, development, and innovation of green technologies such as low-carbon technologies, clean production technologies, and recycling technologies. Simultaneously, according to the changes in regional economic development, it is essential to promote the transformation and upgrading of the industrial structure, as well as the transition from old to new momentum. This can be achieved by increasing the proportion of technology-intensive industries and tertiary industries, enhancing the added value of industries, and fostering long-term, healthy, and sustainable development of the regional economy. Metropolitan areas can attract top-tier human resources through the implementation of a range of preferential policies, while also increasing population density within the limits of environmental carrying capacity. Through the utilization of scale and agglomeration effects, economic and environmental efficiency can be enhanced to promote sustainable development. The government should also further enhance environmental regulations and judiciously attract foreign investments while reducing excess investment in urban greening and planning the greening area of cities reasonably to avoid resource wastage caused by formalism. Furthermore, local governments should carry out reasonable planning of land and enhance the efficiency of urban land [59]. Based on the actual situation, a rational layout of land space should be carried out; this entails a proper distribution of production space, living space, and ecological space within urban areas, promoting coordinated spatial development of the city's economy, people's lives, and ecological environment. The government, in conjunction with enterprises and other market players, should vigorously promote the adoption of clean energy, improve the multi-track system of environmental regulation, reduce industrial pollution emissions, and promote greater awareness of environmental protection among all people.

6. Conclusions

Eco-efficiency is of vital importance in promoting the sustainable and harmonious development of urban agglomerations under the Dual Carbon Target. In this study, we applied the Super-SBM model incorporating undesirable outputs to measure the eco-efficiency and urbanization efficiency of 64 cities located in the four urban agglomerations during 2006–2019. For further analysis, we used an extended STIRPAT model combined with spatial panel Tobit analysis to explore the determinants of eco-efficiency. In terms of comprehensive time series development and spatial distribution, the average *EE* value of the four typical urban agglomerations is 0.866, which is at a relatively high level. However, the eco-efficiency level has demonstrated a declining trend over time, experiencing a reduction of approximately 12.9%. This trend can be attributed to a development model that prioritizes economic growth, leading to unsatisfactory resource allocation, resource depletion, and environmental degradation. There exists a notable regional heterogeneity in the structural distribution of eco-efficiency across each urban agglomeration. Major central cities, such as Beijing, Guangzhou, Shenzhen, and Shanghai, have achieved a commendable equilibrium between economic growth and environmental preservation. Additionally,

these cities have a certain degree of radiation effect on neighboring regions with regards to green development, but the degree of influence varies depending on factors such as differing economic and industrial foundations and geographical locations. The level of technology and urbanization exhibits a significant positive effect on eco-efficiency, while population, industrial structure, *FDI*, and greening level demonstrate a suppressive effect on urban eco-efficiency.

The aforementioned study serves to supplement the extant *EE* research framework and can offer valuable insights and recommendations for the sustainable development of China as well as other nations and holds significant international demonstrative implications. For instance, we can promote coordinated regional development and realize the radiating effects of eco-efficiency through measures such as industrial restructuring and technological efficiency improvements. Alternatively, the government state strategically coordinates the ecological development of urban agglomerations through environmental protection regulations and scientific greening guidelines. However, there are still some limitations in this study: This paper investigates the spatiotemporal variations in *EE* and its influencing factors within China's four primary urban agglomerations, without delving into other regions. The present study's selection of determinants impacting *EE* is not exhaustive, as factors such as residents' consumption and level of education, as well as environmental policies, may also exert a certain degree of influence on *EE*. In the future, there is a pressing need to undertake a more comprehensive and exhaustive investigation of eco-efficiency and its determinants across various regions in China. Specifically, it is imperative to conduct a comprehensive analysis of the discrepancies and formation mechanisms between urban agglomerations at varying levels of development. Only this way will enable the formulation of targeted policy recommendations to facilitate sustainable development.

Author Contributions: Conceptualization, S.X. and C.W. (Chao Wang); methodology, S.X. and C.W. (Chao Wang); software, S.X. and S.Z.; validation, S.X. and C.W. (Chuyao Weng); formal analysis, S.X.; investigation, S.X. and C.W. (Chuyao Weng); resources, S.X.; data curation, S.X.; writing—original draft preparation, S.X. and S.Z.; writing—review and editing, S.X., S.Z., Y.Z. and C.W. (Chuyao Weng); visualization, S.X.; supervision, S.X. and C.W. (Chao Wang); project administration, S.X.; funding acquisition, S.X. and Y.Z. All authors have read and agreed to the published version of the manuscript.

Funding: The research is supported by China University of Geosciences (Beijing) University Student Innovation and Entrepreneurship Training Program (X202211415228) and Capital University of Economics and Business: The Fundamental Research Funds for Beijing Universities [No. XRZ2023066].

Data Availability Statement: Data will be made available on request.

Acknowledgments: Thank you to everyone who contributed to this study.

Conflicts of Interest: The authors declare no conflict of interest.

References

1. Lei, Y.; Chen, J.; Sun, J. Analysis of spatiotemporal evolution characteristics of green development efficiency in China's three major urban agglomerations. *Urban Obs.* **2020**, *1*, 11–18.
2. Fang, C. Important progress and prospects of urbanization and urban agglomeration in China in the past 40 years of reform and opening up. *Econ. Geogr.* **2018**, *38*, 1–9.
3. Yao, S.; Xu, L.; Zheng, T.; Ma, L. Mechanisms and new ideas of rapid growth of Chinese urban agglomerations: A case study of the Yangtze River Delta urban agglomeration. *Hum. Geogr.* **2020**, *35*, 11–18. [CrossRef]
4. Peng, H.; Zhang, J.; Lu, L.; Tang, G.; Yan, B.; Xiao, X.; Han, Y. Eco-efficiency and its determinants at a tourism destination: A case study of Huangshan National Park, China. *Tour. Manag.* **2017**, *60*, 201–211. [CrossRef]
5. Zeng, L. China's Eco-Efficiency: Regional Differences and Influencing Factors Based on a Spatial Panel Data Approach. *Sustainability* **2021**, *13*, 3143. [CrossRef]
6. Yuan, X.; Nie, Y.; Zeng, L.; Lu, C.; Yang, T. Exploring the Impacts of Urbanization on Eco-Efficiency in China. *Land* **2023**, *12*, 687. [CrossRef]
7. Schaltegger, S.; Sturm, A. Ökologische Rationalität: Ansatzpunkte zur Ausgestaltung von ökologieorientierten Managementinstrumenten. *Unternehm. Swiss J. Bus. Res. Pract.* **1990**, *44*, 273–290.

8. WBCSD. *Eco-Efficient Leadership for Improved Economic and Environmental Performance*; WBCSD: Geneva, Switzerland, 1996; pp. 3–16.
9. Halleux, J.M.; Marcinczak, S.; van der Krabben, E. The adaptive efficiency of land use planning measured by the control of urban sprawl. The cases of the Netherlands, Belgium and Poland. *Land Use Policy* **2012**, *29*, 887–898. [CrossRef]
10. Brülhart, M.; Mathys, N.A. Sectoral agglomeration economies in a panel of European regions. *Reg. Sci. Urban Econ.* **2008**, *38*, 348–362. [CrossRef]
11. Mallet, J.S. *Municipal Powers, Land Use Planning, and the Environment: Understanding the Public's Role*; Environmental Law Centre: Edmonton, AB, Canada, 2005.
12. Ma, L.; Long, H.; Chen, K.; Tu, S.; Zhang, Y.; Liao, L. Green growth efficiency of Chinese cities and its spatio-temporal pattern. *Resour. Conserv. Recycl.* **2019**, *146*, 441–451. [CrossRef]
13. Beames, A.; Broekx, S.; Heijungs, R.; Lookman, R.; Boonen, K.; Van Geert, Y.; Dendoncker, K.; Seuntjens, P. Accounting for land-use efficiency and temporal variations between brownfield remediation alternatives in life-cycle assessment. *J. Clean. Prod.* **2015**, *101*, 109–117. [CrossRef]
14. Xie, H.; Wang, W. Spatiotemporal differences and convergence of urban industrial land use efficiency for China's major economic zones. *J. Geogr. Sci.* **2015**, *25*, 1183–1198. [CrossRef]
15. Reinhard, S.; Knox Lovell, C.A.; Thijssen, G.J. Environmental efficiency with multiple environmentally detrimental variables; estimated with SFA and DEA. *Eur. J. Oper. Res.* **2000**, *121*, 287–303. [CrossRef]
16. Wursthorn, S.; Poganietz, W.R.; Schebek, L. Economic-environmental monitoring indicators for European countries: A disaggregated sector-based approach for monitoring eco-efficiency. *Ecol. Econ.* **2011**, *70*, 487–496. [CrossRef]
17. Margarita, R.; Victor, M.; Pedro, M. A new frontier approach to model the eco-efficiency in European countries. *J. Clean. Prod.* **2015**, *103*, 562–573. [CrossRef]
18. Liu, Y.; Qin, M. Comprehensive measurement and comparison of green efficiency of the four major coastal urban agglomerations in eastern China. *China Popul. Resour. Environ.* **2019**, *29*, 11–20.
19. Bai, Y.; Deng, X.; Jiang, S.; Zhang, Q.; Wang, Z. Exploring the relationship between urbanization and urban eco-efficiency: Evidence from prefecture-level cities in China. *J. Clean. Prod.* **2018**, *195*, 1487–1496. [CrossRef]
20. Shi, T.; Zhang, J.; Shi, H. Spatiotemporal evolution and influencing factors of ecological efficiency in the eastern coastal urban agglomerations of China. *Ecol. Econ.* **2023**, *b39*, 90–100+123. (In Chinese)
21. Tone, K. A slacks-based measure of efficiency in data envelopment analysis. *Eur. J. Oper. Res.* **2001**, *130*, 498–509. [CrossRef]
22. Tone, K. A slacks-based measure of super-efficiency in data envelopment analysis. *Eur. J. Oper. Res.* **2002**, *143*, 32–41. [CrossRef]
23. Chunshan, Z.; Chenyi, S.; Shaojian, W.; Guojun, Z. Estimation of eco-efficiency and its influencing factors in Guangdong pr-ovince based on Super-SBM and panel regression models. *Ecol. Indic.* **2018**, *86*, 67–80. [CrossRef]
24. Guan, W.; Xu, S. Study of spatial patterns and spatial effects of energy eco-efficiency in China. *J. Geogr. Sci.* **2016**, *26*, 1362–1376. [CrossRef]
25. Li, G.; Fang, C.; He, S. The influence of environmental efficiency on PM2.5 pollution: Evidence from 283 Chinese prefecture-level cities. *Sci. Total Environ.* **2020**, *748*, 141549. [CrossRef]
26. Luo, Y.; Lu, Z.; Muhammad, S.; Yang, H. The heterogeneous effects of different technological innovations on eco-efficiency: Evidence from 30 China's provinces. *Ecol. Indic.* **2021**, *127*, 107802. [CrossRef]
27. Liao, J.; Yu, C.; Feng, Z.; Zhao, H.; Wu, K.; Ma, X. Spatial differentiation characteristics and driving factors of agricultural eco-efficiency in Chinese provinces from the perspective of ecosystem services. *J. Clean. Prod.* **2021**, *288*, 125466. [CrossRef]
28. Díaz-Villavicencio, G.; Didonet, S.R.; Dodd, A. Influencing factors of eco-efficient urban waste management: Evidence from Spanish municipalities. *J. Clean. Prod.* **2017**, *164*, 1486–1496. [CrossRef]
29. Moutinho, V.; Madaleno, M.; Robaina, M. The economic and environmental efficiency assessment in EU cross-country: Evidence from DEA and quantile regression approach. *Ecol. Indic.* **2017**, *78*, 85–97. [CrossRef]
30. Zhang, Q.; Xiao, Y.; Tang, X.; Huang, H. Evolution and influencing factors of ecological efficiency in the five major urban agglomerations of China. *Econ. Geogr.* **2022**, *42*, 54–63. [CrossRef]
31. Fang, C.; Wang, J. A theoretical analysis of interactive coercing effects between urbanization and eco-environment. *Chin. Geogr. Sci.* **2013**, *23*, 147–162. [CrossRef]
32. Wang, S.; Ma, H.; Zhao, Y. Exploring the relationship between urbanization and the eco-environment-A case study of Beijing-Tianjin-Hebei region. *Ecol. Indic.* **2014**, *45*, 171–183. [CrossRef]
33. York, R.; Rosa, E.A.; Dietz, T. STIRPAT, IPAT and ImPACT: Analytic tools for unpacking the driving forces of environmental impacts. *Ecol. Econ.* **2003**, *46*, 351–365. [CrossRef]
34. Chen, Z.; Wu, S.; Ma, W.; Liu, X.; Cai, B.; Liu, J.; Jia, X.; Zhang, M.; Chen, Y.; Xu, L. Analysis of influencing factors of CO_2 emissions in Chinese cities above prefecture level: Based on the extended STIRPAT model. *China Popul. Resour. Environ.* **2018**, *28*, 45–54.
35. Zhang, F.; Zhan, J.; Li, Z.; Jia, S.; Chen, S. Impacts of urban transformation on water footprint and sustainable energ-y in Shanghai, China. *J. Clean. Prod.* **2018**, *190*, 847–853. [CrossRef]
36. Luo, N.; Li, J.; Luo, F. Empirical analysis on the relationship between the China urbanization and regional eco-efficiency. *China Popul. Resour. Environ.* **2013**, *23*, 60.
37. Grossman, G.M.; Krueger, A.B. Economic Growth and the Environment. *Q. J. Econ.* **1994**, *110*, 353–377. [CrossRef]

38. Jin, X.; Li, X.; Feng, Z.; Wu, J.S.; Wu, K. Linking ecological efficiency and the economic agglomeration of China based on the ecological footprint and nighttime light data. *Ecol. Indic.* **2020**, *111*, 106035. [CrossRef]
39. Ren, Y.; Li, Z. Unraveling the dynamics, heterogeneity, determinants of eco-efficiency in Beijing-Tianjin-He-bei urban agglomeration, China. *J. Environ. Manag.* **2022**, *317*, 115407. [CrossRef]
40. Wu, M.; Ma, J. Measurement of regional ecological efficiency in China and analysis of its influencing factors: Based on DEA-Tobit two-step method. *Technol. Econ.* **2016**, *35*, 75–80.
41. Fang, C. Important progress and future development directions of research on urban agglomerations in China. *Acta Geogr. Sin.* **2014**, *69*, 1130–1144.
42. Fang, C.; Wang, Z.; Ma, H. Theoretical understanding and geographical contribution of the formation and development laws of urban agglomerations in China. *Acta Geogr. Sin.* **2018**, *73*, 651–665.
43. Chen, W.; Si, W.; Chen, Z.M. How technological innovations affect urban eco-efficiency in China: A prefecture- level panel data analysis. *J. Clean. Prod.* **2020**, *270*, 122479. [CrossRef]
44. Huang, T.; Hu, X.; Chen, S.; Wang, Y.; Zhang, B. Evaluation of sustainable development level and its influencing factors in countries along the Belt and Road based on the Super-SBM model and Tobit model: Empirical study. *China Popul. Resour. Environ.* **2020**, *30*, 27–37.
45. Zhang, J.R.; Zeng, W.H.; Wang, J.N.; Yang, F.; Jiang, H. Regional low-carbon economy efficiency in China: Analysis based on the Super-SBM model with CO_2 emissions. *J. Clean. Prod.* **2017**, *163*, 202–211. [CrossRef]
46. Matsumoto, K.I.; Chen, Y. Industrial eco-efficiency and its determinants in China: A two-stage approach. *Ecol. Indic.* **2021**, *130*, 108072. [CrossRef]
47. Verfaillie, H.; Bidwell, R. Measuring eco-efficiency-a guide to reporting company performance. *World Bus. Counc. Sustain. Dev.* **2000**, *2000*, 1–39.
48. Ren, Y.; Fang, C.; Lin, X. Evaluation of ecological efficiency of the four major urban agglomerations in eastern coastal China. *Acta Geogr. Sin.* **2017**, *11*, 2047–2063. [CrossRef]
49. Guo, J.; Chen, F. Research on the mechanism of sub-regional green coordinated development in the middle reaches of the Yangtze River urban agglomeration from a perspective of competition and cooperation. *Ecol. Econ.* **2019**, *35*, 95–99+145.
50. Liu, D.; Zhang, K. Analysis of Spatial Differences and the Influencing Factors in Eco-Efficiency of Urban Agglomerations in China. *Sustainability* **2022**, *14*, 12611. [CrossRef]
51. Chang, X.; Guan, X. Spatiotemporal evolution and influencing factors of ecological efficiency in the Yangtze River Delta urban agglomeration during the new urbanization process. *Econ. Geogr.* **2020**, *40*, 185–195.
52. Han, Y.; Li, Z.; Zhang, F.; Shen, C. Environmental effects of China's two-way FDI. *Resour. Sci.* **2019**, *41*, 2043–2058.
53. Ketteni, E.; Kottaridi, C.; Mamuneas, T.P. Information and communication technology and foreign direct investment: Interactions and contributions to economic growth. *Empir. Econ.* **2015**, *48*, 1525–1539. [CrossRef]
54. Xu, M.; Bao, C. Unveiling the comprehensive resources and environmental efficiency and its influencing factors: Within and across the five urban agglomerations in Northwest China. *Ecol. Indic.* **2023**, *154*, 110466. [CrossRef]
55. Zhang, C.; Chen, Y.; Wang, Y. Spatio-temporal differentiation and influencing factors of ecological efficiency in the Yangtze River Delta urban agglomeration. *J. Nanjing Tech Univ. Soc. Sci. Ed.* **2021**, *20*, 95–108+110. (In Chinese)
56. Guo, K.; Cao, Y.; Wang, Z.; Li, Z. Urban and industrial environmental pollution control in China: An analysis of capital input, efficiency and influencing factors. *J. Environ. Manag.* **2022**, *316*, 115198. [CrossRef] [PubMed]
57. He, D.; Miao, J.; Lu, Y.; Song, Y.; Chen, L.; Liu, Y. Urban greenery mitigates the negative effect of urban density on older adults' life satisfaction: Evidence from Shanghai, China. *Cities* **2022**, *124*, 103607. [CrossRef]
58. Lei, Y.; Chen, J.; Sun, J. Exploring the spatial and temporal evolution of green development efficiency in three major urban agglomerations in China. *Urban Insight* **2020**, *70*, 114–127.
59. Wang, C.; Wang, X.; Wang, Y.; Zhan, J.; Chu, X.; Teng, Y.; Liu, W.; Wang, H. Spatio-temporal analysis of human wellbeing and its coupling relationship with ecosystem services in Shandong province, China. *J. Geogr. Sci.* **2023**, *33*, 392–412. [CrossRef]

land

MDPI

Article

Characteristics and Driving Mechanism of Urban Construction Land Expansion along with Rapid Urbanization and Carbon Neutrality in Beijing, China

Huicai Yang [1,2], Jingtao Ma [2], Xinying Jiao [2,3,4,*], Guofei Shang [2,4] and Haiming Yan [2,4]

[1] Academy of Eco-Civilization Development for Jing-Jin-Ji Megalopolis, Tianjin Normal University, Tianjin 300387, China
[2] School of Land Science and Space Planning, Hebei GEO University, Shijiazhuang 050031, China; haiming.yan@hgu.edu.cn (H.Y.)
[3] Institute of Geographic Sciences and Natural Resources Research, Chinese Academy of Sciences, Beijing 100101, China
[4] Hebei International Joint Research Center for Remote Sensing of Agricultural Drought Monitoring, Hebei GEO University, Shijiazhuang 050031, China
* Correspondence: jiaoxinying@igsnrr.ac.cn

Abstract: Escalating urban issues in Beijing call for comprehensive exploration of urban construction land expansion towards the goal of carbon neutrality. Firstly, urban construction land in Beijing during the period 2005–2020 was accurately detected using Landsat images and impervious surface data, and then its expansion characteristics were revealed. Finally, the driving mechanism of urban construction land expansion was explored using geographically and temporally weighted regression from the input–output perspective. The results showed that the expansion speed and intensity of urban construction land in Beijing showed an overall tendency to slow down, and the center of urban expansion shifted to the new urban development zone and ecological function conservation zone. Urban construction land expansion in the central urban area was first scattered and then compact, while that in the new urban development zone and ecological function conservation zone primarily followed an outward pattern. The permanent population, per capita GDP, and per capita retail sales of social consumer goods were the primary driving factors of urban construction land expansion in Beijing, the impacts of which varied significantly among different districts of Beijing. All these results can provide a solid foundation for improving land use policies towards the goal of carbon neutrality in highly urbanized areas.

Keywords: construction land expansion; landscape pattern; influencing factors; input–output theory; geographically and temporally weighted regression model; Beijing

Citation: Yang, H.; Ma, J.; Jiao, X.; Shang, G.; Yan, H. Characteristics and Driving Mechanism of Urban Construction Land Expansion along with Rapid Urbanization and Carbon Neutrality in Beijing, China. *Land* **2023**, *12*, 1388. https://doi.org/10.3390/land12071388

Academic Editor: Teodoro Semeraro

Received: 8 June 2023
Revised: 4 July 2023
Accepted: 7 July 2023
Published: 12 July 2023

1. Introduction

There has been urban construction land rapid expansion along with accelerated urbanization across the world, which has been one of the important contributors to carbon emissions and climate change [1,2]. Land use change has been the core driving force of carbon storage in terrestrial ecosystems, accounting for one-third of the anthropogenic carbon emission [3,4]. In particular, urban construction land expansion has an increasing impact on ecological carbon storage and carbon emission [5]. On the one hand, there is considerable conversion of cropland, forest, and grassland with higher carbon storage abilities into urban construction land with lower carbon storage abilities in the process of urbanization, greatly reducing the carbon storage capacity of terrestrial ecosystems [1]. On the other hand, the increasing consumption of fossil fuel within urban construction land also leads to a significant increase in carbon emission; for example, the urban areas have accounted for approximately 3/4 of the total carbon emission of the world [6]. Most previous studies have therefore suggested there is generally a strong positive correlation

between urban construction land expansion and carbon emission, and the newly added construction land is an important source of increased carbon emission [7]. However, some other studies have suggested there was an inverted U-shaped trend of the impact of urban construction land expansion on urban carbon emission, which may be due to the spatial heterogeneity to carbon emission efficiency in the urbanization of different dimensions [5,8]. This provides some novel approaches for achieving a balance between rapid urbanization and carbon emission reduction, e.g., regulation of land use change and improvement in carbon emission efficiency [2]. In fact, there are both various influencing factors of urban construction land expansion and heterogeneous impacts of urban construction land on carbon emission across different geographical zones and urban area sizes [5]. It is of great practical significance to accurately reveal the characteristics and driving mechanism of urban construction land expansion, which can provide important theoretical support for low-carbon urbanization and carbon neutrality [4].

Urban construction land expansion as the most direct spatial manifestation of urbanization has been a central topic in urban studies worldwide, and is generally explored with 3S technology [9,10]. For example, some scholars have revealed the spatiotemporal patterns of urban expansion of megacities such as Beijing using remotely sensed land use data and GIS tools [9–12], while other studies have revealed the characteristics of urban land expansion, e.g., the growth rate of urban land, conversion from arable land to of urban land, and expansion process of construction areas in major urban agglomerations based on GIS technology multi-period remote sensing data [13–15]. For example, some previous studies based on remote sensing data such as nighttime light data suggested there has been extensive expansion of urban areas in Beijing in the past decades, with an annual urban expansion rate of 3.46% during the period 1978–2015 [10,15].

There are inevitably some limitations in the traditional retrieval of urban construction land based on remote sensing data, and the increasingly mature 3S technology and abundant multi-source data lay a firm foundation for further improving the retrieval accuracy of urban construction land. For example, there may be considerable differences in the resolution of long time-series remote sensing images from different satellite sensors, and earlier remote sensing images with the same resolution generally exhibited high error rates. In particular, the accuracy of the traditional retrieval of urban construction land is easily affected by the quality of remote sensing images with different cloud amounts in different months, and it costs a lot of human and material resources to carry out the correction of cloud layers, radiation, spectra, and so on. It may be feasible to improve the retrieval accuracy of urban construction land and reduce the cost by supplementing the retrieval results based on traditional methods with multi-source impervious surface data, which can effectively reduce the influence of mixed pixels. In fact, some studies have explored urban expansion using impervious surface data [16–18]. However, there are various impervious surfaces, which may lead to some errors in the retrieval of urban construction land. For example, infrastructure in the periphery of cities may be classified as urban construction land, while parkland within cities may be excluded if the retrieval of urban construction land is solely based on the impervious surface data. There is therefore an urgent need to further improve the retrieval of urban construction land by integrating the impervious surface data with more accurate methods based on 3S technology.

Urban construction land expansion is influenced by various driving factors [19], which have been generally explored with statistical analysis such as regression analysis in and previous studies [20,21]. Specifically, socio-economic factors such as gross domestic product (GDP), income of urban residents, and urban transportation generally have considerable influence on urban construction land expansion [20,21]. For example, there was temporal coevolution of the urban area with the urban population in Beijing, indicating the rising efficiency of urban land use [20]. But these driving factors of urban construction land expansion were generally selected according to previous experience rather than a solid theoretical foundation in most of the previous studies [20,21]. By contrast, the input–output theory suggested that the urbanization process can be regarded as the result of rising

urban output brought on by the social input, which provides a reliable theoretical foundation for improving the rationality of selecting the driving factors of urban construction land expansion [22,23]. It is therefore necessary to carry out more in-depth research on urban construction land expansion on the basis of the input–output theory. Furthermore, previous studies have primarily explored the driving factors of urban construction land expansion via regression analysis such as conventional ordinary least squares regression (OLS) and geographically weighted regression (GWR), which generally fail to capture the non-stationary variation in urban construction land over time or space [24–27]. By contrast, the geographically and temporally weighted regression (GTWR) model, which was further developed based on the GWR model, can effectively reveal the spatiotemporal relationship between independent variables and dependent variables [28]. It is therefore better to explore the driving factors of long-term and non-stationary urban construction land expansion with the GTWR model [28,29].

Beijing, as the capital of China, has experienced substantial urban sprawl in the past decades, where the urbanization rate has been as high as 87.5% in 2021 [23,30,31]. The rapid urban construction land expansion has led to a series of ecological and social problems such as serious environmental pollution, increasing energy consumption, and considerable loss of agricultural land [10]. The concept of reducing construction land while promoting development has been proposed in the new round of national spatial planning of Beijing to cope with the excessive expansion of urban construction land. Previous studies have generally depicted the physical process of urbanization in Beijing with aggregate area change extent or rate from non-urban land to urban uses from the macroscopic and static perspective, providing limited information regarding the internal spatial patterns or driving factors of urban construction land expansion [10]. It is therefore necessary to carry out more in-depth analysis of the characteristics and driving mechanisms of urban construction land expansion in Beijing based on more accurate data and up-to-date technology, which can provide valuable reference information for formulating regional land use policies and achieving carbon neutrality for Beijing and other cities [31]. This study has therefore aimed to (1) detect the urban construction land of Beijing and reveal its expansion characteristics more accurately based on up-to-date remote sensing images and (2) reveal the driving mechanism of urban construction land expansion more accurately based on the input–output theory and the GTWR model. The results of this study can provide a basis for formulating land use policies in Beijing and offer valuable guidance for the optimal utilization of construction land in other areas with high urbanization levels against the background of carbon neutrality.

2. Materials and Methods

2.1. Study Area

Beijing is in the northern part of the North China Plain (115.7–117.4° E, 39.4–41.6° N), with a total area of approximately 16,410 km^2. Beijing is adjacent to Yanshan Mountain, where the elevation generally ranges between 1000 and 1500 m in the mountainous areas and 20 and 60 m in the plain areas, with the elevation declining significantly from northwest to southeast [31]. Beijing includes 16 districts, such as the Dongcheng, Xicheng, and Chaoyang districts and the Beijing Economic-Technological Development Area (BDA) (Figure 1). Beijing is generally divided into four areas, i.e., the capital function core zone, urban function expansion zone, new urban development zone, and ecological function conservation zone, according to the "Main Functional Zone Planning of Beijing". Specifically, the capital function core zone includes the Dongcheng and Xicheng districts, and the urban function expansion zone includes the Haidian, Chaoyang, Fengtai, and Shijingshan districts. The new urban development zone includes the Changping, Shunyi, Tongzhou, BDA, Daxing, and Fangshan districts, and the ecological function conservation zone includes the Mentougou, Yanqing, Huairou, Miyun, and Pinggu districts. The total permanent population of Beijing increased from 15.38 million in 2005 to 21.954 million in 2016, and thereafter gradually decreased to 21.89 million in 2020. But there has been rapid economic

development in Beijing in the past decades, where the regional GDP reached USD 633.40 billion and the per capita regional GDP reached USD 28,514 in 2021. Meanwhile, there was significant urban construction land expansion in Beijing, but with a declining trend in the land use carbon emissions in recent years [31]. For example, the carbon emissions of Beijing reached approximately 2.6 million tons in 2021, and the carbon dioxide emissions per unit GDP decreased by about 4% in comparison to 2020, leading to continuous improvement in the ecological environmental quality.

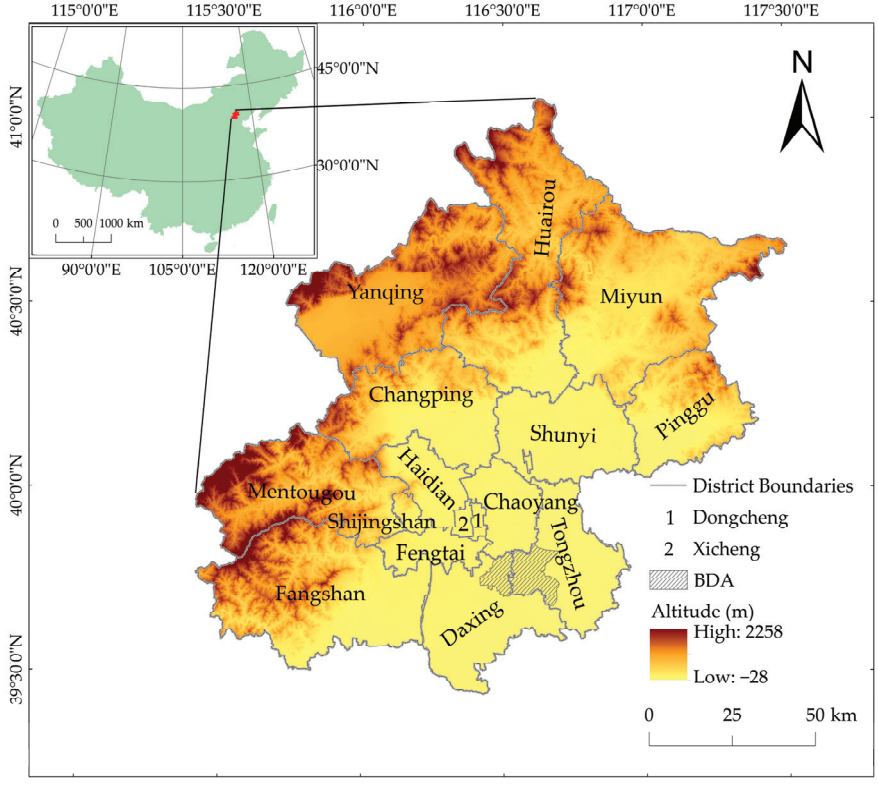

Figure 1. Overview of the study area.

2.2. Data Preparation

This study collected data from the period 2005–2020, which is the implementation period of the "Beijing Urban Master Plan (2004–2020)". This study used remote sensing images with a spatial resolution of 30 m in four periods during the period 2005–2020, which were obtained from the USGS Earth Explorer website (https://earthexplorer.usgs.gov/, accessed on 18 March 2022) (Table 1). This study primarily selected the Landsat images from the first half of May to the middle of June and from the first half of September to the first half of October, considering the growth patterns of vegetation and the planting practices of crops in the study area. Furthermore, the impervious surface data were extracted from China's 30 m Land Cover Dataset from 1990 to 2020 on the Zenodo data sharing platform (https://zenodo.org/, accessed on 20 May 2022). In addition, Beijing's digital elevation model data and administrative division data were obtained from the Resource and Environment Science and Data Center of the Institute of Geographic Sciences and Natural Resources Research, Chinese Academy of Sciences (https://www.resdc.cn/, accessed on 21 May 2022). Finally, the socio-economic data were extracted from the Beijing Statistical Yearbook and the Beijing Regional Statistical Yearbook.

Table 1. Information on remote sensing images used in this study.

Date	Satellite	Sensor	Strip Number/Row Number
2005	Landsat 5	TM	123/32, 123/33
2010	Landsat 5	TM	123/32, 123/33
2015	Landsat 8	OLI	123/32, 123/33, 124/32
2020	Landsat 8	OLI	123/32, 123/33, 124/32

This study detected the urban construction land in the remote sensing images using ENVI 5.3 software (Figure 2). Firstly, data pre-processing of Landsat images was carried out, including radiometric calibration, atmospheric correction, clipping, and mosaicking. Then, the interpretation keys were established, with the land cover classified into six types, i.e., cropland, forest, grassland, construction land, water body, and unused land, and the supervised classification was used to detect the construction land throughout the study area. Finally, this study further processed the detected urban construction land to reduce the error according to the process shown in Figure 2.

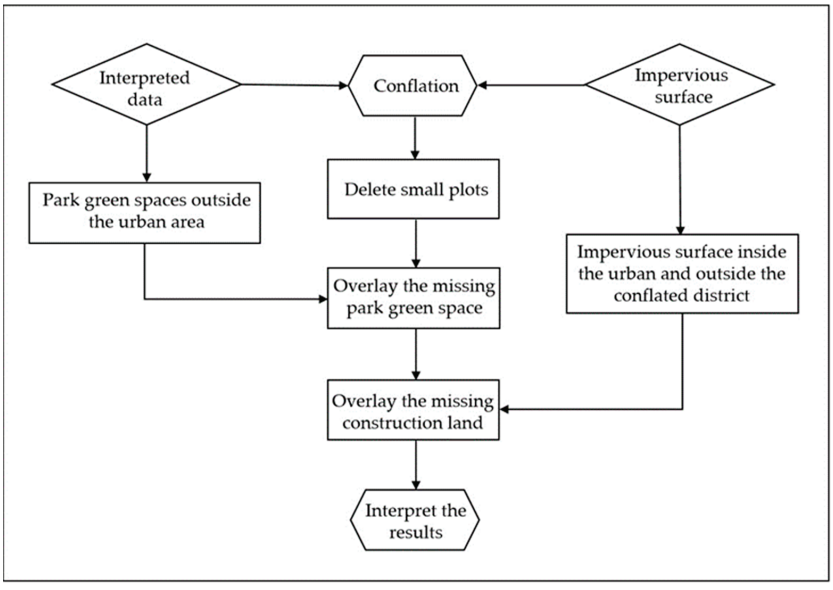

Figure 2. Technical flowchart of the construction land interpretation.

This study focused on the urban core and peripheral areas defined by the "Beijing Urban Master Plan (2004–2020)". The urban core areas include the downtown area and the surrounding ten edge groups, including Beiyuan, Jiuxianqiao, Dongba, Dingfuzhuang, Fatou, Nanyuan, Fengtai, Shijingshan, Xiyuan, and Qinghe as well as Huilongguan and Beiyuan, which are approximately equivalent to the Haidian, Chaoyang, Dongcheng, Xicheng, Fengtai, and Shijingshan districts. At the same time, peripheral areas cover the remaining part of Beijing. This study firstly eliminated the impervious surface data in the peripheral areas, and then intersected the retrieved urban construction land data and the impervious surface data in the urban core areas, eliminating the fragmented patches and obtaining the confirmed urban construction land. Furthermore, the parkland data within the urban core area were extracted from the detected urban construction land, which was used to complete the missing data due to the data intersection. Additionally, the impervious surface in areas outside the areas of data intersection within the core area should be impervious in theory but may be misclassified into other land use types. This

study has therefore included these areas as the missing construction land to form the final urban construction land data. Finally, the retrieval accuracy was evaluated using the Kappa coefficient based on the field survey data.

2.3. Exploration of Urban Construction Land Expansion Characteristics

This study explored the quantitative characteristics of urban construction land expansion using the expansion speed and intensity. The expansion speed of urban construction land refers to the average annual expansion area of construction land during a certain period. The urban construction land expansion intensity refers to the ratio of newly added construction land area during a certain period to the urban construction area of the base period and the time duration of a certain period. It quantifies the rate of change in the urban construction land area [32]. The specific equations are as follows:

$$S_1 = \frac{A_2 - A_1}{T} \tag{1}$$

$$S_2 = \frac{A_2 - A_1}{A_1 \times T} \times 100\% \tag{2}$$

where S_1 represents the expansion speed of urban construction land, S_2 represents the expansion intensity of urban construction land, A_1 is the initial urban construction land area over the initial period, A_2 is the urban construction land area over the ending period, and T is the time duration of a certain period. The dynamic degree was classified into four categories using the natural break classification method: low intensity, relatively low intensity, relatively high intensity, and high intensity.

This study characterized the morphological characteristics of urban construction land using the area-weighted mean fractal dimension (AWMPFD), by splitting the urban construction land into independent patches according to the principle of boundary non-contact [33]. Meanwhile, this study characterized the complexity of urban construction land expansion using the area-weighted mean shape index (AWMSI). Both indices were calculated using Fragstats 4.2 as follows:

$$AWMPFD = \sum_{i=1}^{m}\left[\frac{2\ln(0.25p_i)}{\ln a_i}\left(\frac{a_i}{A}\right)\right] \tag{3}$$

$$AWMSI = \sum_{i=1}^{m}\left[\left(\frac{0.25p_i}{\sqrt{a_i}}\right)\left(\frac{a_i}{A}\right)\right] \tag{4}$$

where A represents the total area of urban construction land and a_i, and p_i represent the area and perimeter of the ith construction land patch, respectively.

2.4. Exploration of the Driving Mechanism of Urban Construction Expansion

This study explored the driving mechanism of urban construction land expansion with the GTWR model since the urban construction land varied both geographically and temporally. The GTWR model can simultaneously reveal the non-stationary relationship between urban construction land expansion and its driving factors in space over time by incorporating the temporal effects into the GWR model as follows [29]:

$$y_i = P_0(x_i, y_i, t_i) + \sum_k P_k(x_i, y_i, t_i)X_{it} + e_i \tag{5}$$

where x_i and y_i represent the spatial coordinates (longitude and latitude) of the ith sample point and t_i represents the time dimension coordinate of the ith sample point; P_0 is the regression constant of the sample point (x_i, y_i, t_i); X_{it} represents the value of the kth indepen-

dent variable at the *i*th sample point; e_i represents the residual value; and $P_k(x_i, y_i, t_i)$ is the *k*th regression parameter of the *i*th sample point, which was estimated as follows:

$$\hat{P}(x_i, y_i, t_i) = [X^T W(x_i, y_i, t_i) X]^{-1} X^T W(x_i, y_i, t_i) Y \quad (6)$$

where $\hat{P}(x_i, y_i, t_i)$ is the estimated value of $P_k(x_i, y_i, t_i)$; X is the matrix of independent variables and X_T is the transpose matrix of X; Y is the sample matrix; and $W(x_i, y_i, t_i)$ is the spatiotemporal weight matrix, which was obtained with the finite Gaussian function, namely the bi-square spatial weight function [8,34]. The optimal bandwidth of the GTWR model was determined with the widely used Akaike information criterion in this study.

The previous studies have generally used the expansion speed or intensity of construction land expansion as the dependent variable [35], and this study accordingly used them as the candidate dependent variables and thereafter selected the one with the higher coefficient of determination (R^2). Moreover, urban development can be regarded as the process of increase in the benefit of industrial aggregates under the constraints of land conditions and the guidance of government policies according to the input–output theory and the theory of urbanization [36]. It is therefore of high scientific importance and operability to select the indicators of driving factors of urban construction land expansion from the input–output perspective, which can effectively reduce the problem of empiricism and make the research results more robust [37]. Specifically, the input factors of urban development include the land, labor, and capital, which jointly influence the output of urban areas according to the extended Cobb–Douglas production function [38,39]. The approaches of increasing the output from the perspective of urban construction land primarily include the increase in the land area and improvement in the utilization efficiency of urban construction land, both of which are closely related to the input and output of economic activities [40]. This study has therefore selected the driving factors of urban construction land expansion from the input–output perspective (Table 2).

Table 2. Selection of influencing factors of urban construction land expansion.

Index Layer	Variable	Index Factor	Index Explanation
Capital input	X_1	Per capita general public budget expenditure	Government support level
	X_2	Per capita fixed asset investment	Overall investment intensity
Labor input	X_3	Permanent population	Human resource foundation
Economic output	X_4	Per capita GDP	Level of economic development
	X_5	Per capita industrial output value	Level of industrial capacity
	X_6	Per capita general public budget revenue	Government revenue and expenditure capacity
Social output	X_7	Per capita disposable income of urban residents	Standard of living for residents
	X_8	Per capita consumption level of urban residents	Consumer demand for residents
	X_9	Per capita social consumer goods retail sales	Level of social consumption
Terrain constraints	X_{10}, X_{11}	Relief degree of land surface, slope	Geological and geomorphic foundation

More specifically, the input index layer included the capital input (per capita general public budget expenditure, per capita fixed asset investment) and labor input (permanent population). Meanwhile, the output index layer included the capital output (per capita GDP, per capita industrial output value, and per capita general public budget revenue) and social output (per capita retail sales of consumer goods, per capita disposable income of urban residents, and per capita consumption expenditure of urban residents). At the same time, the topography was used as the limiting index layer, including the land surface's relief degree and slope (Table 2). In particular, the Economic-Technological Development Area is inconsistent with traditional administrative districts, where the management hierarchy and data acquisition were also inconsistent with other districts and counties. Therefore, this

study explored the driving mechanism of urban construction land expansion based on the administrative district to guarantee scientific validity and calculation convenience. Additionally, this study further filtered these driving factors according to their variance inflation factor (VIF) to ensure the accuracy of the model output, with VIF < 5 as the threshold.

3. Results

3.1. Quantitative Characteristics of Urban Construction Land Expansion in Beijing

The results of this study showed that the overall accuracy of the urban construction land detection was above 95% in all years, indicating the retrieval method used in this study performed better than that in most of the previous studies. For example, the accuracy of the ChinaCover2010 product reached approximately 91% in the first class and 82% in the second class. The overall accuracy of the GlobeLand30 V2010 and GlobeLand30 V2020 data reached 83.50% and 85.72%, with Kappa coefficients of 0.78 and 0.82, respectively, while the accuracy of the land use data provided by the Resource and Environment Science and Data Center (https://www.resdc.cn/, accessed on 22 October 2022), which are the most widely used in China, was above 85% for cropland and construction land and approximately 75% for other land use types. These previous studies generally detected urban construction land solely based on remote sensing images, leading to relatively limited retrieval accuracy. By contrast, the Kappa coefficient in this study reached 0.95 in most years, which met the need of exploration of urban construction land expansion, indicating it is feasible to reduce the retrieval workload and improve the retrieval accuracy of the urban construction land by integrating the remote sensing images and impervious surface data.

The results suggested the total area of urban construction land in the study area in 2005, 2010, 2015, and 2020 reached 2746.58 km^2, 3130.35 km^2, 3429.5 km^2, and 3646.15 km^2, respectively (Figure 3). Moreover, the results showed obvious spatial heterogeneity of the urban construction land expansion in the study area. Specifically, the construction land was concentrated in the central urban area in 2005, and there was remarkable construction land expansion in the Yanqing District and the surrounding areas of the central urban area during the period 2005–2010. However, the urban construction land expansion slowed down during the period 2010–2015, mainly in the Miyun and Yanqing districts. Furthermore, the urban construction land expansion further slowed down during the period 2015–2020, mainly in the southern and southeastern areas around the central urban area and some parts of the Yanqing and Pinggu districts.

The expansion speed of urban construction land varied remarkably among different parts of the study area, and the urban construction land increased most rapidly during the period 2005–2020 in the central urban area, followed by the new urban development zone, e.g., Daxing, the BDA, Shunyi and Changping districts (Table 3). The urban construction land kept expanding rapidly in the central urban area, which contains the major urban core area with a larger spatial scope and more population. Meanwhile, the urban construction land expansion in the new urban development zone was accelerated in Daxing, Shunyi, Changping, and the BDA but was relatively slow in the Tongzhou and Fangshan districts. By contrast, the urban construction land expansion was relatively rapid in Huairou and Miyun and slowed in Mentougou and Yanqing in the ecological function conservation zone. Overall, the urban construction land expansion in the study area slowed down during the period 2005–2020, especially in the central urban area, where the expansion speed continued to slow down significantly.

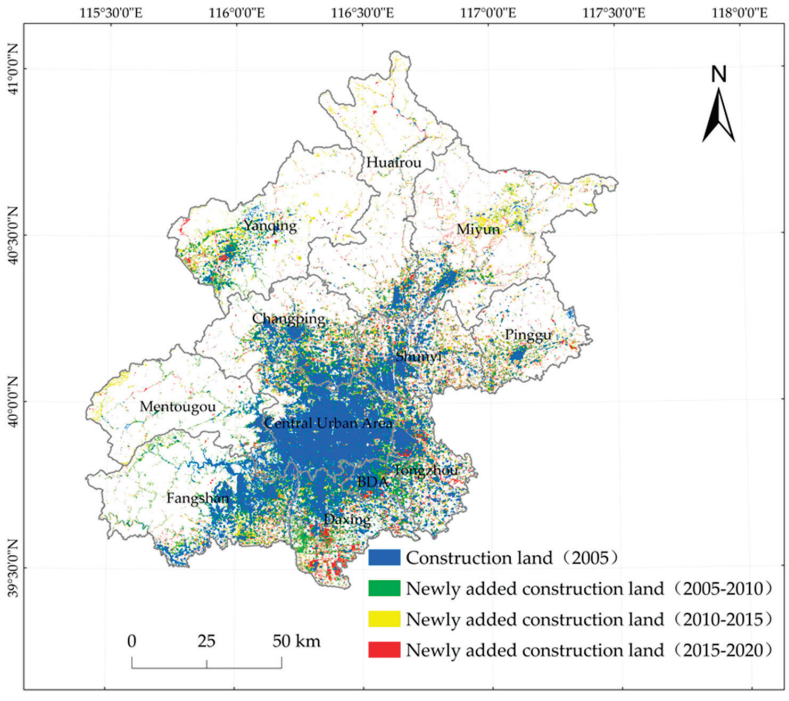

Figure 3. Spatial pattern of construction land expansion in Beijing during the period 2005–2020.

Table 3. Expansion speed of urban construction land in Beijing by districts and counties (unit: km^2/a).

	2005–2010	2010–2015	2015–2020	2005–2020
Central urban area	8.85	6.45	3.64	6.31
Changping District	3.56	1.89	1.41	2.29
Shunyi District	3.68	3.99	1.33	3.00
Tongzhou District	2.76	1.77	1.02	1.85
Daxing District	4.84	3.06	1.82	3.24
Fangshan District	2.55	1.86	0.90	1.77
Mentougou District	0.48	0.68	0.58	0.58
Miyun District	1.37	2.58	1.31	1.75
Pinggu District	1.63	0.94	0.81	1.13
Huairou District	2.70	2.07	1.42	2.06
Yanqing District	1.09	0.70	0.94	0.91
Economic-Technological Development Area	3.66	5.16	1.03	3.28
Overall	37.17	31.15	16.21	28.17

The expansion speed of urban construction land in the study area varied significantly in different periods. Specifically, the urban construction land expansion in the central urban area was considerably more remarkable in the central urban area than in other parts of the study area during the period 2005–2010. The urban construction land expanded relatively rapidly in the Daxing and Shunyi districts, the BDA in the new urban development zone, and Huairou District in the ecological function conservation zone during the period 2005–2010 but much more slowly in the Miyun, Yanqing, and Pinggu districts in the ecological function conservation zone. Consequently, the urban construction land expansion slowed down to some degree. However, it was at a relatively high speed in the central urban area during the period 2010–2015, while it significantly accelerated in the BDA and Shunyi District. The urban construction land expansion slowed down in

Daxing District, while it was still at a low rate in the Mentougou, Pinggu, and Yanqing districts. The urban construction land expansion was at a relatively high speed in the central urban area, Daxing District, Changping District, Shunyi District, Miyun District, Tongzhou District, and the BDA during the period 2015–2020. However, other parts of the study area experienced a relatively low expansion speed.

Considerable spatial heterogeneity was observed in the intensity of the urban construction land expansion across different parts of Beijing (Table 4). During the period 2005–2020, the areas with high intensity of urban construction land expansion primarily included the BDA and the Yanqing, Miyun, Pinggu, and Huairou districts in the ecological function conservation zone. However, the urban construction land expansion intensity was always low in the central urban area and relatively low in the new urban development area districts and Mentougou District. Specifically, the urban construction land expansion intensity was higher than 5% in the Yanqing, Huairou, and Pinggu districts and the BDA during the period 2005–2010, while it was below 2% in Mentougou District. However, the urban construction land expansion intensity was above 5% in Miyun and the BDA and below 2% in Tongzhou, Changping, and Daxing during the period 2010–2015. The urban construction land expansion intensity was the highest in the BDA during the period 2015–2020, followed by the Yanqing, Miyun, Pinggu, Huairou, and Mentougou districts, while it reached only 0.71% in Shunyi District.

Table 4. Urban land expansion intensity in different parts of Beijing.

	2005–2010	**2010–2015**	**2015–2020**	**2005–2020**
Central urban area	0.98%	0.68%	0.37%	0.70%
Changping District	4.30%	1.88%	1.28%	2.76%
Shunyi District	2.48%	2.39%	0.71%	2.02%
Tongzhou District	3.09%	1.71%	0.91%	2.07%
Daxing District	3.59%	1.92%	1.05%	2.40%
Fangshan District	3.38%	2.11%	0.92%	2.35%
Mentougou District	1.78%	2.32%	1.77%	2.15%
Miyun District	3.19%	5.17%	2.08%	4.07%
Pinggu District	5.62%	2.53%	1.93%	3.89%
Huairou District	5.26%	3.19%	1.89%	4.02%
Yanqing District	6.34%	3.10%	3.60%	5.30%
Economic-Technological Development Area	5.02%	5.65%	0.88%	4.50%
Overall	2.22%	1.67%	0.80%	1.68%

The urban construction land expansion intensity was always the lowest in the central urban area, without any change in the intensity level throughout the study period (Figure 4). It was generally high in the new urban development area but decreased throughout the study. The urban construction land expansion intensity was the highest in the ecological function conservation area far from the central urban area but significantly declined during the study period. Overall, the urban construction land expansion intensity in Beijing gradually increased from the central urban area to the peripheral areas, indicating that the pressure for expanding construction land in Beijing gradually shifted outward. It continuously decreased in the central urban area and most districts in the study area.

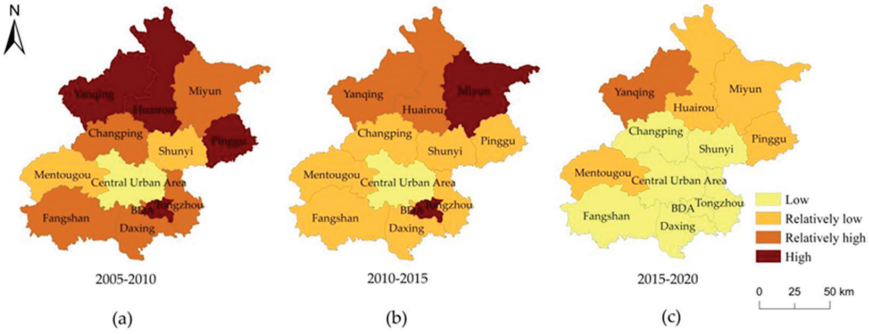

Figure 4. Spatial differentiation of expansion intensity during (**a**) 2005–2010, (**b**) 2010–2015, and (**c**) 2015–2020.

There was slight differentiation in the AWMPFD of different regions of Beijing, which showed an overall increasing trend in most of the study areas (Table 5). Specifically, the AWMPFD of the central urban area and Daxing District exceeded 1.3 in 2005, while that of other regions generally ranged between 1.21 and 1.27. The AWMPFD exceeded 1.3 in three parts of the study area in 2010, i.e., the central urban area, Shunyi District, and Tongzhou District; however, that of Daxing District decreased to 1.29. Meanwhile, the AWMPFD of other districts showed slight variation. In 2015, the number of regions with AWMPFD values over 1.3 reached four: the central urban area, Daxing, Tongzhou, and Shunyi districts. Contrastingly, the number of regions with an AWMPFD of over 1.3 reached five in 2020: the central urban area, Shunyi, Tongzhou, Changping, and Daxing districts. In addition, the variation in the AWMPFD differed remarkably among regions. For example, the AWMPFD of the Changping, Huairou, Shunyi, and Yanqing districts increased continuously. The BDA increased, decreased, and then increased, with an overall increasing trend. By contrast, the AWMPFD of the central urban area, Fangshan, Tongzhou, Daxing, and Mentougou districts first increased and then decreased, as opposed to that of the Miyun and Pinggu districts.

Table 5. Area-weighted mean fractal dimension of different parts of Beijing during the period 2005–2020.

	2005	2010	2015	2020
Central urban area	1.3391	1.3568	1.3644	1.3562
Changping District	1.2498	1.2886	1.2961	1.3095
Shunyi District	1.2606	1.2866	1.3126	1.3247
Tongzhou District	1.2679	1.3115	1.3120	1.3111
Daxing District	1.3160	1.3174	1.3000	1.3012
Fangshan District	1.2534	1.2610	1.2858	1.2766
Mentougou District	1.2602	1.2743	1.2818	1.2646
Miyun District	1.2355	1.2306	1.2264	1.2481
Pinggu District	1.2225	1.2115	1.1812	1.1888
Huairou District	1.2164	1.2298	1.2540	1.2765
Yanqing District	1.2367	1.2447	1.2513	1.2627
Economic-Technological Development Area	1.2484	1.2849	1.2602	1.2949

There was also a remarkable variation in the AWMSI across different parts of the study area during the period 2005–2020 (Table 6). In general, the AWMSI was below 20 in most regions of the study, exceeding 20 in only two or three regions during the study period, and the AWMSI in the central urban area consistently surpassed that of other parts of the study area. Specifically, the AWMSI in most regions ranged from 7.89 to 12.50 in 2005, exceeding 20 in only the central urban area and Daxing. The AWMSI slightly increased in most regions of the study area during the period 2005–2010, ranging between 7.59 and 19.66; however, it

significantly increased in the central urban area. The AWMSI significantly decreased only in Pinggu and slightly increased in other regions during the period 2010–2015, including the central urban area. Meanwhile, the AWMSI slightly increased in most regions of the study area during the period 2015–2020 but showed a significant decrease in the central urban area. In addition, regarding changing trends, the AWMSI increased and then decreased in the central urban area and Mentougou and Tongzhou districts during the study period, while it continuously increased in the Huairou, Shunyi, and Yanqing districts. By contrast, the AWMSI exhibited fluctuations or slight increases in the Changping, Fangshan, and Miyun districts and the BDA. However, in Pinggu District, the AWMSI initially decreased and then increased, consistently maintaining very low values.

Table 6. Area-weighted mean shape index of different parts of Beijing during the period 2005–2020.

	2005	2010	2015	2020
Central urban area	36.1726	43.2899	46.0059	42.0748
Changping District	12.3140	17.9924	17.9322	20.3908
Shunyi District	7.8907	17.1350	23.2845	25.2900
Tongzhou District	12.4957	19.6589	19.3462	19.0957
Daxing District	21.0822	21.5559	17.8593	18.0682
Fangshan District	9.9947	10.2127	12.9806	12.0844
Mentougou District	9.5604	10.9012	12.1469	10.5061
Miyun District	9.5639	10.0908	9.8479	11.8292
Pinggu District	7.8907	7.5955	5.4031	6.0641
Huairou District	8.3947	8.9400	12.7306	15.0203
Yanqing District	7.9808	8.8992	9.4502	10.6989
Economic-Technological Development Area	11.0033	15.7663	13.6771	17.9802

3.2. Driving Mechanisms of Expansion of Urban Construction Land in Beijing

Seven dependent variables were finally selected according to the VIF (Table 7) for ensuring the accuracy of the model output. Specifically, the selected dependent variables were the permanent resident population, per capita consumption expenditure of urban residents, per capita public budget expenditure, per capita fixed asset investment, per capita GDP, per capita industrial output value, and per capita total social consumer goods.

Table 7. VIF values of selected independent variables.

Per Capita General Public Budget Expenditure	Per Capita Fixed Asset Investment	Permanent Population	Per Capita GDP	Per Capita Industrial Output Value	Per Capita Consumption Level of Urban Residents	Per Capita Social Consumer Goods Retail Sales
2.45	1.53	2.11	3.20	1.57	1.60	3.46

The results of the GTWR model suggested the R^2 value of the expansion speed was higher than 0.95, while that of the expansion intensity was lower than 0.80 (Table 8). Therefore, the expansion speed was more appropriate to be used as the dependent variable of the GTWR model. However, the expansion intensity is often influenced by the initial period of construction land area, and the adaptability of this indicator is relatively weak. This study has therefore used the expansion speed of urban construction land as the dependent variable of the GTWR model and further explored its relationship with an independent variable in Beijing.

Table 8. Related parameters of geographically and temporally weighted regression of urban construction expansion.

Model Parameters	Bandwidth	Sigma	AICc	R^2	R^2 Adjusted	Spatiotemporal Distance Ratio
Expansion intensity	0.8186	0.2738	73.0300	0.7887	0.6619	0.2731
Expansion speed	0.2992	0.0453	16.6150	0.9505	0.9366	0.3731

The results of the GTWR model revealed the driving mechanisms behind urban construction land expansion in Beijing as follows (Table 9): (1) the coefficient of per capita general public budget expenditures is relatively stable over time, generally showing a negative impact in the study area except for in the Miyun and Pinggu districts. Specifically, the absolute values of this coefficient were relatively large in the central urban area and new urban development zone. However, its absolute value remained relatively low and stable over time in the ecological conservation zone. (2) The per capita fixed asset investment coefficient significantly varied over time. There was a similarity between the central urban area and new urban development zone, as both areas exhibited a synchronized trend of initially increasing and then decreasing. The per capita fixed asset investment positively affected the urban construction land expansion in the central urban area but negatively affected the ecological conservation zone, except for Yanqing District. (3) The coefficient of the permanent resident population was relatively stable over time but with more remarkable regional differences. This coefficient was relatively low in the central urban area and new urban development zone, which showed some similarity. Moreover, it was high in the ecological conservation zone, indicating this area was susceptible to the influence of the permanent resident population. (4) The coefficients of per capita GDP were all positive and continuously increased during different periods. (5) The per capita industrial output value coefficient was relatively stable over time, with significant spatial differences. This coefficient was generally negative in the central urban area and new urban development zone, whereas it was positive in the ecological conservation zone throughout the study period. (6) The coefficient of per capita urban resident consumption showed a transition from positive to negative in the study area. Specifically, this coefficient was generally negative in the central and new urban development areas. However, it transitioned from negative to positive in the ecological conservation zone in the Miyun and Pinggu districts. (7) The coefficient of per capita retail sales of social consumer goods showed a steady decline over the study period. This coefficient was relatively high in the central urban area and new urban development zone and low in the ecological conservation zone, and it remained relatively stable throughout the study period.

Table 9. Results of geographically and temporally weighted regression.

		X_1	X_2	X_3	X_4	X_5	X_8	X_9
2005–2010	Central urban area	−0.2627	0.0911	0.4581	0.4111	−0.0470	−0.1188	0.3784
	Changping District	−0.1810	0.0507	0.5285	0.5618	0.0027	−0.1306	0.2340
	Shunyi District	−0.1465	−0.0304	0.4790	0.3418	−0.0110	−0.0529	0.2786
	Tongzhou District	−0.2678	0.0707	0.4427	0.2524	−0.0707	−0.1494	0.4573
	Daxing District	−0.3894	0.1460	0.3834	0.1706	−0.0725	−0.1438	0.5815
	Fangshan District	−0.4414	0.1048	0.4116	0.2665	0.0604	−0.0576	0.5264
	Mentougou District	−0.2962	0.0869	0.5388	0.5802	0.0730	−0.1157	0.2878
	Miyun District	0.0335	−0.2138	0.7636	0.3551	0.0966	−0.0751	0.0270
	Pinggu District	0.0052	−0.1401	0.7294	0.3455	0.0710	−0.0636	0.0638
	Huairou District	−0.0442	−0.1048	0.5869	0.3213	0.0822	−0.0906	0.1099
	Yanqing District	−0.1250	0.0272	0.5800	0.4986	0.0770	−0.1538	0.1586

Table 9. *Cont.*

		X_1	X_2	X_3	X_4	X_5	X_8	X_9
2010–2015	Central urban area	−0.2283	0.0666	0.4654	0.4465	−0.0428	−0.1272	0.3669
	Changping District	−0.1692	0.0523	0.5383	0.6209	−0.0036	−0.1363	0.2164
	Shunyi District	−0.1257	−0.0409	0.4740	0.4419	−0.0143	−0.0271	0.2359
	Tongzhou District	−0.2255	0.0371	0.4568	0.3372	−0.0667	−0.1443	0.4183
	Daxing District	−0.3287	0.0990	0.4029	0.2239	−0.0575	−0.1612	0.5518
	Fangshan District	−0.3702	0.0624	0.4105	0.2417	0.0707	−0.0927	0.5476
	Mentougou District	−0.2322	0.0500	0.5361	0.5529	0.0662	−0.1533	0.3234
	Miyun District	0.0362	−0.2434	0.7369	0.4078	0.0936	−0.0436	0.0152
	Pinggu District	0.0110	−0.1818	0.6773	0.4275	0.0707	−0.0028	0.0406
	Huairou District	−0.0496	−0.0982	0.5679	0.3992	0.0704	−0.0937	0.0895
	Yanqing District	−0.1320	0.0432	0.5872	0.5974	0.0594	−0.1669	0.1379
2015–2020	Central urban area	−0.1967	0.0888	0.4788	0.5098	−0.0592	−0.1296	0.3274
	Changping District	−0.1555	0.0826	0.5434	0.6752	−0.0279	−0.1392	0.1928
	Shunyi District	−0.0886	−0.0007	0.4608	0.5114	−0.0417	−0.0200	0.2261
	Tongzhou District	−0.1856	0.0712	0.4645	0.4295	−0.0819	−0.1383	0.3717
	Daxing District	−0.2691	0.1164	0.4326	0.3273	−0.0788	−0.1825	0.4813
	Fangshan District	−0.3072	0.0862	0.4731	0.4229	0.0194	−0.1196	0.4222
	Mentougou District	−0.2102	0.0844	0.5839	0.6991	0.0223	−0.1657	0.2267
	Miyun District	0.0508	−0.1741	0.6566	0.4424	0.0603	0.0013	0.0276
	Pinggu District	0.0346	−0.1124	0.5767	0.4982	0.0220	0.0072	0.0556
	Huairou District	−0.0358	−0.0510	0.5169	0.4572	0.0372	−0.0949	0.0899
	Yanqing District	−0.1330	0.0764	0.5725	0.6647	0.0261	−0.1805	0.1306

The results obtained from the input–output perspective revealed the driving mechanism of urban construction land expansion in Beijing more clearly. On the one hand, from the input perspective, the permanent population was the main driving factor of the urban construction land expansion, indicating the population growth had a stronger promoting effect on urban expansion in Beijing. However, population growth may lead to decreased per capita general public budget expenditure and per capita fixed asset investment. As a result, the coefficient of per capita general public budget expenditure was generally negative. On the other hand, the explanatory power of per capita fixed asset investment was insufficient, and its coefficient was even negative in some districts. This suggested the rapid population growth rather than the overall capital investment from the entire society was the main driver of urban construction land expansion. On the other hand, from the output perspective, per capita GDP was the main factor promoting the urban construction land expansion, indicating the level of economic development strongly promoted urban expansion in Beijing. Meanwhile, per capital retail sales of social consumer goods had explanatory power for the urban construction land expansion only second to per capita GDP, indicating the overall level of social consumption significantly impacted the urban construction land expansion in the study area. But the explanatory power of per capita industrial output value and urban residents' per capita consumption expenditure was insufficient for the urban construction land expansion, which may be related to the special industrial structure of Beijing. In particular, the impact of permanent residents on the urban construction land expansion was relatively less significant in the central urban area with a higher economic development level than that in the ecological function conservation zone, contrary to that of per capita social consumption and retail sales. By contrast, the impact of per capita GDP, which showed an increasing trend, was relatively significant in all districts, indicating that the land use in these urban areas has become more intensive. Overall, urban construction land expansion in Beijing was mainly influenced by three factors, i.e., population, per capita GDP, and per capita retail sales of social consumer goods.

4. Discussion

The urban construction land expansion in the study area has overall slowed down, with a significant decrease in the expansion speed and intensity in the central urban area, which showed an inverted "U-shaped" curve according to previous studies [15]. However, there was an increase in the expansion speed and intensity in the new urban development zone and ecological function conservation zone, thus shifting the center of urban expansion toward these zones. This is consistent with the spatial development strategy proposed by the previous overall urban planning of Beijing, aiming to transfer the strategic development of the old urban area and promote the construction of new urban areas. The expansion intensity in the ecological function conservation zone was significantly higher than that in the central urban area and new urban development zone, primarily due to the significantly lower urbanization baseline in the former.

It is notable that the urban construction land expansion in the central urban area was firstly dispersed and then compact, indicating a gradual shift from outward expansion to inward enhancement. This is primarily consistent with the conclusions of previous studies, i.e., the central urban area of Beijing has entered the later stage of urban construction land expansion with a slower expansion speed but better quality [15]. Furthermore, the AWMPFD declined slightly in a few districts and generally increased in most districts, indicating the urban construction land expansion was mainly in the new urban development zone and ecological conservation zone, which resulted in more complex morphological characteristics of the urban construction land in these zones. Additionally, the topography in some districts limited the urban construction land expansion, leading to complex morphological characteristics of the urban construction land. It is therefore necessary to pay more attention to the rapid urban construction land expansion in these suburban districts, which may lead to new urban sprawl and the destruction of ecological functions in the ecological conservation zone. Moreover, there is generally a close exchange of various elements between the central urban area and suburban districts in Beijing and other highly urbanized regions, but the previous studies generally focused only on the central urban zone, ignoring the role of regional coordinated development. This study more accurately revealed the overall mechanism of the urban construction land expansion by including the central urban zone, the new urban development zone, and the ecological conservation zone.

This study revealed urban construction land more accurately by overlaying the remote sensing data with impervious surface data. However, not only urban construction land expansion but also spatial aggregation of the population, industry, and infrastructure occurred in the urbanization process. It is difficult to comprehensively characterize the expansion of urban space with only the urban construction land expansion. Therefore, it is necessary to consider more factors to better characterize the urbanization process in the future. Moreover, previous studies mostly selected the indicators of driving factors of urban construction land expansion according to the research experience of other scholars, generally lacking a firm theoretical foundation. This study selected these indicators more rationally from the input–output perspective according to the input–output theory, which can effectively reduce the problem of empiricism and make the research results more robust. But this study still failed to take into account the impacts of institutional factors such as policies and city planning, and the influence of transportation factors and planning policies can only be indirectly reflected with some input factors. It is necessary to further improve the framework for selecting the driving factors of urban construction land expansion from the input–output perspective by considering more factors and including more direct characterization indicators in future studies.

5. Conclusions

This study revealed the characteristics of urban construction land expansion in Beijing during the period 2005–2020 based on the data retrieved using Landsat images and impervious surface data and explored its driving mechanism with the (GTWR) model from the input–output perspective. The major conclusions were as follows: (1) the expansion speed

and intensity of urban construction land in Beijing showed an overall tendency to slow down, particularly in the central urban area, and the center of urban expansion shifted to the new urban development zone and ecological function conservation zone. (2) The morphological indices in the central urban area exhibited an initial increase followed by a decrease, indicating the urban construction land expansion in the central urban area was first scattered and then compact. However, the morphological indices increased in most of the new urban development zone and ecological function conservation zone, indicating that the urban construction land expansion in these zones primarily followed an outward pattern. (3) The urban construction land expansion in Beijing was driven by multiple factors, with the permanent population, per capita GDP, and per capita retail sales of social consumer goods being the primary driving factors. The impact of the permanent population was significantly smaller in the central urban area and the new urban development zone than in the ecological function conservation zone, which is contrary to that of per capita retail sales of social consumer goods. By contrast, the impact of per capita GDP was significant in all districts. These findings can make a significant contribution to improving urbanization and land use planning towards the goal of carbon neutrality in Beijing and other cities.

Author Contributions: Conceptualization, H.Y. (Huicai Yang) and X.J.; methodology, J.M.; software, J.M.; validation, X.J. and H.Y. (Haiming Yan); formal analysis, G.S.; investigation, J.M.; resources, G.S.; data curation, J.M. and H.Y. (Haiming Yan); writing—original draft preparation, X.J.; writing—review and editing, X.J.; visualization, J.M.; supervision, G.S.; project administration, X.J. and H.Y. (Haiming Yan). All authors have read and agreed to the published version of the manuscript.

Funding: The China Postdoctoral Science Foundation (2019M650823).

Data Availability Statement: All data, models, and code generated or used during this study are available from the authors upon request.

Conflicts of Interest: The authors declare no conflict of interest.

References

1. Lai, L.; Huang, X.; Yang, H.; Chuai, X.; Zhang, M.; Zhong, T.; Thompson, J.R. Carbon emissions from land-use change and management in China between 1990 and 2010. *Sci. Adv.* **2016**, *2*, e1601063. [CrossRef] [PubMed]
2. Yang, B.; Chen, X.; Wang, Z.; Li, W.; Zhang, C.; Yao, X. Analyzing land use structure efficiency with carbon emissions: A case study in the middle reaches of the Yangtze River, China. *J. Clean. Prod.* **2020**, *274*, 123076. [CrossRef]
3. Huang, S.; Xi, F.; Chen, Y.; Gao, M.; Pan, X.; Ren, C. Land Use Optimization and simulation of low-carbon-oriented—A case study of Jinhua, China. *Land* **2021**, *10*, 1020. [CrossRef]
4. Yang, H.; Huang, J.; Liu, D. Linking climate change and socioeconomic development to urban land use simulation: Analysis of their concurrent effects on carbon storage. *Appl. Geogr.* **2020**, *115*, 102135. [CrossRef]
5. Peng, J.; Zheng, Y.; Liu, C. The Impact of urban construction land use change on carbon emissions: Evidence from the China land market in 2000–2019. *Land* **2022**, *11*, 1440. [CrossRef]
6. Wang, S.; Shi, C.; Fang, C.; Feng, K. Examining the spatial variations of determinants of energy-related CO2 emissions in China at the city level using Geographically Weighted Regression Model. *Appl. Energy* **2018**, *235*, 95–105. [CrossRef]
7. Wang, Q.; Xiao, Y. Has Urban Construction Land achieved low-carbon sustainable development? A case study of North China Plain, China. *Sustainability* **2022**, *14*, 9434. [CrossRef]
8. Zhou, Z.; Cao, L.; Zhao, K.; Li, D.; Ding, C. Spatio-temporal effects of multi-dimensional urbanization on carbon emission efficiency: Analysis based on panel data of 283 cities in China. *Int. J. Environ. Res. Public Health* **2021**, *18*, 12712. [CrossRef]
9. Alqahtany, A. GIS-based assessment of land use for predicting increase in settlements in Al Ahsa Metropolitan Area, Saudi Arabia for the year 2032. *Alex. Eng. J.* **2023**, *62*, 269–277. [CrossRef]
10. Yang, Y.; Liu, Y.; Li, Y.; Du, G. Quantifying spatio-temporal patterns of urban expansion in Beijing during 1985–2013 with rural-urban development transformation. *Land Use Policy* **2018**, *74*, 220–230. [CrossRef]
11. Lin, M.; Shi, Y.; Chen, Y.; Yu, D.Q.; He, Q.; Wang, L. A study on spatial-temporal features of construction land expansion in Changsha urban area. *Geogr. Res.* **2007**, *26*, 265–274.
12. Alqurashi, A.F.; Kumar, L. Spatiotemporal patterns of urban change and associated environmental impacts in five Saudi Arabian cities: A case study using remote sensing data. *Habitat Int.* **2016**, *58*, 75–88. [CrossRef]
13. Al-Bilbisi, H. Spatial monitoring of urban expansion using satellite remote sensing images: A case study of Amman City, Jordan. *Sustainability* **2019**, *11*, 2260. [CrossRef]

14. Abass, K.; Adanu, S.K.; Agyemang, S. Peri-urbanisation and loss of arable land in Kumasi Metropolis in three decades: Evidence from remote sensing image analysis. *Land Use Policy* **2018**, *72*, 470–479. [CrossRef]
15. Zhang, H.; Liang, C.; Pan, Y. Spatial expansion of built-up areas in the beijing–tianjin–hebei urban agglomeration based on nighttime light data: 1992–2020. *Int. J. Environ. Res. Public Health* **2022**, *19*, 3760. [CrossRef]
16. Dutta, D.; Rahman, A.; Paul, S.K.; Kundu, A. Impervious surface growth and its inter-relationship with vegetation cover and land surface temperature in peri-urban areas of Delhi. *Urban Clim.* **2021**, *37*, 100799. [CrossRef]
17. Xia, C.; Zhang, A.; Yeh, A.G. Shape-weighted landscape evolution index: An improved approach for simultaneously analyzing urban land expansion and redevelopment. *J. Clean. Prod.* **2020**, *244*, 118836. [CrossRef]
18. Wu, R.; Li, Y.C.; Wang, S.J. Will the construction of high-speed rail accelerate urban land expansion? Evidences from Chinese cities. *Land Use Policy* **2022**, *114*, 105920. [CrossRef]
19. Ma, Y.L.; Xu, R.S. Remote sensing monitoring and driving force analysis of urban expansion in Guangzhou City, China. *Habitat Int.* **2010**, *34*, 228–235. [CrossRef]
20. Fei, W.; Zhao, S. Urban land expansion in China's six megacities from 1978 to 2015. *Sci. Total Environ.* **2019**, *664*, 60–71. [CrossRef]
21. Chen, L.Y.; Huang, F.; Qi, H.; Zhai, H. Analysis of urban expansion and the driving forces in eastern coastal region of China. In Proceedings of the Conference on Remote Sensing Technologies and Applications in Urban Environments 2018, Berlin, Germany, 9 October 2018. [CrossRef]
22. Zhang, L.Q.; Chen, S.P.; Chen, B.P. The contribution of land to the economic growth and inflection point of its logistic curve in Anhui Province in recent 15 years. *Sci. Geogr. Sin.* **2014**, *1*, 40–46.
23. Liu, Y.S.; Zhang, Z.W.; Zhou, Y. Efficiency of construction land allocation in China: An econometric analysis of panel data. *Land Use Policy* **2018**, *74*, 261–272. [CrossRef]
24. Shu, B.; Zhang, H.; Li, Y.; Qu, Y.; Chen, L. Spatiotemporal variation analysis of driving forces of urban land spatial expansion using logistic regression: A case study of port towns in Taicang City, China. *Habitat Int.* **2014**, *43*, 181–190. [CrossRef]
25. Sarkar, A.; Chouhan, P. Modeling spatial determinants of urban expansion of Siliguri a metropolitan city of India using logistic regression. Model. *Earth Syst. Environ.* **2020**, *6*, 2317–2331. [CrossRef]
26. Peng, W.; Wang, G.; Zhou, J.; Zhao, J.; Yang, C. Studies on the temporal and spatial variations of urban expansion in Chengdu, western China, from 1978 to 2010. *Sustain. Cities Soc.* **2015**, *17*, 141–150. [CrossRef]
27. El-Hamid, H.T.A.; Caiyong, W.; Yongting, Z. Geospatial analysis of land use driving force in coal mining area: Case study in Ningdong, China. *GeoJournal* **2021**, *86*, 605–620. [CrossRef]
28. Brunsdon, C.; Fotheringham, A.S.; Charlton, M.E. Geographically weighted regression: A method for exploring spatial nonstationarity. *Geogr. Anal.* **1996**, *28*, 281–298. [CrossRef]
29. Huang, B.; Wu, B.; Barry, M. Geographically and temporally weighted regression for modeling spatio-temporal variation in house prices. *Int. J. Geogr. Inf. Sci.* **2010**, *24*, 383–401. [CrossRef]
30. Wang, D.G.; Kwan, M.P. Selected studies on urban development issues in China: Introduction. *Urban Geogr.* **2017**, *38*, 360–362. [CrossRef]
31. Zhou, Y.; Chen, M.; Tang, Z.; Mei, Z. Urbanization, land use change, and carbon emissions: Quantitative assessments for city-level carbon emissions in Beijing-Tianjin-Hebei region. *Sustain. Cities Soc.* **2021**, *66*, 102701. [CrossRef]
32. Luo, G.; Chen, X.; Zhou, K.; Ye, M. Temporal and spatial variation and stability of the oasis in the Sangong River Watershed, Xinjiang, China. *Sci. China Ser. D* **2003**, *46*, 62–73. [CrossRef]
33. Cheng, L.X.; Feng, R.Y.; Wang, L.Z. Fractal characteristic analysis of urban land-cover spatial patterns with spatiotemporal remote sensing images in Shenzhen city (1988–2015). *Remote Sens.* **2021**, *13*, 4640. [CrossRef]
34. Zhang, Y.; Chen, X. Spatial and nonlinear effects of new-type urbanization and technological innovation on industrial carbon dioxide emission in the Yangtze River Delta. *Environ. Sci. Pollut. Res.* **2023**, *30*, 29243–29257. [CrossRef] [PubMed]
35. Hu, P.P.; Li, F.; Hu, D.; Sun, X. Spatial and temporal characteristics of urban expansion in pearl River Delta urban agglomeration from 1980 to 2015. *Acta Ecol. Sin.* **2021**, *41*, 7063–7072.
36. Xie, H.; Zhu, Z.; Wang, B.; Liu, G.; Zhai, Q. Does the expansion of urban construction land promote regional economic growth in China? Evidence from 108 cities in the Yangtze River Economic Belt. *Sustainability* **2018**, *10*, 4073. [CrossRef]
37. Jin, G.; Deng, X.; Zhao, X.; Guo, B.; Yang, J. Spatiotemporal patterns in urbanization efficiency within the Yangtze River Economic Belt between 2005 and 2014. *J. Geogr. Sci.* **2018**, *28*, 1113–1126. [CrossRef]
38. Xu, G.; Yin, X.; Wu, G.; Gao, N. Rethinking the contribution of land element to urban economic growth: Evidence from 30 provinces in China. *Land* **2022**, *11*, 801. [CrossRef]
39. Zhu, X.; Zhang, P.; Wei, Y.; Li, Y.; Zhao, H. Measuring the efficiency and driving factors of urban land use based on the DEA method and the PLS-SEM model—A case study of 35 large and medium-sized cities in China. *Sustain. Cities Soc.* **2019**, *50*, 101646. [CrossRef]
40. Liu, S.; Xiao, W.; Li, L.; Ye, Y.; Song, X. Urban land use efficiency and improvement potential in China: A stochastic frontier analysis. *Land Use Policy* **2020**, *99*, 105046. [CrossRef]

land

MDPI

Article

Multi-Scenario Prediction Analysis of Carbon Peak Based on STIRPAT Model-Take South-to-North Water Diversion Central Route Provinces and Cities as an Example

Qingxiang Meng, Baolu Li, Yanna Zheng, Huimin Zhu, Ziyi Xiong, Yingchao Li * and Qingsong Li *

College of Resources and Environment, Henan Agricultural University, Zhengzhou 450046, China; qxmeng@henau.edu.cn (Q.M.); baoluli2023@stu.henau.edu.cn (B.L.); yannazheng2023@stu.henau.edu.cn (Y.Z.); zhm@stu.henau.edu.cn (H.Z.); xiongziyi@stu.henau.edu.cn (Z.X.)
* Correspondence: ycli666@henau.edu.cn (Y.L.); qs.li@henau.edu.cn (Q.L.)

Abstract: With the increase in energy demand, environmental issues such as carbon emissions are becoming more and more prominent. China will scale its intended nationally determined contributions by adopting more vigorous policies and measures. China aims to have CO_2 emissions peak before 2030 and achieve carbon neutrality before 2060. The current challenge and priority of China's high-quality development is to ensure a harmonious balance between the ecological environment and the economy. The South-to-North Water Diversion Project passes through Beijing, Tianjin, Henan, and Hebei, which were chosen as the study sites. The carbon emission data was from the China Carbon Emission Database 2000–2019. Decoupling modeling using statistical yearbook data from four provinces and municipalities. KMO and Bartlett's test used SPSS 27 software. The selection of indicators was based on relevance. Analyses were performed using the extended STIRPAT model and ridge regression. Moreover, projections of carbon peaks in the study area for 2020–2035 under different rates of change were simulated by the scenario analysis method. The results show that: (1) The decoupling analysis of the four provinces and cities from 2000-2019 gradually shifts to strong decoupling; (2) Resident population, energy structure, and secondary industry as a proportion of GDP significantly impact carbon emissions; (3) From 2000–2035, Beijing and Henan experienced carbon peaks. The peak time in Beijing was 96.836 million tons in 2010. The peak time in Henan was 654.1004 million tons in 2011; (4) There was no peak in Hebei from 2000–2035.

Keywords: carbon peaking; decoupling; South-to-North Water Diversion Project; STIRPAT mode

Citation: Meng, Q.; Li, B.; Zheng, Y.; Zhu, H.; Xiong, Z.; Li, Y.; Li, Q. Multi-Scenario Prediction Analysis of Carbon Peak Based on STIRPAT Model-Take South-to-North Water Diversion Central Route Provinces and Cities as an Example. *Land* **2023**, *12*, 2035. https://doi.org/10.3390/land12112035

Academic Editors: Jinyan Zhan, Chao Wang and Xueting Zeng

Received: 10 October 2023
Revised: 28 October 2023
Accepted: 1 November 2023
Published: 8 November 2023

1. Introduction

Against the backdrop of a slowdown in total world carbon emissions, there are significant differences between the developed economy's and the emerging economy's current carbon emissions status and the emissions outlook. Research on carbon emissions has become the attention of scholars at home and abroad [1,2]. The successive establishment of the United Nations Framework Convention on Climate Change, the Kyoto Agreement, and the Paris Agreement demonstrate the international community's collaborative endeavors toward worldwide low-carbon progress. Their ultimate goal is to reduce emissions and save energy, controlling the temperature's rise. In order to achieve green development, it is necessary to study issues such as carbon emissions and their influencing factors [3]. China has made ecological progress an essential part of its 13th Five-Year Plan, implementing the development concepts of innovation, coordination, greenness, openness, and sharing through scientific, technological, and institutional innovation. This includes the implementation of an optimized industrial structure and the building of a low-carbon energy system. Developing green buildings and low-carbon transport establishment of a national carbon emissions trading market and a series of other policy measures will form a new pattern of modernization and construction for the harmonious development of humanity

and nature [4,5]. China is aiming to reach the highest point of its carbon dioxide emissions by 2030 and to become carbon neutral by 2060.

Scholars worldwide have utilized the STIRPAT model to explore the trajectories and peak periods of HCEs in 30 provinces in China until 2040 and have formulated three distinct scenarios (baseline, low, and high) to predict carbon peaks. The findings indicate that in at least one of the scenarios, 25 provinces have the potential to achieve peak HCE by 2030, whereas five provinces would fall short of meeting the 2030 emissions target [6]. Changes in carbon emissions also require more certainty due to uncertainty about future development patterns, making meeting peak targets challenging. Taking Shandong, Henan, and Guangdong as three of China's most populous provinces as examples, the effects of uncertainty in carbon accounting principles, drivers, and simulation mechanisms on achieving peak targets were analyzed [7]. They used the LMDI method to decompose and analyze the driving factors affecting China's carbon dioxide emissions by studying the detailed situation of 41 sub-industries from 2000 to 2016. Based on various official policies and documents, the carbon intensity reduction potential for 2020 and 2030 was predicted [8]. This paper investigates carbon emission peaks in China based on a comparative analysis of energy transition in China and the United States [9]. A novel multifactor decomposition method for carbon emissions is proposed [10]. Multifactor decomposition models based on the Kaya Identity extension and the LMDI decomposition methodology from energy, economic, and social perspectives provide quantitative results. On this basis, an evaluation system was constructed by applying the entropy weight method, and the carbon emission indices of six power generation modes in China were generated from three dimensions: environment, energy, and economy. It also established a carbon emission dynamic model based on the carbon emission data of the past 40 years and, combined with Tapio's decoupling theory, predicted China's carbon emissions under multiple scenarios for the next 40 years. Based on the carbon emission panel data of countries along the "Belt and Road" from 1970 to 2018 and the environmental Kuznets curve (EKC) theory, a panel model was established for each country group for research [11]. The study proposes that carbon substitution, carbon emission reduction, carbon sequestration, and carbon recycling are the four main ways to achieve carbon neutrality, of which carbon substitution will be the backbone of carbon neutrality [12]. According to the high, medium, and low scenarios, China's carbon emissions are projected to fall to 22×10^8, 33×10^8 and 44×10^8 tons in 2060, respectively. Seven implementation recommendations are made for China to achieve carbon neutrality. The results show that the earlier the time of peak carbon emissions, the more significant the economic impact on China; under the three scenarios of peak carbon emissions, government revenues and savings have a significant decline, and the rest of the economic indicators do not cause too much impact; the impact of peak carbon emissions on the output of the construction industry is small, and the output of the other sectors has a slight increase [13]. Focusing on natural resource management under the "dual-carbon" objective, nine experts proposed innovative natural resource management strategies from different perspectives, providing reference and reference for the construction of a low-carbon oriented natural resource management system based on the multi-level perspective of "resource elements-territorial space-ecosystem". This provides a reference for constructing a low-carbon-oriented natural resource management system based on the multi-level perspective of "resource elements, land space, and ecosystem". [14].

In summary, there is still some controversy among many scholars as to whether China can achieve the goals of carbon peaking and carbon neutrality on time, and there are some areas for improvement in the analysis of carbon peaking at the basin level [15]. This study uses the provinces and cities through which the South-to-North Water Diversion Project passes as the study area to analyze, build models, and carry out prediction analyses to provide the government with corresponding carbon peak strategies.

2. Research Area

The four provinces and cities of Beijing, Tianjin, Hebei, and Henan, through which the central line of the South-to-North Water Diversion passes, were used for the study (Figure 1). The provinces and cities through which the South-to-North Water Diversion passes have a significant impact on China's socio-economic development. In the meantime, "Beijing–Tianjin–Hebei" has emerged as the third most significant economic district, following "The Yangtze River Delta" and "Pearl River Delta". The effectiveness of its carbon emission reduction is directly related to the achievement of China's carbon emission reduction targets [16–19]. The South-to-North Water Diversion Mainline Project, an essential part of the National South-to-North Water Diversion Project, is a major strategic infrastructure built to alleviate the severe shortage of water resources in China's Huanghua Hai Plain and optimize the allocation of water resources and is a century-long project related to the sustainable economic and social development of the receiving areas in the provinces and cities of Henan, Hebei, Tianjin, and Beijing and the well-being of the future generations. The regional scope of the South-to-North Water Diversion Project is geographically vast. The spatial differences in each region's resources, population, economy, and industrial structure are apparent, and the specific measures for regional carbon emission reduction are different. Research on land use carbon emissions and influencing factors in the region provide a theoretical and practical basis for its emission reduction.

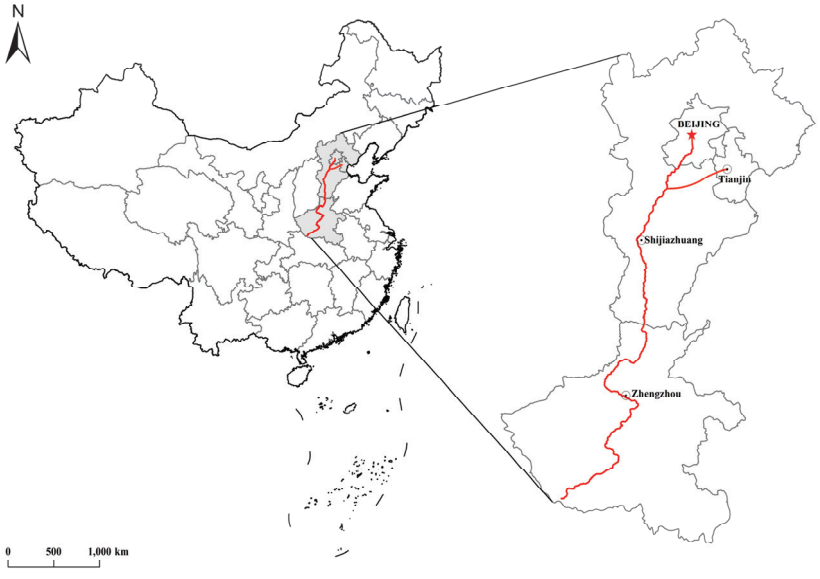

Figure 1. Provinces and cities passing through the South-to-North Water Diversion Central Route.

3. Research Methods and Data

3.1. Analysis of Carbon Emissions

From 2000–2019, Beijing's carbon dioxide emissions have been characterized by a "U" shape, beginning with an increase and then a decrease. The amount increased from 63,471,900 tons in 2000 to its highest point of 96,836,000 tons in 2010 and has since decreased to 70,611,800 tons in 2019. From 2000–2019, Tianjin has seen a steady increase in its CO_2 emissions, with a slight peak from 2010 to 2013 and a total of 151,032,500 tons in 2013. Hebei's carbon dioxide emissions rose steadily from 2000–2019, with the most significant surge occurring between 2000 and 2013. The total amount of CO_2 released in 2013 amounted to 657.72 million tons. From 2014–2017, there was a slight decrease, which kept rising. From 2000–2019, Henan experienced a fluctuating amount of CO_2 emissions.

There was an upward trend from 2000–2011 and a downward trend from 2012–2019. The total amount of CO_2 released in 2019 amounted to 463,998,300 tons (Figure 2).

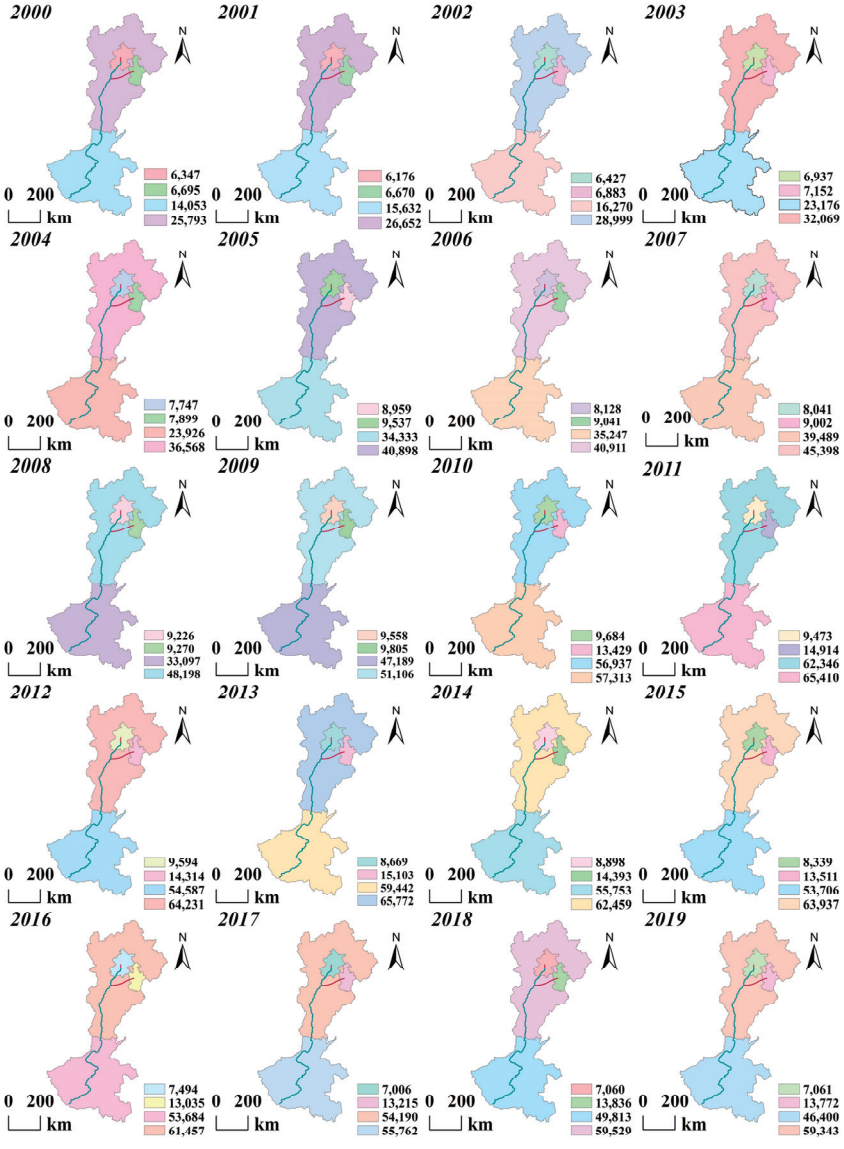

Figure 2. Carbon emissions from Beijing, Tianjin, Hebei, and Henan, 2000–2019 (10^4 t).

Among the four provinces and cities of Beijing, Tianjin, Hebei, and Henan in the period of 2000–2019, Beijing and Tianjin's annual carbon dioxide emissions were relatively small. Hebei's carbon dioxide emissions commonly remained high, and only in 2011, 2012, and 2018 did Henan's carbon dioxide emissions exceed those of Hebei, which shows that Hebei is a large province in terms of carbon dioxide emissions.

3.2. Research Methodology

3.2.1. Decoupling Model

The concept of decoupling was introduced by the Organization for Economic Co-operation and Development in 2002. This concept describes models and demonstrates the correlation between economic growth and environmental quality impairment [20]. Tapio proposed an improved decoupling model in 2005. The decoupling analysis method has been widely used in major industries, and this study uses decoupling analysis to study the relationship between economic growth and carbon emissions, as shown in Equation (1).

$$MI_{t2-t1} = \frac{\%\Delta CE}{\%\Delta GDP} = \frac{\frac{CE_{t2} - CE_{t1}}{CE_{t1}}}{\frac{GDP_{t2} - GDP_{t1}}{GDP_{t1}}} \quad (1)$$

In Equation (1), MI_{t2-t1} is the decoupling index from moment $t1$ to moment $t2$, CE_{t2} and CE_{t1} are the carbon emissions at $t1$ and $t2$. GDP_{t2} and GDP_{t1} are GDP at moments $t1$ and $t2$.

They use elasticity values of 0, 0.8, and 1.2 as thresholds to account for the decoupling of CO_2 from economic growth. For example, when the elasticity value is less than 0, CO_2 shows strong negative or strong decoupling. Therefore, the status and degree of CO_2 decoupling must be determined according to the situation. The specific indicator system [21–23] is shown in Table 1.

Table 1. Tapio Decoupling Indicator System.

Status	Decoupling State	ΔCE	ΔGDP	MI
Decoupling	Strong decoupling	<0	>0	MI < 0
	Weakly decoupling	>0	>0	0 < MI ≤ 0.8
Negative decoupling	Recessive decoupling	<0	<0	MI > 1.2
	Strong negative decoupling	>0	<0	MI < 0
	Weak negative decoupling	<0	<0	0 < MI ≤ 0.8
	Expansion negative decoupling	>0	>0	MI > 1.2
Connection	Expansion connection	>0	>0	0.8 < MI ≤ 1.2
	Recession connection	<0	<0	0.8 < MI ≤ 1.2

3.2.2. STIRPAT Model

The IPAT equation proposed by Western scholars in the 1970s is a classic model for exploring the relationship between economic growth and energy consumption [24,25]. Its expression is shown in Equation (2).

$$I = P \times A \times T \quad (2)$$

In Equation (2), I, P, A, and T represent environmental conditions, population, economic affluence, and technology level, respectively. However, the IPAT equation only considers the relationship between economic development and environmental pressure on energy consumption and sets it as a simple linear relationship with certain limitations. Therefore, in this paper, the STIRPAT model obtained by extending the IPAT model was chosen, and the model's expression is shown in Equation (3).

$$I = aP^b A^c T^d e \quad (3)$$

In Equation (3): a is the model coefficient; b, c, d are prognostic factors; e is the error factor.

3.3. Data Sources

Carbon emissions from the four provinces and cities of Beijing, Tianjin, Hebei, and Henan in 2000–2019 were sourced from the China Carbon Emissions Database (CEADs) [26–29]. Resident population, GDP per capita, energy consumption intensity (energy consumption/GDP), energy structure (coal consumption/total energy consumption), and secondary industry share of GDP are from the China Energy Statistical Yearbook and China Statistical Yearbook (2000–2019).

4. Analysis of Results

4.1. Decoupling Model Analysis

Carbon decoupling refers to the issue of the relationship between changes in CO_2 emissions and economic growth. When economic growth is achieved at the same time that CO_2 emissions grow at a negative rate or a rate less than the economic growth rate, it can be regarded as decoupling, which is essentially a measure of whether economic growth comes at the cost of resource consumption and environmental damage. Through the four provinces and cities through which the South-to-North Water Diversion Project passes, from 2000–2019, carbon emission and GDP data were calculated according to the decoupling model, and the decoupling was calculated as shown in (Figure 3).

	2000-2001	2001-2002	2002-2003	2003-2004	2004-2005	2005-2006	2006-2007	2007-2008	2008-2009	2009-2010
Beijing	V	II	II	II	VI	I	I	VII	II	II
Tianjin	I	II	II	II	II	II	I	II	II	II
Hebei	II	IV	II	II	II	II	II	II	II	II
Henan	VII	II	VI	II	VI	II	II	I	VI	VII
	2010-2011	2011-2012	2012-2013	2013-2014	2014-2015	2015-2016	2016-2017	2017-2018	2018-2019	
Beijing	I	II	I	VI	I	I	I	II	II	
Tianjin	IV	I	II	I	I	I	II	VI	V	
Hebei	VI	II	II	I	VI	I	I	VI	V	
Henan	VII	I	VII	I	I	I	II	I	I	

Decoupling status				
Strong decoupling	I	Weak negative decoupling	V
Weakly decoupling	II	Expansion negative decoupling	VI
Strong negative decoupling	IV	Expansion Connection	VII

Figure 3. Dynamic relationship between carbon emissions and economic growth in four provinces and cities from 2000–2019.

Beijing from 2000–2009 experienced a weak negative decoupling, weak decoupling, expansion negative decoupling, and a strong decoupling stage for a better trend, economic growth, and carbon emissions among the more reasonable. Decoupling mainly alternated between weak and strong decoupling from 2010–2019. Under continuous economic acceleration, the economic growth rate was greater than the growth rate of carbon emissions, indicating that energy conservation and emission reduction efforts achieved the intended results.

Tianjin's carbon emissions and economic development in the 2000–2009 timeframe were mainly weakly decoupling, with a large amount of carbon emitted mainly from the secondary industry, and the growth rate of carbon emissions was greater than that of economic growth, leading to excessive carbon emissions. Expansion of negative decoupling occurred from 2009–2010, and strong decoupling predominated from 2010–2019, indicating significant results in energy conservation, emission reduction, and industrial restructuring. The relationship between carbon emissions and economic growth was within a more reasonable range.

Hebei was mainly weakly decoupled from 2000–2009, closely related to Hebei's energy emissions. Hebei is a traditional industrial province and China's number one iron and steel province, resulting in a continuous increase in carbon emissions. Strong decoupling occurred twice from 2010–2019, in 2016 and 2017, respectively. This demonstrates that Hebei promotes the transformation of old and new kinetic energy, accelerates the pace of transformation and upgrading of traditional industries, and accelerates the development of new industries. It also shows that the industry's momentum toward the middle and

high end is vital. It is necessary to deeply promote the manufacturing industry's high-end, intelligent, and green development.

Henan was mainly dominated by weak decoupling and expansion negative decoupling from 2000–2009, with weak decoupling occurring five times and expansion negative decoupling occurring three times, indicating an irrational match between carbon emissions and economic growth. Strong decoupling occurred six times from 2010–2019. Then, there was a better match between economic growth and carbon emissions, with economic growth being more significant than the rate of carbon emissions and a sustained reduction in carbon emissions. This is closely related to the government's energy-saving and emission-reduction policies, industrial restructuring, and green development. The relationship between economic growth and carbon emissions has been gradually harmonized to promote high-quality development in Henan.

4.2. STIRPAT Model Regression Fit Analysis

4.2.1. Description of Variables

The following is a collection and collation of basic data from four provinces and municipalities: Beijing, Tianjin, Hebei, and Henan carbon emissions, 2000–2019, permanent population, GDP per capita, energy consumption intensity (energy consumption/GDP), and energy structure (coal consumption/total energy consumption). This includes data on the share of the secondary sector in GDP. The maximum, minimum, mean, and standard deviation of each variable after taking the logarithm are shown in (Table 2).

Table 2. Description of variables.

Variant	Abbreviated Symbol	Minimum Value	Maximum Value	Average Value	Standard Deviation
Carbon emissions	I	617.61	6577.2	2754.21	2115.56
Permanent population	P	1001.14	9901	4937.08	3550.22
GDP per capita	A	5450	161,776	45,876.44	35,365.7
Intensity of energy consumption	T	0.21	2.43	1.06	0.58
Energy mix	Y	0.02	1.3	0.81	0.33
Share of secondary sector in GDP	Z	16.2	60.1	44.4	11.93

4.2.2. Variable Correlation Analysis

The base data of the four provinces and cities were logarithmically processed, and factor analyses of the variables by SPSS 27 software, KMO, and Bartlett's test are shown in Table 3. The range of values between 0.7 and 0.8 is barely suitable, and between 0.8 and 0.9 is suitable. The values are 0.8 for Beijing, 0.8 for Tianjin, 0.6 for Hebei, and 0.7 for Henan, all with a significance of 0.000.

Table 3. KMO and Bartlett's test.

		Beijing	Tianjin	Hebei	Henan
KMO Sampling Suitability Measure		0.8	0.6	0.6	0.7
Bartlett's Sphericity test	Approximate Chi-squared value	183.40	238.29	210.19	186.54
	(number of) degrees of freedom (physics)	15	15	15	15
	Significance	0.00	0.00	0.00	0.00

After the KMO and Bartlett tests, the indicators that best reflect the input–output relationship were screened using Pearson correlation coefficients (Figure 4). The closer the absolute value of the Pearson correlation coefficient is to 1, the stronger the correlation between the indicator and carbon emissions.

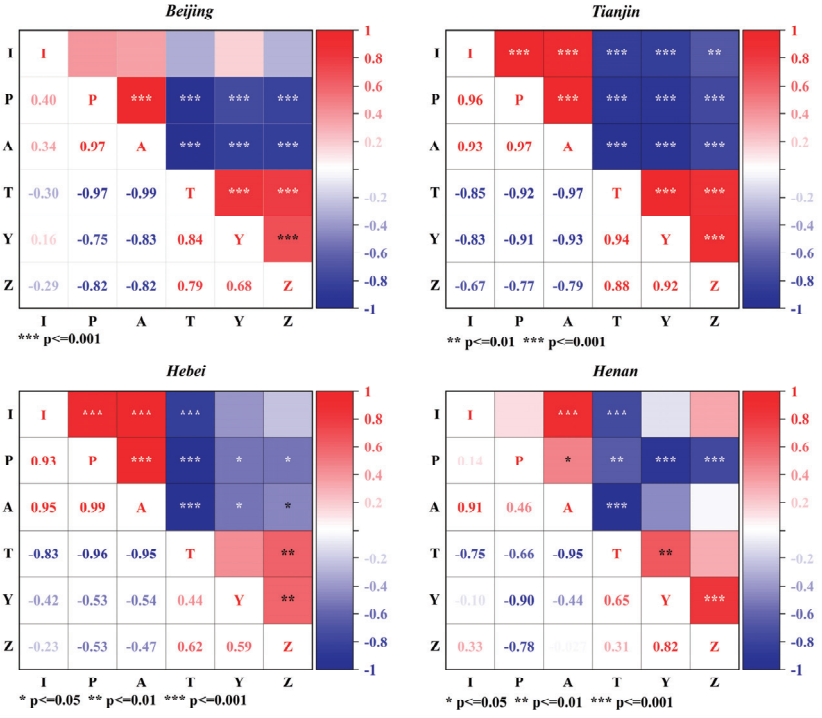

Figure 4. Pearson correlation between indicators.

There is a strong positive correlation of 0.98 between the resident population and GDP per capita in Beijing and a strong negative correlation with energy consumption intensity, energy structure, and the proportion of secondary industry in GDP, which are −0.97, −0.75, and −0.82, respectively. There is a strong negative correlation between per capita GDP and energy consumption intensity, energy structure, and the proportion of the secondary industry. Carbon emissions in Tianjin positively correlate with the resident population and per capita GDP, up to 0.96. A negative correlation exists between permanent population and energy consumption intensity, energy structure, and the proportion of secondary industry in GDP. In Hebei Province, carbon emissions have a strong positive correlation with permanent population and per capita GDP, reaching the highest, 0.95, and a negative correlation with energy consumption intensity, energy structure, and the proportion of secondary industry in GDP. The positive correlation between carbon emission and per capita GDP in Henan Province is 0.91, and the negative correlation between carbon emission and energy consumption intensity and energy structure is 0.91.

4.3. Tapio Decoupling Model Analysis

According to the basic form of the STIRPAT model, the extended STIRPAT model was constructed, and its expression is shown in Equation (4).

$$I = aP^bA^cT^dY^iZ^je \tag{4}$$

In order to facilitate subsequent data analysis and processing, Equation (4) is logarithmic to obtain Equation (5):

$$lnI = blnP + clnA + dlnT + ilnY + jlnZ + lne \tag{5}$$

In formula (5), *b*, *c*, *d*, *i*, and *j* are prediction coefficients representing the amount of change in carbon emissions *b*%, *c*%, *d*%, *i*%, and *j*% that can be induced by a 1% change in the resident population (10 thousand people), GDP per capita (RMB/person), energy consumption intensity (10 thousand tons of standard coal/billions), energy structure (tons of standard coal/tons), and the share of secondary industry in GDP (%). The regression model is used to construct a carbon emission prediction model for the four provinces and municipalities of the South-to-North Water Diversion Project and then to analyze carbon peaking by predicting the future carbon emission trends of the four provinces and municipalities based on the baseline scenario, the green scenario, and the high-speed scenario.

4.4. Ridge Regression Results

The results of the SPSS 27 software test showed that the variance inflation factor between the variables was higher than 10. In order to avoid multicollinearity between the influencing factors, ridge regression analysis was used to fit the carbon emissions to the influencing factors, and the carbon emission prediction models were constructed separately for the study area. Individual carbon emission forecasting models were created for the research region. The pertinent results can be found in Table 4.

Table 4. Carbon emission regression fitting results for four provinces and cities of South-to-North Water Diversion Central Route Project.

Province	P	A	T	Y	Z	Constant	k	R^2
Beijing	0.2561	0.1878 ***	−0.0467	0.1826 ***	−0.0601	5.3592 ***	0.05	0.73
Tianjin	1.0539 ***	0.1522 ***	−0.0229	−0.0764	0.1613	−0.5087	0.15	0.91
Hebei	3.3382 ***	0.2347 ***	−0.1063 **	−0.2363	1.4690 ***	−26.7293 ***	0.10	0.96
Henan	−0.1369	0.3432 ***	−0.3617 ***	0.2525	2.3362 ***	−0.7557	0.15	0.93

Note: ***, ** represent $p < 0.01$ and $p < 0.05$, respectively.

The resulting carbon emission projection models for Beijing, Tianjin, Hebei, and Henan are shown in Equations (6)–(9).

$$\ln I = 0.2561\ln P + 0.1878\ln A - 0.0467\ln T + 0.1826\ln Y - 0.0601\ln Z + 5.3592 \quad (6)$$

$$\ln I = 1.0539\ln P + 0.1522\ln A - 0.0229\ln T - 0.0764\ln Y + 0.1613\ln Z - 0.5087 \quad (7)$$

$$\ln I = 3.3382\ln P + 0.2347\ln A - 0.1063\ln T - 0.2363\ln Y + 1.4690\ln Z - 26.7293 \quad (8)$$

$$\ln I = -0.1369\ln P + 0.3432\ln A - 0.3617\ln T + 0.2525\ln Y + 2.3362\ln Z - 0.7557 \quad (9)$$

According to Equations (6)–(9), the substitution of the data to obtain the carbon emissions and the projected carbon emissions of the four regions of Beijing, Tianjin, Hebei, and Henan from 2000–2019 is shown in (Figure 5).

4.5. Peak Carbon Scenario Projections

Based on the extended STIRPAT model, a forecasting study was conducted with 2020 as the base year and 2035 as the end year. In 2020, due to the impact of "new coronavirus pneumonia", the scenarios were based on the rates of change in the 13th Five-Year Plan, as shown in Tables 5–8. The change characteristics for 2021–2035 were divided into three time periods: 2021–2025, 2026–2030, and 2031–2035, with each period set at five years.

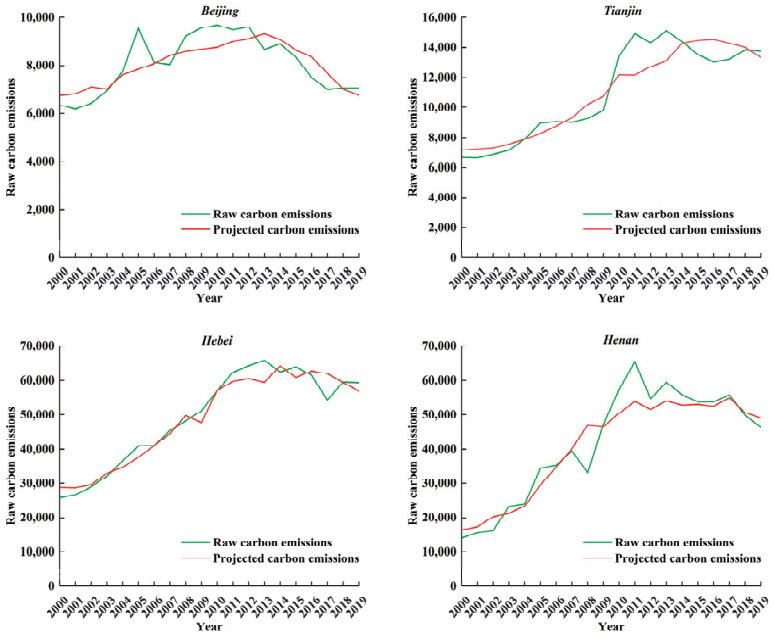

Figure 5. Actual carbon emissions and projections for four provinces and cities, 2000–2019 (10^4t).

4.5.1. Basis for Setting Indicators in Beijing

The setting of various indicators in Beijing is shown in Table 5. The population setting was based on the Beijing Urban Master Plan (2016–2035), which states that the resident population of Beijing will be within 23 million in 2035, and the resident population of Beijing will be 21.9 million in 2019, which allowed us to calculate that the average annual rate of change from 2019–2035 will be controlled to be around 0.3139%. For 2021, the low speed of the population can be set at 0.2800%, the medium speed at 0.3100%, and the high speed at 0.3400%, with a constant annual decline of 0.001% during the forecast period. Per capita GDP was based on the 14th Five-Year Plan for Beijing's National Economic and Social Development and the outline (draft) of the long-term goals for 2035. By 2035, per capita GDP will reach more than 320,000 yuan, and the city's comprehensive competitiveness will rank among the highest in the world. In 2019, the per capita GDP of Beijing was 161,776 yuan. It can be calculated that the average annual change rate from 2019–2035 will be controlled at around 6.1128%. It can be set that the per capita regional gross domestic product in 2021 will decrease at a low speed of 5.9100%, a medium speed of 6.1128%, and a high speed of 6.3100%. During the forecast period, the annual average decline will be 0.28%. The energy consumption intensity in Beijing was 0.46% in 2010 and 0.21% in 2019. Therefore, the change rate between 2010 and 2019 can be calculated to be −5.52%. The energy consumption intensity in 2021 can be set as −5.8200% at low speed, −5.5200% at medium speed, and −5.2200% at high speed. The energy structure in Beijing was 0.38% in 2010 and 0.02% in 2019. Therefore, the change rate between 2010 and 2019 can be calculated to be −9.34%. It can be set that the energy structure in 2021 will have a low speed of −9.5400%, a medium speed of −9.3400%, and a high speed of −9.1400%. In Beijing, the proportion of the secondary industry in GDP was 24% in 2010 and 16.2% in 2019, so the change rate between 2010 and 2019 can be calculated as −3.25% and the proportion of the secondary industry in GDP in 2021 can be set as −3.5500% at low speed, −3.2500% at medium speed and −3.0550% at high speed.

Table 5. Beijing's indicator settings.

Rate of Change	Vintages	Rate of Change Setting				
		Permanent Population	GDP per Capita	Intensity of Energy Consumption	Energy Mix	Share of Secondary Sector in GDP
Low	2019–2020	−0.0569%	7.7771%	−5.7000%	−19.9300%	−3.9744%
	2021–2025	0.2800%	5.9100%	−5.8200%	−9.5400%	−3.5500%
	2026–2030	0.2750%	4.5100%	−5.8250%	−10.0400%	−3.5550%
	2031–2035	0.2700%	3.1100%	−5.8300%	−10.5400%	−3.5600%
Middle	2019–2020	−0.0569%	7.7771%	−5.7000%	−19.9300%	−3.9744%
	2021–2025	0.3100%	6.1128%	−5.5200%	−9.3400%	−3.2500%
	2026–2030	0.3050%	4.7128%	−5.5250%	−8.8400%	−3.2550%
	2031–2035	0.3000%	3.3128%	−5.5300%	−8.3400%	−3.2600%
High	2019–2020	−0.0569%	7.7771%	−5.7000%	−19.9300%	−3.9744%
	2021–2025	0.3400%	6.3100%	−5.2200%	−9.1400%	−3.0500%
	2026–2030	0.3350%	4.9100%	−5.2250%	−8.6400%	−3.0550%
	2031–2035	0.3300%	3.5100%	−5.2300%	−8.1400%	−3.0600%

4.5.2. Basis for Setting Indicators in Tianjin

The indicators of Tianjin are set in Table 6. According to the Tianjin Bureau of Statistics data, by the end of 2021, Tianjin's permanent population had reached 15.6966 million, an increase of 0.4% over the previous year. Since 2016, the resident population of Tianjin has been showing a steady growth trend. Among them, Tianjin's population growth rate dropped slightly in 2020 due to the epidemic. However, with the effective control of the epidemic, Tianjin's population growth rate rose again in 2021. The population will continue to grow in the future as Tianjin's economy continues to develop. According to the plan of the Tianjin municipal government, the permanent population of Tianjin will reach about 20 million by 2035. In 2019, the resident population of Tianjin was 13.85 million. The annual change rate from 2019–2035 will be controlled at about 2.7753%. Then, it can be set that in 2021, the low speed of Tianjin's resident population can be set as 2.5800%, the medium speed can be set as 2.7753%, and the high speed can be set as 2.9800%, with an even annual decline of 0.003% during the forecast period. Gross regional product per capita can be set to be RMB 54,053 per capita in Tianjin in 2010 and RMB 101,557 per capita in Tianjin in 2019; it can be calculated that the average annual rate of change from 2019-2035 will be controlled at about 8.79%. The GDP per capita in 2021 can be set at 8.5884% at low speed, 8.7884% at medium speed, and 8.9884% at high speed. Energy consumption intensity in Tianjin was 1.00% in 2010 and 0.58% in 2019, so the change rate between 2010 and 2019 can be calculated as −4.15%. Energy consumption intensity in 2021 can be set to −4.4462% at low speed, −4.1462% at medium speed, and −3.8462% at high speed. The energy structure in Tianjin was 0.71% in 2010 and 0.46% in 2019, indicating a change rate of −3.52% between 2010 and 2019. The energy structure can be set at −3.8178% for low speed, −3.5178% for medium speed, and −3.2178% for high speed in 2021. In Tianjin, the proportion of the secondary industry in GDP was 52.5% in 2010 and 35.2% in 2019, so the change rate between 2010 and 2019 can be calculated as −3.30%. The proportion of secondary industry in GDP in 2021 can be set as −3.492% at low speed, −3.2957% at medium speed, and −3.0952% at high speed.

4.5.3. Basis for Setting the Indicators in Hebei

The setting of the indicators for Hebei is shown in Table 7. Population setting: According to the Population Development Plan of Hebei Province (2018–2035), the population of Hebei Province will increase to 79.1 million people by 2035. In 2019, the resident population of Hebei Province was 21.9 million people; it can be calculated that the average annual rate of change from 2019–2035 will be controlled at about 0.39%. The population can be set to

have a low speed of 0.3636%, a medium speed of 0.3886%, and a high speed of 0.4086% in 2021, with a predicted annual average decrease of 0.01% during the forecast period. The per capita GDP of Hebei Province was 25,308 yuan in 2010 and 47,036 yuan in 2019, and the change rate from 2010–2019 can be calculated as about 8.59%. It can be set that the per capita regional gross domestic product in 2021 will decrease at a low speed of 8.2854%, a medium speed of 8.5854%, and a high speed of 8.7857%. During the forecast period, the annual average decline will be 0.02%. Energy consumption intensity in Hebei was 1.53% in 2010 and 0.93% in 2019; therefore, the rate of change between 2010–2019 can be calculated to be −3.94%, which can be set as −3.9674% for the low rate of energy consumption intensity in 2021, −3.9374% for the medium rate, and -3.9074% for the high rate. Energy structure in Hebei was 1.00% in 2010 and 0.88% in 2019; then, the rate of change between 2010–2019 can be calculated as −1.15% and the energy structure in 2021 can be set to be −1.5483% for the low rate, −1.1438% for the medium rate, and −0.7483% for the high rate. In 2010, the share of secondary industry in the GDP in Hebei was 52.5%, and in 2019, the share of secondary industry in the GDP in Hebei Province was 38.7%; then, the rate of change between 2010–2019 can be calculated as −2.63%, and it can be set that, in 2021, the share of secondary industry in GDP will be −2.9286% at low speed, −2.6286% at medium speed, and −2.3286% at high speed.

Table 6. Tianjin indicator settings.

Rate of Change	Vintages	Rate of Change Setting				
		Permanent Population	GDP per Capita	Intensity of Energy Consumption	Energy Mix	Share of Secondary Sector in GDP
Low	2019–2020	−1.0000%	6.8772%	7.3418%	−3.1827%	−4.2122%
	2021–2025	2.5800%	8.5884%	−4.4462%	−3.8178%	−3.4952%
	2026–2030	2.4300%	5.0884%	−4.4962%	−1.3178%	−3.4957%
	2031–2035	2.2800%	1.5884%	−4.5462%	1.1822%	−3.4962%
Middle	2019–2020	−1.0000%	6.8772%	7.3418%	−3.1827%	−4.2122%
	2021–2025	2.7753%	8.7884%	−4.1462%	−3.5178%	−3.2952%
	2026–2030	2.6253%	5.2884%	−4.1962%	−1.0178%	−3.2957%
	2031–2035	2.4753%	1.7884%	−4.2462%	1.4822%	−3.2962%
High	2019–2020	−1.0000%	6.8772%	7.3418%	−3.1827%	−4.2122%
	2021–2025	2.9800%	8.9884%	−3.8462%	−3.2178%	−3.0952%
	2026–2030	2.8300%	5.4884%	−3.8962%	−0.7178%	−3.0957%
	2031–2035	2.6800%	1.9884%	−3.9462%	1.7822%	−3.0962%

4.5.4. Basis for Setting the Indicators in Henan

The setting of each indicator in Henan is shown in Table 8. In the population setting, the resident population of Henan Province in 2010 was 94.05 million people, and the resident population of Henan Province in 2019 was 99.01 million. Then, the rate of change between 2010 and 2019 can be calculated as 0.53%, and it can be set that the resident population in 2021 will be 0.4974% at a low rate, 0.5274% at a medium rate, and 0.5574% at a high rate. The uniform rate of decline is 0.001 percent per year over the projection period. The per capita GDP of Henan Province was 41,326 yuan in 2016 and 5,450 yuan in 2019. The annual change rate from 2019–2035 will be controlled at about 7.88%. It can be set that the per capita regional gross domestic product in 2021 will decrease at a low speed of 7.5824%, a medium speed of 7.8824%, and a high speed of 8.1824%, with a predicted average annual decrease of 0.001% during the forecast period. Energy consumption intensity in Henan Province was 0.95% in 2010 and 0.41% in 2019. Then, the rate of change between 2010 and 2019 can be calculated as −5.66%, and it can be set that the low rate of energy consumption intensity in 2021 will be −5.9567%, the medium rate will be −5.6567% and the high rate will be −5.3567%. The energy structure of Henan Province was 1.22% in 2010 and 0.90% in 2019; then, the rate of change between 2010 and 2019 can be calculated as −2.60%, and

it can be set that the low rate of energy structure in 2021 can be set to be −2.9025%, the medium rate can be set to be −2.6025%, and the high rate can be set to be −2.3025%. In Henan Province, the share of secondary industry in GDP was 57.30% in 2010 and 43.50% in 2019. Then, the rate of change between 2010 and 2019 can be calculated to be −2.41%, and it can be set that the share of secondary industry in GDP in 2021 will be −2.7084% at low speed, −2.4084% at medium speed, and −2.1084% at high speed.

Table 7. Setting of indicators in Hebei.

Rate of Change	Vintages	Rate of Change Setting				
		Permanent Population	GDP per Capita	Intensity of Energy Consumption	Energy Mix	Share of Secondary Sector in GDP
Low	2019–2020	0.2441%	5.3944%	−1.5503%	−2.4988%	−4.6629%
	2021–2025	0.3686%	8.2854%	−3.9674%	−1.5483%	−2.9286%
	2026–2030	0.3186%	8.3854%	−4.1674%	−2.0483%	−3.1286%
	2031–2035	0.2686%	8.4854%	−4.3674%	−2.5483%	−3.3286%
Middle	2019–2020	0.2441%	5.3944%	−1.5503%	−2.4988%	−4.6629%
	2021–2025	0.3886%	8.5854%	−3.9374%	−1.1483%	−2.6286%
	2026–2030	0.3836%	8.6854%	−4.1374%	−1.6483%	−2.8286%
	2031–2035	0.3786%	8.7854%	−4.3374%	−2.1483%	−3.0286%
High	2019–2020	0.2441%	5.3944%	−1.5503%	−2.4988%	−4.6629%
	2021–2025	0.4086%	8.7854%	−3.9074%	−0.7483%	−2.3286%
	2026–2030	0.4036%	8.8854%	−4.1074%	−1.2483%	−2.5286%
	2031–2035	0.3986%	8.9854%	−4.3074%	−1.7483%	−2.7286%

Table 8. Setting of Indicators in Henan.

Rate of Change	Vintages	Rate of Change Setting				
		Permanent Population	GDP per Capita	Intensity of Energy Consumption	Energy Mix	Share of Secondary Sector in GDP
Low	2019–2020	0.3145%	7.8824%	−6.5153%	−3.7995%	−2.1667%
	2021–2025	0.4974%	7.5824%	−5.9567%	−2.9025%	−2.7084%
	2026–2030	0.4924%	7.5874%	−6.1567%	−3.4025%	−2.9084%
	2031–2035	0.4874%	7.5924%	−6.3567%	−3.9025%	−3.1084%
Middle	2019–2020	0.3145%	7.8824%	−6.5153%	−3.7995%	−2.1667%
	2021–2025	0.5274%	7.8824%	−5.6567%	−2.6025%	−2.4084%
	2026–2030	0.5224%	7.8874%	−5.8567%	−3.1025%	−2.6084%
	2031–2035	0.5174%	7.8924%	−6.0567%	−3.6025%	−2.8084%
High	2019–2020	0.3145%	7.8824%	−6.5153%	−3.7995%	−2.1667%
	2021–2025	0.5574%	8.1824%	−5.3567%	−2.3025%	−2.1084%
	2026–2030	0.5524%	8.1874%	−5.5567%	−2.8025%	−2.3084%
	2031–2035	0.5474%	8.1924%	−5.7567%	−3.3025%	−2.5084%

4.6. Scenario Building

Based on the impact of the high, medium, and low three rates of change in the four provinces and cities, five scenarios were constructed to carry out the five scenarios for 2020–2035 in each of the four provinces and cities. The results are shown in Table 9.

Low-carbon development scenario (M1): The rates of change between the indicators in this scenario are chosen to be low, exploring the impact of indicators on carbon emissions in a lower scenario. Energy efficiency scenario (M2): Only the resident population and GDP per capita are changed in the low-carbon development scenario, while the rest of the indicators remain unchanged. In the energy-saving scenario, the industrial structure has been optimized, energy consumption has decreased, and the proportion of the secondary

industry to GDP has decreased. Baseline scenario (M3): The median value of changes among the indicators is adopted, and the influence of the original policy intensity on carbon emissions is analyzed without adjustment. Ideal scenario (M4): The ideal scenario has an increase in the resident population, a significant increase in GDP per capita, minimum energy consumption between categories, and green and energy-efficient development. Free development scenario (M5): In this scenario, the variation between the indicators is the highest, and there is no influence from other factors, only from development.

Table 9. Peak carbon forecast scenarios for four provinces and cities, 2020–2035.

Scenarios	Permanent Population	GDP per Capita	Intensity of Energy Consumption	Energy Mix	Share of Secondary Sector in GDP
Low-carbon development scenario (M1)	low	low	low	low	low
Energy efficiency scenario (M2)	middle	middle	low	low	low
Baseline scenario (M3)	middle	middle	middle	middle	middle
Ideal scenario (M4)	middle	high	low	low	low
Freedom to develop scenario (M5)	high	high	high	high	high

4.7. Predictive Analyses

From (Figure 6): Beijing and Henan peaked in the 2000–2035 timeframe under the analysis of different scenarios, with Beijing peaking in 2010 and Henan peaking in 2011. Carbon emissions continued to decline in two regions, Beijing and Henan, over the next 2035 period. The Tianjin data indicated an upward trend in the 2000–2019 timeframe, with a downward trend in carbon emissions under the low-carbon development scenario model over the projection period. Hebei Province did not experience carbon peaking between 2020 and 2035, with an inflection point in 2030 under the low-carbon development model and an upward trend in carbon emissions under the remaining four models.

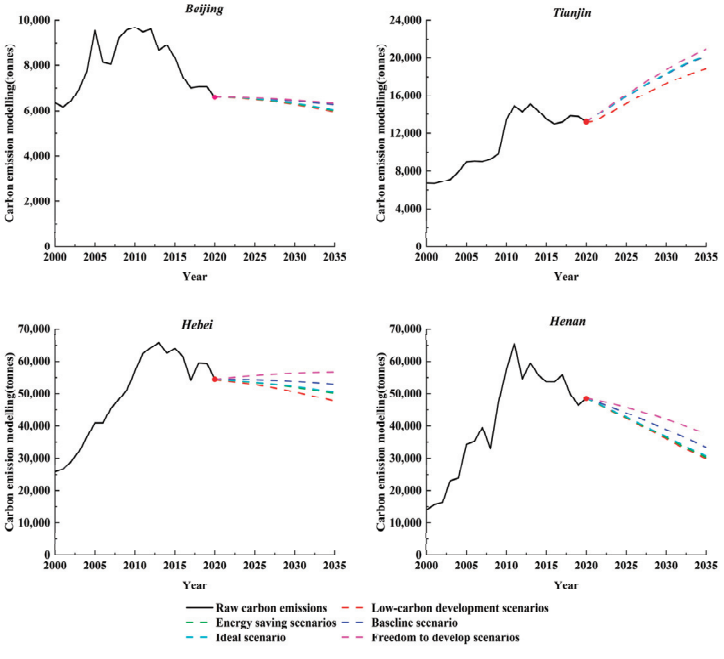

Figure 6. Carbon emission projections for four provinces and municipalities under various scenarios, 2020–2035 (10^4t).

5. Discussion

Wang Wenju et al. analyzed national and provincial governments' overall objectives and critical action plans to promote carbon peaking. They used the Mann–Kendall statistical trend test to examine each province's carbon emission peaking situation [30]. The study found that provincial governments have responded positively to the central government's request to formulate and actively implement action programs for carbon peaking. Beijing and Henan have taken the lead in achieving carbon peaking. Provinces have implemented exceptional government support and financial subsidies, effectively guiding low-carbon development, reducing carbon emissions, and thus achieving carbon peaks. Han Nan et al. constructed a carbon emission system dynamics model by analyzing the relationship between carbon emissions and influencing factors. They set up six scenarios to simulate and predict their impact on the time of carbon peaking in Beijing, Tianjin, and Hebei [31]. The results showed that under the baseline scenario, Beijing has already achieved peak carbon. Tianjin is expected to reach peak carbon by 2023, and Hebei is having difficulty reaching peak carbon by 2035. This is consistent with the findings of this paper.

Our study suggests that Hebei is less likely to reach peak carbon emissions in 2035. However, Beijing, Tianjin, and Henan could reach peak carbon emissions in the 2020–2030 timeframe. Beijing is actively promoting the construction of a green Beijing, deepening the implementation of the functional positioning of the capital city, and taking the lead in establishing the development concept of reduction. Tianjin actively promotes the development of a digital economy, the transformation and upgrading of traditional industries, and the gradual decline of carbon emissions. Henan vigorously promotes energy conservation and emission reduction, accelerates the establishment of a sound economic system of green, low-carbon, and recycling development, promotes the overall green and low-carbon economic and social transformation, and helps to achieve the goal of carbon peak and carbon neutrality. Hebei has formed a diversified pillar industry pattern featuring resource-consuming and polluting industries such as iron and steel, coal, chemicals, and equipment manufacturing. The increased CO_2 emissions from the excessive use of fossil energy sources, such as coal, have put enormous pressure on environmental protection. From the study of decoupling effects, the relationship between economic growth and carbon emissions in provinces and cities along the South-to-North Water Diversion Central Route Project has been generally improving in recent years, and a more desirable decoupling will be achieved in the future.

As of 22 July 2022, the water entering the central canal from the Taocha Canal Headwork of the first phase of the South-to-North Water Diversion Project exceeded 50 billion cubic meters, benefiting a population of more than 85 million. The annual volume of water transferred by the first phase of the Central Route Project has continued to climb from more than 2 billion cubic meters to 9 billion cubic meters. It demonstrates that the South-to-North Water Diversion Project continues to develop highly, providing high-quality water security for the provinces and cities along the route.

In order to reduce energy consumption and achieve carbon reduction goals in the South-to-North Water Diversion Project, consolidating the foundation of green and low-carbon management is fundamental. We should strengthen compliance management, continuously improve green development systems such as environmental protection, pollution control, energy and resource conservation, and efficient utilization, and low-carbon transformation, and guide the implementation of standards and requirements that are conducive to green development. We should also establish and improve a long-term mechanism for green development, actively explore the establishment of effective incentive and constraint mechanisms, promote innovation in green development management and institutional innovation, dynamically monitor energy consumption and carbon emissions, achieve monitoring, reporting, and verification of energy consumption and carbon emissions indicators, and provide decision-making support for green and low-carbon development. Provinces and municipalities along the route should formulate energy-saving and emission-reduction

policies suitable for their provinces according to local conditions to contribute to China's goal of achieving carbon peaking by 2030.

6. Conclusions

This study uses the STIRPAT model to investigate the carbon emissions of provinces and cities along the South-to-North Water Diversion Central Route Project. It also forecasts carbon emissions from 2020–2035 under different scenarios and analyses whether carbon can be peaked by 2035. The main conclusions are as follows:

(1) The four provinces and municipalities were mainly weakly decoupled in the 2000–2009 timeframe, gradually shifting to strong decoupling from 2010–2019. From the perspective of decoupling economic development from carbon emissions, a country or region usually goes through a process progressing from negative decoupling to weak or even strong decoupling. Moreover, the process is often tortuous. For example, recessionary decoupling and negative recessionary decoupling can occur under the influence of political, economic, and environmental factors.

(2) According to the parameters of the model formula for the four provinces and cities, it can be seen that the resident population and per capita GDP have a more significant impact on carbon emissions. Due to this, Beijing's resident population and per capita GDP can cause a change of 0.2561% and 0.1878% for every 1% change. Every 1% change in Tianjin's resident population and GDP per capita can cause a change of 1.0539% and 0.1522%.

(3) There will be carbon peaks in both Beijing and Henan in the 2000–2035 timeframe, with Beijing peaking at 96.836 million tons in 2010 and Henan peaking at 654.104 million tons in 2011. Mainly, the continued optimization of the industrial structure, promoting a clean energy transition, and implementing the Peak Carbon Implementation Program will achieve the Peak Carbon Goal on schedule.

(4) Among the four provinces and cities along the South-to-North Water Diversion Project, only Hebei did not reach its peak during the period under study, which is related to a large amount of energy consumption in Hebei, a traditional industrial province. The total energy consumption in Hebei Province is significant, and its structure is dominated by fossil energy. The proportions of coal consumption per capita and GDP energy consumption are higher than the national level, resulting in more significant carbon emissions.

Author Contributions: Q.M.: Supervision, Project administration, Funding acquisition, Resources. B.L.: Conceptualization, Data curation, Methodology, Software, Visualization, Formal analysis, Writing review & editing. Y.Z.: Writing original draft, Writing review & editing. H.Z.: Investigation, Resources, Writing original draft. Z.X.: Methodology, Validation, Investigation. Y.L.: Writing original draft, Methodology. Q.L.: Data curation, Visualization. All authors have read and agreed to the published version of the manuscript.

Funding: This work was supported by the National Natural Science Foundation of China (Project No.: 42371314), the Research Project of Henan Federation of Social Sciences in 2021 (Project No.: SKL-2021-3196), the Research Project of Humanities and Social Sciences in Colleges and Universities of Henan Province (Project No.: 2021-ZZJH-157), and the Philosophy and Social Science Program of Henan Province (Project No.: 2019CJJ078).

Data Availability Statement: The datasets used and/or analyzed during the current study are available from the corresponding author on reasonable request.

Conflicts of Interest: The authors declare no conflict of interest.

References

1. Hasselmann, K.; Barker, T. The Stern Review and the IPCC fourth assessment report: Implications for interaction between policymakers and climate experts. An editorial essay. *Clim. Chang.* **2008**, *89*, 219–229. [CrossRef]
2. Wang, J. The Establishment of International Emission Trading Mechanism under The Paris Agreement: Process, Challenge and its Implication for China. *Environ. Prot.* **2021**, *49*, 58–62.

3. Wang, C.; Zhang, Y. Implementation Pathway and Policy System of Carbon Neutrality Vision. *Chin. J. Environ. Manag.* **2020**, *12*, 58–64. [CrossRef]
4. Xie, H.; Ren, X.; Xie, Y.; Jiao, X. Development opportunities of the coal industry towards the goal of carbon neutrality. *J. China Coal Soc.* **2021**, *46*, 2197–2211.
5. Ang, H. China's Goal of Achieving Carbon Peak by 2030 and Its Main Approaches. *J. Beijing Univ. Technol. (Soc. Sci. Ed.)* **2021**, *21*, 1–15.
6. Zhao, L.; Zhao, T.; Yuan, R. Scenario simulations for the peak of provincial household CO_2 emissions in China based on the STIRPAT model. *Sci. Total Environ.* **2022**, *809*, 151098. [CrossRef]
7. Zhao, K.; Cui, X.; Zhou, Z.; Huang, P. Impact of uncertainty on regional carbon peak paths: An analysis based on carbon emissions accounting, modeling, and driving factors. *Environ. Sci. Pollut. Res.* **2022**, *29*, 17544–17560. [CrossRef]
8. Zhang, C.; Su, B.; Zhou, K.; Yang, S. Decomposition analysis of China's CO_2 emissions (2000–2016) and scenario analysis of its carbon intensity targets in 2020 and 2030. *Sci. Total Environ.* **2019**, *668*, 432–442. [CrossRef]
9. Fang, G.; Wang, L.; Gao, Z.; Chen, J.; Tian, L. How to advance China's carbon emission peak?—A comparative analysis of energy transition in China and the USA. *Env. Sci. Pollut. Res.* **2022**, *29*, 71487–71501. [CrossRef]
10. Hao, J.; Gao, F.; Fang, X.; Nong, X.; Zhang, Y.; Hong, F. Multi-factor decomposition and multi-scenario prediction decoupling analysis of China's carbon emission under dual carbon goal. *Sci. Total Environ.* **2022**, *841*, 156788. [CrossRef]
11. Chou, J.; Li, Y.; Xu, Y.; Zhao, W.; Li, J.; Hao, Y. Carbon dioxide emission characteristics and peak trend analysis of countries along the Belt and Road. *Environ. Sci. Pollut. Res.* **2023**, *30*, 81881–81895. [CrossRef]
12. Zou, C.; Xiong, B.; Xue, H.; Zheng, D.; Ge, Z.; Wang, Y.; Jiang, L.; Pan, S.; Wu, S. The role of new energy in carbon neutral. *Pet. Explor. Dev.* **2021**, *48*, 411–420. [CrossRef]
13. Wang, Y.; Wang, E.; Bi, Y. Impact of a peak in carbon emissions on China's economy in different situations: Analysis based on CGE model. *Resour. Sci.* **2017**, *39*, 1896–1908.
14. Zhao, R.; Huang, X.; Yun, W.; Wu, k.; Chen, Y.; Wang, S.; Lu, H.; Fang, k.; Li, Y. Key issues in natural resource management under carbon emission peak and carbon neutrality targets. *J. Nat. Resour.* **2022**, *37*, 1123–1136. [CrossRef]
15. Lu, Q.; Lv, T.; Wang, S.; Wei, L. Spatiotemporal Variation and Development Stage of CO_2 Emissions of Urban Agglomerations in the Yangtze River Economic Belt, China. *Land* **2023**, *12*, 1678. [CrossRef]
16. Zhou, J.; Jin, B.; Du, S.; Zhang, P. Scenario Analysis of Carbon Emissions of Beijing-Tianjin-Hebei. *Energies* **2018**, *11*, 1489. [CrossRef]
17. Wang, J.; Qin, L.; Chu, H. Evaluation of Carbon Emission and Carbon Contribution Capacity Based on the Beijing–Tianjin–Hebei Region of China. *Sustainability* **2023**, *15*, 5824. [CrossRef]
18. Liu, Z.; Wang, M.; Wu, L. Countermeasures of Double Carbon Targets in Beijing–Tianjin–Hebei Region by Using Grey Model. *Axioms* **2022**, *11*, 215. [CrossRef]
19. Huang, Y.; Liu, J.; Shi, M. Analysis of influencing factors and prediction of carbon emissions of typical urban agglomerations in China: A case study of Beijing-Tianjin-Hebei region. *Environ. Sci. Pollut. Res.* **2023**, *30*, 52658–52678. [CrossRef] [PubMed]
20. Wang, R.; Xing, J. Study on Decoupling Relationship Between Economic Growth and Dioxide Emissions: Based on the Tapio Decoupling Model. *J. Xi'an Univ. Financ. Econ.* **2013**, *26*, 48–52.
21. Wang, Z.; Li, F.; Xie, Z.; Li, Q.; Zhang, Y.; Dai, M. Decoupling CO_2 Emissions from Economic Growth in China's Cities from 2000 to 2020: A Case Study of the Pearl River Delta Agglomeration. *Land* **2023**, *12*, 1804. [CrossRef]
22. Zhu, S.; Sun, H.; Xia, X.; Yang, Z. Decoupling Analysis of Carbon Emissions and Forest Area in China from 2004 to 2020. *Land* **2023**, *12*, 1458. [CrossRef]
23. Liang, Y.; Cai, W.; Ma, M. Carbon dioxide intensity and income level in the Chinese megacities' residential building sector: Decomposition and decoupling analyses. *Sci. Total Environ.* **2019**, *677*, 315–327. [CrossRef] [PubMed]
24. Yao, M.; Wang, M.; Lei, Y. Research on Shanghai Carbon Peak Forecast Based on STIRPAT Model. *J. Fudan Univ. (Nat. Sci.)* **2023**, *62*, 226–237.
25. Xing, J.; Cheng, Y.; Yao, H. Analysis of Economic Growth and Energy Consumption in Qinghai Province Based on IPAT Model. *Econ. Outlook Bohai Sea* **2020**, *5*, 90–91.
26. Guan, Y.; Shan, Y.; Huang, Q.; Chen, H.; Wang, D.; Hubacek, K. Assessment to China's recent emission pattern shifts. *Earth's Future* **2021**, *9*, e2021EF002241. [CrossRef]
27. Shan, Y.; Liu, J.; Liu, Z.; Xu, X.; Shao, S.; Wang, P.; Guan, D. New provincial CO_2 emission inventories in China based on apparent energy consumption data and updated emission factors. *Appl. Energy* **2016**, *184*, 742–750. [CrossRef]
28. Shan, Y.; Guan, D.; Zheng, H.; Ou, J.; Li, Y.; Meng, J.; Mi, Z.; Liu, Z.; Zhang, Q. China CO_2 emission accounts 1997–2015. *Sci. Data* **2018**, *5*, 170201. [CrossRef]
29. Shan, Y.; Huang, Q.; Guan, D.; Hubacek, K. China CO_2 emission accounts 2016–2017. *Sci. Data* **2020**, *7*, 54. [CrossRef]
30. Wang, W.; Kong, X. Provincial targets, policy tools and path selection for China's carbon peak by 2030. *Social Sci. Front* **2022**, *11*, 78–88.
31. Han, N.; Luo, X. Carbon emission peak prediction and reduction potential in Beijing-Tianjin-Hebei region from the perspective of multiple scenarios. *J. Nat. Resour.* **2022**, *37*, 1277–1288. [CrossRef]

land

MDPI

Article

Spatiotemporal Variation of Per Capita Carbon Emissions and Carbon Compensation Zoning in Chinese Counties

Juan Chen, Sensen Wu * and Laifu Zhang

School of Earth Sciences, Zhejiang University, 866 Yuhangtang Rd., Hangzhou 310058, China; 22038034@zju.edu.cn (J.C.); giserfu@zju.edu.cn (L.Z.)
* Correspondence: wusensengis@zju.edu.cn

Abstract: The per capita carbon balance and carbon compensation zoning of Chinese counties from the perspective of major function-oriented zones is important for realizing the carbon peaking and carbon neutral target. In this study, the Kernel-K-means++ algorithm is used and a more comprehensive per capita carbon compensation zoning model is constructed. Based on this, combined with the major function-oriented zones, Chinese counties are divided into per capita carbon compensation-type zones. Further, spatial and temporal characteristics are detected, and suggestions for optimizing low-carbon development are put forward. The main results are as follows: (1) From 2000 to 2017, the per capita carbon emissions (PCO_2) of Chinese counties were large and showed a trend of stable expansion and a southeast–northwest pattern; (2) the per capita carbon emissions of key development zones accounted for the largest proportion of emissions; (3) there were 1410 payment zones, 170 balanced zones, and 242 compensated zones among China's counties; and (4) 11 types of carbon compensation space optimization zones were finally formed, and low-carbon development directions and strategies were proposed for each type of area. Based on this, this study promotes regional carbon emissions management and reduction in China and provides a reference for other regions to reduce emissions.

Keywords: carbon emission; carbon compensation zoning; Chinese counties; space optimization; major function-oriented zoning

Citation: Chen, J.; Wu, S.; Zhang, L. Spatiotemporal Variation of Per Capita Carbon Emissions and Carbon Compensation Zoning in Chinese Counties. *Land* **2023**, *12*, 1796. https://doi.org/10.3390/land12091796

Academic Editors: Jinyan Zhan, Chao Wang and Xueting Zeng

Received: 15 August 2023
Revised: 6 September 2023
Accepted: 13 September 2023
Published: 16 September 2023

1. Introduction

With the problem of global warming becoming more and more serious, the amount of attention being paid to carbon emissions is gradually increasing. As the basic spatial unit of the population and economic activities and the basic local administrative unit in China, counties are also the basic spatial unit of carbon emissions, and carbon emissions pressures coexist with reduction potential. Carbon compensation is an important measure to achieve CO_2 offsetting of emissions from carbon sources through emissions reduction and other measures in order to achieve a regional carbon balance and thus promote overall national emissions reduction and sustainable development. For extensive study areas, zoning is an effective means of controlling carbon emissions. Categorizing regions with similar carbon emissions and background conditions facilitates localized and centralized management and achieves emissions reduction more efficiently. The study of regional differences in per capita carbon emissions (PCO_2), spatial and temporal patterns, and per capita carbon compensation zoning at the county level in China is crucial to the realization of the carbon peaking and carbon neutral target, the implementation of policies related to carbon control and emissions reduction, and the planning of low-carbon development in counties.

At present, carbon emissions research is a popular research topic in geography, ecology, environmental science, and other disciplines, which is mainly divided into carbon emissions simulation and prediction [1,2], spatial and temporal differentiation characteristics [3,4], driving factors [5,6], and so on. Although the results of carbon emissions simulation in

the existing research differ, the trend of change is relatively consistent, and the relevant research points out that global carbon emissions have shown an upward trend in most previous years. However, there have been decreases or fluctuations in the recent period [7]. The factors driving carbon emissions vary across sectors—for example, in China, carbon emissions from the power sector are mainly driven by economic growth, whereas the effect of technological progress makes a significant contribution to the carbon intensity of the industrial sector [8], and it is important to note that the driving mechanisms of these various factors are changing dynamically over time [9]. In addition, in terms of spatial and temporal carbon emissions variations, existing studies mostly focused on the analysis of spatial aggregation characteristics, patterns, and evolution [10–15]. There are two basic types of such studies, and the first type involves using the boundaries of the administrative region [16], watershed [17], or LUCC [18,19] as the unit to detect the characteristics of the spatial and temporal variations of carbon emissions. There are also studies on the spatialization of carbon emissions statistics by combining nighttime light remote sensing data and other data to detect the spatial and temporal variability of carbon emissions at the raster scale [20,21], and some studies have also combined the two types of data [22,23]. Among them, the study of the spatialization of carbon emissions using nighttime light data is becoming more and more popular. Due to the existence of spatial and temporal variation in carbon emissions, carbon balance has become the focus of carbon emissions reduction research in various regions, and one of the important means of regulating carbon balance is carbon compensation [24].

In terms of carbon compensation, in-depth discussions have been conducted mainly around carbon compensation zoning [24–27], carbon compensation mechanisms [28,29], carbon compensation influencing factors [30], and carbon compensation in different industries, fields, and sectors. The different fields can be divided into forest carbon compensation [31], agricultural carbon compensation [28,29], and ecosystem compensation [32]. Carbon compensation zoning is one of the main focuses of research in the field of carbon compensation at this stage, and it is also a prerequisite and foundation for the implementation of a regional carbon compensation system [27]. With carbon compensation zoning, it is important to implement carbon compensation techniques and carbon compensation policies in terms of empirical evidence. The current zoning research is mainly based on the carbon compensation rate (carbon absorption/carbon emissions) [33], and the zoning evaluation system is established with the carbon compensation rate, the carbon emissions economic contribution coefficient, and the carbon emissions ecological carrying coefficient, and the existing methods to achieve carbon compensation zoning are mainly SOM [34], the SOM-K-means model [24,27], and the three-dimensional magic method [25,35]. In general, the existing carbon compensation studies have two limits: Firstly, the research on regional carbon compensation and compensation zoning is at the exploratory stage, mainly limited to particular fields; secondly, the existing studies focus on compensation zoning based on carbon balance accounting, the economic contribution rate of carbon emissions, the ecological role of the carbon sink, land use, and major functional zones and fail to consider additional factors such as the regional per capita carbon compensation rate and residents' economic and energy consumption level; and thirdly, existing studies do not effectively integrate macroscopic patterns and detailed features, i.e., there is a lack of studies with both large-scale study areas and smaller categorical units (counties).

In this study, based on carbon emissions and carbon sequestration and population–economic statistical data, spatial statistical analysis is used to characterize the spatial and temporal variability of PCO_2 in Chinese counties. The Normalized Revealed Comparative Advantage (NRCA) index is used to quantify data on four dimensions, namely, natural, economic, ecological, and energy attributes, and form comprehensive evaluation indexes of per capita carbon compensation zoning in Chinese counties based on the Kernel-K-means++ algorithm to construct a per capita carbon compensation zoning model of Chinese counties, and the zoning model is used for cluster analysis. Finally, optimization recommendations for low-carbon development in each county are provided based on the zoning results.

2. Materials and Methods

2.1. Study Area

China is located in the eastern part of Asia and on the western coast of the Pacific Ocean, with a total land area of about 9.6 million km^2, ranking third in the world. China has experienced rapid economic growth and large-scale carbon emissions in recent years. However, it has also been subject to a variety of climate, environmental, ecological, urban heat island, and other issues. Therefore, emissions reduction is urgent in order to achieve the carbon peaking and carbon neutral target and to alleviate these conditions. Meanwhile, China's vast area, carbon emissions, and its various types of impact on spatial diversity represent significant challenges. The estimation of China as a research area, exploring carbon compensation zoning methodologies and the optimization of policies, provides strong representative data (Figure 1). Further, considering the accessibility of statistical data, the county level was selected to carry out the research.

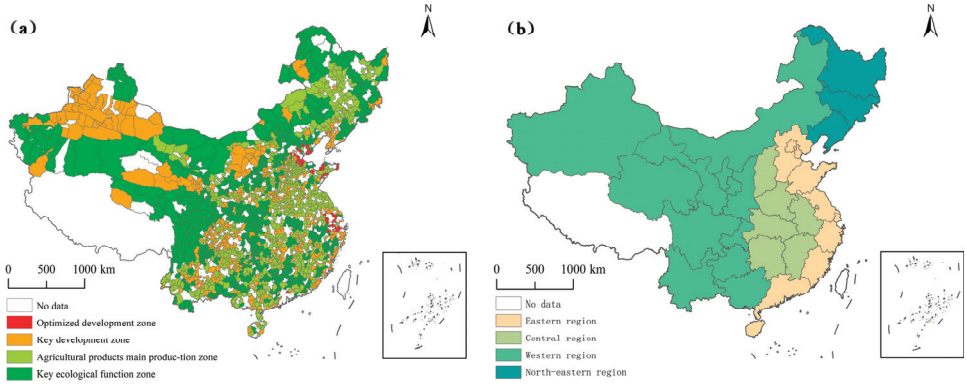

Figure 1. (**a**) shows the study area and the type of main functional area, and (**b**) shows the geographic zoning map of China.

2.2. Data

In this study, based on the feasibility and completeness of the data acquisition, 1822 counties and districts in China were selected as study areas, excluding data from the Tibet Autonomous Region, Taiwan Province, Hong Kong, and the Macao Special Administrative Region, and the study period was 2000–2017. The data used included 2000–2017 China county-level carbon emissions and carbon sequestration data, county-level population data, county-level GDP data, county-level GDP coal consumption data, etc.; 2000–2017 China county-level carbon emissions and sequestration data from the China Carbon Accounting Database (CEADs) (https://www.ceads.net.cn/data/county/, accessed on 15 May 2023), with strong data time series continuity and a uniform calculation caliber; and 2000–2017 China county-level population, GDP, coal consumption, etc., sourced from various official statistical yearbooks, such as the China County Statistical Yearbook and the China Energy Statistical Yearbook (Table 1).

Table 1. Overview of county statistics and sources.

Descriptions	Factors	Years	Sources
Carbon emissions scale indicator	Carbon emissions	2000–2017	CEADs
Carbon sequestration scale indicators	Amount of solid carbon	2000–2017	

Table 1. *Cont.*

Descriptions	Factors	Years	Sources
Population indicators	Population	2001–2018 [1]	China County Statistical Yearbook
Socio-economic indicators	Regional GDP	2001–2018 [1]	
Energy consumption indicators	Regional GDP coal consumption	2001–2018 [1]	
Main functional zone type	Optimized development zone, key development zone, main production zone of agricultural products, key ecological functional zone	\	Government documents on main functional zoning in provinces and cities

[1] The yearbook covers up to the previous year's data. The year of the data is omitted from Table 1 because the official main functional area planning documents were issued at different times in each province and city.

2.3. Methods

In this section, the research process and methodology are presented. The research process of this study is illustrated in Figure 2.

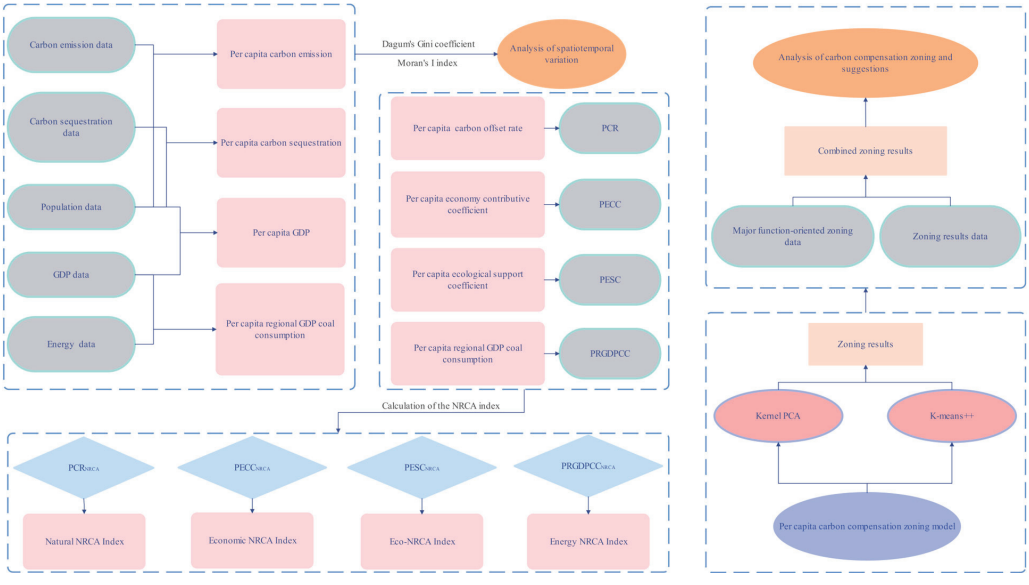

Figure 2. Study process. The gray shapes in Figure 2 represent the data, pale pink shapes represent the interpretation of the data, and light blue shapes represent the NRCA index. While purple shapes represent the model, dark pink shapes represent the algorithms that make up the model, skin tone shapes represent the partitioning results, and orange represents further analysis.

2.3.1. Dagum Gini Coefficient

Dagum [36] decomposed the overall variation into three components of intra-group variation, inter-group variation, and net inter-group variation, and inter-group hypervariable density based on the Gini coefficient was used to effectively address the source of measuring regional variation. In this study, the Dagum Gini coefficient was used as a measure of regional differences in PCO_2 across 1822 county-level units in China, calculated using Equation (1):

$$G_{jh} = \frac{\sum_{i=1}^{nj} \sum_{r=1}^{nh} \left| y_{ji} - y_{hr} \right|}{n_j n_h \left(\overline{y}_j + \overline{y}_h \right)} \quad (1)$$

where j and h are the numbers of two regions; n_j and n_h are the number of county units in j and h, respectively; y_{ji} and y_{hr} are the PCO_2 of the i-th county unit in j and the r-th county unit in h, respectively; and $\overline{y}_j$ and $\overline{y}_h$ represent the average value of PCO_2 of all county units in the corresponding regions.

The Dagum Gini coefficient can be specifically decomposed into three components: the contribution of the within-group Gini coefficient to the overall Gini coefficient G_W, the contribution of the net difference between groups to the overall Gini coefficient G_{nb}, and the contribution of the hypervariable density G_t. The relationship between the three components satisfies $G = G_w + G_{nb} + G_t$, and it is calculated via Equations (2)–(5):

$$G = \sum_{j=1}^{k} G_{jj} P_j S_j + \sum_{j=1}^{k} \sum_{h \neq j} G_{jh} P_j S_h D_{jh} + \sum_{j=1}^{k} \sum_{h \neq j} G_{jh} P_j S_h \left(1 - D_{jh}\right) \quad (2)$$

$$G_w = \sum_{j=1}^{k} G_{jj} P_j S_j \quad (3)$$

$$G_{nb} = \sum_{j=1}^{k} \sum_{h \neq j} G_{jh} P_j S_h D_{jh} \quad (4)$$

$$G_t = \sum_{j=1}^{k} \sum_{h \neq j} G_{jh} P_j S_h (1 - D_{jh}) \quad (5)$$

where $P_j = {}^{n_j}/_{n}$ represents the ratio of carbon emissions per capita of county units within j to the overall carbon emissions per capita of county units n, and $S_h = {}^{n_h \overline{y}_h}/_{n \overline{y}}$ represents the ratio of carbon emissions per capita of county units within h to the overall carbon emissions per capita of county units n.

2.3.2. Moran's I Index

The global Moran's I index is usually used to describe the average degree of association of a spatial unit with its surrounding area over the entire region, and it is calculated via Equation (6):

$$I = \frac{n \sum_{i=1}^{n} \sum_{j \neq i}^{n} W_{ij} \left(X_i - \overline{X}\right) \left(X_j - \overline{X}\right)}{\sum_{i=1}^{n} \sum_{j \neq i}^{n} W_{ij} \sum_{i=1}^{n} \left(X_i - \overline{X}\right)^2} \quad (6)$$

where n is the number of sample counties; X_i and X_j are the per capita carbon emissions of counties i and j, respectively; $\overline{X}$ is the mean value of the per capita carbon emissions; and W_{ij} is the spatial weight matrix (1 if adjacent, 0 if not adjacent). At the given significance level, a positive Moran's I value represents spatial agglomeration (passing the significance test); a negative Moran's I value represents spatial divergence (passing the significance test).

2.3.3. Normalized Revealed Comparative Advantage Index

The NRCA index is primarily an indicator of product competitiveness, obtained by Yu et al. [37] by improving the Revealed Comparative Advantage (RCA) index constructed by Balassa [38], which was used in this study to discriminate the dominant attributes of the per capita carbon compensation zoning in Chinese counties. It is calculated using Equation (7):

$$NRCA_j^i = x_j^i / x - x_j x^i / x x \quad (7)$$

where X_j^i denotes the index value of attribute j of county unit i, X_j denotes the total index value of attribute j of all county units, X^i denotes the total index value of all attributes of county unit i, and X denotes the total index value of all county units and attributes. If $NRCA_j^i > 0$, it means that the county-level unit has a comparative advantage in this attribute; otherwise, it means that the county-level unit does not have a comparative advantage in this attribute.

2.3.4. Comprehensive Evaluation Index of Per Capita Carbon Compensation Zoning

Existing studies point out that the carbon cycle process at the county scale has obvious natural–social binary cycle characteristics [39] and its carbon balance has both natural

and social attributes [40]. Based on the regional binary carbon balance theory [40] and existing studies [24,27], comprehensive evaluation indicators for per capita carbon compensation zones were constructed based on four perspectives: the natural background, socio-economic factors, the ecological environment, and energy consumption construction, and the construction process diagram is shown in Figure 3.

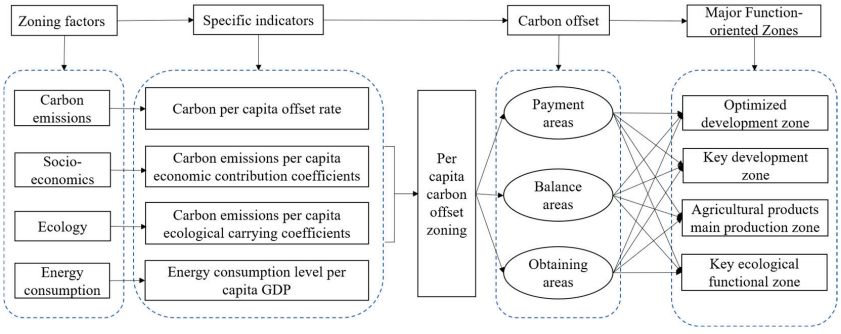

Figure 3. The process of dividing carbon compensation zones.

The per capita carbon compensation rate was used as an indicator of the natural background attributes; the per capita economic contribution coefficient of carbon emissions, calculated based on the GDP, population, and carbon emissions data of the selected regions, was used as an indicator of socio-economic attributes; the per capita ecological support coefficient of carbon emissions calculated based on the selected carbon emissions data and carbon sequestration data was used as an indicator of socio-ecological attributes; and the per capita regional GDP energy consumption level (per capita regional GDP coal consumption), calculated based on selected regional GDP coal consumption and population data, was used as an energy consumption attribute. The mechanism of per capita carbon compensation zoning in Chinese counties was investigated from four perspectives: natural background attributes, socio-economic attributes, ecological and environmental attributes, and energy consumption attributes. The above indicators are shown in Table 2 and Equations (8)–(11).

Table 2. County data on per capita carbon compensation zoning variables.

Descriptions	Factors	Years	Sources
Natural background attribute indicators	Per capita carbon compensation rate (PCR)	2000–2017	Per capita carbon sequestration/per capita carbon emission
Socio-economic attribute indicators	Per capita economic contribution coefficient of carbon emissions (PECC)	2000–2017	(Per capita GDP/per capita total GDP)/(per capita carbon emissions/per capita total carbon emissions)
Socio-ecological attribute indicators	Per capita ecological support coefficient of carbon emissions (PESC)	2000–2017	(Per capita carbon sequestration/per capita total carbon sequestration)/(per capita carbon emissions/per capita total carbon emissions)
Energy consumption attribute indicators	Per capita regional GDP coal consumption (PRGDPCC)	2000–2017	Regional GDP coal consumption/population

The county PCR for China was selected as an indicator reflecting the scale attributes of per capita carbon compensation, PECC was selected as an indicator of the socio-economic

attributes of per capita carbon compensation, PESC was selected as an indicator of the ecological and environmental attributes of per capita carbon compensation, and PRGDPCC was selected as an indicator of the energy consumption attributes of per capita carbon compensation partition. The PCR is calculated using Equation (8):

$$PCR = \frac{PCA_i}{PC_i},\ i = 1, 2, \ldots, n \tag{8}$$

where PCA_i is the per capita carbon sequestration of the i-th county unit, and PC_i is the per capita carbon emissions of the i-th county unit. As shown in Equation (8), the PCR index only considers the relationship between per capita carbon sequestration and per capita carbon emissions in a county itself.

Based on the carbon emissions ecological carrying coefficient and carbon emissions ecological carrying factor proposed by Lu et al. [41], in this study, the per capita carbon emissions economic contribution coefficient (PECC) and per capita carbon emissions ecological carrying coefficient (PESC) are proposed. PECC indicates the socio-economic attributes of per capita carbon compensation and is used to reflect the socio-economic benefits of per capita carbon compensation in the county, and it is calculated via Equation (9):

$$PECC = \frac{PG_i}{PG} / \frac{PC_i}{PC} \tag{9}$$

where PG_i and PG are the GDP per capita of the i-th county unit and the total per capita GDP of 1822 county units, respectively; PC_i and PC are the carbon emissions per capita of the i-th county unit and the total per capita carbon emissions of 1822 county units, respectively.

PESC denotes the eco-environmental attributes of per capita carbon compensation, used to reflect the eco-environmental benefits of per capita carbon compensation in the county, and it is calculated via Equation (10):

$$PESC = \frac{PCA_i}{PCA} / \frac{PC_i}{PC} \tag{10}$$

where PCA_i and PCA are the per capita carbon sequestration of each county unit and the total per capita carbon sequestration of 1822 county units, respectively, and PC_i and PC are the per capita carbon emissions of each county unit and the total per capita carbon emissions of 1822 county units, respectively. As shown in Equation (10), the PESC index takes the correlation between counties into account.

PRGDPCC is used to indicate the level of energy consumption of the residential economy to represent the energy consumption attribute of per capita carbon compensation, and it is calculated via Equation (11):

$$\mathrm{PRGDPCC} = \frac{\mathrm{RGDPCC}_i}{\mathrm{Pop}_i}, i = 1, 2, \ldots, n \tag{11}$$

where $\mathrm{PRGDPCC}_i$ is the level of economic energy consumption of residents in the i-th county unit, Pop_i is the population in the i-th county unit, and there are n county units in total. This index represents the per capita economic energy consumption level of the region.

Based on the natural background attributes, socio-economic attributes, ecological environment attributes, and energy consumption attributes of the per capita carbon compensation in counties, the NRCA index of each attribute was calculated to set the evaluation index of per capita carbon compensation zoning. Considering the four factors of nature, economy, ecology and energy, four comprehensive evaluation indicators for per capita carbon offset zoning were established (Table 3). Regarding the per capita carbon compensation division scheme, the study area was divided into three types: paying, balancing, and receiving [27]. Among them, the payment zone was defined as the area that needs to be compensated by economic or non-economic means in the per capita carbon compensation behavior, the equilibrium area was defined as the area that does not need to pay and receive

compensation in the per capita carbon compensation behavior, and the compensated zone was defined as the area that receives economic or non-economic compensation in the per capita carbon compensation behavior.

Table 3. Comprehensive evaluation index of counties for per capita carbon compensation zoning.

Descriptions	Factors	Years	Interpretation
Natural background property indicators	Natural NRCA index ($NRCA_{PCR}$)	2000–2017	NRCA index of carbon compensation rate per capita for each county unit
Socio-economic attribute indicators	Economic NRCA index ($NRCA_{PECC}$)	2000–2017	NRCA index of economic contribution factor of carbon emissions per capita
Ecological attribute indicators	Ecological NRCA index ($NRCA_{PESC}$)	2000–2017	NRCA index of ecological carrying factor of carbon emissions per capita
Energy consumption attribute indicators	Energy NRCA index ($NRCA_{PRGDPCC}$)	2000–2017	NRCA index of energy consumption levels per capita regional GDP

2.3.5. Per Capita Carbon Compensation Zoning Model Based on Kernel-K-means++ Algorithm

The architecture and implementation strategy of the per capita carbon compensation zoning model designed in this study is shown in Figure 4. A four-dimensional framework of per capita carbon compensation zoning was constructed based on four perspectives, namely, the natural background, socio-economic factors, the ecological environment, and energy consumption (Figure 4), and four indicators, namely, the per capita carbon compensation rate, the per capita carbon emissions economic contribution coefficient, the per capita carbon emissions ecological carrying capacity coefficient, and the per capita economic energy consumption level, to calculate the NRCA index according to the theoretical framework; the NRCA index of four aspects was calculated using Equation (7); and comprehensive evaluation indicators for per capita carbon compensation zoning in Chinese counties were formulated. The dataset was normalized and feature extraction and dimensionality reduction were performed via Kernel PCA; then, the data were clustered using the K-means++ algorithm, and thus, the clustering results were acquired. The specific steps are as follows:

- Step 1: normalizing the raw data so that different features take the same range of values;
- Step 2: using the Kernel PCA method to map the data into the high-dimensional space, selecting the appropriate kernel function, and performing parameter adjustment and experimental verification to obtain better mapping results;
- Step 3: using the K-means++ algorithm to cluster the mapped data, selecting the appropriate number of clusters, and performing experimental verification and adjustment to obtain better clustering results;
- Step 4: analyzing and interpreting the clustering results to gain a deeper understanding of the data.

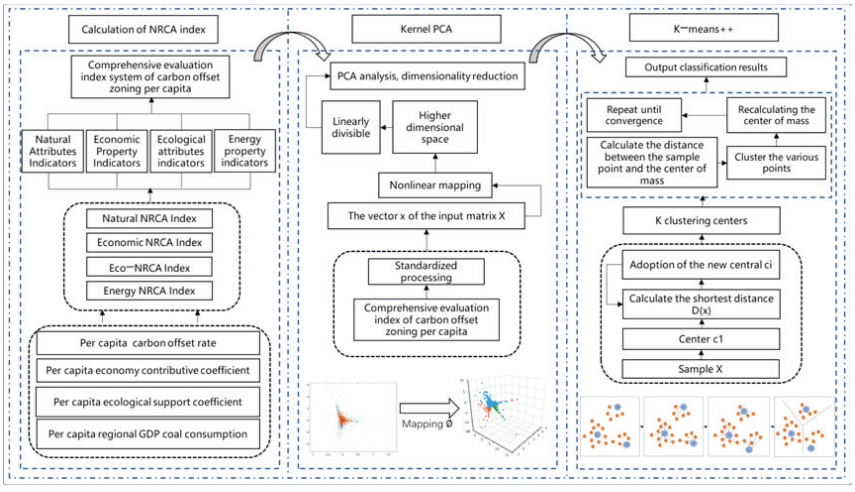

Figure 4. Per capita carbon compensation zoning model structure. In the Kernel PCA section, a two-dimensional map is turned into a three-dimensional map by mapping. The three different colored dots in the map represent different aspects of data, such as economic, ecological, and energy aspects. In the K-means++ section, the blue dots in the small figure represent the center and the orange dots represent the individuals waiting to be clustered.

3. Results

3.1. Analysis of Regional Differences in Carbon Emissions Per Capita in Counties in China

3.1.1. General Differences in PCO_2 in China's Counties

During the study period, the overall Dagum Gini coefficient showed an overall upward trend from 0.48 in 2000 to 0.51 in 2017, although it decreased in 2002 and 2003, indicating a gradual widening of the overall gap in carbon emissions per capita in China's counties (Figure 5).

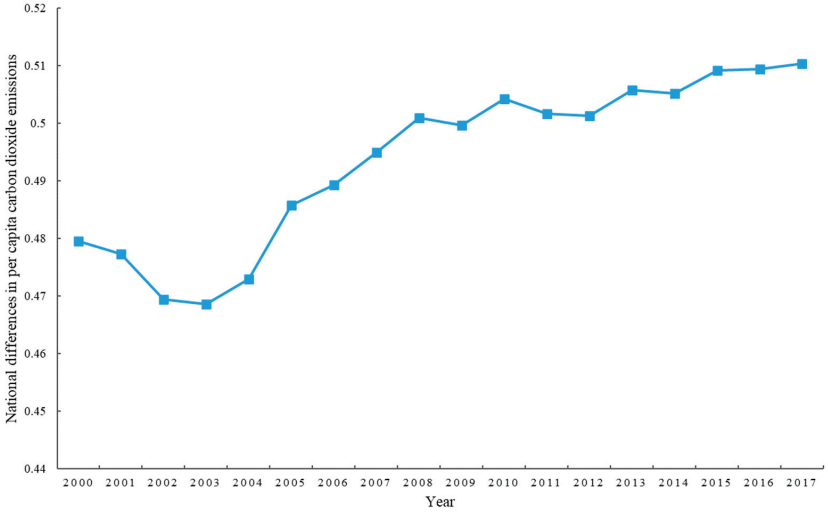

Figure 5. Trends in the general variation of per capita carbon emissions in China's counties (2000–2017).

3.1.2. Spatial Differences in Per Capita Carbon Emissions in China's Counties

According to the geographic zoning map of China (Figure 1b), county PCO_2 was statistically analyzed in the eastern, central, western, and northeastern parts of China.

(1) Intra-economic regional differences. The evolutionary trends of the differences in PCO_2 among the four major economic regions in China's counties from 2000 to 2017 were plotted (Figure 6). First, in terms of the size of the differences, the mean values of the Dagum Gini coefficients of the eastern, central, western, and northeastern regions of the four major economic regions from 2000 to 2017 were 0.423, 0.371, 0.413, and 0.47, respectively, indicating that the difference in PCO_2 was the largest in the northeastern region and the smallest in the central region. In addition, the Dagum Gini coefficients of the central, western, and northeastern regions as a whole showed different degrees of decline, unlike the eastern region, which showed an overall increasing trend. The main changes in Gini coefficients of carbon emissions differences per capita in the region were characterized as follows: (1) That of the eastern region increased abruptly to 0.614 in 2010, (2) that of the central region increased abruptly to 0.6 in 2007 and shrank sharply to 0.265 in 2010, (3) that of the western region fluctuated from 2000 to 2003 and shrank sharply to 0.341 in 2008, (4) and that of the northeastern region fluctuated from 2000 to 2003 and then declined overall.

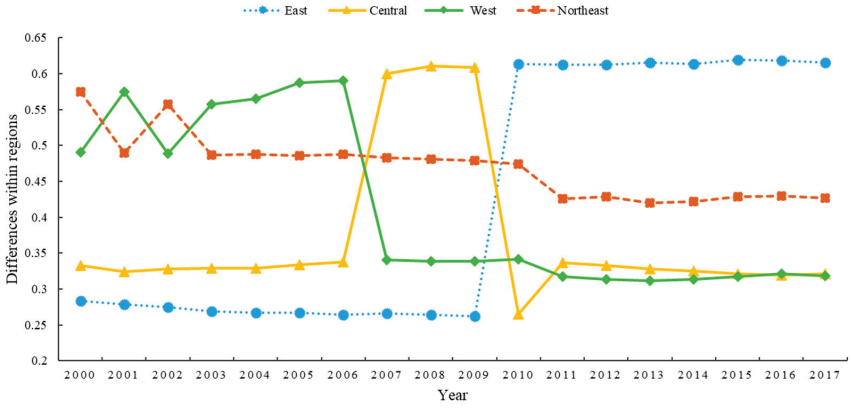

Figure 6. Trends in intra-economic regional variation of carbon emissions per capita by county in China (2000–2017).

(2) Differences between economic regions. Trends in PCO_2 in China's counties during the period of 2000–2017 were plotted for differences between economic regions (Figure 7). In terms of the size of the differences, the order of the differences in carbon emissions per capita between economic regions from 2000 to 2017, from largest to smallest, was east–northeast (0.491), east–west (0.459), west–northeast (0.455), central–northeast (0.451), east–central (0.428), and central–west (0.412). Among them, the differences in PCO_2 between east and central, east and west, and east and northeast showed an overall increasing trend. In 2007, the difference in PCO_2 between east and central expanded sharply and then showed a slowly increasing trend.

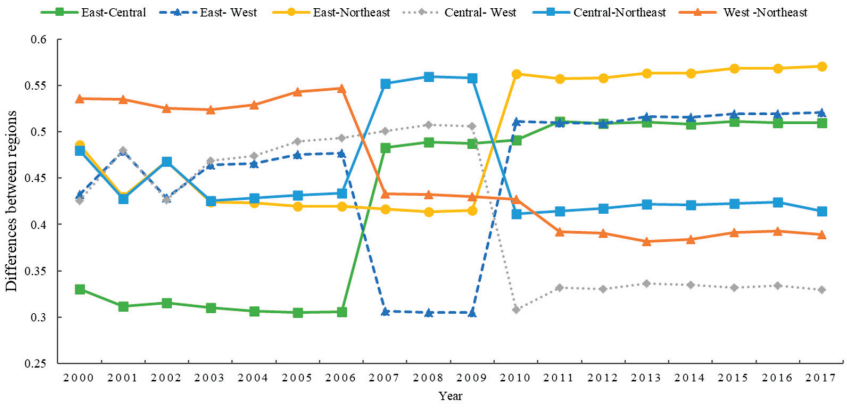

Figure 7. Trends in the variation in carbon emissions per capita among economic regional groups in counties of China (2000–2017).

3.1.3. Sources and Contributions of Differences in PCO_2 by Economic Region in China

Trends in the sources and contributions to differences in PCO_2 across economic regions in China's counties over the period of 2000–2017 were plotted (Figure 8). The mean values of the contribution within each economic region, the contribution between each economic region, and the contribution of hypervariable density were 32.256%, 16.180%, and 51.564%, respectively, indicating that the sources leading to the variation of PCO_2 in Chinese counties included hypervariable density (which accounted for about half of the overall variation), variation within each economic region, and variation between each economic region, in that order.

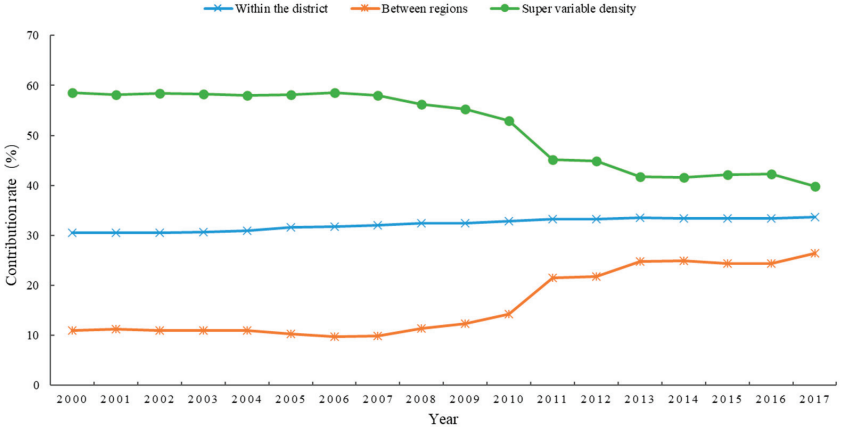

Figure 8. Sources and contributions of differences in PCO_2 by economic regions in counties of China (2000–2017).

In addition, different sources of variation in PCO_2 in China's counties showed different trends that can be derived from Figure 8. Among them, the variance within each economic region and the variance between each economic region showed a stable and increasing trend, whereas the super-variance density showed a more significant decreasing trend, from 58.542% in 2000 to 39.845% in 2017, which is a significant decrease but was located in the main contribution position.

3.2. Spatial and Temporal Patterns of PCO_2 in Chinese Counties

3.2.1. Spatial and Temporal Pattern of Carbon Emissions Per Capita in China's Counties

According to Figure 9, the spatial distribution of per capita carbon emissions in Chinese counties was generally characterized by a high level in the northwest and a low level in the southeast, with high-value counties and regions being more common in the northwest and low-value regions being more common in the southeast. The distribution of per capita carbon emissions in counties was concentrated and clearly differentiated, roughly opposite to the spatial distribution of the Hu Huanyong line (the line of population density comparison) [42]. The counties in northwest China were the areas with high per capita carbon emissions, and this phenomenon became bigger and bigger with time, which may have been caused by many factors. These regions belong to the northwestern half of the Hu Huanyong line and are sparsely populated, with traditional production methods, more carbon sources, and smaller populations, leading to relatively high per capita carbon emissions. The southeast region had low per capita carbon emissions, and its high level of economic development, large population, and well-developed tertiary industry may have led to lower per capita carbon emissions. Over the course of time, per capita carbon emissions in most counties in China showed an increasing trend, especially in some counties in the northwestern region, where per capita carbon emissions increased over time, and the number of high-value counties rose significantly in 2017. This may have been due to the increasing level of China's economic development and the intensity of spatial development of the country's territory over time, leading to increasing natural and anthropogenic carbon sources and increasing per capita carbon emissions.

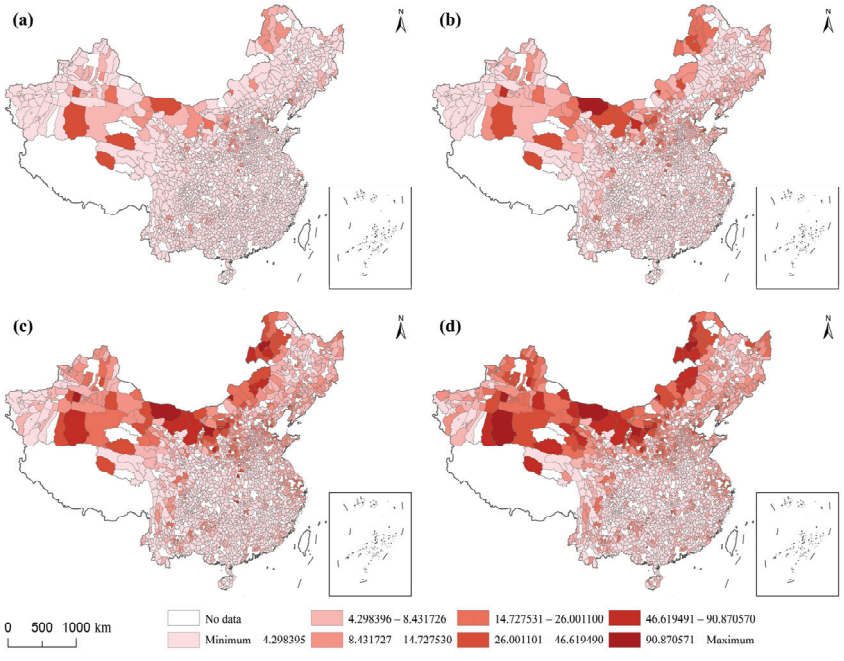

Figure 9. Spatial distribution of carbon emissions per capita in counties in China (unit t): (**a**) 2000; (**b**) 2005; (**c**) 2010; (**d**) 2017.

Looking at the per capita carbon emissions of each main functional area, key development zones ranked third in number but first in per capita carbon emissions, whereas optimized development zones reached a per capita carbon emissions share of about 5% in the period of 2000–2017, with 48 county-level units. Key development zones bore heavy

responsibility for population absorption, economic development, and industrial agglomeration, and their per capita carbon emissions were significantly higher than those of restricted development zones (the main agricultural product-producing zones and key ecological functional zones), which were the main pressure areas for per capita carbon emissions in Chinese counties (Figure 10). The per capita carbon emissions share of key development zones and key ecological functional zones increased year after year, whereas the per capita carbon emissions share of the main agricultural product-producing zones decreased year after year. The increase in per capita carbon emissions in the key ecological functional zones may have been partly due to the gradual increase in the development of the region and the increase in eco-tourism and other industries that generate more carbon emissions. The decrease in per capita carbon emissions in the main agricultural production zones may have been due to the reduction in carbon emissions sources caused by the return of farmland to forests and grasslands and the increase in the abandonment of farmland.

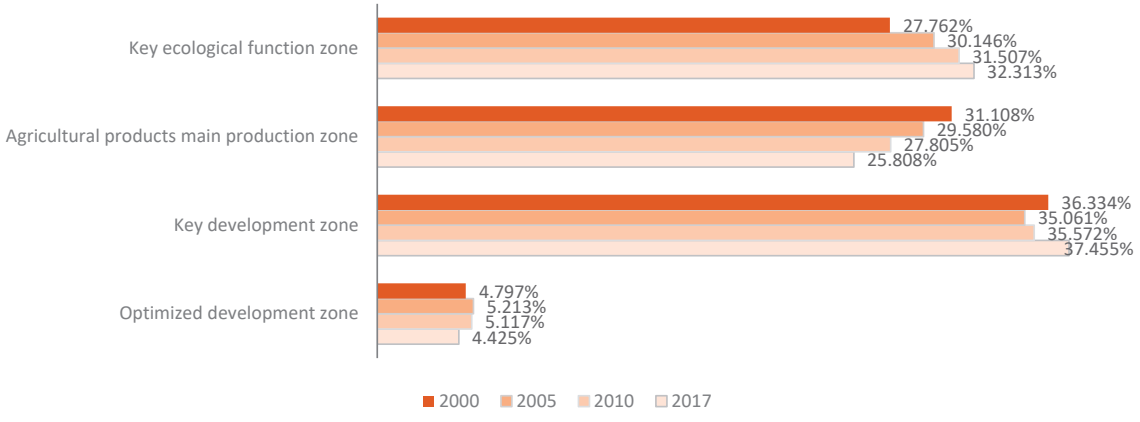

Figure 10. Percentage of carbon emissions per capita in each major function-oriented zone.

3.2.2. Spatial Clustering Characteristics of PCO_2 in Chinese Counties

The global Moran's I indices for 2000–2017 were all greater than 0 and passed the significance test at the 99.99% level, and China's PCO_2 was moderately autocorrelated in space during the study period (Table 4).

Table 4. Moran's I index of per capita county-level carbon emissions in China, 2000–2017.

Years	Moran's I	Z	P
2000	0.302	19.5241	0.000100
2005	0.370	23.7615	0.000100
2010	0.421	27.1650	0.000100
2017	0.511	32.690	0.000100

The global Moran's I index values showed an increasing trend from 2000 to 2017, indicating that the spatial autocorrelation of carbon emissions per capita in China was increasing, and the Moran's I indexes of carbon emissions per capita in Chinese counties were all greater than zero and passed the significance test at the 99.99% level, whereas the districts and counties with similar levels of carbon emissions per capita tended to have a concentrated distribution. Meanwhile, the Moran's I index gradually increased from 2000 to 2017, and the rate of increase for the index was higher in the early period than in the later period (the Moran's I index increased from 0.302 in 2000 to 0.511 in 2017).

3.3. Per Capita Carbon Compensation Zoning and Optimization Analysis in Chinese Counties

3.3.1. Analysis of the NRCA Index

Based on the index values of the natural background attribute, socio-economic attribute, ecological environment attribute, and energy consumption attribute, the NRCA index was used to measure the comparative advantage of each type of attribute in China's counties' per capita carbon compensation zoning, which provided a basis for the zoning and optimization of per capita carbon compensation.

The results show (Figure 11) that most of the dominant areas of natural background attributes in per capita carbon compensation in Chinese counties were located in the southwest, the upper northern part of northeast China, Qinghai, and parts of Xinjiang, indicating that these two major functional zones belonged to the dominant areas of per capita carbon sinks. Most of the disadvantaged areas of the natural background attributes of per capita carbon compensation in Chinese counties were located in the southeast coastal region and parts of the Central Plains and Inner Mongolia, indicating that the per capita carbon compensation rate in these areas was low and that the per capita carbon emissions far exceeded the per capita carbon sequestration, constituting a disadvantaged area of per capita carbon sinks.

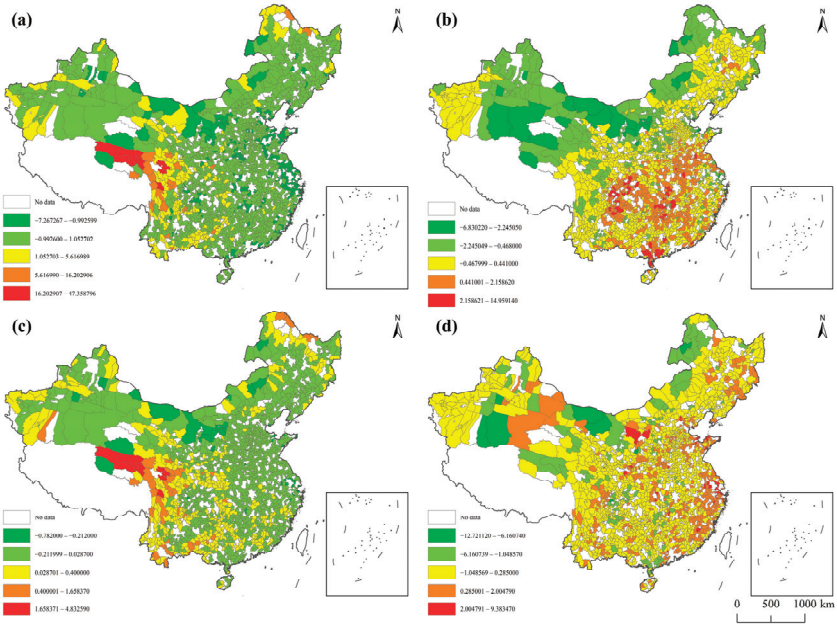

Figure 11. Spatial distribution of NRCA indices in Chinese counties: (**a**) natural background attributes; (**b**) socioeconomic attributes; (**c**) ecological and environmental attributes; (**d**) energy consumption attributes.

The advantageous areas of per capita carbon compensation economic attributes were mainly located in northeastern and central China, western Xinjiang, and southeastern China, where the economic contribution of carbon emissions was high, whereas some areas, such as northwestern Inner Mongolia, Gansu, Qinghai province, and Ningxia province, were the disadvantageous areas of carbon compensation economic attributes, where the economic contribution of carbon emissions was weak, the economic output efficiency was low, and the economic development may have been relatively more sloppy and lagging.

In terms of per capita carbon compensation for ecological attributes, the most advantageous regions were mainly located in the mountainous regions of southwest China, the Daxinganling Mountains in northeast China, the Tianshan Mountains in Xinjiang, and the mountainous regions in the south. These areas play an important ecological role in

water resource protection, wind and sand control, and climate regulation, and have a high ecological carrying capacity of PCO_2.

The areas of per capita carbon compensation where energy consumption attributes were dominant were mainly distributed in the Beijing–Tianjin–Hebei region, the eastern part of the northeast region, the southeastern coastal region, the middle Yellow River Basin region, Qinghai, eastern Gansu, and a few counties in the south of the western region. The areas of per capita carbon compensation where energy consumption attributes were dominant played a major feedback role on the PCO_2 of Chinese counties, and most of the carbon emissions originated from human energy consumption.

3.3.2. Per Capita Carbon Compensation Zoning Results

The per capita carbon compensation zoning model constructed by integrating the Kernel-K-means++ algorithm was used to cluster and analyze the NRCA index of four attributes, and the 1822 county units were classified into 1410 payment zones, 170 balanced zones, and 242 compensated zones. The per capita carbon compensation zoning was then overlaid with the main functional zoning and finally reconstructed into 11 types (Figure 12 and Table 5).

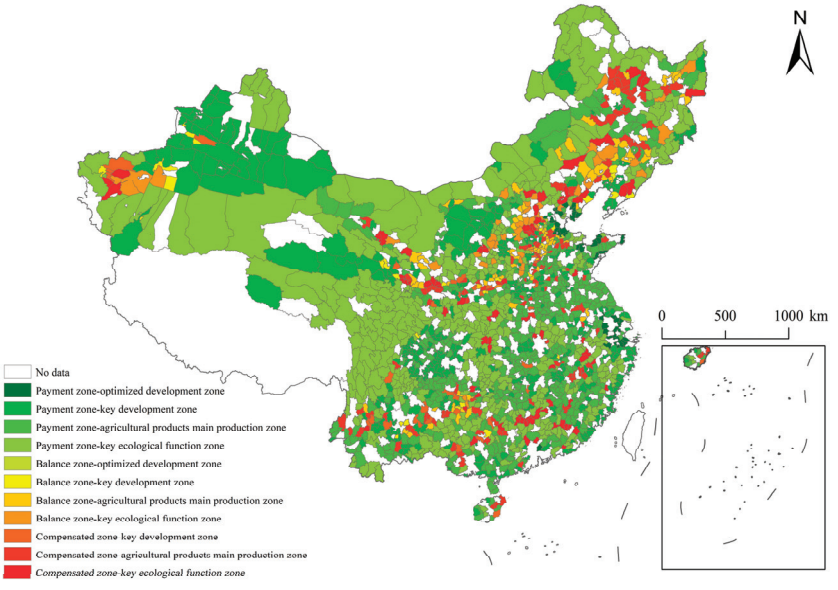

Figure 12. Spatial distribution of per capita carbon compensation zoning.

Table 5. Key indicators of per capita carbon compensation types in county-level regions of China.

Spatial Partitioning of Per Capita Carbon Compensation (Number of Units)	Per Capita Total GDP (%)	Share of Total Per Capita Carbon Emissions (%)	Mean Economic Contribution Factor of Per Capita Carbon Emissions	Mean Ecological Carrying Capacity Coefficient of Per Capita Carbon Emissions
Payment zone—optimized development zone (46)	10.645	4.310	4.106	0.031
Payment zone—key development zone (397)	34.500	34.618	3.588	0.405
Payment zone—main production zone of agricultural products (461)	29.161	17.272	4.47	0.516
Payment zone—key ecological function zone (506)	13.675	27.491	3.128	1.956
Balanced zone—optimized development zone (2)	0.083	0.114	1.39	0.355
Balanced zone—key development zone (29)	0.927	1.652	1.119	0.483
Balanced zone—main production zone of agricultural products (90)	2.131	4.371	0.907	1.697
Balanced zone—key ecological function zone (49)	0.916	2.525	0.697	2.225
Compensated zone—key development zone (33)	1.336	1.218	1.76	1.847
Compensated zone—main production zone of agricultural products (129)	4.681	4.165	1.833	2.435
Compensated zone—key ecological function zone (80)	1.945	2.264	1.526	3.833

3.4. Spatial Optimization Analysis of Per Capita Carbon Compensation Zoning in Chinese Counties

3.4.1. Payment Zone

Based on the zoning results, the payment zone is densely distributed and extensive, mainly located in southeast China, northeast China, and northwest Xinjiang, with a high level of economic development (per capita GDP share of up to 87.981%), high per capita carbon emissions contribution (per capita carbon emissions share of up to 83.691%), high per capita carbon emissions economic contribution capacity, and low per capita carbon emissions ecological carrying capacity. There was a serious mismatch between the two levels (the economic contribution coefficient of carbon emissions per capita was 6.338, and the ecological carrying capacity of carbon emissions per capita was 0.469). This zone includes:

(1) The payment zone—optimized development zone. The payment zone—optimized development zone consists of 46 county-level units, which are mainly located in the Bohai Sea Economic Zone, Yangtze River Delta region, and Pearl River Delta region and belong to highly urbanized and industrialized areas with relatively rapid economic development (the largest per capita total GDP share was 10.645%), large PCO_2 (the per capita total carbon emissions share was 34.618%), and high PCO_2 economic benefits (the average value of the economic contribution coefficient of carbon emissions per capita was 4.106), but the ecological environment is under great pressure (the average value of the ecological bearing coefficient of carbon emissions per capita was 0.031) and facing serious pressure to achieve emissions reduction. The main optimization direction is to promote the construction of industrial agglomeration to improve the economic contribution capacity of carbon emissions per capita and at the same time protect water resources and ecological environment resources and improve ecological environment carrying capacity. A new window and strategic space for opening up to the outside world should be formed while at the same time building an urban green isolation zone and coastal protection forests in order to protect the quality of the water environment in the near-shore sea.

(2) Payment zone—key development zone. The payment zone—key development zone consists of 398 county-level units, which are mainly distributed in the southeast coastal region, the Tianshan region of Xinjiang, the river-loop region, and the Sichuan Basin. This region has a high level of economic development and is the region that had the highest percentage of total GDP per capita among all sub-regions (34.500% of total GDP per capita) and is also the region that had the highest total carbon emissions per capita among all sub-regions (34.618% of total carbon emissions per capita). Although it has a good economic contribution benefit of carbon emissions per capita, it has high ecological and environmental pressure (economic contribution coefficient of carbon emissions per capita. The average value of per capita carbon emissions economic contribution coefficient was 3.588, the average value of the per capita carbon emissions ecological bearing coefficient was 0.405, and the pressure to achieve emissions reduction is greater. The main optimization direction is to form a new window and strategic space for opening up to the outside world. At the same time, it is necessary to build urban green isolation zones and coastal protection forests, strengthen the control of land-based pollutant emissions, and protect the quality of the water environment in the near-shore sea.

(3) Payment zone—agricultural products main production zone. The payment zone—agricultural products main production zone consists of 461 county-level units, mainly located in the northeast region, the North China Plain, and the Middle and Lower Yangtze River Plain. This region is mostly located in the plain area, with excellent agricultural conditions and an agricultural foundation, and is an important agricultural product base, but is more affected by human production activities. Compared with the main agricultural product-producing areas in the balanced zone and the compensated zone, this region has better economic contribution efficiency of carbon emissions per capita (the average value of economic contribution coefficient of carbon emissions per capita was 4.47) and average ecological carrying capacity (the average value of ecological carrying coefficient of carbon emissions per capita was 0.516) and creates the second largest total GDP per capita with lower carbon emissions (the percentage of total GDP per capita was 29.161%,

and the percentage of total carbon emissions per capita was 17.1%). The total carbon emissions per capita was 17.272%. The main optimization direction is the implementation of the geographical indication brand project and origin protection project. At the same time, we should consolidate the achievements of returning farmland to forests, continue to implement the natural forest resources protection project and comprehensive management of small watersheds, and strengthen the construction of wildlife biodiversity reserves.

(4) Payment zone—key ecological function zone. The payment zone—key ecological function zone consists of 505 county-level units, mainly located in the Sichuan Basin, southern Xinjiang, Inner Mongolia, the northern northeastern region, the two lakes region, and the southeastern mountainous region. As the sub-region with the largest share, the economic situation of this zone does not match the carbon emissions situation (the share of total GDP per capita was 13.675%, and the share of total carbon emissions per capita was 27.491%), the economic contribution of carbon emissions per capita is high (the average value of economic contribution coefficient of carbon emissions per capita was 3.128), and the ecological carrying capacity of carbon emissions per capita is high (the average value of ecological carrying coefficient of carbon emissions per capita was 1.956). The main optimization direction is to establish an ecological compensation mechanism, strengthen the natural restoration function of the ecosystem, develop environmentally bearable industries according to local conditions, and export ecological products.

3.4.2. Balanced Zone

The balanced zone is mainly located in parts of northern and northeastern China and some mountainous and hilly areas in southwest China, with an overall sporadic and short linear distribution. The economic development of the equilibrium zone is relatively slow (the percentage of GDP per capita was relatively low, at 4.057% of the total), the percentage of carbon emissions per capita is relatively small (carbon emissions per capita accounted for 8.662% of the total carbon emissions per capita), the ecological function and ecological carrying capacity of the carbon sink per capita are strong (the ecological carrying coefficient of carbon emissions per capita was 1.575), and the economic contribution capacity of carbon emissions per capita and the ecological carrying capacity of carbon emissions per capita are in a relatively matching state (the economic contribution coefficient of per capita carbon emissions was 1.82, and the ecological carrying capacity of per capita carbon emissions was 1.575), indicating that the economic development of the balanced zone is relatively balanced and will not cause an excessive impact on the ecological environment.

(1) Balanced zone—optimized development zone. The number of counties in the balanced zone—optimized development zone is very small. The per capita economic contribution and per capita carbon emissions of this zone are low (0.083% of total GDP per capita and 0.114% of total carbon emissions per capita), and the ecological carrying capacity is weak (the average value of economic contribution coefficient of carbon emissions per capita was 1.39, and the average value of ecological carrying coefficient of carbon emissions per capita was 0.355). The main optimization direction is to optimize the layout of urban functions, focus on the greening of towns and traffic arteries, improve the ecological system of urban forest parks and green channels, and enhance the carrying capacity of the ecosystem.

(2) Balanced zone—key development zone. The balanced zone—key development zone consists of 29 county-level units, showing a sporadic distribution, mainly located in the western region of Xinjiang, the eastern region of Qinghai, the southern region of Liaoning, the North China Plain, and the Yunnan-Guizhou region. This zone constitutes fewer counties and regions, with lower economic development (0.927% of total GDP per capita), lower carbon emissions per capita (1.652% of total carbon emissions per capita), slightly higher economic benefits of carbon emissions per capita (average value of economic contribution coefficient of carbon emissions per capita was 1.119), and a relatively stronger ecological carrying capacity of carbon emissions per capita (the average value of the ecological carrying coefficient of carbon emissions per capita was 0.483). The main opti-

mization directions include forming intensive and efficient urban clusters or dense urban areas, promoting comprehensive water environment management in important watersheds (Wujiang River, Lancang River, etc.), protecting water-bearing areas and biodiversity, and improving the ecological carrying capacity of the environment.

(3) Balanced zone—main production zone of agricultural products. The balanced zone—main production zone of agricultural products consists of 90 county-level units, scattered in the northeast region, the North China Plain, and the southwest mountainous region, whose per capita carbon emissions are more than twice the per capita GDP, with weak economic development and low economic contribution efficiency of per capita carbon emissions (2.131% of total per capita GDP, 4.371% of total per capita carbon emissions, and an average value of economic contribution coefficient of per capita carbon emissions of 0.907), but the ecological carrying capacity is strong (the average value of the ecological carrying coefficient of carbon emissions per capita was 1.697). The main optimization direction is to strengthen ecological protection; maintain a stable landscape system structure of hills, forests, grasses, and farmlands; and correctly handle the relationship between agricultural production, ecological protection, and resource development.

(4) Balanced zone—key ecological functional area. The balanced zone—key ecological functional area consists of 49 county-level units, mainly located near Kashgar in Xinjiang, part of the North China Plain, and part of the Northeast Plain, with a small per capita carbon emissions share (2.525% of total per capita carbon emissions share), weak economic development, and little economic contribution to per capita carbon emissions (0.916% of total per capita GDP and an average value of economic contribution coefficient of per capita carbon emissions of 0.697), but the ecological carrying capacity of carbon emissions per capita is strong (the average value of the ecological carrying coefficient of carbon emissions per capita was 2.225). The main optimization direction is to control the development intensity and carry out integrated management of small watersheds and the construction of silt dams to promote ecosystem restoration.

3.4.3. Compensated Zone

The compensated zone is mainly located in the northeastern plain and mountainous areas of the country's counties, including the mountainous and hilly areas in the southern region, Xinjiang, and some counties in Hainan, and shows a scattered and small cluster-like distribution. The economic development of the compensated zones is relatively limited (the per capita GDP share was relatively low, at 7.962% of the total), the per capita carbon emissions share is the smallest (the per capita carbon emissions accounted for 7.647% of the total per capita carbon emissions), the per capita carbon sink ecological function and ecological carrying capacity is strong (the per capita carbon emissions ecological carrying coefficient was 1.886), and the per capita carbon emissions economic contribution is low (the per capita carbon emissions economic contribution coefficient was 0.286).

(1) Compensated zone—key development zones. The compensated zone—key development zones are composed of 33 county-level units, mainly located in the southwest mountainous region, the middle reaches of the Yellow River, the vicinity of Kashgar in Xinjiang, and the Yili region, whose economic development and PCO_2 are relatively well matched (1.336% of total GDP per capita and 1.218% of total carbon emissions per capita, respectively), with a larger economic contribution of carbon emissions per capita (the average value of the economic contribution coefficient of carbon emissions per capita was 1.76) and stronger ecological and environmental functions (the average value of the ecological bearing coefficient of carbon emissions per capita was 1.847). The main optimization direction is to expand green ecological space; build an ecological pattern of the organic integration of forest, grassland, rivers, and lakes; and improve the carbon sink capacity of the ecosystem.

(2) Compensated zone—main production zone of agricultural products. The compensated zone—main production zone of agricultural products consists of 129 counties. In these areas, the economic development and per capita carbon emissions are well matched

(4.681% of total GDP per capita and 4.165% of total carbon emissions per capita, respectively), the economic contribution of per capita carbon emissions is high (the average value of the economic contribution of per capita carbon emissions was 1.833), and the ecological carrying capacity is strong (the average value of the ecological carrying coefficient of carbon emissions per capita was 2.435). The main direction of optimization includes the rational planning of agricultural land, the comprehensive control of desertification and rock desertification, and the formation of eco-friendly agricultural belts.

(3) Compensated zone—key ecological function zone. The compensated zone—key ecological function zone consists of 80 county-level units, mainly located in the northeast; the center; some parts of Guangdong, Gansu, and Xinjiang; and other northwest areas. The economic development of this zone is at an average level and the per capita carbon emissions are low (1.945% of total GDP per capita and 2.264% of total carbon emissions per capita, respectively), and the economic contribution capacity of per capita carbon emissions is average, whereas the ecological carrying capacity is very strong (the average value of the economic contribution coefficient of per capita carbon emissions was 1.526, and the average value of the ecological carrying coefficient of per capita carbon emissions was 3.833). The main optimization direction is to develop succession and alternative industries, mainly ecological tourism, special breeding, green food processing, etc., to form an ecologically dominant industrial pattern.

4. Discussion

In this study, a new per capita carbon compensation zoning model was proposed and the per capita carbon compensation zoning of Chinese counties was realized, which was verified as being reliable and have the potential to be applied to other similar studies. In addition, the research features and innovations of this study were mainly reflected in the following two aspects:

(1) The per capita carbon compensation rate was selected as a natural background attribute indicator; the level of residential economic energy consumption was selected as an energy consumption indicator to be added to the model; methods such as the K-means and SOM-K-means classification models, which were mostly used in the existing research on carbon compensation zoning, were further developed; a per capita carbon compensation county zoning model incorporating the Kernel-K-means++ algorithm was constructed; and per capita carbon compensation zoning of the counties in China was realized. Previous classification models in this research area did not consider the benefits of integrating data from all input aspects. In contrast, our updated model considers the complexities of multidimensional data and integrates natural context, socio-economic, ecological, and energy consumption aspects. This approach provides an advantage and makes our new model superior to previous models. This new model integrates the main functional zoning of the country with the real background conditions of each county, and the results of regional division have spatial autocorrelation, which is of practical significance in promoting emissions reduction. Additionally, since the new model incorporates nature, ecology, and energy consumption indicators, it is more effective in analyzing and planning sustainable development.

(2) Based on the county scale, results of China's per capita carbon compensation zoning were obtained and an optimization analysis was carried out. Most of the existing studies on carbon compensation zoning in China were conducted at the spatial scale of provinces and urban clusters but not at the spatial scale of counties. This study took the major counties in China as the unit, which provided a more detailed spatial scale and more accurately reflects the characteristics of China's carbon emissions; in addition, 1822 counties were used, which covers most of China's regions, and the study also had great macro-analysis conditions.

Due to the limited research conditions, the time series of the study was only selected as 2000 to 2017, and full time series coverage was not achieved from 2018 to 2023. Since the obtained county-level carbon balance data do not include Tibet, Hong Kong, Macao, and Taiwan and need to be matched with county-level economic data and since the division of

China's county-level units varies with the time series, the carbon balance data and economic data of only 1822 county-level units in China were obtained, which cannot cover all county-level units in China. Considering the availability of data and the applicability of the zoning model, only four indicators, namely, the per capita carbon compensation rate, the per capita carbon emissions ecological carrying coefficient, the per capita carbon emissions economic contribution coefficient, and the level of economic energy consumption of the population, were selected for clustering and partitioning, and population, industrial structure, and technological level were not included in the comprehensive evaluation index. The existing deficiencies of the above study will be further explored in future research. Moreover, there is also potential for future improvement to the new model, which is improved based on the kernel-PCA and K-means++ algorithms due to the kernel-PCA property, so there is also a possibility of overfitting in the new model, which can be further improved in the future.

5. Conclusions

In this study, based on county carbon emissions, carbon sequestration, and economic data, the variable dataset of per capita carbon compensation zoning in Chinese counties was constructed, regional differences in PCO_2 at the county scale were explored, and a four-dimensional framework of carbon compensation zoning was constructed. Based on this, a comprehensive evaluation index and a per capita carbon compensation zoning model were constructed. We also tried to propose a spatial low-carbon optimization strategy to promote carbon neutrality from the perspectives of payment, balanced, and compensated zones.

The main results are as follows: During the period of 2000–2017, the overall differences in PCO_2 were large and showed a steady widening trend in China's counties, generally showing distribution characteristics of low in the southeast and high in the northwest, with obvious spatial autocorrelation. In addition, the model constructed in this study is based on the Kernel-K-means++ algorithm, which integrates natural, economic, ecological, and energy factors and more comprehensively realizes the per capita carbon compensation zoning in Chinese counties. Based on the model, the 1822 counties and districts in China were divided into 1410 payment zones, 170 balanced zones, and 242 compensated zones. By combining the results of carbon compensation zoning with the major function-oriented zones, 11 types of zones were finally formed, and the direction and strategy of low-carbon development for each type of zone were proposed. The improved model and optimization suggestions proposed in this study can contribute to a reduction in China's carbon emissions in order to achieve the target of carbon peaking and carbon neutrality and, at the same time, have certain reference significance for the management of and reduction in carbon emissions in similar regions.

The implementation of sub-regional recommendations should be considered in order to achieve the goal of carbon peaking and carbon neutrality. We suggest that, based on the background characteristics of the study's delineated regions and the recommendations therein, this plan will develop emissions reduction pathways and low-carbon industries. This strategy will keep carbon emissions under control while adapting to local conditions, and with the development of the carbon emissions situation, longer time series studies can be conducted and more appropriate strategies for cutting carbon emissions can be developed.

Author Contributions: Conceptualization, J.C. and S.W.; methodology, J.C.; software, J.C.; validation, J.C., S.W., and L.Z.; formal analysis, J.C.; investigation, J.C.; resources, J.C.; data curation, J.C.; writing—original draft preparation, J.C.; writing—review and editing, J.C., S.W., and L.Z.; visualization, J.C.; supervision, S.W.; project administration, S.W.; funding acquisition, S.W. All authors have read and agreed to the published version of the manuscript.

Funding: This work was supported by the National Key Research and Development Program of China (grant 2021YFB3900900) and the Provincial Key R&D Program of Zhejiang (grant 2021C01031). This work was also supported by the Deep-time Digital Earth (DDE) Big Science Program.

Data Availability Statement: The data presented in this study are available on request from the corresponding author. The data are not publicly available due to privacy.

Conflicts of Interest: The authors declare no conflict of interest.

References

1. O'neill, B.C.; Dalton, M.; Fuchs, R.; Jiang, L.; Pachauri, S.; Zigova, K. Global demographic trends and future carbon emissions. *Proc. Natl. Acad. Sci. USA* **2010**, *107*, 17521–17526. [CrossRef]
2. Zhou, X.; Niu, A.; Lin, C. Optimizing carbon emission forecast for modelling China's 2030 provincial carbon emission quota allocation. *J. Environ. Manag.* **2023**, *325*, 116523. [CrossRef]
3. Lin, Q.; Zhang, L.; Qiu, B.; Zhao, Y.; Wei, C. Spatiotemporal Analysis of Land Use Patterns on Carbon Emissions in China. *Land* **2021**, *10*, 141. [CrossRef]
4. Tian, S.; Wang, S.; Bai, X.; Luo, G.; Li, Q.; Yang, Y.; Hu, Z.; Li, C.; Deng, Y. Global patterns and changes of carbon emissions from land use during 1992–2015. *Environ. Sci. Ecotech.* **2021**, *7*, 100108. [CrossRef]
5. Shi, Q.; Chen, J.; Shen, L. Driving factors of the changes in the carbon emissions in the Chinese construction industry. *J. Clean. Prod.* **2017**, *166*, 615–627. [CrossRef]
6. Ma, X.; Wang, C.; Dong, B.; Gu, G.; Chen, R.; Li, Y.; Zou, H.; Zhang, W.; Li, Q. Carbon emissions from energy consumption in China: Its measurement and driving factors. *Sci. Total Environ.* **2019**, *648*, 1411–1420. [CrossRef]
7. Liu, Z.; Deng, Z.; Davis, S.J.; Giron, C.; Ciais, P. Monitoring global carbon emissions in 2021. *Nat. Rev. Earth Environ.* **2022**, *3*, 217–219. [CrossRef] [PubMed]
8. Pan, X.; Guo, S.; Xu, H.; Tian, M.; Pan, X.; Chu, J. China's carbon intensity factor decomposition and carbon emission decoupling analysis. *Energy* **2022**, *239*, 122175. [CrossRef]
9. Chen, C.; Bi, L. Study on spatio-temporal changes and driving factors of carbon emissions at the building operation stage-A case study of China. *Build. Environ.* **2022**, *219*, 109147. [CrossRef]
10. Liu, C.; Sun, W.; Zhang, L. Spatio-temporal pattern of coupling coordination degree between carbon emissions and vegetation cover and its influencing factors of the Yangtze River Delta. *Sci. Geogr. Sin.* **2023**, *43*, 142–151.
11. Xia, S.; Shao, H.; Wang, H.; Xian, W.; Shao, Q.; Yin, Z.; Qi, J. Spatio-Temporal Dynamics and Driving Forces of Multi-Scale CO_2 Emissions by Integrating DMSP-OLS and NPP-VIIRS Data: A Case Study in Beijing-Tianjin-Hebei, China. *Remote Sens.* **2022**, *14*, 4799. [CrossRef]
12. Zhou, J.; Wang, Y.; Liu, X.; Shi, X.; Cai, C. Spatial Temporal Differences of Carbon Emissions and Carbon Compensation in China Based on Land Use Change. *Sci. Geogr. Sin.* **2019**, *39*, 1955–1961.
13. Wang, X.; Lu, F.; Qin, Y.; Sun, Y. Spatial and temporal changes of carbon sources and sinks in Henan Province. *Prog. Geogr.* **2016**, *35*, 941–951.
14. Wang, S.; Xie, Z.; Wang, Z. The spatiotemporal pattern evolution and influencing factors of CO_2 emissions at the county level of China. *Acta Geogr. Sin.* **2021**, *76*, 3103–3118.
15. Zhang, H.; Peng, Q.; Wang, R.; Qiang, W.; Zhang, J. Spatiotemporal patterns and factors influencing county carbon sinks in China. *Acta Ecol. Sin.* **2020**, *40*, 8988–8998.
16. Long, Z.; Pang, J.; Li, S.; Zhao, J.; Yang, T.; Chen, X.; Zhang, Z.; Sun, Y.; Lang, L.; Wang, N.; et al. Spatiotemporal variations and structural characteristics of carbon emissions at the county scale: A case study of Wu'an City. *Environ. Sci. Pollut.* **2022**, *29*, 65466–65488. [CrossRef] [PubMed]
17. Zhang, B.; Yin, J.; Jiang, H.; Qiu, Y. Spatial–temporal pattern evolution and influencing factors of coupled coordination between carbon emission and economic development along the Pearl River Basin in China. *Environ. Sci. Pollut.* **2023**, *30*, 6875–6890. [CrossRef]
18. Zheng, Y.; Du, S.; Zhang, X.; Bai, L.; Wang, H. Estimating carbon emissions in urban functional zones using multi-source data: A case study in Beijing. *Build. Environ.* **2022**, *212*, 108804. [CrossRef]
19. Zhang, C.; Zhao, L.; Zhang, H.; Chen, M.; Fang, R.; Yao, Y.; Zhang, Q.; Wang, Q. Spatial-temporal characteristics of carbon emissions from land use change in Yellow River Delta region, China. *Ecol. Indic.* **2022**, *136*, 108623. [CrossRef]
20. Zhang, X.; Cai, Z.; Song, W.; Yang, D. Mapping the spatial-temporal changes in energy consumption-related carbon emissions in the Beijing-Tianjin-Hebei region via nighttime light data. *Sustain. Cities Soc.* **2023**, *94*, 104476. [CrossRef]
21. Yang, S.; Yang, X.; Gao, X.; Zhang, J. Spatial and temporal distribution characteristics of carbon emissions and their drivers in shrinking cities in China: Empirical evidence based on the NPP/VIIRS nighttime lighting index. *J. Environ. Manag.* **2022**, *322*, 116082. [CrossRef] [PubMed]
22. Zhu, E.; Qi, Q.; Chen, L.; Wu, X. The spatial-temporal patterns and multiple driving mechanisms of carbon emissions in the process of urbanization: A case study in Zhejiang, China. *J. Clean. Prod.* **2022**, *358*, 131954. [CrossRef]
23. Liu, Q.; Song, J.; Dai, T.; Shi, A.; Xu, J.; Wang, E. Spatio-temporal dynamic evolution of carbon emission intensity and the effectiveness of carbon emission reduction at county level based on nighttime light data. *J. Clean. Prod.* **2022**, *362*, 132301. [CrossRef]
24. Xia, S.; Yang, Y. Spatio-temporal differentiation of carbon budget and carbon compensation zoning in Beijing-Tianjin-Hebei Urban Agglomeration based on the Plan for Major Function-oriented Zones. *Acta Geogr. Sin.* **2022**, *77*, 679–696.

25. Wang, Z.; Qin, M.; Tang, S.; Zhao, Y.; Pang, Y.; Gong, Y. Spatio-temporal Variation of Landuse Carbon Budget and Carbon Compensation Zoning in Beibu Gulf Urban Agglomeration Area. *Bull. Soil Water Conserv.* **2022**, *42*, 348–359.
26. Zhao, R.; Zhang, S.; Huang, X.; Qin, Y.; Liu, Y.; Ding, M.; Jiao, T. Spatial variation of carbon budget and carbon balance zoning of Central Plains Economic Region at county-level. *Acta Geogr. Sin.* **2014**, *69*, 1425–1437.
27. Li, L.; Dong, J.; Xu, L.; Zhang, J. Spatial variation of land use carbon budget and carbon compensation zoning in functional areas: A case study of Wuhan Urban Agglomeration. *J. Nat. Resour.* **2019**, *34*, 1003–1015.
28. Xiong, C.; Chen, S.; Yang, D. Selecting Counties to Participate in Agricultural Carbon Compensation in China. *Pol. J. Environ. Stud.* **2019**, *28*, 1443–1449. [CrossRef]
29. Jing, X.; Tian, G.; Li, M.; Javeed, S.A. Research on the Spatial and Temporal Differences of China's Provincial Carbon Emissions and Ecological Compensation Based on Land Carbon Budget Accounting. *Int. J. Environ. Res. Public Health* **2021**, *18*, 12892. [CrossRef]
30. Keyser, A.R.; Kimball, J.S.; Nemani, R.R.; Running, S.W. Simulating the effects of climate change on the carbon balance of North American high-latitude forests. *Global Change Biol.* **2000**, *6*, 185–195. [CrossRef] [PubMed]
31. Kong, F.; Cao, L.; Xu, C. Compensation Mechanism for Forest Carbon Sink in the Qiantang River Basin Based on Carbon Revenue and Expenditure Accounting. *Sci. Silvae Sin.* **2022**, *58*, 1–15.
32. Piao, S.; Fang, J.; Ciais, P.; Peylin, P.; Huang, Y.; Sitch, S.; Wang, T. The carbon balance of terrestrial ecosystems in China. *Nature* **2009**, *458*, 1009–1013. [CrossRef]
33. Zhao, R.; Liu, Y.; Ma, L.; Li, Y.; Hou, L.; Zhang, Z.; Ding, M. County-level Carbon Compensation of Henan Province Based on Carbon Budget Estimation. *J. Nat. Resour.* **2016**, *31*, 1675–1687.
34. Lin, H.; Zhou, Z.; Chen, S.; Jiang, P. Clustering and assessing carbon peak statuses of typical cities in underdeveloped Western China. *Appl. Energy* **2023**, *329*, 120299. [CrossRef]
35. Ye, J.; Xie, Q.; Tan, N. National land spatial pattern distribution method based on ecological carrying capacity. *Trans. Chin. Soc. Agric. Eng.* **2017**, *33*, 262–271.
36. Dagum, C. *A New Approach to the Decomposition of the Gini Income Inequality Ratio*; Physica-Verlag HD: Heidelberg, Germany, 1998. [CrossRef]
37. Yu, R.; Cai, J.N.; Leung, P.S. The normalized revealed comparative advantage index. *Ann. Regional Sci.* **2009**, *43*, 267–282. [CrossRef]
38. Balassa, B.L. Trade liberalisation and "revealed" comparative advantage. *Manch. Sch.* **1965**, *33*, 99–123. [CrossRef]
39. Zhao, R.; Huang, X. Carbon cycle of urban system: Characteristics, mechanism and theoretical framework. *Acta Ecol. Sin.* **2013**, *33*, 0358–0366. [CrossRef]
40. Zhao, R.; Liu, Y.; Ding, M.; Zhang, Z.; Huang, X.; Qin, Y. Theory, methods, and research progresses of regional carbon budget. *Prog. Geogr.* **2016**, *35*, 554–568.
41. Lu, J.; Huang, X.; Dai, L.; Chen, Z.; Li, Y. Spatio-temporal Scale Analysis on the Equality of Energy Consumption Carbon Emission Distribution in China. *J. Nat. Resour.* **2012**, *27*, 2006–2017.
42. Kong, X.; Fu, M.; Zhao, X.; Wang, J.; Jiang, P. Ecological effects of land-use change on two sides of the Hu Huanyong Line in China. *Land Use Policy* **2022**, *113*, 105895. [CrossRef]

land

MDPI

Article

Understanding Carbon Emissions Reduction in China: Perspectives of Political Mobility

Zhichao Li [1] and Bojia Liu [2,*]

[1] School of International and Public Affairs, Shanghai Jiao Tong University, Shanghai 200030, China
[2] School of Public Administration, South China University of Technology, Guangzhou 510641, China
* Correspondence: 2013040958@ecupl.edu.cn

Abstract: Climate change is one of the largest challenges facing mankind, and the question of how to reduce carbon emissions has raised extensive concern all over the world. However, due to the lack of mechanisms to explain the impact of political factors on environmental regulatory tools, the evaluation of carbon emissions reduction is insufficient in the majority of previous studies. How to better explore the path of carbon emissions reduction has become the key for China to achieve carbon neutralization as soon as possible. Based on a quasi-natural experiment regarding China's carbon emission trading policy, this paper adopts a difference-in-differences model to address the impact of political mobility on China's carbon emissions trading policy, and the selected pilot and non-pilot provinces of this policy in China enabled the model to be matched. Using a panel database with 30 provincial administrative units as the observation objects, the results show that China's carbon emissions trading policy and the horizontal mobility experience of the provincial governors exert a significant positive effect on carbon emission reduction. Additionally, this study identifies a latent factor previously ignored by the existing literature: the correlation between political factors and carbon emissions. This verifies our theoretical hypothesis that officials transferred from the provincial level tend to have higher performance regarding carbon emission reduction. This paper also provides suggestions for the central government to further plan and implement carbon emission reduction policies and mobilize the incentives of local officials in environmental governance.

Keywords: carbon emissions trading; political mobility; difference-in-differences model; policy evaluation

Citation: Li, Z.; Liu, B. Understanding Carbon Emissions Reduction in China: Perspectives of Political Mobility. *Land* **2023**, *12*, 903. https://doi.org/10.3390/land12040903

Academic Editors: Chao Wang, Jinyan Zhan and Xueting Zeng

Received: 12 March 2023
Revised: 7 April 2023
Accepted: 16 April 2023
Published: 18 April 2023

1. Introduction

Human survival and sustainable development face severe challenges. Climate change threatens the lives and environmental conditions of humans worldwide and has become a global concern [1]. Increasing carbon emissions have gradually become the main reason for global climate change. According to the annual report by the United Nations Environment Program, global carbon dioxide emissions showed an upward trend [2]. Correspondingly, to achieve green growth, nations all over the world have enacted a number of environmental laws and emission reduction plans. Therefore, reducing carbon emissions is essential for maintaining a healthy ecological ecosystem.

As the largest source of carbon emissions in the world, China has responded with a series of policies such as instituting emission reduction measures and promoting the establishment of an international carbon market to mitigate global warming [3]. To achieve low-carbon development, China issued the carbon emission reduction plan as guidance for different industrial sectors in terms of achieving the reduction targets in 2012. In 2015, the Chinese central government set the policy target that China's carbon emissions will achieve the peak of domestic carbon emissions by 2030. The Chinese government widened its objectives in 2020 by pledging to achieve carbon neutrality by 2060. To meet these climate targets while trying to pursue economic development, China has implemented a carbon emissions trading system [4]. Since the 11th Five-Year Plan, Chinese central government has

added environmental performance, especially carbon emissions, into the local government performance appraisal, and during the 13th Five-Year Plan it was proposed to establish a national carbon emission trading market by 2020.

Previous studies on carbon emission trading policies have explored the factors that influence carbon emission performance, such as technology development [5], total energy consumption [6] and energy consumption structure [7]. Studies on the impact of carbon emission trading policies mainly focused on two categories, which contains sectors and environmental governance. For the sectoral impact, existing studies have mainly focused on the power sector and transport sector [8,9]. However, it can be found that the existing empirical research was limited to certain sectors related to carbon trading policies while ignoring interactions with other perspectives, or was concentrated on macro-economic simulation instead of specific environmental activities and behaviors based on different perspectives.

Regarding the overall impact on a national level, research on the driving mechanism of China's carbon emissions reduction is relatively lacking and has insufficient evidence. Previous studies ignored the role of government officials in carbon emission reduction. Few studies chose to use factors such as government performance and human behavior to explore an in-depth explanation of China's carbon emissions reduction, especially the impact of political leaders on environmental governance. The literature shows that in a political system, the attention distribution of political leaders may affect or even change policy objectives, their implementation methods and performance [10]. The most persuasive theory about China's economic growth miracle is the "Promotion Tournament Model Theory" [11], which points out that the incentive of local officials is a fundamental motivation of China's economic development. To improve economic performance, Chinese central government has established the promotion tournament incentive structure, which has motived local officials with GDP growth as the core indicator. Understanding the influence of local officials on carbon emissions is very important for policy implication. However, considering the political tournament mechanism in China, local officials face two kinds of promotion incentives, including economic development and emissions reduction: can the implementation of policies on carbon emission trading effectively promote the performance of carbon emission reduction?

In this study, we explored whether the current carbon emissions trading policy can promote emission reduction performance, and we proposed a theoretical framework that explains the relations among political mobility, tenure, and carbon emission performance. In areas with similar natural resources, human capital and technological innovation capacity, local carbon emission performance may be different due to the different political experiences of leaders. By understanding the possible motivations of these key actors, we hoped to better understand the key factors in environmental governance, such as political arrangements and incentives.

2. Literature Review and the Theoretical Framework: Understanding Carbon Emissions in the Context of the Chinese Political Environment

2.1. Carbon Emissions Trading System

Traditional regulation tools and policies such as environmental tax and industrial energy prices were inefficient due to information asymmetry [12]. Existing studies have discussed that using a market-oriented mechanism is more efficient and economical on the realization of carbon emissions reduction compared to policies directly led by government, such as environmental protection administrative penalties and pollution charges [13]. Therefore, it is imperative to design effective market-oriented regulation policies for reducing carbon emissions.

During the past decades, carbon emissions trading systems have become important tools in market-oriented environmental regulation to address the issues of inefficient carbon emission allocation. Building on Coase's option theory, John Dales proposed a system of carbon emissions trading in 1968 [14]. Introducing property rights into environmental pollution control was meant to internalize the cost of carbon dioxide emissions [15]. The

literature on carbon trading mechanisms has mainly focused on the effects of regional carbon emissions reduction programs in developed countries. The markets were often the research objects, especially carbon trading in Europe's EU-ETS program, which operates through auctions. To better quantify and empirically study the utility of carbon trading mechanisms, scholars began to use different models such as the dynamic decision-making model, the general equilibrium model, and the network analysis model [16]. For example, Dong et al.'s study of China's carbon emissions trading policy found that market scale and reduction costs were negatively correlated [17]. Martin et al. focused on the impact of emissions trading on enterprise [18]. Other scholars used different models to explore the impacts of carbon trading on other affected groups.

The effectiveness of carbon emissions trading is relatively unexamined. The majority of the existing studies are qualitative research, predictive simulations, or are focused on specific industries or regions. At the national level, empirical research is scarce. Few empirical studies have analyzed the effectiveness of pilot emission trading systems on politics. Additionally, the performance of carbon emissions trading systems remains controversial. Even so, scholars have generally determined that China's carbon emissions trading system has successfully promoted carbon emission reductions [19].

Despite the fact that these studies investigated the efficiency of policies, the results they reached differed substantially due to discrepancies in their data and techniques. The emission reduction results of these systems under diverse viewpoints varied since some researchers concentrated on various core objects. Others adopted different policy evaluation methods, making it difficult to obtain unbiased estimates for the variable of carbon emissions. Similarly, the literature also provides a theoretical framework for the study of carbon emissions trading systems. Theoretical arguments for the emission reduction effects of these systems can certainly be made. However, they are frequently biased and ineffective. Stated another way, the majority of studies have focused on the direct impact of carbon emission trading systems while disregarding politics.

2.2. Political Mobility in the Context of China's Politics

Government officials actively participate in environmental governance as managers of society and advocates for government policies. The reasons behind their acts will inevitably have an impact on both their work performance and the government's. In most Western democracies, the political reputation model can explain how political incentives affect environmental governance [20]. Officials may decide to modify tax and environmental governance policies in accordance with the preferences of their constituencies to protect their chances of being re-appointed or re-elected.

Different from Western democracies, local officials in China are appointed by higher-level authorities, but local governments nevertheless retain a lot of power. Sometimes referred to as federalism with Chinese characteristics, this division of authority makes China's economic growth possible through administrative and fiscal decentralization [21]. However, this theory relies upon a high degree of institutional stability, which creates its own motivating effect. The Chinese promotion tournament theory proposes a Principal-agent relationship among the levels of government. China's administrative level-by-level contract system represents a typical type of strong incentive contract from the perspective of economics [22]. The central government, as the employer, holds political tournaments among provincial governments by virtue of personnel appointment or the recommendation power of the administrative head. From this point of view, in a political environment where vertical contracting and horizontal competition are highly unified, the extensiveness and unity of local government power provided by the administrative subject contract system gives the administrative subject enough space to play a significant role. Many studies have found that economic growth is the primary indicator of political promotion. Hence, local governments frequently devote their main resources to fostering economic growth [23]. Projects that result in short-term economic growth will be approved by local officials, regardless of any long-term environmental implications.

This situation is changing. Environmental protection has been a focal point since the Chinese government shifted its goals. Environmental protection is now included in the performance evaluation of local officials. This is important because the promotion tournament incentive structure has had severe consequences for environmental governance, such as global warming [24], excessive energy consumption and environmental pollution. Therefore, understanding the initial impact of carbon emissions on local officials is important for China's policy response to climate change. Strangely, the role of local officials in emissions reduction has largely been ignored by researchers.

2.3. Theoretical Framework and Research Hypothesis

2.3.1. The Performance of the Carbon Emissions Trading System

The implementation of a carbon emissions trading policy may improve the environmental circumstances in the pilot region in a market-oriented way. Because carbon emissions can be measured, it is possible to compare regional carbon emission controls on a horizontal scale. While pursuing political promotion, local officials in areas with fewer emission reductions experience higher pressure. Simply said, regional environmental quality improvements can help officials get promoted. Therefore, local officials will compete with other officials at the same level on environmental protection issues in order to gain promotion opportunities [25]. Where once they competed to demonstrate economic progress, officials must now show environmental stewardship. At the same time, poor performance in an environmental quality evaluation will likely attract the attention of environmental protection departments.

From the industry perspective, carbon emissions trading policy has improved the incentives to reduce production costs through emission reduction. Enterprises have also gained a measure of autonomy through trading carbon emissions. There will be significant external pressure on the government in regions with high carbon emissions to improve local environmental governance. Under the joint action of the above two subjects, local governments will make every effort to implement the carbon emission trading policy, improve regional environmental quality, strengthen regional environmental governance and supervision, and strive to reverse the bad environmental situation in the region. This behavior is conducive to promoting the reduction of carbon dioxide emissions. Based on this, we propose the first hypothesis:

Hypothesis 1. *China's carbon emissions trading system has a significantly positive effect on reducing China's carbon emissions.*

2.3.2. Effect of Political Mobility on Carbon Emission Reduction Performance

With the opening up of China in the late 1970s, local officials have taken an active role in constructing a new economic system, developing the private economy and reforming the local government performance evaluation system. For the carbon emission reduction scheme, efficiency incentives were to be provided to local officials. It was necessary to link reductions to political promotion. Previous studies of provincial officials noted that the performance of local officials may be affected by their tenure, which is highly influenced by economic performance. Chen et al. focused on the relationship between performance evaluation and the tenure of local officials [26]; their tenure depended on local economic performance. Similarly, He et al. proved that the higher the completion ratio of economic growth targets, the higher the probability of promotion, and the higher the probability of political promotion in the case of higher economic growth targets [27].

Moreover, according to the multi-task principal-agent theory, when there are multiple tasks to accomplish local officials always decide on the action with the highest expected utility and obvious results. The period for achieving political goals through economic growth is brief and simple to track. Environmental protection requires a long period and high investment. Hence, rational local government officials will prioritize economic growth and reduce investment in environmental governance due to the constraints of multi-

dimensional political goals assessment and limited financial resources. This will in turn affect environmental quality. Thus, due to the externality characteristics of environmental protection, local officials may choose to disregard environmental issues. Extensive growth patterns even have a crowding out effect on environmental governance expenditure, which is not conducive to the improvement of environmental quality. The central government could change this. Local officials might focus on environmental regulation performance if it had an impact on their political tenure [28]. This leads to our second set of hypotheses:

Hypothesis 2-a. *Carbon emission reduction performance is negatively associated with the tenure of local officials.*

Hypothesis 2-b. *Carbon emission reduction performance is positively associated with the tenure of local officials.*

How do local officials get into positions of power in China? Previous studies provided two models to explain political mobility: the factional model and the performance model. The factional model considers personal relationships to central leaders as the key to career success [29]. However, just as Teiwes advocated the utility of the factional concept, the efficiency of the factional model has not been systematically tested [30]. The performance model is the current mainstream explanation. Bo insisted on using the performance model to challenge the traditional factional model [31]. Based on the performance model, the political mobility of local officials mainly included the following five movements: promotion (vertical mobility from a lower rank to a higher one); demotion (includes demotions and purges or dismissals); lateral transfer (horizontal mobility without change in rank); retirement; and continuing without movement. Local officials faced different promotion incentives depending on their experiences, which might affect their environmental governance performance [32]. In this study, we sought to observe whether and how political mobility incentives affect carbon emission reduction performance, so we chose promotion and lateral transfer as the main types for our research.

Officials who are promoted within their home region are more familiar with local circumstances and therefore tend to set higher performance targets. Compared to locally promoted officials, officials transferred from higher authorities and other localities tend to avoid more challenging tasks or taking risks to achieve higher goals due to their unfamiliarity with the area [33]. Therefore, we assumed that locally promoted officials were more likely to set higher government performance goals than transferred officials.

In China's public personnel system, if a central government official was appointed to be a governor, he/she would probably regard this experience as compulsory training that would enable further promotion within the bureaucratic system. Thus, local officials connected with the central government have more chances of promotion. As a result, officials with close ties to the central government tend to make more conservative decisions to safeguard their chances of promotion [34].

The paths taken by officials transferred horizontally from other provinces are more complicated. Some scholars believe that the political mobility system helps higher-level government officials accomplish their long-term strategic goals. The active mobility of officials avoids nepotism, which is typically caused by the long-term employment of officials in one place. In addition, officials also tend to set higher goals as they gain more ability by learning, exchanging experiences and updating their governance concepts. Therefore, they usually formulate strategies to show their unique views, highlight their potential, and help realize the intention of coordinating regional development. This is reflected in the completely different emission reduction governance methods of those who were locally promoted and those who were transferred from the central government. Therefore, contrary to previous conclusions, there is evidence that officials transferred to new provinces can achieve higher performance [35].

Hence, we set dummy variables and propose a third set of hypotheses by taking "officials promoted from other provinces" as the reference group:

Hypothesis 3-a. *Compared with officials in the control group, locally promoted officials will have higher carbon emission reduction performance.*

Hypothesis 3-b. *Compared with officials in the control group, officials transferred from the central government will have lower carbon emission reduction performance.*

Hypothesis 3-c. *Compared with officials in the control group, officials transferred from other provinces will have higher carbon emission reduction performance.*

Additionally, educational background is important for cadre selection and political mobility in China, and local officials are therefore often keen to obtain a high academic level [36]. Thus, an improvement of the educational background of local officials results in a higher likelihood of cadres being more aware of the basic needs of citizens, understanding the connotations of economic development more openly and comprehensively, and paying more attention to the coordinated development of the environment and the economy. Based on this, we proposed the following hypothesis:

Hypothesis 4. *Local officials with a higher level of education will show more resolve to achieve carbon emission reductions.*

The above theoretical hypotheses were proposed through theoretical analysis. The theoretical research framework of this study was obtained and tested using the empirical analysis described below.

3. Materials and Methods

3.1. Statistical Modeling

To assess the net effect of the carbon emissions trading policy, we measured the difference between the state of the pilot provinces following intervention by the carbon emissions trading mechanism and the assumed state without policy trials. The latter kind of state, known as the counterfactual state, is not observable, but can be estimated via comparison with a control group (i.e., the non-pilot provinces) [37].

The carbon trading mechanism trials in the pilot provinces commenced in 2013, so this paper takes 2013 as the policy implementation year. From 2013 to the national introduction of the carbon market in 2017, the policy only applied to the pilot provinces; all non-pilot provinces were unaffected. Thus, the non-pilot provinces and cities were taken as the control group. Based on Hypothesis 1, we used the DID method to compare the carbon reduction performance before and after the launch of the carbon trading policy. Since the study has two groups with divided research objects, it can be considered a "quasi-experimental" design. The DID method is suitable for the causal effect estimation of the quasi-experiment because it can avoid endogeneity. That is, it can effectively control the interaction effect between the explained variable and the explanatory variable. In the DID model of panel data, the exogenous explanatory variable can be used to control the unobservable individual heterogeneity between samples. It can also control the influence of unobservable factors which change with time, so it can produce an unbiased estimation of the policy effect. To ensure the robustness of the results, we verified the estimation results through different test methods.

Based on the DID model expressed in econometrics, we established the following model Formula (1) to evaluate the emission reduction performance of the carbon emissions trading policy:

$$Y = \alpha + \beta_1 \times policy \times (G_i \times D_t) + \Sigma\beta_j \times control + \gamma G_i + \lambda D_t + \varepsilon_{it} \quad (1)$$

Y is the explained variable carbon emission and Control represents a series of control variables. Based on the above theoretical assumptions, the control variables included in the policy evaluation Model (1) are the economic, social and political factors that affect carbon emissions. G_i is the grouping dummy variable. If $G_i = 1$, it is a pilot province, which is the intervention group; if $G_i = 0$, it is a non-pilot province, which is the control group. This parameter indicates that even without the influence of this policy, there would still be unchangeable differences between the two comparison groups due to some other uncontrollable factors. D_t is the staging dummy variable (after policy implementation $D_t = 1$, before policy implementation $D_t = 0$), representing the time difference before and after policy implementation. The interaction term $G_i \cdot D_t$ (policy) represents the net effect of the carbon emissions trading policy. ε_{it} is the random interference term. If the coefficient β_1 of the policy is not significantly equal to 0, it means that China's carbon emissions trading policy has a significant impact on carbon emission reduction. However, if $\beta_1 = 0$, this indicates that China's carbon emissions trading policy is invalid.

Based on the analysis and assumptions of the relevant variables affecting carbon emissions, we constructed multiple regression models to estimate the coefficients. Model (2) is set as follows:

$$Y = \alpha + \beta_1 policy + \beta_2 pergdp + \beta_3 population + \beta_4 energy + \beta_5 secindustry + \beta_6 tenure + \beta_7 edu + \beta_8 local + \beta_9 center + \beta_{10} intertrans + \varepsilon_{it} \quad (2)$$

Y is the explained variable carbon emission, α is a constant term, β_i ($i = 1, 2, 3, \ldots, 10$) represents the regression coefficient of the explanatory variable and the control variable and ε_{it} is the random error term. Specifically, *policy* represents the implementation of a carbon trading policy, while *tenure*, *edu*, *local*, *center* and *intertrans* are the variables reflecting officials' characteristics. For *pergdp*, *population*, *energy* and *secindustry* denote the control variables. Table 1 provides the detailed variable definitions.

Table 1. Definitions of variables of used to measure the effectiveness of China's carbon emissions trading system and their measurement methods.

	Variable Name	Variable Meaning	Variable Operation	Data Source	Direction
Dependent variable	Emission	Carbon emission	Unit: million tons	CEADs	/
Political factors	Tenure	Official's tenure	Measured by number of years that the official holds his/her position	China Political Elite Database (CPED)	/
	Edu	Official's education background	Measured using sequencing variables, divided into 1 (senior high school or below), 2 (junior college or bachelor's degree), 3 (master's degree), 4 (doctorate)	China Political Elite Database (CPED)	−
	Local	Promoted form local province	Vertical promotion from a local province is recorded as "1", otherwise it is recorded as "0".	China Political Elite Database (CPED)	−
	Center	Transferred from central government	Horizontal transfer from central government is recorded as "1", otherwise it is recorded as "0".	China Political Elite Database (CPED)	+
	Intertrans	Transferred from another province	Horizontal transfer from another province is recorded as "1", otherwise it is recorded as "0".	China Political Elite Database (CPED)	

Table 1. *Cont.*

	Variable Name	Variable Meaning	Variable Operation	Data Source	Direction
Economic and social factors	Pergdp	GDP per capita	Unit: CNY/person	National Bureau of Statistics	+
	Population	Resident population at year end	Unit: ten thousand	National Bureau of Statistics	+
	Energy	Energy consumption per unit of GDP	Ratio of regional energy consumption to regional GDP (unit: ton of standard coal/10,000 CNY)	China Statistical Yearbook	+
	Secindustry	Secondary industry added value	Ratio of added value of secondary industry to regional GDP	National Bureau of Statistics	+

Note: The + and − in the last column indicate that the expected relationship between independent variables and dependent variables is positive or negative, respectively.

3.2. Data and Variables

Considering the comparability and accessibility of the known data, we selected the carbon emissions of 30 provincial administrative units in China as the explanatory variables, including Shenzhen, Beijing, Tianjin, Shanghai, Chongqing, Guangdong and Hubei, all of which have implemented the pilot carbon trading system. In 2003, China proposed the concept of "scientific development". Given the nation's authoritarian political environment, this concept was set to become the new direction of local governments. As a result, local officials attached great importance to the concept of environment protection at this time. In the future, 2003 may be seen as an important turning point in the trajectory of carbon emissions. Given this history, we examined the changes in carbon emissions in selected provinces from 2004 to 2015.

Since the calculation method for carbon emissions is complex and involves a highly specific discipline, the carbon emissions data for each province in this study were obtained from the database website China Emission Accounts and Datasets (CEADs). The independent variable and control variable data were obtained from the following databases: the Chinese Statistical Yearbook, the National Bureau of Statistics, and the Chinese Political Elite Database.

The variables of carbon emissions, economic factors, and social factors were continuous variables obtained from the databases mentioned above, whereas the variables of political factors were obtained by the author through the selected database and quantified for measurement. Among them, the length of an official's term was defined using the method in the existing relevant literature (i.e., the number of years from the beginning of the post to final departure from the position). Since the official appointment and departure time usually occurs in a certain month of a certain year, if the official takes office in the first half of the year (January–June), the year was taken as the starting year of his/her appointment; otherwise, the official term was calculated from the next year. Based on the previous studies, officials' education was measured by sequencing variables and we divided them into 1 (senior high school or below), 2 (junior college or bachelor's degree), 3 (master's degree) and 4 (doctorate) [38]. The sources of the provincial governors were measured by setting dummy variables, in which the reference group was composed of officials promoted from other provinces.

Previous studies have shown that carbon dioxide emissions are affected by various economic and social factors. The consensus is that there is a negative correlation between economic and social development and carbon emissions. This study considers influencing factors as control variables, including the variables of per capita GDP, population, GDP energy consumption and added value of secondary industries.

Per capita GDP (per GDP) was used to reflect the level of economic development in a region. As for the correlation between the economy and carbon dioxide emissions, the mainstream view supports an inverted "U" relationship, namely, the Environmental Kuznets Curve [39]. This means that the environmental quality degrades with an increase in income within a certain range, then improves after the income reaches a certain level. However, another stream of research opposes these findings and rejects the Environmental Kuznets Curve [40]. No consensus has been reached regarding the relationship between economic growth and an increase in carbon dioxide emissions, which may be due to the different economic development stages of the research objects. Because the levels of economic development differed from region to region within China, we believe that provinces and cities with a higher per capita GDP have a greater demand for economic development, and rapid economic development will increase carbon emissions; thus, per capita GDP is positively correlated with greenhouse gas emissions.

Regarding population, Birdsall stated that population growth can affect greenhouse gas emissions in two ways [41]. First, a larger population will have a higher energy demand, which is accompanied by an increase in carbon emissions. Second, rapid population growth often leads to environmental destruction, which is not conducive to the reduction of carbon dioxide. Kaya established the correlation between greenhouse gas emissions and population through the identity of factor decomposition [42]. Through the modified Kaya identity, STIRPAT, and other models, follow-up research has shown that there is a stable and long-term positive correlation between population growth and the urbanization process and carbon emissions. Therefore, we expect a positive correlation between population and carbon emissions.

In terms of GDP energy consumption, the production of carbon dioxide mainly comes from energy consumption, and the carbon emissions of a region are inevitably affected by local energy utilization. The energy consumption per unit of GDP measures the energy utilization of provinces and cities. The measurement unit is the energy consumption per ten thousand CNY of GDP, which reflects the economic benefits of energy consumption. Based on this, we expected a positive correlation between GDP energy consumption and carbon emissions.

As for the added value of secondary industries, empirical studies have proven that secondary industries play an important role in carbon emissions, and the adjustment of industrial structure is an important driving factor of changes in carbon emissions [43]. We used the secondary industry value added ratio to measure the level of industrial structure. Compared with primary and tertiary industries, the energy demand of secondary industries is relatively high. Therefore, it was more intuitive to select the added value of the secondary industries. Based on this, we expected the value-added ratio of the secondary industries to be proportional to carbon emissions. The variables are shown in Table 1 above.

3.3. Descriptive Statistics

Table 2 shows the descriptive statistical analysis of each variable conducted in this study. The diagnosis results of collinearity among variables shows that the variance expansion factor (VIF) is much smaller than 10, indicating that there was no significant collinearity between variables. Based on this, further conclusions were obtained using the econometric regression model.

Table 2. Descriptive statistics of main variables.

Variable Name	Observations	Mean	Standard Deviation	Minimum Value	Maximum Value
Tenure	360	3.186	1.854	1	10
Edu	360	2.743	0.637	2	4
Local	360	0.700	0.459	0	1

Table 2. *Cont.*

Variable Name	Observations	Mean	Standard Deviation	Minimum Value	Maximum Value
Center	360	0.156	0.362	0	1
Intertrans	360	0.097	0.297	0	1
Emission	360	288.91	234.56	5.80	1553.80
Pergdp	360	33,215.43	21,617.04	4317	107,960
Population	360	4413.62	2651.96	539	10,849
Energy	360	1.166	0.651	0.298	4.324
Secindustry	360	0.471	0.077	0.197	0.590

4. Results and Discussions

4.1. Analysis of Parallel Trend Test and DID Results

In this study, based on Formula (1) we used the DID model to test the impact of the carbon emissions trading policy on carbon emissions. However, to be consistent, a key assumption for the DID estimator was the parallel trend hypothesis, also known as the common trend assumption. It states that if there is no policy impact, then the trend of the treatment and control should be parallel and have the same time trend. Otherwise, if the model fails to meet this assumption, this estimation will be biased. Therefore, a parallel trend check was performed for the DID model.

As shown in Figure 1, we drew a comparison diagram of changes in the carbon emission trend between pilot provinces and non-pilot provinces to illustrate the changes before and after the pilot trading system. Figure 1 intuitively shows that prior to the implementation of the carbon emissions trading system in 2013, the growth trend of carbon emissions in the two groups was almost identical; there was no systematic difference over time. However, after initiation of the pilot in 2013, the trends in the pilot provinces changed and carbon emissions were stable or even declining. The non-pilot provinces maintained their pre-2013 growth trends. Therefore, we believe that these data meet the premise of using the DID method, which can successfully identify the net effect of a carbon emissions trading mechanism.

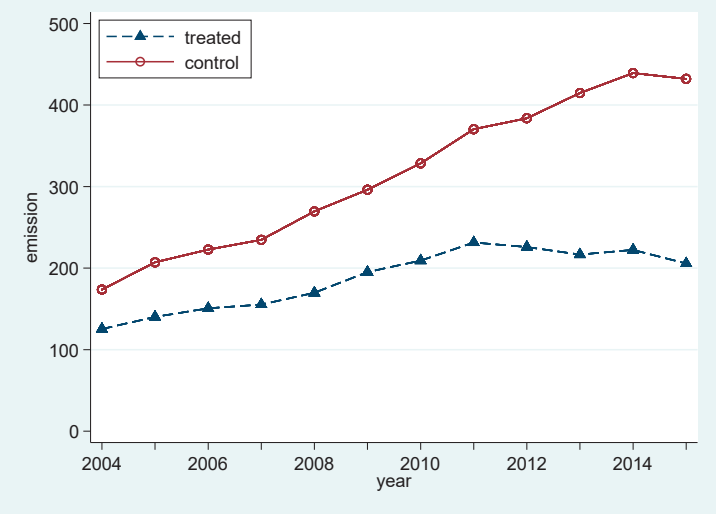

Figure 1. Time trend of carbon emissions in pilot and non-pilot provinces from 2004 to 2015.

The carbon emissions trading system pilot provides us with a quasi-natural experiment. In this study, the effect of this policy was analyzed using the DID method, and the results are shown in Table 3.

Table 3. Effect test of the carbon trading mechanism pilot.

Variable	Model 1	Model 2
Policy	−109.12 ** (41.93)	−147.50 ** (54.24)
Control variables	No	Yes
Individual effect	Yes	Yes
Time effect	Yes	Yes
Constant	262.79 *** (36.62)	−519.70 (262.49)
N	360	355
R^2	0.126	0.535

Note: *** $p < 0.01$, ** $p < 0.05$; Outside the brackets are the coefficients, and within the brackets are the robust standard errors aggregated at the provincial level.

In Table 3, Model 1 is the estimated result without the control variables, while Model 2 is the estimated result by adding in the control variables. The regression coefficient of the carbon emissions trading system policy is significantly negative at the 5% level, indicating that the carbon trading system has a significant effect on carbon emissions reduction in the pilot provinces. Compared with the non-pilot provinces, the carbon trading system reduced carbon emissions in the pilot provinces by an average of more than 140 million tons. Hypothesis 1 is therefore verified, which indicates that China's carbon emissions trading system has a significantly positive effect on reducing China's carbon emissions.

4.2. Effect Test of Related Variables

4.2.1. Regression Results

Based on Formula (2), the regression results are shown in Table 4. Model 3 is a regression result that includes only economic and social factors; Model 4 presents the regression result that includes only the factors of political mobility; finally, Model 5 is the whole model with both dependent and control variables.

Table 4. Influence of the carbon emission trading policy on carbon emission reduction performance.

Variable	Model 3	Model 4	Model 5
$G_i \cdot D_t$	−155.61 *** (43.20)	−100.47 (78.39)	−130.95 ** (48.86)
Tenure		4.28 (9.21)	−6.90 (7.45)
Edu		16.76 (40.98)	−1.10 (35.38)
Local		−79.93 (76.27)	−29.79 (56.01)
Center		−9.15 (94.14)	−6.68 (61.48)
Intertrans		−209.74 ** (85.33)	−152.06 * (72.94)
Pergdp	0.005 *** (0.001)		0.005 *** (0.001)
Population	0.045 *** (0.010)		0.044 *** (0.011)
Energy	79.55 * (42.94)		88.53 ** (39.20)
Secindustry	651.99 *** (226.94)		776.21 *** (224.34)
Constant	−457.54 *** (144.57)	365.58 (264.82)	−509.95 ** (267.16)
N	360	355	355
R^2	0.491	0.166	0.527

Note: *** $p < 0.01$, ** $p < 0.05$, * $p < 0.1$; The robust standard errors aggregated at the provincial level are reported in the parentheses.

The results show that local official tenure has no significant relationship with carbon emissions reduction. As a consequence, Hypothesis 2 cannot be proved. The results also indicate that only the officials transferred from other provinces had a significant negative impact on carbon emissions, thus supporting Hypothesis 3-c. Officials who were promoted from within their provinces tended to have higher carbon emissions reduction performance

than those from the central agencies; this is consistent with the hypothetical direction, but the differences are not significant. Thus, the effectiveness of carbon emissions for officials promoted from different sources suggests that political mobility influences the provincial government leaders' environmental governance performance. Although the influence coefficient of education in Model 5 on the performance of carbon emissions is negative, it is not significant so Hypothesis 4 cannot be proved. Generally, these results validate the logic behind the actions of government officials. However, most of them failed to pass the significance test because local officials usually must pursue many vague and pluralistic goals. Environmental performance is not yet the core focus of China's official assessment indicators. As such, the exact role that an official's characteristics play in environment performance cannot be well understood.

The results of the control variables related to the economy and society were all in line with expectations. The coefficient of the per capita GDP of the region was significantly positive at the 1% level. This indicates that China's economic development level is still in a relatively early stage, and is highly dependent on the sacrifice of environmental resources. China's economic growth has not passed the stage of "exchanging environmental quality for economic growth". The coefficient of the variable population is significantly positive, which indicates that China, as a country with a large population, undoubtedly contributes significantly to the emission of carbon dioxide. The coefficients of energy per unit of GDP and value added of secondary industries are also significantly positive, which is also in line with general experience. Currently, China's energy structure is not especially advanced, and the further development of secondary industries will still primarily depend on energy consumption. In sum, the conflict between economic development and the capability of environment governance has become increasingly evident, which has caused a negative impact on the overall level of carbon emissions.

4.2.2. Interaction Effect Test

To test the interaction effect between the political factors and carbon emissions, this study examined the moderating effects of official sources on the correlation between tenure and career path on carbon emissions by referring to the test method of interaction effects in the regression analysis. Table 5 reports the test results.

Table 5. Regression results of interaction effects of the variables regarding political mobility.

Variable	Model 6	Model 7	Model 8
Local	28.59 (28.12)		
Local × tenure	26.80 ** (12.10)		
Local × tenure^2	−0.12 (1.67)		
Center		52.70 (39.73)	
Center × tenure		−20.54 * (11.78)	
Center × tenure^2		−10.13 * (5.07)	
Intertrans			−120.27 ** (44.67)
Intertrans × tenure			−22.79 ** (9.72)
Intertrans × tenure^2			−2.52 (8.03)
Constant	−516.80 ** (188.01)	−451.45 ** (165.55)	−467.97 *** (155.17)
N	355	355	355
R^2	0.502	0.496	0.512

Note: *** $p < 0.01$, ** $p < 0.05$, * $p < 0.1$; Outside the brackets are the coefficients, and within the brackets are the robust standard errors aggregated at the provincial level.

The regression results show that the interaction effect between the source and the term of the selected governor has passed the significance test, thus verifying the regulatory effect of official sources on government performance. The interaction effect between local promotion and tenure was significantly positive, while the transfers of central and provincial and tenure were both significantly negative. That is to say, the longer the tenure of the local official who was promoted, the more carbon emissions tended to increase. On

the other hand, officials moving from the central government and those moving to a new province had the opposite result. This indicates that government officials from different sources have different carbon emissions reduction performance levels.

4.3. Robustness Test

In this study, robustness tests were carried out, including the widely used single-difference test, counter-fact test and matching method, to ensure the reliability of the results.

4.3.1. Single Difference Test

According to the traditional treatment method, we used the single difference method to estimate the impact of the carbon emissions trading system on carbon emissions. The regression results are shown in Table 6. As expected, the single difference test overestimates the effectiveness of the carbon emissions trading system. Meanwhile, it proves the validity of our DID estimation results.

Table 6. Single difference test estimation results of the impact of the carbon emissions trading system.

Variable	Model 9	Model 10
Policy	−127.08 * (62.92)	−146.87 ** (62.75)
Control variables	No	Yes
Individual effect	Yes	Yes
Time effect	No	No
Constant	314.32 *** (43.54)	49.14 (25,765.05)
N	360	343
R^2	0.047	0.287

Note: *** $p < 0.01$, ** $p < 0.05$, * $p < 0.1$; Outside the brackets are the coefficients, and within the brackets are the robust standard errors aggregated at the provincial level.

4.3.2. Counterfactual Test

Drawing on the robustness of the test methods used in previous research, we conducted counterfactual tests by changing the setting of policy pilot provinces. If the coefficient of the carbon emissions trading system was still significantly negative, it indicated that carbon emission decline may be a result of other policies or random factors, but not necessarily a result of the carbon emissions trading mechanism. The test results are listed in Table 7. Six pilot provinces were chosen: Zhejiang, Anhui, Jiangxi, Shandong, Henan and Hunan. Model 12 and Model 11 are the estimated results with and without the addition of control variables, respectively. Six additional pilot provinces were then chosen: Yunnan, Qinghai, Shaanxi, Gansu, Ningxia and Xinjiang. Model 14 and Model 13 are the estimated results with and without the addition of control variables, respectively. The coefficients of the four models were not significant. This indicates that the downward trend of carbon emissions in the pilot provinces and selected cities was caused by the carbon emissions trading system rather than other factors.

Table 7. Results of the counterfactual test.

Variable	Model 11	Model 12	Model 13	Model 14
Policy	−21.39 (45.01)	−79.05 (52.50)	−5.91 (58.28)	34.99 (61.23)
Control variables	No	Yes	No	Yes
Individual effect	Yes	Yes	Yes	Yes
Time effect	Yes	Yes	Yes	Yes
Constant	221.93 *** (28.81)	−571.20 * (264.69)	270.84 *** (36.23)	−543.08 ** (307.57)
N	360	355	360	355
R^2	0.104	0.495	0.123	0.502

Note: *** $p < 0.01$, ** $p < 0.05$, * $p < 0.1$; Outside the brackets are the coefficients, and within the brackets are the robust standard errors aggregated at the provincial level.

4.3.3. Matching Test

Although the carbon emissions trading system pilot successfully met the conditions necessary to be considered a quasi-experiment, the choice of pilot provinces may have had endogenous problems, leading to selection bias. Matching pre-processing prior to estimating the causal effect can solve this problem under non-random experimental conditions and thus overcome the problem of choice. The idea of the matching method was derived from the matching estimator of the counterfactual framework. The basic idea was to find the individual belonging to the control group so that the value of the measurable variable was as close as possible to the value of the experimental group. That is, the matching method could be used to separate a matching sample with relatively balanced covariates to find randomized experimental samples hidden in the observed data. Therefore, it became obvious which samples could be used to estimate the matching estimators, and the resulting matching estimators could be interpreted as the individual causal effects [44]. In addition, the use of matching samples for analysis can make the estimation results more robust and less sensitive to functional forms, as well as reduce the model dependence of the subsequent regression analysis to estimate causal effects.

This study used the ebalance command to perform matching, and the matching principle was the entropy balancing method. The entropy balancing method is a multivariate weighting method which overcomes some of the problems encountered in traditional matching methods, such as nearest neighbor matching and propensity score matching. Traditional matching methods involve a long matching process in which it is difficult to balance all the covariates. In practice, the matching covariate balance is often low.

The entropy balancing method directly integrated the covariate balance into the weight function used to adjust the control group data. Based on the maximum entropy weight, the data can satisfy as large a balance constraint as possible. Compared with the traditional matching method, the entropy balance method has some advantages. Because the weight value in the entropy balance is directly adjusted to the known sample moment, the covariate balance of the traditional processing method under the constraint of a given moment is improved; therefore, a balance test is not required. In addition, because the entropy balance weight changes smoothly between each element, this method retains more information than other methods and the estimated result after matching is more accurate.

Table 8 shows the balanced results of the matched variables. As mentioned above, due to the particularity of the value of the political and business relationship in the variable, multiple matching methods still cannot achieve effective matching, which increases the overall matching difficulty. Therefore, this variable is not included in the matching process. Compared with the results before matching, the deviations of the matched treated group and the control group are effectively reduced, and the mean and standard deviation of the matching variables are also very close, indicating that the selected matching method is appropriate. Therefore, the estimation results are reliable.

Table 8. Results of covariate equilibrium.

Variable	Means			Variances			Skewness		
	Treated	Control		Treated	Control		Treated	Control	
		Pre	Post		Pre	Post		Pre	Post
Tenure	3.972	3.011	3.972	4.816	2.933	3.407	0.696	0.828	0.698
Edu	2.917	2.700	2.917	0.416	0.395	0.084	0.075	0.330	−2.566
Local	0.639	0.717	0.639	0.234	0.204	0.232	−0.578	−0.965	−0.578
Center	0.056	0.184	0.056	0.053	0.151	0.053	3.881	1.663	3.880
Intertrans	0.181	0.071	0.180	0.150	0.066	0.149	1.661	3.351	1.661
Pergdp	52,746	28,448	52,744	7.67×10^8	2.77×10^8	3.77×10^8	0.338	1.020	0.179
Population	4012	4467	4012	9,668,793	6,210,363	8,951,918	1.123	0.397	0.434
Energy	0.771	1.266	0.771	0.092	0.467	0.160	0.885	1.521	1.432
Secindustry	0.438	0.480	0.438	0.010	0.005	0.013	−1.123	−1.235	−0.872

After matching, we again estimated the effectiveness of the carbon emissions trading system on emissions reduction. The results are shown in Table 9. Model 15 is the estimated result without the addition of control variables after matching, and Model 16 is the estimated result after considering other relevant influencing factors after matching. Regardless of whether control variables were added, the coefficient of policy was significantly negative. That is, the carbon emissions trading system promoted carbon emission reduction in pilot provinces, which was consistent with the estimation result of DID. In other words, after considering the problem of sample selection bias, Hypothesis 1 of this paper was still valid, which further indicated that the DID estimation results were robust and reliable.

Table 9. Net effect test of carbon trading system after matching.

Variable	Model 15	Model 16
Policy	−173.97 ** (68.45)	−128.21 *** (25.06)
Control variables	No	Yes
Individual effect	Yes	Yes
Time effect	Yes	Yes
Constant	361.22 *** (66.98)	224.44 (150.61)
N	355	355
R^2	0.140	0.790

Note: *** $p < 0.01$, ** $p < 0.05$; Outside the brackets are the coefficients, and within the brackets are the robust standard errors aggregated at the provincial level.

5. Conclusions and Policy Implications

China attaches great importance to and plays a constructive role in climate change. In the Paris Agreement, the Chinese government committed to the target of achieving peak carbon emissions by 2030 [45]. The central government has gradually improved the mechanisms of carbon emissions reduction by implementing a market-oriented carbon trading system. The environmental regulation tools and the concept of low carbon have made progress in controlling carbon emissions and adapting to climate change.

Starting with the development of carbon neutrality strategies in China, this paper constructed a quasi-natural experiment based on the DID method to evaluate the effectiveness of carbon emission reductions by China's carbon trading system from a perspective of political mobility with panel data for 30 provinces in China from 2004 to 2015, and it conducted a robustness test using the counterfactual test and matching test to further test the robustness of the results. This paper mainly makes contributions in three aspects. First, on the theoretical side, in addition to examining the impact of the carbon trading system on carbon emissions, this study's findings help to explain the impact of political factors on environmental governance. Second, on the methodology side, the DID model and various robustness tests this paper conducted have expanded the processes available to evaluate the policy's net effect on carbon emissions and revealed the effect of officials' incentives to reduce emissions. Finally, on the practical side, this paper helps the central government to gain a deeper understanding of carbon emissions trading, so as to design more effective and targeted strategies for motivating officials and supervising policy implementation to promote carbon neutralization and environmental development. This paper aimed to explore potential feasible ways to reduce carbon emissions to promote the realization of carbon neutrality as soon as possible. Therefore, the main implications based on the empirical results are as follows. Throughout the research, the results demonstrated that political mobility has significant effects on the reductions of carbon dioxide emissions in the context of local promotion. The target of carbon neutrality indicated that in the long run the government and local officials will face continuous pressures, so their behavior should no longer be ignored. First, the Chinese central government should pay more attention to the environmental performance of local officials through the appraisal system. GDP can no longer be the most important indicator of political mobility. Second, the behavior of local officials should also be of concern. The promotion path of provincial leaders influences their political performance. By optimizing the appraisal system and rationalizing

how assessment proportions are weighted, local officials can be made to focus on carbon emissions reduction through political mobility. Finally, environmental protection indicators should become the priority during the assessment of government officials.

Furthermore, the carbon emissions trading system is an effective policy tool to reduce carbon intensity and promote carbon neutrality. Several policy implications and suggestions based on this policy can also be drawn. First, due to China's outdated development mode and its secondary industries, which are important causes of its recent energy consumption and carbon emission increases, it is necessary for China to maintain energy conservation and emissions reduction to achieve the goal of carbon neutrality. Second, with the implementation of the carbon emissions trading system, enterprises should develop the new industrialization path and accelerate the transformation of the industrial structure in order to improve the utilization efficiency of energy based on this new type of market-orientated policy emissions reduction policy. Third, by vigorously developing technology-intensive industries to replace pollution-intensive industries and increasing reliance on large-scale and advanced industrial enterprises, the utilization rate of resources can be improved. In short, the carbon trading system and other market-oriented governance tools can serve an important role in dealing with carbon emissions challenges in achieving carbon neutrality. Moreover, the application of advanced technology to secondary industries and emission reduction targets is an additional and more effective way to fundamentally reduce carbon emissions. In other words, the realization of carbon neutrality needs diversified paths, as well as suitable incentive mechanisms.

However, this paper also has some limitations. Owing to limited data availability, this study used provincial panel data to evaluate the effect of carbon trading on emissions reduction. However, there may have been other factors affecting carbon emissions. Future researchers could test other factors based on this study's findings. Carbon emissions trading in a variety of cities should also be investigated to assess its reduction effectiveness. Additionally, more impact variables should be used to establish a larger and more comprehensive database. These approaches could be helpful in obtaining more significant results.

Author Contributions: Conceptualization, Z.L.; methodology, Z.L. and B.L.; formal analysis, B.L.; writing—original draft preparation, B.L.; writing—review and editing, Z.L.; supervision, Z.L.; funding acquisition, Z.L. All authors have read and agreed to the published version of the manuscript.

Funding: This research has been supported by the National Natural Science Foundation of China (NO. 71974057) and the 'Shu Guang' project (Grant No. 21SG49) supported by the Shanghai Municipal Education Commission and the Shanghai Education Development Foundation.

Data Availability Statement: The datasets generated and/or analyzed during the current study are available from the corresponding author on reasonable request.

Conflicts of Interest: The authors declare that they have no known competing financial interest or personal relationships that could have appeared to influence the work reported in this paper.

Abbreviations

CEAD, China Emission Accounts & Datasets; DID, difference-in-differences model; VIF, variance inflation factor.

References

1. Friedlingstein, P.; Andrew, R.; Rogelj, J.; Peters, G.; Canadell, J.; Knutti, R.; Luderer, G.; Raupach, M.; Schaeffer, M.; van Vuuren, D.P.; et al. Persistent growth of CO_2 emissions and implications for reaching climate targets. *Nat. Geosci.* **2014**, *7*, 709–715. [CrossRef]
2. Bronselaer, B.; Zanna, L. Heat and carbon coupling reveals ocean warming due to circulation changes. *Nature* **2020**, *584*, 227–233. [CrossRef]
3. Gao, Z.; Li, S.; Cao, X.; Li, Y. Carbon Emission Intensity Characteristics and Spatial Spillover Effects in Counties in Northeast China: Based on a Spatial Econometric Model. *Land* **2022**, *11*, 753. [CrossRef]
4. Mallapaty, S. How China could Be carbon neutral by mid-century. *Nature* **2020**, *586*, 482–483. [CrossRef] [PubMed]

5. Matthias, D.; Baumgartner, R.J. Intra-sectoral differences in climate change strategies: Evidence from the global automotive industry. *Bus. Strat. Environ.* **2018**, *27*, 265–281.
6. Rojas Sanchez, D.; Hoadley, A.F.A.; Khalilpour, K.R. A multi-objective extended input-output model for a regional economy. *Sustain. Prod. Consum.* **2019**, *20*, 15–28. [CrossRef]
7. Feng, K.; Davis, S.; Sun, L.; Hubacek, K. Drivers of the US CO_2 emissions 1997–2013. *Nat. Commun.* **2015**, *6*, 7714. [CrossRef] [PubMed]
8. Schaefer, S. Decoupling the EU ETS from subsidized renewables and other demand side effects: Lessons from the impact of the EU ETS on CO_2 emissions in the German electricity sector. *Energy Policy* **2019**, *133*, 110858. [CrossRef]
9. Dorta Antequera, P.; Díaz Pacheco, J.; López Díez, A.; Bethencourt Herrera, C. Tourism, Transport and Climate Change: The Carbon Footprint of International Air Traffic on Islands. *Sustainability* **2021**, *13*, 1795. [CrossRef]
10. Newig, J. Public Attention, Political Action: The Example of Environmental Regulation. *Ration. Soc.* **2004**, *16*, 149–190. [CrossRef]
11. Li, X.; Liu, C.; Weng, X.; Zhou, L. Target Setting In Tournaments: Theory And Evidence From China. *Econ. J.* **2019**, *129*, 2888–2915. [CrossRef]
12. Vine, E.; Hamrin, J. Energy savings certificates: A market-based tool for reducing greenhouse gas emissions. *Energy Policy* **2008**, *36*, 467–476. [CrossRef]
13. Gersbach, H.; Glazer, A. Markets and regulatory hold-up problems. *J. Environ. Econ. Manag.* **1999**, *37*, 151–164. [CrossRef]
14. Dales, J.H. *Pollution, Property and Prices: An Essay in Policy-Making and Economics*; Edward Elgar Publishing: Northampton, MA, USA, 1968.
15. Montgomery, W.D. Markets in licenses and efficient pollution control programs. *J. Econ. Theory* **1972**, *5*, 395–418. [CrossRef]
16. Tang, L.; Wang, H.; Li, L.; Yang, K.; Mi, Z. Quantitative models in emission trading system research: A literature review. *Renew. Sustain. Energy Rev.* **2020**, *132*, 110052. [CrossRef]
17. Dong, Z.; Wang, S.; Zhang, W.; Shen, H. The dynamic effect of environmental regulation on firms' energy consumption behavior-Evidence from China's industrial firms. *Renew. Sustain. Energy Rev.* **2021**, *156*, 111966. [CrossRef]
18. Martin, R.; Muuls, M.; Wagner, U.J. The impact of the European Union emissions trading scheme on regulated firms: What is the evidence after ten years? *Rev. Environ. Econ. Policy* **2016**, *10*, 129–148. [CrossRef]
19. Nie, X.; Chen, Z.; Yang, L.; Wang, Q.; He, J.; Qin, H.; Wang, H. Impact of Carbon Trading System on Green Economic Growth in China. *Land* **2022**, *11*, 1199. [CrossRef]
20. Ales, L.; Maziero, P.; Yared, P. A theory of political and economic cycles. *J. Econ. Theory* **2014**, *153*, 224–251. [CrossRef]
21. Yang, X.; Yan, J.; Tian, K.; Yu, Z.; Li, R.; Xia, S. Centralization or decentralization? the impact of different distributions of authority on China's environmental regulation. *Technol. Forecast. Soc.* **2021**, *173*, 121172. [CrossRef]
22. Wang, X.; Lei, P. Does strict environmental regulation lead to incentive contradiction?—Evidence from China. *J. Environ. Manag.* **2020**, *269*, 110632. [CrossRef] [PubMed]
23. Zhang, Y.; Zhu, X. The Moderating Role of Top-Down Supports in Horizontal Innovation Diffusion. *Public Adm. Rev.* **2020**, *80*, 209–221. [CrossRef]
24. Duan, H.; Zhang, G.; Wang, S.; Fan, Y. Integrated benefit-cost analysis of China's optimal adaptation and targeted mitigation. *Ecol. Econ.* **2019**, *160*, 76–86. [CrossRef]
25. Zhang, J.; Fan, H.C.; Xu, Z.W.; Zhou, L.F. The structural reduction of GDP growth: From the perspective of official assessment mechanism. *Econ. Res. J.* **2020**, *55*, 31–48.
26. Chen, Y.; Li, H.; Zhou, L.A. Relative performance evaluation and the turnover of provincial leaders in China. *Econ. Lett.* **2005**, *88*, 421–425. [CrossRef]
27. He, L.; Wan, H.; Zhou, X. How are political connections valued in China? Evidence from market reaction to CEO succession. *Int. Rev. Financ. Anal.* **2014**, *36*, 141–152. [CrossRef]
28. Davis, F.L.; Wurth, A.H. Voting preferences and the environment in the American electorate: The discussion extended. *Soc. Nat. Resour.* **2003**, *16*, 729–740. [CrossRef]
29. Nathan, A.J. A factionalism model for CCP politics. *China Q.* **1973**, *53*, 34–66. [CrossRef]
30. Teiwes, F. Normal politics with Chinese characteristics. *China J.* **2001**, *45*, 69–82. [CrossRef]
31. Bo, Z. *Chinese Provincial Leaders: Economic Performance and Political Mobility Since 1949: Economic Performance and Political Mobility Since 1949*; Routledge: Abingdon, UK, 2019.
32. Meier, K.J.; Favero, N.; Zhu, L. Performance Gaps and Managerial Decisions: A Bayesian Decision Theory of Managerial Action. *J. Public Adm. Res. Theory* **2015**, *25*, 1221–1246. [CrossRef]
33. Duan, H.; Hu, Q. Local officials' concerns of climate change issues in China: A case from Jiangsu. *J. Clean. Prod.* **2014**, *64*, 545–551. [CrossRef]
34. Zhou, Q.; Zeng, J. *Promotion Incentives, GDP Manipulation and Economic Growth in China: How Does Sub-National Officials Behave When They Have Performance Pressure?* SSRN: Rochester, NY, USA, 2018.
35. Xi, T.; Yao, Y.; Zhang, M. Capability and opportunism: Evidence from city officials in China. *J. Comp. Econ.* **2018**, *46*, 1046–1061. [CrossRef]
36. Spilerman, S.; Lunde, T. Features of educational attainment and job promotion prospects. *Am. J. Sociol.* **1991**, *97*, 689–720. [CrossRef]

37. Johnson, P.; Durlauf, S.N.; Temple, J. Growth Econometrics. In *Handbook of Economic Growth*; Elservier: Amsterdam, The Netherlands, 2005; Volume 1, Part A(1); pp. 65–69.
38. Shan, Y.; Guan, D.; Zheng, H.; Ou, J.; Li, Y.; Meng, J.; Mi, Z.; Liu, Z.; Zhang, Q. China CO2 emission accounts 1997–2015. *Sci. Data* **2018**, *5*, 170201. [CrossRef]
39. Ota, T. Economic growth, income inequality and environment: Assessing the applicability of the Kuznets hypotheses to Asia. *Palgrave Commun.* **2017**, *3*, 17069. [CrossRef]
40. Saqib, M.; Benhmad, F. Updated meta-analysis of environmental kuznets curve: Where do we stand? Environ. *Impact Assess. Rev.* **2021**, *86*, 106503. [CrossRef]
41. Birdsall, N. Another Look at Population and Global Warming: Population, Health and Nutrition Policy Research. In *Working Paper*; WPS 1020; World Bank: Washington, DC, USA, 1992.
42. Kaya, Y. *Impact of Carbon Dioxide Emission Control on GNP Growth: Interpretation of Proposed Scenarios*; IPCC: Paris, France, 1990.
43. Han, F.; Huang, M. Land Misallocation and Carbon Emissions: Evidence from China. *Land* **2022**, *11*, 1189. [CrossRef]
44. Hainmueller, J. Ebalance: A Stata package for entropy balancing. *J. Stat. Softw.* **2013**, *54*, 1–17. [CrossRef]
45. UNFCCC, 2018. Intended Nationally Determined Contributions (INDCs). Available online: https://unfccc.int/documents/4107 (accessed on 1 April 2023).

land

MDPI

Article

Research on Forest Ecological Product Value Evaluation and Conversion Efficiency: Case Study from Pearl River Delta, China

Jingyu Wang [1,2], Wei Liu [3] and Fanbing Kong [1,2,4,*]

[1] Institute of Ecological Civilization, Zhejiang A & F University, Hangzhou 311300, China; wangjy@zafu.edu.cn
[2] College of Economics and Management, Zhejiang A & F University, Hangzhou 311300, China
[3] College of Geography and Environment, Shandong Normal University, Jinan 250358, China
[4] Institute of Digital Forestry & Green Development, Nanjing Forestry University, Nanjing 210037, China
* Correspondence: kongfanbin@aliyun.com

Abstract: Exploring an effective scientific method to measure the economic benefits of ecological products is of great significance for green development. Based on the InVEST model, this paper, taking the Pearl River Delta (PRD) as an example, evaluated the FEPs value in the PRD from 2000 to 2015; using a super-efficient DEA model, the conversion efficiency of ecological products was estimated, and its temporal and spatial variation characteristics were analyzed using the Malmquist index. The results showed that the value of FEPs in the PRD shot up during 2000–2015, and that the regulation services value is the main part of FEPs, followed by the value of cultural service. The overall conversion efficiency of FEPs is improving. However, cities differ greatly. Technical efficiency is the key driving factor for improving forest product conversion efficiency. The main reasons for the current efficiency loss are redundant inputs and insufficient outputs. This paper also suggests that conversion efficiency is a convincing method to evaluate the degree of transformation of ecological environment resources into economic benefits and the degree of ecological and economic coordinated development.

Keywords: forest ecological product; value evaluation; conversion efficiency; Pearl River Delta

Citation: Wang, J.; Liu, W.; Kong, F. Research on Forest Ecological Product Value Evaluation and Conversion Efficiency: Case Study from Pearl River Delta, China. *Land* **2023**, *12*, 1803. https://doi.org/10.3390/land12091803

Academic Editor: Eusebio Cano Carmona

Received: 7 August 2023
Revised: 11 September 2023
Accepted: 12 September 2023
Published: 18 September 2023

1. Introduction

With the advancements in urbanization and industrialization in China, the conflict between human beings and ecology has become increasingly prominent [1]. These problems include poor infrastructure [2], poor air quality [3], severe soil pollution [4], and the growth in energy consumption far exceeding domestic energy production [5]. Resolving the conflict between economic development and ecological environment protection is undoubtedly a major challenge. As a factor of production in the economic system, the influence of ecological capital on the regional economy has attracted widespread attention from scholars [6,7]. Through comprehensive governance of the ecological environment, the international community promotes the coordinated development of ecological construction while improving the local socio-economic level, environmental protection, and socio-economic systems [8]. Therefore, an indicator is needed to evaluate the degree of transformation of ecological environment resources into economic benefits to measure the degree of ecological and economic coordinated development in this region [9].

The concept of ecological products has not yet been uniformly defined. Research is more focused on ecosystem services [10] or environmental services (Environmental Services) [11], and some of these are expressed as eco-label products [12]. Ecosystem services refer to the benefits that humans derive directly or indirectly from ecosystems [13], including the provision, regulation, support, and cultural services necessary to sustain life and protect the integrity of ecosystems [14]. As far as the relationship between ecosystem

services and ecological products is concerned, on the one hand, ecological products are equated with ecosystem services that generate positive externalities and are collectively referred to as tangible material products and intangible services provided by pure, natural systems; on the other hand, ecological products are divided into narrow and broad concepts. Ecosystem services in the narrow sense are equivalent to ecological products, and ecological products in the broad sense include products or services produced by human activities, in addition to products or services produced by natural systems, including artificial attributes and human labor [15]. Ecological products refer to the collection of goods and services for the purpose of human consumption and utilization through the interaction between ecosystem production and human social production, and constitute the necessities of human life together with agricultural products and industrial products. Forest ecological products are considered to be ecosystem services that use forest resources to provide human beings with high-quality life and production factors within a certain period of time. Forest ecological products have three main characteristics: tradability, which has the transaction attributes of human economic activities [16]; consumption, which has the consumption attributes of human economic activities and contains added value; relevance, which is the relationship between natural resources and human activities. The recognition of ecological products is not only necessary to enhance the supply of ecological services, but also to convert ecological products into economic gains [17,18]. At the national level, converting ecological products into economic benefits has become a priority.

The value conversion of ecological products relies on scientific calculations of the ecological services value. The accounting methods are various. Some scholars adopt the equivalence factor method on the basis of ecosystem classification; this is the service value equivalent for an overall accounting of different ecosystems [19,20]. The functional value method has also been recognized by scholars [21]. Based on field measurements and statistical data, the physical quantity and service quantity of products provided by the ecosystem are calculated, and the total value is obtained by summing them up [22,23]. The former method is widely comparable; however, it is difficult to distinguish the value of each service. The calculation results of the latter method are more authentic and credible, but too many parameters and data are required [24,25]. Research on ecological products mainly focuses on the supply of ecosystem products, ecosystem regulation services, cultural services, and gross ecosystem product (GEP).

Research on the conversion of ecological products to economic value focuses on the analysis of the transformation path. Considering the public goods characteristics of ecological products, a variety of policy tools have been used to convert ecological products into economic profit [26–28]. However, there are defects, such as policy support system construction, and lagged market evolution; additionally, competition incentives struggle to meet diversified needs [29]. Other conversion paths include the market path [30] and the social path. The specific conversion methods mainly include ecological protection compensation [31], ecological ownership transactions [32], commercial development [33], green financial support [34], policy incentives [35], and other measures [36]. Different implementation methods for the same ecological product have different effects [37]. Research on the value conversion evaluation of ecological products is still in its infancy, and the evaluation methods mainly include two types based on numerical ratio and efficiency. The former mainly includes the green (green water and lush mountains) gold (gold and silver mountains) index represented by the ratio of GEP to EDP (gross domestic product adjusted by ecological environment factors) [38]. The latter incorporates GEP into the economic efficiency system to measure the value-conversion efficiency of ecological products [39]. The former only uses simple mathematical ratios for evaluation, and the economic significance of the conclusion is slightly insufficient, while the latter can still be further improved in the construction of the evaluation system.

As a production factor existing in the economic system, ecological capital affects the growth of the regional economy [40], and promotes the welfare of the people and wealth accumulation [41]. Therefore, based on the framework of ecological efficiency [42], ecological

capital is included in the variables of the ecological economic growth model, and, together with traditional production factors, is the main factor to enhance the coordination between ecology and economy [43]. The ecological product conversion efficiency, representing the efficiency of converting GEP into GDP, was selected to evaluate the degree of transformation of ecological environment resources into economic benefits to measure the degree of ecological and economic coordinated development [44], which is an important basis for the scientific evaluation and continuous optimization of ecological product value. To empirically analyze the forest ecological products (hereafter referred to as FEPs) conversion efficiency, this paper uses the Pearl River Delta (hereafter referred to as PRD) region as an example.

2. Materials and Methods

2.1. Study Area

The nine cities in the PRD are Guangzhou, Shenzhen, Foshan, Zhaoqin, Dongguan, Zhongshan, Zhuhai, Jiangmen, and Huizhou [45] (Figure 1), and they make up the main component of the Guangdong–Hong Kong–Macao Greater Bay Area [46]. In 2020, the PRD had a total land area of 54,766 km^2, a regional GDP of CNY 8952.4 billion, and a resident population of 78,235,400. With a land area of 0.57%, it houses 5.12% of the population and is responsible for 7.82% of the GDP. The area of forest land is 2.83 million hectares, with a forest-coverage rate of 51.73%. All nine cities have been named "National Forest Cities" and have basically built the country's first "National-level Forest City Cluster Demonstration Zone" [47]. Therefore, taking the PRD as an example by quantitatively evaluating the value of FEPs and value conversion efficiency in large-scale urban agglomerations, and proposing optimization countermeasures to promote the development of an ecological socio-economic system of high quality, this study will provide a reference for large-scale urban agglomerations to explore the ecological product value conversion mechanisms.

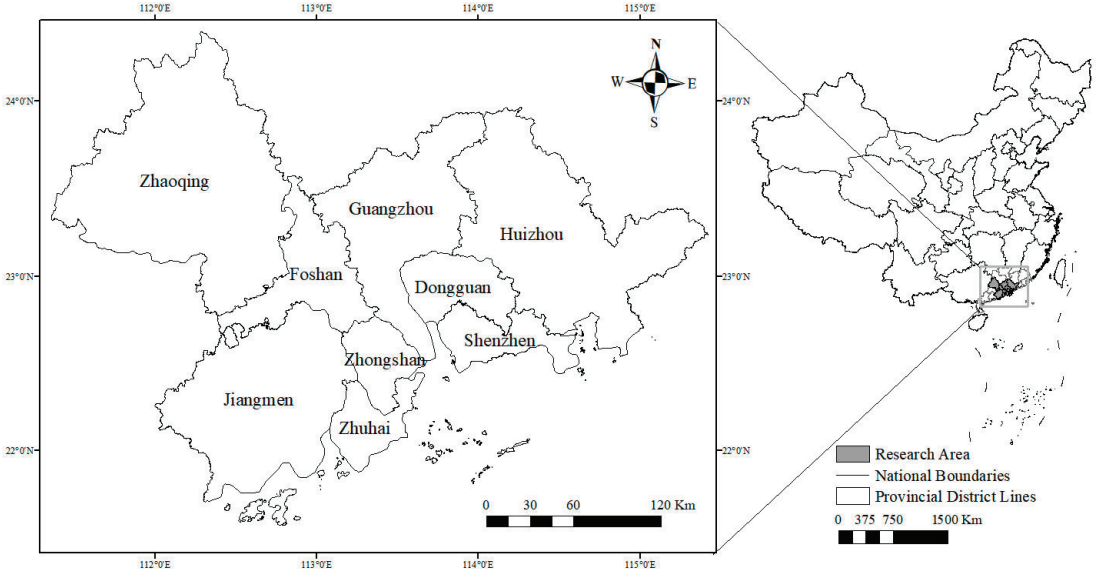

Figure 1. Location of Pearl River Delta.

2.2. Method

2.2.1. Calculation Method of GEP

The calculation of GEP refers to the methods of Ouyang [48] and divides GEP into three parts: the value of material products, regulation services products, and cultural

products [49] (Table 1). The physical quantity and its distribution characteristics are calculated based on the InVEST model and GIS technology.

$$V_m = \sum_{i=1}^{n} F_i \times P_i \quad (1)$$

where V_m is the value of forest material products. F_i is the yield of forest product i. P_i is the market price of forest product i.

Table 1. GEP calculation method.

GEP	Index	Methods
Material product value	Forest products	Market value method
Regulating service value	Conservation of water sources	Shadow price method
	Carbon fixation and oxygen release	Alternative costing method
	Air purification	Alternative costing method
	Soil conservation	Alternative costing method
Cultural service value	Forestry tourism	Travel expense method

The regulating service consists of four parts: the conservation of water sources; carbon fixation and oxygen release; air purification; and soil conservation. Using the shadow price method, we estimated the value of the forest ecosystem's water conservation services. According to previous studies, the storage cost per unit is 1.5 CNY/m^3 [50]. The Water Balance Equation was used to estimate the output of aquatic products. Monthly water production is as follows:

$$WY = PPT - ET \pm S \approx PPT - ET \quad (2)$$

where S is the change in water storage capacity. PPT is monthly precipitation. ET is the actual monthly evaporation amount, which can be estimated as follow:

$$ET(R,t) = \frac{A * R}{A + B * R^2 * EXP\left(-\frac{C*t}{235+t}\right)} \quad (3)$$

Among them, A, B, and C are empirical coefficients, which are related to the temperature in various places. Therefore, the values in the PRD region are 3100, 1.8, and 34.4, respectively. R is the monthly precipitation (mm), and t is the monthly average temperature (°C).

The calculation of the carbon fixation and oxygen release value adopts the method of alternative cost. This study uses the average value of CNY 272.65/t of China's afforestation cost per ton of CO_2 fixed in the forest ecosystem calculated in the relevant research [51]. The net primary production (NPP) of the ecosystem was evaluated to measure its carbon sequestration and oxygen release. The productivity of vegetation is influenced by natural factors such as climate, soil, topography, and human factors [52]. This study used the CASA (Carnegie Ames Stanford Approach) model [53] to estimate NPP and further calculate the CO_2 absorption of vegetation.

Alternative cost methods have also been used to calculate the value of air purification based on an assessment of the amount of air pollutant purification by the forest ecosystem. With reference to relevant research, the treatment costs of SO_2, NO_X, and retained dust are 1200, 630, and CNY 150/t, respectively, and the purification amounts per unit area of forest ecosystem for SO_2, NO_X, and retained dust are 22.64, 0.82, and 3831.7 t/(km^2·a), respectively.

The soil conservation value of forest ecosystems is mainly reflected by a reduction in sediment deposition in rivers and lakes, and a reduction in soil-erosion-induced reservoir loss and soil fertility loss. Soil loss is calculated using the restoration cost method, which is a substitute for the value of soil protection. Potential soil erosion is estimated as:

$$A_p = R \times K \times LS \tag{4}$$

Actual soil erosion is estimated as:

$$A_r = R \times K \times LS \times C \times P \tag{5}$$

The soil conservation service capacity provided by the ecosystem is

$$A_c = A_p - A_r \tag{6}$$

where R is the rainfall erosion factor, which is related to rainfall amount, rainfall duration, intensity and kinetic energy. It is generally reflected by the product of heavy rain kinetic energy and the maximum 30 min rainfall intensity. The daily rainfall erosivity model is applied to calculate rainfall erosion:

$$R_i = \alpha \sum_{j=1}^{k} (P_j)^{\beta} \tag{7}$$

where R_i is the erosive force in the i-th half-month period (MJ mm hm^{-2} h^{-1}), k and P_j, respectively represent the number of rainfall days in the half-month period and the daily rainfall on the j-th day. The daily rainfall is required to be $\geq$12 mm, otherwise it will not be calculated. α and β are model parameters, estimated based on rainfall characteristics:

$$\begin{gathered} \beta = 0.8363 + \frac{18.144}{p_{d12}} + \frac{24.455}{p_{y12}} \\ \alpha = 21.586\beta^{-7.1891} \end{gathered} \tag{8}$$

where p_{d12} is the daily average rainfall with daily rainfall $\geq$12 mm, and p_{y12} is the annual rainfall with daily rainfall $\geq$12 mm.

K is the soil erodibility factor, which reflects the ease with which soil is eroded and transported by rainwater. The EPCI model for estimating soil erodibility is established based on the physical structure of the soil (percentage of sand, silt, and clay) and the content of organic matter:

$$\begin{aligned} K = \{0.2 + 0.3exp[-0.0256S_d(1 - S_i/100)]\} \times \left[\frac{S_i}{(Cl+S_i)}\right]^{0.3} \times \left\{1 - \frac{0.25C}{[C+\exp(3.72-2.95C]}\right\} \times \\ \left\{1 - \frac{0.7 \times \left(1 - \frac{S_d}{100}\right)}{\left\{1 - \frac{S_d}{100} + exp[-5.51+22.9[-5.51+22.9(1-S_d/100)]]\right\}}\right\} \end{aligned} \tag{9}$$

where S_d is the sand content, S_i is the powder content, Cl is the clay content, and C is the organic carbon content. L and S are slope length and slope factor, respectively, reflecting the impact of topography and landforms on soil erosion. The slope length factor is calculated as follows:

$$L = (\lambda/22.13)^{\alpha} \tag{10}$$

where L is the amount of soil erosion normalized to a slope length of 22.13 m; λ is the slope length.

S is the slope factor, calculated as follows:

$$S = \begin{cases} 10.8\sin\theta + 0.03 \ (\theta < 5^{\circ}) \\ 16.8\sin\theta - 0.50 \ (5^{\circ} \leq \theta \leq 10^{\circ}) \\ 21.9\sin\theta - 0.96 \ (\theta \geq 10^{\circ}) \end{cases} \tag{11}$$

C is the vegetation coverage and management factor, which is mainly affected by surface land use type and vegetation coverage. *P* is the soil and water conservation measure factor. The values of *C* and *P* are derived from relevant research on the PRD region [54].

According to the "Forest Ecosystem Service Function Evaluation Specification", the cost of manually digging 1 m^3 of Class I and II soil is CNY 8.4/m^3 [55]. The soil conservation amount is converted into the volume of the topsoil layer, and is then multiplied by the cost of excavating 1 m^3 of soil to obtain the annual soil conservation value of the ecosystem.

2.2.2. Method of Evaluation for Ecological Product Conversion Efficiency

Data envelopment analysis (DEA) is a method of operations research and is used in the study of economic production boundaries. This method is generally used to measure the production efficiency of some decision-making units. The DEA model can effectively identify multiple inputs and multiple outputs of efficiency and is currently the most well-constructed efficiency measurement method, widely used by scholars in many research fields [56]. The super-efficient DEA model further evaluates units that are at the same frontier [57]. Therefore, the DEA model with input-oriented constant returns to scale is used in this paper, and can be specifically expressed as

$$\begin{cases} \min\left[\theta - \varepsilon\left(\sum_{i=1}^{m} S_i^- + \sum_{r=1}^{s} S_r^+\right)\right] \\ s.t. \sum_{\substack{j=1 \\ j\neq k}}^{n} \lambda j x i j + S_i^- = \theta x 0, i = 1, 2, \cdots, m \\ \sum_{\substack{j=1 \\ j\neq k}}^{n} \lambda j y r j - S_r^+ = y 0, r = 1, 2, \cdots, s \\ \lambda j \geq 0, j = 1, 2, \cdots, n, S_r^+ \geq 0, S_i^- \geq 0 \end{cases} \tag{12}$$

where the decision-making unit's super-efficiency value is given by θ, which represents the relative forest ecological product value-conversion efficiency of each city; the non-Archimedean infinitesimal is given by ε; m, s, n stand for input variable dimension, output variable dimension, and number of decision-making units, respectively; S_i^- S_r^+ represents the slack variable; the input variables and output variables are given by xij and yij, respectively; λ is the weight coefficient. $\theta < 1$ means that the decision-making unit has not achieved the optimal efficiency, while $\theta > 1$ means that it has achieved the optimal efficiency.

Based on the Total Factor Productivity (TFP) index, this study uses the productivity index decomposition method to identify the main factors leading to production inefficiency. Referring to Cooper et al. [58], the sources of the inefficiency items of multi-agent and multi-efficiency units are disassembled.

$$\begin{aligned} IE = \overrightarrow{S^t} &= IE^x + IE^y \\ &= \frac{1}{2N}\sum_n^N \frac{s_n^x}{q_n^x} + \frac{1}{2M}\sum_m^M \frac{s_m^y}{q_m^y} \end{aligned} \tag{13}$$

where IE^x and IE^y are the inefficiency values of factor input and output, respectively.

Since there are input variables such as ecological products, land, labor, and capital, Formula (13) can be further disassembled to obtain detailed information that leads to inefficiency.

$$IE = IE_{GEP} + IE_{land} + IE_{labour} + IE_{capital} \tag{14}$$

Combined with the constructed directional distance function and the characteristics of the Malmquist–Luenberge productivity index, the efficiency subject is disassembled.

$$ML_t^{t+1} = \underbrace{IE^x(t) - IE^x(t+1)}_{TFP^x} + \underbrace{IE^y(t) - IE^y(t+1)}_{TFP^y} \quad (15)$$

By dismantling the efficiency subject, the influence of the input factor (TFP^x) and output (TFP^y) on the total output (TFP) can be analyzed.

The Malmquist index can clearly reflect the trend and composition of efficiency changes [44]. TFP consists of Comprehensive Technical Efficiency (EC) and Technical Progress (TC), among which EC can be disassembled into Scale Efficiency (SE) and Pure Technical Efficiency (PE). Therefore, to dynamically analyze the changes in FEPs conversion efficiency in the PRD, this paper used the Malmquist index.

2.3. Index Construction

The indicator system used to estimate forest ecological product value conversion efficiency includes input and output parts (Table 2). The input indicators are regional GEP, completed investment in forestry fixed assets, and the number of forestry industry employees. Considering that economic growth is mostly reflected in the growth of the industry, this paper chooses the output value of forestry as an indicator.

Table 2. Input–output indicators of forest ecological product value conversion efficiency.

Category	Primary Index	Secondary Index	Tertiary Index
Input indicators	The value of forest ecological products	Material product value	Forest products
		Regulating service value	Conservation of water sources Carbon fixation and oxygen release Air purification Soil conservation
		Cultural service value	Forestry tourism
	Labor	Number of forestry practitioners	
	Physical capital	Amount of forestry fixed assets investment	
Output indicators	Economic growth	Output value of forestry industry	

2.4. Data Sources

This paper used socioeconomic data, meteorological data, remote sensing data, soil data, etc., to estimate the value of forestry products and their conservation efficiency (Table 3). Socioeconomic data mainly came from the "China Forestry Statistical Yearbook", "Guangdong Statistical Yearbook", "Guangdong Rural Statistical Yearbook", and the "Statistical Yearbook" of various cities from 2000 to 2016. Meteorological data including the daily average rainfall, solar radiation, and monthly average temperature were collected from meteorological stations in Guangdong Province through the National Meteorological Science Data Center. The data on land use were sourced from the Chinese Academy of Sciences cloud platform for resources and the environment. The NDVI data were obtained from NASA MODIS (MOD13Q product). The soil physical structure components were from the scientific data center of cold and dry areas. The DEM data were taken from the geospatial data cloud.

Table 3. Data sources.

Classification	Data	Data Sources
Socioeconomic data	Forest products Number of forestry practitioners Forestry fixed assets investment GDP	China Forestry Statistical Yearbook; Guangdong Statistical Yearbook; Guangdong Rural Statistical Yearbook; Statistical Yearbook of various cities (http://stats.gd.gov.cn/gdtjnj/index.html (accessed on 20 August 2019))
Meteorological data	Daily average rainfall Solar radiation monthly average temperature	National Meteorological Science Data Center (http://data.cma.cn/ (accessed on 20 August 2019))
Remote sensing data	land use NDVI data Soil physical structure components DEM data	Chinese Academy of Sciences cloud platform NASA MODIS (MOD13Q product) scientific data center of cold and dry areas (http://bdc.casnw.net/ (accessed on 20 August 2019)) geospatial data cloud (https://www.gscloud.cn/ (accessed on 20 August 2019))

3. Results and Analysis

3.1. Forest Ecological Product Value

During the period 2000 to 2015, the value of FEPs in the PRD ranged from CNY 222.381 billion to 314.051 billion (calculated at constant prices in 2000) (Figure 2). In 2015, the total value of forestry ecological products in the PRD was about 0.97 times the total forestry output value. Among them, the regulatory services value was the highest, CNY 242.844 billion, accounting for 77.33% of the total value; the value of cultural services was CNY 66.36 billion, accounting for 21.13% of the total value; the value of material products was CNY 4.847 billion, accounting for 1.54% of the total value (Table 4). Six ecological products can be ranked in order of value: soil conservation > cultural service > carbon fixation and oxygen release > air purification > material product > water retention. Among them, the values of soil conservation and cultural services accounted for 87.40% of the total, making up the largest proportion.

Table 4. FEPs value in the PRD in 2015.

Ecological Products	Value/RMB 100 Million	Proportion (%)
Material products	48.47	1.54%
Regulatory services	2428.44	77.33%
Water retention	47.25	1.50%
Carbon fixation and oxygen release	222.7	7.09%
Air purification	77.21	2.46%
Soil conservation	2081.27	66.27%
Cultural services	663.6	21.13%
Sum	3140.51	100%

During the period 2000 to 2015, a fluctuating upward trend was seen in the value of FEPs in the PRD (Figure 3). Following a slow increase in 2000–2005, there was a downward trend in 2010, but then a substantial increase. The total value increased from CNY 232.381 to 314.051 billion from 2000 to 2015, with an increase of 35.14%. In terms of ecological product composition, material products and cultural services values both showed an upward trend, while the value of regulatory services rose slightly but fluctuated. Specifically, the value of material products increased from CNY 2.183 billion to 4.837 billion from 2000 to 2015,

an increase of 122%. The regulatory products showed a fluctuating upward trend, while the value of carbon fixation and oxygen release showed a slow upward trend after a sharp decline. As for cultural services, the value shot up from CNY 35 million in 2000 to CNY 66.35 billion in 2020, showing the most significant increase.

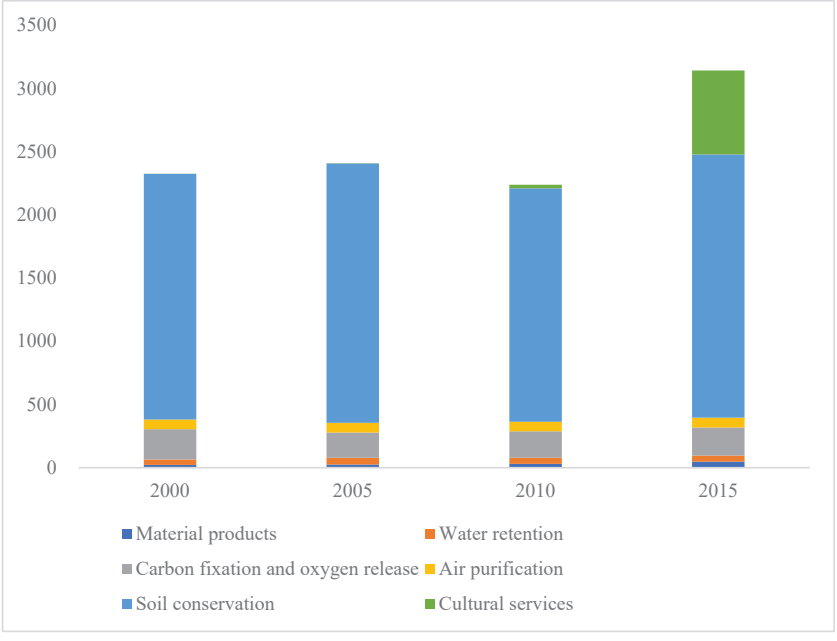

Figure 2. Changes in the value compositions of forest ecological products in the Pearl River Delta from 2000 to 2015.

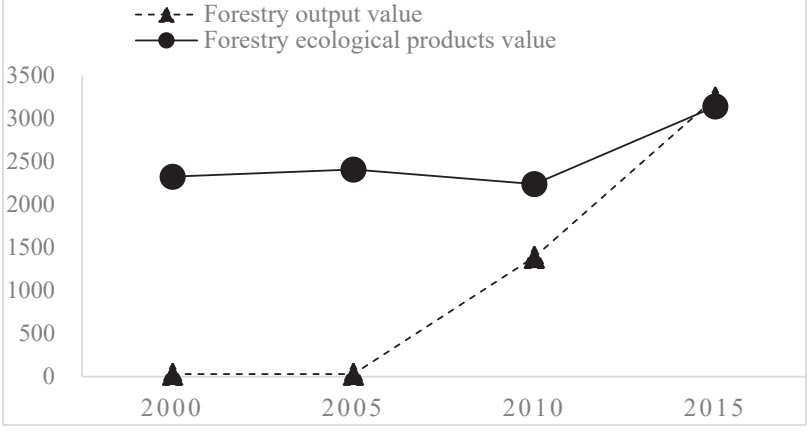

Figure 3. Forestry output value and FEPs value in the PRD.

The distribution of FEPs in the PRD is quite different (Table 5), being higher in Guangzhou, Zhaoqing, and Huizhou. The main ecological products in Guangzhou are cultural service products, while in Huizhou and Zhaoqing, they are regulatory service products with a high soil conservation value. The FEPs values in Zhuhai, Dongguan, and Zhongshan are relatively low.

Table 5. The value of forest ecological products in the Pearl River Delta cities in 2015.

City	Guangzhou	Shenzhen	Zhuhai	Foshan	Jiangmen	Zhaoqin	Dongguan	Zhongshan	Huizhou
Material products	2.47	0.12	0.2	0.78	4.83	37.02	0.21	0.01	2.84
Regulatory services	269.57	55.62	31.27	54.09	365.92	986.11	35.17	29.26	601.43
Water retention	6.29	0.99	0.51	1.34	6.91	18.11	0.91	0.52	11.67
Carbon fixation and oxygen release	23.64	5.76	2.58	6.06	37.01	86	3.47	2.58	55.61
Air purification	8.14	2.08	1.38	1.84	11.69	29.88	2.1	0.85	19.26
Soil conservation	231.51	46.78	26.8	44.85	310.31	852.13	28.69	25.31	514.89
Cultural services	293.26	46.78	28.9	56.95	37.37	26.05	40.6	22.52	33.19
Sum	565.3	180.5	60.37	111.81	408.11	1049.18	75.98	51.79	637.46

3.2. Comparison of Forestry Output Value and Forest Ecological Product Value

Different from FEPs, the total output value of forestry in the PRD showed a continuous upward trend (Figure 4). From 2005 to 2015, the output of the forestry industry rose rapidly, benefiting from the rapid development of the secondary and tertiary industries, while the value of FEPs showed a downward trend between 2005 and 2010, mainly due to the decline in the regulating services value; water conservation, and carbon fixation and oxygen release values also declined. However, in the following five years, the FEPs value greatly improved. This growth mainly came from the improvements in cultural value. In terms of cities, the output values of Guangzhou, Jiangmen, Zhaoqing, and Huizhou are higher than the value of FEPs, while the value of FEPs is higher in other cities.

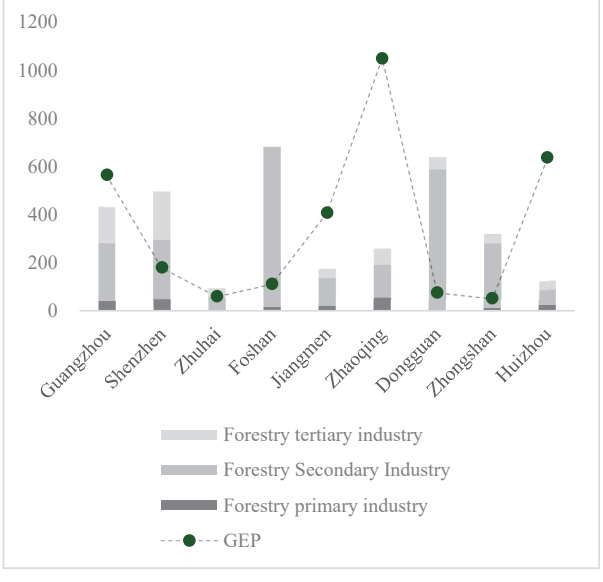

Figure 4. Forestry output value and FEPs value of each city in the PRD.

3.3. Spatio-Temporal Characteristics of FEPs Value-Conversion Efficiency

3.3.1. FEPs Value-Conversion Efficiency

Based on the index in Table 2, this paper used MATLAB to measure the value-conversion efficiency of FEPs every five years from 2000 to 2015 in nine cities in the PRD. The conversion efficiency of FEPs in the PRD differs. Specifically, Guangzhou, Shenzhen, Zhaoqing, Dongguan, and Zhongshan achieved relatively high efficiencies, while Zhuhai, Foshan, Jiangmen, and Huizhou achieved relatively low efficiencies (Table 6). In 2015, among the nine prefectures and cities in the PRD, five cities with a high efficiency remained

effective, while the conversion efficiency of FEPs in Huizhou in 2015 was only 4.8%. From the perspective of changing trends, the conversion efficiency showed a downward trend for Zhaoqing and Huizhou, from 2.253 and 0.445 in 2000 to 1.001 and 0.048 in 2015, respectively. Guangdong, Shenzhen, Dongguan, and Zhongshan maintained a continuous growth trend, rising from 0.028, 0.013, 0.046, and 0.029 in 2000 to 1.936, 2.772, 4.502, and 1.493 in 2015, respectively. Zhuhai, Foshan, and Jiangmen, which also had an increasing trend, reached their peak efficiencies in 2010, being 0.358, 2.805, and 2.270, respectively; however, these values dropped to lower levels in the following five years. It is worth mentioning that although Zhaoqing experienced a fluctuating downward trend, in 2000, 2005, and 2015, its conversion efficiency was effective. Nevertheless, there are large differences in conversion efficiency between cities in the PRD, and the overall trend of fluctuating growth can be seen.

Table 6. FEPs value conversion efficiency from 2000 to 2015.

City	2000	2005	2010	2015	Average
Guangzhou	0.028	0.032	0.186	1.936	0.546
Shenzhen	0.013	0.006	1.121	2.772	0.978
Zhuhai	0.028	0.004	0.358	0.137	0.132
Foshan	0.073	0.018	2.805	0.406	0.826
Jiangmen	0.132	0.059	2.270	0.321	0.696
Zhaoqin	2.253	1.075	0.423	1.001	1.188
Dongguan	0.046	0.003	1.320	4.502	1.468
Zhongshan	0.029	0.005	1.258	1.493	0.696
Huizhou	0.444	0.163	0.524	0.048	0.295
Average	0.338	0.152	1.141	1.402	

3.3.2. Dynamic Analysis of Value-Conversion Efficiency of FEPs

The dynamic analysis of the conversion efficiency of FEPs in the PRD was conducted using the Malmquist index. From a regional perspective (Table 7), the average TFP of the conversion efficiency of the PRD is 0.924, indicating that during the study period, the value of FEPs did not significantly correspond to an economic benefit. This varied greatly in other years, from 2.477 in 2000–2005, and rapidly dropping to 0.218 in 2005–2010. However, in 2010–2015, it rose quickly to 1.456, showing a more violent fluctuation trend. Specifically, the average value of the technical efficiency change index (EC) is 1.245, indicating that the level of resource utilization in the PRD has improved significantly. The technical efficiency fluctuated from 2000 to 2015. Due to the double impact of the pure technical efficiency change index (PE) and scale efficiency change index (SE), it rose from 0.528 to 2.885 during 2000–2010, and then fell to 1.276 in 2015. The average technological progress index (TE) is 0.724, and the lowest value is seen in the 2005–2010 period, which shows a synchronous fluctuation in the total factor productivity change index (TFP), indicating a limited level of technological advancement; therefore, the promotion effect of technological innovation on improving conversion efficiency is not obvious.

Table 7. TFP of FEPs in 2000–2015.

	EFF	TE	PE	SE	TFP
2000–2005	0.524	4.725	0.838	0.626	2.477
2005–2010	2.885	0.076	1.285	2.245	0.218
2010–2015	1.276	1.141	1.105	1.155	1.456
Average	1.245	0.742	1.06	1.175	0.924

The difference in the pure technical efficiency change index between cities in the PRD is small, and the change in the EFF is mainly caused by the change in SE (Table 8). The differences between cities are mainly reflected in the TE. The TFP values of Guangzhou, Zhuhai, Foshan, Dongguan, Shenzhen, and Zhongshan all exceeded 1, Zhaoqing was close to 1, at 0.989, and, in Shenzhen and Dongguan, the values were less than 1. The city with the

highest TFP was Foshan. Regarding the changing trends, the TFP of each city was relatively high during 2000–2005 and 2010–2015, and fell sharply during 2005–2010. Overall, the TFP of most cities showed a downward trend between 2000 and 2015.

Table 8. TFP of FEPs of each city in 2000–2015.

	EFF	TE	PE	SE	TFP
Guangzhou	1.557	0.671	1.524	1.021	1.044
Shenzhen	0.803	0.816	1	0.803	0.655
Zhuhai	2.134	0.491	1.018	2.095	1.049
Foshan	2.563	0.759	1.022	2.507	1.946
Jiangmen	0.978	1.087	1.060	0.922	1.063
Zhaoqin	1	0.989	1	1	0.989
Dongguan	0.571	0.418	1	0.571	0.239
Zhongshan	1.883	0.591	1	1.883	1.112
Huizhou	1	1.254	1	1	1.254
Average	1.245	0.742	1.060	1.175	0.924

3.3.3. The Input–Output Slack Rate of the Conversion Efficiency of FEPs Products

All cities in the PRD have experienced redundant input and insufficient output during FEPs value conversion (Table 9). The lack of output is more prominent. Zhuhai, Foshan, Jiangmen, and Huizhou have not realized the effective allocation of resources, and there are many deficiencies in their input and output indicators. Both Zhuhai and Huizhou have a large deficit in their forestry output value. Foshan has a 90% redundancy in fixed capital investment. Jiangmen has a surplus of more than 90% in both cultural service value and labor input. The conversion efficiency of FEPs in Guangzhou, Shenzhen, Zhaoqing, Dongguan, and Zhongshan has reached the production front, and the efficiency of production resource allocation has reached an effective level, but there is still room for optimization in terms of input. Guangzhou, Shenzhen, and Dongguan all have a certain degree of overinvestment in material products, while overinvestment in regulatory services has appeared in Dongguan. There is also a certain degree of redundancy in cultural service investment in Dongguan and Zhongshan. The surplus of forestry labor is more prominent in Shenzhen, as is the investment in fixed capital. Therefore, it is still necessary to optimize investments in ecological products across various cities.

Table 9. Redundancy rate and insufficient rate of each city in 2015.

City	Redundancy Rate					Insufficient Rate
	Material Products	Regulatory Products	City	Material Products	Regulatory Products	City
Guangzhou	3.31	1.37	Guangzhou	3.31	1.37	Guangzhou
Shenzhen	2.48	0.02	Shenzhen	2.48	0.02	Shenzhen
Zhuhai	0.99	0.99	Zhuhai	0.99	0.99	Zhuhai
Foshan	0.56	0.72	Foshan	0.56	0.72	Foshan
Jiangmen	0.44	0.45	Jiangmen	0.44	0.45	Jiangmen
Zhaoqing	0	0.01	Zhaoqing	0	0.01	Zhaoqing
Dongguan	2.53	12.06	Dongguan	2.53	12.06	Dongguan
Zhongshan	0	0	Zhongshan	0	0	Zhongshan
Huizhou	0.99	0.85	Huizhou	0.99	0.85	Huizhou

4. Conclusions

This paper evaluates the forestry ecological products values of the PRD from 2000 to 2015, and bases these on the input–output perspective to estimate the conversion efficiency of FEPs using the Super-SBM model, Malmquist index, and InVEST model. The conclusions are noted below.

First, the total value of FEPs in the PRD is fluctuating upwards. In 2015, the value of FEPs reached CNY 314.051 billion, with an increase of 1.35 times compared with the value of CNY 2321.381 billion in 2000. The regulatory service value is the main component of FEPs, followed by the cultural service value. Specifically, soil conservation and forest recreation are the main FEPs in the PRD, indicating that forests regulate climate in a significant way, especially in regard to water and soil conservation. With the development of the economy, the value of cultural services in FEPs has become increasingly prominent, and is inseparable from the construction of the PRD National Forest City Group [47] and forest parks, and the excavation of ecological space. However, the value of FEPs is still slightly lower than the total output value of the forestry industry, suggesting that the development of the forest ecological industry is lagging, and that there is still room for improvement in ecological civilization construction and value conversion for ecological products in the PRD.

Second, the conversion efficiency of FEPs in the PRD has continued to rise, and it achieved overall efficiency in 2010, indicating that the PRD has made remarkable achievements in the exploration and construction of the forest cities cluster. However, the imbalance in conversion efficiency among cities cannot be ignored. Although the overall conversion efficiency of FEPs in the four cities—Zhuhai, Foshan, Jiangmen, and Huizhou—is relatively low, other cities still show a trend of fluctuating growth. With the comprehensive construction of the national forest city group agglomeration and the in-depth development of the "Forest Chief System", the PRD will be able to make better use of its forest ecological resources, thereby promoting forest product value conversion. Regardless of whether this development involves the construction of forest parks or forest towns, it will vigorously activate FEPs and provide multiple paths for the conversion of their values.

Third, the TFP of FEPs in the PRD fluctuates greatly. The total factor productivity is below one, but technical efficiency is above one, and the technological progress is below one, indicating that FEP conversion efficiency has been changed primarily due to forestry technical efficiency improvements in the PRD. Technology advancements in forestry, however, have yet to show positive results. Through enhancing the efficiency of FEP conversion, it is necessary to establish a corresponding forestry technology service system urgently, increase the promotion and application of new technology, and improve the conversion efficiency of FEPs through technological progress.

Fourth, the PRD's loss of conversion efficiency is primarily due to excessive inputs and insufficient outputs, with specific reasons for variation in the loss of efficiency.

5. Discussion

Based on the value calculation of the forest ecological products, this paper constructs an input-output index system from the perspective of efficiency, which provides a new perspective for evaluating the value transformation of forest ecological products.

The forest ecosystem is the main body of the terrestrial ecosystem. It provides humans with a variety of regulatory ecological products such as water conservation, carbon fixation and oxygen release, wind and soil fixation, air purification, and climate regulation, as well as supply ecological products such as timber, economic forest fruits, and biomass energy [59]; and cultural ecological products such as tourism and health care, landscape value, etc. [60]. However, areas rich in forest resources and ecological products are mostly areas with relatively backward economic development [61]. Considering that forest ecological products maintain the livelihood of forest farmers, the evaluation of the value conversion of ecological products is an important factor in measuring the economic development of forest areas. Through the calculation of the value of forest ecological products in the PRD region, we found that during the research period, cultural services showed a significant increase. The development of forest tourism resources is an explicit means to realize the economic development of forest areas [62,63]. Government departments can promote the value of ecological products by innovating forest ecological industries.

The economic benefits brought by forestry material products and cultural products have been taken into consideration, but the role of regulating services in realizing eco-

nomic benefits is not yet obvious [64]. With the development of the carbon trading market, carbon sinks play an important role in forest environmental benefits, and their economic value should be included in the forest ecological product value conversion evaluation system [65]. Government departments should further improve the forest ecological protection compensation mechanism and promotion mechanism.

From the perspective of conversion efficiency, it is urgent to establish a forestry technology service system, promote the application of new technologies and new products, and improve conversion efficiency through technological progress. Institutional innovation is another effective means to improve conversion efficiency. The focus should be on developing the "Forest Chief System", the development and construction of forest parks and forest towns, promoting the precise connection between the supply and demand of forest ecological boards, promoting the trading of forest ecological resources rights and interests, and improving the protection level of forest ecological resources.

This study is a useful attempt to evaluate the value transformation of forest ecological products in large-scale urban agglomerations, and there is still room for optimization. Restricted by existing data, forestry output can be further refined, and the indirect economic benefits could be included. At the same time, the cost of ecological damage caused by forestry economic development could also be taken into consideration.

Author Contributions: Methodology, W.L.; Writing—original draft, J.W.; Writing—review & editing, F.K. All authors have read and agreed to the published version of the manuscript.

Funding: This research was funded by the National Natural Science Foundation of China (Grant No. 42071283) and Fundamental Research Funds for the Provincial Universities of Zhejiang, grant number 22FR013.

Data Availability Statement: Not applicable.

Conflicts of Interest: The authors declare no conflict of interest.

References

1. Zhang, C.; Li, J.; Zhou, Z.; Sun, Y. Application of Ecosystem Service Flows Model in Water Security Assessment: A Case Study in Weihe River Basin, China. *Ecol. Indic.* **2021**, *120*, 106974. [CrossRef]
2. Wang, Y.; Zhou, L. Assessment of the Coordination Ability of Sustainable Social-Ecological Systems Development Based on a Set Pair Analysis: A Case Study in Yanchi County, China. *Sustainability* **2016**, *8*, 733. [CrossRef]
3. Carpenter, A.; Wagner, M. Environmental Justice in the Oil Refinery Industry: A Panel Analysis across United States Counties. *Ecol. Econ.* **2019**, *159*, 101–109. [CrossRef]
4. da Silva, A.M.; Manfre, L.A.; Urban, R.C.; Silva, V.H.O.; Manzatto, M.P.; Norton, L.D. Organic Farm Does Not Improve Neither Soil, or Water Quality in Rural Watersheds from Southeastern Brazil. *Ecol. Indic.* **2015**, *48*, 132–146. [CrossRef]
5. Kuriqi, A.; Pinheiro, A.N.; Sordo-Ward, A.; Garrote, L. Flow Regime Aspects in Determining Environmental Flows and Maximising Energy Production at Run-of-River Hydropower Plants. *Appl. Energy* **2019**, *256*, 113980. [CrossRef]
6. Wang, L.; Su, K.; Jiang, X.; Zhou, X.; Yu, Z.; Chen, Z.; Wei, C.; Zhang, Y.; Liao, Z. Measuring Gross Ecosystem Product (GEP) in Guangxi, China, from 2005 to 2020. *Land* **2022**, *11*, 1213. [CrossRef]
7. Fan, Y.; Fang, C.; Zhang, Q. Coupling Coordinated Development between Social Economy and Ecological Environment in Chinese Provincial Capital Cities-Assessment and Policy Implications. *J. Clean. Prod.* **2019**, *229*, 289–298. [CrossRef]
8. Yang, Y.; Wang, L.; Yang, F.; Hu, N.; Liang, L. Evaluation of the Coordination between Eco-Environment and Socioeconomy under the "Ecological County Strategy" in Western China: A Case Study of Meixian. *Ecol. Indic.* **2021**, *125*, 107585. [CrossRef]
9. Geall, S. *Clear Waters and Green Mountains: Will Xi Jinping Take the Lead on Climate Change?* Lowy Institute for International Policy: Sydney, Australia, 2017.
10. Ehrlich, P.R.; Mooney, H.A. Extinction, Substitution, and Ecosystem Services. *BioScience* **1983**, *33*, 248–254. [CrossRef]
11. Wunder, S. Revisiting the Concept of Payments for Environmental Services. *Ecol. Econ.* **2015**, *117*, 234–243. [CrossRef]
12. Higgins, K.; Hutchinson, W.G.; Longo, A. Willingness-to-Pay for Eco-Labelled Forest Products in Northern Ireland: An Experimental Auction Approach. *J. Behav. Exp. Econ.* **2020**, *87*, 101572. [CrossRef]
13. Costanza, R.; d'Arge, R.; De Groot, R.; Farber, S.; Grasso, M.; Hannon, B.; Limburg, K.; Naeem, S.; O'neill, R.V.; Paruelo, J. The Value of the World's Ecosystem Services and Natural Capital. *Nature* **1997**, *387*, 253–260. [CrossRef]
14. Costanza, R.; De Groot, R.; Sutton, P.; Van der Ploeg, S.; Anderson, S.J.; Kubiszewski, I.; Farber, S.; Turner, R.K. Changes in the Global Value of Ecosystem Services. *Glob. Environ. Change* **2014**, *26*, 152–158. [CrossRef]
15. Ma, G.; Wang, J.; Yu, F.; Yang, W.; Ning, J.; Peng, F.; Zhou, X.; Zhou, Y.; Cao, D. Framework Construction and Application of China's Gross Economic-Ecological Product Accounting. *J. Environ. Manag.* **2020**, *264*, 109852. [CrossRef] [PubMed]

16. Łaszkiewicz, E.; Czembrowski, P.; Kronenberg, J. Can Proximity to Urban Green Spaces Be Considered a Luxury? Classifying a Non-Tradable Good with the Use of Hedonic Pricing Method. *Ecol. Econ.* **2019**, *161*, 237–247. [CrossRef]
17. Polasky, S.; Kling, C.L.; Levin, S.A.; Carpenter, S.R.; Daily, G.C.; Ehrlich, P.R.; Heal, G.M.; Lubchenco, J. Role of Economics in Analyzing the Environment and Sustainable Development. *Proc. Natl. Acad. Sci. USA* **2019**, *116*, 5233–5238. [CrossRef]
18. Liu, Y.; Zhu, J.; Li, E.Y.; Meng, Z.; Song, Y. Environmental Regulation, Green Technological Innovation, and Eco-Efficiency: The Case of Yangtze River Economic Belt in China. *Technol. Forecast. Soc. Change* **2020**, *155*, 119993. [CrossRef]
19. Liu, M.; Li, W. Calculation of Equivalence Factor Used in Ecological Footprint for China and Its Provinces Based on Net Primary Production. *J. Ecol. Rural Environ.* **2010**, *26*, 401–406.
20. Jia, Y.; Liu, Y.; Zhang, S. Evaluation of Agricultural Ecosystem Service Value in Arid and Semiarid Regions of Northwest China Based on the Equivalent Factor Method. *Environ. Process.* **2021**, *8*, 713–727. [CrossRef]
21. Barbier, E.B.; Baumgärtner, S.; Chopra, K.; Costello, C.; Duraiappah, A.; Hassan, R.; Kinzig, A.; Lehman, M.; Pascual, U.; Polasky, S. The Valuation of Ecosystem Services. In *Biodiversity, Ecosystem Functioning, and Human Wellbeing: An Ecological and Economic Perspective*; Oxford University Press: Oxford, UK, 2009; Volume 10.
22. Wong, C.P.; Jiang, B.; Kinzig, A.P.; Lee, K.N.; Ouyang, Z. Linking Ecosystem Characteristics to Final Ecosystem Services for Public Policy. *Ecol. Lett.* **2015**, *18*, 108–118. [CrossRef] [PubMed]
23. Hao, F.; Lai, X.; Ouyang, W.; Xu, Y.; Wei, X.; Song, K. Effects of Land Use Changes on the Ecosystem Service Values of a Reclamation Farm in Northeast China. *Environ. Manag.* **2012**, *50*, 888–899. [CrossRef]
24. Viglizzo, E.F.; Paruelo, J.M.; Laterra, P.; Jobbágy, E.G. Ecosystem Service Evaluation to Support Land-Use Policy. *Agric. Ecosyst. Environ.* **2012**, *154*, 78–84. [CrossRef]
25. Hao, C.; Wu, S.; Zhang, W.; Chen, Y.; Ren, Y.; Chen, X.; Wang, H.; Zhang, L. A Critical Review of Gross Ecosystem Product Accounting in China: Status Quo, Problems and Future Directions. *J. Environ. Manag.* **2022**, *322*, 115995. [CrossRef]
26. Merlo, M.; Briales, E.R. Public Goods and Externalities Linked to Mediterranean Forests: Economic Nature and Policy. *Land Use Policy* **2000**, *17*, 197–208. [CrossRef]
27. Czyżewski, B.; Matuszczak, A.; Miśkiewicz, R. Public Goods versus the Farm Price-Cost Squeeze: Shaping the Sustainability of the EU's Common Agricultural Policy. *Technol. Econ. Dev. Econ.* **2019**, *25*, 82–102. [CrossRef]
28. Xie, H.; Li, Z.; Xu, Y. Study on the Coupling and Coordination Relationship between Gross Ecosystem Product (GEP) and Regional Economic System: A Case Study of Jiangxi Province. *Land* **2022**, *11*, 1540. [CrossRef]
29. Sun, X.; Loh, L.; Chen, Z. Effect of Market Fragmentation on Ecological Efficiency: Evidence from Environmental Pollution in China. *Environ. Sci. Pollut. Res.* **2020**, *27*, 4944–4957. [CrossRef] [PubMed]
30. Sierra, R.; Russman, E. On the Efficiency of Environmental Service Payments: A Forest Conservation Assessment in the Osa Peninsula, Costa Rica. *Ecol. Econ.* **2006**, *59*, 131–141. [CrossRef]
31. Le, W.; Leshan, J. How Eco-Compensation Contribute to Poverty Reduction: A Perspective from Different Income Group of Rural Households in Guizhou, China. *J. Clean. Prod.* **2020**, *275*, 122962. [CrossRef]
32. Fan, S.; Yang, J.; Liu, W.; Wang, H. Institutional Credibility Measurement Based on Structure of Transaction Costs: A Case Study of Ongniud Banner in the Inner Mongolia Autonomous Region. *Ecol. Econ.* **2019**, *159*, 212–225. [CrossRef]
33. Pan, H.; Zhang, L.; Cong, C.; Deal, B.; Wang, Y. A Dynamic and Spatially Explicit Modeling Approach to Identify the Ecosystem Service Implications of Complex Urban Systems Interactions. *Ecol. Indic.* **2019**, *102*, 426–436. [CrossRef]
34. Cui, H.; Wang, R.; Wang, H. An Evolutionary Analysis of Green Finance Sustainability Based on Multi-Agent Game. *J. Clean. Prod.* **2020**, *269*, 121799. [CrossRef]
35. Piñeiro, V.; Arias, J.; Dürr, J.; Elverdin, P.; Ibáñez, A.M.; Kinengyere, A.; Opazo, C.M.; Owoo, N.; Page, J.R.; Prager, S.D. A Scoping Review on Incentives for Adoption of Sustainable Agricultural Practices and Their Outcomes. *Nat. Sustain.* **2020**, *3*, 809–820. [CrossRef]
36. Samii, C.; Lisiecki, M.; Kulkarni, P.; Paler, L.; Chavis, L.; Snilstveit, B.; Vojtkova, M.; Gallagher, E. Effects of Payment for Environmental Services (PES) on Deforestation and Poverty in Low and Middle Income Countries: A Systematic Review. *Campbell Syst. Rev.* **2014**, *10*, 1–95. [CrossRef]
37. Geng, J.; Liang, C. Analysis of the Internal Relationship between Ecological Value and Economic Value Based on the Forest Resources in China. *Sustainability* **2021**, *13*, 6795. [CrossRef]
38. Jinnan, W.; Guoxia, M.A.; Zhikai, W.; Xiahui, W.; Fang, Y.U.; Guihuan, L.I.U.; Yunhao, Z.; Wu, Y.; Minjun, S.H.I.; Jingsong, D. Development and Application of Indicator System about the Quaternary Industry of Ecological Products in China. *China Popul. Resour. Environ.* **2021**, *31*.
39. Caiado, R.G.G.; de Freitas Dias, R.; Mattos, L.V.; Quelhas, O.L.G.; Leal Filho, W. Towards Sustainable Development through the Perspective of Eco-Efficiency-A Systematic Literature Review. *J. Clean. Prod.* **2017**, *165*, 890–904. [CrossRef]
40. Jahanger, A.; Usman, M.; Murshed, M.; Mahmood, H.; Balsalobre-Lorente, D. The Linkages between Natural Resources, Human Capital, Globalization, Economic Growth, Financial Development, and Ecological Footprint: The Moderating Role of Technological Innovations. *Resour. Policy* **2022**, *76*, 102569. [CrossRef]
41. Costanza, R. Valuing Natural Capital and Ecosystem Services toward the Goals of Efficiency, Fairness, and Sustainability. *Ecosyst. Serv.* **2020**, *43*, 101096. [CrossRef]
42. Coluccia, B.; Valente, D.; Fusco, G.; De Leo, F.; Porrini, D. Assessing Agricultural Eco-Efficiency in Italian Regions. *Ecol. Indic.* **2020**, *116*, 106483. [CrossRef]

43. Wang, C.; Wang, X.; Wang, Y.; Zhan, J.; Chu, X.; Teng, Y.; Liu, W.; Wang, H. Spatio-Temporal Analysis of Human Wellbeing and Its Coupling Relationship with Ecosystem Services in Shandong Province, China. *J. Geogr. Sci.* **2023**, *33*, 392–412. [CrossRef]
44. Zang, Z.; Zhang, Y.; Xi, X. Analysis of the Gross Ecosystem Product—Gross Domestic Product Synergistic States, Evolutionary Process, and Their Regional Contribution to the Chinese Mainland. *Land* **2022**, *11*, 732. [CrossRef]
45. Wang, M.-X.; Zhao, H.-H.; Cui, J.-X.; Fan, D.; Lv, B.; Wang, G.; Li, Z.-H.; Zhou, G.-J. Evaluating Green Development Level of Nine Cities within the Pearl River Delta, China. *J. Clean. Prod.* **2018**, *174*, 315–323. [CrossRef]
46. Zhou, Y.; Wei, T.; Chen, S.; Wang, S.; Qiu, R. Pathways to a More Efficient and Cleaner Energy System in Guangdong-Hong Kong-Macao Greater Bay Area: A System-Based Simulation during 2015-2035. *Resour. Conserv. Recycl.* **2021**, *174*, 105835. [CrossRef]
47. Li, X.; Luo, Y.; Wu, J. Decoupling Relationship between Urbanization and Carbon Sequestration in the Pearl River Delta from 2000 to 2020. *Remote Sens.* **2022**, *14*, 526. [CrossRef]
48. Ouyang, Z.; Song, C.; Zheng, H.; Polasky, S.; Xiao, Y.; Bateman, I.J.; Liu, J.; Ruckelshaus, M.; Shi, F.; Xiao, Y.; et al. Using Gross Ecosystem Product (GEP) to Value Nature in Decision Making. *Proc. Natl. Acad. Sci. USA* **2020**, *117*, 14593–14601. [CrossRef]
49. Zou, Z.; Wu, T.; Xiao, Y.; Song, C.; Wang, K.; Ouyang, Z. Valuing Natural Capital amidst Rapid Urbanization: Assessing the Gross Ecosystem Product (GEP) of China's 'Chang-Zhu-Tan'Megacity. *Environ. Res. Lett.* **2020**, *15*, 124019. [CrossRef]
50. Tang, Z.; Shi, Y.; Nan, Z.; Xu, Z. The Economic Potential of Payments for Ecosystem Services in Water Conservation: A Case Study in the Upper Reaches of Shiyang River Basin, Northwest China. *Environ. Dev. Econ.* **2012**, *17*, 445–460. [CrossRef]
51. Lei, N.; Zhang, Y.; Li, J. Research on Ecological Compensation for Construction Land from a Carbon Emission Perspective. 2022. Available online: https://www.researchsquare.com/article/rs-2161826/v1 (accessed on 1 January 2023).
52. Peng, W.; Kuang, T.; Tao, S. Quantifying Influences of Natural Factors on Vegetation NDVI Changes Based on Geographical Detector in Sichuan, Western China. *J. Clean. Prod.* **2019**, *233*, 353–367. [CrossRef]
53. Yuan, J.; Niu, Z.; Wang, C. Vegetation NPP Distribution Based on MODIS Data and CASA Model—A Case Study of Northern Hebei Province. *Chin. Geogr. Sci.* **2006**, *16*, 334–341. [CrossRef]
54. Hu, M.; Li, Z.; Wang, Y.; Jiao, M.; Li, M.; Xia, B. Spatio-Temporal Changes in Ecosystem Service Value in Response to Land-Use/Cover Changes in the Pearl River Delta. *Resour. Conserv. Recycl.* **2019**, *149*, 106–114. [CrossRef]
55. Huang, J.; Fan, J.; Furbo, S. emonstration and Optimization of a Solar District Heating System with Ground Source Heat Pump. *Solar Energy* **2020**, *202*, 171–189. [CrossRef]
56. He, J.; Wan, Y.; Feng, L.; Ai, J.; Wang, Y. An Integrated Data Envelopment Analysis and Emergy-Based Ecological Footprint Methodology in Evaluating Sustainable Development, a Case Study of Jiangsu Province, China. *Ecol. Indic.* **2016**, *70*, 23–34. [CrossRef]
57. Tone, K. A Strange Case of the Cost and Allocative Efficiencies in DEA. *J. Oper. Res. Soc.* **2002**, *53*, 1225–1231. [CrossRef]
58. Cooper, W.W.; Seiford, L.M.; Tone, K.; Zhu, J. Some Models and Measures for Evaluating Performances with DEA: Past Accomplishments and Future Prospects. *J. Product. Anal.* **2007**, *28*, 151–163. [CrossRef]
59. Pearce, D.W. The Economic Value of Forest Ecosystems. *Ecosyst. Health* **2001**, *7*, 284–296. [CrossRef]
60. López-Santiago, C.A.; Oteros-Rozas, E.; Martín-López, B.; Plieninger, T.; Martín, E.G.; González, A.J. Using Visual Stimuli to Explore the Social Perceptions of Ecosystem Services in Cultural Landscapes: The Case of Transhumance in Mediterranean Spain. *Ecol. Soc.* **2014**, *19*. [CrossRef]
61. Zameer, H.; Yasmeen, H.; Wang, R.; Tao, J.; Malik, M.N. An Empirical Investigation of the Coordinated Development of Natural Resources, Financial Development and Ecological Efficiency in China. *Resour. Policy* **2020**, *65*, 101580. [CrossRef]
62. Bhaktikul, K.; Aroonsrimorakot, S.; Laiphrakpam, M.; Paisantanakij, W. Toward a Low-Carbon Tourism for Sustainable Development: A Study Based on a Royal Project for Highland Community Development in Chiang Rai, Thailand. *Environ. Dev. Sustain.* **2021**, *23*, 10743–10762. [CrossRef]
63. Morán-Ordóñez, A.; Hermoso, V.; Martínez-Salinas, A. Multi-Objective Forest Restoration Planning in Costa Rica: Balancing Landscape Connectivity and Ecosystem Service Provisioning with Sustainable Development. *J. Environ. Manag.* **2022**, *310*, 114717. [CrossRef]
64. Sannigrahi, S.; Zhang, Q.; Joshi, P.K.; Sutton, P.C.; Keesstra, S.; Roy, P.S.; Pilla, F.; Basu, B.; Wang, Y.; Jha, S. Examining Effects of Climate Change and Land Use Dynamic on Biophysical and Economic Values of Ecosystem Services of a Natural Reserve Region. *J. Clean. Prod.* **2020**, *257*, 120424. [CrossRef]
65. Yin, S.; Gong, Z.; Gu, L.; Deng, Y.; Niu, Y. Driving Forces of the Efficiency of Forest Carbon Sequestration Production: Spatial Panel Data from the National Forest Inventory in China. *J. Clean. Prod.* **2022**, *330*, 129776. [CrossRef]

land

MDPI

Article

Domestic Regional Synergy in Achieving National Climate Goals—The Role of Comparative Advantage in Emission Reduction

Dongxu Chen [1,*], Xiaoying Chang [2], Tao Hong [1] and Tao Ma [1,*]

[1] School of Management, Harbin Institute of Technology, Harbin 150001, China; hongtao_hit@163.com
[2] School of Humanities, Social Sciences & Law, Harbin Institute of Technology, Harbin 150001, China; changxiaoying@hit.edu.cn
* Correspondence: 18b910049@stu.hit.edu.cn (D.C.); matao@hit.edu.cn (T.M.); Tel.: +86-18249041276 (D.C.); +86-451-86414009 (T.M.)

Abstract: Domestic regional synergistic emission reduction is important in achieving national climate goals. This study constructed a game theory-based model for regional synergistic emission reduction, modified the Basic Climate Game using the exact-hat algebra method, and expanded the game model using a general spatial equilibrium model to incorporate cross-regional economic impacts generated by emission reduction actions through factors and product flows. The formation of regional comparative advantages in emission reductions and their impact on synergistic emission reductions were revealed through regional characteristics such as emission elasticity, sectoral structure, regional trade shares, and green total factor productivity. A form of synergy was then proposed that utilizes the comparative advantages of different regions, allowing for synergistic emission reductions across different income regions and engagement with regions that are still at the carbon-peaking stage in cooperation. Moreover, the model was created to be as close to the economic reality as possible to provide a trade, industry, and economic growth policy that complements emission-reduction policies.

Keywords: regional synergy; carbon neutrality; comparative advantage; emission reduction; regional economic growth; regional trade; scenario analysis

Citation: Chen, D.; Chang, X.; Hong, T.; Ma, T. Domestic Regional Synergy in Achieving National Climate Goals—The Role of Comparative Advantage in Emission Reduction. *Land* **2023**, *12*, 1723. https://doi.org/10.3390/land12091723

Academic Editors: Jinyan Zhan, Chao Wang and Xueting Zeng

Received: 12 August 2023
Revised: 28 August 2023
Accepted: 3 September 2023
Published: 4 September 2023

1. Introduction

Domestic regional synergy is an effective mechanism for achieving national emission reduction goals (in this paper, "emissions" specifically refers to CO_2 emissions) [1]. An imbalance between regional economic development and emission characteristics leads to varying tradeoffs between mitigating climate change and promoting economic growth in different regions [2]. This requires a reasonable emission reduction path and policy design to avoid economic development constraints resulting from achieving climate goals [3]. Thus, to achieve national emission reduction goals, the interests of different regions must be coordinated, and appropriate regional cooperation paths must be identified to achieve the dual goals of economic growth and emission reduction [4]. Regions with different levels of economic development and resource endowments should have different timelines for achieving climate goals. Leveraging the unique advantages of each region based on their development for regional synergistic emission reduction is necessary. The formation of these unique advantages does not solely depend on geographical proximity but also on the economic interdependence between regions, including factors such as technological level [5], industrial structures [6], carbon emission characteristics, and regional trade relationships [7]. These factors cannot be ignored in regional synergistic emission reduction.

Similar to international cooperation on climate change, regional synergy within a country to reduce emissions faces issues of public good attributes of climate change and trade-offs between emission reduction benefits and costs. In national climate governance,

local government actions determine the achievement of climate change targets [8]. Due to the short-term economic losses caused by climate policies [9], non-exclusivity of emission reduction benefits, and emission reduction costs borne by regions, free-riding is widespread in climate change, creating resistance to unilateral emission reduction actions by regions [10]. Climate change is an environmental and developmental problem and different stages of regional development result in different emission reduction costs. Independent emission-reduction actions lead to higher emission reduction costs for regions with lower emission-reduction potential. Therefore, regional synergy is required to reduce overall emission reduction costs [11]. Cooperation not only achieves emission reduction goals but also generates economic benefits, mainly reflected in the promotion of economic growth. Some studies have quantified the environmental benefits and gross domestic product (GDP) impacts of cooperative actions in the Paris Agreement [12,13]. In this process, regional spillover effects caused by trade cannot be ignored [14]. Under the flow of factors and products between regions, emission reduction costs, and economic losses and benefits caused by emission reduction constitute a comparative advantage of emission reduction in regions. Policies aimed at regional trade should be the primary method of promoting regional climate cooperation [15–17].

Regional synergistic emission reduction in a country exhibits unique characteristics that differ from those of international climate cooperation, as the actions of different regions can be managed by the national government [18], which faces less resistance than international cooperation. Furthermore, under a tighter flow of factors and products, regional cooperation on carbon reduction is more vulnerable to the influence of inter-regional trade. The current resource mismatch in regional factors and product markets limits the achievement of climate goals in some countries [19]. Therefore, regional synergy is needed to optimize the flow of factors and products among regions and promote emission reduction. Local governments are concerned with short-term economic growth and tend to develop high-carbon emission sectors with high output values [20]. Therefore, regional synergistic emission reduction needs to consider the differentiated climate goal realization paths and coordinate policies, industries, technologies, energy, and ecology among regions.

Game theory and its modeling methods could explain regional cooperation issues related to climate change [21,22]. DeCanio and Fremstad [23] analyzed 25 basic game theory models for climate cooperation and provided a theoretical foundation for analyzing regional cooperation issues related to climate change. Subsequent research has extended the formalism of models, including incorporating irreversible environmental degradation into participant payoffs [24], using N-player bargaining games based on learning dynamics to test international climate agreements [25], adding climate disaster risk to bargaining games to analyze the possibility of cooperation [26], constructing game models with foresight alliances [27], allowing multi-round negotiations and using dynamic games to explain the formation of large coalitions [28], proposing a dynamic differential game to model the transboundary pollution control between two asymmetric regions [29], and incorporating international leadership, domestic energy security, domestic economy, and domestic environment in games to explain participants' strategic choices [30]. Although these model forms are diverse, the core problem is the trade-off between regional development and emission reduction. The most intuitive model is the Basic Climate Game, which defines the payoffs of regions in climate cooperation as the benefits and harms of carbon emissions [31]. Although these game models provide a refined description of the theoretical mechanism of regional climate cooperation, their strict assumptions limit their explanatory power, whereas overly simple models are unable to provide useful policy recommendations [32]. In particular, when analyzing synergistic emission reduction among various regions within a country, cross-regional flows of goods and factors must be considered. Some studies have introduced trade models and new economic geography theories into game models to examine the relationships between carbon tariffs, trade barriers, and climate cooperation alliances [33–35]. These studies simulate and analyze cooperative behavior using assumed parameters, which cannot provide accurate characterizations of cooperative behavior based

on real data; however, they provide support for studying regional synergistic emission reduction from a trade perspective.

This study aimed to make several contributions to existing research. First, current theories on climate change cooperation mainly analyze cooperative emission reduction behaviors between countries, whereas research on regional synergistic emission reduction under the guidance and coordination of the state is scarce. Regional synergistic emission reduction should consider the process of achieving climate goals through regionally graded and orderly measures. This requires a new explanation of the relationship between the local and global optima in regional synergistic emission reduction. This study constructed a game model for regional synergistic emission reduction and used the exact-hat algebra method to construct the payoff function of game subjects. This method appropriately described the changes in emissions and their growth rates while achieving climate change targets and explained the differences in emission reduction actions between regions in different stages of development.

Second, although some studies on regional climate cooperation have considered trade issues, considerations of cross-regional economic impacts of factors and product flows of regional emission reduction are scarce. This study drew on the payoff function construction method of the Basic Climate Game proposed by Molina et al. [31] and used changes in economic growth and damage caused by emission reduction to characterize regional payoffs. The general spatial equilibrium model was incorporated into the game model to analyze the changes in regional economic growth caused by emission reduction, reveal the formation of regional comparative advantages in emission reduction, and investigate the impact of these advantages on regional synergistic emission reduction.

Third, achieving regional synergy requires the formation of multifaceted policy efforts; however, current simplified game models do not effectively support policy combinations. The general spatial equilibrium model is an extension of that used by Caliendo et al. [36], which uses conclusions derived from data on carbon emission elasticity [37,38], sectoral structures, trade shares, trade costs, and green total factor productivity (TFP) to support policies.

This study aimed to answer the following questions:

(1) What type of regional synergistic emission reduction meets the phased climate-change mitigation targets for different regions within a country?
(2) Considering the cross-regional impacts of emission reduction actions caused by regional economic interdependence, how can the comparative advantages of emission reduction among regions be utilized to achieve effective regional synergistic emission reduction while maintaining economic growth?
(3) What factors influence the formation of comparative advantages in emission reduction among regions? What insights do these factors provide for policies that promote synergistic regional emission reduction?

2. Model Construction

2.1. Assumptions of the Regional Synergistic Emission Reduction Game Model

2.1.1. Strategy and Payoff

Based on the Basic Climate Game, a regional synergistic emission reduction game model was constructed, and trade relations between regions were incorporated as factors affecting regional strategy based on a general spatial equilibrium model. Assuming that there are N regions, as is common in regional cooperative game models, the focus is on the strategy between two regions, denoted as Regions 1 and 2. The emission level of each region is denoted as e_n, and negative net emissions are allowed for each region (e.g., carbon capture from the atmosphere) [39].

Each region's strategy is a Synergistic Action (SA) or Unilateral Action (UA). Molina et al. [31] found that the difference in payoffs for different strategies depended on regional emissions. The Basic Climate Game sets the total payoff for region n as $G_n(e_n) - D_n(e)$, where $G_n(e_n)$ and $D_n(e)$ represent the benefits and damages of emissions,

respectively. The benefits of emissions for a region come primarily from economic growth driven by emissions, which is a function of regional emissions, e_n. However, the damage of regional emissions is a function of the total emissions, e, which represents the damages caused by climate change resulting from total emissions. This study improved this assumption by introducing the exact-hat algebra method, which expresses changes in x after an economic and environmental change as $\hat{x} = x'/x$, where x' denotes the new value of x after the change. We assumed that the regional payoff function, denoted as Π_n, is the difference between the changes in GDP and damages caused by emissions. In other words, when a region chooses a strategy, it focuses on the impact of emission-reduction actions on economic growth and the reduction in damage caused by emissions. The payoff function is expressed as:

$$\Pi_n = \widehat{G}_n - \widehat{D}_n \tag{1}$$

Improving the model using the exact-hat algebra method has four advantages. First, it can better reflect the actual emission reduction behavior of regions in response to climate change. The variable $\hat{e}$ can describe changes in the growth rate and quantity of emissions and accurately represent the stage of regional emission reduction. The goals of emission reduction in the second half of this century under the Paris Agreement for all countries are a long-term process that considers a decrease in total emissions and emission growth rate; a typical case is China's carbon peaking and carbon-neutral targets. Second, this method can eliminate the numerical differences between G_n and D_n and effectively reflect the tradeoff between economic growth and climate change mitigation in a region. The calculation methods and units of measurement for G_n and D_n differ. A large difference between the two can cause an excessive emphasis or underestimation of their impact. Third, this method is more appropriate for GDP change caused by emission changes in the general spatial equilibrium model, highlighting the role of key variables more accurately by simplifying the model. Fourth, considering only the change in damage caused by emissions, $\widehat{D}_n$, it ensures a more concise model analysis, relaxing the research assumptions regarding damage caused by emissions. Calculating damage caused by emissions is complex. General damage includes negative economic effects represented by GDP loss and the loss of the ecological environment and social welfare.

2.1.2. Comparative Advantage in Regional Synergistic Emission Reduction

The overall change in emissions in the two regions is expressed as $\hat{e}_{1+2} = (e_1/e)\hat{e}_1 + (e_2/e)\hat{e}_2$. The relationships between regional and aggregate emissions indicate that, in the process of achieving the overall goal of reducing emissions or decelerating emissions growth, regional emissions and trends may be in different stages. Therefore, allowing for regional differences in emission reduction efforts is key to achieving overall climate change targets through regional synergy.

We assume that when two regions achieve synergy in mitigating climate change, changes in total emission reduction, denoted as ($\hat{e}_{1+2}$), are lower than the emission reduction resulting from each region acting unilaterally. This can be divided into two scenarios. If $\hat{e}_{1+2}$ decreases, $\hat{e}_1$ and $\hat{e}_2$ may both decrease (Scenario 1), or $\hat{e}_1$ may decrease while $\hat{e}_2$ increase (Scenario 2). Scenario 1 is the basic form of regional cooperation for emission reduction in previous studies, where Regions 1 and 2 are required to reduce $\hat{e}_n$ in synergy. Conversely, Scenario 2 considers the comparative advantage of regional synergistic emission reduction. In regional synergistic emission reduction, if Region 2 does not have an absolute advantage in emission reduction over Region 1, increasing $\hat{e}_2$ in Region 2 provides both regions better overall payoffs than decreasing $\hat{e}_2$. This increase in total payoffs is due to the higher overall economic growth in both regions, caused by the increase in $\hat{e}_2$, including regional economic growth and cross-regional economic impact through trade. Furthermore, a decrease in $\hat{e}_1$ in Region 1 reduces damage caused by emissions more than an increase in $\hat{e}_1$, providing both regions with better overall payoffs.

2.2. Impact of Emission Reduction on Economic Growth in Payoff

2.2.1. Emissions and Economic Growth in General Spatial Equilibrium Models

According to the Environmental Kuznets Curve [40], an inverted U-shaped relationship between emissions and economic growth determines the complexity of connections with government payoff. Changes in emissions and economic growth depend on the level of economic development in the region. However, the flow of factors and products between regions creates regional spillover effects on the impact of emission changes on economic growth. A general spatial equilibrium model is an effective method to address this issue.

Following the methods proposed by Duan et al. [37] and Shapiro and Walker [38] to incorporate emissions into a trade equilibrium model, the government controls the emissions of sector j in region n, denoted as e_n^j, through emission reduction policies, denoted as t_n (including environmental taxes and emission penalties), where $e_n = \sum_{j=1}^{J} e_n^j$. Changes in regional emissions, denoted as $\hat{e}_n$, are determined by changes in the intensity of environmental regulations, denoted as $\hat{t}_n$, where an increase in $\hat{t}_n$ represents an increase in the level of emission reduction efforts, resulting in a decrease in emissions. Changes in the intensity of regional environmental regulations may affect the economic growth of another region due to regional trade. This further specifies government action compared with the Basic Climate Game, making it more realistic. Let α_n^j be the emission elasticity. The relationship between emissions and environmental regulation is given by

$$e_n^j = \frac{\alpha_n^j}{t_n} Y_n^j \tag{2}$$

In contrast to general equilibrium models in international trade, examining regional economic relations in a country requires consideration of labor mobility and transfer payments. Caliendo et al. [36] made pioneering efforts in this field, and this study extended their model.

2.2.2. Production of Intermediate Goods with Emissions as a Byproduct

Following the approach of Copeland and Taylor [41], we introduced emissions as a byproduct of the production function of intermediate goods. The potential output function is expressed as:

$$y_n^j\left(z_n^j\right) = z_n^j\left[T_n^j\left[h_n^j\left(z_n^j\right)\right]^{\beta_n}\left[l_n^j\left(z_n^j\right)\right]^{(1-\beta_n)}\right]^{\gamma_n^j}\prod_{k=1}^{J}\left[M_n^{jk}\left(z_n^j\right)\right]^{\gamma_n^{jk}} \tag{3}$$

where the productivity level, z_n^j, follows the Fréchet distribution, T_n^j is the fundamental productivity, $h_n^j(\cdot)$ and $l_n^j(\cdot)$ denote the demand for land and labor, respectively, $M_n^{jk}(\cdot)$ is the demand for final material inputs by firms in sector j from sector k, $\gamma_n^{jk} \geq 0$ is the share of sector j goods spent on materials from sector k, and $\gamma_n^j \geq 0$ is the share of value added to the gross output. We assume that the production function has constant returns to scale, namely that $\gamma_n^j + \sum_{j=1}^{J} \gamma_n^{jk} = 1$. Based on potential output, a producer can allocate a fraction ϵ_n^j of $y_n^j\left(z_n^j\right)$ to emission-reduction activities to reduce payments. The remaining $1 - \epsilon_n^j$ fraction is the net output. We denote the net production after abatement investment using $q_n^j\left(z_n^j\right) = \left(1 - \epsilon_n^j\right) y_n^j\left(z_n^j\right)$. We assume that the emissions are also affected by z_n^j. Advanced production technologies can improve resource utilization efficiency, leading to positive externalities in emission reduction. Research on the technology list for China's response to climate change supports this assumption [42]. Under this assumption, emissions from output at different technological levels differ. Let α_n^j denote the emission elasticity of

sector j in region n. Then, the relationship between emissions and potential output can be expressed as:

$$e_n^j\left(z_n^j\right) = \left(\frac{1}{z_n^j}\right)\left(1-\epsilon_n^j\right)^{\frac{1}{\alpha_n^j}} y_n^j\left(z_n^j\right) \tag{4}$$

The net production of intermediate goods is obtained, where z_n^j includes the technical level of potential output ${z_n^j}^{1-\alpha_n^j}$ and the technical level of emission reduction ${z_n^j}^{\alpha_n^j}$:

$$q_n^j\left(z_n^j\right) = z_n^j\left(\left[T_n^j\left[h_n^j\left(z_n^j\right)\right]^{\beta_n}\left[l_n^j\left(z_n^j\right)\right]^{(1-\beta_n)}\right]^{\gamma_n^j}\prod_{k=1}^{J}\left[M_n^{jk}\left(z_n^j\right)\right]^{\gamma_n^{jk}}\right)^{1-\alpha_n^j}\left[e_n^j\left(z_n^j\right)\right]^{\alpha_n^j} \tag{5}$$

2.2.3. Prices of Final Goods, Trade Share, and Transfer Payment

We use x_n^j to denote the cost of the input bundle needed to produce intermediate good varieties. Let $B_{1,n}^j = \left(\alpha_n^j\right)^{-\alpha_n^j}\left(1-\alpha_n^j\right)^{\alpha_n^j-1}$, $B_{2,n}^j = \left[\gamma_n^j(1-\beta_n)^{(1-\beta_n)}\beta_n{}^{\beta_n}\right]^{-\gamma_n^j}\prod_{k=1}^{J}\left(\gamma_n^{jk}\right)^{-\gamma_n^{jk}}$. Then:

$$x_n^j = B_{1,n}^j(\iota_n)^{\alpha_n^j}\left(\varsigma_n^j\right)^{1-\alpha_n^j} \tag{6}$$

$$\varsigma_n^j = B_{2,n}^j\left(r_n^{\beta_n}w_n^{1-\beta_n}\right)^{\gamma_n^j}\prod_{k=1}^{J}\left(P_n^k\right)^{\gamma_n^{jk}}$$

where κ_{ni}^j is the transport cost of intermediate goods. Let $B_3^j = \left[\Gamma\left(1+\frac{1-\eta_n^j}{\theta^j}\right)\right]^{\frac{1}{1-\eta_n^j}}$. We define P_n^j as the unit price of sectoral composite goods:

$$P_n^j = B_3^j\left[\sum_{i=1}^{N}\left(x_i^j\kappa_{ni}^j\right)^{-\theta^j}\left(T_i^j\right)^{(1-\alpha_i^j)\gamma_i^j\theta^j}\right]^{-\frac{1}{\theta^j}} \tag{7}$$

Let π_{ni}^j denote the share of region n's expenditure on sector j composite goods purchased from region i.:

$$\pi_{ni}^j = \frac{\left(x_i^j\kappa_{ni}^j\right)^{-\theta^j}{T_i^j}^{(1-\alpha_i^j)\theta^j\gamma_i^j}}{\sum_{m=1}^{N}\left(x_m^j\kappa_{nm}^j\right)^{-\theta^j}{T_m^j}^{(1-\alpha_i^j)\theta^j\gamma_m^j}} \tag{8}$$

We used F_n^j to denote the revenue from emission penalties or carbon taxes received by region n from sector j through environmental regulations; that is, $F_n^j = t_n e_n^j$. The total environmental regulation revenue in region n is $F_n = \sum_{j=1}^{J}F_n^j$. The term χ represents the return per person from the national portfolio of land and structures in all regions. In particular, $\chi = \frac{\sum_{i=1}^{N}t_i r_i H_i}{\sum_{i=1}^{N}L_i}$. The income of an agent residing in region n is:

$$I_n = w_n + \chi + (1-\iota_n)r_n H_n/L_n + F_n/L_n \tag{9}$$

2.2.4. Changes in Regional GDP

In the constructed model, the impact of green TFP denoted as A_n^j, is reflected in economic growth. A_n^j incorporates emission elasticity, which allows for the inclusion of non-expected outputs, such as emissions, into the calculation, in contrast to TFP, which only considers expected outputs. The green TFP of sector j in region n can be derived from the equilibrium conditions, as follows:

$$A_n^j = \frac{x_n^j}{P_n^j} \tag{10}$$

As $\widehat{\pi}_{nn}^j = \left(\frac{\hat{x}_n^j}{\hat{P}_n^j}\right)^{-\theta^j} \left(\widehat{T}_i^j\right)^{(1-\alpha_i^j)\gamma_i^j\theta^j}$, changes in green TFP can be expressed as:

$$\hat{A}_n^j = \frac{\hat{x}_n^j}{\widehat{P}_n^j} = \frac{\left(\widehat{T}_i^j\right)^{(1-\alpha_i^j)\gamma_i^j}}{\left(\widehat{\pi}_{nn}^j\right)^{\frac{1}{\theta^j}}} \tag{11}$$

The GDP in a given region-sector pair is the difference between gross production and expenditure on materials, $\frac{w_n L_n^j + r_n H_n^j}{P_n^j}$. As, in equilibrium, $L_n = \frac{(1-\beta_n) r_n H_n}{\beta_n w_n}$, GDP of sector j in region n is: $GDP_n^j = \left(\frac{1}{1-\beta_n}\right)\frac{w_n L_n}{P_n^j}$. Based on the changes in the price level and green TFP derived from the equilibrium condition, actual GDP changes in sector j in region n can be expressed as:

$$\widehat{GDP}_n^j = \hat{A}_n^j \hat{L}_n^j \left(\frac{\widehat{w}_n}{\hat{x}_n^j}\right) \tag{12}$$

Sectors are categorized according to their emission characteristics into carbon-intensive sector j and low-emission sector k, and ψ_n^j and ψ_n^k are used to represent their respective shares of GDP in the region. Thus, changes in regional GDP can be expressed as:

$$\widehat{GDP}_n = \psi_n^j \widehat{GDP}_n^j + \psi_n^k \widehat{GDP}_n^k \tag{13}$$

According to this model, local governments can influence economic growth and emissions by changing the intensity of their environmental regulations, $\hat{t}_n$, and can affect economic growth by changing $\hat{A}_n^j$ and $\hat{\kappa}_{ni}^j$. This process is influenced by regional characteristics, including emission characteristics, which are explained in the model using emission elasticity, α_n^j, sectoral structure, which is explained in the model using the proportion of sector j to the total GDP, ψ_n^j, and trade relationship between two regions, which is explained in the model using the sector trade share between regions, π_{ni}^j.

2.3. Emission Damage in Payoff

As previously mentioned, the impact of global warming caused by climate change on region n is not solely determined by its own emissions, e_n, but also by total emissions. Therefore, damage from emissions is a function of the overall emissions. Considering the complexity of factors and processes involved in the impact of climate change on a region, this study did not aim to construct an exact function to explore these issues. Instead, a simple model was used to elucidate the mechanism, and previous assumptions were leveraged to simplify the analysis using the exact-hat algebra method. This analysis focused on changes in damage caused by emissions rather than on precise emissions. We posited that a linear relationship between damage caused by emissions and emissions would exist. Thus, variation in damage caused by emissions was expressed as:

$$\widehat{D}_n = \frac{e_1}{e}\hat{e}_1 + \frac{e_2}{e}\hat{e}_2 + \cdots + \frac{e_n}{e}\hat{e}_n \tag{14}$$

2.4. Data

2.4.1. Numerical Settings of the Payoff Matrix

As with most game model studies, we set values to analyze different Nash equilibrium outcomes. From the perspective of 2 × 2 static games, the model constructed in this study corresponds to the 25 climate cooperation 2 × 2 games proposed by DeCanio and Fremstad [23]. These games can be mainly classified as No-Conflict, Prisoner's Dilemma,

Coordination, Chicken, and Unhappy Games. In this study, the game form depended on the numerical values of the payoff matrices. The payoff matrices for the game between the two regions are shown in Table 1, where Π_n^A, Π_n^B, Π_n^C, and Π_n^D represent the regional profits under the four strategy combinations.

Table 1. Payoff Matrix of the 2 × 2 game.

		Region 2	
		Synergistic Action (SA)	Unilateral Action (UA)
Region 1	Synergistic Action (SA)	Π_1^A, Π_2^A	Π_1^B, Π_2^B
	Unilateral Action (UA)	Π_1^C, Π_2^C	Π_1^D, Π_2^D

To clarify the relationship between emissions and economic growth under different strategies, this study used different payoff values, following the analysis method of complete information static games. In this study, game payoffs were ordinal or cardinal. In the studies by DeCanio and Fremstad [23] and Madani [32], ordinal numbers ranging from one to four were used to represent the payoffs of agents in climate games, with the government as a game participant ranking the sequential results. This approach is commonly used in static games with perfect information. Using ordinal values as payoffs in climate change games avoids the comparison of utilities between regions with significantly different income levels, thereby overcoming the shortcomings of traditional cost-benefit analyses. Therefore, we set the payoff values under different strategies to 0.01, 0.02, 0.03, and 0.04. This was consistent with the calculated values of our model, which effectively explained the economic meaning implied in the data, namely, the difference between changes in GDP and damages, both caused by emissions. Furthermore, this setting was similar to ordinal results, representing the utilities of local governments at four levels under different strategies and making the game results more intuitive. Based on these settings, values for emissions, damage caused by emissions, and economic growth were assigned. Although this value setting is only one of many results, it is consistent in interpreting the relationship between different strategies, emissions, and economic growth in models.

For both regions, the numerical settings of emission changes were provided according to the two scenarios assumed above. As shown in Table 2, in Scenario 1, $\hat{e}_n = 0.8$ if the region chose the SA strategy, and $\hat{e}_n = 1$ if the region chose the UA strategy. Regional synergy in Scenario 1 indicated that both players increased their emission reduction efforts to minimize the overall emissions of both regions. In Scenario 2, $\hat{e}_1 = 0.7$ and $\hat{e}_2 = 1.1$ if both regions chose the SA strategy, $\hat{e}_1 = 0.9$ and $\hat{e}_2 = 1$ if Region 1 chose SA and Region 2 chose UA, and $\hat{e}_1 = 1$ and $\hat{e}_2 = 1.1$ if Region 1 chose UA and Region 2 chose SA. The form of regional synergistic emission reduction in Scenario 2 indicated that some regions could increase their emissions appropriately when synergistic, considering the overall decrease in the emissions increase in both regions. According to the model, if changes in emissions are determined, changes in damage caused by emissions can be obtained. If $\hat{e}_{1+2} = 0.8$, $\widehat{D}_n = 0.96$; if $\hat{e}_{1+2} = 0.9$, $\widehat{D}_n = 0.97$; if $\hat{e}_{1+2} = 0.95$, $\widehat{D}_n = 0.98$; if $\hat{e}_{1+2} = 1$, $\widehat{D}_n = 0.99$. The reason for this setting is that while Regions 1 and 2 did not change their emissions, emission reduction actions in other regions reduced total emissions; if $\hat{e}_{1+2} = 1.05$, $\widehat{D}_n = 1$. Thus, the difference in the payoff matrix is mainly determined by the difference in changes in GDP due to abatement actions.

Table 2. Nash equilibrium, emissions, and economic growth of synergistic emission reduction.

Type of Game		No-Conflict Game		Prisoner's Dilemma Game		Coordination Game		Chicken Game		Unhappy Game	
Nash Equilibrium		(SA, SA)		(UA, UA)		(SA, SA) and (UA, UA)		(SA, UA) and (UA, SA)		(SA, UA)	
Region		1	2	1	2	1	2	1	2	1	2
Payoff	Π_n^A	0.04	0.04	0.03	0.03	0.04	0.04	0.03	0.03	0.03	0.03
	Π_n^B	0.02	0.03	0.01	0.04	0.01	0.03	0.02	0.04	0.02	0.04
	Π_n^C	0.03	0.02	0.04	0.01	0.03	0.01	0.04	0.02	0.04	0.01
	Π_n^D	0.01	0.01	0.02	0.02	0.02	0.02	0.01	0.01	0.01	0.02
Scenario 1	$\hat{e}_n$	0.8	0.8	1	1	0.8 (1)	0.8 (1)	0.8 (1)	1 (0.8)	0.8	1
	$\hat{e}_{1+2}$	0.8		1		0.8 (1)		0.9		0.9	
	$\widehat{D}_{\mathrm{n}}$	0.96		0.99		0.96 (0.99)		0.97		0.97	
	$\widehat{G}_n$	1	1	1	1	1 (1.01)	1 (1.01)	0.99 (1.01)	1.01 (0.99)	0.99	1.01
	$\widehat{G}_{1+2}$	1		1		1 (1.01)		1 (1)		1	
Scenario 2	$\hat{e}_n$	0.7	1.1	1	1	0.7 (1)	1.1 (1)	0.9 (1)	1 (1.1)	0.9	1
	$\hat{e}_{1+2}$	0.9		1		0.9 (1)		0.95 (1.05)		0.95	
	$\widehat{D}_{\mathrm{n}}$	0.97		0.99		0.97 (0.99)		0.98 (1)		0.98	
	$\widehat{G}_n$	1.01	1.01	1.01	1.01	1.01	1.01	1 (1.04)	1.02 (1.02)	1	1.02
	$\widehat{G}_{1+2}$	1.01		1.01		1.01		1.01 (1.03)		1.01	

2.4.2. Parameter Settings

As the design of the regional economic growth part of the model in this study is based on a general spatial equilibrium model, realistic data can be used for the analysis. To obtain more general findings, we use a range of key parameters and values from existing studies, including trade elasticity [43] and emissions elasticity [37]. The object of our analysis is still assumed to be the two general regions, 1 and 2, and all other regions are grouped into Region 3. We establish a set of parameters based on the current state of the economy as a baseline, where $\theta^j = \theta^k = 4$, $\alpha_n^j = 0.6$, $\alpha_n^k = 0$, $\pi_{11}^j = \pi_{12}^j = \pi_{21}^j = \pi_{21}^j = 0.3$, $\pi_{13}^j = \pi_{23}^j = 0.4$, $\gamma_n^{jk} = \gamma_n^{jj} = \gamma_n^{kk} = 0.1$, $\gamma_n^{kj} = 0.4$, $\gamma_n^j = 0.6$, $\psi_n^j = 0.5$, and $\beta_n = 0.17$. In this baseline, we take two values for each parameter to compare the results and thus analyze the impact of each factor on the comparative advantage of emission reduction. The specific settings are given in the later analysis.

3. Results

3.1. Nash Equilibrium of Regional Synergistic Emission Reduction

3.1.1. Equilibrium Results in the Basic Synergistic Form

The results of the game analysis are presented in Table 2 (a more detailed analysis of the process and results can be found in Appendix A). Changes in the GDP caused by abatement actions determine regional strategies, resulting in different Nash equilibrium

outcomes. In Scenario 1, for the No-Conflict Game, when the changes in GDP of the two regions are less affected by the abatement action ($\widehat{G}_1 = \widehat{G}_2 = 1$, $\hat{e}_1 = \hat{e}_2 = 0.8$), unilateral actions of the free-riding regions do not cause an increase in their own GDP but generate a loss of economic growth for regions that choose SA ($\widehat{G}_1 = 0.99$, $\widehat{G}_2 = 1$, $\hat{e}_1 = 0.8$, $\hat{e}_2 = 1$). There was no significant boost to economic growth when both sides maintained their existing emission reduction plans ($\widehat{G}_1 = \widehat{G}_2 = 1$, $\hat{e}_1 = \hat{e}_2 = 1$), and rational players settled on the (SA, SA) strategy pair in Nash equilibrium.

When the payoff of free-riding is greater than the payoff of synergistic emission reduction ($\Pi_1^C = 0.04 > 0.03 = \Pi_1^A$ and $\Pi_2^B = 0.04 > 0.03 = \Pi_2^A$), and benefiting from the overall reduction in emissions from global mitigation actions, two regions taking unilateral action can achieve a decrease in changes in damage from emissions ($\widehat{D}_1 = \widehat{D}_2 = 0.98$). In other words, both regions can benefit from the overall reduction in emissions by choosing the UA strategy ($\Pi_1^D = \Pi_2^D = 0.02$), even if this payoff is smaller than the payoff from the synergistic emission reduction ($\Pi_1^A = \Pi_2^A = 0.03$). In this case, the game falls into a prisoner's dilemma.

Unlike the prisoner's dilemma, although there is an equilibrium outcome (UA, UA) in the Coordination Game, there is also a Pareto-optimal equilibrium for the (SA, SA) strategy pair; that is, when both regions reach a synergistic emission reduction, they gain the highest payoff. When one region chooses SA and the other chooses UA in the Coordination Game, the region loses economic growth to reduce emissions ($\widehat{G}_n = 0.98$) and fails to benefit from the other region's lenient environmental policy. At this point, this region has the lowest payoff ($\Pi_n^B = 0.01$); therefore, this game reflects the nature of collective action in both regions.

In addition, when either player in the game is able to achieve a greater increase in economic growth by free-riding ($\widehat{G}_n = 1.01$) and gaining the highest payoff, a Chicken or Unhappy Game is formed, and it is difficult for the two regions to reach an equilibrium result of synergistic emission reduction.

In summary, the mitigation actions of the two regions impact each other's economic growth, and the extent to which the two regions can achieve synergistic emission reduction depends on the changes in economic growth resulting from emission reduction. Achieving the regional synergistic emission reduction described in Scenario 1 requires both parties to achieve higher economic growth under strict environmental policies while reducing emissions. It is important to avoid high economic growth in a region through free-rider behavior.

3.1.2. Equilibrium Results Considering the Comparative Advantage of Emission Reduction

Unlike Scenario 1, Scenario 2 describes two regions that exploit their respective comparative advantages to reduce emissions. For Region 2, increasing $\hat{e}_2$ rather than decreasing $\hat{e}_2$ allows for more overall economic growth in both regions. For Region 1, decreasing $\hat{e}_1$ compared to increasing $\hat{e}_1$ can reduce the damage from emissions by significantly reducing emissions and does not result in a greater loss of economic growth. Consequently, both regions reap greater overall payoffs.

In Scenario 2, the synergistic emission reduction in the two regions allows one region to increase emissions in the short term. This means that the (SA, SA) Nash equilibrium strategy pair in Scenario 2 is easier to achieve than in Scenario 1, and both players in the game are more likely to form regional synergistic emission reduction. It is easier to form No-Conflict and Coordination Games. When a region has a comparative advantage in emission reduction, the implementation of strict emission reduction policies can still lead to economic growth ($\widehat{G}_1 = 1.01$). Even if another region increases some of its emissions, it is an effective synergistic emission reduction as long as the overall emission change of both regions ($\hat{e}_{1+2}$) decreases. This means that the conditions for achieving regional synergistic emission reduction have been relaxed, allowing regions that are still in the process of reaching their carbon peaks to participate. However, other payoff matrices in Scenario 2 that cannot achieve the (SA, SA) Nash equilibrium strategy pair are less likely to

occur in reality than in Scenario 1. To achieve Prisoner's Dilemma, Chicken, and Unhappy Games, regions that do not have a comparative advantage in reducing emissions must achieve higher economic growth ($\widehat{G}_2 = 1$ when $\hat{e}_2 = 1.1$, $\widehat{G}_2 = 1.02$ when $\hat{e}_2 = 1$), which is challenging.

Different comparative advantages of emission reduction between two regions form a differentiated pattern of regional emissions and economic growth. The Nash equilibrium that achieves regional synergistic emission reduction has the lowest overall emissions of the two regions ($\hat{e}_{1+2} = 0.8$) compared to the other equilibrium strategy pairs, enabling faster achievement of the carbon neutrality target while maintaining economic growth. However, Scenario 1 has better reduction results than Scenario 2 ($0.8 < 0.9$), whereas the economic growth of the two regions under Scenario 2 is better than that of Scenario 1 ($1.01 > 1$). Although reducing emissions as quickly as possible is an important pathway to achieving carbon-neutrality goals, for some regions, the pursuit of faster emission reduction comes at a higher cost in terms of lost economic growth. Therefore, regional synergistic emission reduction requires a trade-off between economic growth and emission reduction and the pursuit of a global optimum rather than a local optimum.

3.2. Factors Influencing the Comparative Advantage of Emission Reduction in Regional Synergy

The game analysis demonstrated that effective regional synergy relies on the ability of a region to form a comparative advantage in emission reduction, mainly in terms of the impact of different emission reduction actions on local and other regions' economic growth. This avoids a sharp decline in economic growth when implementing strict environmental regulations and exchanges a lower increase in emissions for faster economic growth in both regions. Therefore, we analyzed the effects of various factors on the formation of a comparative advantage in emission reduction, including the regional characteristics determined by the emission elasticity, α_1^j, the GDP of sector j in region n as a share of the total regional GDP, ψ_n^j, and the trade share, π_{ni}^j. Local governments increase economic growth by changing green TFP, $\hat{A}_n^j$, and trade costs, $\hat{\kappa}_{ni}^j$, and reduce the recession in economic growth from changes in the intensity of environmental regulations, $\hat{t}_n$.

3.2.1. Emission Elasticities

First, in carbon-intensive sectors, low emission elasticities attenuate the impact of changes in the intensity of environmental regulations on economic growth, whereas high emission elasticities amplify the loss of economic growth from abatement. In Figure 1a, the horizontal axis represents the change in the intensity of environmental regulations in Region 1, $\hat{t}_1$, which indicates regional efforts to mitigate climate change. The vertical axis represents the GDP change in Region 1, $\widehat{GDP}_1$. According to Duan et al. [37], who estimated the emission elasticity of sectors in major countries, most of the values of α_n^j range from 0.01 to 0.11. When $\alpha_1^j = 0.01$, an increase in $\hat{t}_1$ causes a smaller decrease in $\widehat{GDP}_1$, whereas when $\alpha_1^j = 0.11$, an increase in $\hat{t}_1$ causes a larger decrease in $\widehat{GDP}_1$. This is because high emission elasticity means that manufacturers in carbon-intensive sectors produce more emissions as by-products when producing intermediate products, which entails higher production costs and results in higher prices for products in carbon-intensive sectors.

Second, when sectors in a region have higher emission elasticity values, the impact of emission reduction actions on economic growth spills over to other regions. As shown in Figure 1b, when $\alpha_1^j = 0.01$, the curves of $\hat{t}_1$ and $\widehat{GDP}_2$ are close to horizontal, which means that changes in the intensity of environmental regulations in Region 1 have little effect on the changes in GDP in Region 2. In contrast, when $\alpha_1^j = 0.11$, an increase in $\hat{t}_1$ causes a decrease in $\widehat{GDP}_2$, which means that the implementation of more stringent environmental regulations in Region 1 causes a loss of economic growth in Region 2. This is because under the trade linkage of carbon-intensive products between the two regions, Region 2 faces the same product price increase owing to strict environmental regulations when purchasing

products from Region 1's carbon-intensive sectors. In addition, as shown in Figure 1c, the value of the emission elasticity of another region had little effect on the relationship between $\hat{t}_1$ and $\widehat{GDP}_1$ in this region.

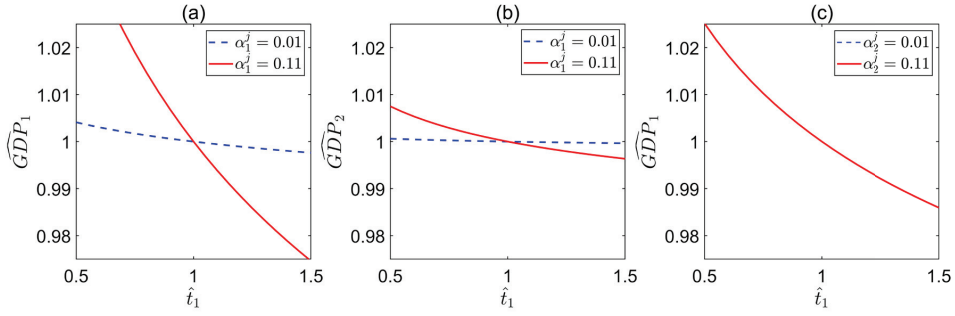

Figure 1. Relationship between $\hat{t}_n$ and $\widehat{GDP}_n$ under different α_n^j. (**a**) Relationship between $\hat{t}_1$ and $\widehat{GDP}_1$ under different α_1^j; (**b**) Relationship between $\hat{t}_1$ and $\widehat{GDP}_2$ under different α_1^j; (**c**) Relationship between $\hat{t}_1$ and $\widehat{GDP}_1$ under different α_2^j.

Third, the value of the emission elasticity portrays the emission characteristics of the sector. When the emission elasticity tends to zero, carbon-intensive sectors gradually transform into low-emission sectors, generating fewer emissions during production. Therefore, the emission elasticity of carbon-intensive sectors is reduced by upgrading technology to decrease the share of byproducts produced effectively in intermediate goods to achieve economic growth under emission reduction constraints.

3.2.2. Sectoral Structures

First, the sectoral structure of a region determines the extent to which changes in environmental regulations affect its economic growth. When a region's sectors are predominantly carbon intensive, enhanced efforts to reduce emissions through strict environmental regulations can lead to a significant decline in economic growth in the region. As shown in Figure 2a, when the share of carbon-intensive sectors in the region is $\psi_1^j = 0.7$, $\hat{t}_1$ increases, causing a larger decrease in $\widehat{GDP}_1$, whereas when $\psi_1^j = 0.3$, $\hat{t}_1$ increases, causing a smaller decrease in $\widehat{GDP}_1$. Regions with a low-emission sectoral structure will not bear a disproportionate economic loss from significant emission reduction compared to regions with carbon-intensive sectors as their mainstay.

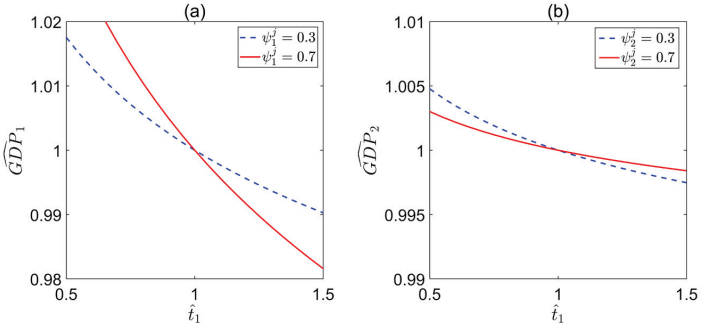

Figure 2. Relationship between $\hat{t}_n$ and $\widehat{GDP}_n$ under different ψ_n^j. (**a**) Relationship between $\hat{t}_1$ and $\widehat{GDP}_1$ under different ψ_1^j; (**b**) Relationship between $\hat{t}_1$ and $\widehat{GDP}_2$ under different ψ_2^j.

Second, regions with low-emission sectoral structures are more vulnerable to changes in the strength of environmental regulations in other regions. As shown in Figure 2b,

comparing the values of different ψ_2^j, when $\psi_2^j = 0.3$, an increase in $\hat{t}_1$ causes a greater decrease in $\widehat{GDP}_2$. This suggests that when the sectoral structure of Region 2 has a low share of carbon-intensive sectors, its economy is more vulnerable to the cross-regional impacts of the environmental regulations in Region 1. This is because Region 2 has fewer carbon-intensive sectors, and its demand for carbon-intensive products is more likely to be met by the supply from Region 1. When Region 1 enforces strict environmental regulations, it raises the price of the products produced by its carbon-intensive sectors, which in turn increases the cost of production in Region 2. A specific example is the inter-regional transmission of electricity, where increased environmental regulations in the power-exporting location increase the cost of electricity production, raising the price of purchased electricity in the power-importing location and further increasing the production costs of other industries in the power-importing location, thereby affecting economic growth.

3.2.3. Trade Shares

First, when regional demand for carbon-intensive intermediate goods is mainly supplied by other regions, changes in the intensity of environmental regulation in the region have less impact on its economic growth. Conversely, when a region purchases a higher share of carbon-intensive intermediate goods from local sources, changes in the intensity of environmental regulations in that region are greater for economic growth.

Figure 3a shows two extreme cases of the trade share of the carbon-intensive sector j. $\pi_{11}^j = 0$ means that all the products of sector j required in the region come from other regions, at which time the increase in $\hat{t}_1$ causes a smaller decrease in $\widehat{GDP}_1$. Moreover, $\pi_{11}^j = 1$ means that all the products of sector j required by the region come from itself, and the increase in $\hat{t}_1$ causes a larger decrease in $\widehat{GDP}_1$. This is because strict environmental regulations increase the price of intermediate products by increasing the production cost of sector j. In the absence of trade in sector j, the region can only buy local intermediate products from sector j at higher prices, which slows economic growth. When the share of intermediate goods purchased from other regions in sector j increases, the demand for local high-priced intermediate goods in sector j gradually decreases and regional economic growth is less affected by environmental regulations.

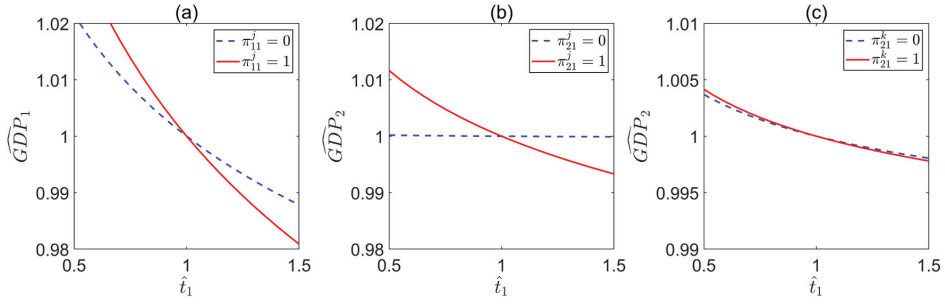

Figure 3. Relationship between $\hat{t}_n$ and $\widehat{GDP}_n$ under different π_{ni}^j. (**a**) Relationship between $\hat{t}_1$ and $\widehat{GDP}_1$ under different π_{11}^j; (**b**) Relationship between $\hat{t}_1$ and $\widehat{GDP}_2$ under different π_{21}^j; (**c**) Relationship between $\hat{t}_1$ and $\widehat{GDP}_2$ under different π_{21}^k.

Second, the cross-regional spillover effects of environmental regulations on economic growth are constrained by trade share. If strong trade links exist between the two regions in carbon-intensive intermediate goods, changes in the intensity of environmental regulations in one region may have a larger impact on economic growth in the other. As shown in the two extreme cases in Figure 3b, $\pi_{21}^j = 0$ indicates that the share of products in sector j purchased by Region 2 from Region 1 is 0. $\hat{t}_1$ has almost no effect on $\widehat{GDP}_2$ in this case. When $\pi_{21}^j = 1$, all the intermediate goods of sector j are purchased by Region 2

from Region 1; at this time, the strengthening of environmental regulations in Region 1 leads to the loss of economic growth in Region 2. In addition, the cross-regional spillover effects of environmental regulations on economic growth are closely related to the emission characteristics of the sectors, as shown in Figure 3c. Changes in the trade shares of the low-carbon sectors in the two regions do not significantly alter the cross-regional economic impact of environmental regulation.

3.2.4. Green Total Factor Productivity

First, an increase in green TFP in carbon-intensive sectors can reduce the negative impact of climate-change mitigation measures on economic growth. As shown in Figure 4a, $\hat{t}_1 = 1.5$ and $\hat{t}_1 = 0.5$ represents the increase and decrease, respectively, in environmental regulations to control the growth of emissions by regional agents. Changes in the intensity of local governments' efforts to control emissions affect the relationship between green TFP and economic growth in carbon-intensive sectors. Achieving the same level of economic growth under strict environmental regulations requires a higher green TFP in carbon-intensive sectors. Although stronger environmental regulations reduce economic growth, $\widehat{GDP}_n$ is greater than 1 when $\hat{A}_n^j$ is higher, which maintains a positive change in GDP.

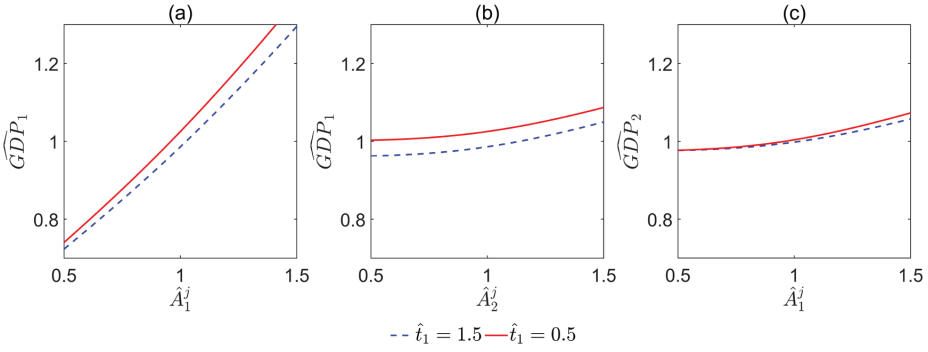

Figure 4. Relationship between $\hat{A}_n^j$ and $\widehat{GDP}_n$ under different $\hat{t}_n$. (**a**) Relationship between $\hat{A}_1^j$ and $\widehat{GDP}_1$; (**b**) Relationship between $\hat{A}_2^j$ and $\widehat{GDP}_1$; (**c**) Relationship between $\hat{A}_1^j$ and $\widehat{GDP}_2$.

Second, the mitigating effect of increased green TFP on the negative impacts of environmental regulations has a regional spillover effect. As shown in Figure 4b, changes in the green TFP $\hat{A}_1^j$ and GDP $\widehat{GDP}_1$ of Region 1 are positively correlated. A higher level of green TFP gains in carbon-intensive sector j leads to a higher level of economic growth. Furthermore, under exact-hat algebra assumptions, the numerical magnitude relationship between the variable and 1 determines the direction of change in the variable. If t_1 is constant, $\hat{A}_1^j > 1$ (or $\hat{A}_1^j < 1$) indicates that an increase (decrease) in green TFP leads to an increase (decrease) in GDP. As can be seen from (b) and (c) in Figure 4, an increase in $\hat{A}_n^j$ positively affects changes in GDP in the other region, $\widehat{GDP}_i$.

3.2.5. Trade Costs

Reducing the cost of trade in carbon-intensive sectors may lead to the relocation of carbon-intensive industries between regions, thereby affecting regional economic growth. According to current spatial economics theory, lower inter-regional trade costs contribute to economic growth. As shown in Figure 5, $\hat{\kappa}_{ni}^j$ has an inverse effect on $\widehat{GDP}_n$. Comparing (a) and (d) with (c) and (f), the impact curve of the change in trade costs on the change in local GDP is steeper than that of the other regions. Lower trade costs result in lower prices for local purchases of intermediate goods from other regions, leading to local economic growth. However, for regions with strict environmental regulations, in which environmental regulations increase the cost of production in local carbon-intensive sectors, lower

trade costs imply that carbon-intensive products can be purchased from other regions at lower prices. This reduces the production of carbon-intensive products in the local area and increases those produced in areas with relatively lax emissions regulations. While the relocation of carbon-intensive industries creates carbon leakage problems for the latter, buying higher-emission products from other regions at lower prices allows the former to continue to grow economically under strict environmental regulations. As shown in Figure 5a, although a tendency towards more stringent environmental regulations ($\hat{t}_1 = 1.5$) reduces economic growth, when $\hat{\kappa}_{12}^{j}$ is lower, $\widehat{GDP}_1$ is greater than 1, and the GDP can maintain its original level of growth. Furthermore, for different industries, comparing (a) and (d) with (b) and (e) in Figure 5, changes in trade costs $\hat{\kappa}_{ni}^{j}$ for the carbon-intensive sector j has a greater impact on economic growth than changes in trade costs $\hat{\kappa}_{ni}^{k}$ for other sectors k.

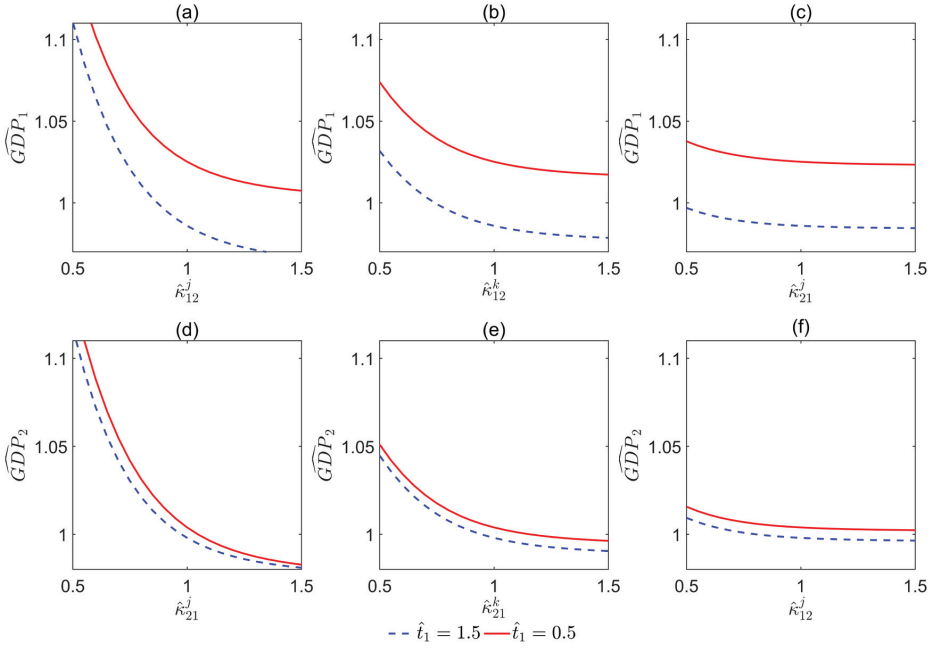

Figure 5. Relationship between $\hat{\kappa}_{ni}^{j}$ and $\widehat{GDP}_n$ under different $\hat{t}_n$. (**a**) Relationship between $\hat{\kappa}_{12}^{j}$ and $\widehat{GDP}_1$; (**b**) Relationship between $\hat{\kappa}_{12}^{k}$ and $\widehat{GDP}_1$; (**c**) Relationship between $\hat{\kappa}_{21}^{j}$ and $\widehat{GDP}_1$; (**d**) Relationship between $\hat{\kappa}_{21}^{j}$ and $\widehat{GDP}_2$; (**e**) Relationship between $\hat{\kappa}_{21}^{k}$ and $\widehat{GDP}_2$; (**f**) Relationship between $\hat{\kappa}_{12}^{j}$ and $\widehat{GDP}_2$.

4. Discussion

4.1. Discussion of the Case of China

The results of our analysis can explain the current regions where synergistic emission reductions have been developed. China has set the goal of "carbon peaking and carbon neutrality" to mitigate climate change [44]. However, the unique complexity of China's economy as a large country determines the complexity and uniqueness of its regional cooperation in emission reduction [45]. Mitigating climate change is usually assigned to China's administrative regions, and the different resource endowments of each region lead to significant differences in their performance in mitigating climate change [46]. In this context, regional synergistic emission reduction is beginning in some regions of China. A typical example is the collaborative management of air pollution in Beijing, Tianjin, and Hebei. The Action Plan for the Prevention and Control of Air Pollution ("Ten Measures

for the Atmosphere") was promulgated in 2013, and the Beijing-Tianjin-Hebei Synergistic Development was elevated to a national strategy in 2014. With the joint efforts between regions, the implementation of "Ten Measures for the Atmosphere" reduced 352.7 Mt of CO_2 emissions in the Beijing-Tianjin-Hebei regions [47]. Although these three regions are in different stages of development, effective synergistic climate change governance has been achieved. Among them, Beijing and Hebei play different roles. Beijing adopts strict environmental regulations to control emissions, while Hebei increases the growth rate of emissions in the short term by taking over some of Beijing's industries [48], with more lenient emission reduction policies to maintain stable economic growth in both regions. According to emissions data published by Carbon Emission Accounts and Datasets [49], the change in Beijing's carbon emissions has decreased from 1.026 in 2013–2014 to 0.937 in 2014–2015 since the enactment of the Air Pollution Control Action Plan in 2013. In contrast, the change in carbon emissions in Hebei saw a brief increase, from 0.95 in 2013–2014 to 1.024 in 2014–2015.

This validates the form of synergistic emission reduction proposed by our model. Compared to Beijing, which has completed industrialization, Hebei has more industries with high carbon emission intensity [50], which means that strict environmental regulations can significantly increase the production costs of firms. The trade link between the two regions is deeper with the industrial transfer, and increasing the emission growth rate in Hebei in the short term will provide better overall returns for both regions than decreasing the emission growth rate. Whether through appropriate regional cost-sharing of emission reductions [51] or horizontal transfer payments from Beijing to Hebei [52], stable synergistic emission reductions must allow Hebei to reap additional gains from cooperative emission reductions. This part of the gains is mainly captured by economic growth in our study.

4.2. Further Discussion of the Findings

Consistent with the findings of Da Zhu [30], Molina et al. [31], and others, the results of our model analysis emphasize the importance of economic growth in the choice of regional synergy strategies. Furthermore, we include changes in GDP caused by changes in emissions in the payoff function and define the formation condition of synergistic emissions reduction as a decrease in changes in total emissions in both regions. This enhancement expands the eligibility for participation in synergistic emission reductions to cover the case of the region reaching peak emissions through synergy.

Recent research on national climate change cooperation concludes that it is difficult to establish stable cooperation between countries with large differences in income levels [24,53]. However, we find that regional synergistic emissions reductions within a country are more flexible in form than cooperation between countries. This allows our model to allow regions with differing incomes to achieve synergistic emissions reductions. Under national-level climate change targets, some regions will appropriately relax constraints on emissions reductions and increase the rate of emissions growth in the short term [46] to ensure smooth economic growth while reaching peak emissions as soon as possible. For such areas, we propose a form of cooperation that exploits the comparative advantages of regional emissions reductions. That is, by increasing the growth rate of emissions, such regions stimulate the economic growth of their own region and the synergistic region, thereby reducing the economic loss of the synergistic region due to emission reduction and helping the two regions to jointly achieve the emission reduction target.

Although game models are considered divorced from policy practice in the analysis of climate cooperation issues [33], as in Carrozzo Magli and Manfredi [24], Verendel et al. [26], and others, more detailed games also strengthen the policy guidance implications of the models. Starting from the base game form proposed by DeCanio and Fremstad [23], our study enriches the current game model in terms of regional characteristics and inter-regional economic relations. By adding a general spatial equilibrium model to the game model, the model is made as close to the economic reality as possible to provide trade, industry, and economic growth policy complement to emissions reduction policy.

The model developed in this study can be used for future analyses. As this study aimed to explain general regional synergistic emission reduction theoretical mechanisms, although a quantitative general spatial equilibrium model was incorporated into the game model, the results of the simulations were derived by assigning values to the parameters in the analysis. Future studies could apply this model to calculate the economic impact of emission-reduction actions using real statistics from specific regions, extend the damage from emissions not analyzed in detail in this study, and make precise calculations. This would allow the analysis of synergistic emission reduction between specific regions and the prediction of synergistic emission reduction potential of different regions. The model is also applicable to other regions and countries, providing methodological support for the analysis of inter-regional cooperation on climate change mitigation. However, the model proposed in this study still has some limitations. First, our model is based on short-term static analyses and is unable to analyze the long-term dynamic problem of stable cooperation. Future research can extend our study with dynamic games and dynamic general equilibrium models. In addition, our model does not focus on socio-political factors and constructs a utility function using only economic gains and climate change damages. Socio-political factors are undeniably critical in climate change cooperation, and issues such as public attitudes toward climate change and environmental issues, mechanisms for the promotion of officials, and the right to development in the region all influence the formation of cooperation. These factors could be used to enrich our model in future research.

5. Conclusions

This study constructed a game model of regional synergistic emission reduction. The Basic Climate Game was modified using the exact-hat algebra method, with changes in GDP and damage caused by emissions included in the payoff function. This allows for a more rational description of changes in emissions during the process of achieving climate change targets and tradeoffs between economic growth and emission reduction by regional agents. A general spatial equilibrium model incorporating emissions and environmental regulations was constructed to extend the game model and analyze the changes in regional economic growth under emission reduction actions to explain the formation of comparative advantages of emission reduction and impact on regional synergistic emission reduction.

Whether synergistic emission reduction can be achieved between regions depends on whether regions can achieve the dual goals of reducing emissions and maintaining economic growth in the process of regional synergistic emission reduction. The synergy between the two regions means that, while maintaining stable economic growth, the overall increase in emissions of the two regions or the total amount of emissions is reduced.

Regional action to reduce emissions using environmental regulations as a policy tool not only impacts local economic growth but also has a cross-regional economic impact in the context of regional trade. Different economic impacts of emission reduction reflect the comparative advantages of regional emission reduction, including faster emission reduction with lower economic growth losses and faster economic growth with fewer incremental emissions.

Pursuing the optimal emission reduction effect locally is difficult and inefficient; the overall optimal emission reduction effect should be pursued to effectively achieve the carbon neutrality target. This requires using the comparative advantage of each region to reduce emissions. Regions where a small increase in emissions can effectively drive the overall economic growth of the two synergistic regions can appropriately increase their emissions. This can lower the threshold for regional participation in synergistic emission reduction and enable more regions to join the synergy. Regions that can maintain economic growth despite significant emission reduction, can undertake more emission reduction in regional synergy. This form of synergy can maintain the overall economic growth of both regions while reducing total emissions.

The formation of a comparative advantage in emission reduction depends on characteristics such as emissions elasticity, sectoral structure, and trade share in a region.

Considering the economic linkages between the two regions, these characteristics affect not only fluctuations in local economic growth due to environmental regulations but also the extent of cross-regional economic shocks due to environmental regulations. Regions must consider these characteristics and choose an appropriate way to participate in collaborative emission reduction.

Regional synergistic emission reduction requires not only emission reduction policies but a combination of policies. Regional trade and economic growth policies should not be neglected in the process of synergistic emission reduction, including improving green TFP, guiding industrial upgrading and inter-regional relocation, and reducing trade costs in key sectors between regions with synergistic emission reduction.

Supplementary Materials: The following supporting information can be downloaded at: https://www.mdpi.com/article/10.3390/land12091723/s1. Title: Supplementary Material—Details of the model.

Author Contributions: Conceptualization, T.M. and D.C.; methodology, D.C.; software, X.C.; validation, D.C., T.H. and T.M.; formal analysis, D.C.; investigation, T.H.; resources, T.M.; data curation, D.C.; writing—original draft preparation, D.C.; writing—review and editing, T.M.; visualization, X.C.; supervision, T.M. and T.H.; project administration, T.M.; funding acquisition, T.M. All authors have read and agreed to the published version of the manuscript.

Funding: This research was funded by the National Natural Science Foundation of China, grant numbers 71974046, 71950001, and the Heilongjiang Province Philosophy and Social Science Research Planning Project, grant number 21JYB143.

Data Availability Statement: All data generated or analysed during this study are included in this published article [and its Supplementary Information Files].

Conflicts of Interest: The authors have no relevant financial or non-financial interests to disclose.

Appendix A

Tables A1–A10 show the game models and the results of changes in emission, damage caused by emissions, and GDP for scenarios 1 and scenarios 2.

Table A1. No-conflict game in scenario 1.

		Region 2					
		Synergistic Action (SA)			Unilateral Action (UA)		
Region 1	Synergistic Action (SA)	0.04, 0.04 *			0.02, 0.03		
	Unilateral Action (UA)	0.03, 0.02			0.01, 0.01		
		$\hat{e}_n$		$\widehat{D}_n$		$\widehat{G}_n$	
		Region 1	Region 2	Region 1	Region 2	Region 1	Region 2
SA, SA		0.8	0.8	0.96	0.96	1	1
SA, UA		0.8	1	0.97	0.97	0.99	1
UA, SA		1	0.8	0.97	0.97	1	0.99
UA, UA		1	1	0.99	0.99	1	1

* Nash Equilibrium.

Table A2. Prisoner's dilemma game in scenario 1.

		Region 2					
		SA				UA	
Region 1	SA	0.03, 0.03				0.01, 0.04	
	UA	0.04, 0.01				0.02, 0.02 *	
		$\hat{e}_n$		$\widehat{D}_n$		$\widehat{G}_n$	
		Region 1	Region 2	Region 1	Region 2	Region 1	Region 2
SA, SA		0.8	0.8	0.96	0.96	0.99	0.99
SA, UA		0.8	1	0.97	0.97	0.98	1.01
UA, SA		1	0.8	0.97	0.97	1.01	0.98
UA, UA		1	1	0.98	0.98	1	1

* Nash Equilibrium.

Table A3. Coordination game in scenario 1.

		Region 2					
		SA				UA	
Region 1	SA	0.04, 0.04 *				0.01, 0.03	
	UA	0.03, 0.01				0.02, 0.02 *	
		$\hat{e}_n$		$\widehat{D}_n$		$\widehat{G}_n$	
		Region 1	Region 2	Region 1	Region 2	Region 1	Region 2
SA, SA		0.8	0.8	0.96	0.96	1	1
SA, UA		0.8	1	0.97	0.97	0.98	1
UA, SA		1	0.8	0.97	0.97	1	0.98
UA, UA		1	1	0.99	0.99	1.01	1.01

* Nash Equilibrium.

Table A4. Chicken game in scenario 1.

		Region 2					
		SA				UA	
Region 1	SA	0.03, 0.03				0.02, 0.04 *	
	UA	0.04, 0.02 *				0.01, 0.01	
		$\hat{e}_n$		$\widehat{D}_n$		$\widehat{G}_n$	
		Region 1	Region 2	Region 1	Region 2	Region 1	Region 2
SA, SA		0.8	0.8	0.96	0.96	0.98	0.98
SA, UA		0.8	1	0.97	0.97	0.99	1.01
UA, SA		1	0.8	0.97	0.97	1.01	0.99
UA, UA		1	1	0.99	0.99	1	1

* Nash Equilibrium.

Table A5. Unhappy game in scenario 1.

		Region 2					
		SA				UA	
Region 1	SA	0.03, 0.03				0.02, 0.04 *	
	UA	0.04, 0.01				0.01, 0.02	
		$\hat{e}_n$		$\widehat{D}_n$		$\widehat{G}_n$	
		Region 1	Region 2	Region 1	Region 2	Region 1	Region 2
SA, SA		0.8	0.8	0.96	0.96	0.99	0.99
SA, UA		0.8	1	0.97	0.97	0.99	1.01
UA, SA		1	0.8	0.97	0.97	1.01	0.98
UA, UA		1	1	0.99	0.99	1	1.01

* Nash Equilibrium.

Table A6. No-conflict game in scenario 2.

		Region 2					
		SA				UA	
Region 1	SA	0.04, 0.04 *				0.02, 0.03	
	UA	0.03, 0.02				0.01, 0.01	
		$\hat{e}_n$		$\widehat{D}_n$		$\widehat{G}_n$	
		Region 1	Region 2	Region 1	Region 2	Region 1	Region 2
SA, SA		0.7	1.1	0.97	0.97	1.01	1.01
SA, UA		0.9	1	0.98	0.98	1	1.01
UA, SA		1	1.1	1	1	1.03	1.02
UA, UA		1	1	0.99	0.99	1	1

* Nash Equilibrium.

Table A7. Prisoner's dilemma game in scenario 2.

		Region 2					
		SA				UA	
Region 1	SA	0.03, 0.03				0.01, 0.04	
	UA	0.04, 0.01				0.02, 0.02 *	
		$\hat{e}_n$		$\widehat{D}_n$		$\widehat{G}_n$	
		Region 1	Region 2	Region 1	Region 2	Region 1	Region 2
SA, SA		0.7	1.1	0.97	0.97	1	1
SA, UA		0.9	1	0.98	0.98	0.99	1.02
UA, SA		1	1.1	1	1	1.04	1.01
UA, UA		1	1	0.99	0.99	1.01	1.01

* Nash Equilibrium.

Table A8. Coordination game in scenario 2.

		Region 2					
		SA				UA	
Region 1	SA	0.04, 0.04 *				0.01, 0.03	
	UA	0.03, 0.01				0.02, 0.02 *	
		$\hat{e}_n$		$\widehat{D}_n$		$\widehat{G}_n$	
		Region 1	Region 2	Region 1	Region 2	Region 1	Region 2
SA, SA		0.7	1.1	0.97	0.97	1.01	1.01
SA, UA		0.9	1	0.98	0.98	0.99	1.01
UA, SA		1	1.1	1	1	1.03	1.02
UA, UA		1	1	0.99	0.99	1.01	1.01

* Nash Equilibrium.

Table A9. Chicken game in scenario 2.

		Region 2					
		SA				UA	
Region 1	SA	0.03, 0.03				0.02, 0.04 *	
	UA	0.04, 0.02 *				0.01, 0.01	
		$\hat{e}_n$		$\widehat{D}_n$		$\widehat{G}_n$	
		Region 1	Region 2	Region 1	Region 2	Region 1	Region 2
SA, SA		0.7	1.1	0.97	0.97	1	1
SA, UA		0.9	1	0.98	0.98	1	1.02
UA, SA		1	1.1	1	1	1.04	1.02
UA, UA		1	1	0.99	0.99	1	1

* Nash Equilibrium.

Table A10. Unhappy game in scenario 2.

		Region 2					
		SA				UA	
Region 1	SA	0.03, 0.03				0.02, 0.04 *	
	UA	0.04, 0.01				0.01, 0.02	
		$\hat{e}_n$		$\widehat{D}_n$		$\widehat{G}_n$	
		Region 1	Region 2	Region 1	Region 2	Region 1	Region 2
SA, SA		0.7	1.1	0.97	0.97	1	1
SA, UA		0.9	1	0.98	0.98	1	1.02
UA, SA		1	1.1	1	1	1.04	1.01
UA, UA		1	1	0.99	0.99	1	1.01

* Nash Equilibrium.

References

1. Wang, X.; Chen, Y.; Chen, J.; Mao, B.; Peng, L.; Yu, A. China's CO_2 regional synergistic emission reduction: Killing two birds with one stone? *Energy Policy* **2022**, *168*, 113149. [CrossRef]
2. Zheng, J.; Mi, Z.; Coffman, D.M.; Milcheva, S.; Shan, Y.; Guan, D.; Wang, S. Regional development and carbon emissions in China. *Energy Econ.* **2019**, *81*, 25–36. [CrossRef]
3. Auffhammer, M.; Carson, R.T. Forecasting the path of China's CO_2 emissions using province-level information. *J. Environ. Econ. Manag.* **2008**, *55*, 229–247. [CrossRef]
4. Dong, K.; Hochman, G.; Zhang, Y.; Sun, R.; Li, H.; Liao, H. CO_2 emissions, economic and population growth, and renewable energy: Empirical evidence across regions. *Energy Econ.* **2018**, *75*, 180–192. [CrossRef]
5. Wang, S.; Zeng, J.; Liu, X. Examining the multiple impacts of technological progress on CO_2 emissions in China: A panel quantile regression approach. *Renew. Sustain. Energy Rev.* **2019**, *103*, 140–150. [CrossRef]
6. Mi, Z.; Sun, X. Provinces with transitions in industrial structure and energy mix performed best in climate change mitigation in China. *Commun. Earth Environ.* **2021**, *2*, 1–12. [CrossRef]
7. Zhou, D.; Zhou, X.; Xu, Q.; Wu, F.; Wang, Q.; Zha, D. Regional embodied carbon emissions and their transfer characteristics in China. *Struct. Change Econ. Dyn.* **2018**, *46*, 180–193. [CrossRef]
8. Wu, S. A systematic review of climate policies in China: Evolution, effectiveness, and challenges. *Environ. Impact Assess. Rev.* **2023**, *99*, 107030. [CrossRef]
9. Lin, B.; Jia, Z. What will China's carbon emission trading market affect with only electricity sector involvement? A CGE based study. *Energy Econ.* **2019**, *78*, 301–311. [CrossRef]
10. Stavins, R.; Zou, J.; Brewer, T.; Conte Grand, M.; den Elzen, M.; Finus, M.; Gupta, J.; Höhne, N.; Lee, M.K.; Michaelowa, A.; et al. International cooperation: Agreements and instruments. *Clim. Change* **2014**, *7*, 1001–1082.
11. Mehling, M.A.; Metcalf, G.E.; Stavins, R.N. Linking climate policies to advance global mitigation. *Science* **2018**, *359*, 997–998. [CrossRef] [PubMed]
12. Akimoto, K.; Sano, F.; Tehrani, B.S. The analyses on the economic costs for achieving the nationally determined contributions and the expected global emission pathways. *Evol. Inst. Econ. Rev.* **2017**, *14*, 193–206. [CrossRef]
13. Fujimori, S.; Kubota, I.; Dai, H.; Takahashi, K.; Hasegawa, T.; Liu, J.; Hijioka, Y.; Masui, T.; Takimi, M. Will international emissions trading help achieve the objectives of the Paris Agreement? *Environ. Res. Lett.* **2016**, *11*, 104001. [CrossRef]
14. Thube, S.D.; Delzeit, R.; Henning, C.H.C.A. Economic gains from global cooperation in fulfilling climate pledges. *Energy Policy* **2022**, *160*, 112673. [CrossRef]
15. Barrett, S. Rethinking climate change governance and its relationship to the world trading system. *World Econ.* **2011**, *34*, 1863–1882. [CrossRef]
16. Hagen, A.; Schneider, J. Small climate clubs should not use trade sanctions. *Energy Res. Soc. Sci.* **2022**, *92*, 102777. [CrossRef]
17. Nordhaus, W. Dynamic climate clubs: On the effectiveness of incentives in global climate agreements. *Proc. Natl. Acad. Sci. USA* **2021**, *118*, e2109988118. [CrossRef]
18. Sun, X.; Wang, W.; Pang, J.; Liu, X.; Zhang, M. Study on the evolutionary game of central government and local governments under central environmental supervision system. *J. Clean. Prod.* **2021**, *296*, 126574. [CrossRef]
19. Wang, M.; Feng, C. The consequences of industrial restructuring, regional balanced development, and market-oriented reform for China's carbon dioxide emissions: A multi-tier meta-frontier DEA-based decomposition analysis. *Technol. Forecast. Soc. Change* **2021**, *164*, 120507. [CrossRef]
20. Li, B.; Wu, S. Effects of local and civil environmental regulation on green total factor productivity in China: A spatial Durbin econometric analysis. *J. Clean. Prod.* **2017**, *153*, 342–353. [CrossRef]
21. Finus, M. Game theoretic research on the design of international environmental agreements: Insights, critical remarks, and future challenges. *Int. Rev. Environ. Resour. Econ.* **2008**, *2*, 29–67. [CrossRef]
22. Heitzig, J.; Lessmann, K.; Zou, Y. Self-enforcing strategies to deter free-riding in the climate change mitigation game and other repeated public good games. *Proc. Natl. Acad. Sci. USA* **2011**, *108*, 15739–15744. [CrossRef] [PubMed]
23. Decanio, S.J.; Fremstad, A. Game theory and climate diplomacy. *Ecol. Econ.* **2013**, *85*, 177–187. [CrossRef]
24. Carrozzo Magli, A.C.; Manfredi, P. Coordination games vs prisoner's dilemma in sustainability games: A critique of recent contributions and a discussion of policy implications. *Ecol. Econ.* **2022**, *192*, 107268. [CrossRef]
25. Smead, R.; Sandler, R.L.; Forber, P.; Basl, J. A bargaining game analysis of international climate negotiations. *Nat. Clim. Change* **2014**, *4*, 442–445. [CrossRef]
26. Verendel, V.; Johansson, D.J.A.; Lindgren, K. Strategic reasoning and bargaining in catastrophic climate change games. *Nat. Clim. Change* **2016**, *6*, 265–268. [CrossRef]
27. Heitzig, J.; Kornek, U. Bottom-up linking of carbon markets under far-sighted cap coordination and reversibility. *Nat. Clim. Change* **2018**, *8*, 204–209. [CrossRef]
28. Kováč, E.; Schmidt, R.C. A simple dynamic climate cooperation model. *J. Public. Econ.* **2021**, *194*, 104329. [CrossRef]
29. Xiao, L.; Chen, Y.; Wang, C.; Wang, J. Transboundary pollution control in asymmetric countries: Do assistant investments help? *Environ. Sci. Pollut. Res. Int.* **2022**, *29*, 8323–8333. [CrossRef]
30. Da Zhu, J. Cooperative equilibrium of the China-US–EU climate game. *Energy Strategy Rev.* **2022**, *39*, 100797. [CrossRef]

31. Molina, C.; Akçay, E.; Dieckmann, U.; Levin, S.A.; Rovenskaya, E.A. Combating climate change with matching-commitment agreements. *Sci. Rep.* **2020**, *10*, 10251. [CrossRef]
32. Madani, K. Modeling international climate change negotiations more responsibly: Can highly simplified game theory models provide reliable policy insights? *Ecol. Econ.* **2013**, *90*, 68–76. [CrossRef]
33. Helm, D.; Hepburn, C.; Ruta, G. Trade, climate change, and the political game theory of border carbon adjustments. *Oxf. Rev. Econ. Policy* **2012**, *28*, 368–394. [CrossRef]
34. Kuhn, T.; Pestow, R.; Zenker, A. Building climate coalitions on preferential free trade agreements. *Environ. Resour. Econ.* **2019**, *74*, 539–569. [CrossRef]
35. Lessmann, K.; Marschinski, R.; Edenhofer, O. The effects of tariffs on coalition formation in a dynamic global warming game. *Econ. Modell.* **2009**, *26*, 641–649. [CrossRef]
36. Caliendo, L.; Parro, F.; Rossi-Hansberg, E.; Sarte, P. The impact of regional and sectoral productivity changes on the U.S. economy. *Rev. Econ. Stud.* **2018**, *85*, 2042–2096. [CrossRef]
37. Duan, Y.; Ji, T.; Lu, Y.; Wang, S. Environmental regulations and international trade: A quantitative economic analysis of world pollution emissions. *J. Public. Econ.* **2021**, *203*, 104521. [CrossRef]
38. Shapiro, J.S.; Walker, R. Why is pollution from US manufacturing declining? The roles of environmental regulation, productivity, and trade. *Am. Econ. Rev.* **2018**, *108*, 3814–3854. [CrossRef]
39. Van Vuuren, D.P.; Stehfest, E.; Gernaat, D.E.H.J.; van den Berg, M.; Bijl, D.L.; de Boer, H.S.; Daioglou, V.; Doelman, J.C.; Edelenbosch, O.Y.; Harmsen, M.; et al. Alternative pathways to the 1.5 °C target reduce the need for negative emission technologies. *Nat. Clim. Change* **2018**, *8*, 391–397. [CrossRef]
40. Dinda, S. Environmental Kuznets Curve Hypothesis: A Survey. *Ecol. Econ.* **2004**, *49*, 431–455. [CrossRef]
41. Copeland, B.R.; Taylor, M.S. *Trade and the Environment: Theory and Evidence*; Princeton University Press: Princeton, NJ, USA, 2003.
42. Wang, C.; Cong, J.; Wang, K.; Qi, Y.; Cai, W.; Li, Y.; Fu, S.; Wang, W.; Wei, Y.; Zheng, X.; et al. Research on China's technology lists for addressing climate change. *Chin. J. Popul. Resour. Environ.* **2021**, *19*, 151–161. [CrossRef]
43. Giri, R.; Yi, K.M.; Yilmazkuday, H. Gains from trade: Does sectoral heterogeneity matter? *J. Int. Econ.* **2021**, *129*, 103429. [CrossRef]
44. The State Council of the People's Republic of China. Opinions of the Central Committee of the Communist Party of China and the State Council on Completely, Accurately, and Comprehensively Implementing the New Development Concept and Doing a Good Job of Carbon Peak and Carbon Neutrality. 2021. Available online: https://www.gov.cn/zhengce/2021-10/24/content_5644613.htm (accessed on 1 July 2023).
45. Shi, Q.; Zheng, B.; Zheng, Y.; Tong, D.; Liu, Y.; Ma, H.; Hong, C.; Geng, G.; Guan, D.; He, K.; et al. Co-benefits of CO_2 emission reduction from China's clean air actions between 2013–2020. *Nat. Commun.* **2022**, *13*, 5061. [CrossRef] [PubMed]
46. Mi, Z.F.; Wei, Y.M.; He, C.Q.; Li, H.; Yuan, X.; Liao, H. Regional efforts to mitigate climate change in China: A multi-criteria assessment approach. *Mitig. Adapt. Strateg. Glob. Change* **2017**, *22*, 45–66. [CrossRef]
47. Lu, Z.; Huang, L.; Liu, J.; Zhou, Y.; Chen, M.; Hu, J. Carbon dioxide mitigation co-benefit analysis of energy-related measures in the air pollution prevention and control action plan in the Jing-Jin-Ji region of China. *Resour. Conserv. Recy* **2019**, *1*, 100006. [CrossRef]
48. Liu, T.; Pan, S.; Hou, H.; Xu, H. Analyzing the environmental and economic impact of industrial transfer based on an improved CGE model: Taking the Beijing-Tianjin-Hebei region as an example. *Environ. Impact Assess. Rev.* **2020**, *83*, 106386. [CrossRef]
49. Guan, Y.; Shan, Y.; Huang, Q.; Chen, H.; Wang, D.; Hubacek, K. Assessment to China's recent emission pattern shifts. *Earths Future* **2021**, *9*, EF002241. [CrossRef]
50. Wang, C.; Zhan, J.; Li, Z.; Zhang, F.; Zhang, Y. Structural decomposition analysis of carbon emissions from residential consumption in the Beijing-Tianjin-Hebei region, China. *J. Clean. Prod.* **2019**, *208*, 1357–1364. [CrossRef]
51. Liu, X.; Yang, M.; Niu, Q.; Wang, Y.; Zhang, J. Cost accounting and sharing of air pollution collaborative emission reduction: A case study of Beijing-Tianjin-Hebei region in China. *Urban. Clim.* **2022**, *43*, 101166. [CrossRef]
52. Chu, Z.; Bian, C.; Yang, J. Joint prevention and control mechanism for air pollution regulations in China: A policy simulation approach with evolutionary game. *Environ. Impact Assess. Rev.* **2021**, *91*, 106668. [CrossRef]
53. Gross, J.; Böhm, R. Voluntary restrictions on self-reliance increase cooperation and mitigate wealth inequality. *Proc. Natl. Acad. Sci. USA* **2020**, *117*, 29202–29211. [CrossRef] [PubMed]

MDPI AG
Grosspeteranlage 5
4052 Basel
Switzerland
Tel.: +41 61 683 77 34

Land Editorial Office
E-mail: land@mdpi.com
www.mdpi.com/journal/land

Academic Open
Access Publishing

mdpi.com

ISBN 978-3-7258-2642-1